LABORATORY EVALUATION OF THE UNCONFINED COMPRESSION STRENGTH OF POLYMERIC FIBER REINFORCED SOILS

by

Robert Emmett Kral

A thesis submitted to the faculty of
The University of North Carolina at Charlotte
In partial fulfillment of the requirements
for the degree of Master of Science in
Civil Engineering

Charlotte

2014

Approved by:

_____
Dr. Kimberly Warren

_____
Dr. Vincent Ogunro

_____
Dr. Miguel Pando

© 2014
Robert Emmett Kral
ALL RIGHTS RESERVED

ABSTRACT

ROBERT EMMETT KRAL. Laboratory evaluation of the unconfined compression strength of polymeric fiber reinforced soils. (Under the direction of DR. KIMBERLY WARREN)

Geosynthetic fiber reinforced soil can be used to remediate weak, near-surface soils. The purpose of this study was to determine the impact that the geofibers had on the unconfined compressive strength (UCS) of various soil types. To distinguish this work from previous studies, a larger diameter test mold was utilized to eliminate boundary effects, soils were reinforced with 12.7 mm (0.5 in) long polypropylene fibrillated fiber (PFF) inclusions, a wider range of fiber contents was tested, test specimens were carefully molded using select kaolin clay and Ottawa sand materials, and the controlled specimens were compared to the performance of four field soils. A total of 165 UCS tests were performed at both optimum moisture content (OMC) and Soaked soil conditions. In comparison to unreinforced test specimens, fiber reinforced test specimens clearly showed an increase in UCS ranging from 4% to 820% as the fiber content increased from 0.5% to 2% by mass. The data also displayed an optimum UCS, dependent upon the fine content in the soil and the percentage of fiber inclusions. As the fiber content increased, an increase in axial strain and ductility of the reinforced soil was observed due to the interaction between the soil particles and the PFFs, which also affected the failure mode of each test specimen. Specimens tested under soaked soil conditions displayed an increase in strength with increased reinforcement, but the magnitude was lower than the specimens tested at OMC conditions. The data acquired as part of this study correlated well with data presented in the literature.

ACKNOWLEDGEMENTS

Foremost, my sincerest thank you goes to Professor Kimberly Warren for the continued support, patience, and motivation. Her enthusiasm and immense expertise in Geotechnical Engineering made it very intriguing and the reason I wanted to concentrate in the field and pursue my Masters. It has been a struggle with schedules and life for both of us and I am grateful that we were able to make this final push and produce this thesis.

I would like to thank the University of North Carolina at Charlotte, Civil and Environmental Engineering Department, for granting and funding the pursuit of my academic dreams which led me to a Masters of Science in Civil Engineering. I would also like to thank my committee members, Professor Tobi Ogunro and Professor Miguel Pando, who were able to allocate the time and support in order to better my thesis. In addition, I want to thank Professor Srinivas Pulugurtha and James Birkett for their support and understanding in the effort to grant my graduation request for Fall 2014.

I would also like to express my deepest gratitude to my dad (watching over me from above), mom, twin brother, and two youngest sisters. They have always shown support and encouragement through the years of my Masters pursuit and life in general. I would also like to acknowledge the love and support given to me from my close relatives and friends.

Finally, I would like to thank Kelly Nealon for the unrelenting motivation and support to overcome the exhaustion of a long work day and helping me find the drive to stay steadfast in the completion of this thesis.

TABLE OF CONTENTS

LIST OF FIGURES		vii
LIST OF TABLES		x
CHAPTER 1:	INTRODUCTION	1
1.1	Description of the Problem Statement	1
1.2	Summary of the Research Method	2
1.3	Research Scope	4
CHAPTER 2:	LITERATURE REVIEW	5
2.1	Introduction	5
2.2	Previously Conducted Unconfined Compression (UC) Testing	11
2.3	Previously Conducted Triaxial Testing	17
2.4	Previously Conducted Full-Scale Field Studies	22
CHAPTER 3:	LABORATORY TEST MATERIALS AND CONFIGURATION	26
3.1	Introduction	26
3.2	Ottawa Sand Mixed with Kaolin Clay	28
3.3	Field Soils	30
3.4	Polypropylene Fibrillated Geosynthetic Fiber	33
3.5	Test Specimen Preparation	36
3.6	Unconfined Compression Configuration and Test Procedure	47
3.7	Rigaku Miniflex+ X-Ray Diffractometer Procedure	52
CHAPTER 4:	ANALYSIS OF FIBER-REINFORCED SOIL DATA	60
4.1	Potential Research Contribution	60
4.2	Analysis Overview	62

4.3 Unconfined Compressive Strength as a Function of Varying the Fiber Content 64

4.4 Unconfined Compressive Strength as a Function of the Fines Content 74

4.5 Soil Strain and Elastic Modulus as a Function of Varying Fiber Content 77

4.6 Test Specimen Failure Modes 84

4.7 Soaked Test Specimens 90

CHAPTER 5: SUMMARY AND CONCLUSIONS 96

5.1 Research Summary 96

5.2 Research Conclusions 97

5.3 Recommendations for Future Research 101

REFERENCES 102

APPENDIX A: COMPACTION CURVES 105

APPENDIX B: TEST MATRIX 114

APPENDIX C: UNCONFINED COMPRESSION CURVES AND PHOTOS 118

APPENDIX D: TEST DATA 283

LIST OF FIGURES

FIGURE 3.1:	Grain size distribution curves for all kaolin clay-Ottawa sand soils and the Ottawa sand	29
FIGURE 3.2:	North Carolina field soil county locations	30
FIGURE 3.3:	Field soil grain size distribution curves	31
FIGURE 3.4:	Examples of various geosynthetic fibers: (a) Monofilament (after tunneltalk.com); (b) Fibrillated (after nycon.com); (c) Multifilament 1 (after sciencedirect.com); (d) Multifilament 2 (after sciencedirect.com)	34
FIGURE 3.5:	FIBERCAST 500™ polypropylene fibrillated fiber	35
FIGURE 3.6:	Custom compaction mold used to generate the test specimens	37
FIGURE 3.7:	Test specimen soaking process: (a) Lincoln County samples prior to water submersion; (b) Soil swell for a 30% kaolin clay-Ottawa sand mixture; (c) Soil trim, prior to fiber trimming	39
FIGURE 3.8:	Hobart mixer	40
FIGURE 3.9:	Mixed kaolin clay-Ottawa sand soil beginning to cohere	41
FIGURE 3.10:	Final soil mix after the addition of fiber reinforcement	43
FIGURE 3.11:	Fibers floating on top of the soil	43
FIGURE 3.12:	Fibers adhering to the side of the mixing bowl	44
FIGURE 3.13:	Example of where separation occurs in samples with a high percentage of reinforcement (39R): (a) General view of test specimen; (b) Detailed view of separation 1; (c) Detailed view of separation 2	46
FIGURE 3.14:	Test specimen extruded successfully without issues	47
FIGURE 3.15:	ELE Digital Tritest load frame	49
FIGURE 3.16:	A prepared test specimen inside the load frame	50
FIGURE 3.17:	Load cell used during the UC testing	51

FIGURE 3.18: Rigaku Miniflex+ XRD 52

FIGURE 3.19: Rigaku Miniflex+ interior 53

FIGURE 4.1: Unconfined compressive strength with varying fiber content for the 10% kaolin clay-90% Ottawa sand material 65

FIGURE 4.2: Unconfined compressive strength with varying fiber content for the 15% kaolin clay-85% Ottawa sand material 66

FIGURE 4.3: Unconfined compressive strength with varying fiber content for the 20% kaolin clay-80% Ottawa sand material 66

FIGURE 4.4: Unconfined compressive strength with varying fiber content for the 25% kaolin clay-75% Ottawa sand material 67

FIGURE 4.5: Unconfined compressive strength with varying fiber content for the 30% kaolin clay-70% Ottawa sand material 67

FIGURE 4.6: Unconfined compressive strength with varying fiber content (kaolin clay-Ottawa sand samples): (a) Raw data; (b) Percent increase 69

FIGURE 4.7: Unconfined compressive strength with varying fiber content (field soils): (a) Raw data; (b) Percent increase 72

FIGURE 4.8: Varying fine content with constant fiber content 75

FIGURE 4.9: Axial strain with varying fiber content (kaolin clay-Ottawa sand samples): (a) Raw data; (b) Percent increase 78

FIGURE 4.10: Axial strain with varying fiber content (field soils): (a) Raw data; (b) Percent increase 80

FIGURE 4.11: Unconfined compressive strength as a function of axial strain (1.25% fiber content versus control specimens): (a) 20% kaolin clay-80% Ottawa sand; (b) Lincoln County field soil 82

FIGURE 4.12: Typical failures: (a) Angular shear; (b) Bulging with horizontal separation 86

FIGURE 4.13: Maximum fiber content associated with an angular failure surface 87

FIGURE 4.14: 10% kaolin clay-90% Ottawa sand specimen: (a) 1.5% fiber angular failure surface; (b) 1.75% fiber bulging failure surface 88

FIGURE 4.15: 15% kaolin clay-85% Ottawa sand specimen: (a) 1.25% fiber angular failure surface; (b) 1.5% fiber bulging failure surface 88

FIGURE 4.16: Guilford County test specimen: (a) Unreinforced angular failure surface; (b) 0.75% fiber bulging failure surface 89

FIGURE 4.17: Unconfined compressive strength as a function of fiber content for specimens prepared at optimum moisture content and soaked soil conditions (30% kaolin clay-Ottawa sand) 91

FIGURE 4.18: Unconfined compressive strength as a function of fiber content for specimens prepared at optimum moisture content and soaked soil conditions (Guilford County) 92

FIGURE 4.19: Unconfined compressive strength as a function of fiber content for specimens prepared at optimum moisture content and soaked soil conditions (Johnston County) 92

FIGURE 4.20: Unconfined compressive strength as a function of fiber content for specimens prepared at optimum moisture content and soaked soil conditions (Lincoln County) 93

FIGURE 4.21: Unconfined compressive strength as a function of fiber content for specimens prepared at optimum moisture content and soaked soil conditions (Buncombe County) 93

LIST OF TABLES

TABLE 2.1:	Summary of the cited references	8
TABLE 3.1:	Kaolin clay and Ottawa sand properties (after U.S. Silica)	28
TABLE 3.2:	Summary of the index testing results for all soils	32
TABLE 3.3:	FIBERCAST 500 polypropylene fiber specifications (after www.fibermesh.com)	35
TABLE 3.4:	Number of tests performed for each unconfined compression test configuration	48
TABLE 3.5:	MDI JADE 6.5 output table (30% kaolin clay-70% Ottawa sand mixture)	55
TABLE 3.6:	MDI JADE 6.5 output table (Guilford County)	56
TABLE 3.7:	MDI JADE 6.5 output table (Johnston County)	57
TABLE 3.8:	MDI JADE 6.5 output table (Lincoln County)	58
TABLE 3.9:	MDI JADE 6.5 output table (Buncombe County)	59
TABLE 4.1:	Unconfined compressive strength (kaolin clay-Ottawa sand mixtures)	68
TABLE 4.2:	Percent increase in unconfined compressive strength (field soils) as a function of fiber content	73
TABLE 4.3:	Maximum unconfined compressive strength for each optimum fines content	76
TABLE 4.4:	Percent increase in axial strain at failure for the kaolin clay-Ottawa sand specimens	79
TABLE 4.5:	Percent increase in axial strain at failure (field soils)	81
TABLE 4.6:	Calculation of secant modulus	83
TABLE 4.7:	Percent increase in soaked unconfined compressive strength as a function of fiber content	94

TABLE 4.8: Percent decrease in unconfined compressive strength (optimum moisture content versus post soak conditions) 94

CHAPTER 1: INTRODUCTION

1.1. Description of the Problem Statement

Geosynthetics have been utilized as a soil strengthening and/or stabilizing admixture in a variety of applications that include everything from the mitigation of slope hazards to increasing the stability of subgrade materials in roadways. Conventional methods of earth reinforcement often introduce continuous, layered inclusions including strips, fabrics, and/or grids into an earth mass (Maher and Gray (1990)) that are oriented in a particular direction. While the use of geotextiles and geogrids are well established in roadways and other earth retaining structures, geofibers serve as a randomly oriented reinforcement alternative that can be incorporated into a weak material to increase bearing capacity and/or soil strength. An earth mass stabilized with discrete, randomly distributed fibers resembles traditional earth reinforcement in many of its' properties (Gary and Al-Refeai (1986)), but mimics admixture stabilization in its preparation (Maher and Gray (1990)). Similar to cement or lime admixtures, geosynthetic fibers can easily be dispersed in the near surface soils, and the use of randomly distributed fibers can benefit the maintenance of strength isotropy and help minimize potential planes of weakness that develop parallel to oriented reinforcement (Gray and Maher (1989)).

Geosynthetic and natural fibers have been utilized in field applications. While Chapter 2 provides a full literature review, a few examples are named here. Polypropylene fibrillated fibers were blended with fat clay (CH) along a section of Highway LA 15 to

repair shallow slope failures (Zhang et al. (2003)). Tingle et al. (1999) investigated the use of reinforcing fibers for military airstrips and roadways as a quick and easy solution to mitigate unsuitable subgrade soils. Two full-scale mechanically stabilized earth (MSE) retaining walls that were constructed using horizontal geogrid inclusions in a silty sand backfill blended with randomly distributed fibers to create a stronger and stiffer material were tested by the Korea Railway Research Institute (Park and Tan (2005)).

As fiber inclusions become more prevalent as a viable soil strengthening and/or stabilizing admixture, laboratory strength data for different fiber types, fiber dosages, and fiber lengths are needed. Some testing has been conducted on geosynthetic and natural fiber soil inclusions using triaxial, unconfined compression, California bearing ratio, direct shear, tensile and flexural strength testing protocols in previous studies, but the extents of these evaluations are limited. The research provided herein presents an in depth evaluation of the unconfined compressive strength of various soil types over a wide range of reinforcement dosages using a common 12.7 mm (0.5 in) long polypropylene fibrillated fiber.

1.2. Summary of the Research Method

The work described herein investigates the use of polypropylene fibrillated fibers as randomly distributed geosynthetic reinforcement in soil with the goal of evaluating unconfined compressive strength gain and material behavior. While the literature provides limited test results for SP-SM, CH, and CL soils reinforced with polypropylene fibrillated fibers at the lower dosage rates, a conclusive unconfined compressive strength dataset does not exist for different types of soils reinforced using various dosage amounts with 12.7 mm (0.5 in) long polypropylene fibrillated fiber inclusions.

Initially as part of this study, Ottawa sand was mixed with 10% - 30% kaolin clay percentages at a consistent moisture content to generate a series of highly controlled test specimens both with and without the geosynthetic inclusions. Geosynthetic inclusions were varied between 0.5% and 2% by mass and all tests were repeated three times to ensure consistency in the test procedure and repeatability in the test results.

Subsequently, these results were compared to remolded test specimens generated using four different field soils collected from Buncombe, Johnston, Guilford, and Lincoln Counties in North Carolina. Field soil test specimens were included in the matrix to evaluate differences in behavior resulting from soils that have more inconsistent properties in comparison to the Ottawa sand and kaolin clay mixtures. Geosynthetic inclusions were varied between 0.75% and 2% by mass.

While all tests (controlled materials and field soils) were performed at the optimum moisture content measured for each respective soil using standard Proctor compaction effort, 25 additional tests were subsequently repeated after soaking the test specimens inside the compaction mold for a 24 hour time period to further evaluate the change in the unconfined compressive strength both with and without geosynthetic inclusions.

A total of 120 unconfined compression tests were performed on the kaolin clay-Ottawa sand mixtures and 20 unconfined compression tests were performed on the field soils. In addition, a total of 25 unconfined compression tests were performed on soaked test specimens. While this report will display the unconfined compressive strength as a function of fine content and as a function of fiber content, the failure surface/mode was also noted and photographed for each unconfined compression test to determine patterns and behavior.

1.3. Research Scope

A brief description of each section in this thesis is included below.

- Chapter 2 provides an outline of the results obtained during the literature review conducted as part of this research project;
- Chapter 3 summarizes the physical properties of the kaolin clay, Ottawa sand, North Carolina field soils, and the geosynthetic fiber utilized during this study, and describes the preparation procedures and testing protocol in detail;
- Chapter 4 presents and discusses the wealth of data collected from the 165 unconfined compression tests conducted as part of this study;
- Chapter 5 provides a research summary, enumerates the conclusions from the work conducted herein, and presents recommendations for future work;
- The References chapter provides the bibliographic information for all cited references;
- Appendix A includes the standard Proctor compaction curves for all soils tested;
- Appendix B includes the full test matrix;
- Appendix C provides detailed information from each test specimen including the pre and post-test photographs, and the raw stress-strain data from each unconfined compression test;
- Appendix D provides a summary table of important test result information for each test performed including the test date, unit weight, moisture content, peak unconfined compressive strength, axial strain at failure, and degree of saturation.

CHAPTER 2: LITERATURE REVIEW

2.1. Introduction

UC testing is a simple way to determine the unconsolidated, undrained shear strength and/or the unconfined compressive (UC) strength of a cohesive soil specimen. Several researchers have utilized UC testing to determine strength parameters of soils reinforced with natural or synthetic fibers distributed throughout the sample either randomly or in a particular direction. Ang and Loehr (2003), Iasbik et al. (2002), Jiang et al. (2010), Kumar et al. (2006), Maher and Ho (1994), Nataraj and McManis (1997), Rafalko et al. (2008), and Tang et al. (2007) have contributed in some way to this database. These cited studies investigated synthetic fibers (i.e., polypropylene, nylon, polyester, glass, poly vinyl alcohol, and plastic waste) with fiber content percentages ranging from 0.05% to 4% by dry mass of the soil, and fiber lengths ranging from approximately 3 mm to 52 mm (0.2 in to 2 in). However, the majority of these studies look at reinforced soils with less than 1% fiber by mass. In general, it was determined that fibers increased the UC strength and the test specimens experienced larger axial strains at failure when compared with unreinforced soil specimens.

Researchers that have utilized either Consolidated Drained (CD) or Consolidated Undrained (CU) triaxial testing protocols with fiber inclusions include Freilich et al. (2010), Gary and Al-Refeai (1986), Gregory (2006), Maher and Gray (1990), Michalowski and Cermak (2003), Ranjan et al. (1994), and Romero (2003). They focused on synthetic

fibers that were manufactured using polypropylene (i.e., monofilament, multifilament, tape, and fibrillated), rubber (i.e., Buna-N), polyamide, glass, and steel. Fiber percentages ranged from 0.1% to 4% by dry mass, and the lengths ranged from 12 mm to 38 mm (0.5 in to 1.5 in). In general, their test results corresponded well with Mohr-Coulomb failure criterion. Linear peak stress increases were observed with increased fiber contents up to 2%. Subsequently, the failure curve went to an asymptotic upper limit when additional fiber was added. Modified stress-strain behavior was observed from a brittle to a more ductile behavior. Gregory (2006) did not note a significant trend in cohesion, but did observe an increase in the internal angle of friction due to the fiber inclusions. Triaxial testing also revealed that the samples may experience a change in behavior from strain hardening to strain softening.

Additional fiber reinforced testing includes CBR and swell pressure and volumetric change testing. Nataraj and McManis (1997) conducted CBR testing in conjunction with UC testing and direct shear testing. Iasbik et al. (2002) conducted resilient modulus testing on fiber reinforced soils. Monofilament and fibrillated polypropylene fiber contents ranging from 0.1% to 0.75% and fiber lengths ranging from 20 mm to 25 mm (0.75 in to 1 in) were investigated. Greater CBR values and decreased resilient modulus values were observed.

Research conducted by Puppala and Musenda (2000) emphasized the effects of fibers on high plasticity soil and the swell potential of that soil. Fibrillated polypropylene fiber lengths equal to 13 mm and 50 mm (0.5 in and 2 in, respectively) were introduced into two highly plastic clays from Texas. Fiber contents ranged from 0% to 0.9%. The purpose of this study was to determine the swell pressure and volumetric change in expansive clays

after a 48-hour saturation period. Deformation readings were recorded as the samples were soaked. Puppala and Musenda (2000) observed greater swelling as the fiber content was increased in the specimens. They concluded that it was "attributed to the fact that the fibers within the clayey soil mass create paths that allow a better distribution of moisture within the soil sample." Puppala and Musenda (2000) did not explore the saturated UC strength characteristics of reinforced test specimens as was done in the current study.

Full-scale field studies were performed by Consoli et al. (2003), Gregory and Chill (1998), Park and Tan (2005), Tingle et al. (1999), and Zhang et al. (2003). Prior to the full-scale field testing, laboratory testing was performed to better quantify the reinforcement parameters of the fibrillated, monofilament, and tape polypropylene fibers. They investigated fiber lengths ranging from 25 mm to 76 mm (1 in to 3 in) at fiber contents ranging from 0.2% to 1%.

The Consoli et al. (2003) study showed that the polypropylene fibers significantly improved soil behavior when it was subjected to a plate load test. Gregory and Chill (1998) repaired two embankment slopes; one embankment slope had fiber reinforced backfill and the other was unreinforced. The fiber-reinforced backfill showed no signs of movement while the unreinforced slope ended up failing. Park and Tan (2005) concluded that a retaining wall reinforced with geogrid layers in addition to a polypropylene fiber treated backfill produced a stiffer and stronger composite. In a study by Tingle et al. (1999), polypropylene fibrillated fibers reduced rutting more significantly than other types of fibers tested in a full-scale roadway subgrade stabilization project, and the CBR values were also greatly improved with the use of the geofiber. Unfortunately, the field results produced by Zhang et al. (2003) were inconclusive due to failures that occurred outside their repaired,

fiber reinforced slope. It was also noted that water trapped in 'fissures' and 'cracks' caused adjacent soils to become soaked, resulting in the slope failure. Table 2.1 summarizes the laboratory investigations and field demonstrations pertinent to the work conducted herein and the following section attempts to discuss these studies in more detail.

Table 2.1: Summary of the Cited References

Authors	**Research Contribution**
Ang, E. C. and Loehr, J. E. (2003)	UC testing was performed to determine if the test specimen size impacts test results in a sandy clay reinforced with 52 mm (2 in) long polypropylene fibrillated fibers. The authors recommended using a specimen diameter size greater than or equal to 70 mm (2.75 in), and reported increases in the UC strength with increases in fiber content.
Iasbik, I., De Lima, D. C., Carvalho, C. A., Silva, C. H., Minette, E. and P.S.A. (2002)	Determined the optimum parameters for use in repeated-loading triaxial and resilient modulus tests conducted on clayey soil. They used 20 mm (0.75 in) long polypropylene monofilament fibers with fiber contents up to 2%. Reinforcing fibers were responsible for a substantial decrease in the resilient modulus and an increase the UC strength.
Jiang, H., Cai, Y. and Liu, J. (2010)	Conducted UC testing on fiber reinforced clayey soil while varying fiber length, fiber content, and aggregate size. They used polypropylene monofilament fiber reinforcement with fiber contents up to 0.4%. The fibers increased the UC strength, cohesion, and the friction angle. An optimum fiber content equal to 0.3% was reported.
Kumar, A., Walia, B. S. and Mohan, J. (2006)	Conducted UC testing on clay soil reinforced with four different polyester fibers. Fiber lengths ranged from 0.3 mm to 13 mm (0.1 in to 0.5 in) and fiber contents ranged from 0.5% to 2%. UC strength increased with increasing fiber content.
Maher, M. H. and Ho, Y. C. (1994)	Performed UC testing on blocks of kaolin clay using three different fibers (polypropylene monofilament, glass, and softwood pulp) at fiber contents ranging from 0.5% to 4%. Fiber lengths ranged from 6 mm to 25 mm (0.25 in to 1 in). The increase in peak UC strength was greatest with the use of shorter fibers at lower moisture contents.

Table 2.1: Summary of the Cited References (continued)

Authors	Research Contribution
Nataraj, M. S. and McManis, K. L. (1997)	UC testing was conducted on sandy clay and poorly graded sand. Optimum results were realized with a 25 mm (1 in) polypropylene fibrillated fiber using a 0.3% content fiber content. Direct shear and CBR tests were also performed. Reinforced SP test specimens experienced greater UC strengths, friction angles, and CBR values. Bulging failure surfaces were observed.
Rafalko, S. D., Brandon, T. L., Filz, G. M. and Mitchell, J. K. (2008)	UC testing was conducted on clay specimens using five different fibers (fibrillated and monofilament polypropylene fibers, nylon fibers, and 2 poly vinyl alcohol fibers) and three different chemical additives. Fiber contents ranged from 0.5% to 1% and fiber lengths ranged from 8 mm to 19 mm (0.33 in to 0.75 in). Increasing the fiber content while holding the chemical stabilizer constant increased UC strength and 'toughness'.
Tang, C., Shi, B., Gao, W., Chen, F. and Cai, Y. (2007)	UC testing was conducted on sandy clay reinforced with 12 mm long polypropylene monofilament fiber using fiber contents equal to 0.05%, 0.15%, and 0.25%. Increasing the fiber content increased the UC strength, shear strength, and axial strain at failure.
Freilich, B. J., Li, C. and Zornberg, J. G. (2010)	Triaxial testing was conducted to study the long term effective stress conditions for two different clays reinforced with 25 mm (1 in) long polypropylene fibrillated fibers at a fiber content equal to 0.5%. The authors concluded that soils reinforced with fibers will experience reduced effective stress over long term conditions when compared to short term. Bulging failure surfaces were observed.
Gary, D. H. and Al-Refeai, T. O. (1986)	CD triaxial tests were performed to investigate the responses of dry sand reinforced with reed and glass filament fibers and 35 mm (1.3 in) diameter woven and nonwoven polypropylene and glass monofilament fibers. Fibers ranged in length from 12 mm to 36 mm (0.5 in to 1.5 in) and fiber contents ranged from 0% to 2%. The authors observed a linear increase in strength with an increase in fiber content to an asymptotic upper limit.
Gregory, G. H. (2006)	The observations of 278 triaxial tests conducted by Gregory (2006) and AGT Laboratories were summarized. 52 mm (2 in) long polypropylene monofilament fibers at 0.3 kg to 3.2 kg of fiber per cubic meter (0.17 lb to 2 lb of fiber per cubic foot) of soil were utilized as reinforcement. Direct shear, creep, and shear interface tests were also performed. Triaxial data showed a 16% to 64% increase in the friction angle. Direct shear data showed a 19% to 26% increase in the friction angle.

Table 2. 1: Summary of the Cited References (continued)

Authors	Research Contribution
Maher, M. H. and Gray, D. H. (1990)	180 triaxial tests were conducted on nine sands using Buna, palm, and glass fiber reinforcement with lengths ranging from 12 mm to 45 mm (0.5 in to 1.75 in) and fiber contents ranging from 1% to 5%. Shear strength increased linearly with increasing fiber content to an asymptotic upper limit.
Michalowski, R. L. and Čermák, J. (2003)	Triaxial tests were conducted on sands reinforced with steel wire, polyamide monofilament, and polypropylene fibrillated fibers randomly distributed or oriented in a particular direction. Most fibers were 25 mm (1 in) in length and fiber contents up to 2% by volume were investigated. Results demonstrated shear strength increases up to 70%, and increased strain levels at failure.
Puppala, A. J. and Musenda, C. (2000)	Swell pressures and volumetric changes on high plasticity clays reinforced with polypropylene fibrillated fiber inclusions were investigated using 13 mm and 50 mm (0.5 in and 2 in, respectively) long fibers with up to 0.9% fiber contents. The authors observed greater swelling as the fiber content was increased.
Ranjan, G., Vasan, R. M. and Charan, H. D. (1994)	Triaxial tests were conducted on a poorly graded, fine sand samples reinforced with four different plastic fibers. Fiber lengths ranged from 18 mm to 38 mm (0.75 in to 1.5 in) and fiber contents ranged from 0% to 4%. The shear strength increased linearly as the fiber content increased.
Romero, R. J. (2003)	46 triaxial tests were performed to evaluate the effective stress, strain, pore pressure, and volumetric changes unreinforced and reinforced soil specimens to develop a model. Clayey silt was reinforced with up to 0.4% fiber content using a 52 mm (2 in) long polypropylene fibrillated fiber. Test specimens experienced increases in the strain at failure, the friction angle, and the cohesion.
Zhang, Z., Farrag, K. and Morvant, M. (2003)	Direct shear and triaxial tests were conducted on samples reinforced with 25 mm (1 in) long polypropylene fibrillated fibers using 0.1% and 0.2% fiber contents prior to a field repair. With the addition of 0.1% fiber content, a minimum increase of 50% to the ultimate shear strength was observed.

Table 2. 1: Summary of the Cited References (continued)

Authors	Research Contribution
Consoli, N. C., Casagrande, M. D., Prietto, P. D. and Thome, A. (2003)	Plate load tests were carried out on two sandy soil test sites subsequent to preliminary triaxial testing. An unreinforced site was compared to a site reinforced with 25 mm (1 in) long polypropylene monofilament fibers installed using a 0.5% fiber content. The reinforced soil displayed a noticeably stiffer response with increasing settlements due to the continuous increase in strength at larger deformations.
Gregory, G. H. and Chill, D. S. (1998)	A consistently failing slope in Beaumont, Texas was reinforced with fibers. The clayey soil from the slope underwent 32 triaxial and 86 direct shear tests prior to field implementation. 25 mm and 50 mm (1 in and 2 in, respectively) long polypropylene fibrillated fibers were blended into the clay with fiber contents up to 0.25%. The repaired fiber-reinforced slope has shown no signs of movement but the unreinforced slope in the same area has failed.
Park, T. and Tan, S. A. (2005)	Two mechanically stabilized earth walls were constructed in Korea to compare a normally constructed SM backfill with a second wall reinforced with 60 mm (2.5 in) long polypropylene monofilament fibers at 0.2% fiber content. UC and CD triaxial tests were performed on representative samples of the backfill prior to constructing the full-scale walls. Reinforced walls constructed with geogrid layers in conjunction with the polypropylene monofilament fibers produced a stronger and stiffer material.
Tingle, J. S., Webster, S. L. and Santoni, R. L. (1999)	Two roadway sections were constructed to validate previously performed UC testing. Six different sand types, four polypropylene fiber types (fibrillated, monofilament, tape, and mesh), six different deniers, and five different fiber contents (0.2% to 1%, by dry mass) with fiber lengths ranging from 13 mm to 76 mm (0.5 in to 3 in) were evaluated. Fibrillated fibers proved superior to alternative synthetic additives in regard to rut resistance. The CBR results of geofiber stabilized concrete sand improved 6% to 35%.

2.2. Previously Conducted Unconfined Compression (UC) Testing

Ang and Loehr (2003) conducted several UC tests using a sandy clay (CL) to determine if the specimen size would affect the strength characteristics of a soil sample. A 52 mm (2

in) long polypropylene fibrillated fiber was investigated using 0.2% and 0.4% fiber contents by mass. Ang and Loehr (2003) found that the UC strength increased as the fiber content increased, in line with the results of the current study. Ang and Loehr (2003) concluded that specimen diameter sizes greater than or equal to 70 mm (2.75 in) are "reasonably representative of the true mass strengths for fiber reinforced soils." They conducted UC tests to a maximum 25% strain limit to observe the behavior of the compression curve post failure. It is important to note that the test specimen size for the current study exceeds the minimum diameter recommended by Ang and Loehr (2003).

Iasbik et al. (2003) focused on the influence of fiber content and fiber length on the UC strength of an elastic silt (MH) to determine the optimum parameters for use in repeated-loading triaxial and resilient modulus (MR) tests. Iasbik et al. (2003) reported that the optimum moisture content measured during standard Proctor compaction testing varied less than 1% when polypropylene monofilament fibers were added to the soil. For this reason, the same optimum moisture content was used for the elastic silt soil both reinforced and unreinforced with geosynthetic fibers. Based on this finding, the current study also utilizes one optimum moisture content condition for each soil type regardless of fiber content. Subsequently, Iasbik et al. (2003) determined that the polypropylene monofilament fibers increased the UC strength, and that the fibers were responsible for a substantial decrease in the MR values. An approximate 65% decrease in MR was observed when 0.25% fiber was added to the soil at a deviator stress of 52.5 kPa (7.6 psi). The authors also concluded that a fiber length of 20 mm (0.75 in) with a fiber content equal to 0.25% was the optimum combination. However, this study only investigated impacts on

UC strength using fiber contents ranging from 0.5% to 0.75%. The current study investigates fiber contents up to 2%.

Jiang et al. (2010) varied fiber length, fiber content, and aggregate size in a series of UC tests to determine the engineering properties of a reinforced clayey soil acquired from the Nanjing region of China. Two testing plans were developed. Plan A used polypropylene monofilament fibers with lengths equal to 10 mm, 15 mm, 20 mm, and 25 mm (0.4 in, 0.6 in, 0.8 in, and 1 in, respectively). As part of this testing matrix, each fiber length was added to the soil using 0.1%, 0.2%, 0.3%, and 0.4% fiber contents. Plan B was designed to determine the strength characteristics of the soil specimens after varying aggregate sizes. Four different aggregate sizes were mixed into the clayey soil, each tested with a 15 mm (0.6 in) polypropylene fiber at a 0.4% fiber content. Jiang et al. (2010) determined that the inclusion of the polypropylene monofilament fibers produced greater results for UC strength, cohesion, and internal angle of friction when compared with the unreinforced test specimens. They reported a 0.3% optimum fiber content by dry mass of the soil for all fiber lengths. They also reported a preference for the 15 mm (0.6 in) long polypropylene monofilament fiber. Regarding Plan B, UC strength decreased with increasing aggregate size, but the 3.5 mm (0.14 in) aggregate produced the greatest increase in cohesion and angle of internal friction for the clayey soil.

Kumar et al. (2006) utilized four different polyester fibers in soft, highly compressible clay test specimens prepared at several densities for UC testing. They tested a 0.3 mm (0.1 in) long plain fiber, a 0.6 mm (0.2 in) long plain fiber, a 0.6 mm (0.2 in) long crimped fiber, and a 12 mm (0.5 in) plain fiber. Kumar et al. (2006) mixed the clay with up to 12% Ottawa sand to mold various soil types, and used fiber contents equal to 0.5%, 1%, 1.5%, and 2%

of the dry mass. Based on the results from this study, the highly compressible clay experienced significant increases in UC strength ranging from 50% - 68% using the 3 mm (0.2 in) long fibers at 0.5% to 2% fiber contents. Increases in UC strength ranging from 70% to 115% were observed using the 6 mm (0.2 in) long plain and crimped fibers as well as the 12 mm (0.5 in) long polyester fiber. Overall, the UC strength increased with increasing fiber content. The authors reported that the largest percent increase in UC strength relative to the unreinforced control test specimens without Ottawa sand was 180% with the following combinations of admixtures: 2% of the 6 mm (0.2 in) long plain polyester fibers in a 10% Ottawa sand mixture, 1.5% of the 6 mm (0.2 in) long crimped polyester fibers in a 10% Ottawa sand mixture, and 1% of the 2 mm (0.5 in) plain long polyester fibers in a 10% Ottawa sand mixture.

Maher and Ho (1994) evaluated a kaolinite clay from Macon, Georgia to determine the mechanical properties of the soil when reinforced with polypropylene monofilament, glass, and softwood pulp fibers. The kaolinite was mixed at a water content twice the liquid limit, placed in 305 mm by 305 mm by 254 mm (12 in by 12 in by 10 in) blocks, and kept at room temperature for two weeks. The blocks were then trimmed to specific sizes for UC testing. It was observed that the results of preliminary standard Proctor compaction testing (i.e., the maximum dry density and optimum moisture content) were not altered when the fiber reinforcement increased from 0.5% to 4% or when the fiber length increased from 6 mm to 25 mm (0.25 in to 1 in). The increase in peak UC strength was greatest with the use of shorter fibers and lower moisture contents.

Nataraj and McManis (1997) performed UC testing on sandy clay (CL) and poorly graded sand (SP). Initial compaction tests verified that there was not a significant change

in compaction behavior, optimum moisture content, or the maximum dry density when comparing reinforced to unreinforced soil specimens. UC testing was conducted on the following test specimen sizes (diameter by height): 33 mm by 72 mm (1.25 in by 2.75 in), 70 mm by 140 mm (2.75 in by 5.5 in), and 100 mm by 117 mm (4 in by 4.5 in). Angular failure planes were observed for the unreinforced clay specimens while bulging failures occurred in the reinforced clay specimens. Direct shear and CBR tests were also performed on the CL material; increases in strength were observed as a result of the fiber inclusions. The UC strength of the SP was tested using the Harvard Miniature apparatus, which is 33 mm by 72 mm (1.25 in by 2.75 in). Reinforced SP test specimens experienced greater friction angles and CBR values than the unreinforced SP. Overall, Nataraj and McManis (1997) reported an optimum fiber content equal to 0.3% using 25 mm (1 in) long polypropylene fibrillated fibers, but indicate that further investigation is needed. It should be noted that Ang and Loehr (2003) have concluded that the diameters of these test specimens are not "reasonably representative of the true mass strengths for fiber reinforced soils" due to their specimen size.

Rafalko et al. (2008) investigated fiber reinforced soils in combination with other stabilizers in two different soft clays to develop a rapid construction technique for military airfields constructed on soft subgrade materials. The authors were concerned with the ability for the stabilized soil to withstand the air traffic over a 72-hour period post-construction. The list of stabilizing inclusions/additives included fibrillated and monofilament polypropylene fibers, nylon fibers, poly vinyl alcohol (PVA) fibers (PVA1 and PVA2), Portland cement (Type I/II and III), lime (pelletized and pulverized), and calcium carbide. Fiber lengths ranged from 8 mm to 19 mm (0.33 in to 0.75 in), and the

fiber content percentages ranged from 0.5% to 1%. All test specimens were prepared at the optimum moisture content and compacted to the maximum dry density of the clay based on the results of the standard Proctor compaction testing for this material. The moisture content was not adjusted with the addition of the stabilizers. Test specimens were permitted to cure for 3 days prior to UC testing. Primary stabilizers were applied at a dosage rate of 5% with the use of chemical stabilizers or a dosage rate of 0.5% to 1% by dry mass of the soil with the use of fibers. Fibers utilized as a secondary stabilizer were applied at a dosage rate of 1% by dry mass. UC strength increased and the soil became more brittle with the help of primary chemical stabilizer; the addition to fiber increased the 'toughness' of the soil, but the peak strength was unaffected. Increasing the fiber content while holding the chemical stabilizer constant also increased UC strength and 'toughness'. The authors reported that fibers used as the primary stabilizer may not provide enough strength increase to a soft clay to support military airfield traffic.

Tang et al. (2007) performed UC and direct shear tests on 12 groups of soils from Nanjing, China. The test specimens were either uncemented or cemented with 5% or 8% Portland cement by dry mass of the soil. A 12 mm (0.5 in) long polypropylene monofilament fiber was added using fiber percentages equal to 0.05%, 0.15%, and 0.25% by dry mass. Once prepared, they were cured for either 7, 14, or 28 days prior to UC testing. Results indicate that the inclusion of the polypropylene monofilament fibers within the uncemented and cemented samples increased the UC strength, shear strength, and axial strain at failure. The fiber inclusions also decreased sample brittleness, stiffness, and the loss of post-peak strength. Utilizing a scanning electron microscopy (SEM), the interactions between the fiber surface and the soil matrix were investigated. It was

determined that the bond strength and friction at the soil-fiber interface are the dominant mechanism controlling the reinforcement benefit.

2.3. Previously Conducted Triaxial Testing

Freilich et al. (2010) studied the long term effective stress conditions for two different clay soils (plasticity indices equal to 49 and 54) while utilizing a polypropylene fibrillated fiber that was 25 mm (1 in) in length at a 0.5% fiber content by dry mass. Samples were compacted at approximately 2% dry of the standard Proctor effort optimum moisture content in a 71 mm by 142 mm (2.80 in by 5.60 in) sample (diameter by height). Each test specimen was loaded until it reached a maximum of 20% axial strain. During triaxial testing, the unreinforced test specimens exhibited an angular shear surface at failure while the reinforced test specimens bulged until failure. The bulging was attributed to the increase in soil ductility due to the presence of fiber reinforcement. Freilich et al. (2010) concluded that soils reinforced with fibers will experience reduced effective stress over long term conditions when compared to short term. The results indicate that the effect of the fibers on the pore pressure during CU triaxial testing may produce a higher estimation of effective strength.

Gary and Al-Refeai (1986) tested a variety of geosynthetics in a battery of CD triaxial tests to investigate the stress-strain responses of dry sand from Muskegon, Michigan. Woven and nonwoven polypropylene multifilament, woven and nonwoven polypropylene tape, and glass yarn woven monofilament geotextiles were cut into 35 mm (1.3 in) diameter specimens and placed within the soil sample at specified lift heights. Among the randomly distributed discrete fibers used in this study were No. 1 reed, No. 2 reed, and No. 204 glass filament fibers with lengths that varied from 12 mm to 36 mm (0.5 in to 1.5 in) and fiber

contents that ranged from 0% to 2%. Test results indicated that all reinforcing inclusions increased the strength and modified the stress-deformation behavior of the sand significantly. Results showed an increase in ultimate strength for fiber reinforced test specimens. There was a linear increase in strength resulting from an increase in fiber content up to 2% by mass. Thereafter, it followed an asymptotic upper limit. Additionally, the authors reported that "rougher (not stiffer)" fibers were more effective in terms of increasing the ultimate strength of the specimen.

Gregory (2006) performed extensive laboratory testing to refine and extend a fiber reinforced design model he developed previously. A total of 101 triaxial tests were performed using a 73 mm (2.875 in) diameter test specimen size that was 147 mm (5.8 in) in height. A fat clay with a liquid limit of 59, plastic limit of 20, and fine content equal to 94%, and a non-plastic silty sand with a 13% fine content were tested. A 52 mm (2 in) long polypropylene monofilament fiber was used to reinforce the soils using 0.3 kg to 3.2 kg of fiber per cubic meter (0.17 lb to 2 lb of fiber per cubic foot) of soil. During the mixing process, fibers were pre-mixed into the fat clay while fibers were added during compaction of the silty sand.

Gregory (2006) also summarized the results of 177 triaxial tests performed by the AGT Laboratory in Chattanooga, Tennessee. The AGT Laboratory used three different soils during their testing: a fat clay (liquid limit = 68, plastic limit = 28, and fine content = 96%), a poorly graded sand (non-plastic with <2% fine content), and a sandy clay (liquid limit = 27, plastic limit = 12, and fine content = 55%). It was noted that the AGT Laboratory developed mixing methods based on producing 4 to 6 samples or "batches" at once. Gregory (2006) noted that this could be the cause for the variability in the AGT Laboratory

results. Based on the discussion provided by Gregory (2006), triaxial data showed a 16% to 64% increase in the internal angle of friction relative to the unreinforced test specimens, depending on the material tested and the quantity of fiber inclusions. Direct shear results showed a 19% to 26% increase in the internal angle of friction relative to unreinforced test specimens for test specimens that had fiber contents with 0.4 kg to 8 kg of fiber per cubic meter (0.25 lb to 0.5 lb of fiber per cubic foot) of soil.

Maher and Gray (1990) conducted 180 triaxial tests using nine sands reinforced with 12 mm to 45 mm (0.5 in to 1.75 in) long fibers at fiber contents ranging from 1% to 5% by dry mass. Fibers including Buna-N (aspect ratio of 20), reed No. 0 (aspect ratio of 20), reed No. 3 (aspect ratio of 20), Palmyra palm (aspect ratio of 20), glass No. 1 (aspect ratio of 60), glass No. 2 (aspect ratio of 80), and glass No. 3 (aspect ratio of 125) were investigated. Failure surfaces appeared to follow Mohr-Coulomb failure criterion. They observed an isotropic reinforcing action with no development of preferred planes of weakness or strength. Larger fiber aspect ratios increased the fiber's ability to contribute to an increase in shear strength. Fibers with a low modulus did not contribute significantly to an increase in soil strength. Similar to another study reported herein, shear strength increased linearly with increasing fiber content to an asymptotic upper limit. An increase in the uniformity of the sand exhibited an increase in the contribution to the shear strength. A reduction in shear strength was noted for sands with a larger soil grain size.

Michalowski and Cermak (2003) performed CD triaxial tests to assess the strength characteristics of fine and medium sands reinforced with galvanized steel wire that had a specific gravity of 7.85, polyamide monofilament with a specific gravity of 1.28, and polypropylene fibrillated fiber with a specific gravity of 0.91. Most reinforcing fibers were

25 mm (1 in) in length, uniformly distributed or oriented in a particular direction, and were added in 0.5% to 2% fiber contents by volume of the specimen. CD test results demonstrated shear strength increases up to 70% with the addition of 2% fiber content by volume. It was also observed that the fine sand test specimens were stronger than the coarse sand specimens with low 0.5% fiber contents, but the opposite occurs at larger 2% fiber contents. It was also discovered that larger fiber aspect ratios have a greater contribution to the strength gain. Michalowski and Cermak (2003) reported that fiber length needs to be one order of magnitude greater than the size of the soil particles to allow for a more effective soil-reinforcement interaction. They also observed a decrease in initial stress with the addition of fiber, but an increase in failure stress was measured. The strain level at failure was also increased with the addition of the fiber.

Ranjan et al. (1994) conducted several CU triaxial tests on a poorly graded fine sand (SP-SM) soil reinforced with four different plastic fibers with lengths ranging between 18 mm to 38 mm (0.75 in to 1.5 in). Each plastic fiber had a different aspect ratio (length/width) and fiber contents ranged up to 4% by dry mass of the soil. The authors reported that plastic fiber reinforcements never ruptured and they were responsible for the increase in peak shear strength and residual strength relative to the unreinforced control specimens. Each fiber reinforced test specimen experienced a particular confining stress referred to as the ‘critical confining stress’, which would result in the fibers slipping or pulling out. Ranjan et al. (1994) observed fibers stretching or yielding at confining stresses greater than their ‘critical confining stress’. Increasing the fiber aspect ratio correlated to an increase in shear strength contribution and a reduction in the ‘critical confining stress’.

Similar to other studies, the authors also report an increasing linear trend in shear strength with increasing fiber content up to 2%.

Romero (2003) studied the effective stress, strain, pore pressure, and volume change behavior of unreinforced and reinforced soil specimens to develop a model that would predict the behaviors of fiber reinforced soils. CD and CU triaxial testing was conducted on a clayey silt (liquid limit = 32, plastic limit = 25, and the clay content = 12%) using a 74 mm (2.9 in) diameter by 143 mm (5.6 in) tall mold. During soil preparation, 80% of the total water was added and the sample was permitted to hydrate overnight. The remaining 20% of total water was added the next day, and the sample was permitted to hydrate over a second evening time period. Samples were either prepared 2% wet or 2% dry of the standard Proctor optimum moisture content. A 2-inch long polypropylene fibrillated fiber was added to the reinforced test specimens using fiber contents up to 0.4% by dry mass of the soil. A total of 26 CU tests were performed to evaluate the stress-strain behaviors of fiber reinforced soils. Additionally, stress-strain behaviors were observed during 20 CD triaxial tests. Significant axial strains were required to mobilize the resistance provided by the fibers under the undrained loading conditions. A much smaller axial strain was required to mobilize the fiber resistance under the drained testing conditions. The addition of fiber reinforcement increased the friction angle and cohesion significantly during undrained testing conditions while the fibers impacted the friction angle only slightly and the cohesion significantly under drained testing conditions.

Zhang et al. (2003) identified an embankment constructed of fat clay (CH) on a section of Highway LA 15 next to the Mississippi River levee in Concordia Parish that has experienced a high frequency of slope failures. During the field observations, the authors

reported that water trapped in ‘fissures’ and ‘cracks likely caused the slope failures. The authors developed a laboratory testing program to evaluate the use of randomly oriented synthetic fibrillated fibers and non-woven geotextile fabric in the Concordia Parish soils compacted at different moisture contents, soil densities, and confining pressures. Testing involved direct shear and CD triaxial testing of samples reinforced with 25 mm (1 in) long polypropylene fibrillated fibers at 0.1% and 0.2% fiber contents by mass. With the addition of 0.1% fiber content, a minimum increase of 50% to the ultimate shear strength was gained.

2.4. Previously Conducted Full-Scale Field Studies

Consoli et al. (2003) performed two plate load tests on a sandy soil from Porto Alegre, Brazil. Each test was constructed in a 4 m^2 (43 ft^2) test area using 12 compaction lifts. One sample remained unreinforced while the other contained 25 mm (1 in) long polypropylene monofilament fibers at a 0.5% fiber content by dry mass. The test areas were subjected to a plate load test using a 0.3 m (1 ft) diameter steel plate. In addition, static CD triaxial tests were performed on the reinforced and unreinforced soil at four different confining pressures, low axial strain, and at a minimum 97% saturation. The plate load test demonstrated that the polypropylene monofilament fibers significantly improved the behavior of the soil. The reinforced soil displayed a noticeably stiffer response with increasing settlements due to the continuous increase in strength at larger deformations. The triaxial testing also verified the observation noted from the field test. The polypropylene monofilament fiber reinforced samples experienced strain hardening at axial strains larger than 20%. Conversely, the unreinforced soil samples demonstrated plastic behaviors at larger strains. Data from the triaxial tests also revealed a 530% increase

in the cohesion with the addition of the fibers while the friction angle only experienced a 3% increase.

Gregory and Chill (1998) collected clay samples from a failing highway embankment slope in Beaumont, TX. They subjected this soil to 32 CD triaxial tests and 86 direct shear tests. Fibrillated polypropylene fibers that were 25 mm and 50 mm (1 in and 2 in, respectively) long were blended into the clay at fiber contents up to 0.25% of the dry mass. At the completion of laboratory testing, a field case study was performed on the failing embankment slope. The slope was re-constructed by removing up to 0.6 m (2 ft) of clay below the primary failure surface. The excavated soil was loosely placed in 200 mm (8 in) lifts. A pre-determined dosage of fiber was mixed in to each lift, which was compacted to 95% of the maximum dry density in accordance with standard Proctor compaction testing protocol. The authors observed a 20% to 50% increase in effective shear strength with the polypropylene fibrillated fiber inclusions. The fibers increased the factor of safety by 50% based on a slope stability analysis due to the increased friction angle and cohesion. The repaired fiber-reinforced slope has shown no signs of movement but the remaining unreinforced backfilled slope in the same area has failed.

Park and Tan (2005) explored the use of geogrid layers with randomly oriented synthetic monofilament fibers in a silty sand (SM) backfill. Two full-scale walls were constructed. One wall was constructed using conventional mechanically stabilized backfill with the geogrid only. The second wall was constructed in the same way, but the 60 mm (2.5 in) long polypropylene monofilament fibers were added to the backfill using a 0.2% fiber content. UC and CD triaxial tests were performed on representative samples of the backfill prior to constructing the full-scale walls. The specimens were prepared at standard

Proctor compaction specifications. Polypropylene fibers and geogrid were installed at the center of the reinforced samples as needed. The strength characteristic data acquired from the laboratory testing were used as inputs during a Finite Element Modeling (FEM) effort to predict and compare the behavior of the full-scale walls. After evaluation of the two full-scale reinforced walls, it was concluded that the reinforced walls constructed with geogrid layers in conjunction with the polypropylene monofilament fibers produced a stronger and stiffer material. There was reasonable agreement between FEM predictions and field measurements.

Tingle et al. (1999) conducted UC tests on six different sand types, using four fiber types, five fiber lengths, six different deniers, and five different fiber contents in preparation for the construction of full-scale road sections to be reinforced with fibrillated, monofilament, and tape polypropylene fibers. Fiber lengths and contents ranged from 52 mm to 76 mm (2 in to 3 in) and fiber contents ranged from 0.6% to 1% by dry mass of the soil. The results from the laboratory testing indicate that the four types of fiber inclusions improved the load bearing capacity in the following order from best to worst: fibrillated, tape, monofilament, and mesh. Improvement was observed in all six types of sands tested. The authors observed an optimum fiber length equal to 51 mm (2 in) with an optimum fiber content between 0.6% and 1% by dry mass. It was noted that the denier of the fiber does not affect its reinforcement capacity. Sands that contain up to 8% silt will increase the effectiveness of the fiber reinforcement. The density of the samples was decreased with increasing fiber content, but the density of a fiber reinforced fine sand was less affected than the density of a fiber reinforced coarse sand.

Two full-scale roadway sections were constructed under Hangar 4 at the US Army Corps of Engineer Waterways Experiment Station in Vicksburg, Mississippi to validate the laboratory testing results. At the completion of the field testing, fibrillated fibers proved superior to alternative synthetic additives in regard to rut resistance. Resistance to rutting was maximized with a 1% fiber content. There was no significant difference in results between the 51 mm (2 in) and the 76 mm (3 in) fibrillated fibers, but it was noted that the 76 mm (3 in) fibrillated fibers tended to get hung up on the mixing equipment. Densification of the stabilized sands and supporting sand layers also attributed to the permanent rutting of the test sections. It was found that fiber stabilized materials had a resistance to compaction, hence increased deformations during testing due to densification. CBR results of the geofiber stabilized concrete sand had improvements on the order of 6% to 35%, which correlated to a 583% increase over the unstabilized sand shoulder at similar depths.

CHAPTER 3: LABORATORY TEST MATERIALS AND CONFIGURATION

3.1. Introduction

The intent of this chapter is to describe the materials and testing procedures utilized as part of this project. To assess the unconfined compressive strength of geosynthetic-reinforced soil, two types of soil specimens were compacted using a standard Proctor compaction effort, and subsequently tested in the laboratory to determine the unconfined compressive strength.

For Dataset 1, bags of ASTM certified Ottawa sand and kaolin clay were purchased to generate soil specimens easily controlled in terms of their grain size distribution and material properties. To generate the unconfined compression test specimens, the kaolin clay was systematically mixed with the sand in different percentages to simulate various grain size distributions and compacted using a standard Proctor effort. These specimens were tested both with and without the reinforcing polypropylene fibrillated fibers in varying amounts.

More specifically, 120 tests were performed on the kaolin clay-Ottawa sand test specimens at the optimum moisture content determined during the standard Proctor compaction testing conducted for these soils. These test specimens were generated using kaolin clay percentages equal to 0%, 10%, 15%, 20%, 25%, and 30%, and mixed with fiber percentages equal to 0% (referred to as the control specimens), 0.5%, 0.75%, 1%, 1.25%, 1.5%, 1.75%, and 2%. Additionally, unconfined compression tests were repeated after

soaking five additional 30% kaolin clay-70% Ottawa sand test specimens to measure any difference in the unconfined compressive strength. The full test matrix is displayed in Appendix B.

For comparison to the kaolin clay-Ottawa sand test specimens, field soils acquired from four counties including 1) Buncombe County (located in the mountains of North Carolina), 2) Johnston County (located in the eastern piedmont), 3) Guilford County (located in the western piedmont), and 4) Lincoln County (located northwest of Charlotte) were tested. Similar to the laboratory generated soils, all four field soils were tested both with and without the polypropylene fibrillated fiber reinforcement to determine the unconfined compressive strength of geosynthetic-reinforced soils collected from the field.

More specifically, 20 tests were performed on the four field soils at the optimum moisture content determined during the standard Proctor compaction testing conducted for these soils. The test specimens were mixed with geosynthetic fiber percentages equal to 0%, 0.75%, 1.25%, 1.75%, and 2%. Additionally, 25 unconfined compression tests were repeated using the same field soils after they were soaked.

In summary, a total of 125 ASTM kaolin clay-Ottawa sand test specimens and a total of 40 field soil specimens were tested as part of the extensive test matrix displayed in Appendix B. It should be noted that any mention of an optimum moisture content in this thesis refers to the value acquired during standard Proctor compaction testing, representing a standard Proctor compaction effort. This chapter will outline the specifications of all test materials, summarize the soil and test specimen preparation procedures, and describe the test configuration and matrix in detail.

3.2. Ottawa Sand Mixed with Kaolin Clay

The Ottawa sand was purchased from U.S. Silica, which distributes ASTM graded sand from Ottawa, Illinois conforming to the ASTM C 778 (Standard Specification for Standard Sand). Additionally, the U.S. Silica plant in Kosse, Texas supplied the Kaolin B. Table 3.1 displays the specifications for each material provided from U.S. Silica.

Table 3.1: Kaolin Clay and Ottawa Sand Properties (after U.S. Silica)

Ottawa Sand	
Color	White
Grain Shape	Round
Hardness, Mohs	7
Melting Point, °F	3100
Mineral	Quartz
pH	7
Specific Gravity	2.65
Kaolin B	
Median Particle Size, μm	1.00
Bulk Density, kN/m^3	
Untapped	7.85
Tapped	10.68
Color	White
pH (ASTM D 1208-78)	6
Specific Gravity (ASTM C 329-75)	2.58

Figure 3.1 displays the grain size distribution for the kaolin clay-Ottawa sand mixtures and for the Ottawa sand. For example, the 30% kaolin curve on Figure 3.1 represents the 30% kaolin-70% Ottawa sand mixture. The data was generated using the procedures outlined in ASTM D 422 (Standard Test Method for Particle-Size Analysis of Soils) while varying the kaolin clay percentages between 10% and 30%. A hydrometer analysis was utilized to determine the kaolin clay particle sizes that were less than 0.075 mm, which is the No. 200 sieve. The hydrometer analysis was performed in accordance with ASTM D 422 (Standard Test Method for Particle-Size Analysis).

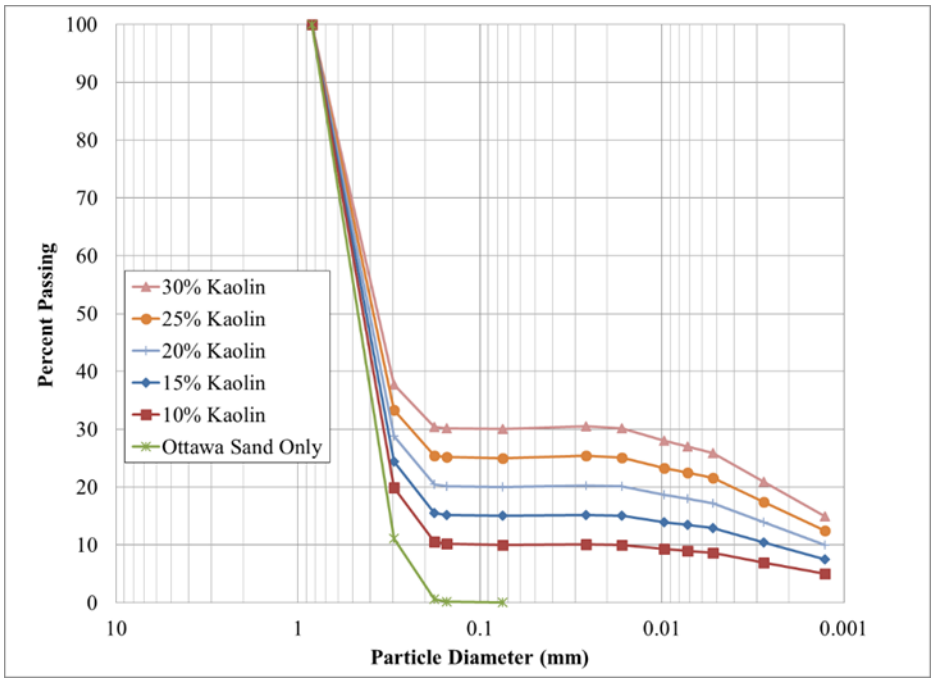

Figure 3.1: Grain Size Distribution Curves for all Kaolin Clay-Ottawa Sand Soils and the Ottawa Sand

3.3. Field Soils

The location of each field soil county within the state of North Carolina is displayed on Figure 3.2. Buncombe County (1) is located in western North Carolina near the Appalachian Mountains. Johnston County (2) is the farthest east and those soils are predominately coastal plain soils according to a Soil Survey of Johnston County, NC. Guilford County (3) is located in the North Carolina Piedmont region and Lincoln County (4) soils consist primarily of clay underlain by weathered rock.

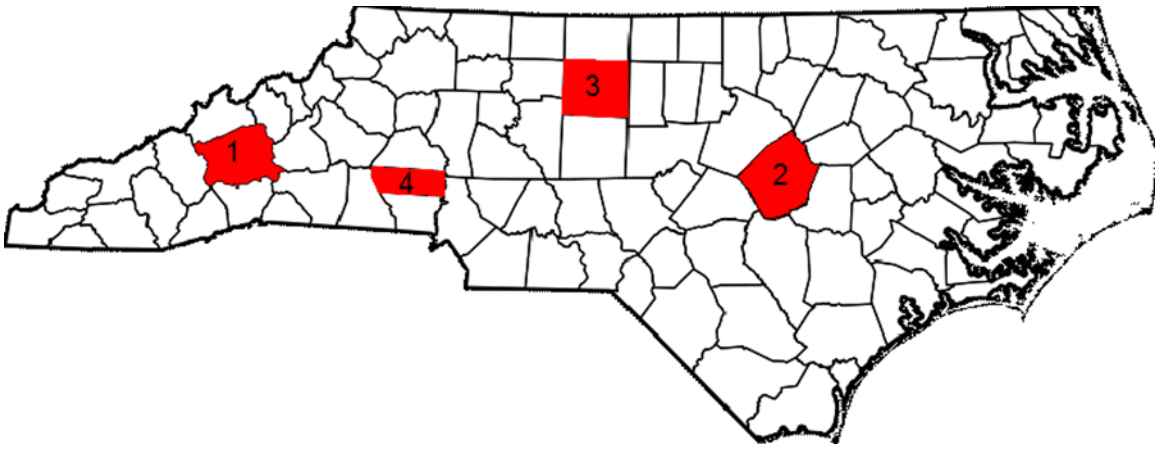

Figure 3.2: North Carolina Field Soil County Locations

For all field soils, grain size distribution testing was conducted in accordance with ASTM D 422 (i.e., Standard Test Method for Particle-Size Analysis of Soils), Atterberg limit tests were performed in accordance with ASTM D 4318 (i.e., Standard Test Methods for Liquid Limit, Plastic Limit, and Plasticity Index of Soils), and standard Proctor compaction tests were performed in accordance with ASTM D 698 (i.e., Standard Test Methods for Laboratory Compaction Characteristics of Soil Using Standard Effort). The grain size distribution curve for each field soil is displayed in Figure 3.3. Note that two of

the field soils are designated as ‘sandy silt (ML)’ and the other two are classified as ‘silty sand (SM)’ in accordance with ASTM D 2487 (i.e., Standard Practice for Classification of Soils for Engineering Purposes (Unified Soil Classification System)). Table 3.2 summarizes the results of the index tests performed on all five kaolin clay-Ottawa sand mixtures and the four North Carolina field soils tested during this study. Note that a 30% kaolin clay soil indicates that the remaining fraction of the soil is Ottawa sand.

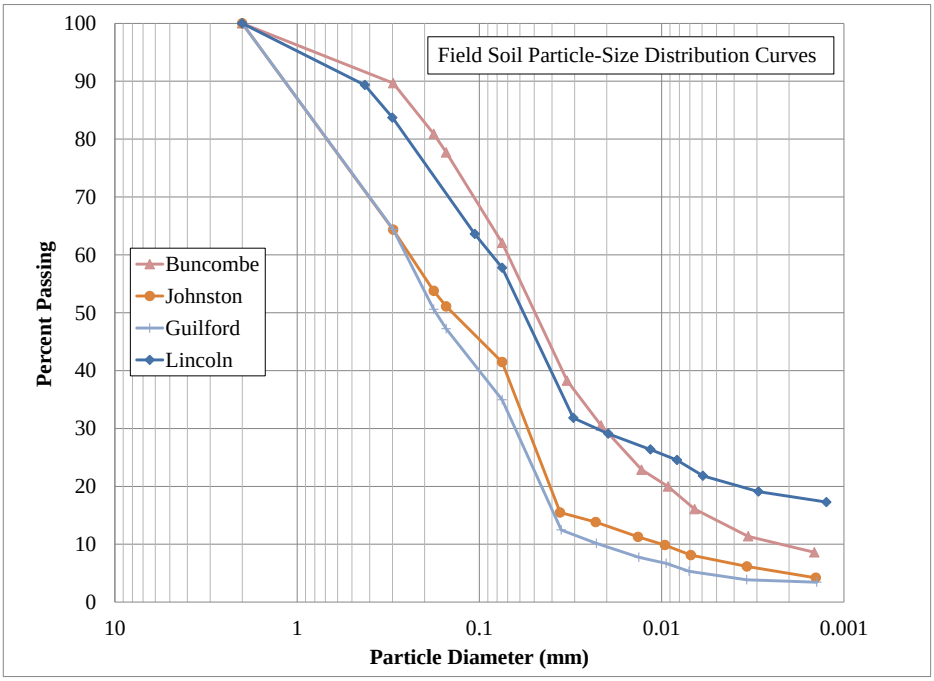

Figure 3.3: Field Soil Grain Size Distribution Curves

Table 3.2: Summary of the Index Testing Results for all Soils

Soil	**Liquid Limit (ASTM D4318)**	**Plastic Limit (ASTM D4318)**	**Plasticity Index (ASTM D4318)**	**D_{50} (mm)**	**$\gamma_{d\,(max)}$, kN/m^3 (ASTM D698)**	**Optimum Moisture Content (ASTM D698)**	**USCS Soil Classification (ASTM D2487)**
Field Soils							
Buncombe	48	42	6	0.050	14.6	24.0	ML
Guilford	37	29	7	0.180	17.5	15.9	SM
Johnston	34	28	6	0.150	17.6	14.2	SM
Lincoln	43	36	7	0.058	14.8	22.5	ML
Kaolin Clay-Ottawa Sand Soils							
30% Kaolin	22	15	7	0.360	19.5	11.0	SC-SM
25% Kaolin	21	14	7	0.380	19.7	10.0	SC-SM
20% Kaolin	19	14	5	0.400	20.1	9.1	SC-SM
15% Kaolin	14	13	1	0.420	19.5	8.3	SM
10% Kaolin	13	12	1	0.440	18.7	7.4	SP-SM

3.4. Polypropylene Fibrillated Geosynthetic Fiber

Fiber reinforcement was first introduced into cementatious materials to enhance the brittle nature of the material. More recently, fiber reinforcement has been introduced into soils as geosynthetic fiber reinforcement. Field studies have been performed to evaluate slope rehabilitation using geosynthetic fibers (Gregory and Chill, 1998). The fibers have also been studied in temporary and/or low-volume roads (Tingle et al., 2002).

Reinforcing fibers can be composed of various materials including steel, polypropylene, nylon, and polyethylene, and are also classified by structure. Examples of various fiber structures include monofilament, fibrillated, multifilament, tape, hooked end (steel only), and crimped (steel only). Figure 3.4 displays a variety of geosynthetic reinforcing fibers, but the polypropylene fibrillated fiber displayed in Figure 3.5 is the one utilized in this study. When the fibrillated fiber is pulled apart, the structure appears to have a web-like appearance.

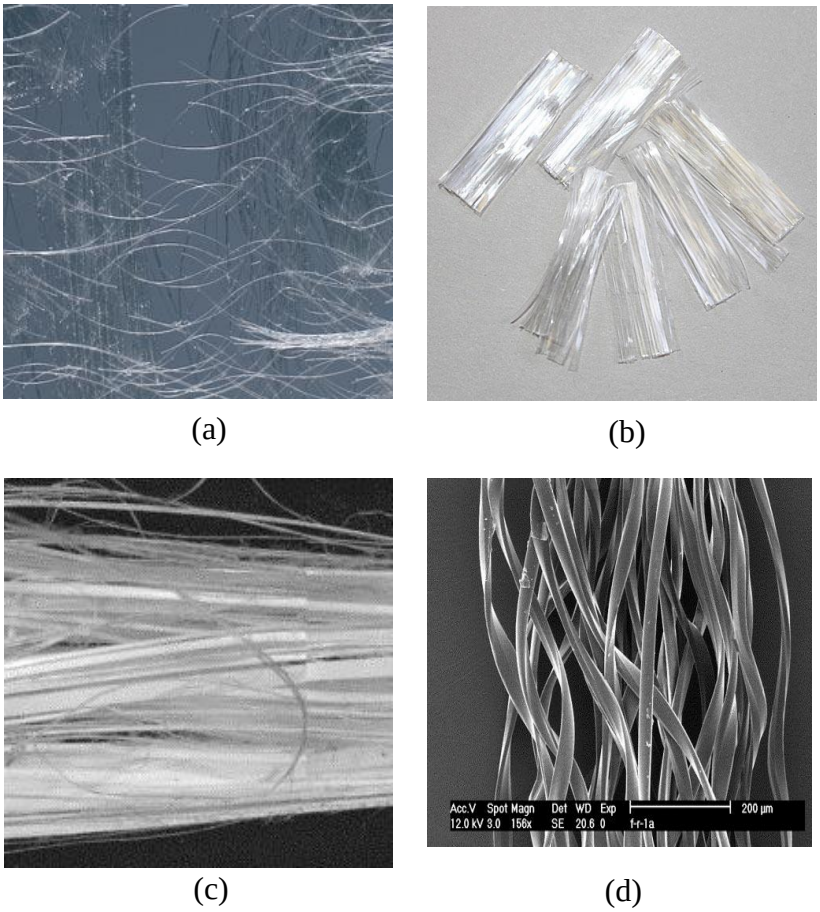

Figure 3.4: Examples of Various Geosynthetic Fibers: (a) Monofilament (after tunneltalk.com); (b) Fibrillated (after nycon.com); (c) Multifilament 1 (after sciencedirect.com); (d) Multifilament 2 (after sciencedirect.com)

In this study, the Propex Concrete Systems FIBERCAST 500™ fibrillated fiber was utilized to reinforce all test specimens (see Figure 3.5). The polypropylene fibrillated fiber was used in this study because past field research has shown that it exhibits the most strength benefit when used in roadway subgrade (Tingle et al., 1999) and slope repair (Gregory and Chill, 1998). Additionally, there is a limited amount of unconfined compression strength data for this type of fiber. The specifications of this polypropylene fibrillated fiber (displayed in Table 3.3) meet the requirements of ASTM C 1116, Type III 4.1.3 (i.e., Standard Specification for Fiber-Reinforced Concrete).

Figure 3.5: FIBERCAST 500™ Polypropylene Fibrillated Fiber

Table 3.3: FIBERCAST 500 Polypropylene Fiber Specifications
(after www.fibermesh.com)

Property	Test Method	Values
Denier	ASTM D 1907	360 grams/9000 meters
Length	Measured	12.7 mm (0.5 in)
Tensile Strength	ASTM D 2256	1.5 kg (3.2 lbs)
Elongation-at-Break	ASTM D 2256	15%

3.5. Test Specimen Preparation

In general, the reinforcing fibers were carefully mixed into the test specimens using the following specimen preparation procedures, and subsequently, subjected to unconfined compression testing in accordance with ASTM D 2166 (i.e., Standard Test Method for Unconfined Compressive Strength of Cohesive Soils). The specimen preparation procedures were carefully configured to ensure each test specimen was generated consistently and that the fiber inclusions were thoroughly mixed throughout the test specimen.

All soils were oven dried for at least 24 hours at a temperature of 110 °C. Once dried, soils were sieved using a No. 10 sieve (1651 µm particle size). Any soil particles retained on this sieve were discarded, and the remaining soil was utilized to generate the test specimens. Note that the Ottawa sand and kaolin clay materials passed the No. 10 sieve (1651 µm) entirely.

Test specimen size will affect the results of an unconfined compression test. According to Ang and Loehr (2003), specimens with diameters larger than 70 mm (2.75 in) and fiber lengths less than 50 mm (1.97 in) are more likely to produce strength data representative of the contribution it would have to a larger mass of soil in the field. In this study, the polypropylene fibrillated fibers were 12.7 mm (0.5 in) long and the compaction mold was 203 mm (8 in) long by and 102 mm (4 in) in diameter as displayed in Figure 3.6. To generate a compaction mold with these dimensions, a custom generated coextruded polyvinyl chloride (PVC) pipe was utilized as a mold to compact the test specimens. The schedule 40 PVC pipe was manufactured in accordance with ASTM F 891 (i.e., Standard Specification for Coextruded Poly Vinyl Chloride (PVC) Plastic Pipe with a Cellular Core).

Figure 3.6: Custom Compaction Mold Used to Generate the Test Specimens

Because the 203 mm (8 in) long PVC compaction mold utilized in this study was taller than a standard Proctor mold, the drop count of the standard Proctor hammer had to be recalculated to ensure each test specimen received a 'standard' level of compaction effort (600 kN-m/m^3 or 12,400 ft-lb$_f$/ft^3) during sample preparation. Using the same three compaction lifts, Equation 3.1 was utilized to calculate the number of hammer drops that would be required to reach the standard Proctor effort for each lift inside the custom PVC mold.

$$N = \frac{E * V}{H * P * L} \qquad (1)$$

Where:

E = Energy from 25 drops = 593.11 kN-m/m^3 (12,387.39 ft-lb_f/ft^3)
N = Number of Drops = 44
H = Fall Height = 304.8 mm (12 in)
P = Hammer Weight = 1.24 N (5.5 lb)
V = Volume of Mold = 0.001647 m^3 (0.058177 ft^3)
L = Number of Lifts = 3

In this study, all soils were prepared at the optimum moisture contents determined for each soil during standard Proctor compaction testing, but a select number of tests were repeated to simulate soaked conditions. According to Iasbik et al. (2002) and Maher and Ho (1994), the addition of polypropylene fibers alters the optimum moisture content by less than 1% so the small effect on the optimum moisture content related to the inclusion of reinforcing fibers was not considered during this compaction evaluation.

The soaked test specimens were compacted at the same optimum moisture contents using the PVC mold, bound on both ends with filter paper and a porous stone, and placed in a large water bath for 24 hours. It is important to note that the specimens remained in the PVC mold during the soaking period so the change in saturation would likely be less than if the specimens had been removed. Values of saturation for each test specimen are summarized Appendix D. Figure 3.7(a) displays the Lincoln County samples prepared to be soaked. After the specimens were soaked, it was evident that the soil swelled during the soak process (Figure 3.7(b)) so care was taken to remove excess soil (Figure 3.7(c)). Subsequently, an unconfined compression test was performed on the soaked soil specimen to determine the impact on unconfined compressive soil strength.

(a)

(b)

(c)

Figure 3.7: Test Specimen Soaking Process: (a) Lincoln County Samples Prior to Water Submersion; (b) Soil Swell for a 30% Kaolin Clay-Ottawa Sand Mixture; (c) Soil Trim, Prior to Fiber Trimming

To ensure repeatable test results and consistent fiber mixes, test specimens were prepared and mixed in a Hobart mixer (see Figure 3.8) using a three batch process that included one batch for each lift in the compaction mold. Field soils were passed through the No. 10 sieve (1651 µm) and divided into three parts for each of the compaction lifts. Comparatively, the constituents of the kaolin clay-Ottawa sand test specimens were individually measured and mixed for each of the three batches to ensure consistency between the three lifts in the compaction mold. The fiber reinforcement was measured for each compaction lift for all specimens. In total, approximately 3.7 kg (8.1 lbs) of soil was needed to generate both the field soils and the kaolin clay-Ottawa sand soil test specimens. The following paragraphs provide more detail regarding the preparation procedures.

Figure 3.8: Hobart Mixer

More specifically, the kaolin clay and the Ottawa sand was independently measured and placed in a clean mixing bowl, mixed by hand initially, and then placed inside the mixer. Subsequently, the water required to achieve the optimum moisture content was mixed into the material at a low speed for approximately 30 seconds or until the largest soil clumps were the approximate size of peas and the water was incorporated throughout the mixture. The mixer speed was increased to a medium speed, and mixed for an additional 30 seconds while soil that was stuck to the sides of the bowl was removed and added to the mixture. Any clay clumps were broken apart using the tips of the fingers, and then mixing resumed at medium speed for an additional 45 seconds. At this stage, the soil took on the appearance of granola clusters (small cohesive clumps that stuck together in groups), and the soil also started to cohere into larger masses that climbed up the sides of the mixer as shown in Figure 3.9.

Figure 3.9: Mixed Kaolin Clay-Ottawa Sand Soil Beginning to Cohere

With the exception of the control specimens (i.e., no fiber reinforcement), the correct geofiber mass was poured into the bowl and mixed on low speed for up to 45 seconds, depending on how long it took the fibers to lose their luster. Figure 3.10 displays an example of a mixture at the end of the mixing phase. A loss of luster provided a qualitative indicator that the soil had begun to migrate into the fibrillations of the fiber. By trial and error, it appeared that additional mixing beyond this state produced uneven clumping and fiber grouping. Any existing soil-fiber clumps were manually broken up and all contents inside the bowl were further mixed by hand. There was a tendency for the fibers to 'float' on top of the soil (see Figure 3.11) so care was taken to tumble the soil over top of the fibers. The fibers also had a tendency to adhere to the walls of the bowl (see Figure 3.12) so they were removed and added back to the mixture.

Figure 3.10: Final Soil Mix after the Addition of Fiber Reinforcement

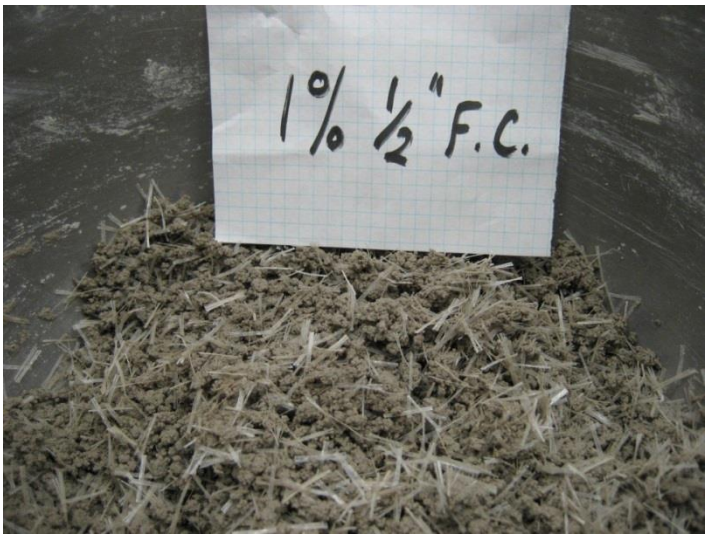

Figure 3.11: Fibers Floating on Top of the Soil

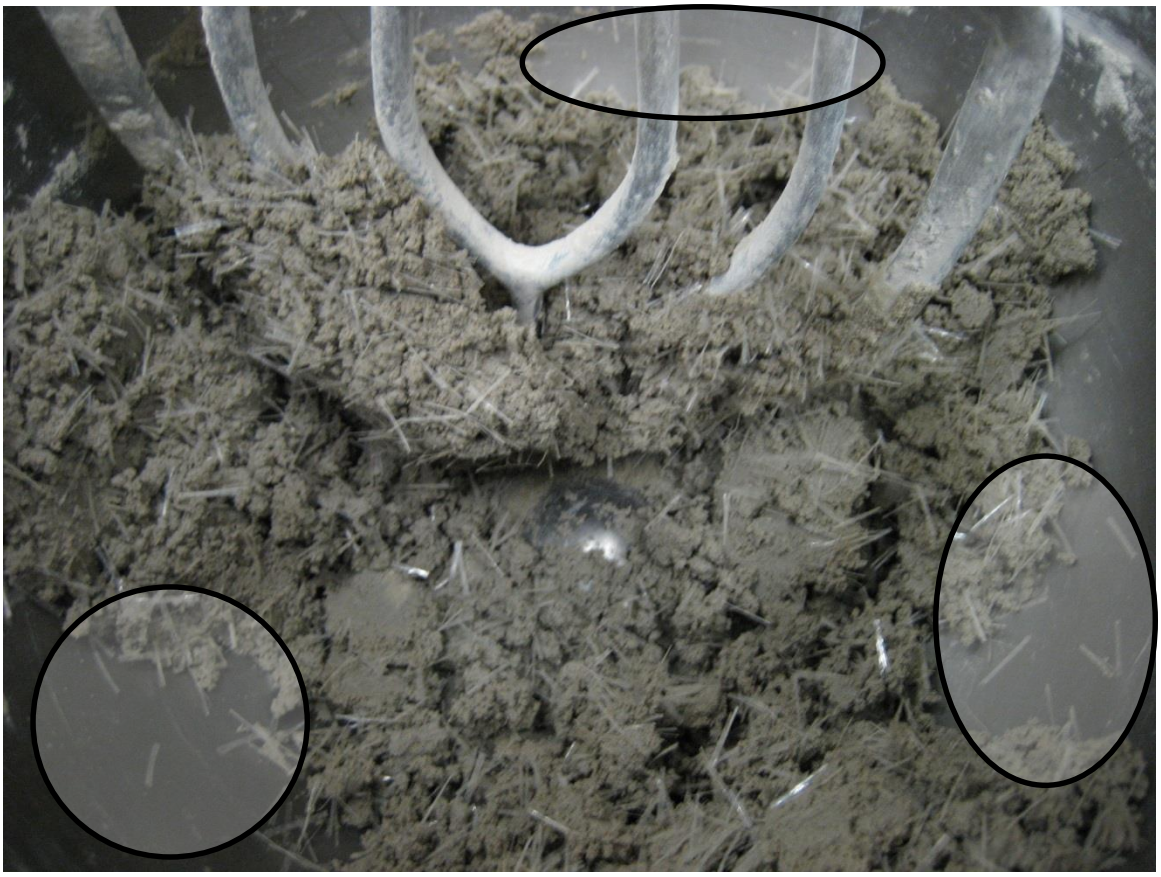

Figure 3.12: Fibers Adhering to the Side of the Mixing Bowl

The process used to transfer the soil from the mixing bowl to the PVC compaction mold varied depending on whether the soil was reinforced or not. Unreinforced soil was placed in the mold using a hand trowel while carefully avoiding wasted soil. For the reinforced soil specimens, it was necessary to maintain the fiber distribution that was carefully achieved during the mixing process. If the soil was simply poured into the mold by trowel, there was a tendency for the heavier soil particles to drop to the bottom and the majority of the fibers would 'float' on top. In order to prevent this issue, one handful of soil was manually compressed and placed in the mold at a time. This locked the fibers into their current configuration and maintained the distribution as the soil was placed in the mold.

Between lifts, the soil was scarified or roughened with a flat-head screwdriver prior to placement of the next lift. For the final lift, the soil was slightly compressed by hand and carefully placed so there was a slight crown over the top of the mold before compaction. This detail ensured that there was sufficient soil to fill the mold post compaction.

After the soil was compacted, a wire saw was used to trim the outside edge of the specimen around the circumference of the mold, and a flat striker bar was used to trim the excess soil from the top of the specimen (using a sawing action) and smooth the top of the sample (using the beveled edge). The sample was rotated while using the straightedge in order to avoid pulling the fibers from the top of the sample. Small voids were filled with cuttings and carefully leveled. Extra precautions had to be taken for the fiber reinforced specimens. Fibers that extended over the edge of the mold were trimmed with scissors to avoid trapping fibers between the edge of the mold and the extruder retaining ring during extrusion. Without this step, the trapped fibers would scour the face of the extruded specimen. For the test specimens that were soaked, the material swelled so an extra step was taken to trim the excess soil before extrusion to maintain the same test specimen dimensions.

Each sample was extruded using a manual hydraulic hand pump while care was taken to avoid possible breakage of the sample. Samples with a larger volume of fibers and higher sand percentage (e.g., 10% kaolin clay-90% Ottawa sand mixture with 2% fiber) tended to have separation issues, particularly at the lift interfaces, if excessively tilted off the vertical axis when removed from the sample extruder and transported to the load frame. Figure 3.13 displays a photograph of a sample with separation issues. The top photograph (Figure 3.13(a)) shows the entire specimen while Figure 3.13(b) and (c) highlight the

separations created. Alternatively, Figure 3.14 displays a photograph of test specimen 35R post extrusion without separation issues.

(a)

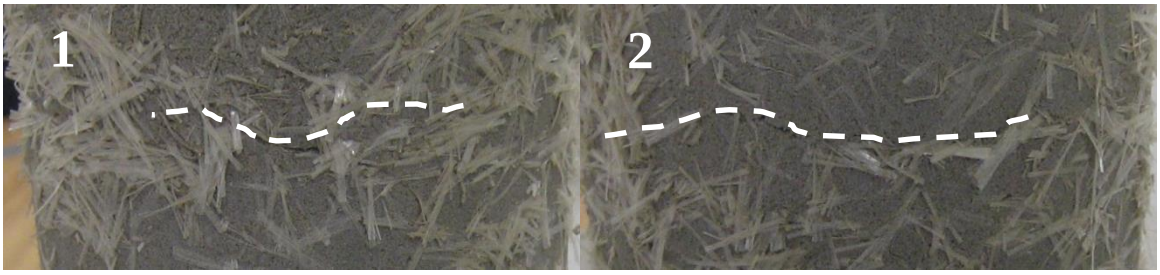

(b) (c)

Figure 3.13: Example of Where Separation Occurs in Samples with a High Percentage of Reinforcement (39R): (a) General View of Test Specimen; (b) Detailed View of Separation 1; (c) Detailed View of Separation 2

Figure 3.14: Test Specimen Extruded Successfully without Issues

3.6. Unconfined Compression Configuration and Test Procedure

While the previous section highlights the details of the preparation process for all test specimens, this section describes the testing configuration and procedures while highlighting any modifications to the ASTM standards. Unconfined compression tests were performed on the test specimens in accordance with ASTM D 2166 (i.e., Standard Test Method for Unconfined Compressive Strength of Cohesive Soils) immediately after they were extruded from the PVC compaction mold to minimize moisture content changes in the test specimen. The full test matrix is included in Appendix B but Table 3.4 provides a summary. For example, for the 30% kaolin clay row in Table 3.4, the 30% kaolin clay-70% Ottawa sand was molded at the optimum moisture content, and was tested three times using each with the following fiber contents: 0%, 0.5%, 0.75%, 1%, 1.25%, 1.5%, 1.75%, and 2%.

Table 3.4: Number of Tests Performed for Each Unconfined Compression Test Configuration

	Fiber Content							
	0.00%	**0.50%**	**0.75%**	**1.00%**	**1.25%**	**1.50%**	**1.75%**	**2.00%**
Optimum Water Content								
Buncombe	1	-	1	-	1	-	1	1
Johnston	1	-	1	-	1	-	1	1
Guilford	1	-	1	-	1	-	1	1
Lincoln	1	-	1	-	1	-	1	1
30% Kaolin	3	3	3	3	3	3	3	3
25% Kaolin	3	3	3	3	3	3	3	3
20% Kaolin*	3	3	3	3	3	3	3	3
15% Kaolin	3	3	3	3	3	3	3	3
10% Kaolin	3	3	3	3	3	3	3	3
Soaked								
Buncombe	1	-	1	-	1	-	1	1
Johnston	1	-	1	-	1	-	1	1
Guilford	1	-	1	-	1	-	1	1
Lincoln	1	-	1	-	1	-	1	1
30% Kaolin	1	-	1	-	1	-	1	1

* 7 additional samples were tested at fiber contents greater than 2.0% (3 @ 2.25%, 3 @ 3.00%, and 1 @ 3.50% fiber content)

The ELE Digital Tritest load frame utilized during this study is displayed in Figure 3.15, and a test specimen configured inside the load frame is displayed in Figure 3.16. The upper cross bar of the load frame was adjusted to ensure the retaining nuts were secure and there was sufficient clearance to mount the soil specimen. The LVDT displayed in Figure 3.16 was adjusted so that the tip rested on the square metal plate and was clear of any obstructions. The first 12.7 mm (0.5 in) of stroke was retracted to minimize potential over-extension readings at the end of the LVDT stroke range, which could result in false voltage

readings. After this was accounted for, the LVDT stroke was 50.8 mm (2 in). The load frame was adjusted to produce a 2.032 mm/minute strain rate, corresponding to a 1% strain/min rate for the 203.2 mm (8 in) sample as recommended by ASTM D 2166.

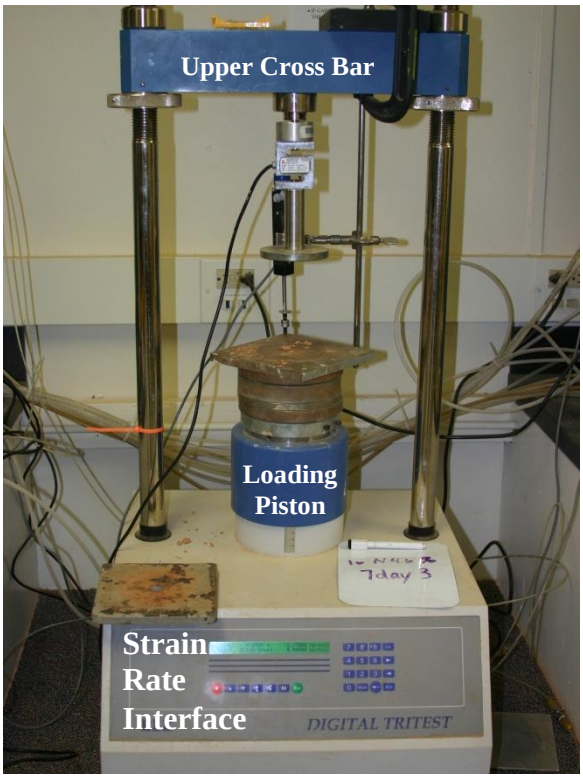

Figure 3.15: ELE Digital Tritest Load Frame

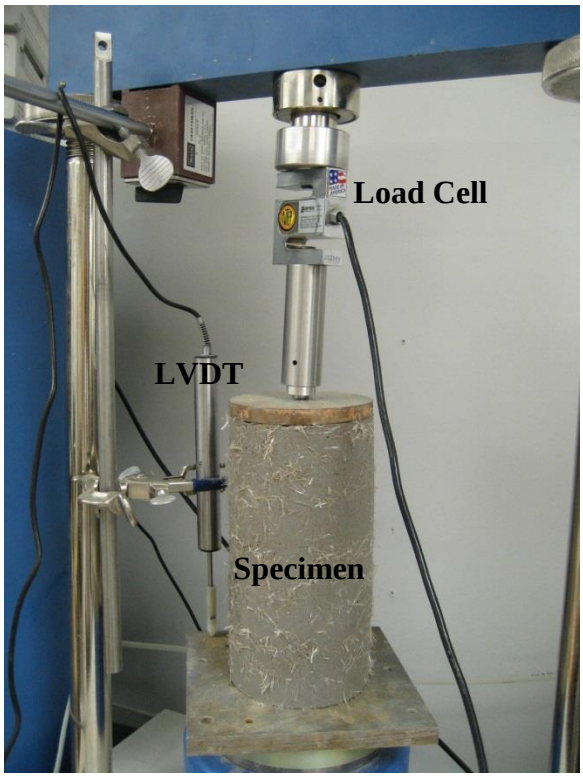

Figure 3.16: A Prepared Test Specimen inside the Load Frame

The test specimen was centered on the 152.4 mm (6 in) square plate displayed in Figure 3.16 and the loading piston, plate, and test specimen were raised until the circular plate on top of the test specimen just touched the 8.9 kN (2000 lb) load cell displayed in Figure 3.16 and Figure 3.17. It is important to apply a seating load to prevent the load cell from shifting, but the seating load should be limited to 0.45 to 0.91 kg (1 to 2 lbs) of force. Prior to the initiation of each test, the LVDT and load cell were set to zero.

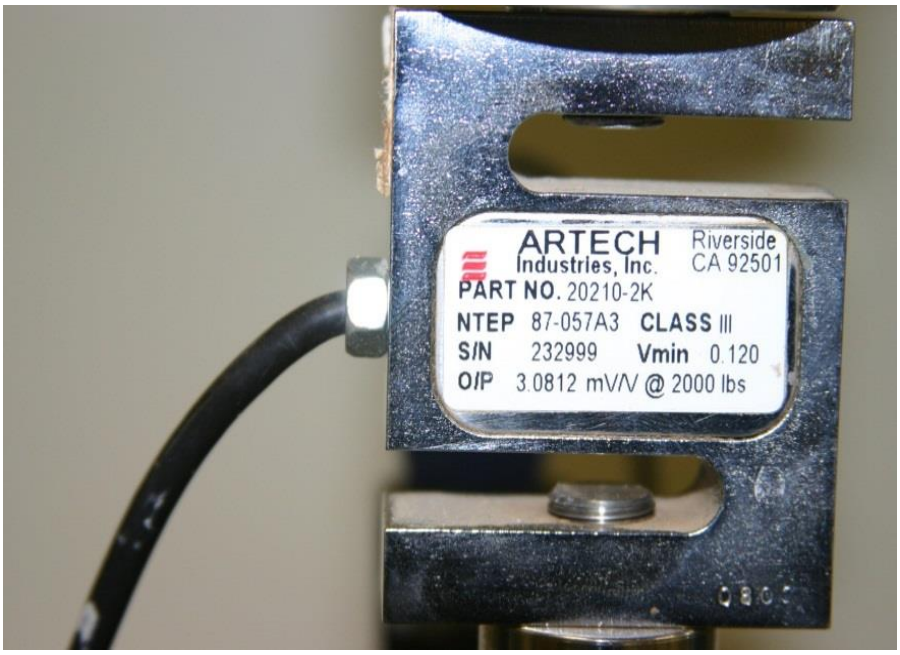

Figure 3.17: Load Cell Used During the UC Testing

A data acquisition system with LabVIEW was utilized to monitor the raw voltage data streaming from the load cell and the LVDT. Conversion factors provided by the manufacturer (i.e., Artech Industries, Inc.) converted the raw voltage values into engineering units of measurement inside the LabVIEW program. Each test was conducted well beyond failure. In several cases, failure was not reached within the 15 minute time frame established by ASTM D 2166, but the test continued until the stroke of the LVDT was exceeded.

Following each test, photographs of the test specimen were acquired. The pre and post-test photographs and the raw stress-strain data for each test specimen are presented in Appendix C. Soil samples were obtained from the top, middle and bottom of the test specimen to measure the water content at the end of each test. The test data was then imported into an Excel spreadsheet for further analysis.

3.7. Rigaku Miniflex+ X-Ray Diffractometer Procedure

This section describes a separate evaluation aimed at determining the mineral content of the field soils. The Miniflex+ X-Ray Diffractometer (XRD) displayed in Figure 3.18 was utilized with the help of the UNC Charlotte Engineering and Geology Department to develop a better understanding of the chemical makeup of the soils tested during this study. The XRD is composed of 1) the X-ray generator, which generates the radiation, 2) the goniometer, which measures the angles of the diffracted beams, and 3) the electronic circuit panel, which controls the intensity of the returning diffracted x-rays. The XRD emits a beam of radiation at the material, and as it strikes the crystal within the specimen being tested, it causes the beam to scatter in different directions. From the angle and intensities of these scattered beams, a three-dimensional picture of the density of electrons within the crystal can be produced. Once this image has been produced, it is used to determine the mean positions of the atoms and the chemical bonds that make up the crystals within the sample.

Figure 3.18: Rigaku Miniflex+ XRD

For each XRD test, the field soil samples acquired from Guilford, Johnston, Lincoln, and Buncombe counties were prepared by oven drying the soil for a 24 hour time period, and sieving the sample using a No. 200 sieve (0.075 mm particle size). Each processed sample was then placed in a plastic sampler the size of quarter, and placed inside the XRD machine as displayed in Figure 3.19. The circular plate within the machine rotates, allowing the X-ray to strike the sample at angles almost perpendicular to the samples. The XRD then communicates to a Windows platform software (i.e., MDI JADE 6.5) to deliver and analyze the raw data.

Figure 3.19: Rigaku Miniflex+ Interior

The MDI JADE 6.5 software program uses the raw diffracted intensities and scattered angles to develop diffraction patterns that can be compared to more than 5,000 minerals with known 'fingerprints'. Soil specimens are multi-phase materials that will consist of more than one mineral. Comparing the raw data of the sample to the known 'fingerprints' within the MDI JADE 6.5 software allows for identification of the sample based on multiple superposed patterns. This comparison is performed by taking the multi-phased mixture peaks on the diffraction pattern and using the known diffraction patterns within the software to develop a list of possible minerals and their concentration within the sample being tested. These known "fingerprint" patterns are also called Powder Diffraction Files (PDF). The output from the MDI JADE 6.5 software results in a table that provides the element name, chemical formula, figure-of-merit, the number of hits, and other parameters related to the XRD result.

Tables 3.5 through Table 3.9 present the XRD outputs for the kaolin clay-Ottawa sand mixtures and all field soils. The 'Figure-of-Merit' (FOM) column represents the confidence in the analysis for each multi-phased mixture listed. For example, Guilford County (Table 3.6) appears to have a diffraction curve similar to that of Kaolinite clay. This is assumed due to the low FOM value. The lower the FOM value, the closer the peak diffraction points match the known mineral diffraction points in the MDI JADE 6.5 software. The last column labeled 'Hits' represents the number of lines from the tested sample that match the PDF peaks. For Guilford County (Table 3.6), there were 27 lines that matched the PDF of Kaolinite. Based on this analysis, it was determined that all four field soils predominately contained the Kaolinite element.

Table 3.5: MDI JADE 6.5 Output Table (30% Kaolin Clay-70% Ottawa Sand Mixture)

10 Hits Sorted on Figure-Of-Merit	Chemical Formula	FOM	J	D	PDF-#	Hits	#d/I	I%	2T(0)	RIR	Space Group	a	b	c	Z	CSD#
Quartz	Si O2	2.7	+	C	99-0088	24	29	94	0.06	2.11	P3221 (154)	4.913	4.913	5.405	3	88
Kaolinite	Al4 (O H)8 (Si4 O10)	3.3	+	C	99-0067	27	200	76	0.04	0.43	P1 (1)	5.149	8.934	7.384	1	67
Rhodochrosite	Mn (C O3)	6	+	C	99-0089	3	29	15	0.06	1.65	R-3c (167)	5.905	5.905	5.905	2	89
Vermiculite 2M	Mg3 (Si4 O10) (O H)2	6.7	+	C	99-0106	0	200	2	0	11.15	Cc (9)	5.33	9.18	28.85	4	106
Cryolite	Na3 (Al F6)	8.8	+	C	99-0040	0	183	15	-0.08	0.26	P21/n (14)	5.402	5.596	7.756	2	40
Diopside	Ca Mg Si2 O6	8.9	+	C	99-0045	0	173	15	-0.08	0.58	C2/c (15)	9.75	8.926	5.251	4	45
Nepheline	NaAlSiO4	9	+	C	99-0083	0	140	15	-0.08	0.37	P63 (173)	9.98	9.98	8.332	1	83
Sodalite	Na4 Cl (Al3 Si3 O12)	9.6	+	C	99-0096	5	45	15	-0.04	1.64	P-43n (218)	8.869	8.869	8.869	2	96
Muscovite 2M	Kal2[Si3Al]O10(OH)2	9.8	+	C	99-0082	1	200	15	0.12	0.2	C2/c (15)	5.189	8.996	20.096	4	82
Celestine	Sr (S O4)	10.4	+	C	99-0025	0	133	15	-0.04	1.05	Pnma (62)	8.36	5.352	6.858	4	25

Table 3.6: MDI JADE 6.5 Output Table (Guilford County)

23 Hits Sorted on Figure-Of-Merit	Chemical Formula	FOM	J	D	PDF-#	Hits	#d/I	I%	2T(0)	RIR	Space Group	a	b	c	Z	CSD#
Kaolinite	Al4 (O H)8 (Si4 O10)	3.7	+	C	99-0067	27	200	50	0.08	0.43	P1 (1)	5.149	8.934	7.384	1	67
Quartz	Si O2	6	+	C	99-0088	24	29	31	0.12	2.11	P3221 (154)	4.913	4.913	5.405	3	88
Litharge	Pb O	7.7	+	C	99-0071	0	28	62	0.08	12.56	P4/nmm (129)	3.964	3.964	4.996	2	71
Barite	BaSO4	8	+	C	99-0016	0	163	43	0	1.53	Pnma (62)	8.884	5.456	7.157	4	16
Brookite	Ti O2	8.1	+	C	99-0020	7	101	31	0.04	0.76	Pbca (61)	9.174	5.449	5.138	8	20
Enstatite	Mg (Si O3)	9.9	+	C	99-0047	0	200	41	0.1	0.29	Pbca (61)	18.225	8.813	5.18	16	47
Alunogen	(Al (H2 O)6)2 (S O4)3 (H2 O)4.4	13.8	+	C	99-0006	6	200	66	-0.06	0.3	P-1 (2)	7.425	26.975	6.061	2	6
Anorthite	Ca (Al2 Si2 O8)	14.6	+	C	99-0012	1	200	92	0.1	0.28	P-1 (2)	8.177	12.877	14.169	8	12
Topaz	Al2 (Si O4) (O H)2	16.5	+	C	99-0104	0	146	23	0	0.33	Pbnm (62)	4.724	8.947	8.39	4	104
Cerussite	Pb C O3	17.6	+	C	99-0026	6	111	34	-0.12	5.87	Pmcn (62)	5.179	8.492	6.141	4	26
Albite - high	Na (Al Si3 O8)	23.4	+	C	99-0001	0	200	40	0.08	0.32	C-1 (2)	8.149	12.88	7.106	4	1
Microcline	K (Al Si3 O8)	23.7	+	C	99-0078	0	200	28	-0.1	0.31	C-1 (2)	8.573	12.983	7.22	4	78
Ankerite	Ca Mg0.27 Fe0.73 (C O3)2	24.3	+	C	99-0011	1	45	68	-0.1	1.45	R-3 (148)	4.831	4.831	16.166	3	11
Zoisite	Ca2Al3[Si3O12]OH	24.5	+	C	99-0113	0	200	100	0.04	0.34	Pnma (62)	16.212	5.559	10.036	4	113
Arsenopyrite	As Fe S	29.2	+	C	99-0014	1	144	72	-0.02	1.04	P-1 (2)	5.744	5.675	5.785	4	14
Cancrinite	Na8 (Al6 Si6 O24) (O H)2.04 (H2 O)2.66	31	+	C	99-0023	0	136	34	0.02	0.58	P63 (173)	12.664	12.664	5.159	1	23
Hemimorphite	Zn4 Si2 O7 (O H)2 (H2 O)	32.9	+	C	99-0061	0	128	100	-0.1	1.06	Imm2 (44)	8.366	10.714	5.113	2	61
Pickeringite	Mg0.93Mn0.07 Al2 (S O4)4 (H2 O)22	33	+	C	99-0086	0	200	62	0.06	0.3	P21/c (14)	6.184	24.272	21.226	4	86
Kyanite	Al2 Si O5	38.3	+	C	99-0068	3	200	79	0.04	0.17	P-1 (2)	7.119	7.847	5.572	4	68
Forsterite	Mg2 (Si O4)	43.2	+	C	99-0052	0	129	83	-0.04	0.38	Pbnm (62)	4.756	10.207	5.98	4	52
Muscovite 2M	Kal2[Si3Al]O10(OH)2	45.1	+	C	99-0082	1	200	10	0.12	0.2	C2/c (15)	5.189	8.996	20.096	4	82
Gypsum	Ca (S O4) (H2 O)2	45.3	+	C	99-0058	1	186	100	-0.12	0.99	I2/c (15)	5.68	15.18	6.52	4	58
Celestine	Sr (S O4)	48	+	C	99-0025	0	133	18	0.12	1.05	Pnma (62)	8.36	5.352	6.858	4	25

Table 3.7: MDI JADE 6.5 Output Table (Johnston County)

4 Hits Sorted on Figure-Of-Merit	Chemical Formula	FOM	J	D	PDF-#	Hits	#d/I	I%	2T(0)	RIR	Space Group	a	b	c	Z	CSD#
Kaolinite	Al4 (O H)8 (Si4 O10)	2.3	+	C	99-0067	27	200	31	0.08	0.43	P1 (1)	5.149	8.934	7.384	1	67
Quartz	Si O2	5.9	+	C	99-0088	24	29	76	0.06	2.11	P3221 (154)	4.913	4.913	5.405	3	88
Alunogen	(Al (H2 O)6)2 (S O4)3 (H2 O)4.4	6.9	+	C	99-0006	6	200	52	-0.08	0.3	P-1 (2)	7.425	26.975	6.061	2	6
Cerussite	Pb C O3	17.6	+	C	99-0026	6	111	23	0.1	5.87	Pmcn (62)	5.179	8.492	6.141	4	26

Table 3.8: MDI JADE 6.5 Output Table (Lincoln County)

5 Hits Sorted on Figure-Of-Merit	Chemical Formula	FOM	J	D	PDF-#	Hits	#d/I	I%	2T(0)	RIR	Space Group	a	b	c	Z	CSD#
Quartz	Si O2	13.4	+	C	99-0088	24	29	46	0.1	2.11	P3221 (154)	4.913	4.913	5.405	3	88
Kaolinite	Al4 (O H)8 (Si4 O10)	20	+	C	99-0067	27	200	63	0.1	0.43	P1 (1)	5.149	8.934	7.384	1	67
Anatase	TiO2	31.9	+	C	99-0008	10	18	20	0.02	2.55	I41/amd (141)	3.785	3.785	9.514	4	8
Goethite	Fe O (O H)	46.2	+	C	99-0055	1	70	46	-0.02	1.32	Pbnm (62)	4.605	9.96	3.023	4	55
Graphite	C	49.3	+	C	99-0057	7	11	40	0.12	1.24	P63/mmc (194)	2.456	2.456	6.696	4	57

Table 3.9: MDI JADE 6.5 Output Table (Buncombe County)

27 Hits Sorted on Figure-Of-Merit	Chemical Formula	FOM	J	D	PDF-#	Hits	#d/I	I%	2T(0)	RIR	Space Group	a	b	c	Z	CSD#
Kaolinite	Al4 (O H)8 (Si4 O10)	4.5	+	C	99-0067	27	200	64	-0.02	0.43	P1 (1)	5.149	8.934	7.384	1	67
Graphite	C	7.1	+	C	99-0057	7	11	46	0.06	1.24	P63/mmc (194)	2.456	2.456	6.696	4	57
Quartz	Si O2	8.1	+	C	99-0088	24	29	41	0.1	2.11	P3221 (154)	4.913	4.913	5.405	3	88
Aragonite	Ca C O3	12.2	+	C	99-0013	4	105	20	-0.04	0.56	Pmcn (62)	4.962	7.97	5.739	4	13
Muscovite 1M	KAl2[Si3B]O10](OH)2	14.9	+	C	99-0081	3	197	18	0	0.47	C2/m (12)	5.102	8.788	10.076	1	81
Biotite	K(Mg,Fe)3Al[Si3O10]F2	18.3	+	C	99-0019	4	200	21	-0.1	0.63	C2/m (12)	5.329	9.23	10.219	2	19
Sillimanite	Al2 (Si O4) O	18.6	+	C	99-0093	7	144	30	-0.06	0.55	Pbnm (62)	7.486	7.674	5.77	4	93
Alum	K Al (S O4)2 (H2 O)12	19.9	+	C	99-0004	3	100	43	0.12	0.71	Pa-3 (205)	12.157	12.157	12.157	4	4
Molybdite	Mo O3	20.8	+	C	99-0080	2	99	46	-0.12	2.06	Pbnm (62)	3.964	13.857	3.697	4	80
Analcime	Na (Al Si2 O6) (H2 O)	21.7	+	C	99-0007	2	58	25	0.1	0.98	Ia-3d (230)	13.73	13.73	13.73	16	7
Orthoclase	K (Al Si3 O8)	24.6	+	C	99-0085	2	200	68	0.02	0.34	C2/m (12)	8.562	12.996	7.193	4	85
Topaz	Al2 (Si O4) (O H)2	25.7	+	C	99-0104	0	146	18	0.1	0.33	Pbnm (62)	4.724	8.947	8.39	4	104
Celestine	Sr (S O4)	26.1	+	C	99-0025	0	133	55	0.12	1.05	Pnma (62)	8.36	5.352	6.858	4	25
Kyanite	Al2 Si O5	26.7	+	C	99-0068	3	200	28	-0.12	0.17	P-1 (2)	7.119	7.847	5.572	4	68
Cassiterite	Sn O2	29.4	+	C	99-0024	2	22	37	0	4.77	P42/mnm (136)	4.739	4.739	3.187	2	24
Diopside	Ca Mg Si2 O6	30.2	+	C	99-0045	0	173	100	0.02	0.58	C2/c (15)	9.75	8.926	5.251	4	45
Cancrinite	Na8 (Al6 Si6 O24) (O H)2.04 (H2 O)2.66	30.5	+	C	99-0023	0	136	36	0.04	0.58	P63 (173)	12.664	12.664	5.159	1	23
Bayerite	Al (O H)3	32.5	+	C	99-0017	5	153	17	-0.1	0.68	P21/a (14)	5.062	8.671	4.713	4	17
Muscovite 2M	Kal2[Si3Al]O10(OH)2	36.7	+	C	99-0082	1	200	33	0	0.2	C2/c (15)	5.189	8.996	20.096	4	82
Pickeringite	Mg0.93Mn0.07 Al2 (S O4)4 (H2 O)22	38.4	+	C	99-0086	0	200	20	0.02	0.3	P21/c (14)	6.184	24.272	21.226	4	86
Nepheline	NaAlSiO4	43.7	+	C	99-0083	0	140	9	-0.02	0.37	P63 (173)	9.98	9.98	8.332	1	83
Hemimorphite	Zn4 Si2 O7 (O H)2 (H2 O)	43.9	+	C	99-0061	0	128	50	0.12	1.06	Imm2 (44)	8.366	10.714	5.113	2	61
Chabazite	Ca1.95 Al3.9 Si8.1 O24 (H2 O)13	46.7	+	C	99-0027	0	200	46	-0.1	0.5	R-3m (166)	9.42	9.42	9.42	1	27
Sulfur	S	47.6	+	C	99-0100	0	200	100	0	1	Fddd (70)	10.465	12.866	24.486	16	100
Microcline	K (Al Si3 O8)	47.9	+	C	99-0078	0	200	15	0.1	0.31	C-1 (2)	8.573	12.983	7.22	4	78
Albite - low	Na (Al Si3 O8)	48.9	+	C	99-0002	0	200	20	-0.1	0.32	C-1 (2)	8.137	12.785	7.158	4	2
Anorthite	Ca (Al2 Si2 O8)	49.3	+	C	99-0012	1	200	20	-0.1	0.28	P-1 (2)	8.177	12.877	14.169	8	12

CHAPTER 4: ANALYSIS OF FIBER-REINFORCED SOIL DATA

4.1. Potential Research Contribution

At the completion of the literature review, it was determined that several test methods have been utilized to measure the benefits of fiber inclusions in soil. Synthetic fibers evaluated in previous studies include polypropylene, nylon, polyester, glass, and plastic waste. Natural fibers including coconut husk and softwood pulp have also been investigated. The literature indicates that there is a limited dataset of unconfined compressive (UC) strength (q_u) laboratory data available using polypropylene fibrillated fibers (PFF) as reinforcement.

Ang and Loehr (2003) used 52 mm (2 in) fibers in 0.2% and 0.4% dosages by dry mass and compared them to control samples. While their data presented an increase in q_u with increasing fiber content similar to the data that will be presented in this report, the data presented herein also includes fiber contents greater than 0.4%. Nataraj and McManis (1997) performed UC tests on Harvard miniature CL and SP soil samples (33 mm by 72 mm) using 25 mm (1 in) PFFs in dosage rates ranging from 0.1% to 0.3%. However, it should be noted that Ang and Loehr (2003) showed that samples tested below a 70 mm (2.75 in) diameter are not "reasonably representative of the true 'mass' strengths for fiber reinforced soils." Additionally, Nataraj and McManis (1997) did not explore fiber contents greater than 0.3%. Rafalko et al. (2008) conducted UC testing using 8.4 mm to 19 mm (0.33 in to 0.75 in) long PFFs with fiber contents ranging from 0.5% to 1%. The Staunton

clay (CH) q_u increased from 110 kPa (26 psi) to 228 kPa (33 psi) with 1% fiber content and no primary stabilizer, equivalent to an approximate 106% strength increase.

Other studies (e.g., Gary and Al-Refeai (1986); Freilich et al. (2010); Iasbik et al. (2002); Maher and Gray (1990); Michalowski and Cermak (2003); Ranjan et al. (1994); Nataraj and McManis (1997); Tang et al. (2007); and Puppala and Musenda (2000)) utilized alternative testing methods that include the California Bearing Ratio (CBR), direct shear, and triaxial testing methods to evaluate geofiber reinforcement in soil.

PFFs are typically used in full-scale field applications that include slope repairs and subgrade stabilization of roadway construction. Zhang et al. (2003) underwent a full-scale field study of a roadway embankment on Highway LA 15 that was notorious for failures. Prior to developing a remediation plan for the failure, Zhang et al. (2003) performed laboratory testing that included direct shear and consolidated drained (CU) triaxial testing. The direct shear results revealed an increase in shear strength ranging from 48% to 248% for a fat clay (CH) with almost 90% fines by incorporating a 25 mm (1 in) PFF using a 0.1% fiber content. The same soil mixture also produced a 241% increase in friction angle and a 203% increase in cohesion from triaxial testing.

A strength increase resulting from fiber inclusions can be used to remediate weak, near-surface soils unable to achieve specified allowable net bearing pressure requirements for a project using typical compaction procedures. Rather than importing structural fill from an offsite location, PFFs may be a suitable in-situ remediation alternative since it can be blended into near surface soils relatively easily.

A field study performed by Consoli et al. (2003) investigated the effect that fiber reinforced sand has on the bearing capacity of the material. They used a polypropylene

monofilament fiber as the reinforcing inclusion in a plate load test to verify triaxial lab testing performed on a sandy soil with approximately 38.3% fines (consisting mostly of kaolinite). The triaxial testing consisted of unreinforced and reinforced samples with 24 mm (1 in) long polypropylene monofilament fibers at 0.5% fiber content. Strength increases were observed from both the laboratory and the field test. The literature indicates that fiber inclusions increase the overall strength of the soil when compared to an identical unreinforced counterpart.

The data presented in this chapter will add to the current database of information to better understand geofiber reinforcement in cohesive soils. To distinguish this work from previous studies, a larger 102 mm (4 in) diameter test mold was utilized to eliminate boundary effects, a wider range of fiber contents up to 2% was tested, and the soil content was carefully controlled using select kaolin clay and Ottawa sand materials. These controlled material test specimens were subsequently compared to the performance of reinforced field soils for four different counties. The effect of soaking the test specimens was also explored.

4.2. Analysis Overview

UC testing was performed on two types of soil at their respective optimum water contents: 1) Ottawa sand mixed with kaolin clay in various percentages by mass; and 2) North Carolina field soils (locations previously displayed in Figure 3.2). Prior to the UC tests, index tests that included standard Proctor compaction, Atterberg limits, water content measurements, and grain size analyses were conducted. From this point forward, Dataset 1 refers to the kaolin clay-Ottawa sand specimens and Dataset 2 refers to the field soil specimens.

For Dataset 1, test specimens were remolded using Ottawa sand mixed with 10%, 15%, 20%, 25%, and 30% kaolin clay. For each of these mixtures, control specimens with no reinforcement were compared to test specimens reinforced with 12.7 mm (0.5 in) long PFFs using 0.5%, 0.75%, 1%, 1.25%, 1.5%, 1.75%, and 2% fiber contents by mass (details provided in Chapter 3). Three tests were performed for each clay and fiber combination to ensure repeatability, resulting in 120 UC tests performed on kaolin clay-Ottawa sand test specimens. The test numbers are designated 19_1R through 156R on the summary test matrix presented in Appendix B.

For Dataset 2, unreinforced control specimens generated from the Guilford, Johnston, Lincoln, and Buncombe county field soils were compared to field soil test specimens reinforced with the same geofiber using 0.75%, 1.25%, 1.75%, and 2% fiber contents by mass. The goal was to compare the behaviors of a natural field soil to the behaviors of a more controlled laboratory mixed material. There were 20 UC tests performed on these four field soils, designated as test specimens 157R through 176R on the summary test matrix presented in Appendix B.

In addition to these tests, which were conducted at the optimum water content determined during each standard Proctor compaction test, additional tests were performed to evaluate changes in strength due to soaked conditions. Field soils from Guilford, Johnston, Lincoln, and Buncombe counties in addition to specimens molded using the 30% kaolin-70% Ottawa sand mixture were investigated. The 30% kaolin clay-Ottawa sand mixture was selected because it was more comparable to the field soils that had fine contents greater than 30%. As part of the soaking process, all test specimens were initially prepared at their optimum moisture content with the same fiber content percentages

reported for Dataset 2, and then subsequently soaked. There were 25 soaked UC tests performed, designated by test specimens 177R through 201R on the UC Test Matrix presented in Appendix B. A total of 165 UC tests were performed as part of the research presented herein. Appendix C presents the pre and post-test photographs and the stress-strain curves for each test specimen. Appendix D presents a summary table of important test specimen results. The following sections present q_u results as a function of varying the fiber content and varying the fine content of the kaolin clay-Ottawa sand mixtures.

4.3. Unconfined Compressive Strength as a Function of Varying the Fiber Content

Figure 4.1 through Figure 4.5 displays q_u as a function of fiber content for the 10%, 15%, 20%, 25%, and 30% kaolin clay mixtures, respectively. For each of the three tests performed at each fiber content, the minimum, first quartile, median (second quartile), third quartile, and maximum of the UC strengths are displayed on these Figures for each material. The first quartile is essentially the middle number between the smallest q_u and the median q_u. The number between the maximum q_u and the median q_u is defined as the third quartile. Additionally, the averages, minimums, maximums, and the standard deviations of the UC strengths are displayed in Table 4.1. Every measure was taken to create the test specimens as consistently as possible, but it is important to point out that the orientation of the fibers was random and variable from one specimen to the next. Also, it should be noted that due to the limitation of the LVDT, the maximum allowable strain was 25% (mm/mm). If a sample reached the 25% axial strain maximum, the test was terminated, and the final q_u was recorded as the maximum q_u.

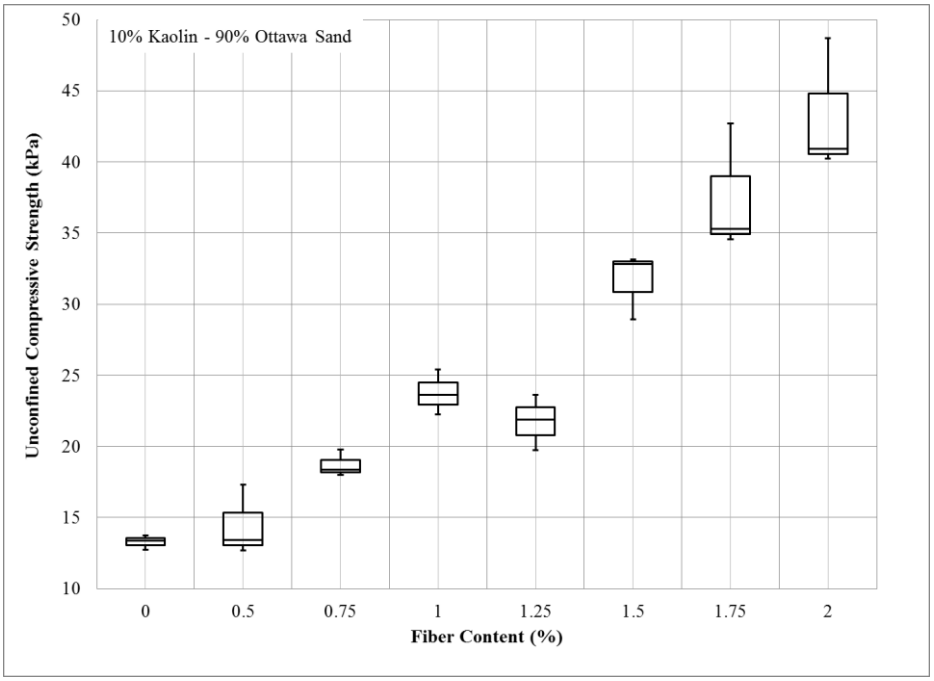

Figure 4.1: Unconfined Compressive Strength with Varying Fiber Content for the 10% Kaolin Clay-90% Ottawa Sand Material

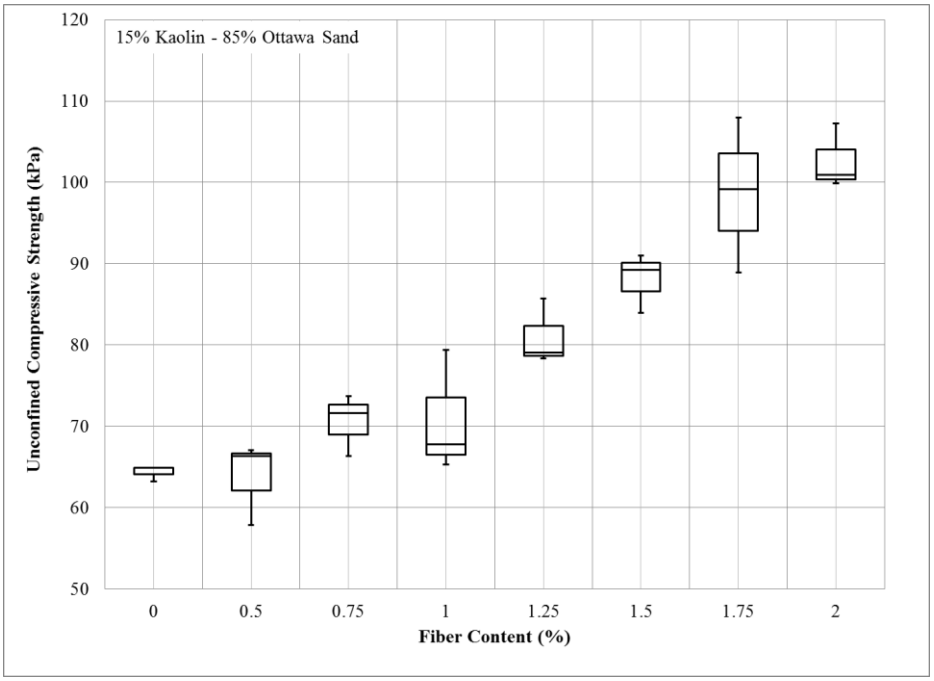

Figure 4.2: Unconfined Compressive Strength with Varying Fiber Content for the 15% Kaolin Clay-85% Ottawa Sand Material

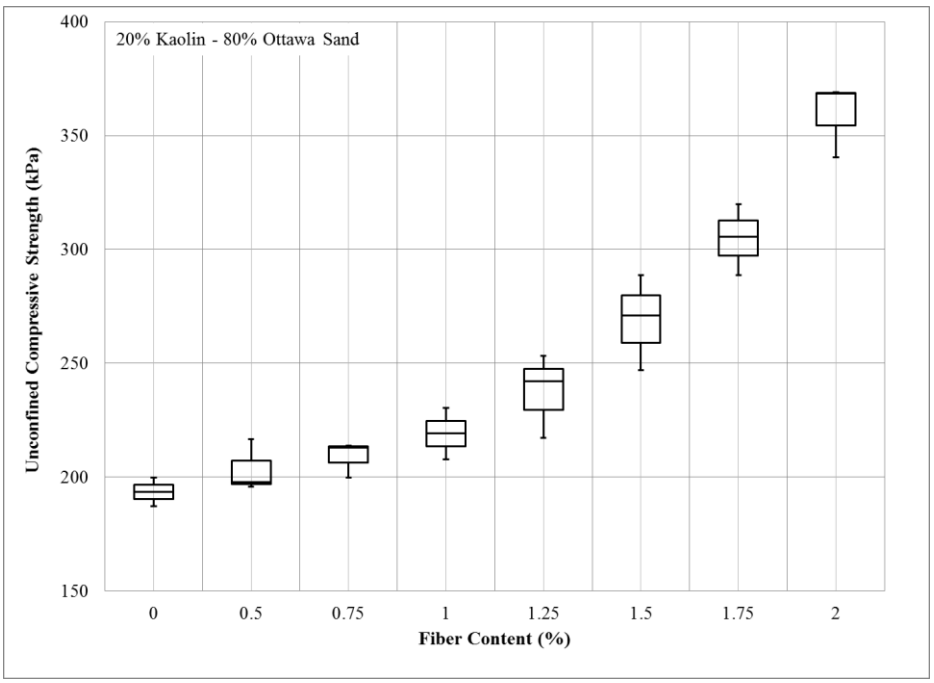

Figure 4.3: Unconfined Compressive Strength with Varying Fiber Content for the 20% Kaolin Clay-80% Ottawa Sand Material

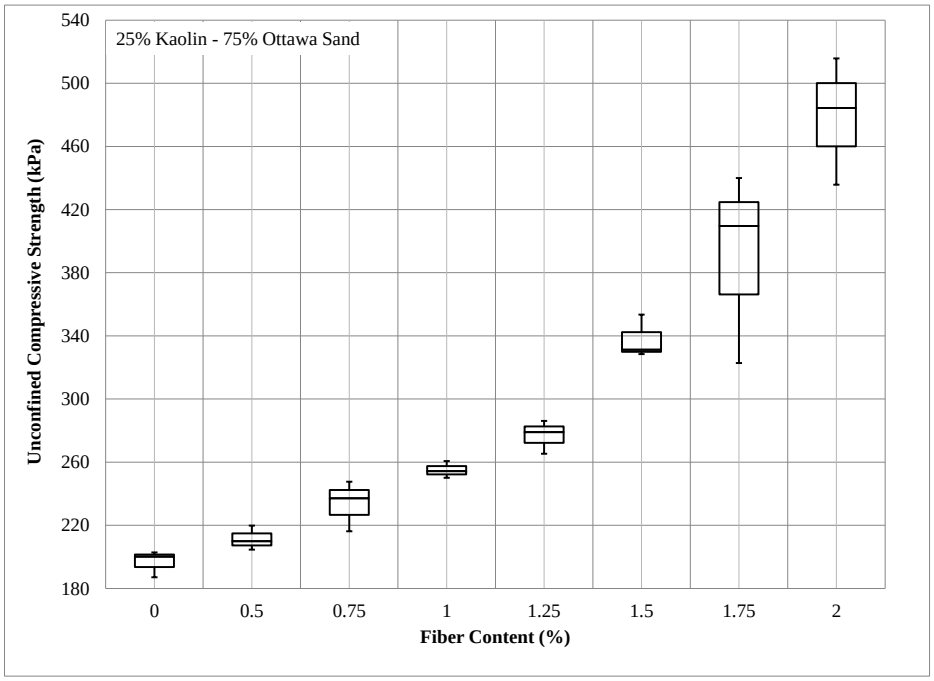

Figure 4.4: Unconfined Compressive Strength with Varying Fiber Content for the 25% Kaolin Clay-75% Ottawa Sand Material

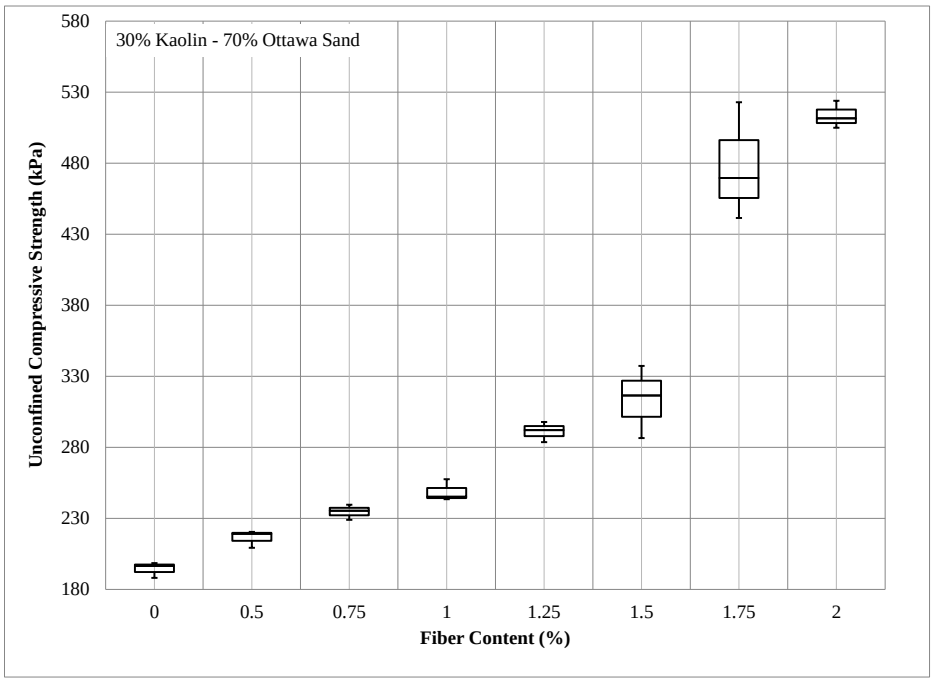

Figure 4.5: Unconfined Compressive Strength with Varying Fiber Content for the 30% Kaolin Clay-70% Ottawa Sand Material

Table 4.1: Unconfined Compressive Strength (Kaolin Clay-Ottawa Sand Mixtures)

% Fines (USCS)		Fiber Content (%)							
		0.00	0.50	0.75	1.00	1.25	1.50	1.75	2.00
		Unconfined Compressive Strength							
10 (SP-SM)	Increase	-	9%	41%	79%	64%	138%	183%	226%
	Avg. (kPa)	13.28	14.47	18.70	23.75	21.75	31.63	37.51	43.28
	Min. (kPa)	12.72	12.70	18.00	22.23	19.74	28.93	34.57	40.22
	Max (kPa)	13.72	17.29	19.76	25.40	23.64	33.16	42.69	48.69
	S.D. (kPa)	0.51	2.47	0.93	1.59	1.95	2.35	4.50	4.70
15 (SM)	Increase	-	-1%	10%	10%	26%	37%	53%	59%
	Avg. (kPa)	64.37	63.74	70.56	70.80	81.03	88.08	98.67	102.66
	Min. (kPa)	63.25	57.86	66.33	65.27	78.32	83.97	88.91	99.84
	Max (kPa)	64.93	67.03	73.74	79.38	85.73	91.02	107.96	107.25
	S.D. (kPa)	0.97	5.10	3.81	7.54	4.09	3.67	9.53	4.01
20 (SC-SM)	Increase	-	5%	8%	13%	23%	39%	58%	86%
	Avg. (kPa)	193.44	203.37	208.84	219.10	237.51	268.96	304.77	359.32
	Min. (kPa)	187.08	204.63	214.86	250.14	252.26	314.70	322.82	435.72
	Max (kPa)	202.81	205.33	236.03	254.37	275.54	343.63	439.95	515.80
	S.D. (kPa)	6.36	11.44	7.84	11.21	18.48	21.00	15.58	16.43
25 (SC-SM)	Increase	-	4%	15%	28%	36%	68%	97%	143%
	Avg. (kPa)	196.68	204.98	226.50	251.55	267.78	329.87	387.74	478.64
	Min. (kPa)	187.08	204.63	214.86	250.14	252.26	314.70	322.82	435.72
	Max (kPa)	202.81	205.33	236.03	254.37	275.54	343.63	439.95	515.80
	S.D. (kPa)	8.42	0.35	10.74	2.44	13.44	14.52	59.59	40.35
30 (SC-SM)	Increase	-	7%	18%	28%	48%	61%	145%	164%
	Avg. (kPa)	194.33	208.62	230.27	248.73	288.36	313.41	475.49	513.45
	Min. (kPa)	188.09	203.92	222.27	243.44	275.19	286.48	441.36	504.87
	Max (kPa)	198.46	211.68	239.56	257.55	297.77	337.28	522.86	523.92
	S.D. (kPa)	5.50	4.13	8.72	7.69	11.75	25.54	42.33	9.66

Figure 4.6(a) displays q_u as a function of all fiber contents tested for all kaolin clay-Ottawa sand test specimens, and Figure 4.6(b) displays the percent increase in q_u as a function of fiber content. Note that the field soil data are not included in either Figure and that the average of the three tests performed for each test combination displayed on Figure 4.6(a) is displayed in Figure 4.6(b).

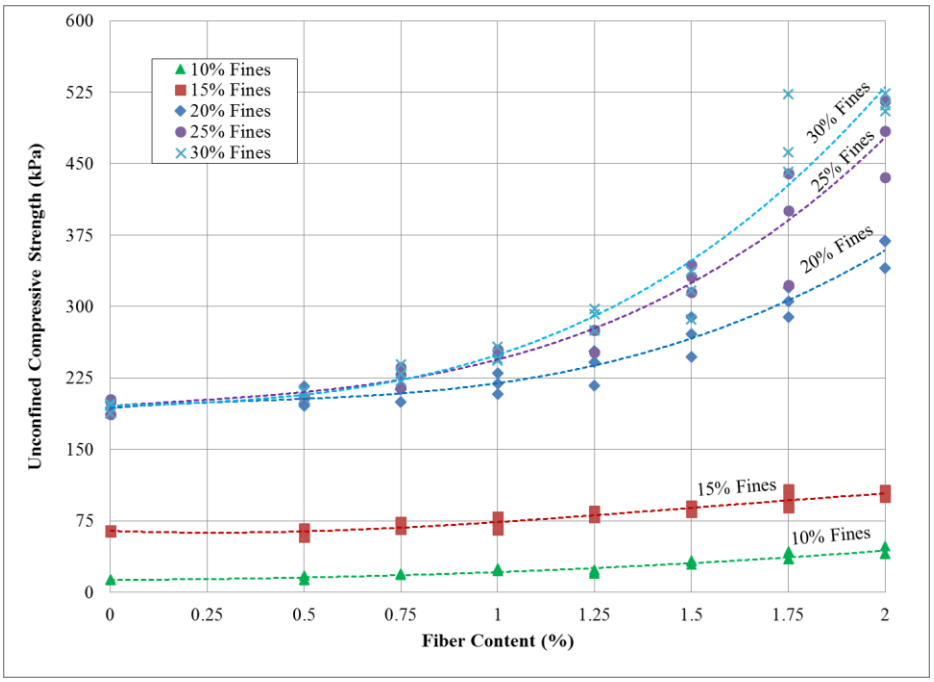

(a)

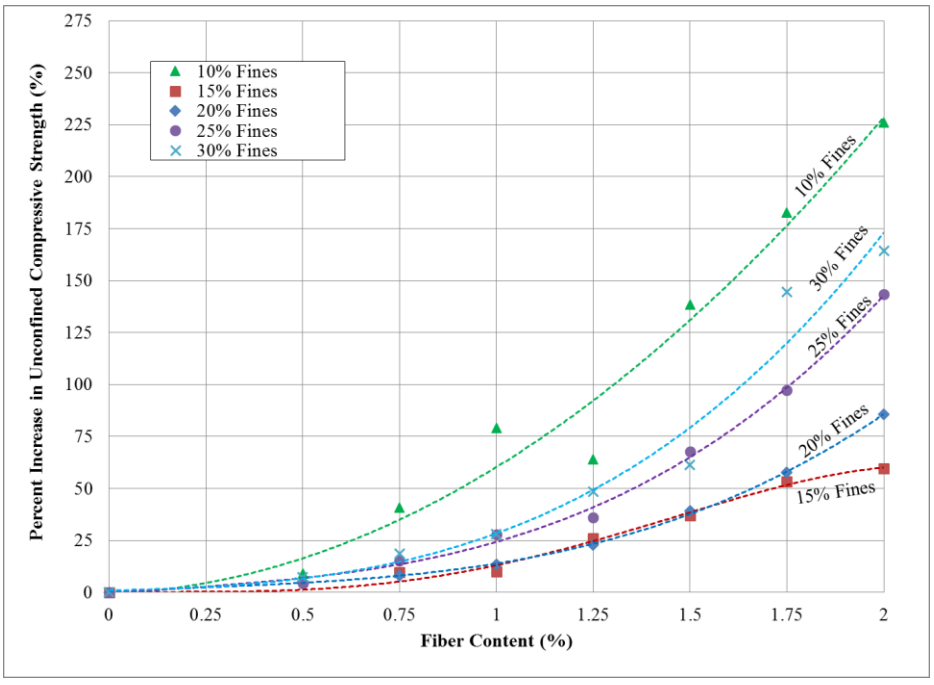

(b)

Figure 4.6: Unconfined Compressive Strength with Varying Fiber Content (Kaolin Clay-Ottawa Sand Samples): (a) Raw Data; (b) Percent Increase

In comparison to the unreinforced test specimens, the q_u increased approximately 4% (e.g., 25% fines specimen that had a 0.5% fiber content) to 226% (e.g., 10% fines specimen that had a 2% fiber content) depending upon the fiber percentage and fines content. While the increase in q_u does not visually appear to be significant for the 10% fines soil on Figure 4.6(a) due to the low initial strength value for the unreinforced soil, the 10% fines material achieved the highest percent increase in q_u as displayed in Figure 4.6(b). The average q_u for the unreinforced 10% fines material was approximately 13.28 kPa (1.93 psi). The average jumped to 43.28 kPa (6.28 psi) for the same soil having 2% fiber content, resulting in a 226% increase in q_u. With the exception of the 10% fines content material, q_u appears to increase as the fines content increases.

Gary and Al-Refeai (1986) tested an SP-SM material that had less than a 10% fines content reinforced with a 27 mm (1.1 in) plastic fiber. An increase in their fiber content from 0% to 0.5% increased their measured q_u approximately 33%, compared to the 9% increase recorded for the 10% kaolin clay-Ottawa sand material in this study. An increase in their fiber content from 0% to 1% increased their measured q_u approximately 83%, compared to the 79% measured in this study. Finally, an increase in fiber content from 0% to 2% increased their measured q_u approximately 200%, compared to 226% reported on Figure 4.6(b). The data presented as part of this study appears to compare well with data reported in the literature.

Geofibers are commonly utilized to repair slopes and roadway embankments, for subgrade stabilization in roadways and foundations, and in retaining wall backfill material. A review of the literature reveals that the majority of field studies utilize PFF with fiber contents ranging from approximately 0.2% to 0.5%, but PFF contents as high as 1% have

been reported. This study indicates that fiber percentages up to 2% may provide additional benefits to soil strength. Based on the literature, PFF fibers are typically 25 mm (1 in) in length. A previous field study by Tingle et al. (1999) showed that fiber lengths greater than 76 mm (3 in) tend to get hung up in the field mixing equipment, and they recommended using fibers that are 25 mm (1 in) or less to facilitate field mixing.

Similar to Figure 4.6(a), Figure 4.7(a) displays q_u as a function of fiber content for all four field soils in addition to the tests performed using the 30% kaolin clay-70% Ottawa sand mixture. Because the Guilford, Johnston, Lincoln, and Buncombe county field soils contain approximately 35%, 42%, 58%, and 62% fines, respectively, the 30% kaolin clay test specimens were utilized for comparison since the fine content for this mixture was the highest. Similar to Figure 4.6(b), Figure 4.7(b) displays the percent increase in q_u as a function of fiber content. Table 4.2 summarizes the statistical q_u information related to these tests for each soil mixture and fiber content. Recall that field soils were only tested using the 0.75%, 1.25%, 1.75%, and 2% fiber percentages, and tests were not repeated.

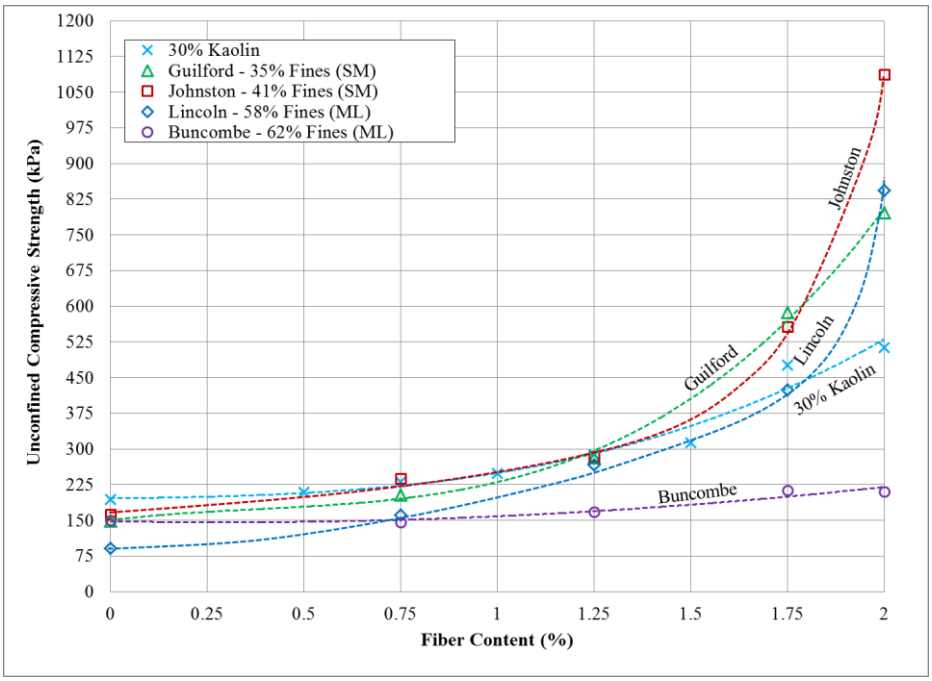

(a)

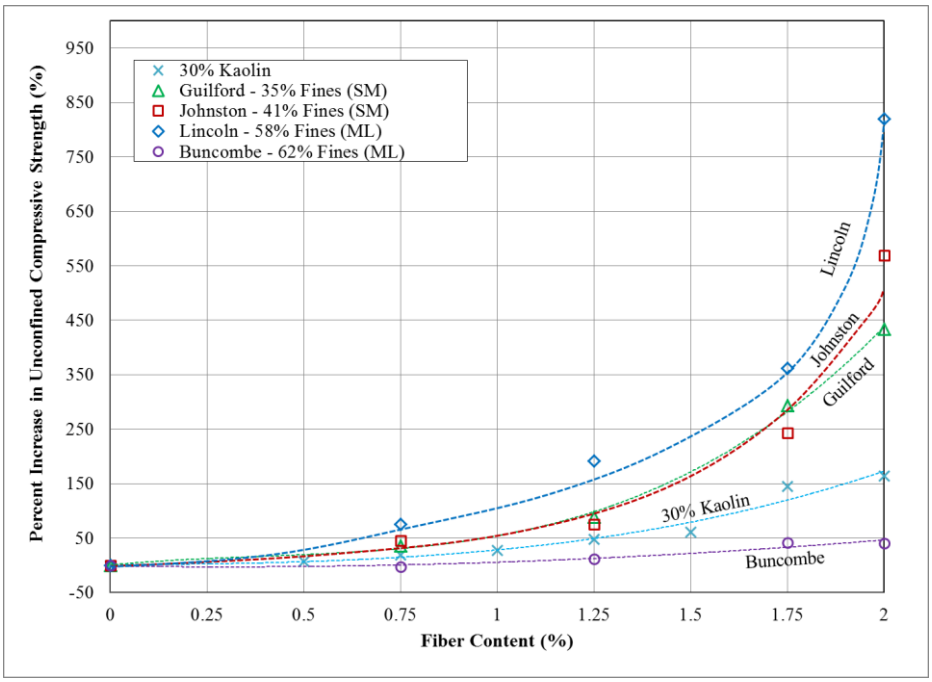

(b)

Figure 4.7: Unconfined Compressive Strength with Varying Fiber Content (Field Soils): (a) Raw Data; (b) Percent Increase

Table 4.2: Percent Increase in Unconfined Compressive Strength (Field Soils) as a Function of Fiber Content

% Fines (USCS) NC County	Fiber Content (%)				
	0.00	**0.75**	**1.25**	**1.75**	**2.00**
	Percent Increase in Unconfined Compressive Strength (Unconfined Compressive Strength, kPa)				
30* (SC-SM)	- (194.33)	21% (234.62)	50% (291.18)	146% (477.93)	164% (513.45)
35 (SM) Guilford	- (149.24)	36% (202.86)	88% (281.19)	293% (586.72)	434% (796.28)
41 (SM) Johnston	- (162.64)	46% (237.44)	75% (284.36)	243% (557.43)	569% (1087.70)
58 (ML) Lincoln	- (91.73)	75% (160.88)	191% (267.07)	362% (424.07)	820% (843.91)
62 (ML) Buncombe	- (149.94)	-3% (146.06)	12% (167.94)	42% (213.10)	41% (210.98)

* 30% Kaolin Clay-70% Ottawa Sand Tests Included for Comparison

Similar to the data presented for the kaolin clay-Ottawa sand materials, the data shows an increase in q_u with an increase in fiber content for all field soils. Nataraj and McManis (1997) performed similar testing on a CL material. While the fine content of their clay was not reported, the Buncombe County test data was utilized for comparison because their reported liquid limits were close (i.e., 44% for Nataraj and McManis (1997) and 48% for Buncombe County) and both were classified as a fine-grained soil. Based on the data provided by Nataraj and McManis (1997), a 200% fiber content increase from 0.1% to 0.3% generated an approximate 55% increase in q_u. In comparison, the Buncombe County soil experienced a 44% increase in qu when a 167% increase in fiber content was made from 0.75% to 2%.

4.4. Unconfined Compressive Strength as a Function of the Fines Content

While the previous section presented q_u as a function of fiber content, this section presents it as a function of fine content. Figure 4.8 displays q_u as a function of the fine content for the control test specimens for the 0.75%, 1.25%, 1.75%, and 2% fiber contents. All five kaolin clay-Ottawa sand materials (i.e., 10%, 15%, 20%, 25%, and 30% kaolin clay mixtures) and all four field soils (i.e., Guilford = 35% fines, Johnston = 42% fines, Lincoln = 58% fines, and Buncombe = 62% fines) are included on this figure. The transfer in data from the kaolin clay-Ottawa sand tests to the field soil tests is labeled clearly at the top of Figure 4.8 and the field soil data is also shaded to clearly establish the different datasets. It is important to note that each point on a single curve on Figure 4.8 represents a different soil type (i.e., different fine content) that was prepared at a different optimum moisture content, in accordance with the standard Proctor compaction test results for each soil. For this reason, the optimum moisture content for each soil is presented at the bottom of Figure 4.8.

Recall that the kaolin clay-Ottawa sand test specimens were utilized to ensure consistency between test specimens, and the field soils were added to the test matrix to validate the trends of the controlled materials using in-situ materials that inherently have increased variability. Even though the limitations of the data presented in Figure 4.8 has been clearly stated, this Figure demonstrates that while there are two datasets and each point is prepared at a slightly varying moisture content, the relationship between q_u and fine content appears to naturally transition from one side to the other for each fiber content displayed on Figure 4.8.

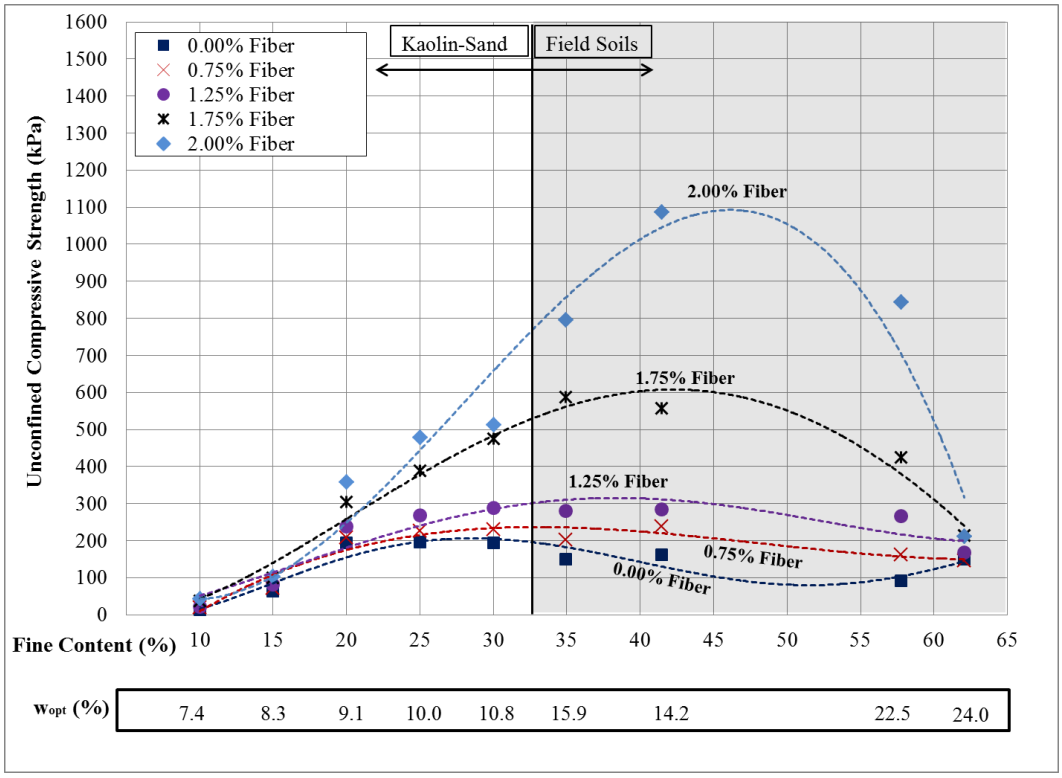

Figure 4.8: Varying Fine Content with Constant Fiber Content

Having stated the above limitations to this Figure, Figure 4.8 shows a general increase in q_u as the fiber content increases regardless of material type with the exception of the soil containing greater than 60% fines. The differences in the q_u for all Buncombe soil test specimens (62% fines) were significantly reduced in comparison to all other soils tested. It should be noted that Jiang et al. (2010), Puppala and Musenda (2000), and Tang et al. (2007) conducted UC tests on clayey soils with fine contents ranging from 80% to 98%. They observed UC strengths ranging from 195 to 383 kPa (28 to 56 psi) compared to the 150 to 211 kPa (22 to 31 psi) range observed on Figure 4.8 for the Buncombe County soil so the results appear to fall inside a reasonable range. Maher and Ho (1994) experienced the same phenomenon with samples having high fine contents. Maher and Ho (1994) utilized pure kaolin clay (95% to 100% clay content) and discovered that the effect on

increase in strength was greater in sandy soils in comparison to soils with very high fine contents. Both Maher and Ho (1994) and Maher and Gray (1990) discovered that the mechanism for transfer of load from soil to fiber is via interface friction.

With the exception of the high fine content soils previously discussed, Figure 4.8 provides an initial reference to estimate values of q_u for varying soil types and different fiber contents up to 2%, which is not currently available in the literature. However, a continuation of this type of testing would strengthen the value of this Figure for practical use in the field.

The data on Figure 4.8 also indicate that there may be an optimum unconfined compressive strength that is dependent on the fine content in the soil and the percentage of fiber inclusions. The maximum q_u appears to increase as the fiber content increases. Additionally, the optimum value of q_u is reached at a higher fine content for each increase in fiber content. More specifically, the 0.75%, 1.25%, 1.75%, and the 2% fiber content curves appear reach their maximums at approximately the 25%, 30%, 35%, and 42% fine content marks, respectively, on Figure 4.8. Table 4.3 summarizes the maximum q_u and the percent increase over the baseline achieved at each of these optimum points.

Table 4.3: Maximum Unconfined Compressive Strength for Each Optimum Fines Content

Fiber Content (%)	**Optimum Fine Content (%)**	**Maximum q_u (kPa)**	**Increase in q_u (%)**
0.00	20	200	-
0.75	25	240	20%
1.25	30	300	50%
1.75	35	590	195%
2.00	42	1088	444%

The higher fiber content soils appear to reach significantly higher levels of q_u, and the increase can be more significant for soils with higher fine contents. For the 42% fine content in Figure 4.8, the q_u is approximately 284 kPa (41 psi), 557 kPa (81 psi), and 1088 kPa (158 psi) for the 1.25%, 1.75%, and 2% fiber content specimens, respectively, resulting in a 75%, 243%, and 569% increase over the control specimens, respectively. In comparison, at the 20% fines content in Figure 4.8, the q_u is approximately 238 kPa (35 psi), 305 kPa (44 psi), and 359 kPa (52 psi) for the 1.25%, 1.75%, and 2% fiber content specimens, respectively, resulting in a 23%, 58%, and 86% increase over the control specimens, respectively. It is important to point out that the workability of mixing these fibers in the field at percentages greater than 1% is unknown.

4.5. Soil Strain and Elastic Modulus as a Function of Varying Fiber Content

Figure 4.9(a) displays the average axial strain at failure as a function of fiber content for all kaolin clay-Ottawa sand test specimens. Similarly, Figure 4.9(b) displays the percent increase in axial strain at failure. Note that the field soil data are not included on this Figure. While there is a slight increase in the defined axial strain level at failure for the 10% and 15% kaolin mixtures as the fiber content increases up to 2%, the fibers appear to induce a more significant non-linear increase in the defined axial strain level for the 20% to 30% kaolin specimens on Figure 4.9(a). Table 4.4 presents the average axial strain and the percent increase in axial strain measured for all kaolin clay-Ottawa sand data. Negative values in Table 4.4 indicate that the failure strains are lower than the failure strains for the control test specimens.

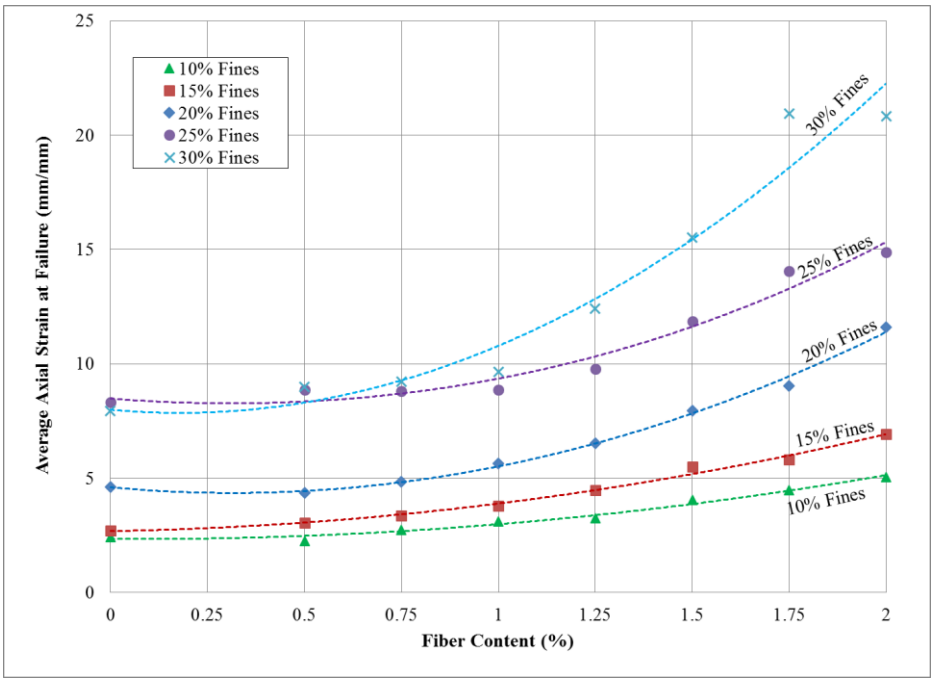

(a)

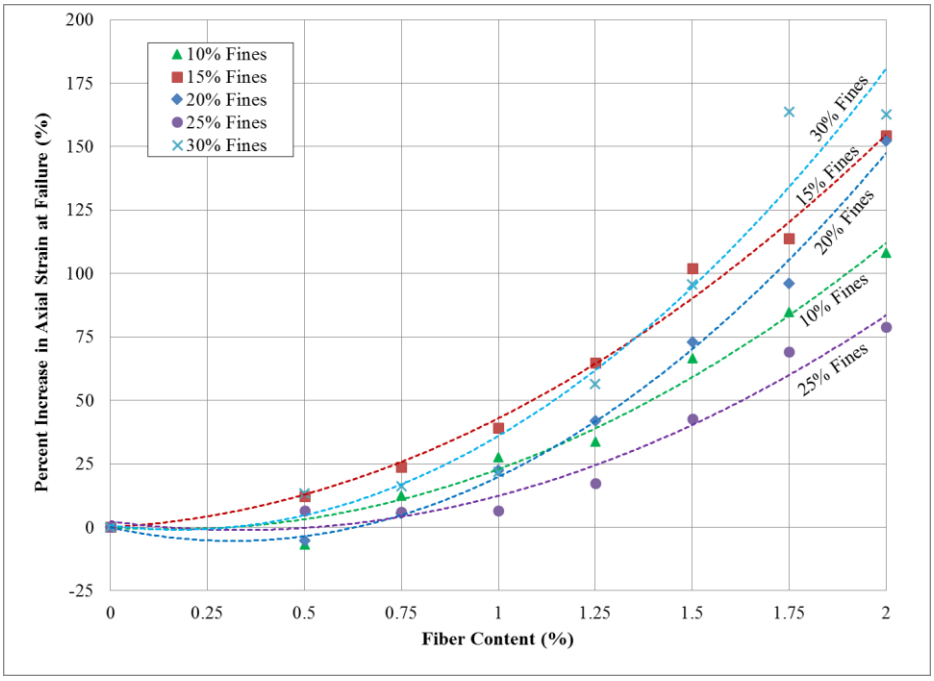

(b)

Figure 4.9: Axial Strain with Varying Fiber Content (Kaolin Clay-Ottawa Sand Samples): (a) Raw Data; (b) Percent Increase

Table 4.4: Percent Increase in Axial Strain at Failure for the Kaolin Clay-Ottawa Sand Specimens

% Fines (USCS)	Fiber Content (%)							
	0.00	**0.50**	**0.75**	**1.00**	**1.25**	**1.50**	**1.75**	**2.00**
	Percent Increase in Strain at Failure (Strain at Failure mm/mm)							
10 (SP-SM)	- (2.43)	-7% (2.26)	12% (2.73)	28% (3.10)	34% (3.25)	67% (4.04)	85% (4.48)	108% (5.05)
15 (SM)	- (2.72)	12% (3.05)	24% (3.36)	39% (3.79)	65% (4.48)	102% (5.49)	114% (5.82)	154% (6.92)
20 (SC-SM)	- (4.60)	-5% (4.36)	5% (4.85)	22% (5.63)	42% (6.53)	73% (7.96)	96% (9.03)	152% (11.61)
25 (SC-SM)	- (8.32)	2% (8.86)	4% (8.81)	8% (8.88)	13% (9.76)	41% (11.87)	77% (14.07)	79% (14.88)
30 (SC-SM)	- (7.93)	14% (9.00)	15% (9.21)	22% (9.66)	53% (12.40)	96% (15.52)	162% (20.93)	163% (20.84)

Similar to Figure 4.9(a), Figure 4.10(a) displays axial strain at failure as a function of fiber content for all four field soils in addition to the suite of tests performed with the averaged results of the 30% kaolin clay-70% Ottawa sand material. Figure 4.10(b) displays the percent increase in axial strain at failure. Similar to Dataset 1, there is an increase in the axial strain level at failure with an increase in fiber content for all field soils. The averages and the percent increases in the axial strains at failure are summarized in Table 4.5. These data indicate that the ductility of the reinforced soil increases due to the interaction between the soil particles and the PFFs.

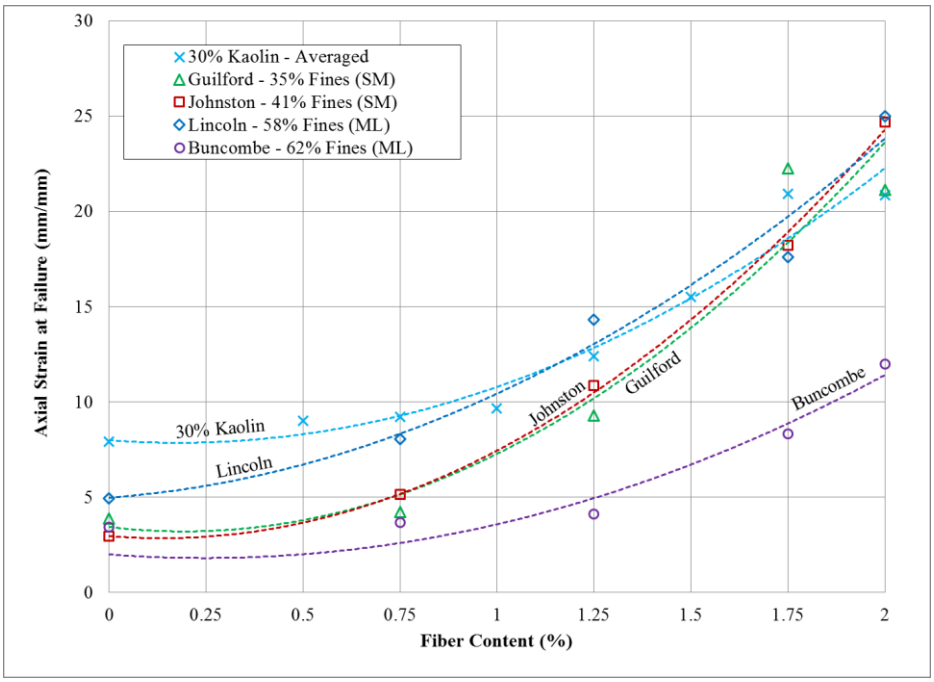

(a)

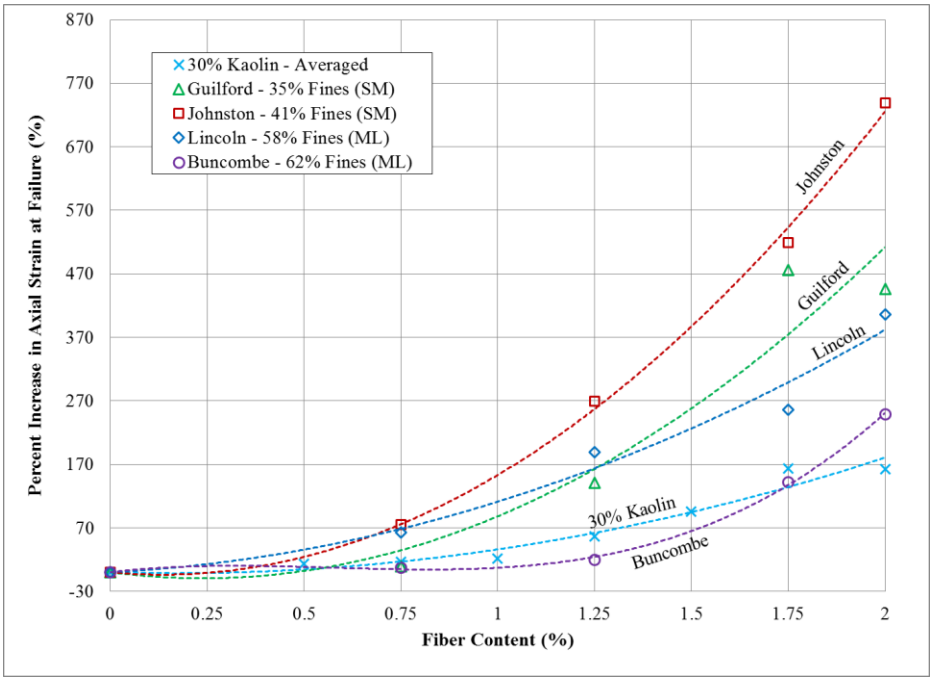

(b)

Figure 4.10: Axial Strain with Varying Fiber Content (Field Soils): (a) Raw Data; (b) Percent Increase

Table 4.5: Percent Increase in Axial Strain at Failure (Field Soils)

% Fines (USCS) NC County	Fiber Content (%)							
	0.00	**0.50**	**0.75**	**1.00**	**1.25**	**1.50**	**1.75**	**2.00**
	Percent Increase in Strain at Failure (Strain at Failure, mm/mm)							
30* **(SC-SM)**	- (7.93)	14% (9.00)	15% (9.21)	22% (9.66)	53% (12.40)	96% (15.52)	162% (20.93)	163% (20.84)
35 **(SM)** **Guilford**	- (3.86)	- -	9% (4.23)	- -	140% (9.29)	- -	476% (22.27)	446% (21.11)
41 **(SM)** **Johnston**	- (4.94)	- -	63% (8.06)	- -	189% (14.31)	- -	256% (17.59)	406% (25.00)
58 **(ML)** **Lincoln**	- (2.94)	- -	75% (5.14)	- -	269% (10.85)	- -	519% (18.21)	739% (24.68)
62 **(ML)** **Buncombe**	- (3.44)	- -	7% (3.68)	- -	20% (4.12)	- -	142% (8.34)	248% (11.99)

* 30% Kaolin Clay-70% Ottawa Sand Tests Included for Comparison

For each test conducted, the secant modulus was determined in accordance with Lambe and Whitman (1969). More specifically, the secant modulus was determined from the slope of a line that begins at the zero stress level and extends to a stress equal to half of the peak stress. Utilizing the 50% strength for the secant modulus represents a safety factor of 2. Figure 4.11 provides a visual example of how the secant modulus is determined in this study. Figure 4.11(a) displays q_u as a function of axial strain for the 20% kaolin clay-80% Ottawa sand mixture. Figure 4.11(b) displays the same data for the Lincoln County field soil. In each figure, the unreinforced test data are compared to test data for soils reinforced with 1.25% fiber content. Raw data curves are displayed using solid lines in both figures and the lines utilized to calculate the secant modulus for each soil type are illustrated using dashed lines. There are 3 data curves for each condition in Figure 4.11(a) because the controlled soils were repeated three times. The secant modulus values for all soils tested are presented in Table 4.6.

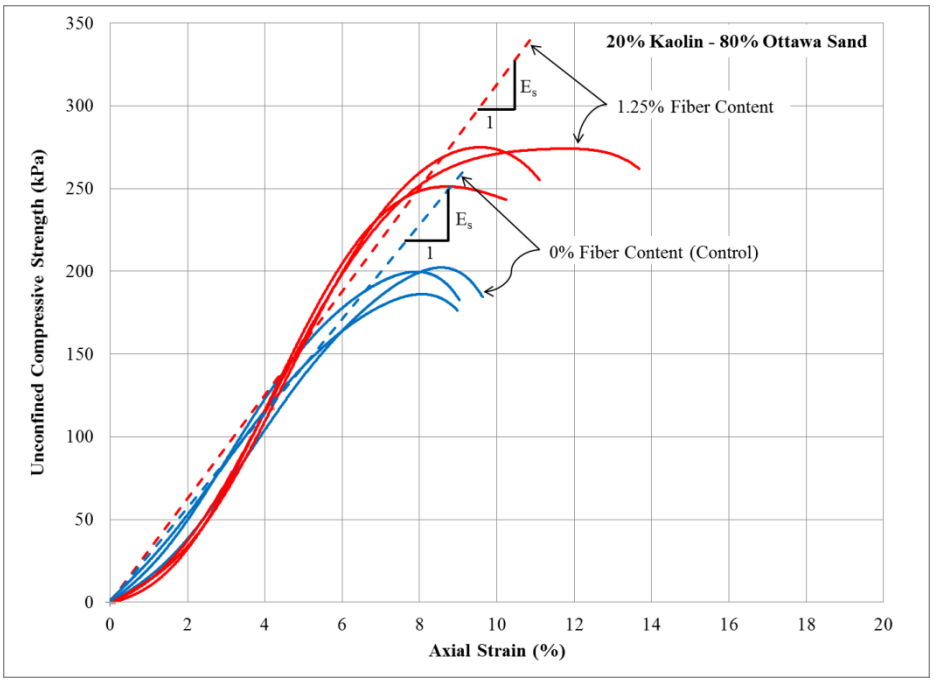

(a)

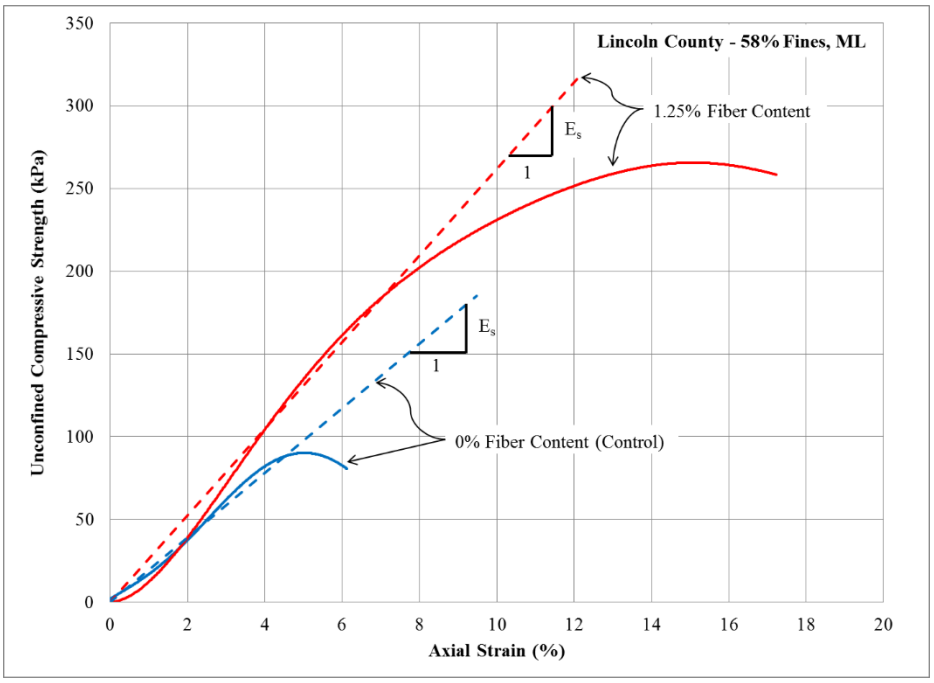

(b)

Figure 4.11: Unconfined Compressive Strength as a Function of Axial Strain (1.25% Fiber Content versus Control Specimens): (a) 20% Kaolin Clay-80% Ottawa Sand; (b) Lincoln County Field Soil

Table 4.6: Calculation of Secant Modulus

% Fines (USCS) NC County	Fiber Content (%)							
	0.00	0.50	0.75	1.00	1.25	1.50	1.75	2.00
	Percent Change in Modulus of Elasticity (Modulus of Elasticity, kPa)							
10 (SP-SM)	- (1018)	-15% (863)	-11% (906)	2% (1036)	-7% (946)	-30% (708)	-33% (679)	-29% (724)
15 (SM)	- (2907)	-25% (2194)	-26% (2160)	-46% (1581)	-47% (1547)	-55% (1310)	-55% (1313)	-64% (1037)
20 (SC-SM)	- (3855)	23% (4749)	1% (3912)	-9% (3523)	-21% (3049)	-30% (2693)	-30% (2694)	-35% (2516)
25 (SC-SM)	- (2857)	-12% (2522)	4% (2984)	10% (3139)	9% (3120)	19% (3402)	20% (3421)	21% (3451)
30 (SC-SM)	- (3394)	-3% (3297)	4% (3530)	5% (3549)	2% (3464)	-8% (3111)	-6% (3190)	-5% (3216)
35 (SM) Guilford	- (4419)	- -	23% (5456)	- -	16% (5130)	- -	-13% (3840)	5% (4625)
41 (SM) Johnston	- (6696)	- -	-34% (4432)	- -	-39% (4059)	- -	-40% (3987)	-36% (4306)
58 (ML) Lincoln	- (1956)	- -	28% (2504)	- -	34% (2618)	- -	61% (3158)	74% (3401)
62 (ML) Buncombe	- (5305)	- -	-3% (5166)	- -	-18% (4341)	- -	-41% (3154)	-46% (2877)

While the axial strain at failure increased with fiber content, the secant modulus values reported in Table 4.6 do not support a clear trend in modulus with an increase in fiber content. Six out of the nine soils reported in Table 4.6 show a decrease in the secant modulus relative to the unreinforced specimens. For example, the secant moduli calculated

for the Johnston County soil decreased 34% to 40% as the fiber content increased from 0% to 2% by mass.

In a study conducted by Iasbik et al. (2003), polypropylene monofilament fibers increased the overall UC strength, but a 0.25% fiber content was responsible for a 65% decrease in the resilient modulus values determined from this study, indicating that the stiffness of the soil decreased. The results from the Tang et al. (2007) study indicate that the inclusion of polypropylene monofilament fibers increased the UC strength, shear strength, and axial strain at failure, but decreased sample brittleness, stiffness, and the loss of post-peak strength. Tang et al. (2007) analyzed the interactions between the fiber surface and the soil matrix, and determined that the bond strength and friction at the soil-fiber interface was the dominant mechanism controlling the reinforcement benefit.

4.6. Test Specimen Failure Modes

At the completion of each UC test, the direction of the failure surface and any observations were noted and photographed for each test specimen. Typically, an angular shear surface failure plane transitioned into a bulging failure that included some horizontal separation at the lift interface, depending upon the percentage of fiber incorporated in the sample. The increase in the ductility of the material could provide an explanation for the transitional failure modes observed.

Nataraj and McManis (1997) observed the same bulging failure described in this section while testing the UC characteristics of a poorly graded sand (SP) and a sandy clay (CL). They used a 25 mm (1 in) long PFF with a maximum fiber content of 0.3%, and concluded this to be the optimum fiber content even though their results show an increasing trend in q_u. Nataraj and McManus (1997) did not indicate whether all specimens with PFF

bulged nor did they illustrate through picture or diagram the severity of any bulging that occurred. However, Ang and Loehr (2003) were of the opinion that the sample sizes utilized in Nataraj and McManus study were not "reasonably representative of the true 'mass' strengths for fiber reinforced soils." Ang and Loehr (2003) recommended using a 100 mm by 117 mm (4 in by 4.5 in) diameter by height sample size, the same diameter size utilized in this study.

Bulging may have also been triggered in the Nataraj and McManus study (1997) at lower fiber contents when compared to results in this study due to the sample length used. A longer sample length may be able to absorb more of the axial deformation prolonging the failure, thus prolonging the bulging. Michalowski and Cermak (2003) experienced the same type of bulging effect in their triaxial testing utilizing fine and coarse sand specimens. Additionally, the Nataraj and McManis (1997) test specimens were stored in a humidity room for 18 hours prior to testing, which may have impacted the overall strength of the samples.

Figure 4.12(a) displays a typical angular failure plane for an unreinforced soil specimen with 20% kaolin clay and 80% Ottawa sand. Figure 4.12(b) displays a typical bulge failure with horizontal separation for a 1.5% fiber reinforced soil specimen that has 25% kaolin clay and 75% Ottawa sand.

(a) (b)

Figure 4.12: Typical Failures: (a) Angular Shear; (b) Bulging with Horizontal Separation

While a different laboratory test method was utilized, previous studies performed by Freilich et al. (2010) observed bulging at failure during consolidated drained CD and CU triaxial testing of fiber reinforced clayey soils. They also noted that samples without reinforcement experienced an angular failure surface similar to the results observed in Figure 4.12(a). Freilich et al. (2010) attributed the bulging failure behavior to an increase in the ductility of the soil as a result of the fiber inclusions (i.e., the deformation required to reach failure).

For each of the five kaolin clay-Ottawa sand mixtures, the transition from a typical angular shear failure surface to a bulging failure surface occurred at different fiber contents. Figure 4.13 displays the maximum fiber content associated with an angular failure surface for each of the kaolin clay-Ottawa sand mixtures tested. For example, the 10% kaolin clay-90% Ottawa sand test specimen transitioned from a typical angular shear failure surface

(Figure 4.14(a)) to a bulging failure surface (Figure 4.14(b)) at fiber contents higher than 1.5%. For the 15% kaolin clay-85% Ottawa sand test specimens, a typical angular shear failure surface (Figure 4.15(a)) was observed for fiber contents up to 1.25% and all test specimens with 1.5% fiber contents or higher showed a bulging failure (Figure 4.15(b)). In a similar pattern, the maximum fiber contents for which an angular failure surface developed for the 20%, 25%, and 30% kaolin clay test specimens were 1%, 0.75%, and 0.5%, respectively.

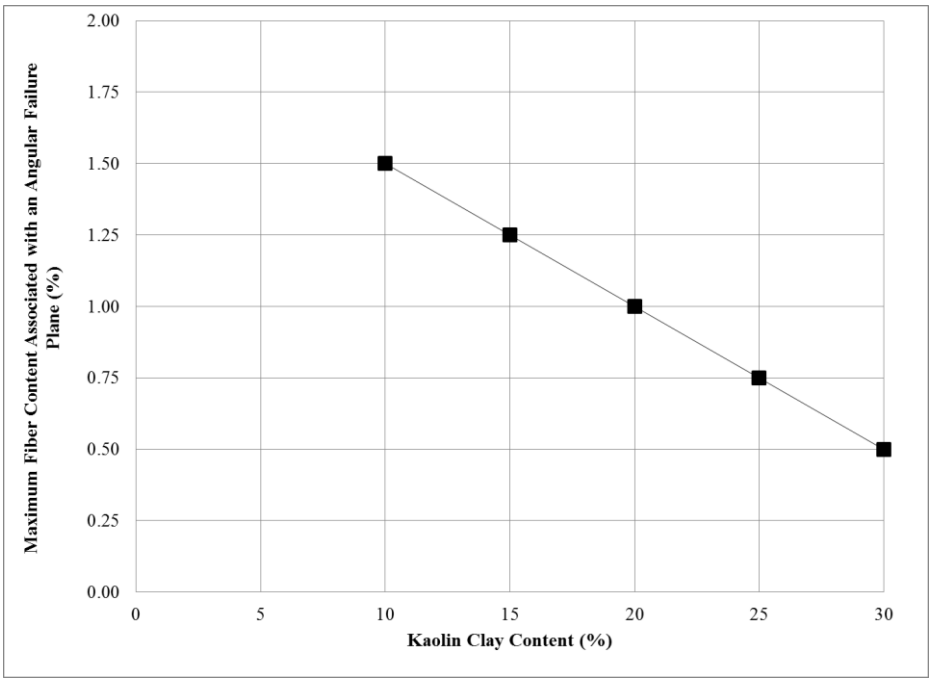

Figure 4.13: Maximum Fiber Content Associated with an Angular Failure Surface

(a) (b)

Figure 4.14: 10% Kaolin Clay-90% Ottawa Sand Specimen: (a) 1.5% Fiber Angular Failure Surface; (b) 1.75% Fiber Bulging Failure Surface

(a) (b)

Figure 4.15: 15% Kaolin Clay-85% Ottawa Sand Specimen: (a) 1.25% Fiber Angular Failure Surface; (b) 1.5% Fiber Bulging Failure Surface

For all field soils tested, the failure surface appeared to bulge at all levels of reinforcement because of the high fine content. Recall that the maximum fiber content associated with an angular failure surface for the 30% kaolin clay-70% Ottawa sand sample was 0.5% (see Figure 4.13). By extrapolating the same curve, one can hypothesize that the transition will take place at extremely low fiber percentages in high fine content soils including the ones tested in this study. The photographs of the field soils support this hypothesis. A typical angular shear failure surface was observed for all unreinforced control test specimens generated using field soils, but with the addition of 0.75% fiber content, a bulging failure surface developed in all specimens. Figure 4.16(a) and Figure 4.16(b) demonstrates the angular failure surface for the unreinforced condition and the bulging failure surface with the addition of 0.75% fiber content, respectively, for the Guilford County field soil.

(a) (b)

Figure 4.16: Guilford County Test Specimen: (a) Unreinforced Angular Failure Surface; (b) 0.75% Fiber Bulging Failure Surface

4.7. Soaked Test Specimens

The Figures in this section display q_u as a function of fiber content for the soil specimens tested after the specimens are soaked for a 24 hour time period. The 30% kaolin clay-70% Ottawa sand test specimens and the four field soils are included in these Figures. Figure 4.17 displays q_u as a function of fiber content for the 30% kaolin clay-70% Ottawa sand mixture tested at both optimum moisture content and post-soak soil conditions. For comparison with the 30% kaolin clay-70% Ottawa sand material, Figures 4.18, 4.19, 4.20, and 4.21 display q_u as a function of fiber content for the field soils tested at both optimum moisture content and post-soak soil conditions.

Similar to Table 4.2, Table 4.7 summarizes the increase in q_u as a function of fiber content relative to the q_u for the unreinforced control test specimens for the soaked test specimens. These numbers strictly quantify the effect of the fiber content. Recall that field soils were only tested using 0.75%, 1.25%, 1.75%, and 2% fiber percentages and tests were not repeated. For example, the q_u for the Johnston County soil increased 70% with 0.75% fiber content but it increased 629% when 2% fiber content was added. For the same soil and fiber contents in Table 4.2 (tests conducted at optimum moisture content), the increase in q_u ranged from 46% to 569% so the impact of the fiber inclusions does not appear to be impacted by the moisture content when tested. Table 4.8 summarizes the decrease in q_u as a result of soaking the test specimen. While Table 4.7 compares a fiber reinforced test specimen to one that is not for all soaked test specimens, Table 4.8 reports the decrease in strength resulting from the soaking process. For example, at a 0.75% fiber content, the q_u for the Johnston County soil decreases 52% (nearly 124 kPa) as a result of soaking the test specimen.

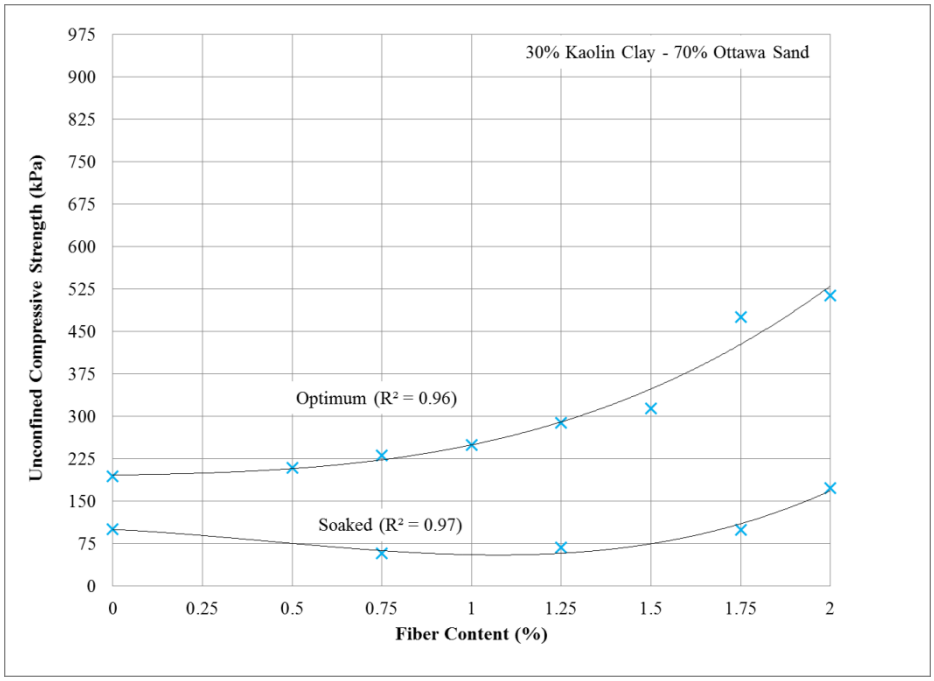

Figure 4.17: Unconfined Compressive Strength as a Function of Fiber Content for Specimens Prepared at Optimum Moisture Content and Soaked Soil Conditions (30% Kaolin Clay-Ottawa Sand)

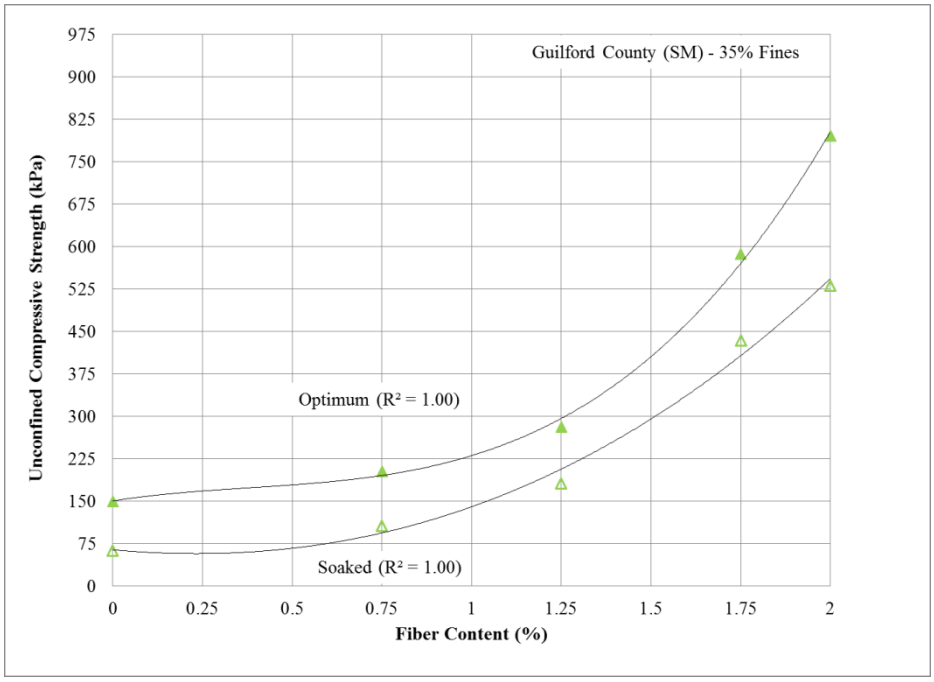

Figure 4.18: Unconfined Compressive Strength as a Function of Fiber Content for Specimens Prepared at Optimum Moisture Content and Soaked Soil Conditions (Guilford County)

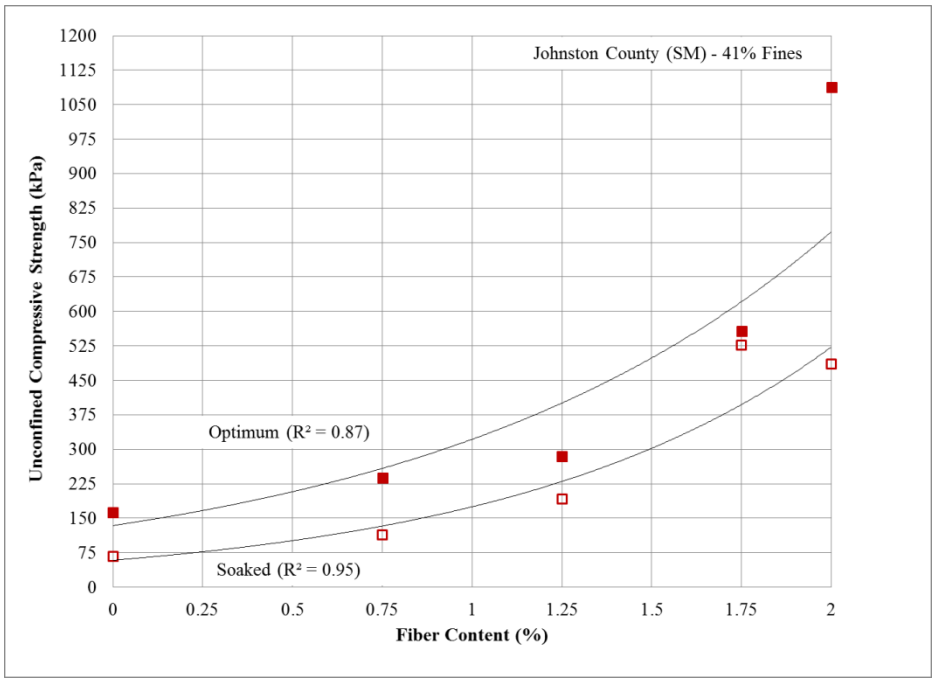

Figure 4.19: Unconfined Compressive Strength as a Function of Fiber Content for Specimens Prepared at Optimum Moisture Content and Soaked Soil Conditions (Johnston County)

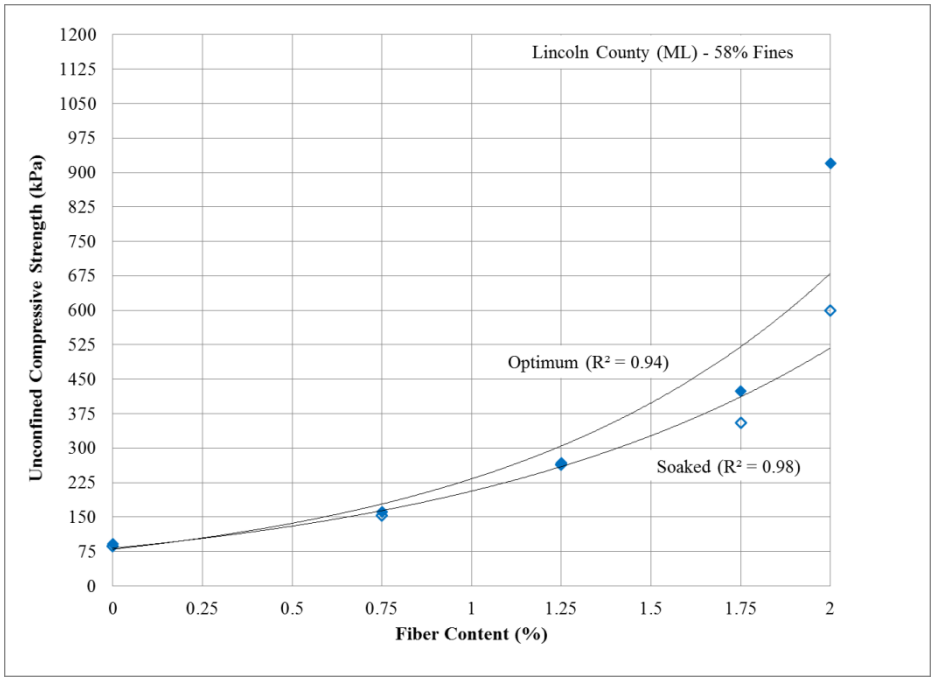

Figure 4.20: Unconfined Compressive Strength as a Function of Fiber Content for Specimens Prepared at Optimum Moisture Content and Soaked Soil Conditions (Lincoln County)

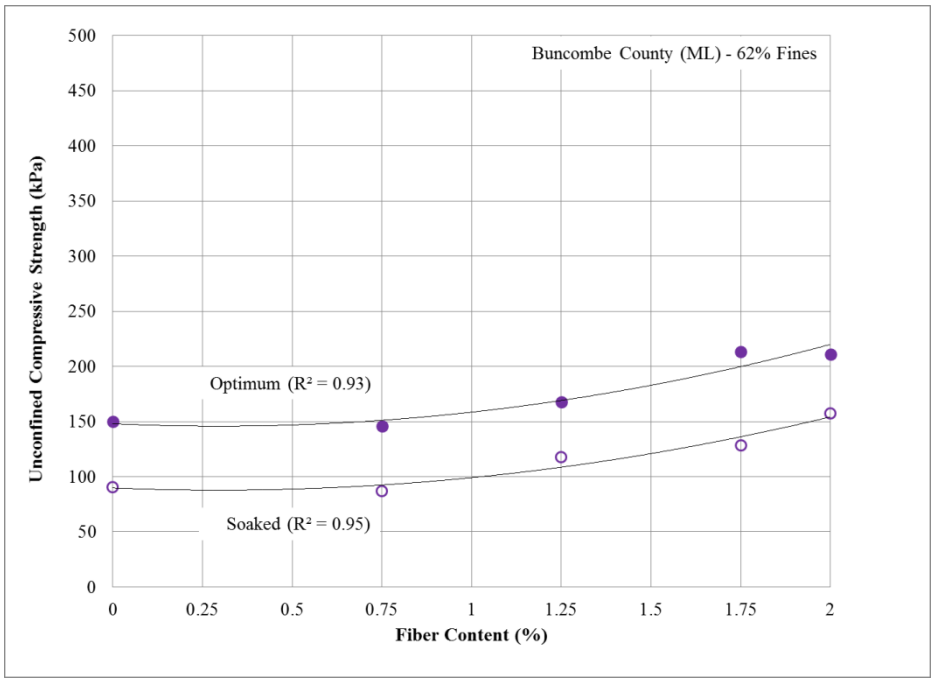

Figure 4.21: Unconfined Compressive Strength as a Function of Fiber Content for Specimens Prepared at Optimum Moisture Content and Soaked Soil Conditions (Buncombe County)

Table 4.7: Percent Increase in Soaked Unconfined Compressive Strength as a Function of Fiber Content

% Fines (USCS) NC County	Fiber Content (%)				
	0.00	0.75	1.25	1.75	2.00
	Percent Increase in Unconfined Compressive Strength (Unconfined Compressive Strength, kPa)				
30 (SC-SM)	- (100.55)	-43% (57.15)	-32% (68.09)	-2% (98.79)	73% (173.58)
35 (SM) Guilford	- (62.08)	71% (106.19)	193% (181.70)	599% (433.95)	756% (531.33)
41 (SM) Johnston	- (66.68)	70% (113.60)	187% (191.57)	689% (526.39)	629% (485.81)
58 (ML) Lincoln	- (86.82)	76% (153.12)	204% (263.55)	309% (355.28)	590% (599.42)
62 (ML) Buncombe	- (90.67)	-4% (87.14)	30% (117.48)	42% (128.42)	74% (157.35)

Table 4.8: Percent Decrease in Unconfined Compressive Strength (Optimum Moisture Content versus Post Soak Conditions)

% Fines (USCS) NC County	Fiber Content (%)				
	0.00	0.75	1.25	1.75	2.00
	Percent Decrease in the Unconfined Compressive Strength Due to Soaked Conditions (Decrease = Optimum – Soaked, kPa)				
30 (SC-SM)	48% (93.78)	76% (177.47)	77% (223.09)	79% (379.14)	66% (339.87)
35 (SM) Guilford	58% (87.16)	48% (96.67)	35% (99.49)	26% (152.76)	33% (264.95)
41 (SM) Johnston	59% (95.96)	52% (123.84)	33% (92.79)	6% (31.05)	55% (601.89)
58 (ML) Lincoln	5% (4.91)	5% (7.76)	1% (3.52)	16% (68.79)	29% (244.49)
62 (ML) Buncombe	40% (59.27)	40% (58.92)	30% (50.46)	40% (84.68)	25% (53.63)

At soaked moisture conditions, the unconfined compressive strength steadily increases from 101 kPa (15 psi) to 174 kPa (25 psi) for the 30% kaolin clay-70% Ottawa sand material and it increases from 62 kPa (9 psi) to 531 kPa (77 psi) for the Guilford County field soil as the fiber content increases from 0% to 2%. While specimens tested under soaked conditions display an increase in strength due to an increase in reinforcement, the magnitude of the unconfined compressive strength is lower in all cases (Figures 4.17 through 4.21) compared to the optimum moisture conditions. In line with the results of a study conducted by Maher and Ho (1994), the loss in strength can be attributed to the lubricating effects of the water and the fibers, decreasing the load transfer between the clay particles and fibers. The difference between the kaolin clay material and the field soil can potentially be attributed to the inherent variability in the field soil, which may be providing more shear strength regardless of saturation level.

CHAPTER 5: SUMMARY AND CONCLUSIONS

5.1. Research Summary

The literature indicates that there is limited unconfined compressive strength laboratory data for polypropylene fibrillated fiber (PFF) reinforced soil. Fiber reinforced soil can be used to remediate weak, near-surface soils that are normally unable to achieve specified allowable net bearing pressure requirements using typical compaction procedures. Rather than importing structural fill from an offsite location, PFF may be a suitable in-situ remediation alternative since they can be blended into near-surface soils.

The data presented in this thesis will supplement the current database of information to better understand geofiber reinforcement in soils. To distinguish this work from previous studies, a larger 102 mm (4 in) diameter test mold was utilized to eliminate boundary effects, soils were reinforced with 12.7 mm (0.5 in) long fibrillated PPF inclusions, a wider range of fiber contents ranging from 0.5% to 2% was tested, and test specimens were carefully generated using select kaolin clay and Ottawa sand materials with controlled fine content fractions ranging between 10% - 30% by mass. These controlled material test specimens were subsequently compared to the performance of four North Carolina field soils collected from Buncombe, Johnston, Guilford, and Lincoln Counties. A total of 140 unconfined compression strength tests were performed at the optimum moisture content as determined using a standard Proctor compaction effort, and 25 additional unconfined

compression strength tests were performed on samples soaked for 24 hours with varying fine and fiber contents.

The purpose of this study was to determine the impact that the PFF had on the unconfined compressive strength using various soil types. In this body of work, the unconfined compressive strength was displayed as a function of fine content (i.e., soil type) as well as fiber content, the axial strain at failure and secant modulus values were reported, and patterns associated with the failure surfaces that developed during these tests were also noted and photographed. Finally, the unconfined compression strengths of soaked test specimens were compared to the unconfined compressive strength of the soil samples tested at the optimum moisture content. The following conclusions can be advanced from the data acquired during this study.

5.2. Research Conclusions

1. A total of 165 unconfined compression tests were performed on fiber reinforced soils with varying fine contents at both the optimum moisture content and post-soak soil conditions. While an ASTM preparation procedure was not available, a detailed specimen preparation procedure was created as part of this study to ensure repeatability of the data. It is important to note that the orientation of the fibers was random and variable from one specimen to the next. Figure 4.1 through Figure 4.5 and Table 4.1 display and summarize the data associated with test repeatability.
2. In comparison to unreinforced test specimens, the controlled kaolin clay – Ottawa sand test data clearly showed an increase in the unconfined compressive strength ranging from 9% to 226% as the fiber content increased from 0.5% to 2% (Figure 4.6 and Table 4.1). The test data acquired using the field soils also showed an increase in the

unconfined compressive strength up to 820% with the same fiber content range (Figure 4.7 and Table 4.2). These data correlate well with the limited data available in the literature, and the trends indicate that fiber percentages as high as 2% may provide added benefit to soil strength.

3. With the exception of the 10% kaolin clay-90% Ottawa sand controlled test specimens and the Buncombe County field soil test specimens, the percent increase in the unconfined compressive strength increased with the fine content in the soil as displayed in Figure 4.6 and Figure 4.7.
4. Figure 4.8 displays a general increase in the unconfined compressive strength as the fiber content increases regardless of material type with the exception of the Buncombe County soil (62% fines). Similar results were reported in several studies including Jiang et al. (2010), Puppala and Musenda (2000), Tang et al. (2007), and Maher and Ho (1994). Both Maher and Ho (1994) and Maher and Gray (1990) reported that the transfer of load from soil to fiber was primarily due to the interface friction.
5. The controlled kaolin clay-Ottawa sand test specimens were included in this study to ensure consistency/repeatability. The field soils were added to the test matrix to validate their trends using in-situ materials that inherently have increased variability. Figure 4.8 displays the unconfined compressive strength as a function of fine content for all soil types tested in this study. While the transfer in data from the controlled material tests to the field soil tests is clearly labeled and there appears to be smooth transition between the two datasets, it is important to note that each point on a single curve represents a different soil type prepared at a different optimum moisture content. Figure 4.8 should be used with caution, but provides an initial reference to estimate

values of q_u for varying soil types and different fiber contents up to 2%, which is not currently available in the literature. A continuation of this testing would strengthen the validity of this reference for practical use in the field.

6. There appeared to be an optimum unconfined compressive strength dependent on the fine content in the soil and the percentage of fiber inclusions. The maximum unconfined compressive strength increased as the fiber content increased and the optimum was reached at a higher fine content for each increase in fiber content. More specifically, the 0.75%, 1.25%, 1.75%, and the 2% fiber content curves reached their maximums at approximately 25%, 30%, 35%, and 42% fine content, respectively (see Figure 4.8).
7. The axial strain at failure increased with an increase in fiber content for all tests as displayed in Figure 4.9 and Figure 4.10. It appears that the ductility of the reinforced soil increased due to the interaction between the soil particles and the polypropylene fibrillated fibers.
8. Some test specimens generated an angular failure plane while others experienced a failure bulge. The observed increase in the ductility of the material could provide an explanation for the transitional failure modes that were detected. The maximum fiber content at which an angular failure surface was observed increased with a decrease in the fines content of the soil (Figure 4.13). Bulging failures were observed for all field soils due to their high fine contents.
9. While the axial strain at failure increased with fiber content, the secant modulus values reported in Table 4.6 do not support a clear trend in modulus with an increase in fiber content. Six out of the nine soils reported in Table 4.6 show a decrease in the secant

modulus relative to the unreinforced specimens. In a study conducted by Iasbik et al. (2003), polypropylene monofilament fibers increased the overall UC strength, but a 0.25% fiber content was responsible for a 65% decrease in the resilient modulus values determined from this study, indicating that the stiffness of the soil decreased. The results from the Tang et al. (2007) study indicate that the inclusion of polypropylene monofilament fibers increased the UC strength, shear strength, and axial strain at failure, but decreased sample brittleness, stiffness, and the loss of post-peak strength. Tang et al. (2007) analyzed the interactions between the fiber surface and the soil matrix, and determined that the bond strength and friction at the soil-fiber interface was the dominant mechanism controlling the reinforcement benefit.

10. When tested at the optimum moisture content using fiber contents ranging from 0% to 2% by mass, the unconfined compressive strength steadily increased from 101 kPa (15 psi) to 174 kPa (25 psi) for the 30% kaolin clay-70% Ottawa sand material, and it increased from 62 kPa (9 psi) to 564 kPa (82 psi) for the Guilford County field soil. While specimens tested under soaked conditions displayed an increase in strength due to an increase in reinforcement, the magnitude of the unconfined compressive strength was lower than the values measured at optimum moisture in all cases (Figures 4.17 through 4.21). In line with the results of a study conducted by Maher and Ho (1994), the loss in strength can be attributed to the lubricating effects of the water and the fibers, which likely decreased the load transfer between the clay particles and fibers. The differences between the controlled materials and the field soils can potentially be attributed to the inherent variability in the field soil, which may have provided more shear strength regardless of the saturation level.

5.3 Recommendations for Future Research

The following suggestions are recommended for future research:

- Extend the test matrix to include additional field soils to validate the unconfined compression strengths presented herein.
- Extend the test matrix to include various geosynthetic fiber lengths.
- Investigate the interaction between soil solid and fiber on a microscopic level.
- Investigate the installation process in the field for the purpose of recommending best practices for installation dependent upon fiber length.

REFERENCES

Ang, E. C. and Loehr, J. E. (2003). "Specimen Size Effects for Fiber-Reinforced Silty Clay in Unconfined Compression." *Geotechnical Testing Journal,* 26(2): 191-200.

ASTM C 1116 (2010). "Standard Specification for Fiber-Reinforced Concrete." *ASTM International,* West Conshohocken, PA, U.S.A.

ASTM D 422 (2002). "Standard Test Method for Particle-Size Analysis of Soils." *ASTM International,* West Conshohocken, PA, U.S.A.

ASTM D 698 (2000). "Standard Test Methods for Laboratory Compaction Characteristics of Soil Using Standard Effort (12,400 ft-lbf/ft3 (600 kN-m/m3))." *ASTM International,* West Conshohocken, PA, U.S.A.

ASTM D 788 (2006). "Standard Specification for Standard Sand." *ASTM International,* West Conshohocken, PA, U.S.A.

ASTM D 2166 (2006). "Standard Test Method for Unconfined Compressive Strength of Cohesive Soil." *ASTM International,* West Conshohocken, PA, U.S.A.

ASTM D 2487 (2010). "Standard Practice for Classification of Soils for Engineering Purposes (Unified Soil Classification System)." *ASTM International,* West Conshohocken, PA, U.S.A.

ASTM D 4318 (2010). "Standard Test Methods for Liquid Limit, Plastic Limit, and Plasticity Index of Soils." *ASTM International,* West Conshohocken, PA, U.S.A.

ASTM F 891 (2010). "Standard Specification for Coextruded Poly(Vinyl Chloride) (PVC) Plastic Pipe with a Cellular Core." *ASTM International,* West Conshohocken, PA, U.S.A.

Consoli, N. C., Casagrande, M. D., Prietto, P. D. and Thome, A. (2003). "Plate Load Test on Fiber-Reinforced Soil." *Journal of Geotechnical and Geoenvironmental Engineering,* 129(10): 951-955.

Freilich, B. J., Li, C. and Zornberg, J. G. (2010). "Effective Shear Strength of Fiber-Reinforced Clays." *Proceedings of the 9th International Conference on Geosynthetics,* 9ICG, Guarujá, Brazil, 4: 1997-2000.

Gary, D. H. and Al-Refeai, T. O. (1986). "Behavior of Fabric-Versus Fiber-Reinforced Sand." *Journal of Geotechnical Engineering,* 112(8): 804-820.

Gregory, G. H. (2006). "Shear Strength, Creep, and Stability of Fiber-Reinforced Soil Slopes." Doctoral dissertation submitted to the faculty of the Graduate College of Oklahoma State University in partial fulfillment of the requirements for the degree of Doctor of Philosophy. Stillwater, Oklahoma, May 2006, 225 pp.

Gregory, G. H. and Chill, D. S. (1998). "Stabilization of Earth Slopes with Fiber Reinforcement." *Proceedings of the 6th International Conference on Geosynthetics*, pp. 1073-1078. Atlanta, GA, USA.

Iasbik, I., De Lima, D. C., Carvalho, C. A., Silva, C. H., Minette, E. and P. S. A. (2002). "Geotechnical Characterization of a Clayey Soil Stabilized with Polypropylene Fiber Using Unconfined Compression and Resilient Modulus Testing Data." *ASTM Special Technical Publication*, 1437: 114-125.

Jiang, H., Cai, Y. and Liu, J. (2010). "Engineering Properties of Soils Reinforced by Short Discrete Polypropylene Fiber." *Journal of Materials in Civil Engineering*, 31: 1315-1322.

Kumar, A., Walia, B. S. and Mohan, J. (2006). "Compressive Strength of Fiber Reinforced Highly Compressible Clay." *Construction and Building Materials*, 20(10): 1063-1068.

Lambe, T. W. and Whitman, R. V. (1969). "Soil Mechanics." John Wiley and Sons, Inc., New York.

Maher, M. H. and Gray, D. H. (1990). "Static Response of Sand Reinforced with Randomly Distributed Fibers." *Journal of Geotechnical Engineering*, 116(11): 1661-1677.

Maher, M. H. and Ho, Y. C. (1994). "Mechanical Properties of Kaolinite/Fiber Soil Composite." *Journal of Geotechnical Engineering*, 120(8): 1381-1393.

Michalowski, R. L. and Čermák, J. (2003). "Triaxial Compression of Sand Reinforced with Fibers." *Journal of Geotechnical and Geoenvironmental Engineering*, 129(2): 125-136.

Nataraj, M. S. and McManis, K. L. (1997). "Strength and Deformation Properties of Soils Reinforced with Fibrillated Fibers." *Geosynthetics International*, 4(1): 65-79.

Park, T. and Tan, S. A. (2005). "Enhanced Performance of Reinforced Soil Walls by the Inclusion of Short Fiber." *Geotextiles and Geomembranes*, 23(4): 348-361.

Puppala, A. J. and Musenda, C. (2000). "Effects of Fiber Reinforcement on Strength and Volume Change in Expansive Soils." *Transportation Research Record*, 1736: 134-140.

Rafalko, S. D., Brandon, T. L., Filz, G. M. and Mitchell, J. K. (2008). "Fiber Reinforcement for Rapid Stabilization of Soft Clay Soils." *Journal of the Transportation Research Board*, 2026: 21-29.

Ranjan, G., Vasan, R. M. and Charan, H. D. (1994). "Behaviour of Plastic-Fibre-Reinforced Sand." *Geotextiles and Geomembranes,* 13(8): 555-565.

Romero, Ricardo J. (2003). "Development of a Constitutive Model for Fiber-Reinforced Soils." Doctoral dissertation submitted to the faculty of the Graduate College of the University of Missouri in partial fulfillment of the requirements for the degree of Doctor of Philosophy. Columbia, Missouri, 2003, 157 pp.

Tang, C., Shi, B., Gao, W., Chen, F. and Cai, Y. (2007). "Strength and Mechanical Behavior of Short Polypropylene Fiber Reinforced and Cement Stabilized Clayey Soil." *Geotextiles and Geomembranes*, 25(3): 194-202.

Tingle, J. S., Webster, S. L. and Santoni, R. L. (1999). "Discrete Fiber Reinforcement of Sands for Expedient Road Construction." *Technical Report GL-99-3*. U.S. Army Corps of Engineers Waterways Experiment Station, Vicksburg, VA U.S.A.

Zhang, Z., Farrag, K. and Morvant, M. (2003). "Evaluation of the Effects of Synthetic Fibers and Nonwoven Geotextile Reinforcement on the Stability of Heavy Clay Embankments." *Report No. FHWA/LA.03/337*, Louisiana Transportation Research Center, Baton Rouge, LA U.S.A.

APPENDIX A: COMPACTION CURVES

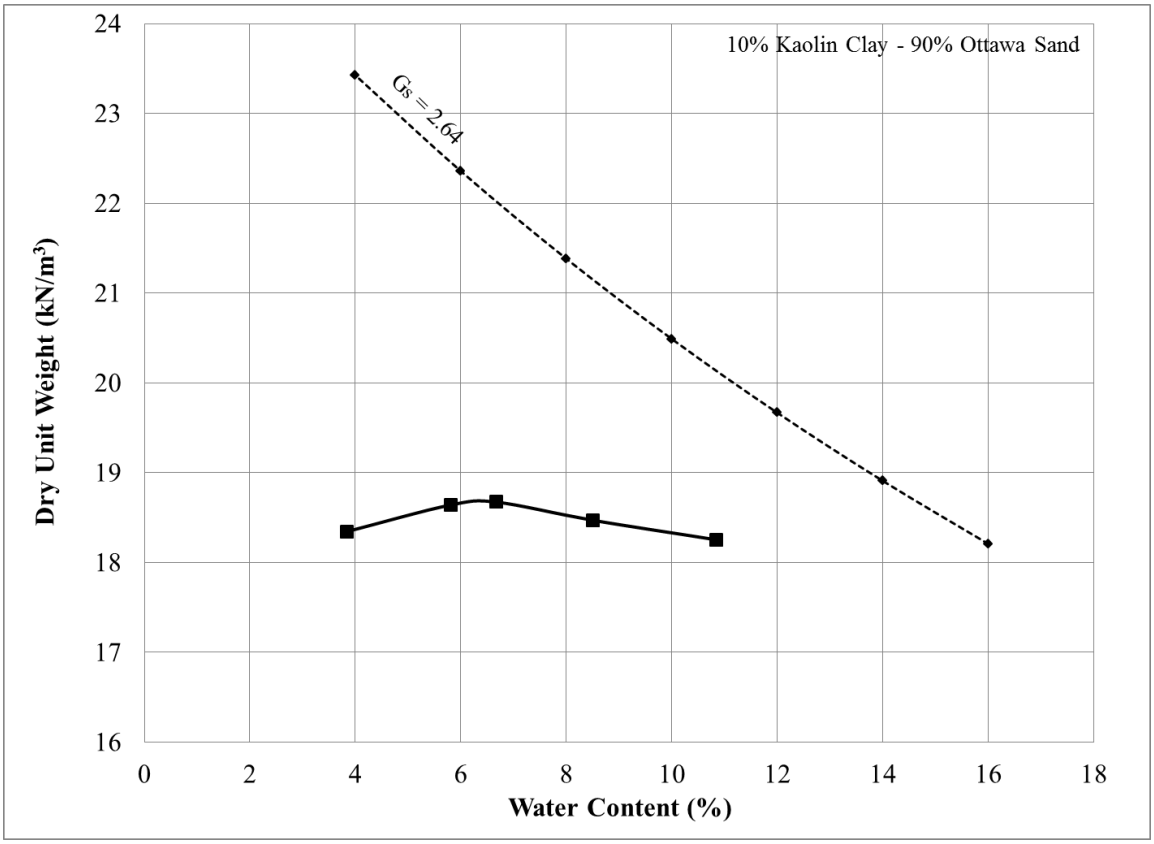

Figure A.1: 10% Kaolin Clay-90% Ottawa Sand Standard Proctor (ASTM D 698) Compaction Curve (0% Fiber Content)

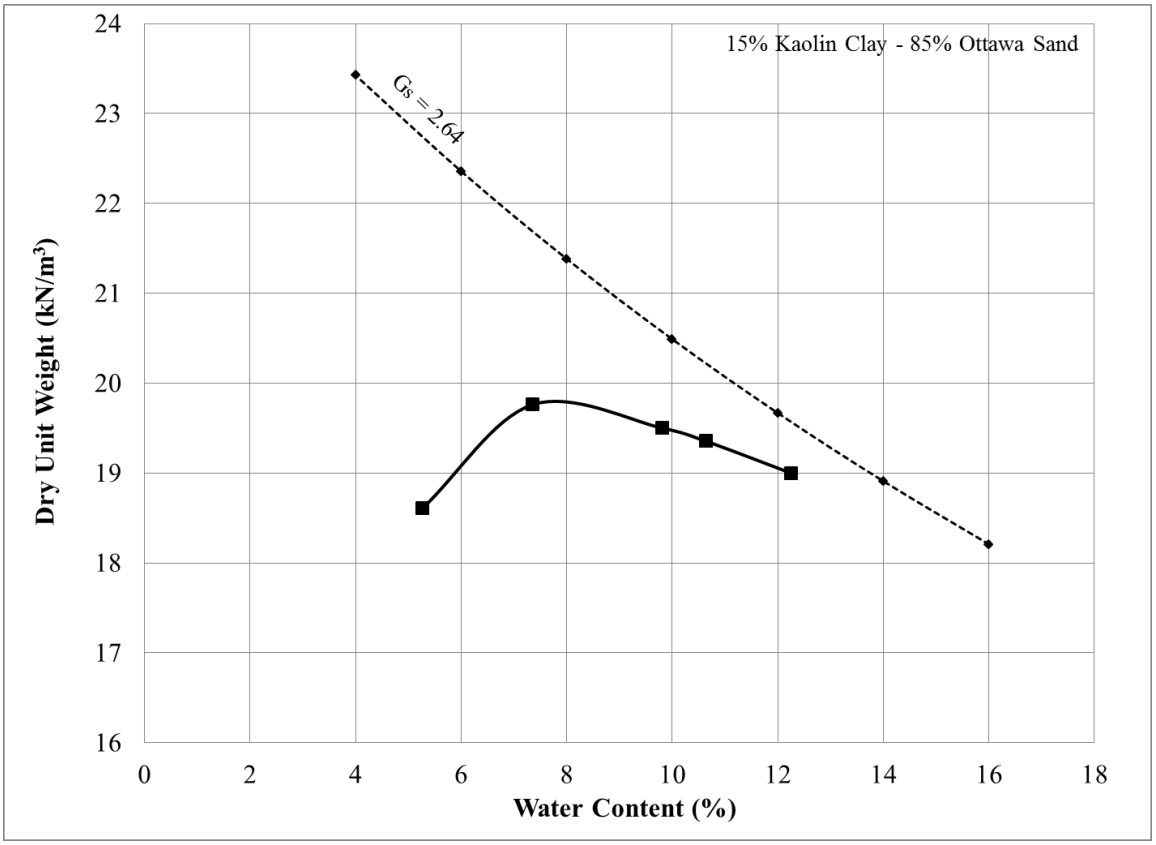

Figure A.2: 15% Kaolin Clay-85% Ottawa Sand Standard Proctor (ASTM D 698) Compaction Curve (0% Fiber Content)

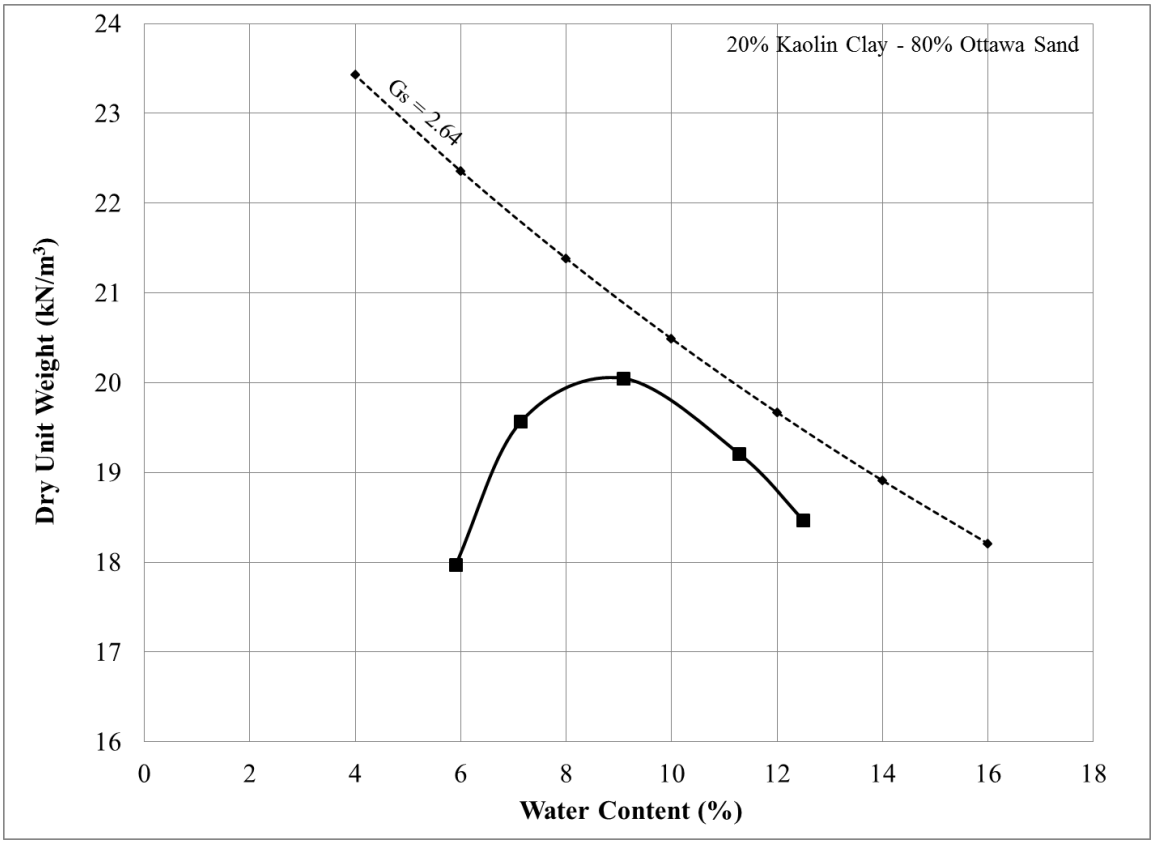

Figure A.3: 20% Kaolin Clay-80% Ottawa Sand Standard Proctor (ASTM D 698) Compaction Curve (0% Fiber Content)

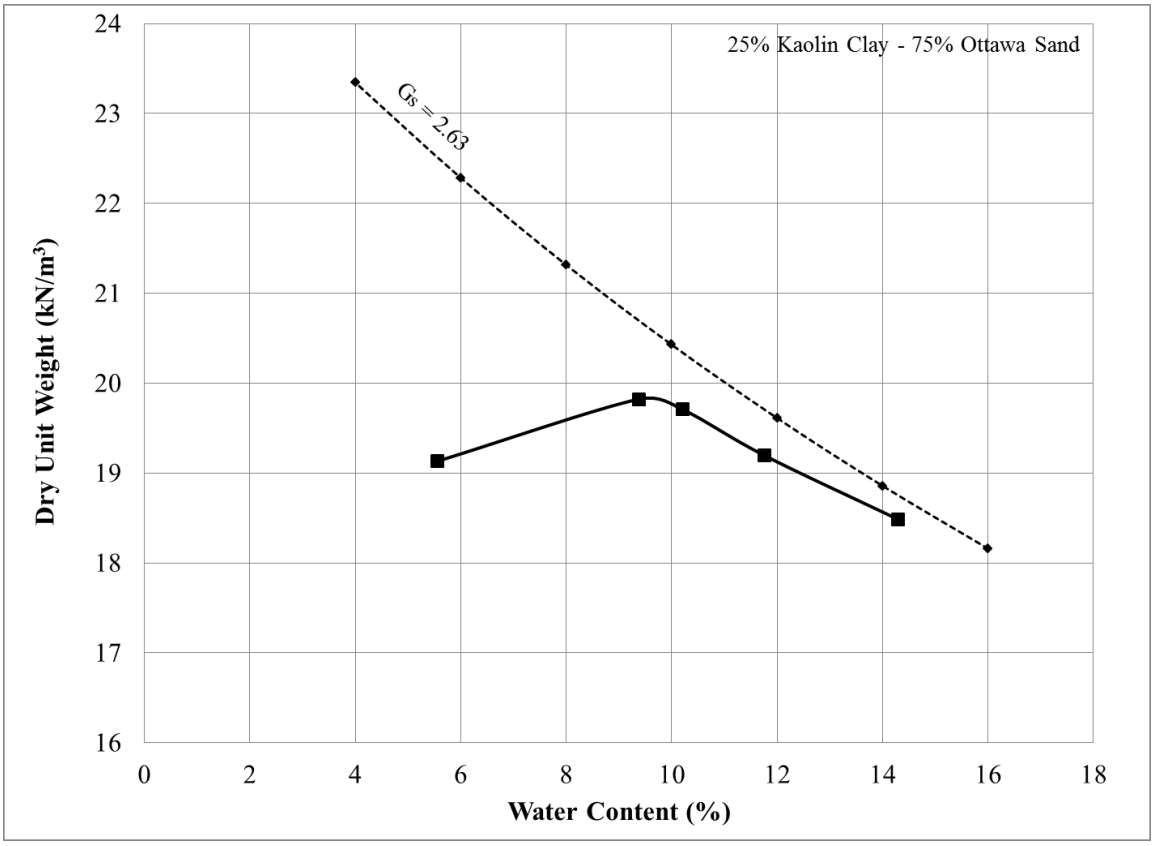

Figure A.4: 25% Kaolin Clay-75% Ottawa Sand Standard Proctor (ASTM D 698) Compaction Curve (0% Fiber Content)

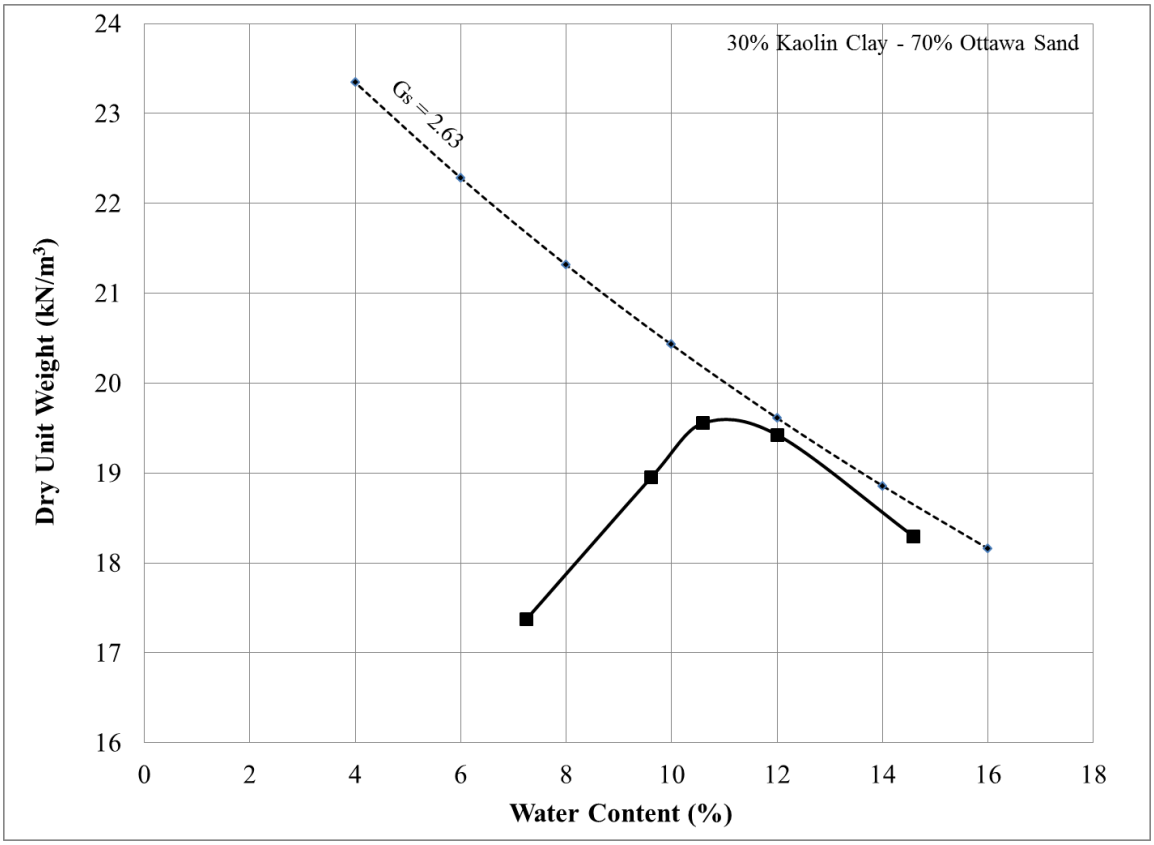

Figure A.5: 30% Kaolin Clay-70% Ottawa Sand Standard Proctor (ASTM D 698) Compaction Curve (0% Fiber Content)

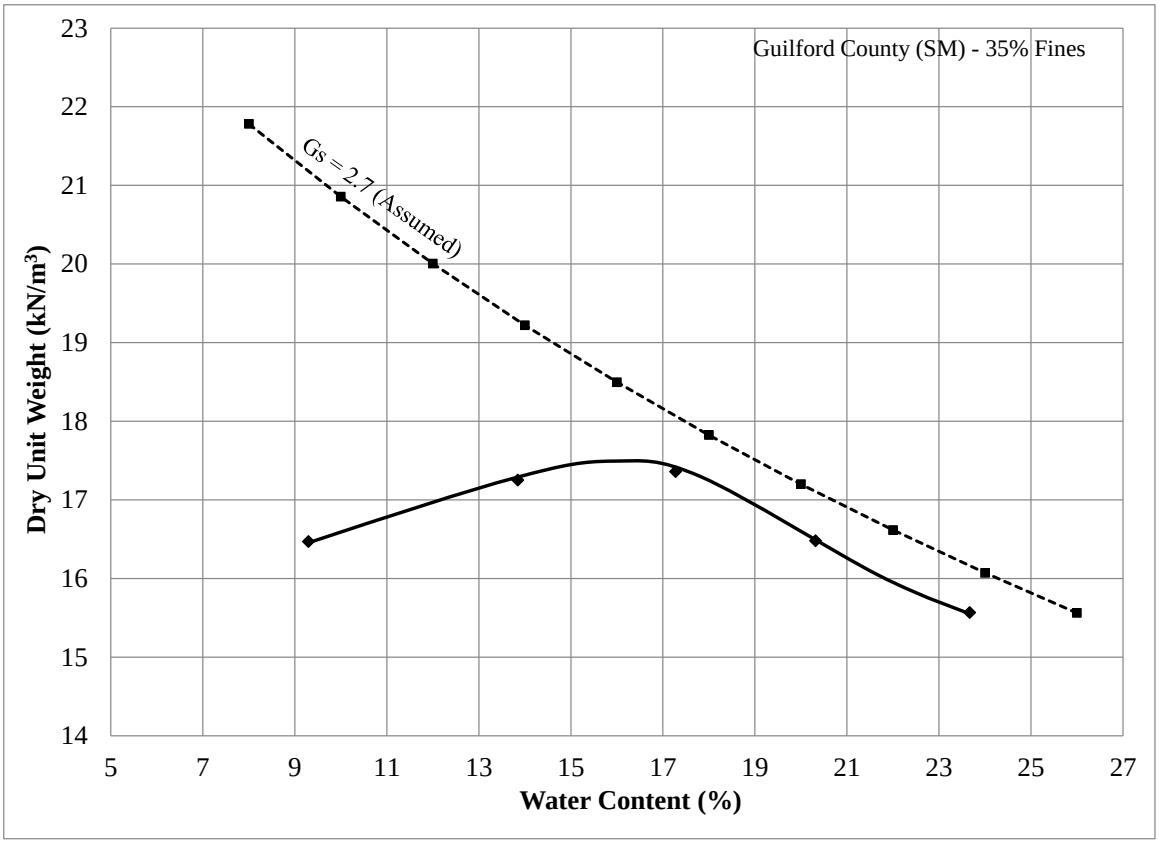

Figure A.6: Guilford County Standard Proctor (ASTM D 698) Compaction Curve (0% Fiber Content)

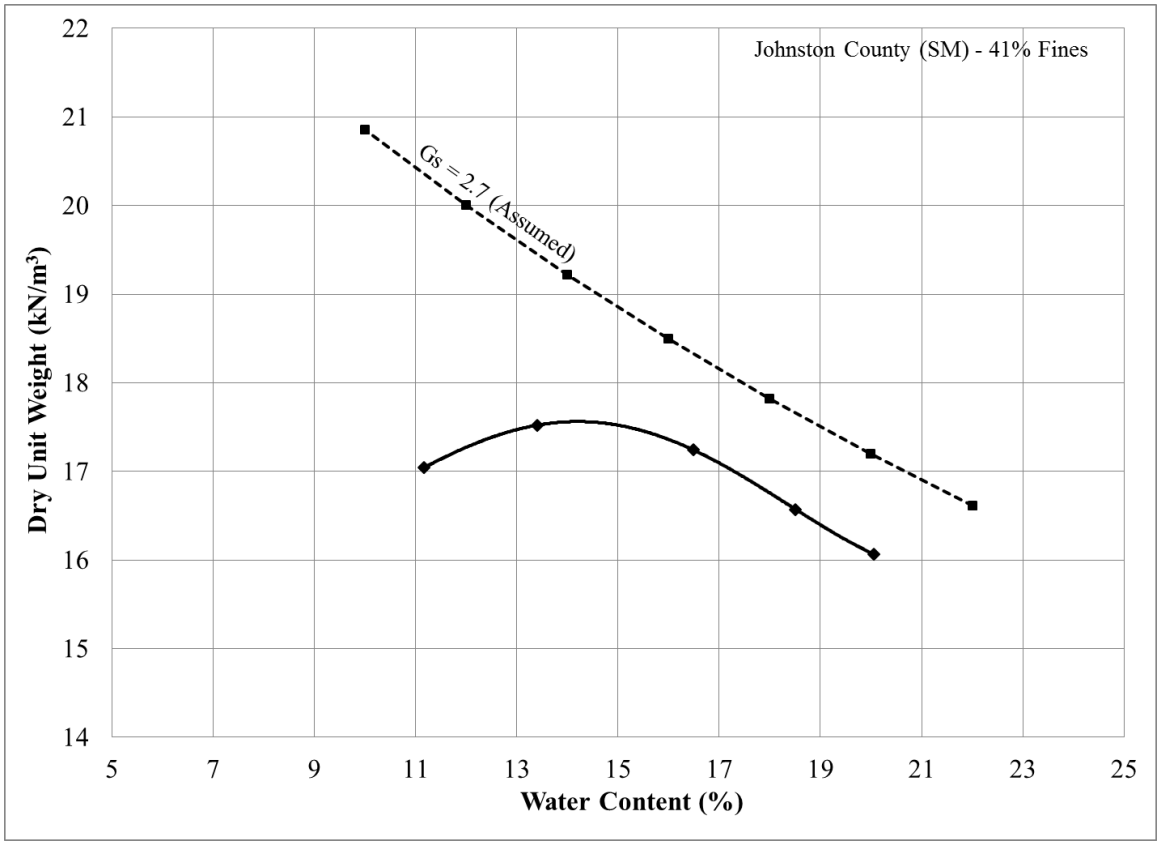

Figure A.7: Johnston County Standard Proctor (ASTM D 698) Compaction Curve (0% Fiber Content)

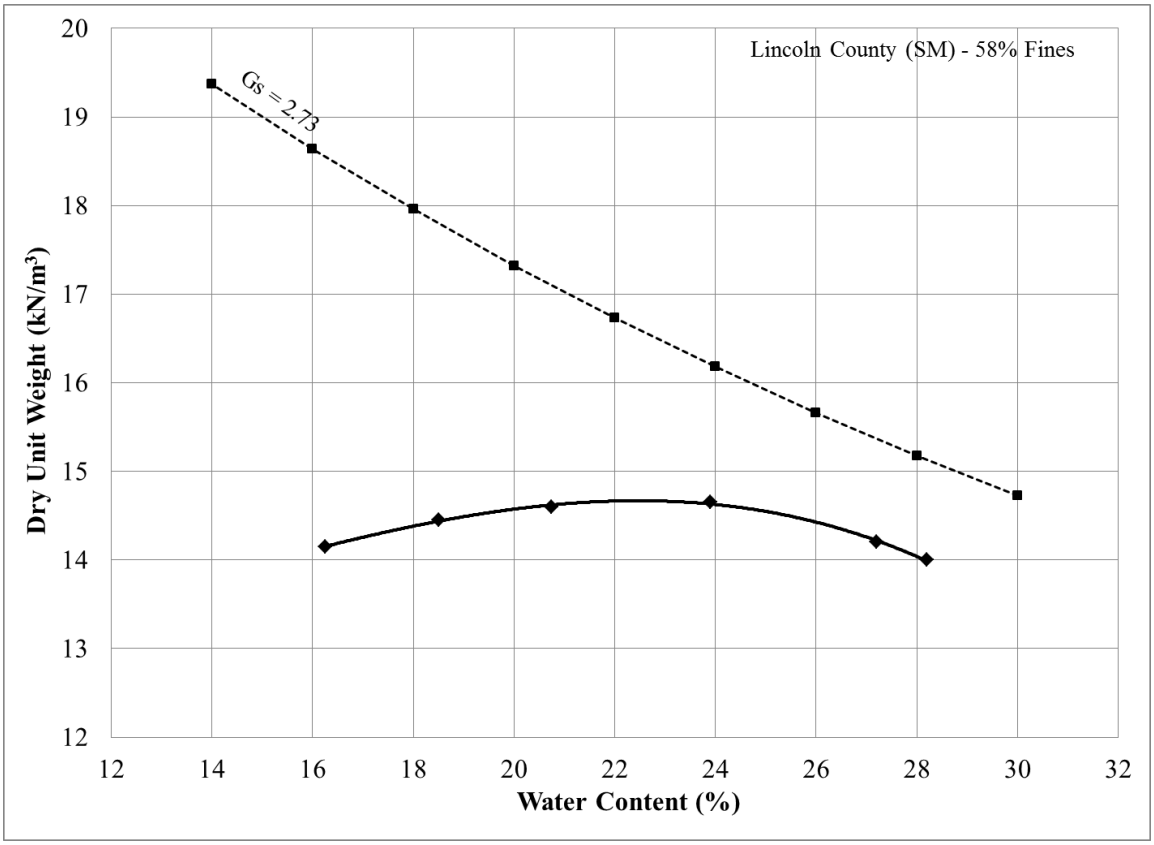

Figure A.8: Lincoln County Standard Proctor (ASTM D 698) Compaction Curve (0% Fiber Content)

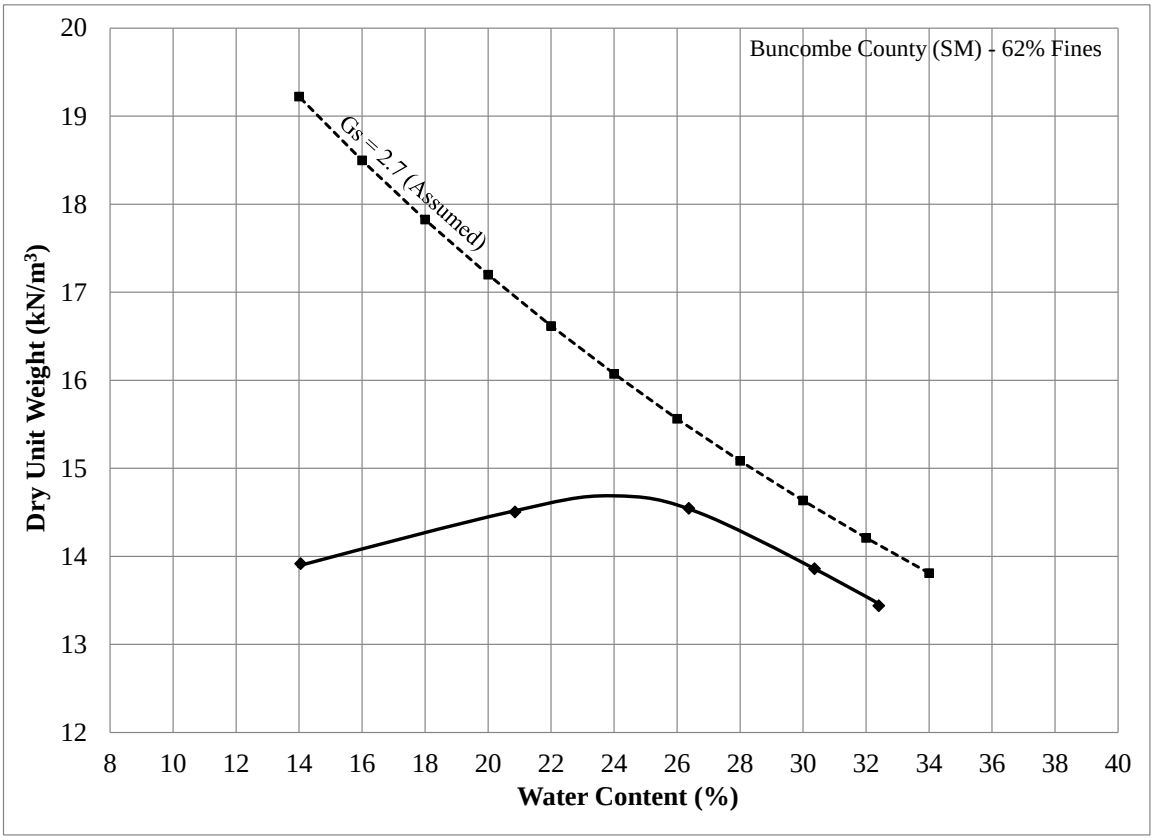

Figure A.9: Buncombe County Standard Proctor (ASTM D 698) Compaction Curve (0% Fiber Content)

APPENDIX B: TEST MATRIX

Table B.1: Unconfined Compression Test Matrix

Test Completion Date	Specimen No.	Fine Content (%)	Water Content (%)	Fiber Length (mm)	Fiber Content (%)	Group Description
08/11/09	19_1R	10	Optimum	No Fiber	Control	Control (0% Fiber) Vary Kaolin %
08/11/09	20_1R	20	Optimum	No Fiber	Control	
08/11/09	21_1R	30	Optimum	No Fiber	Control	
08/11/09	22_1R	25	Optimum	No Fiber	Control	
08/11/09	23_1R	15	Optimum	No Fiber	Control	
07/29/09	24R	10	Optimum	No Fiber	Control	
07/29/09	25R	15	Optimum	No Fiber	Control	
07/29/09	26R	20	Optimum	No Fiber	Control	
07/29/09	27R	25	Optimum	No Fiber	Control	
07/29/09	28R	30	Optimum	No Fiber	Control	
07/30/09	29R	10	Optimum	No Fiber	Control	
07/30/09	30R	15	Optimum	No Fiber	Control	
07/30/09	31R	20	Optimum	No Fiber	Control	
07/30/09	32R	25	Optimum	No Fiber	Control	
07/30/09	33R	30	Optimum	No Fiber	Control	
08/05/09	34R	20	Optimum	12.7	0.50	20% Kaolin Vary Fiber %
08/05/09	35R	20	Optimum	12.7	0.75	
08/05/09	36R	20	Optimum	12.7	1.00	
08/05/09	37R	20	Optimum	12.7	1.25	
08/17/09	38_1R	20	Optimum	12.7	1.50	
08/17/09	39_1R	20	Optimum	12.7	1.75	
08/17/09	40_1R	20	Optimum	12.7	2.00	
08/06/09	41R	20	Optimum	12.7	0.50	
08/06/09	42R	20	Optimum	12.7	0.75	
08/06/09	43R	20	Optimum	12.7	1.00	
08/06/09	44R	20	Optimum	12.7	1.25	
08/06/09	45R	20	Optimum	12.7	1.50	
08/06/09	46R	20	Optimum	12.7	1.75	
08/07/09	47R	20	Optimum	12.7	2.00	
08/07/09	48R	20	Optimum	12.7	0.50	
08/07/09	49R	20	Optimum	12.7	0.75	
08/10/09	50R	20	Optimum	12.7	1.00	
08/10/09	51R	20	Optimum	12.7	1.25	
08/10/09	52R	20	Optimum	12.7	1.50	
08/10/09	53R	20	Optimum	12.7	1.75	
08/10/09	54R	20	Optimum	12.7	2.00	

Table B.1: Unconfined Compression Test Matrix (continued)

Test Completion Date	Specimen No.	Fine Content (%)	Water Content (%)	Fiber Length (mm)	Fiber Content (%)	Group Description
02/18/10	73R	10	Optimum	12.7	0.50	10% Kaolin Vary Fiber %
02/23/10	74R	10	Optimum	12.7	0.75	
02/23/10	75R	10	Optimum	12.7	1.00	
02/23/10	76R	10	Optimum	12.7	1.25	
02/23/10	77R	10	Optimum	12.7	1.50	
02/25/10	78R	10	Optimum	12.7	1.75	
02/25/10	79R	10	Optimum	12.7	2.00	
02/25/10	80R	10	Optimum	12.7	0.50	
02/25/10	81R	10	Optimum	12.7	0.75	
02/25/10	82R	10	Optimum	12.7	1.00	
05/19/10	83R	10	Optimum	12.7	1.25	
05/24/10	84R	10	Optimum	12.7	1.50	
05/24/10	85R	10	Optimum	12.7	1.75	
05/24/10	86R	10	Optimum	12.7	0.50	
05/24/10	87R	10	Optimum	12.7	0.75	
05/24/10	88R	10	Optimum	12.7	2.00	
05/24/10	89R	10	Optimum	12.7	1.00	
05/24/10	90R	10	Optimum	12.7	1.25	
05/24/10	91R	10	Optimum	12.7	1.50	
05/26/10	92R	10	Optimum	12.7	1.75	
05/26/10	93R	10	Optimum	12.7	2.00	
05/26/10	94R	15	Optimum	12.7	0.50	15% Kaolin Vary Fiber %
05/26/10	95R	15	Optimum	12.7	0.75	
05/26/10	96R	15	Optimum	12.7	1.00	
05/26/10	97R	15	Optimum	12.7	1.25	
05/26/10	98R	15	Optimum	12.7	1.50	
05/26/10	99R	15	Optimum	12.7	1.75	
05/26/10	100R	15	Optimum	12.7	2.00	
06/03/10	101R	15	Optimum	12.7	0.50	
06/03/10	102R	15	Optimum	12.7	0.75	
06/03/10	103R	15	Optimum	12.7	1.00	
06/03/10	104R	15	Optimum	12.7	1.25	
06/03/10	105R	15	Optimum	12.7	1.50	
06/03/10	106R	15	Optimum	12.7	1.75	
06/03/10	107R	15	Optimum	12.7	2.00	
06/09/10	108R	15	Optimum	12.7	0.50	
06/09/10	109R	15	Optimum	12.7	0.75	
06/09/10	110R	15	Optimum	12.7	1.00	
06/10/10	111R	15	Optimum	12.7	1.25	
06/10/10	112R	15	Optimum	12.7	1.50	
06/10/10	113R	15	Optimum	12.7	1.75	
06/10/10	114R	15	Optimum	12.7	2.00	

Table B.1: Unconfined Compression Test Matrix (continued)

Test Completion Date	Specimen No.	Fine Content (%)	Water Content (%)	Fiber Length (mm)	Fiber Content (%)	Group Description
06/22/10	115R	25	Optimum	12.7	0.50	25% Kaolin Vary Fiber %
06/22/10	116R	25	Optimum	12.7	0.75	
06/22/10	117R	25	Optimum	12.7	1.00	
06/22/10	118R	25	Optimum	12.7	1.25	
06/22/10	119R	25	Optimum	12.7	1.50	
06/23/10	120R	25	Optimum	12.7	1.75	
06/23/10	121R	25	Optimum	12.7	2.00	
06/29/10	122R	25	Optimum	12.7	0.50	
06/29/10	123R	25	Optimum	12.7	0.75	
06/29/10	124R	25	Optimum	12.7	1.00	
06/29/10	125R	25	Optimum	12.7	1.25	
06/29/10	126R	25	Optimum	12.7	1.50	
06/29/10	127R	25	Optimum	12.7	1.75	
06/29/10	128R	25	Optimum	12.7	2.00	
06/29/10	129R	25	Optimum	12.7	0.50	
06/29/10	130R	25	Optimum	12.7	0.75	
06/29/10	131R	25	Optimum	12.7	1.00	
06/29/10	132R	25	Optimum	12.7	1.25	
06/30/10	133R	25	Optimum	12.7	1.50	
06/30/10	134R	25	Optimum	12.7	1.75	
06/30/10	135R	25	Optimum	12.7	2.00	
07/07/10	136R	30	Optimum	12.7	0.50	30% Kaolin Vary Fiber %
07/07/10	137R	30	Optimum	12.7	0.75	
07/07/10	138R	30	Optimum	12.7	1.00	
07/07/10	139R	30	Optimum	12.7	1.25	
07/07/10	140R	30	Optimum	12.7	1.50	
08/05/10	141R	30	Optimum	12.7	1.75	
07/07/10	142R	30	Optimum	12.7	2.00	
07/12/10	143R	30	Optimum	12.7	0.50	
07/12/10	144R	30	Optimum	12.7	0.75	
07/12/10	145R	30	Optimum	12.7	1.00	
08/02/10	146R	30	Optimum	12.7	1.25	
08/02/10	147R	30	Optimum	12.7	1.50	
08/02/10	148R	30	Optimum	12.7	1.75	
08/05/10	149R	30	Optimum	12.7	2.00	
08/03/10	150R	30	Optimum	12.7	0.50	
08/03/10	151R	30	Optimum	12.7	0.75	
08/03/10	152R	30	Optimum	12.7	1.00	
08/03/10	153R	30	Optimum	12.7	1.25	
08/05/10	154R	30	Optimum	12.7	1.50	
08/05/10	155R	30	Optimum	12.7	1.75	
08/05/10	156R	30	Optimum	12.7	2.00	

Table B.1: Unconfined Compression Test Matrix (continued)

Test Completion Date	Specimen No.	Fine Content (%)	Water Content (%)	Fiber Length (mm)	Fiber Content (%)	Group Description
10/02/10	157R	41.5	Optimum	12.7	0.75	Field Soils Vary Fiber %
10/02/10	158R	41.5	Optimum	12.7	1.25	
10/02/10	159R	41.5	Optimum	12.7	1.75	
10/02/10	160R	62.1	Optimum	12.7	0.75	
10/02/10	161R	62.1	Optimum	12.7	1.25	
10/02/10	162R	62.1	Optimum	12.7	1.75	
10/02/10	163R	35.0	Optimum	12.7	0.75	
10/02/10	164R	35.0	Optimum	12.7	1.25	
10/03/10	165R	35.0	Optimum	12.7	1.75	
10/20/10	166R	41.5	Optimum	12.7	0.00	
10/20/10	167R	41.5	Optimum	12.7	2.00	
10/20/10	168R	62.1	Optimum	12.7	0.00	
10/20/10	169R	62.1	Optimum	12.7	2.00	
10/20/10	170R	35.0	Optimum	12.7	0.00	
10/20/10	171R	35.0	Optimum	12.7	2.00	
11/17/10	172R	57.8	Optimum	12.7	0.00	
11/17/10	173R	57.8	Optimum	12.7	0.75	
11/17/10	174R	57.8	Optimum	12.7	1.25	
11/17/10	175R	57.8	Optimum	12.7	1.75	
11/17/10	176R	57.8	Optimum	12.7	2.00	
12/07/10	177R	41.5	Soaked	12.7	0.00	Field Soils Vary Fiber % 24 Hour Soak
12/07/10	178R	41.5	Soaked	12.7	0.75	
12/07/10	179R	41.5	Soaked	12.7	1.25	
12/07/10	180R	41.5	Soaked	12.7	1.75	
12/07/10	181R	41.5	Soaked	12.7	2.00	
12/14/10	182R	62.1	Soaked	12.7	0.00	
12/14/10	183R	62.1	Soaked	12.7	0.75	
12/14/10	184R	62.1	Soaked	12.7	1.25	
12/14/10	185R	62.1	Soaked	12.7	1.75	
12/14/10	186R	62.1	Soaked	12.7	2.00	
12/15/10	187R	35.0	Soaked	12.7	0.00	
12/15/10	188R	35.0	Soaked	12.7	0.75	
12/15/10	189R	35.0	Soaked	12.7	1.25	
12/15/10	190R	35.0	Soaked	12.7	1.75	
12/15/10	191R	35.0	Soaked	12.7	2.00	
12/16/10	192R	57.8	Soaked	12.7	0.00	
12/16/10	193R	57.8	Soaked	12.7	0.75	
12/16/10	194R	57.8	Soaked	12.7	1.75	
12/16/10	195R	57.8	Soaked	12.7	1.25	
12/16/10	196R	57.8	Soaked	12.7	2.00	
12/16/10	197R	30	Soaked	12.7	0.00	30% Kaolin Vary Fiber % 24 Hour Soak
12/17/10	198R	30	Soaked	12.7	0.75	
12/17/10	199R	30	Soaked	12.7	1.25	
12/17/10	200R	30	Soaked	12.7	1.75	
12/17/10	201R	30	Soaked	12.7	2.00	

APPENDIX C: UNCONFINED COMPRESSION CURVES AND PHOTOS

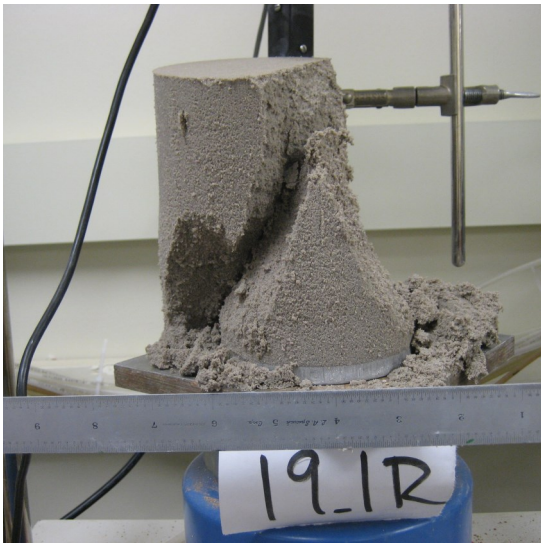

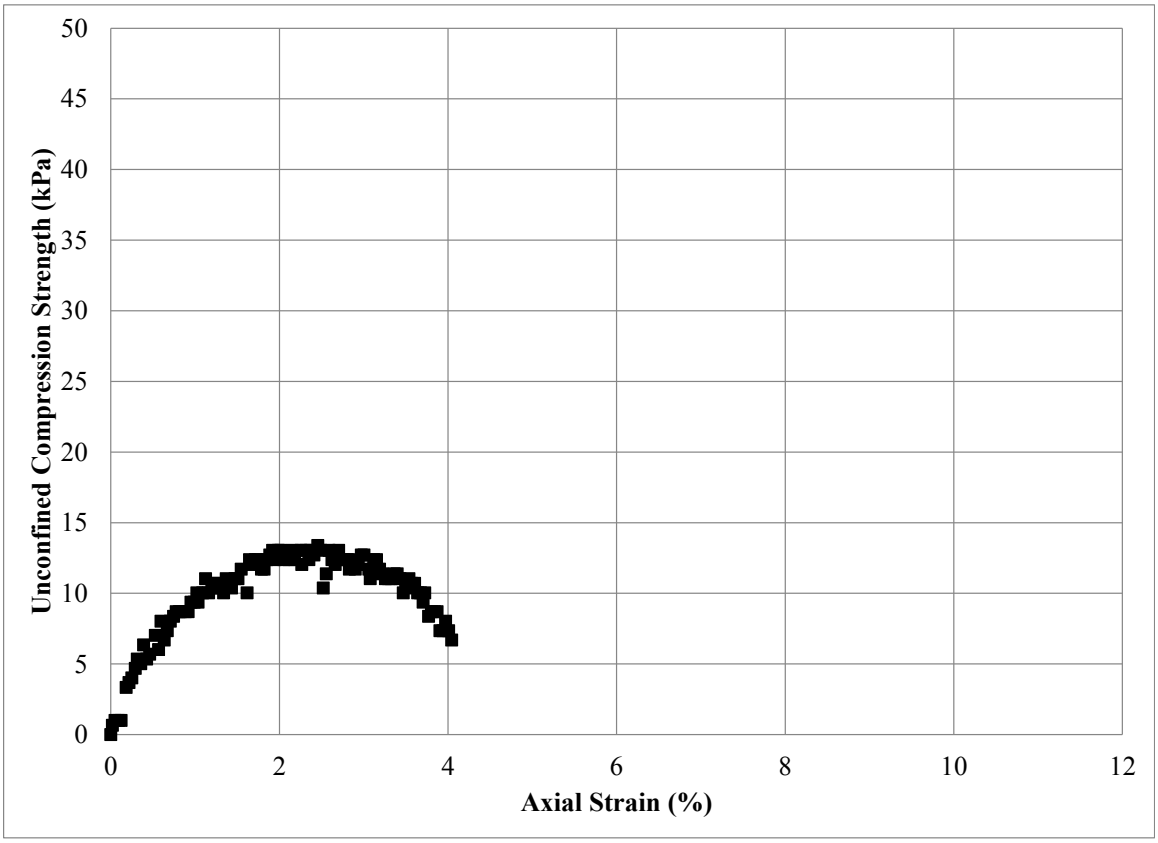

Figure C.1: Unconfined Compression Test Specimen No. 19_1R: (a) Photograph Prior to Testing; (b) Photograph Post Testing; and (c) Stress – Strain Data

(a)

(b)

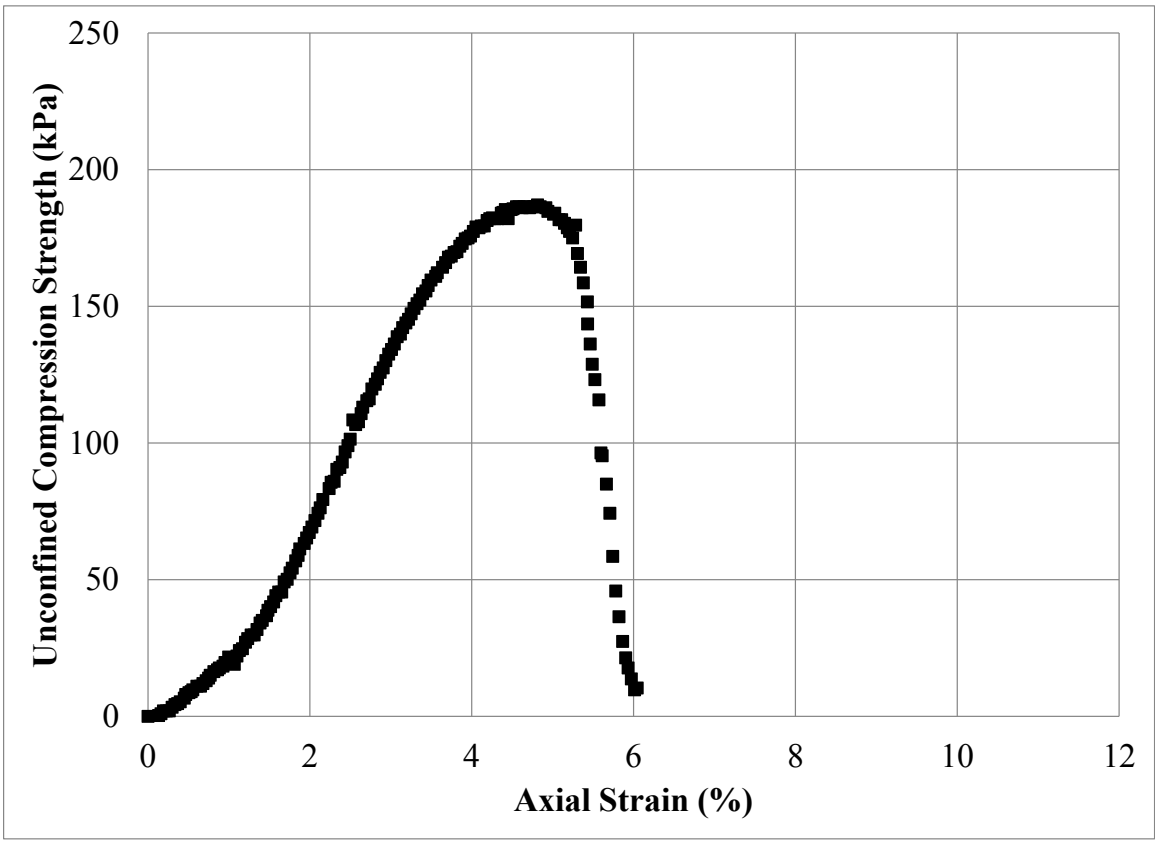

(c)

Figure C.2: Unconfined Compression Test Specimen No. 20_1R: (a) Photograph Prior to Testing; (b) Photograph Post Testing; and (c) Stress – Strain Data

(a)

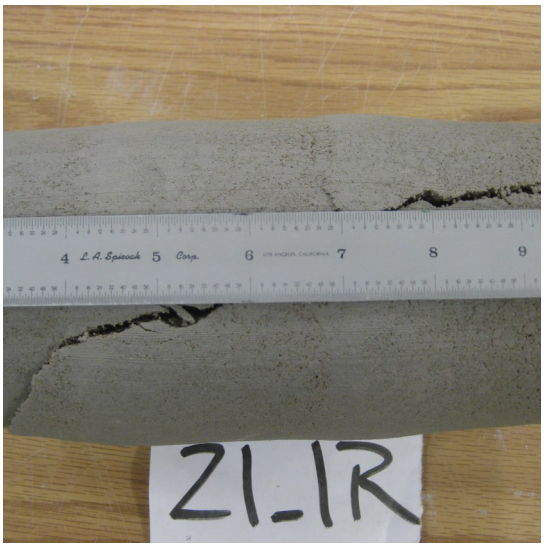

(b)

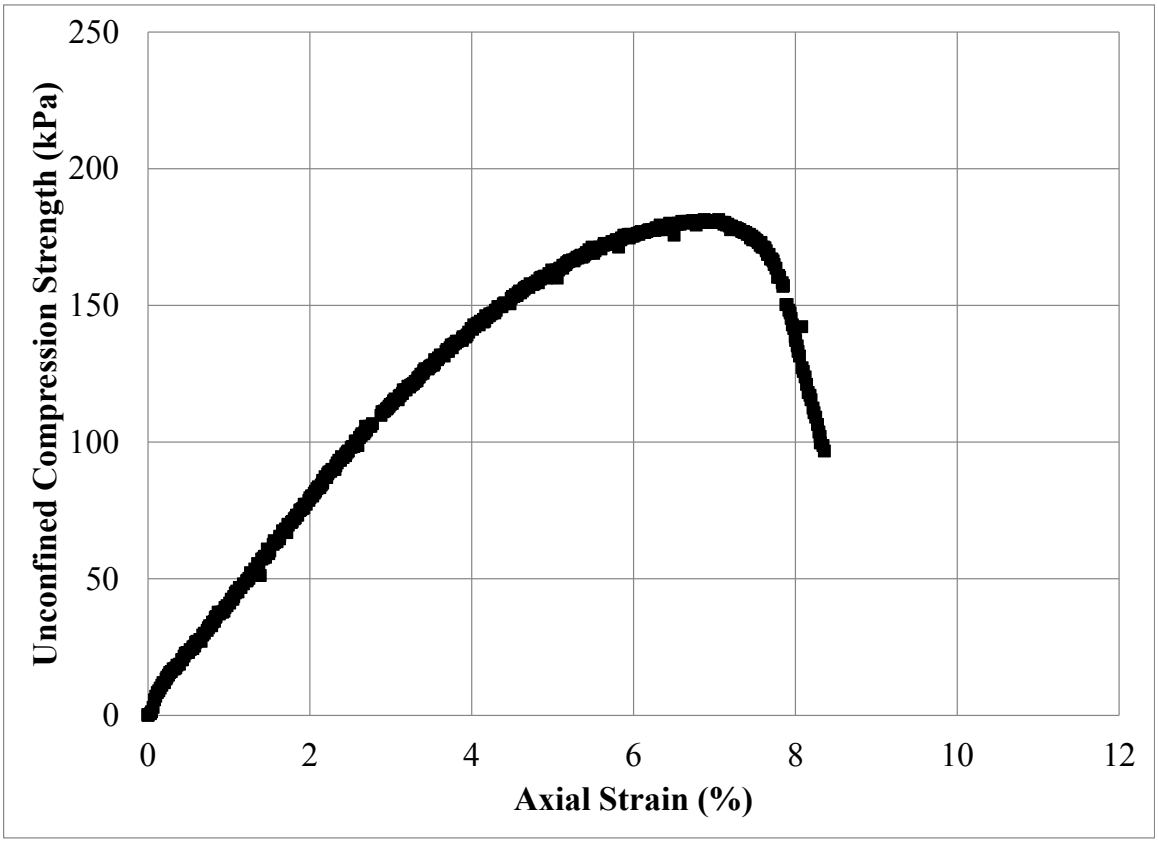

(c)

Figure C.3: Unconfined Compression Test Specimen No. 21_1R: (a) Photograph Prior to Testing; (b) Photograph Post Testing; and (c) Stress – Strain Data

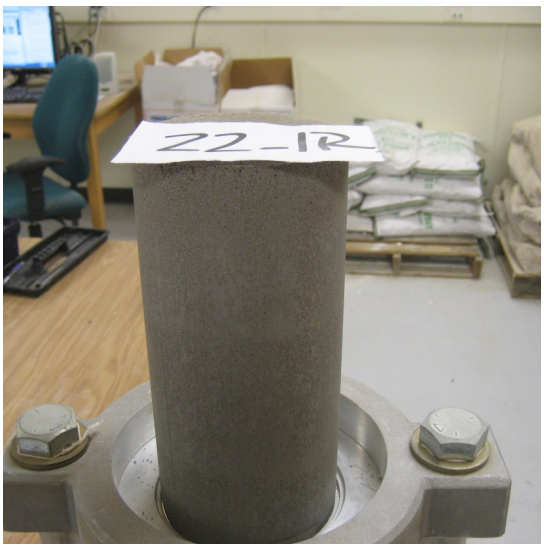

(a)

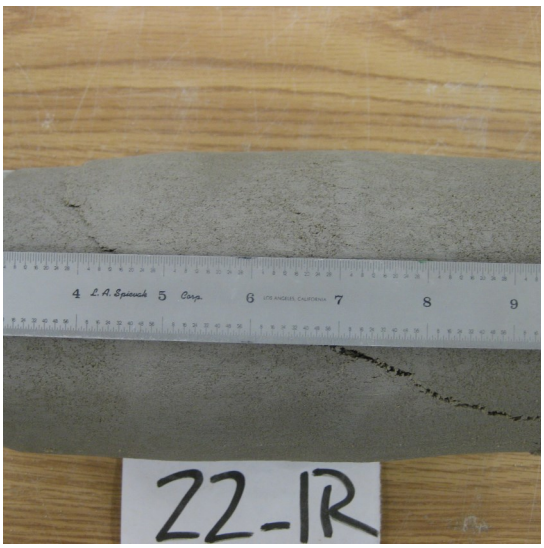

(b)

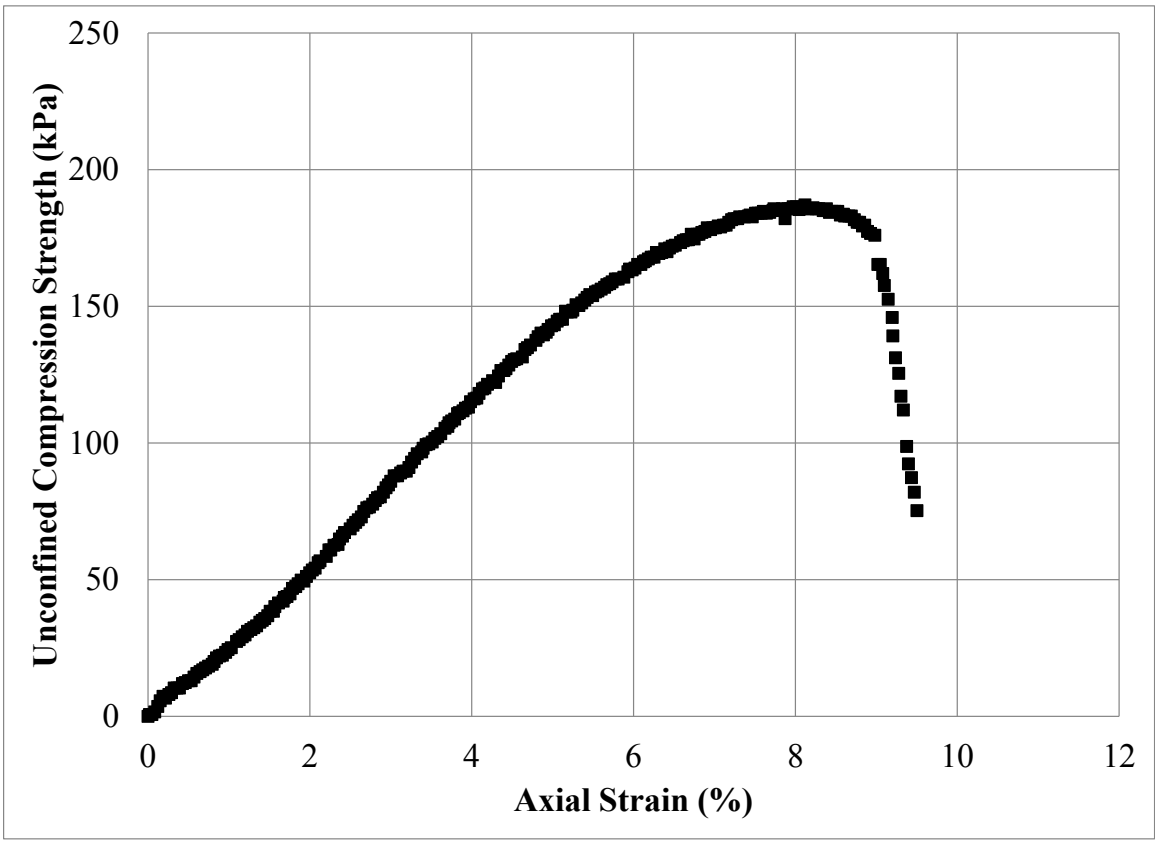

(c)

Figure C.4: Unconfined Compression Test Specimen No. 22_1R: (a) Photograph Prior to Testing; (b) Photograph Post Testing; and (c) Stress – Strain Data

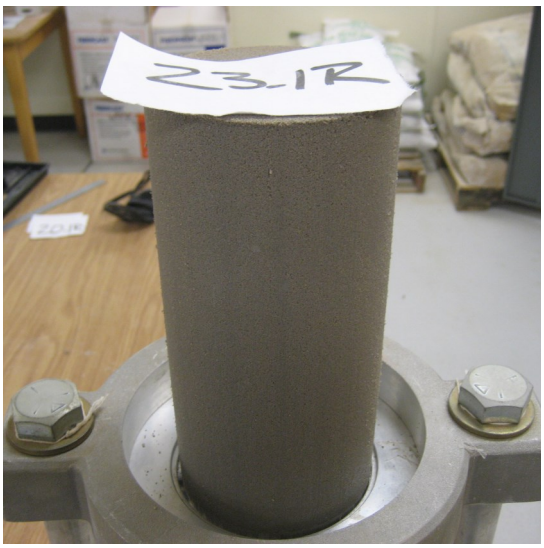

(a)

(b)

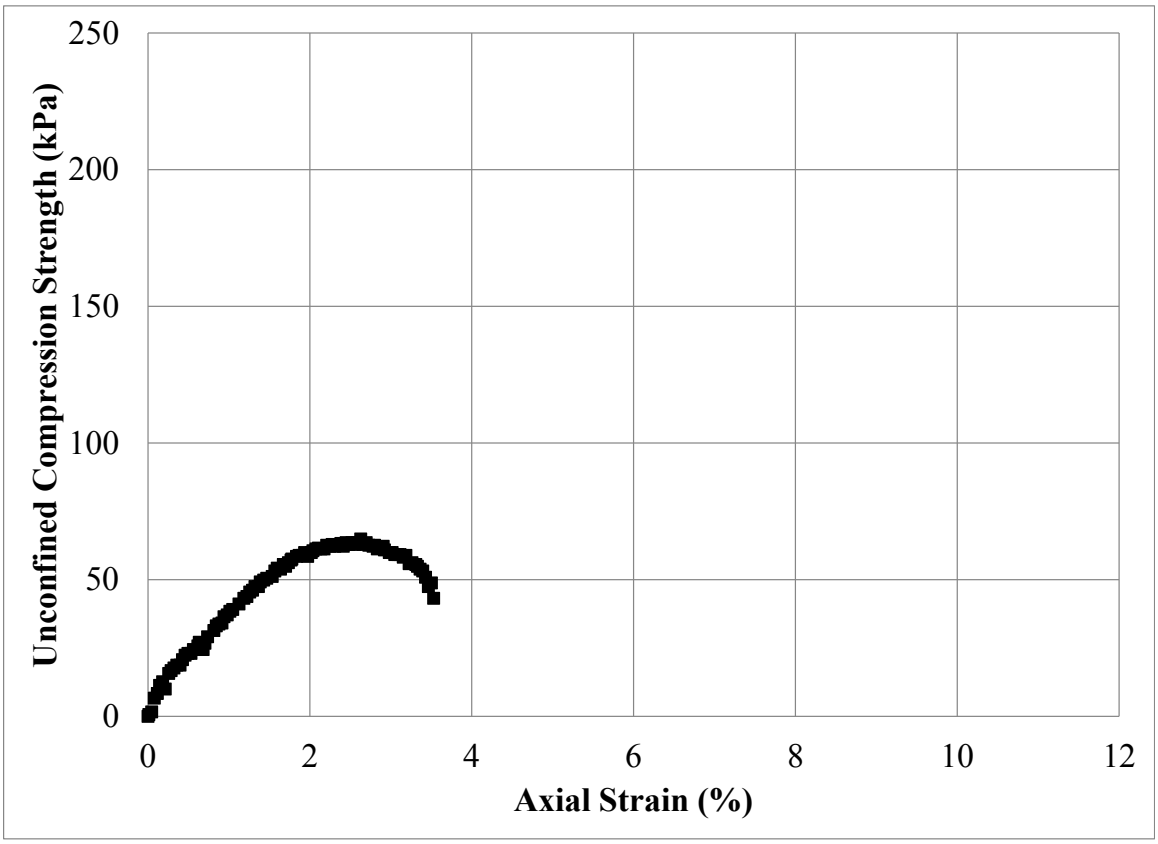

(c)

Figure C.5: Unconfined Compression Test Specimen No. 23_1R: (a) Photograph Prior to Testing; (b) Photograph Post Testing; and (c) Stress – Strain Data

(a)

(b)

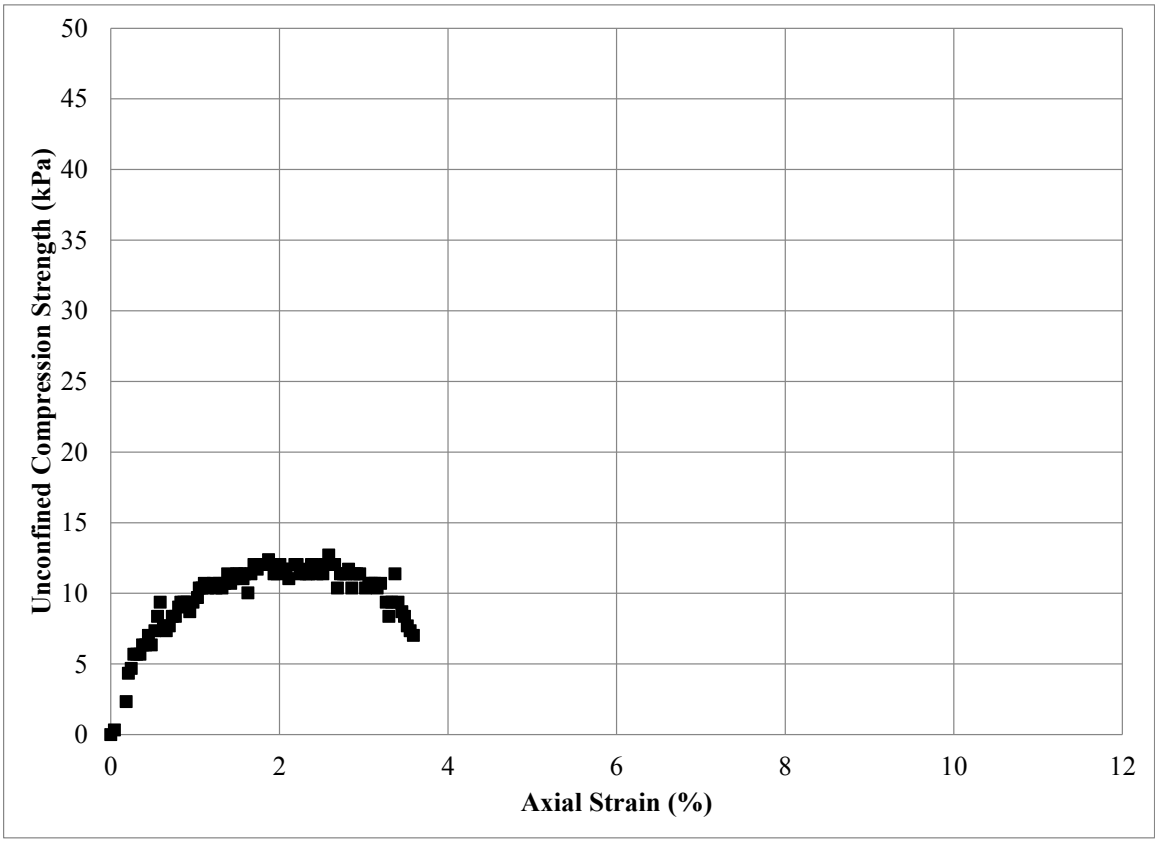

(c)

Figure C.6: Unconfined Compression Test Specimen No. 24R: (a) Photograph Prior to Testing; (b) Photograph Post Testing; and (c) Stress – Strain Data

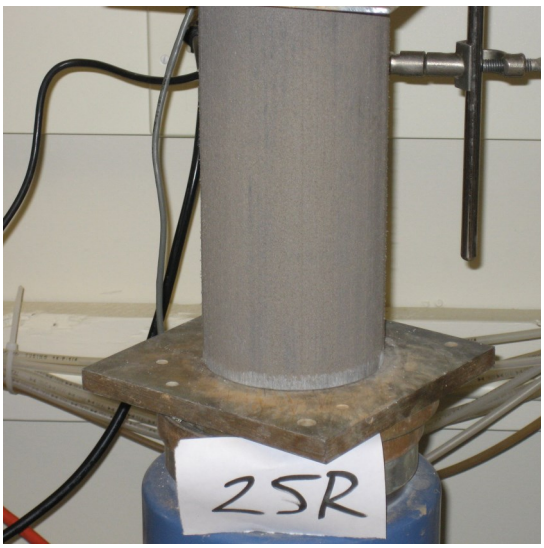

(a)

(b)

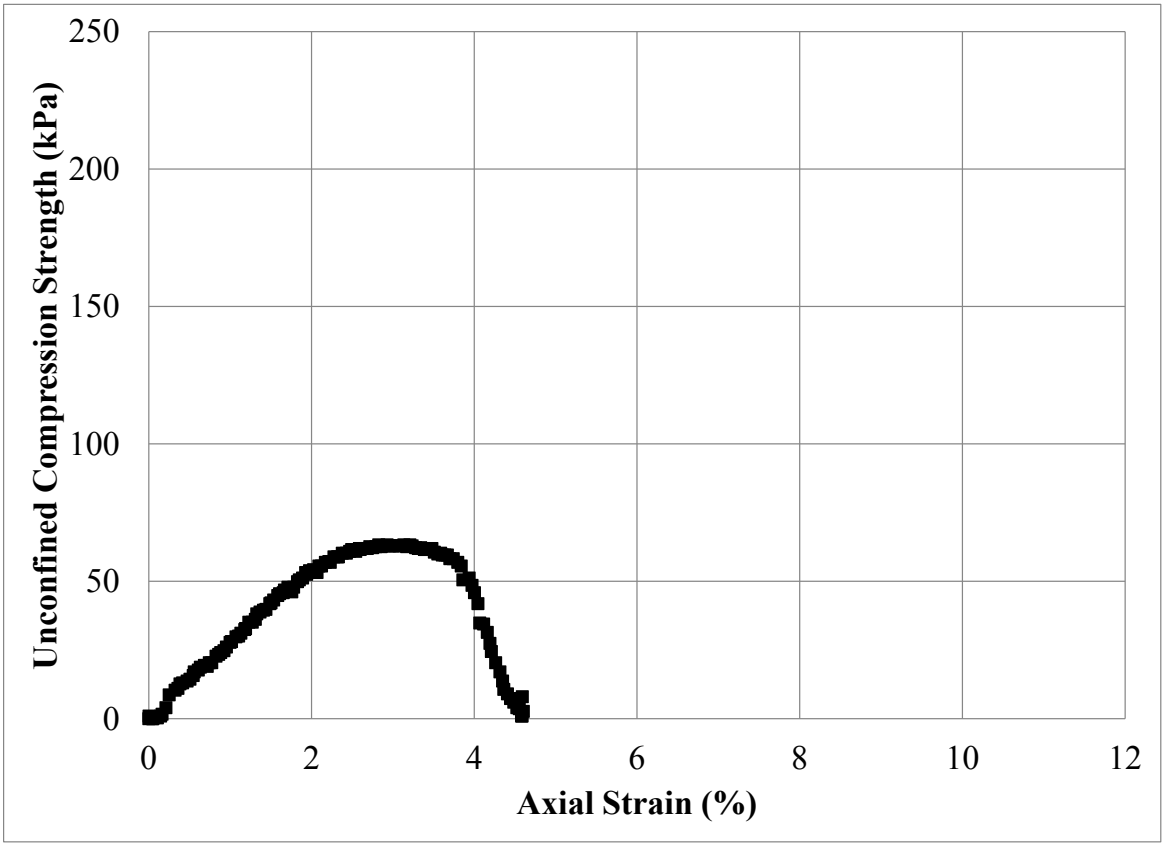

(c)

Figure C.7: Unconfined Compression Test Specimen No. 25R: (a) Photograph Prior to Testing; (b) Photograph Post Testing; and (c) Stress – Strain Data

(a)

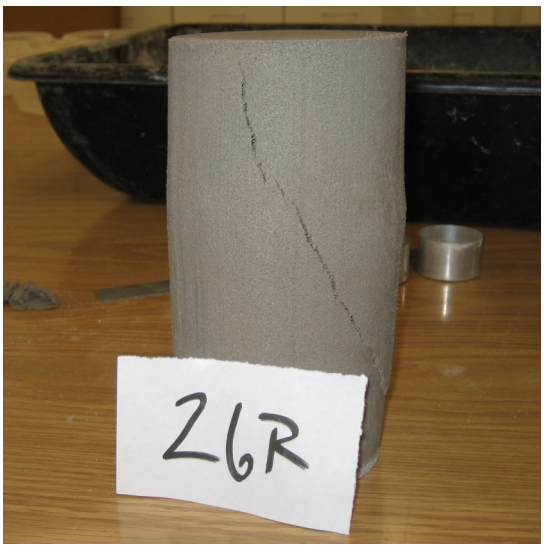

(b)

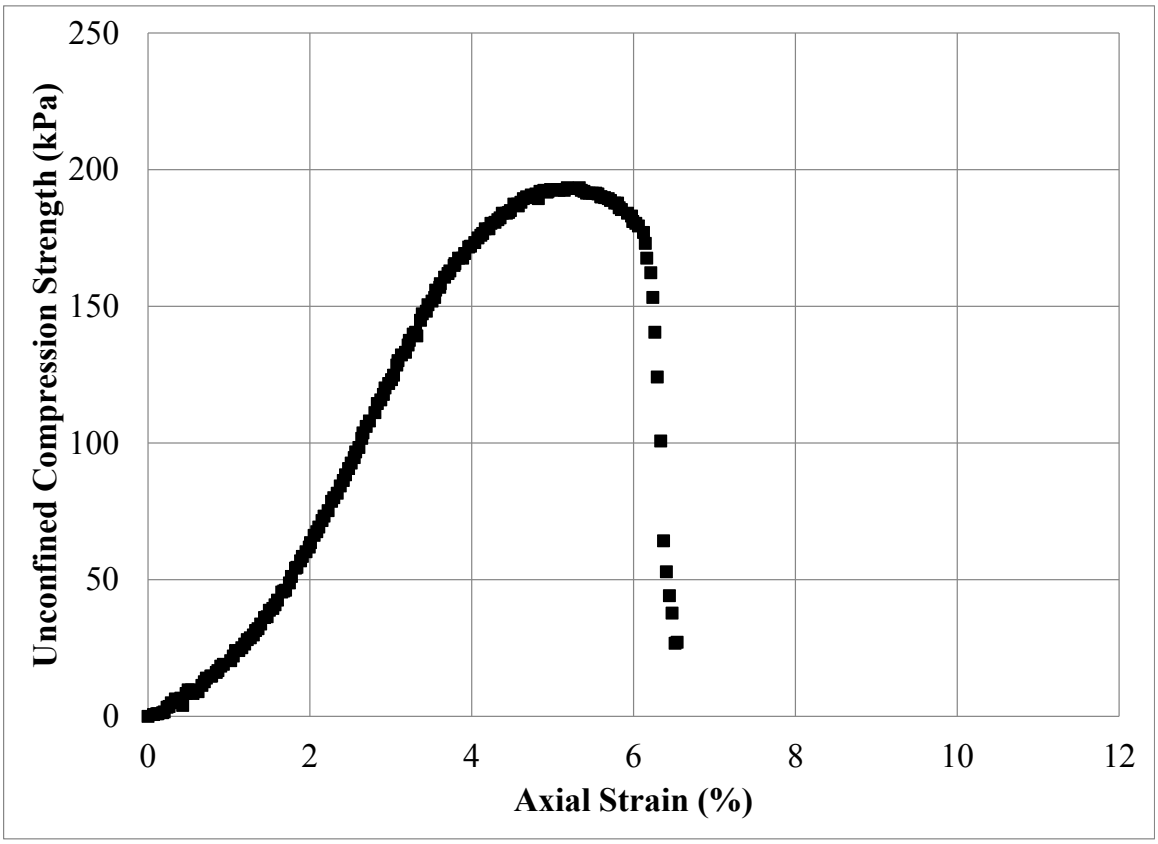

(c)

Figure C.8: Unconfined Compression Test Specimen No. 26R: (a) Photograph Prior to Testing; (b) Photograph Post Testing; and (c) Stress – Strain Data

(a)

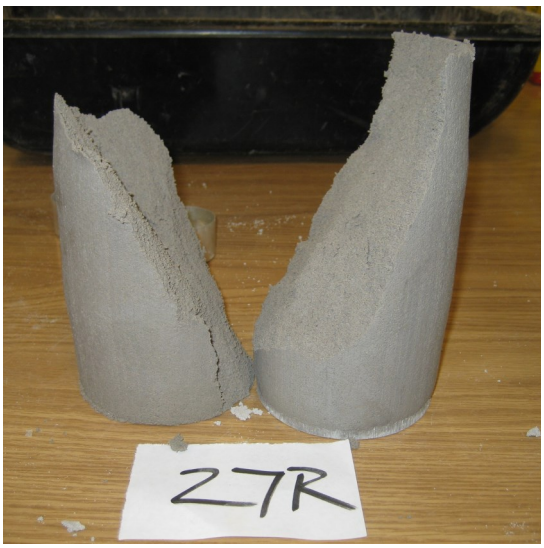

(b)

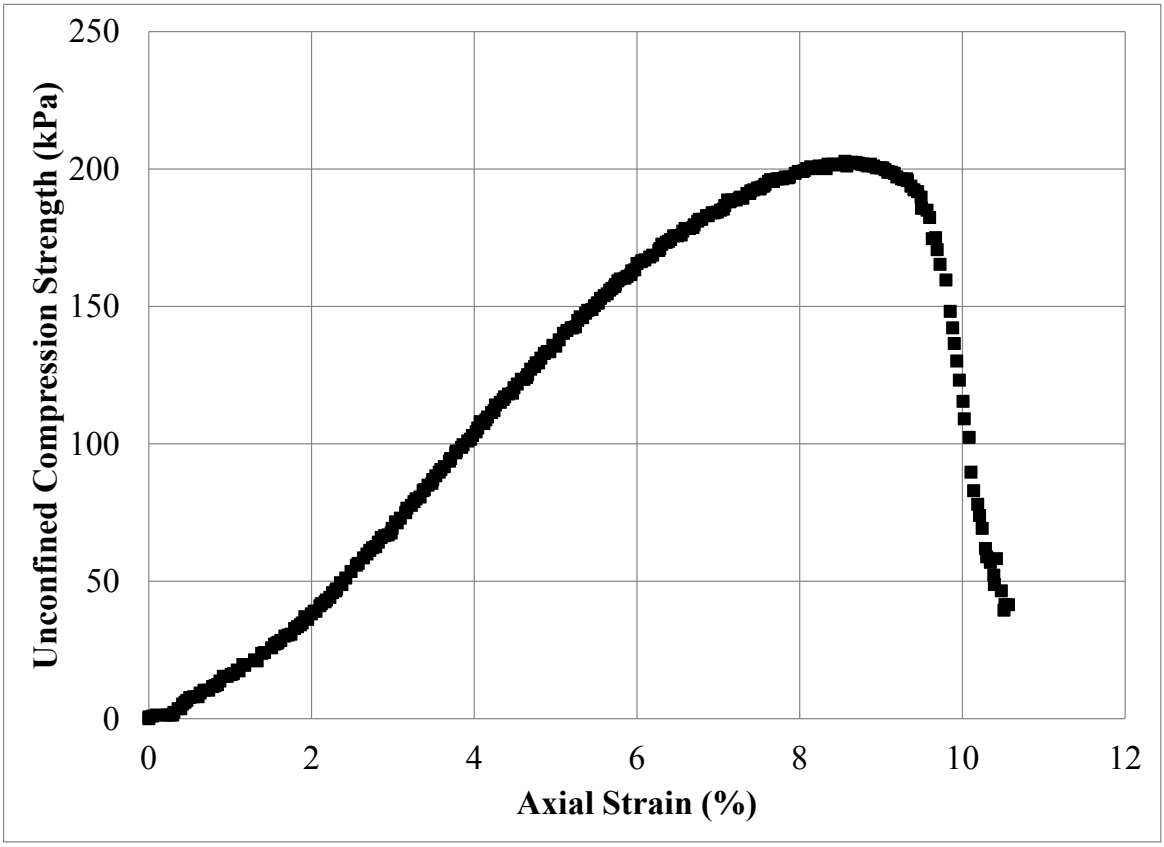

(c)

Figure C.9: Unconfined Compression Test Specimen No. 27R: (a) Photograph Prior to Testing; (b) Photograph Post Testing; and (c) Stress – Strain Data

(a)

(b)

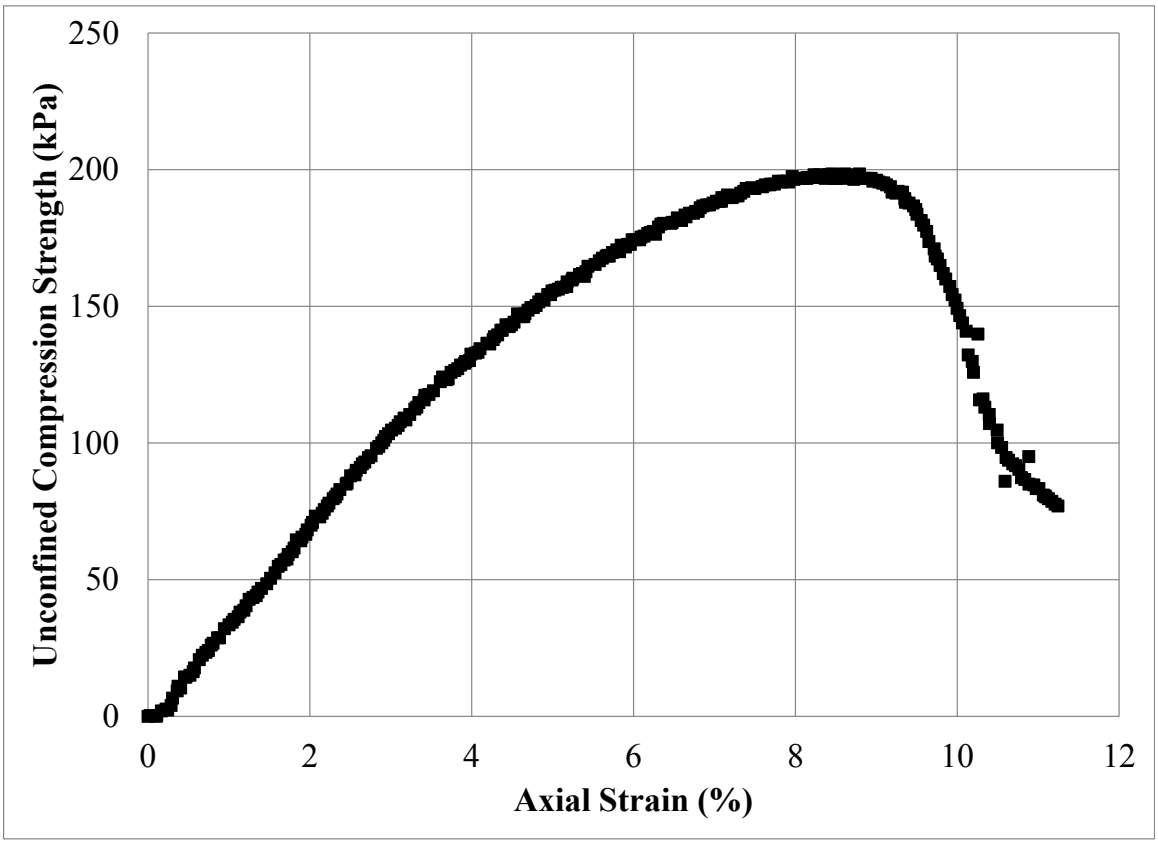

(c)

Figure C.10: Unconfined Compression Test Specimen No. 28R: (a) Photograph Prior to Testing; (b) Photograph Post Testing; and (c) Stress – Strain Data

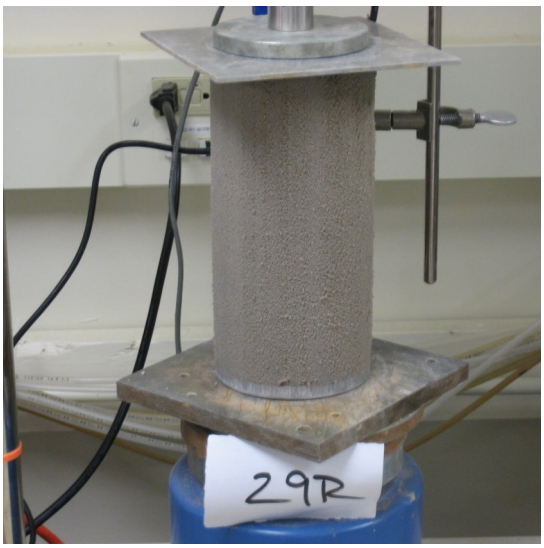

(a)

(b)

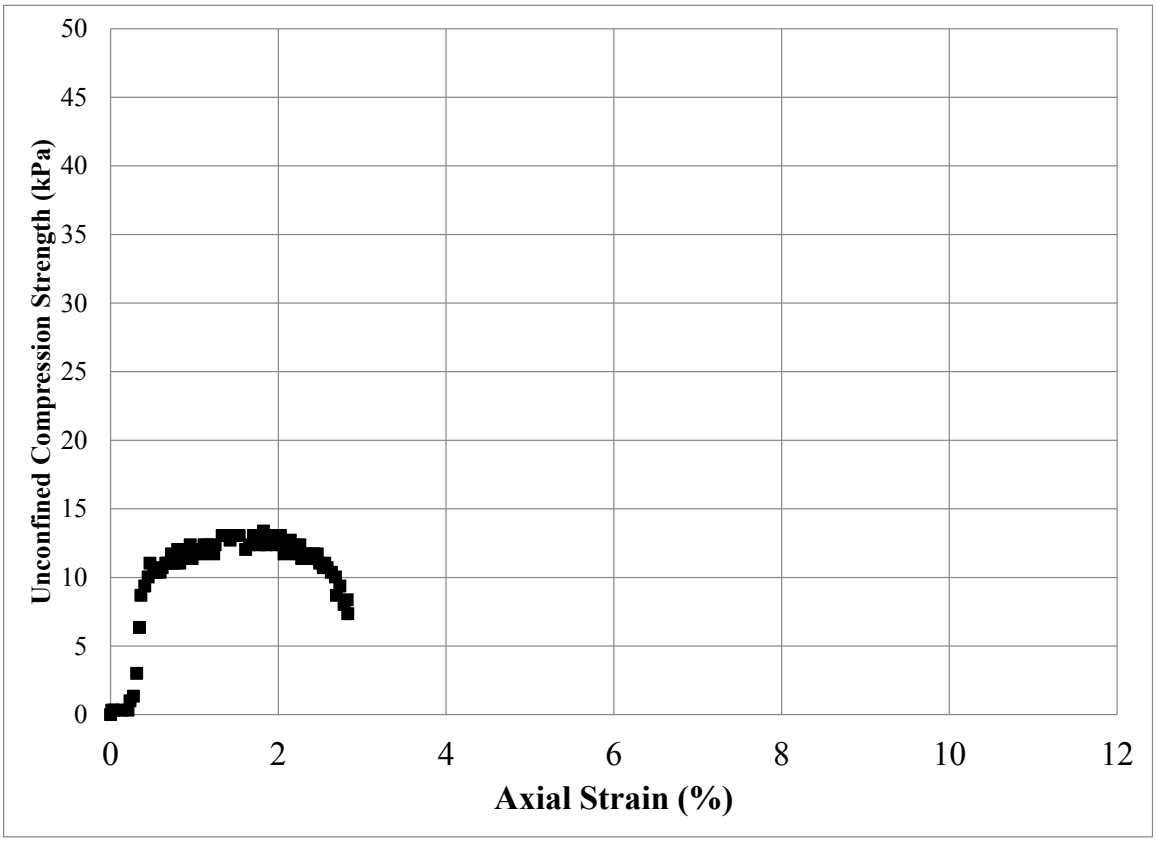

(c)

Figure C.11: Unconfined Compression Test Specimen No. 29R: (a) Photograph Prior to Testing; (b) Photograph Post Testing; and (c) Stress – Strain Data

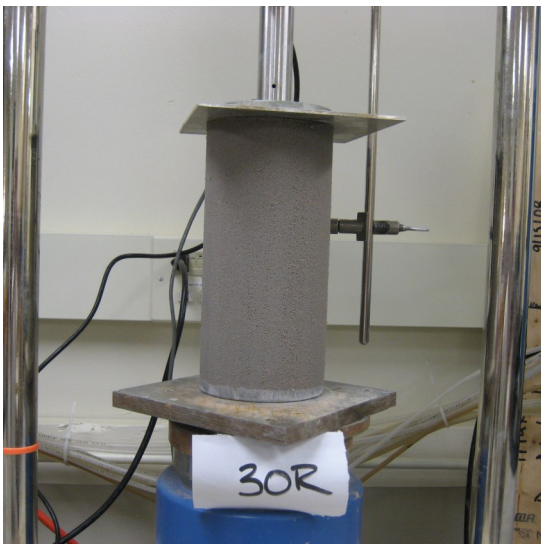

(a)

(b)

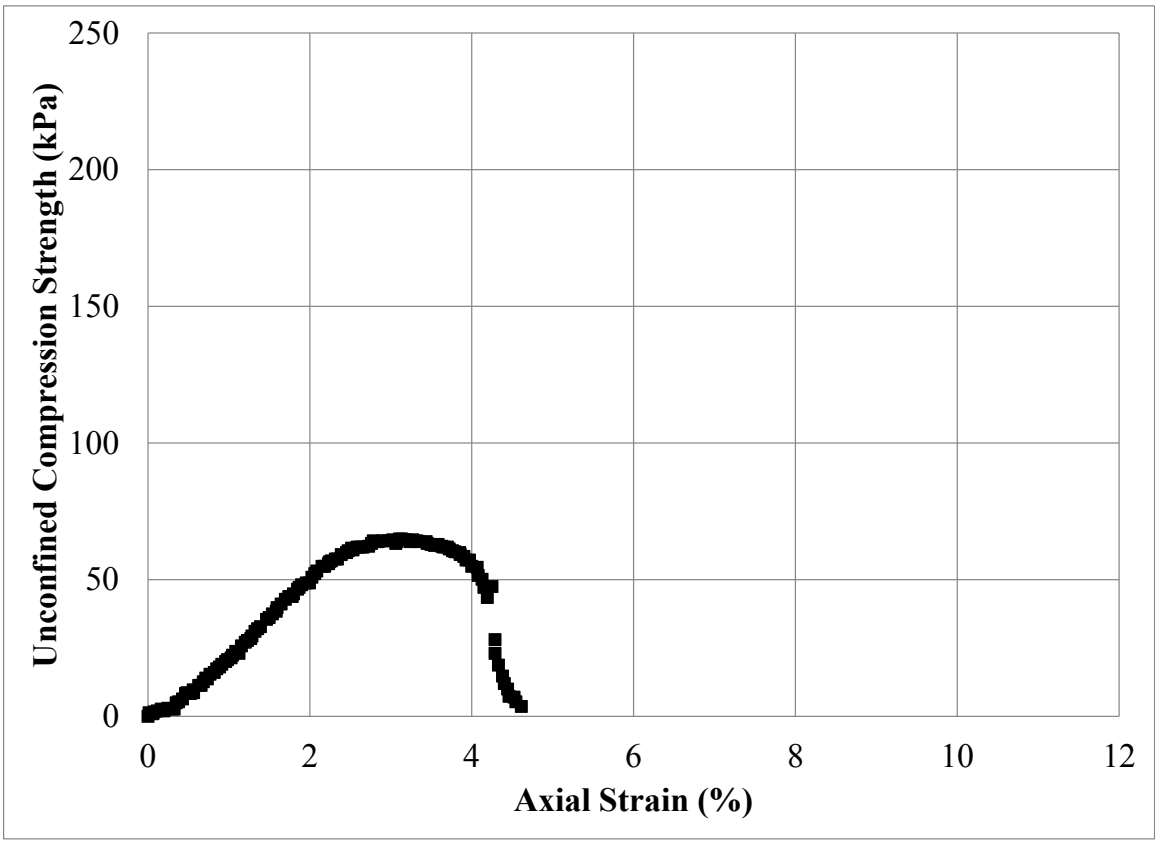

(c)

Figure C.12: Unconfined Compression Test Specimen No. 30R: (a) Photograph Prior to Testing; (b) Photograph Post Testing; and (c) Stress – Strain Data

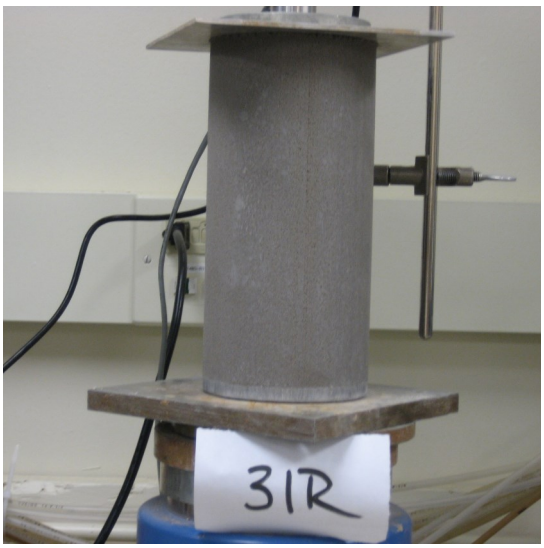

(a)

(b)

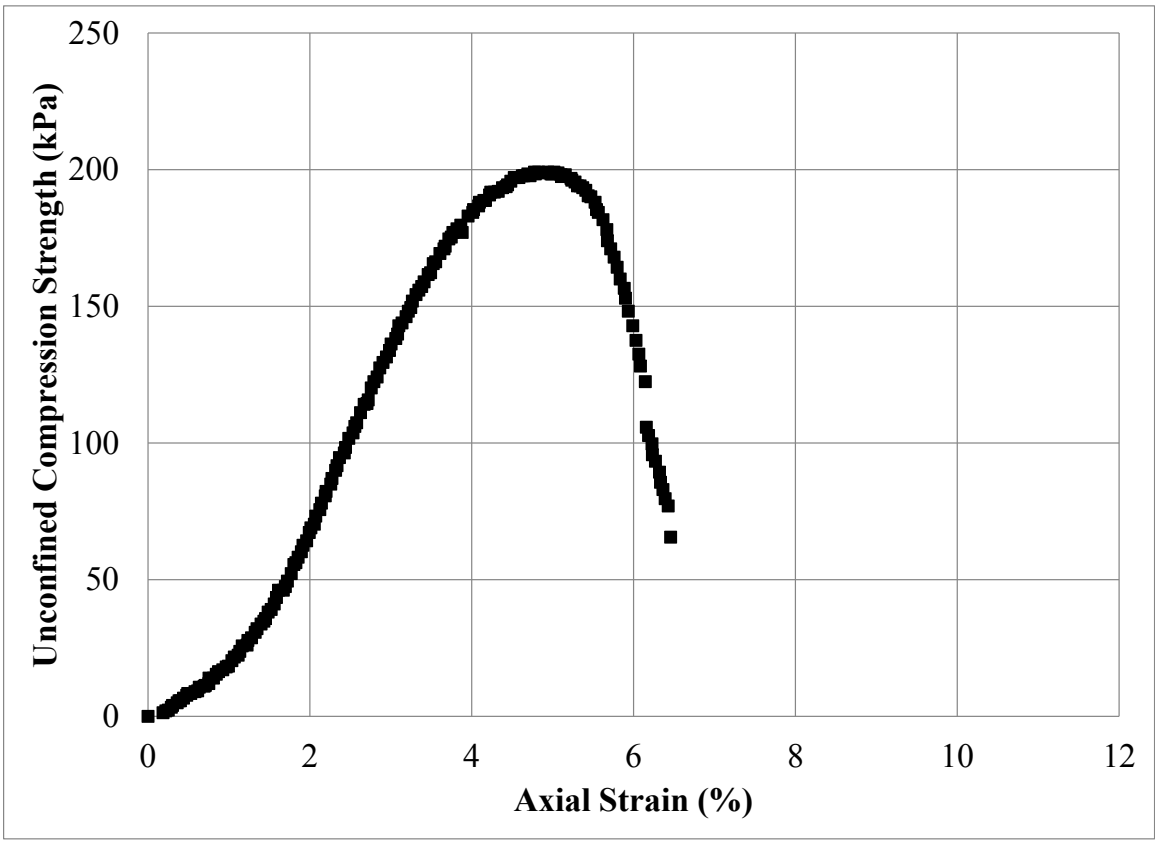

(c)

Figure C.13: Unconfined Compression Test Specimen No. 31R: (a) Photograph Prior to Testing; (b) Photograph Post Testing; and (c) Stress – Strain Data

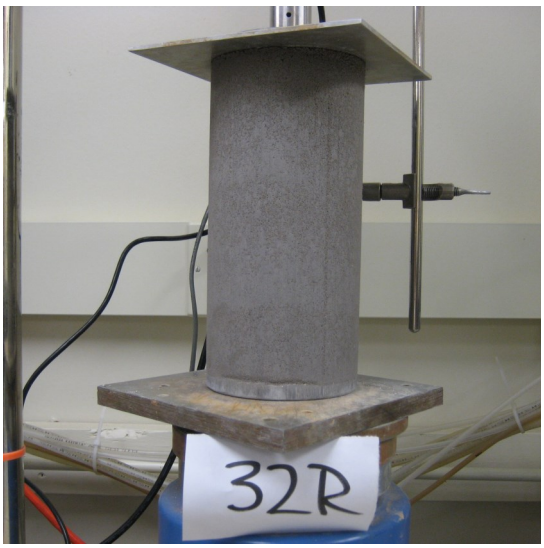

(a)

(b)

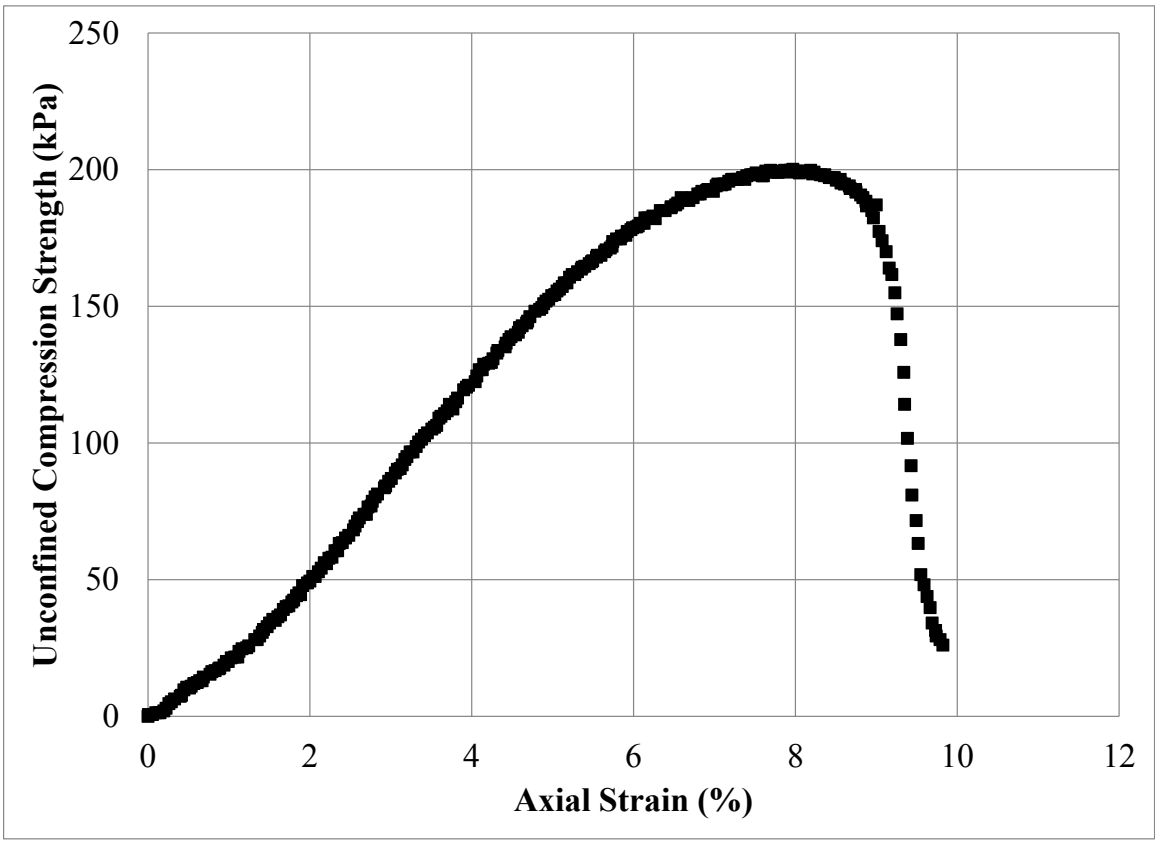

(c)

Figure C.14: Unconfined Compression Test Specimen No. 32R: (a) Photograph Prior to Testing; (b) Photograph Post Testing; and (c) Stress – Strain Data

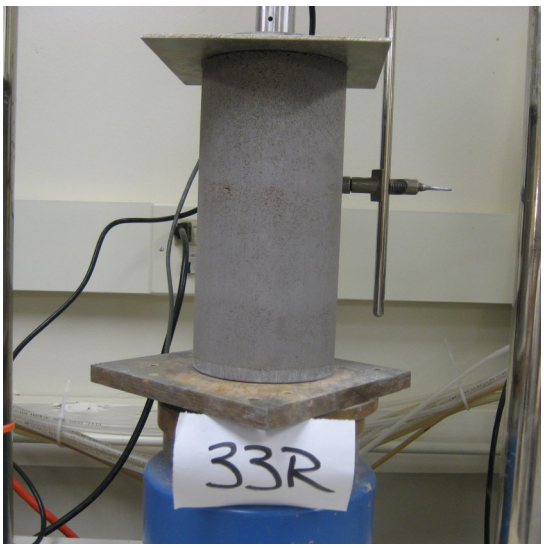

(a)

(b)

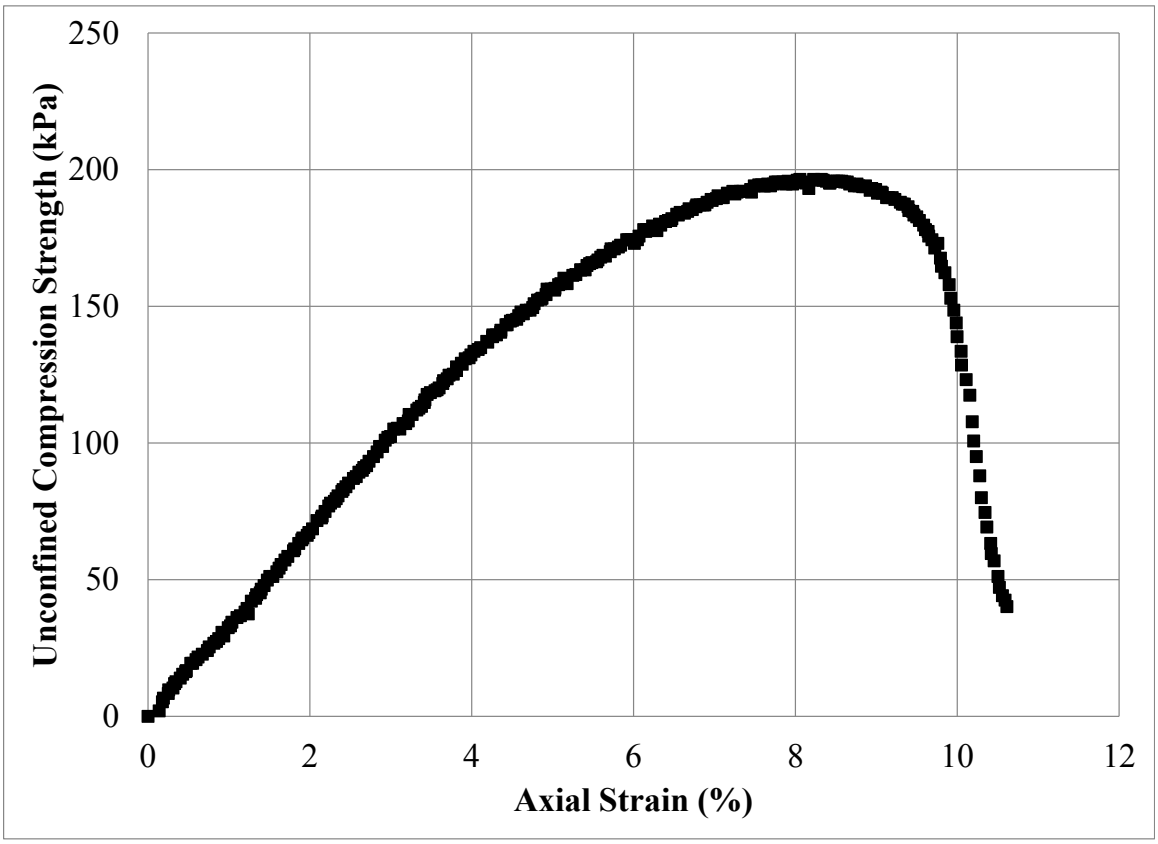

(c)

Figure C.15: Unconfined Compression Test Specimen No. 33R: (a) Photograph Prior to Testing; (b) Photograph Post Testing; and (c) Stress – Strain Data

(a)

(b)

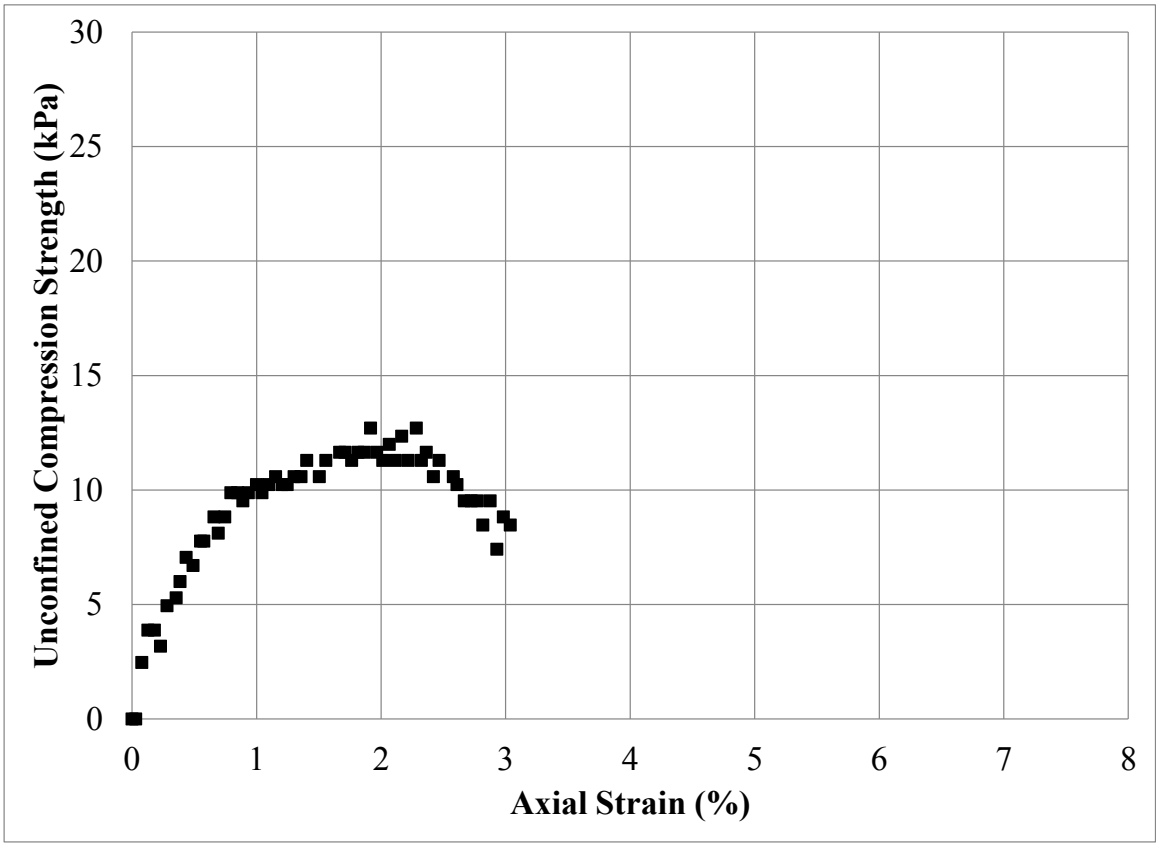

(c)

Figure C.16: Unconfined Compression Test Specimen No. 73R: (a) Photograph Prior to Testing; (b) Photograph Post Testing; and (c) Stress – Strain Data

(a)

(b)

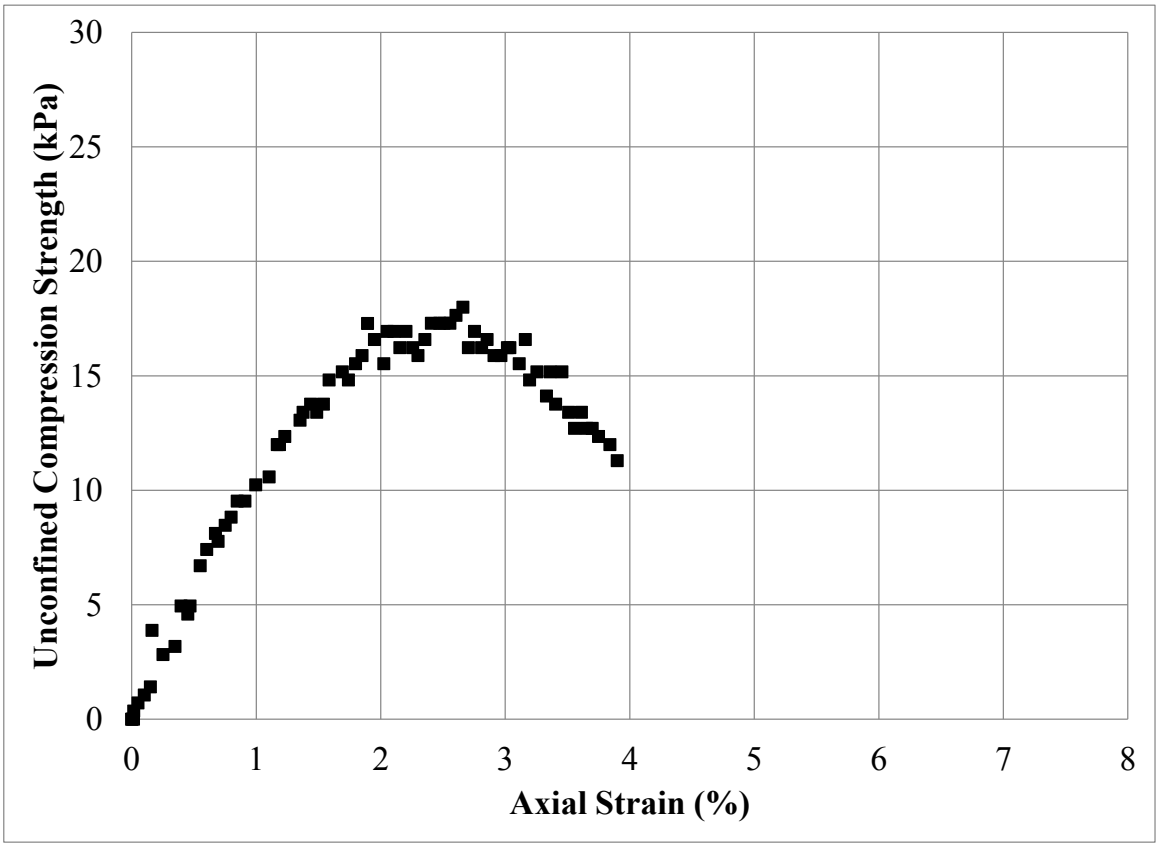

(c)

Figure C.17: Unconfined Compression Test Specimen No. 74R: (a) Photograph Prior to Testing; (b) Photograph Post Testing; and (c) Stress – Strain Data

(a)

(b)

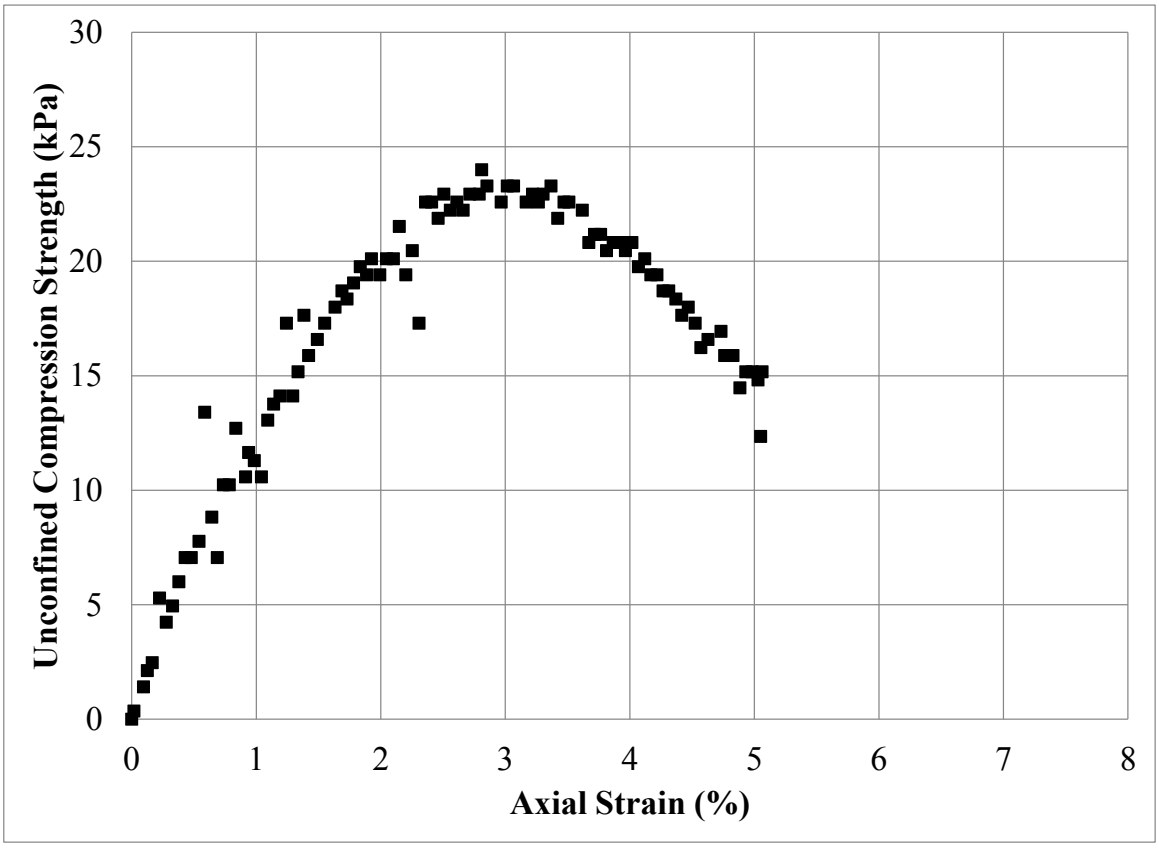

(c)

Figure C.18: Unconfined Compression Test Specimen No. 75R: (a) Photograph Prior to Testing; (b) Photograph Post Testing; and (c) Stress – Strain Data

(a)

(b)

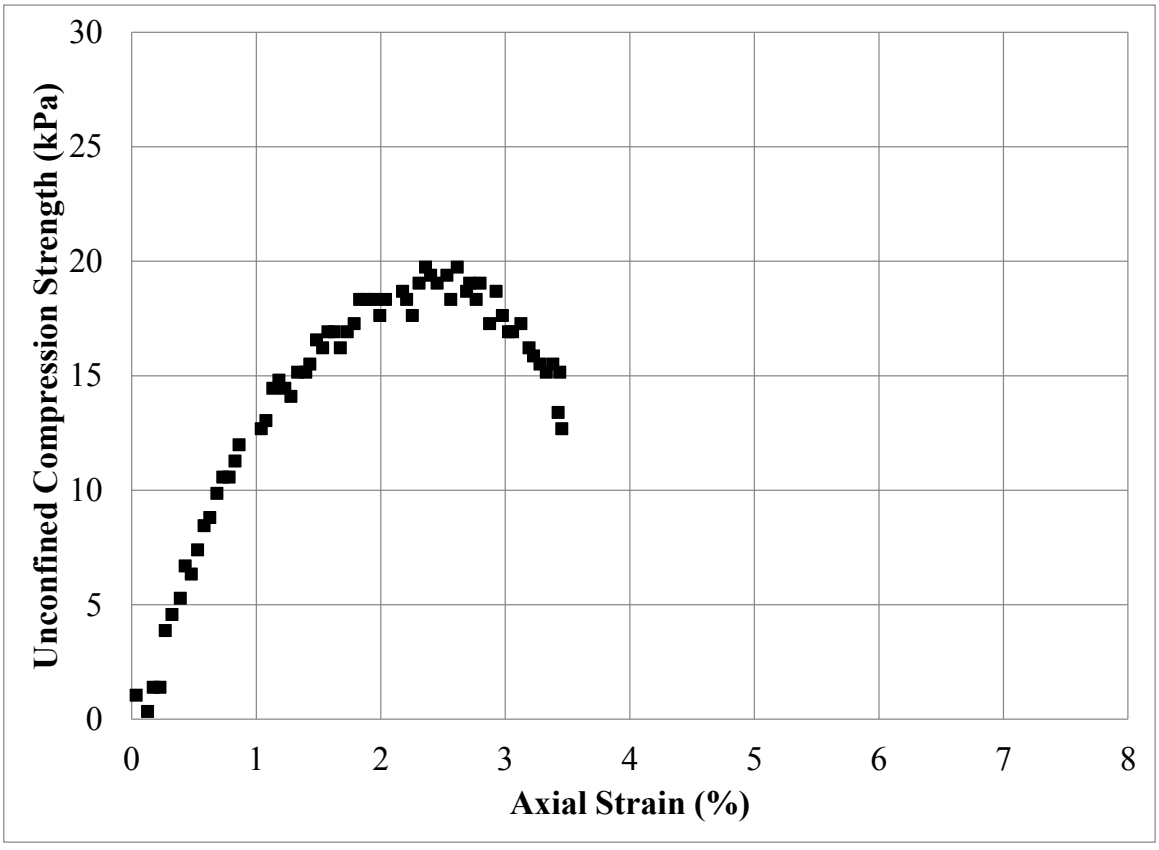

(c)

Figure C.19: Unconfined Compression Test Specimen No. 76R: (a) Photograph Prior to Testing; (b) Photograph Post Testing; and (c) Stress – Strain Data

(a)

(b)

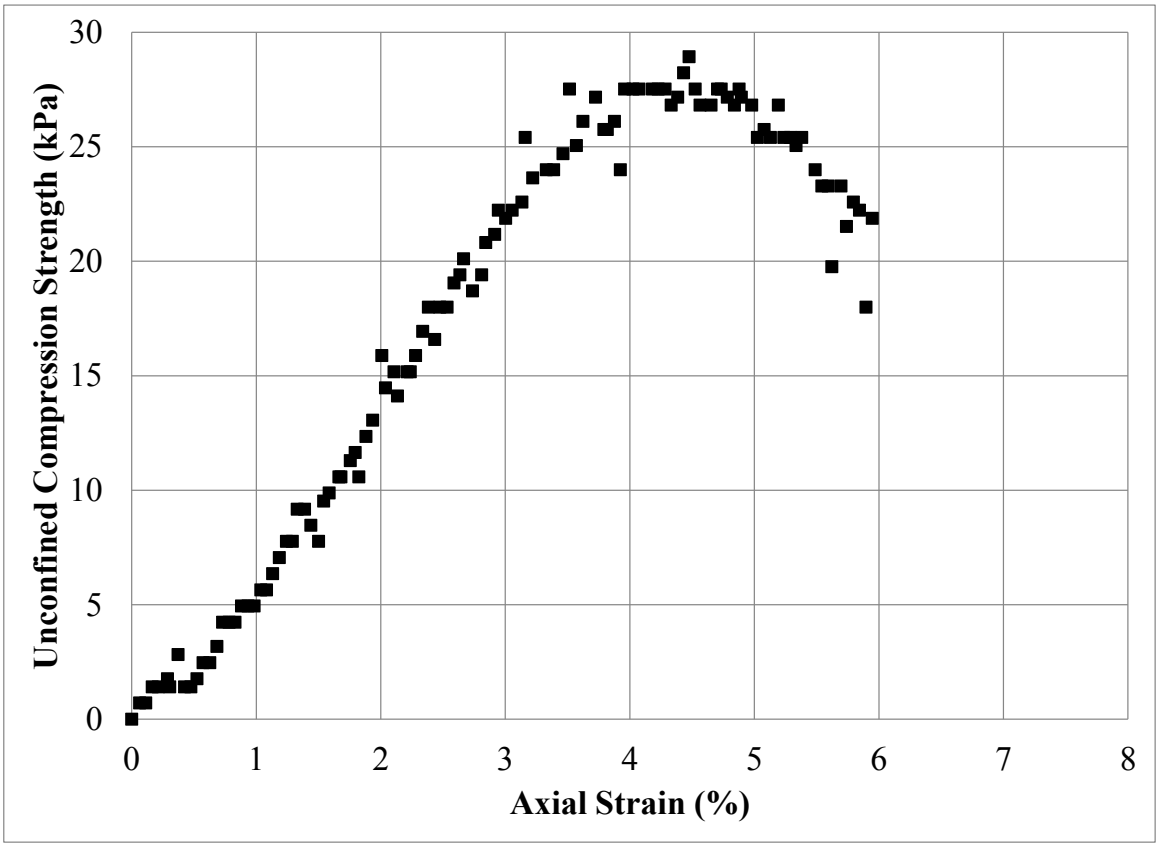

(c)

Figure C.20: Unconfined Compression Test Specimen No. 77R: (a) Photograph Prior to Testing; (b) Photograph Post Testing; and (c) Stress – Strain Data

(a)

(b)

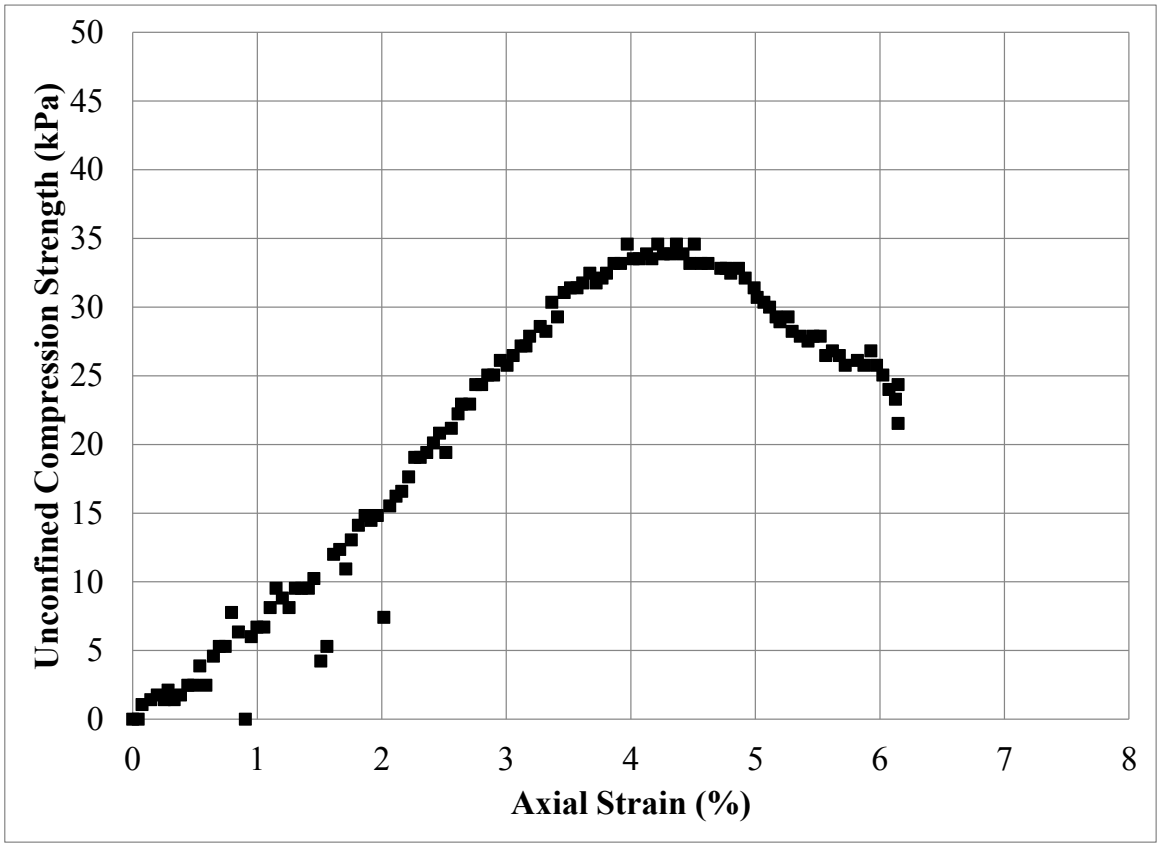

(c)

Figure C.21: Unconfined Compression Test Specimen No. 78R: (a) Photograph Prior to Testing; (b) Photograph Post Testing; and (c) Stress – Strain Data

(a)

(b)

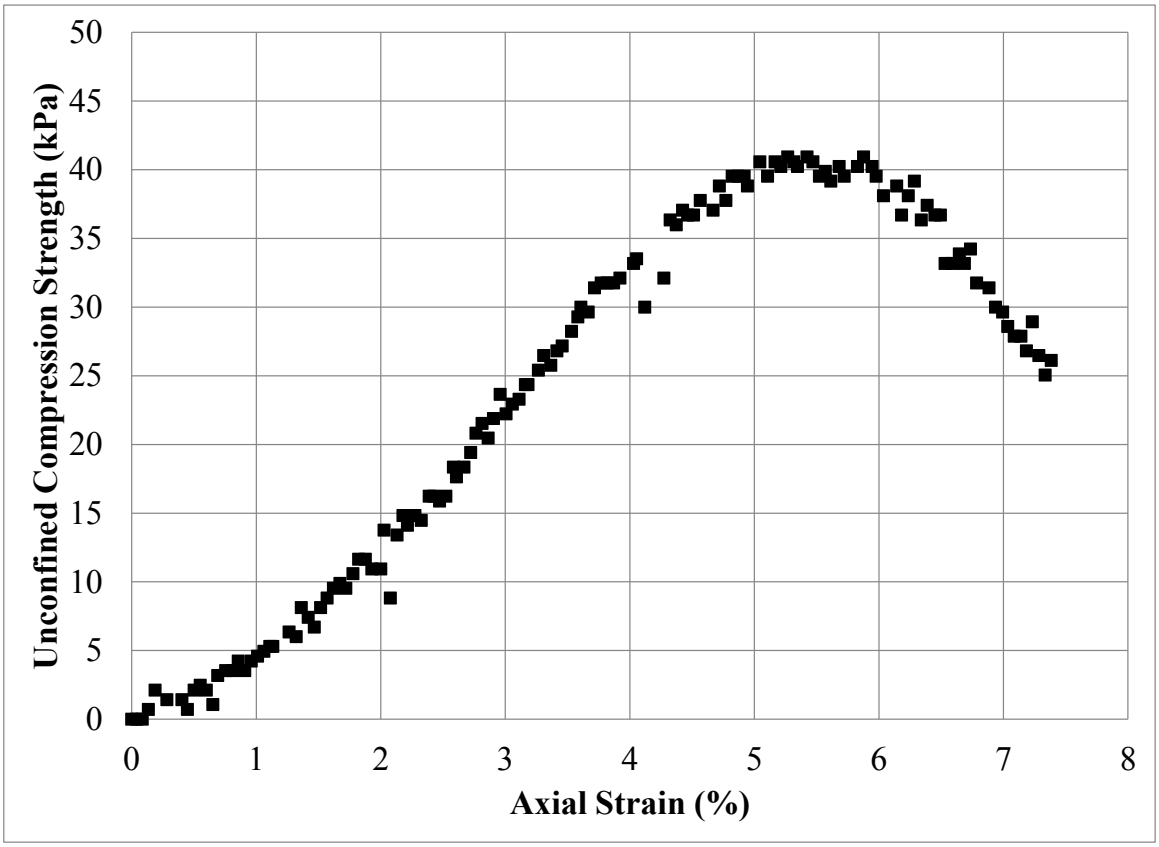

(c)

Figure C.22: Unconfined Compression Test Specimen No. 79R: (a) Photograph Prior to Testing; (b) Photograph Post Testing; and (c) Stress – Strain Data

Photographs for Test Specimen 80R are not Available

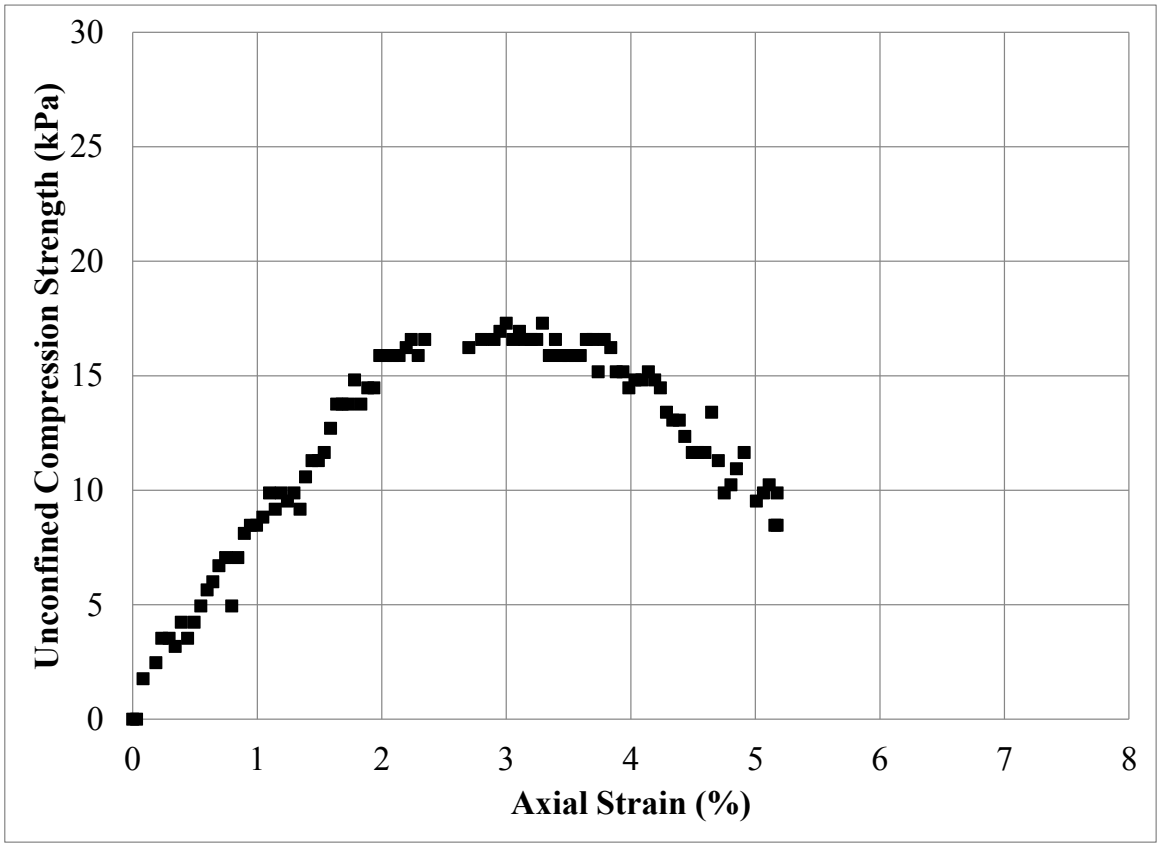

Figure C.23: Unconfined Compression Test Specimen No. 80R: Stress – Strain Data

(a)

(b)

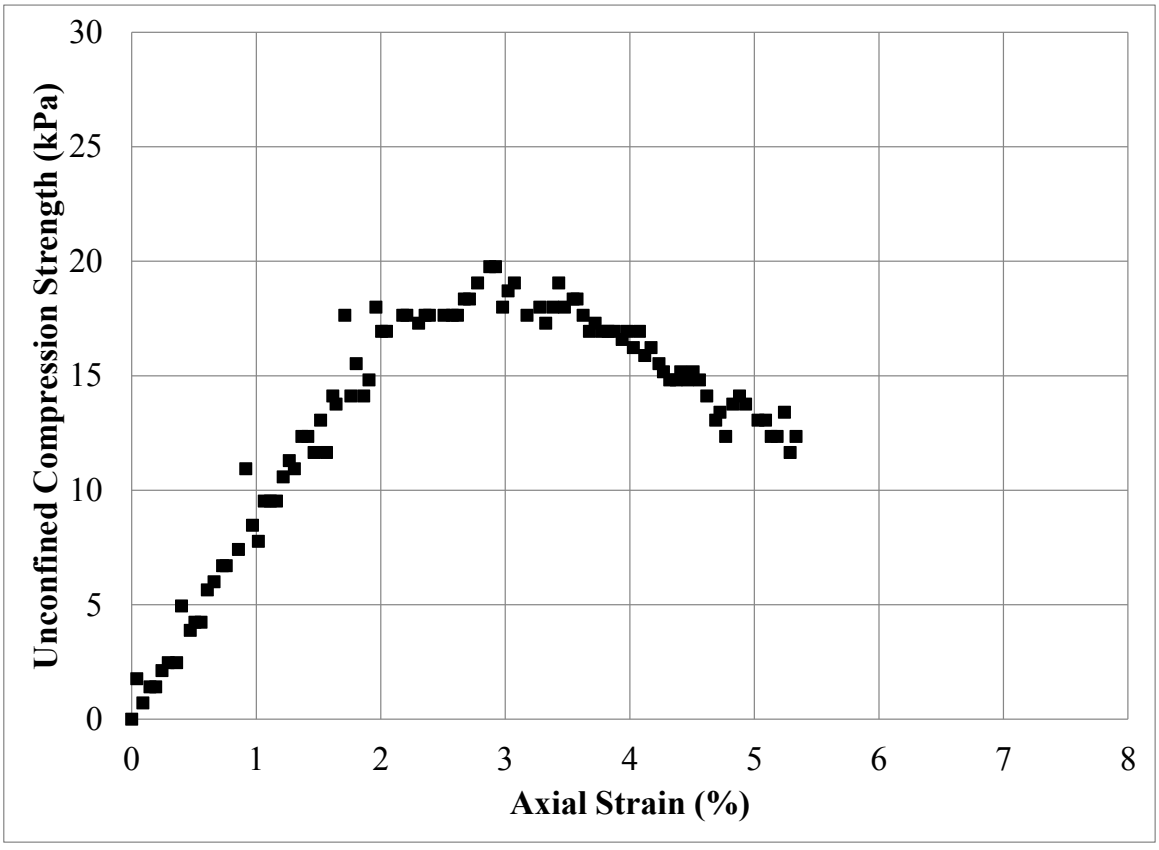

(c)

Figure C.24: Unconfined Compression Test Specimen No. 81R: (a) Photograph Prior to Testing; (b) Photograph Post Testing; and (c) Stress – Strain Data

(a)

(b)

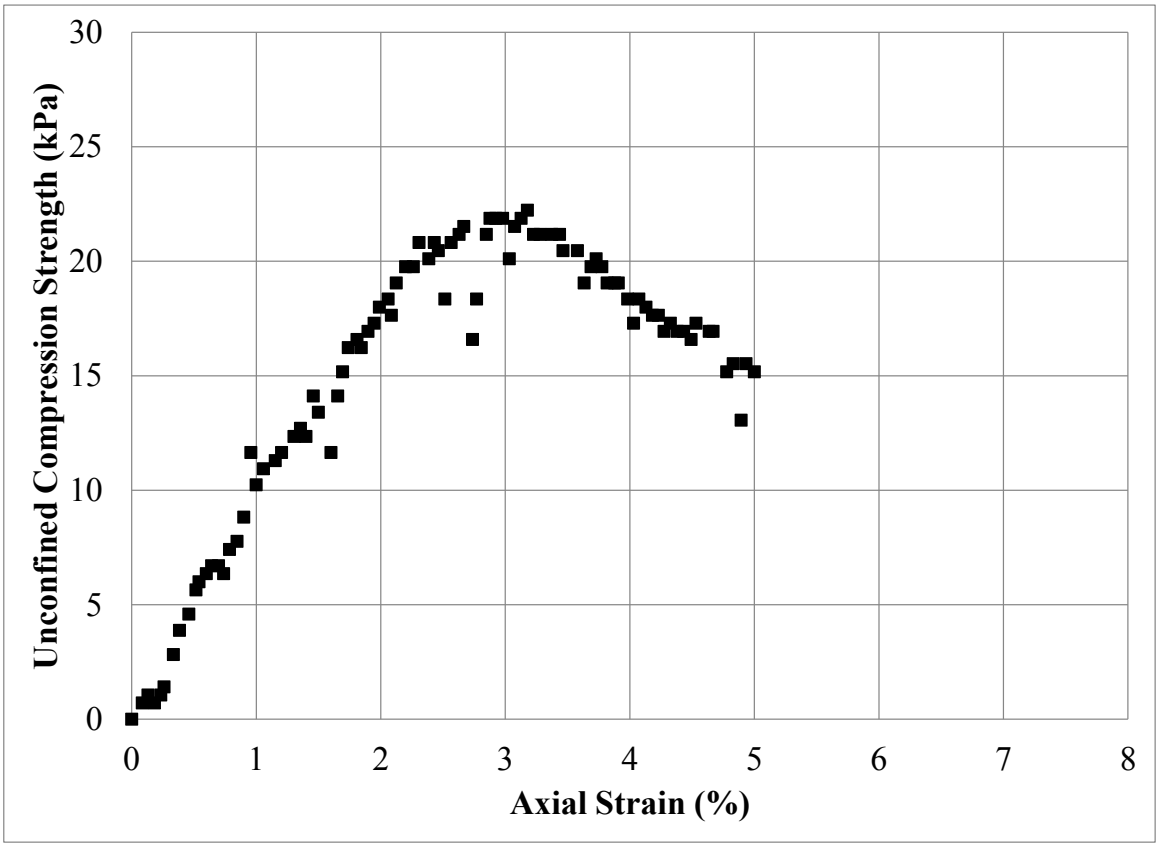

(c)

Figure C.25: Unconfined Compression Test Specimen No. 82R: (a) Photograph Prior to Testing; (b) Photograph Post Testing; and (c) Stress – Strain Data

(a)

(b)

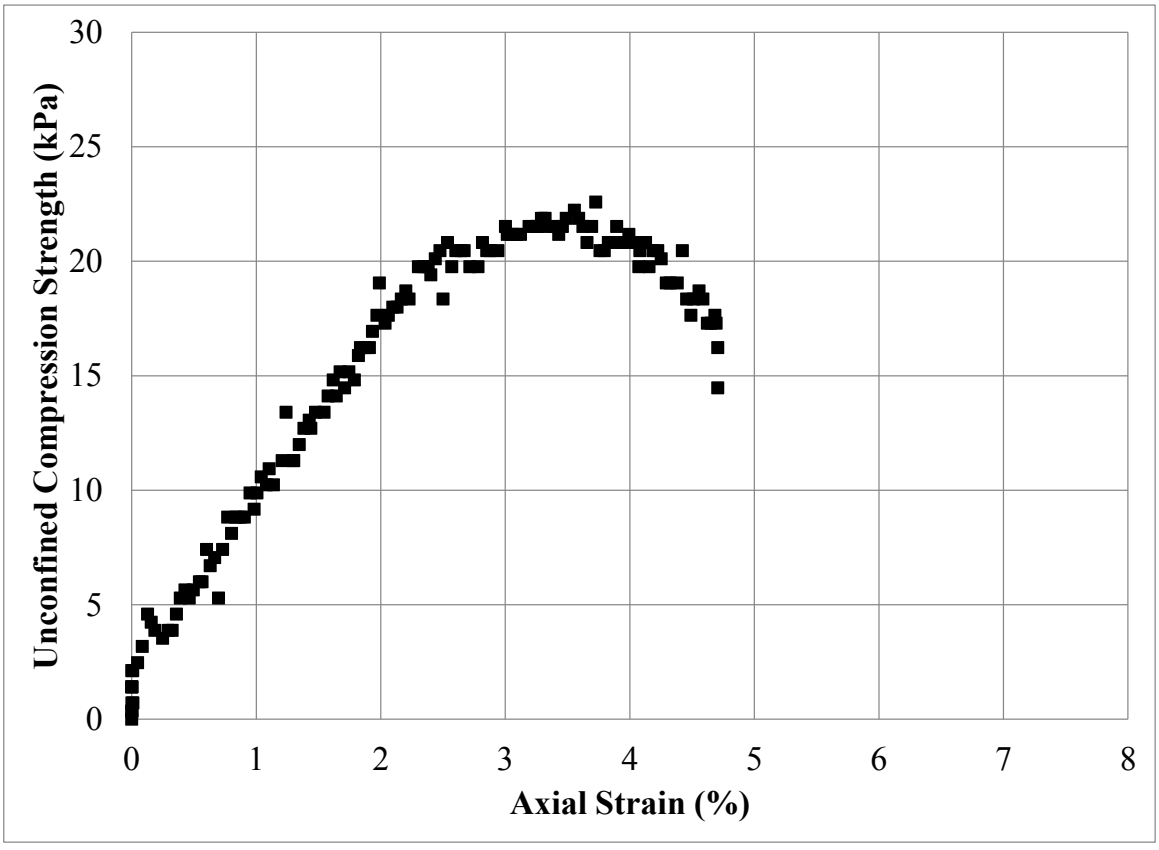

(c)

Figure C.26: Unconfined Compression Test Specimen No. 83R: (a) Photograph Prior to Testing; (b) Photograph Post Testing; and (c) Stress – Strain Data

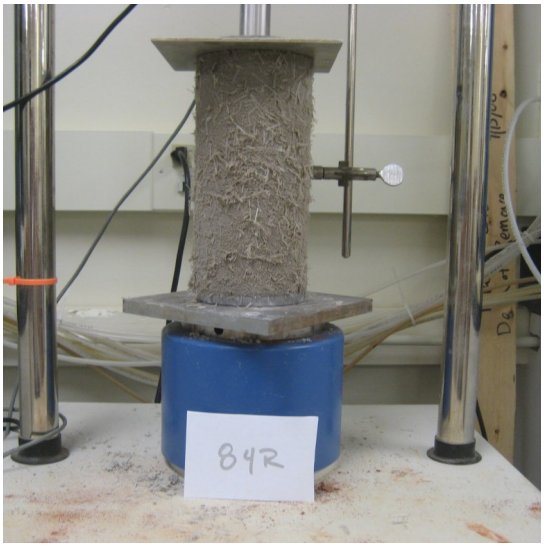

(a)

(b)

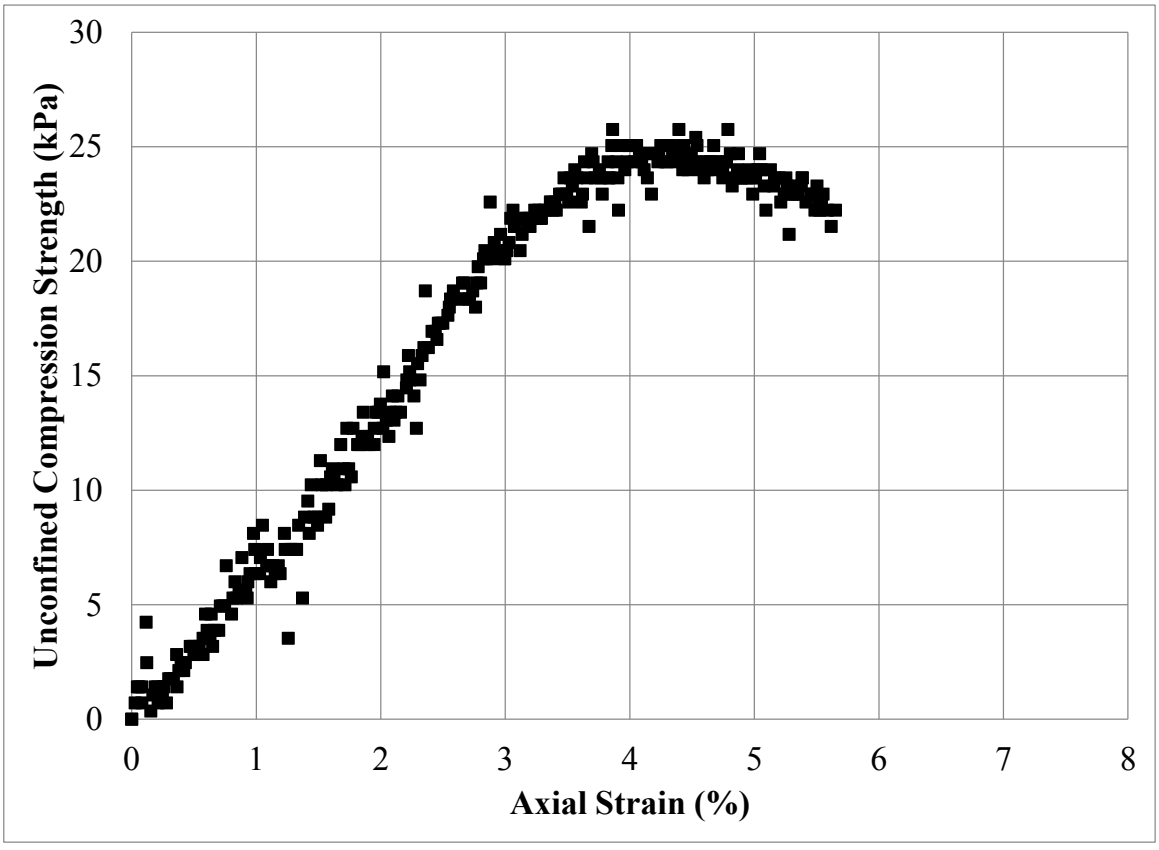

(c)

Figure C.27: Unconfined Compression Test Specimen No. 84R: (a) Photograph Prior to Testing; (b) Photograph Post Testing; and (c) Stress – Strain Data

(a)

(b)

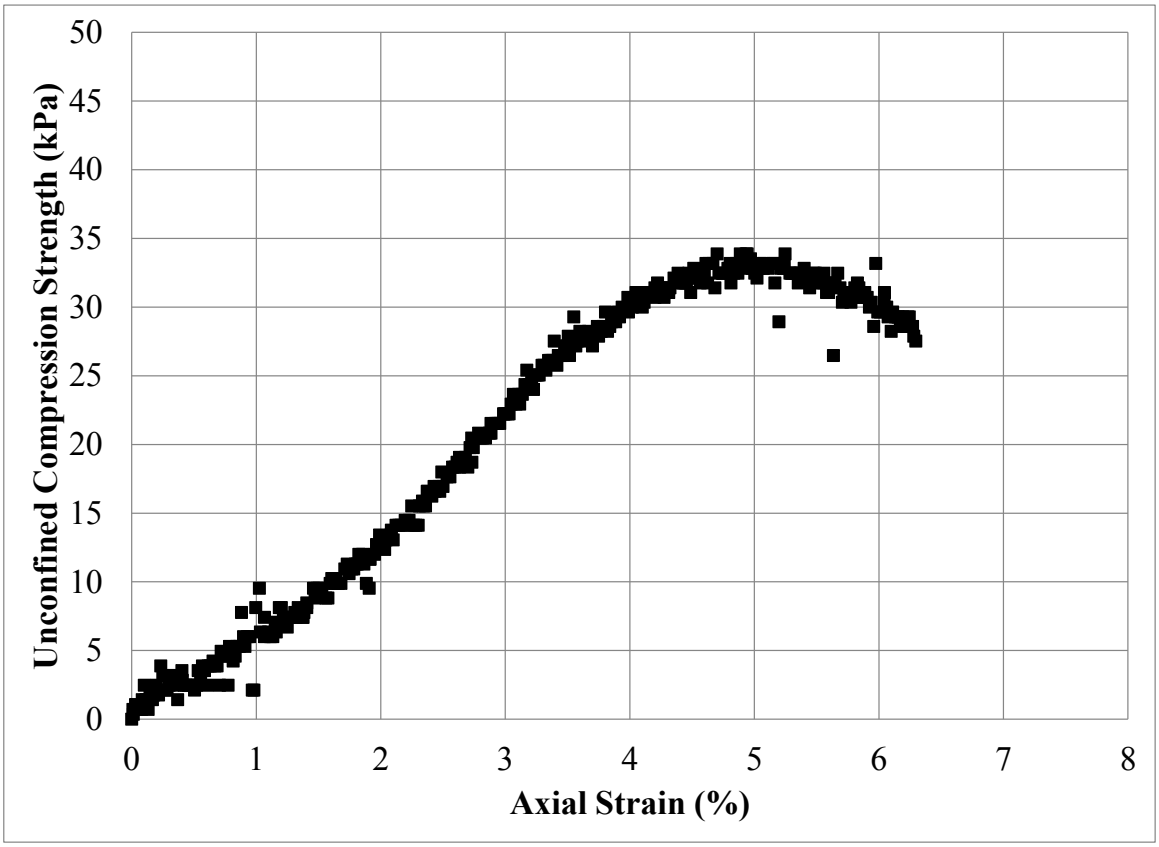

(c)

Figure C.28: Unconfined Compression Test Specimen No. 85R: (a) Photograph Prior to Testing; (b) Photograph Post Testing; and (c) Stress – Strain Data

(a)

(b)

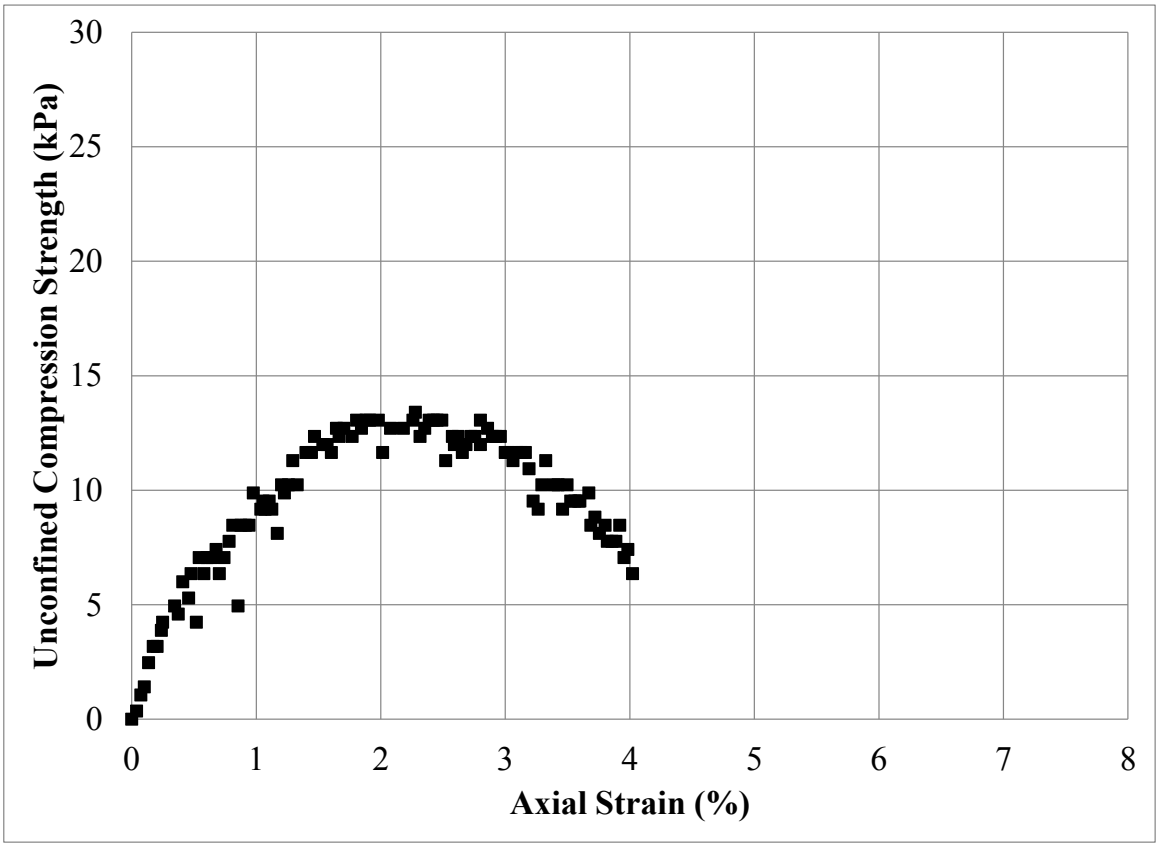

(c)

Figure C.29: Unconfined Compression Test Specimen No. 86R: (a) Photograph Prior to Testing; (b) Photograph Post Testing; and (c) Stress – Strain Data

(a)

(b)

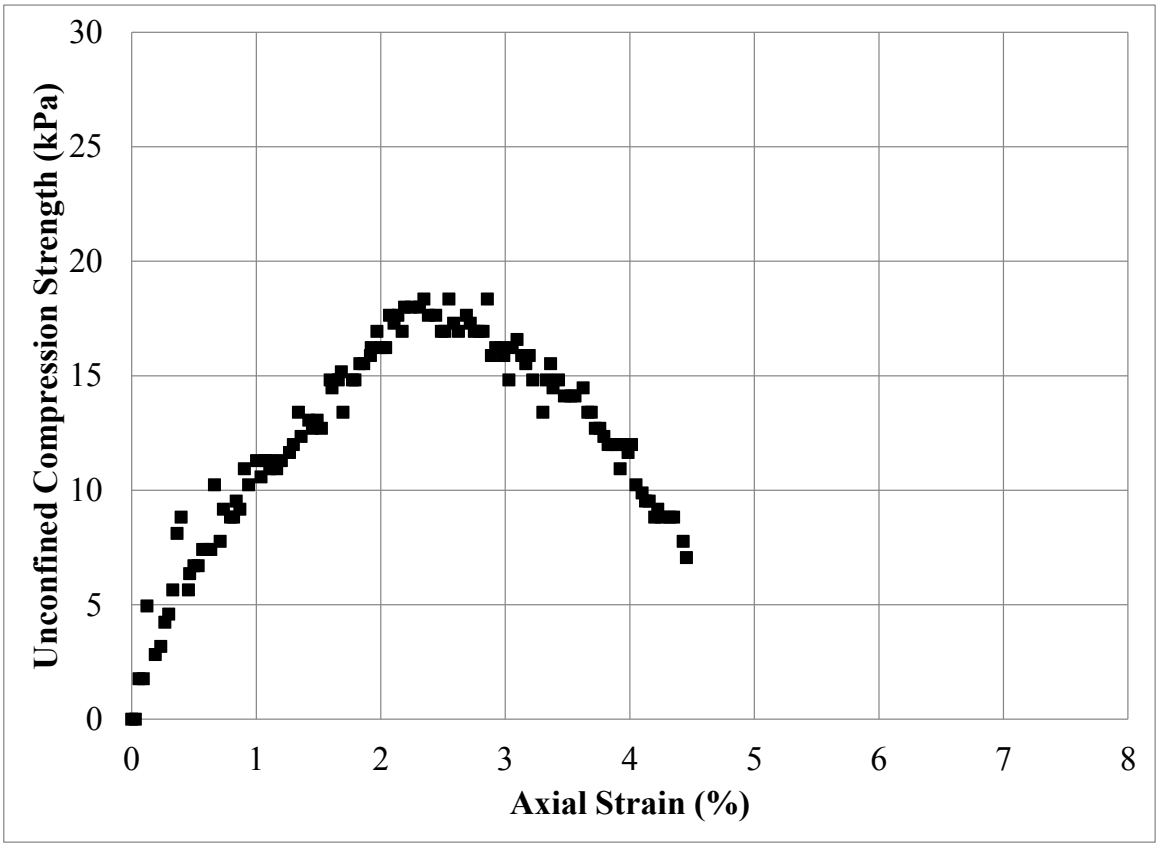

(c)

Figure C.30: Unconfined Compression Test Specimen No. 87R: (a) Photograph Prior to Testing; (b) Photograph Post Testing; and (c) Stress – Strain Data

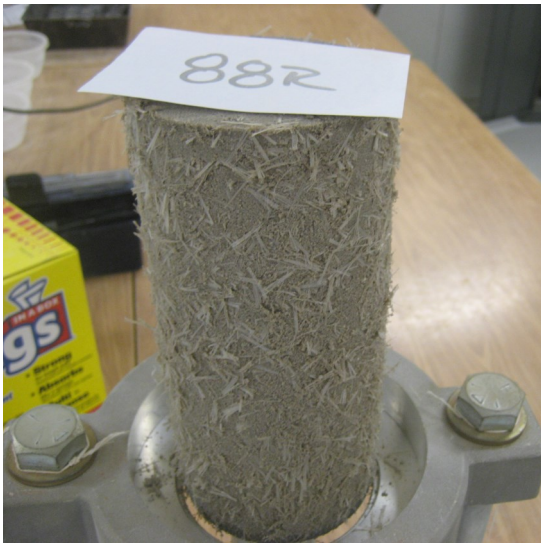

(a)

(b)

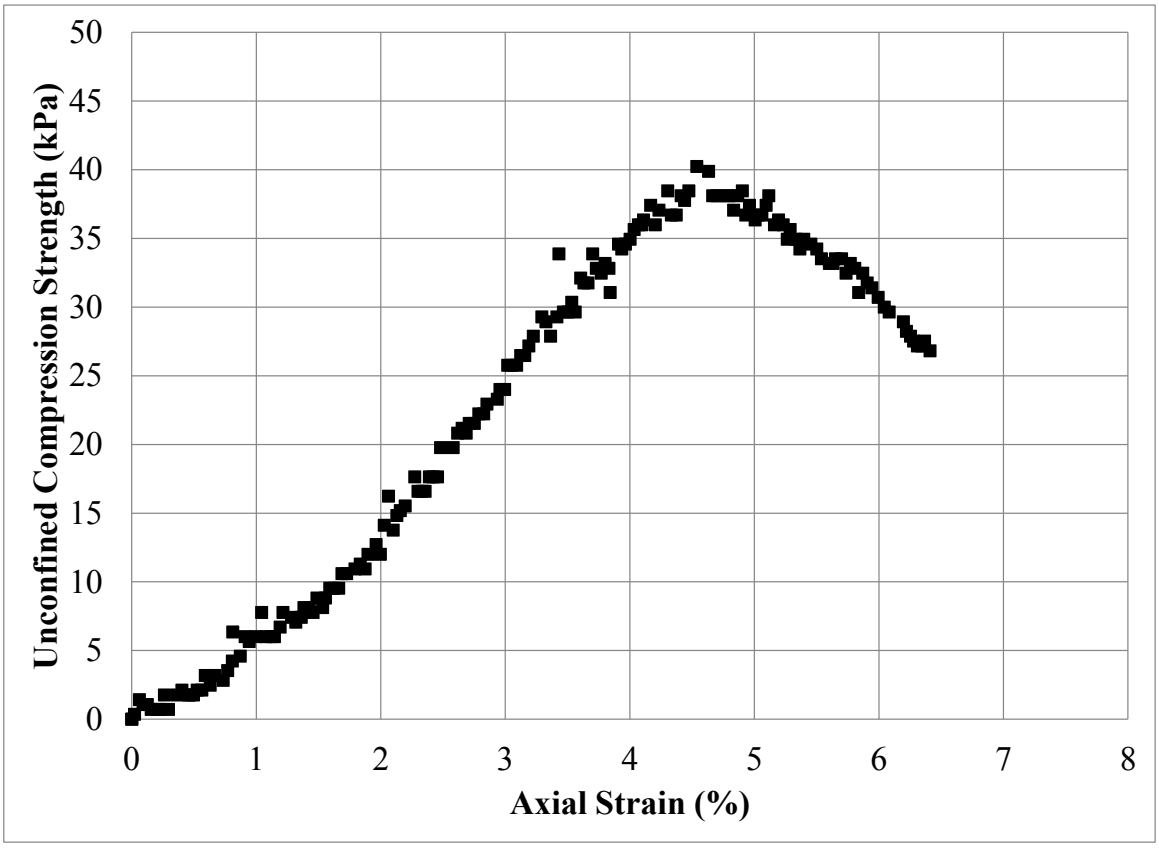

(c)

Figure C.31: Unconfined Compression Test Specimen No. 88R: (a) Photograph Prior to Testing; (b) Photograph Post Testing; and (c) Stress – Strain Data

(a)

(b)

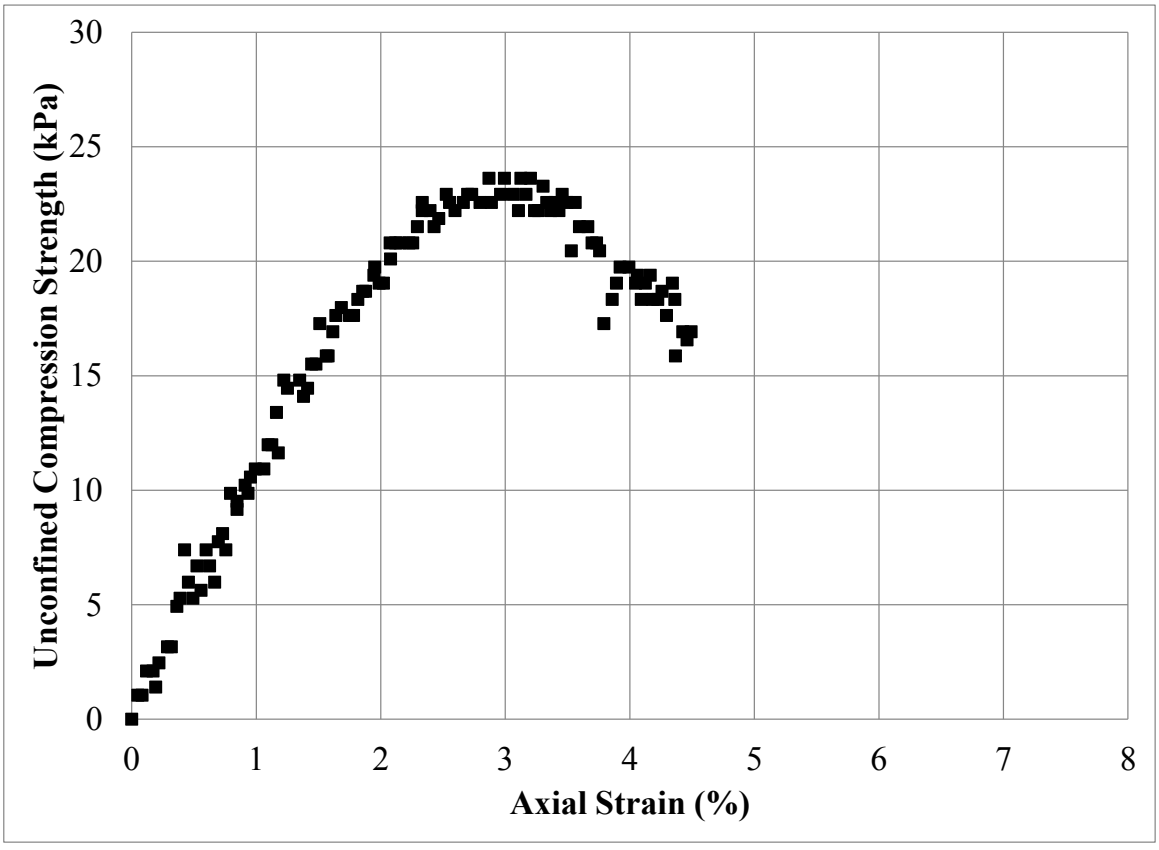

(c)

Figure C.32: Unconfined Compression Test Specimen No. 89R: (a) Photograph Prior to Testing; (b) Photograph Post Testing; and (c) Stress – Strain Data

(a)

(b)

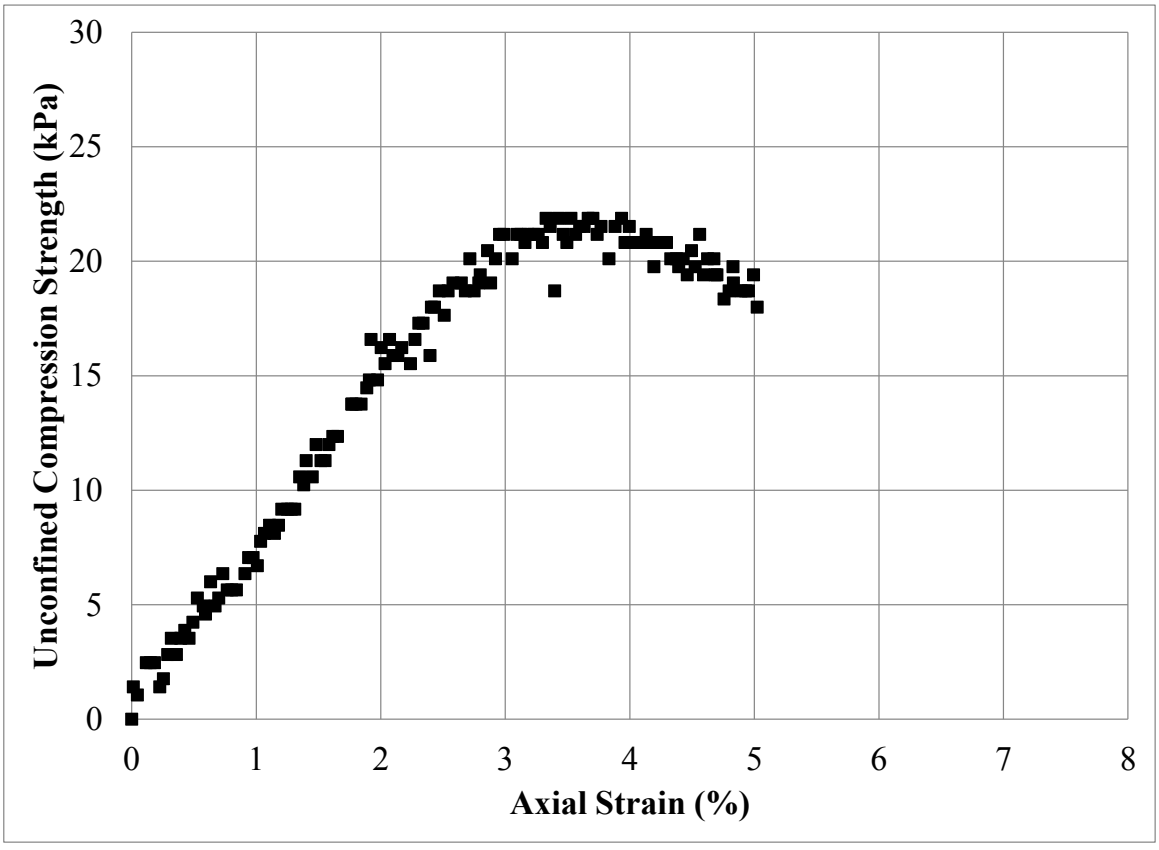

(c)

Figure C.33: Unconfined Compression Test Specimen No. 90R: (a) Photograph Prior to Testing; (b) Photograph Post Testing; and (c) Stress – Strain Data

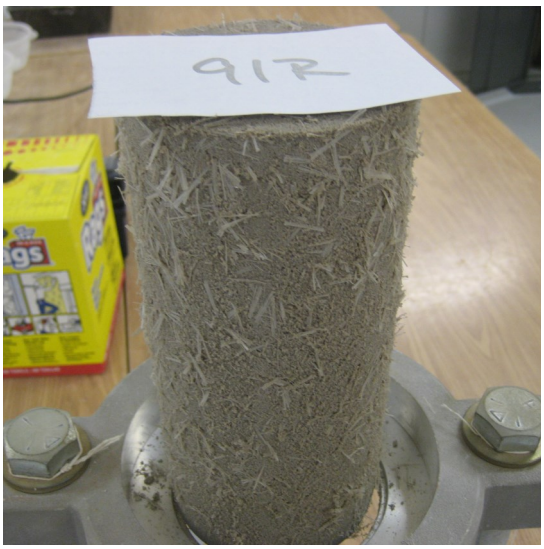

(a)

(b)

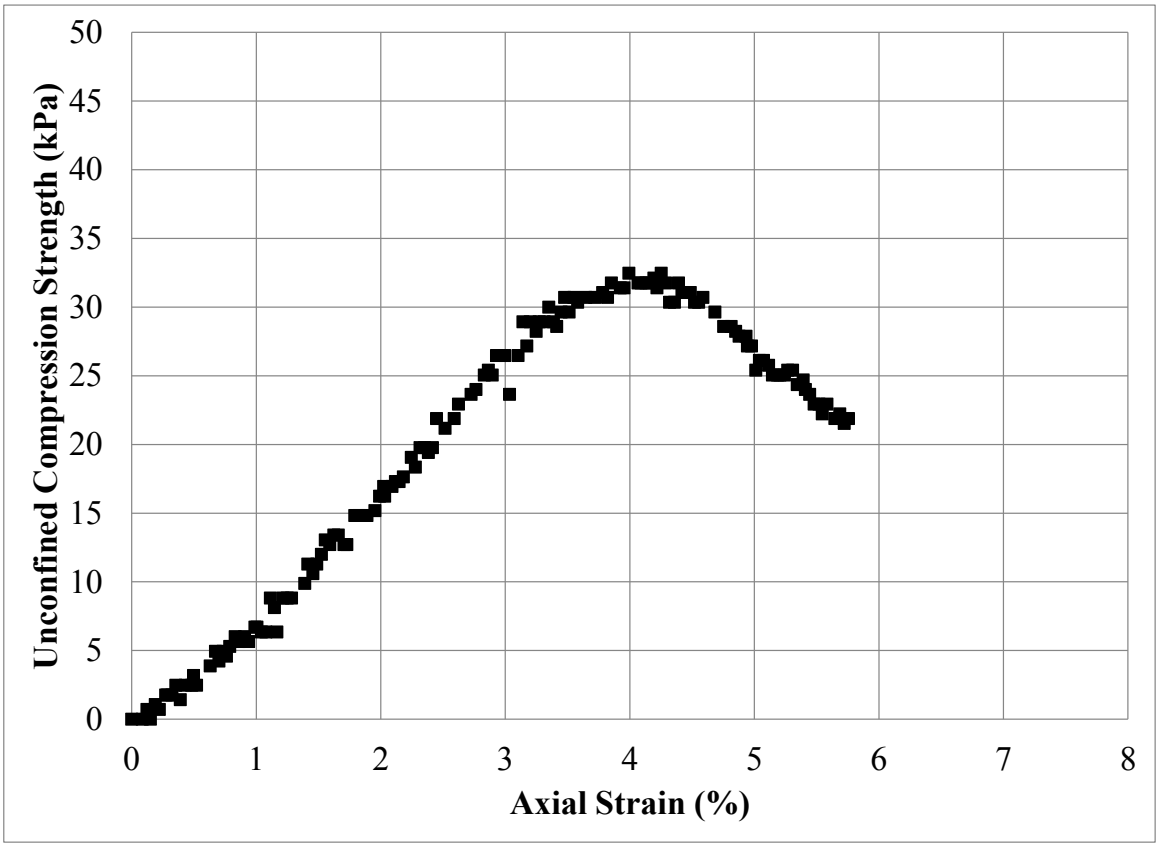

(c)

Figure C.34: Unconfined Compression Test Specimen No. 91R: (a) Photograph Prior to Testing; (b) Photograph Post Testing; and (c) Stress – Strain Data

(a)

(b)

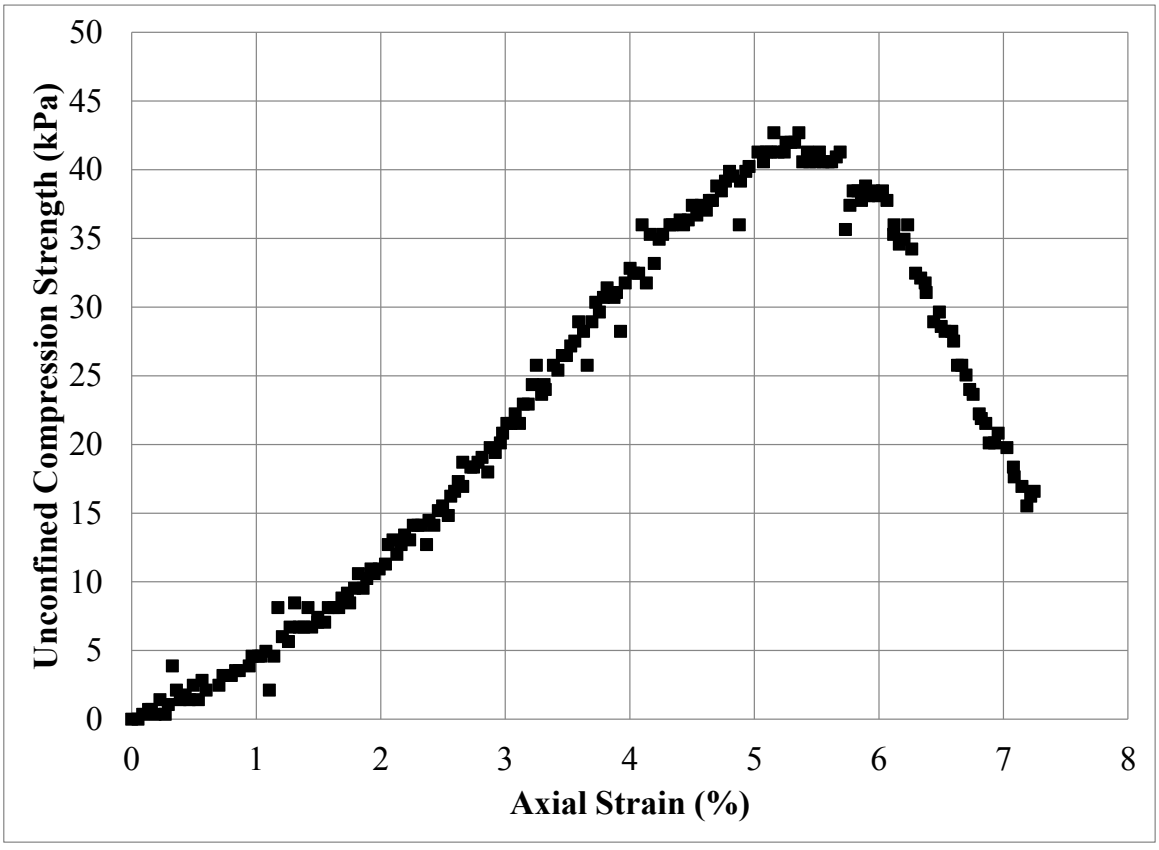

(c)

Figure C.35: Unconfined Compression Test Specimen No. 92R: (a) Photograph Prior to Testing; (b) Photograph Post Testing; and (c) Stress – Strain Data

(a)

(b)

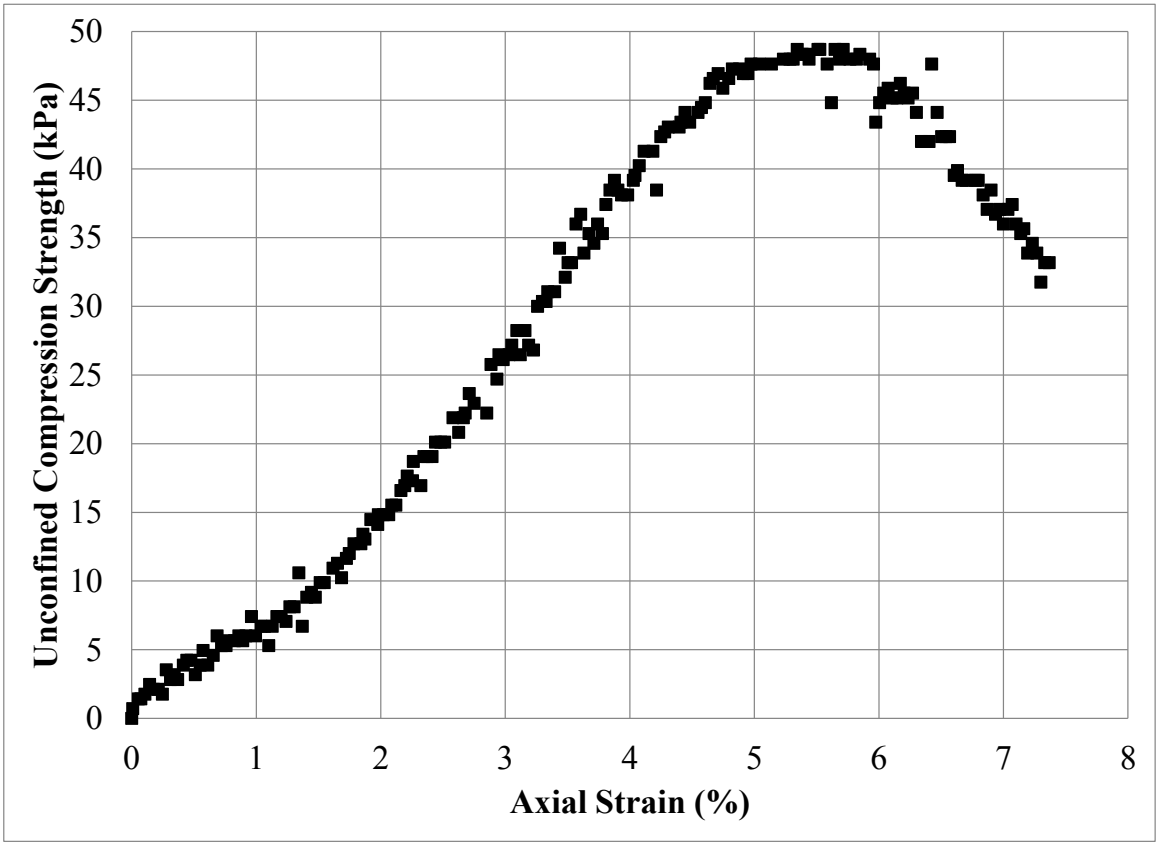

(c)

Figure C.36: Unconfined Compression Test Specimen No. 93R: (a) Photograph Prior to Testing; (b) Photograph Post Testing; and (c) Stress – Strain Data

(a)

(b)

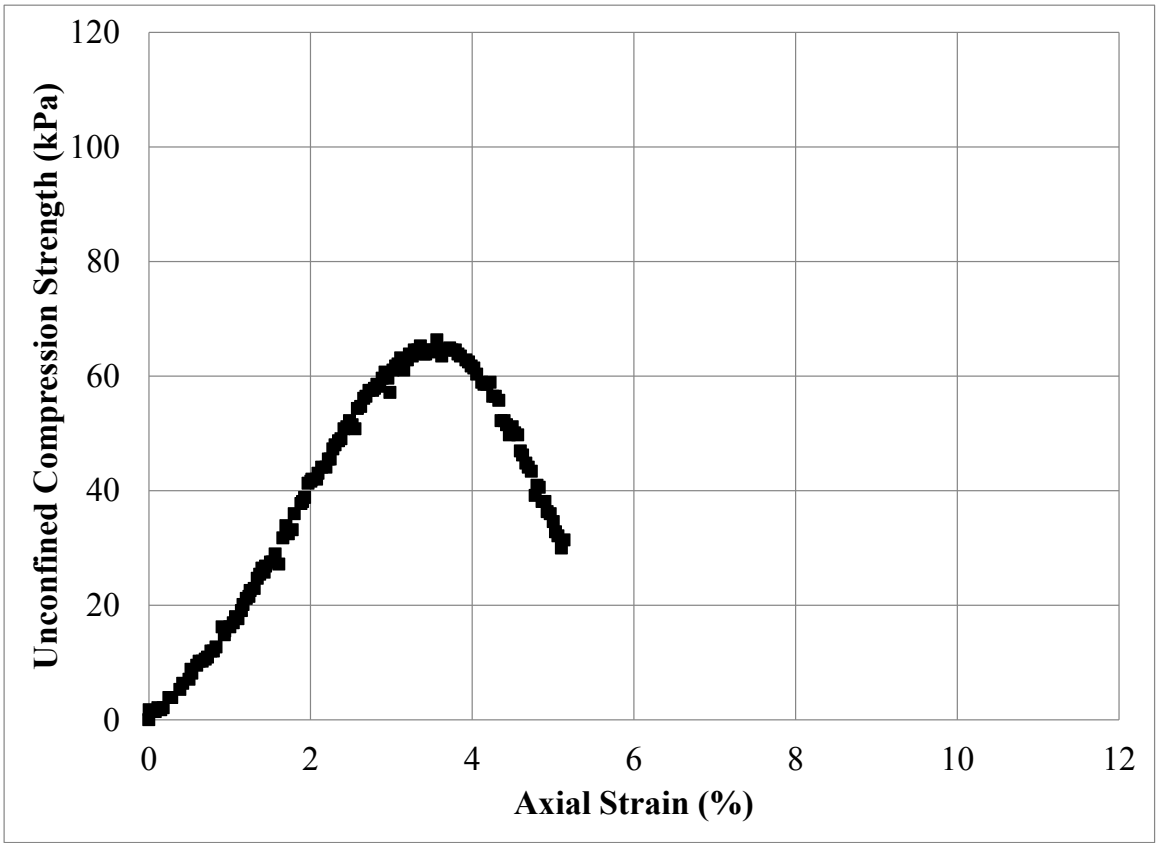

(c)

Figure C.37: Unconfined Compression Test Specimen No. 94R: (a) Photograph Prior to Testing; (b) Photograph Post Testing; and (c) Stress – Strain Data

(a)

(b)

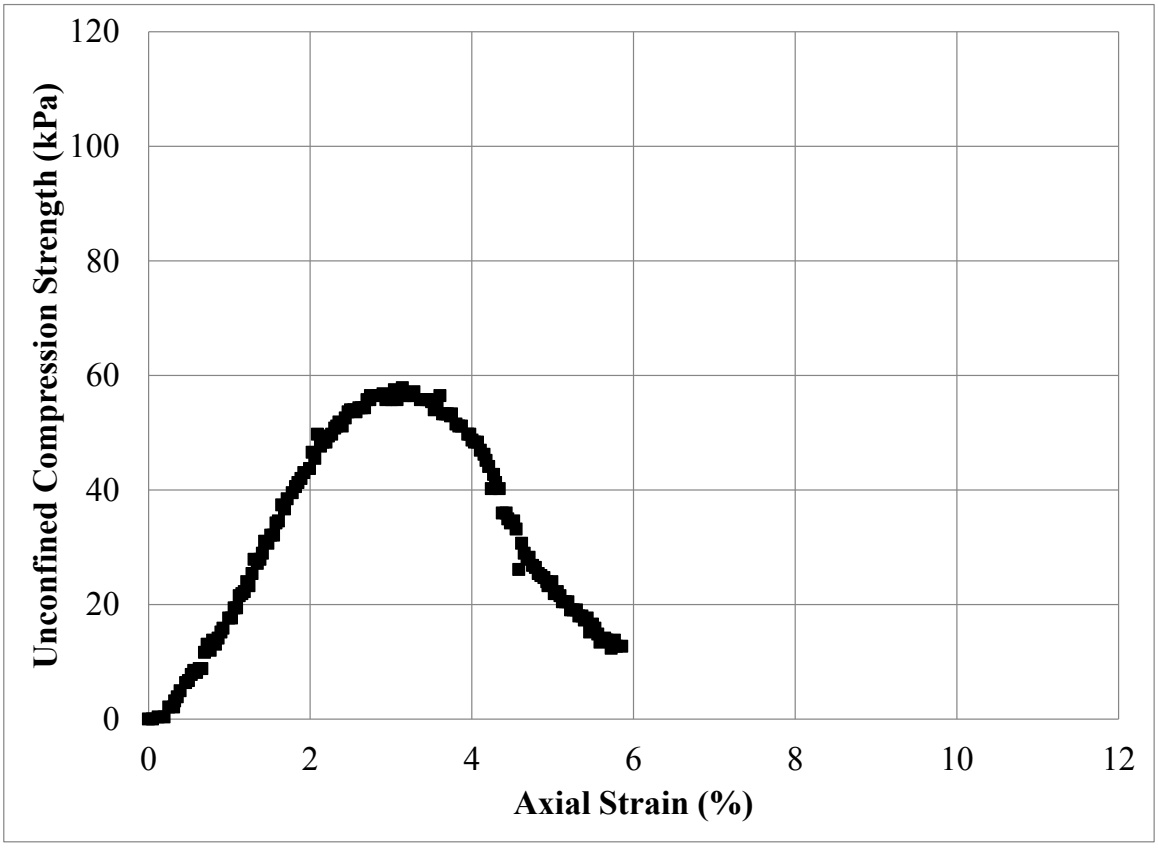

(c)

Figure C.38: Unconfined Compression Test Specimen No. 95R: (a) Photograph Prior to Testing; (b) Photograph Post Testing; and (c) Stress – Strain Data

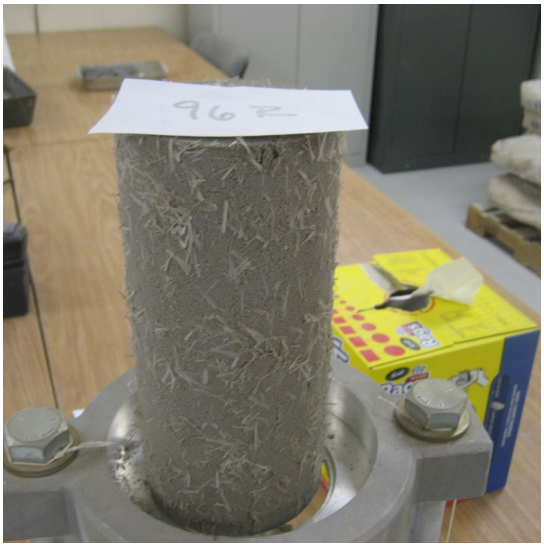

(a)

(b)

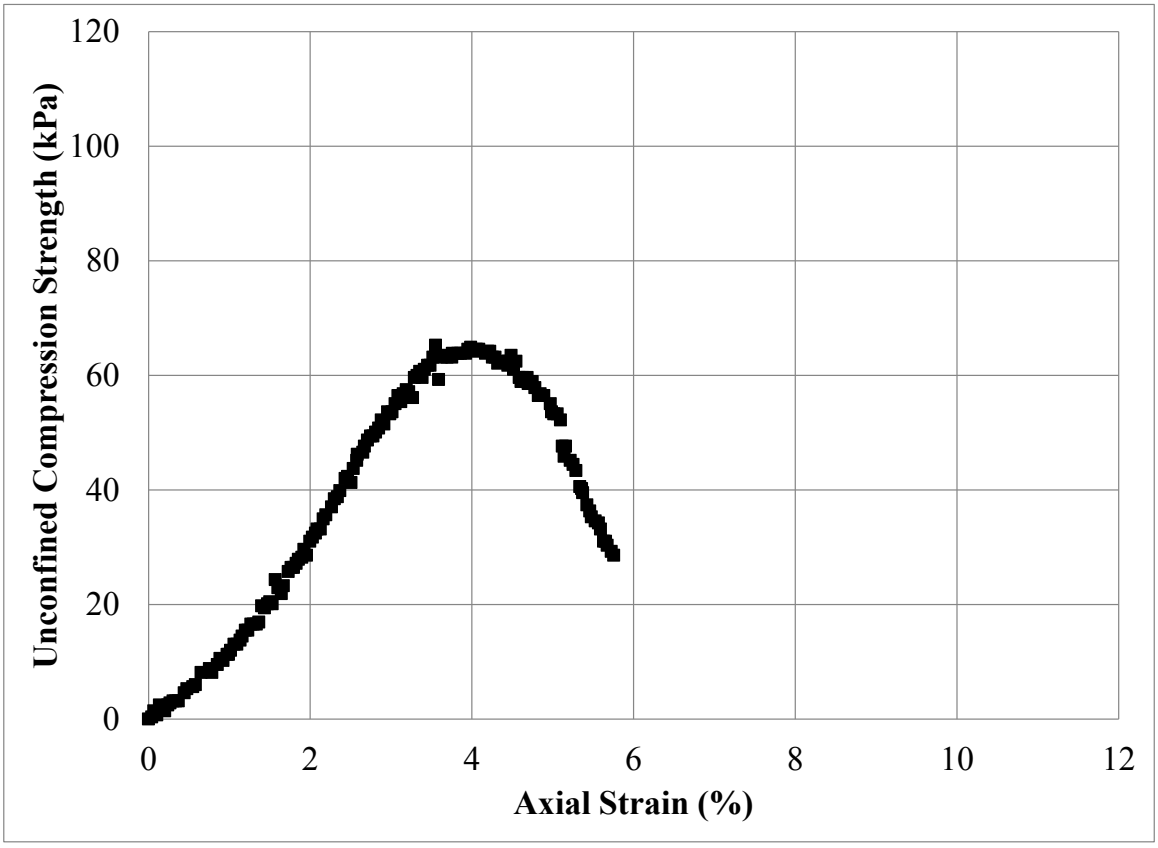

(c)

Figure C.39: Unconfined Compression Test Specimen No. 96R: (a) Photograph Prior to Testing; (b) Photograph Post Testing; and (c) Stress – Strain Data

(a)

(b)

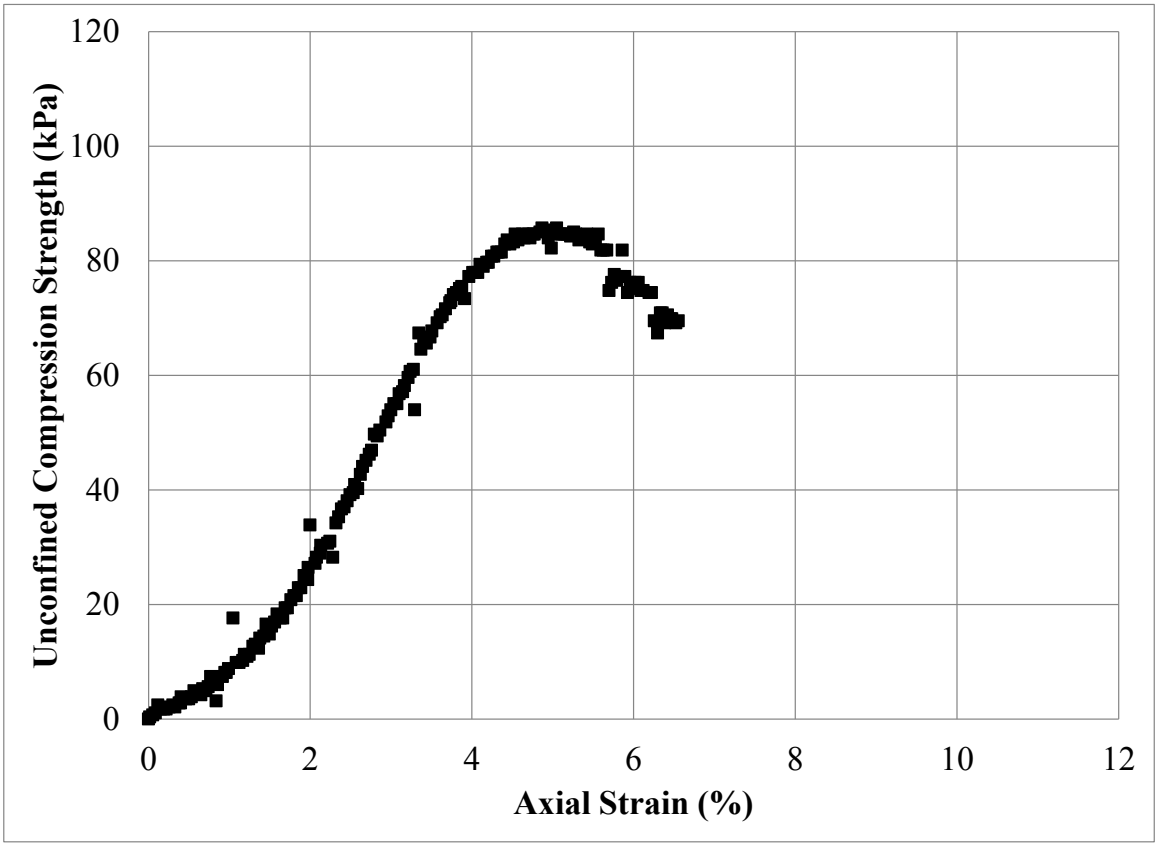

(c)

Figure C.40: Unconfined Compression Test Specimen No. 97R: (a) Photograph Prior to Testing; (b) Photograph Post Testing; and (c) Stress – Strain Data

(a)

(b)

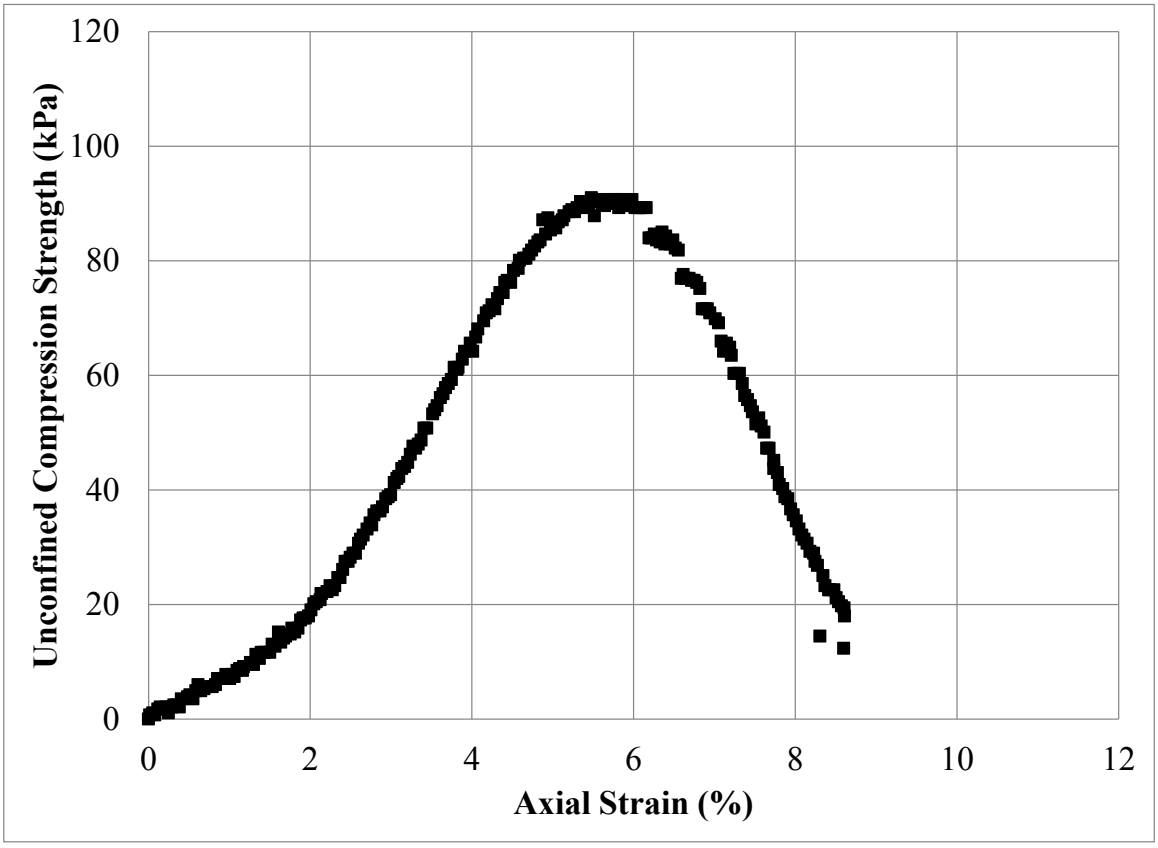

(c)

Figure C.41: Unconfined Compression Test Specimen No. 98R: (a) Photograph Prior to Testing; (b) Photograph Post Testing; and (c) Stress – Strain Data

(a)

(b)

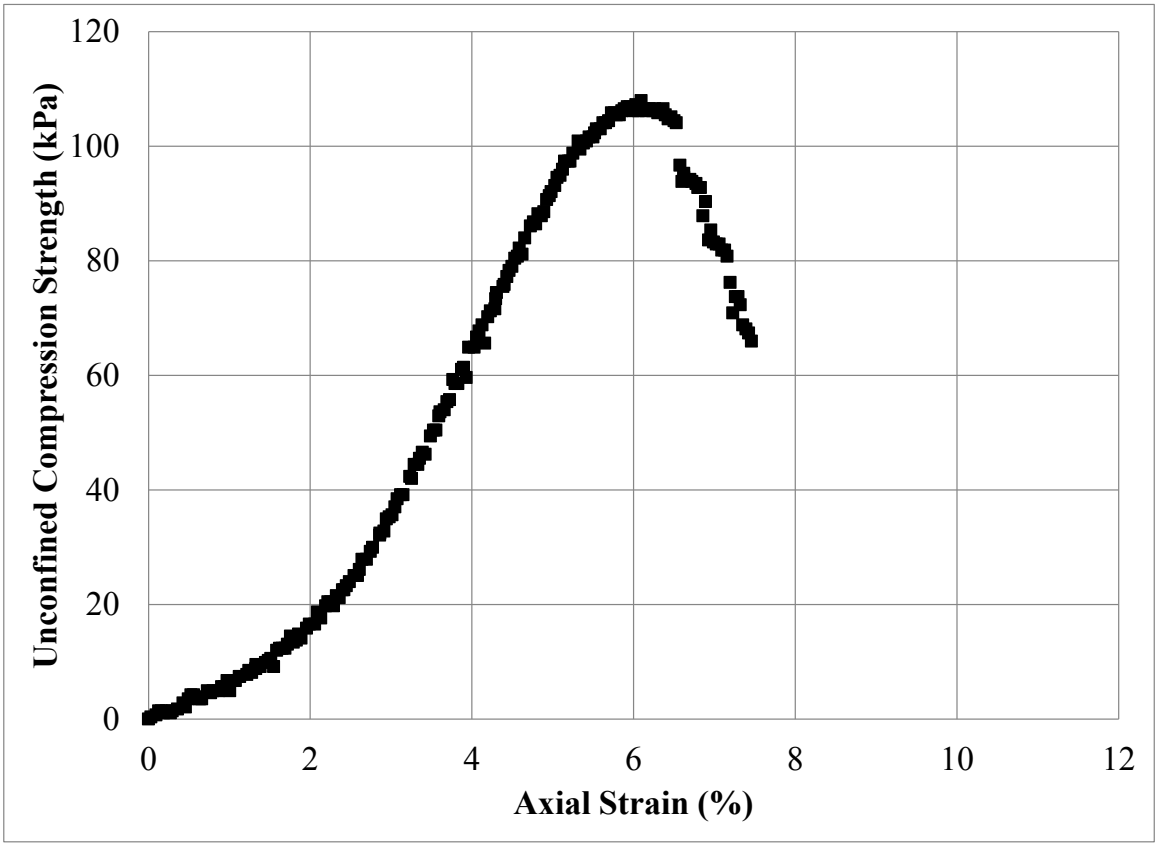

(c)

Figure C.42: Unconfined Compression Test Specimen No. 99R: (a) Photograph Prior to Testing; (b) Photograph Post Testing; and (c) Stress – Strain Data

(a)

(b)

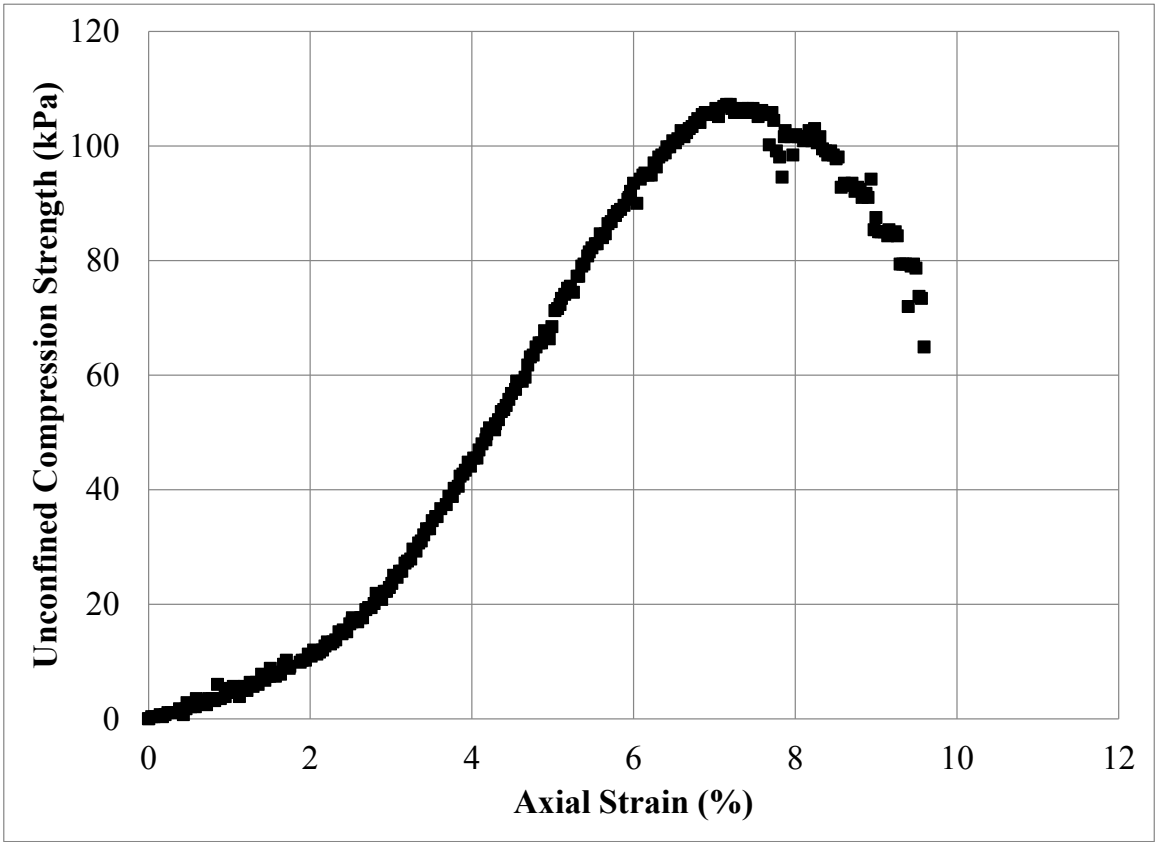

(c)

Figure C.43: Unconfined Compression Test Specimen No. 100R: (a) Photograph Prior to Testing; (b) Photograph Post Testing; and (c) Stress – Strain Data

(a)

(b)

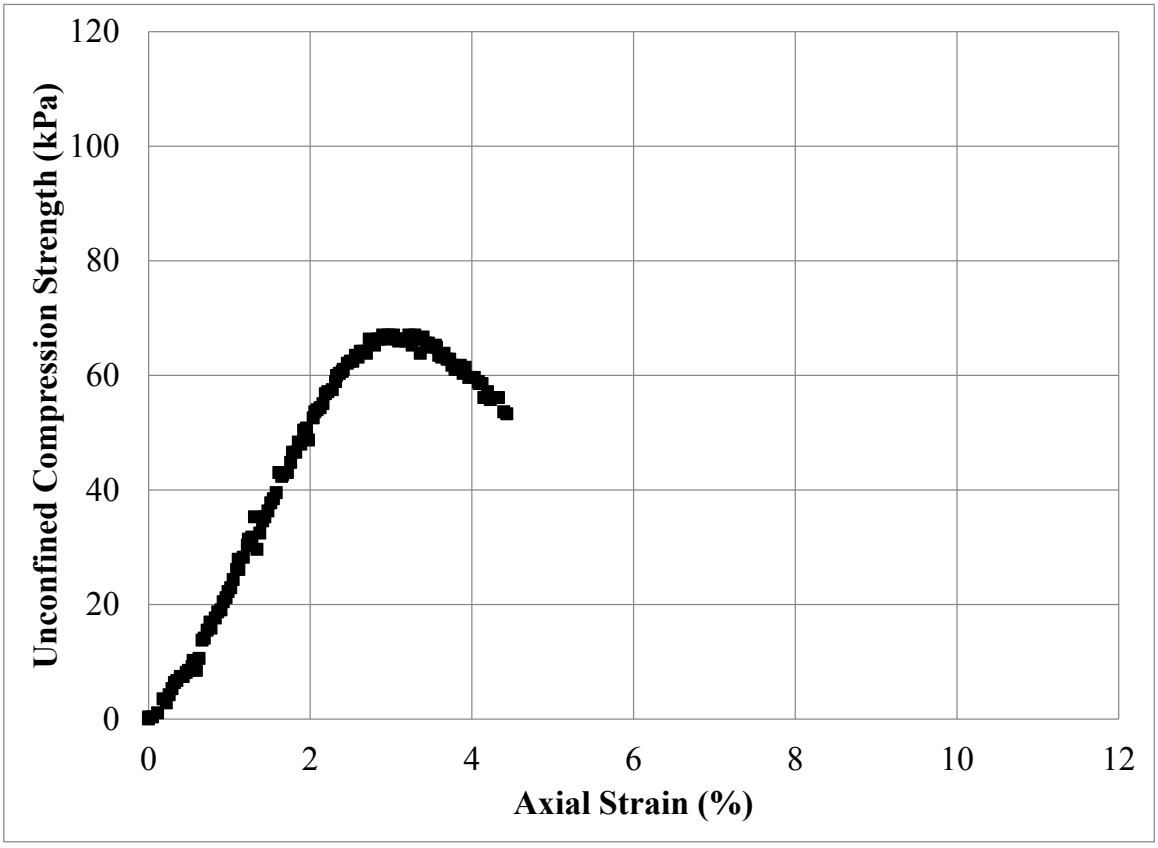

(c)

Figure C.44: Unconfined Compression Test Specimen No. 101R: (a) Photograph Prior to Testing; (b) Photograph Post Testing; and (c) Stress – Strain Data

(a)

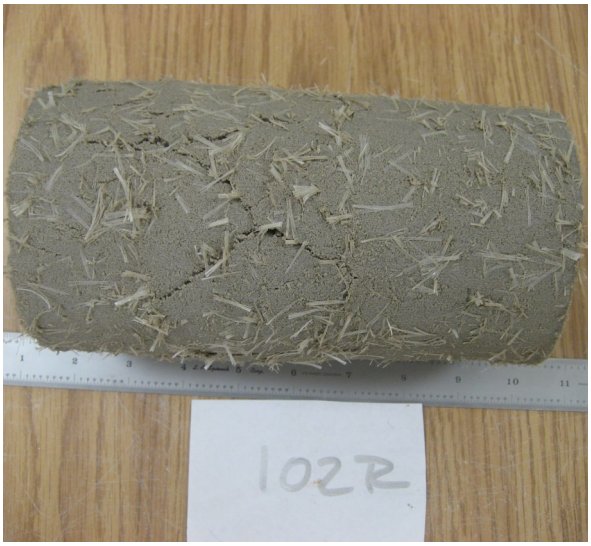

(b)

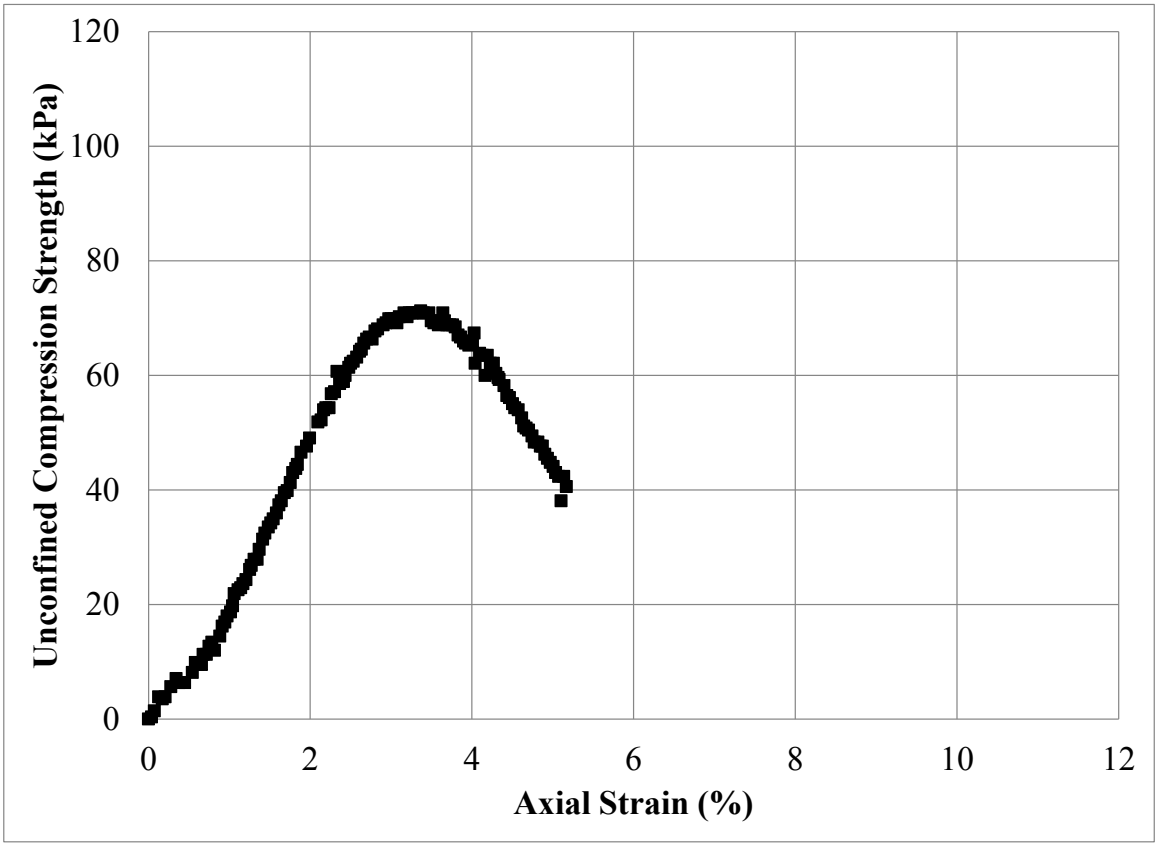

(c)

Figure C.45: Unconfined Compression Test Specimen No. 102R: (a) Photograph Prior to Testing; (b) Photograph Post Testing; and (c) Stress – Strain Data

(a)

(b)

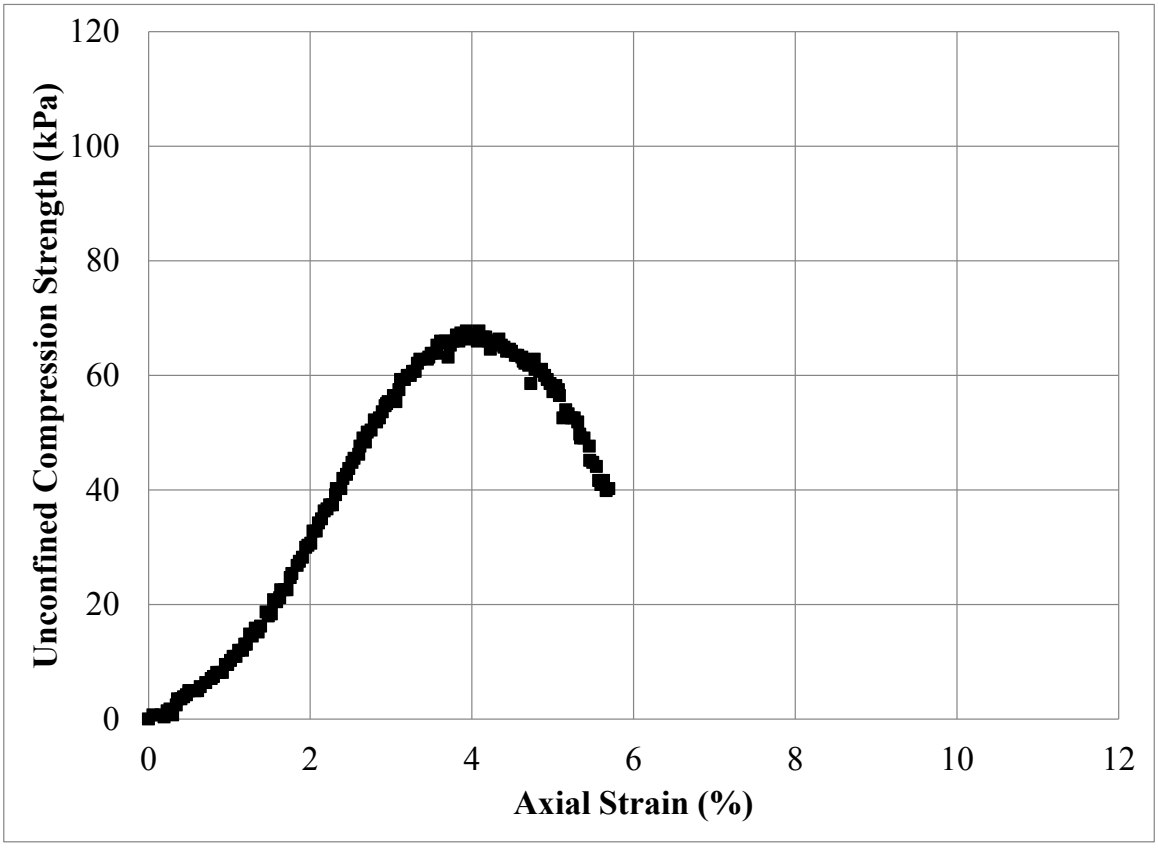

(c)

Figure C.46: Unconfined Compression Test Specimen No. 103R: (a) Photograph Prior to Testing; (b) Photograph Post Testing; and (c) Stress – Strain Data

(a)

(b)

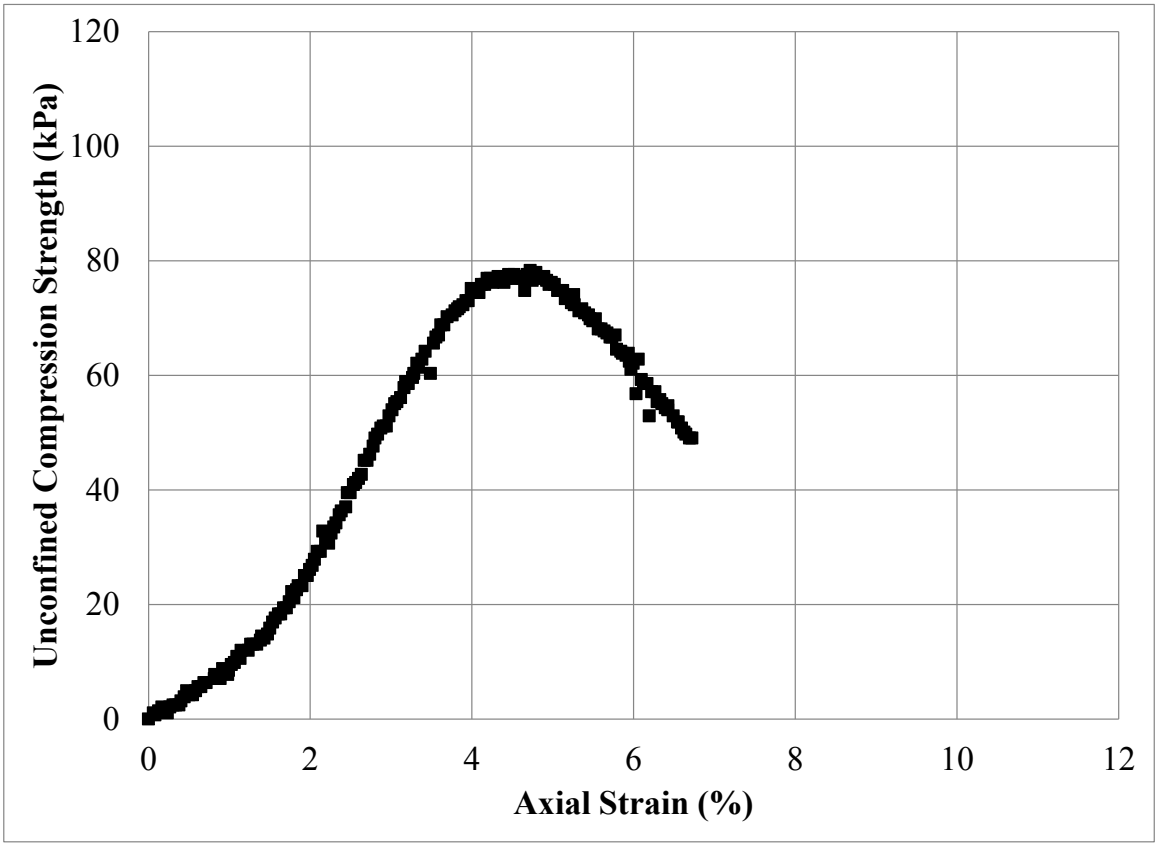

(c)

Figure C.47: Unconfined Compression Test Specimen No. 104R: (a) Photograph Prior to Testing; (b) Photograph Post Testing; and (c) Stress – Strain Data

(a)

(b)

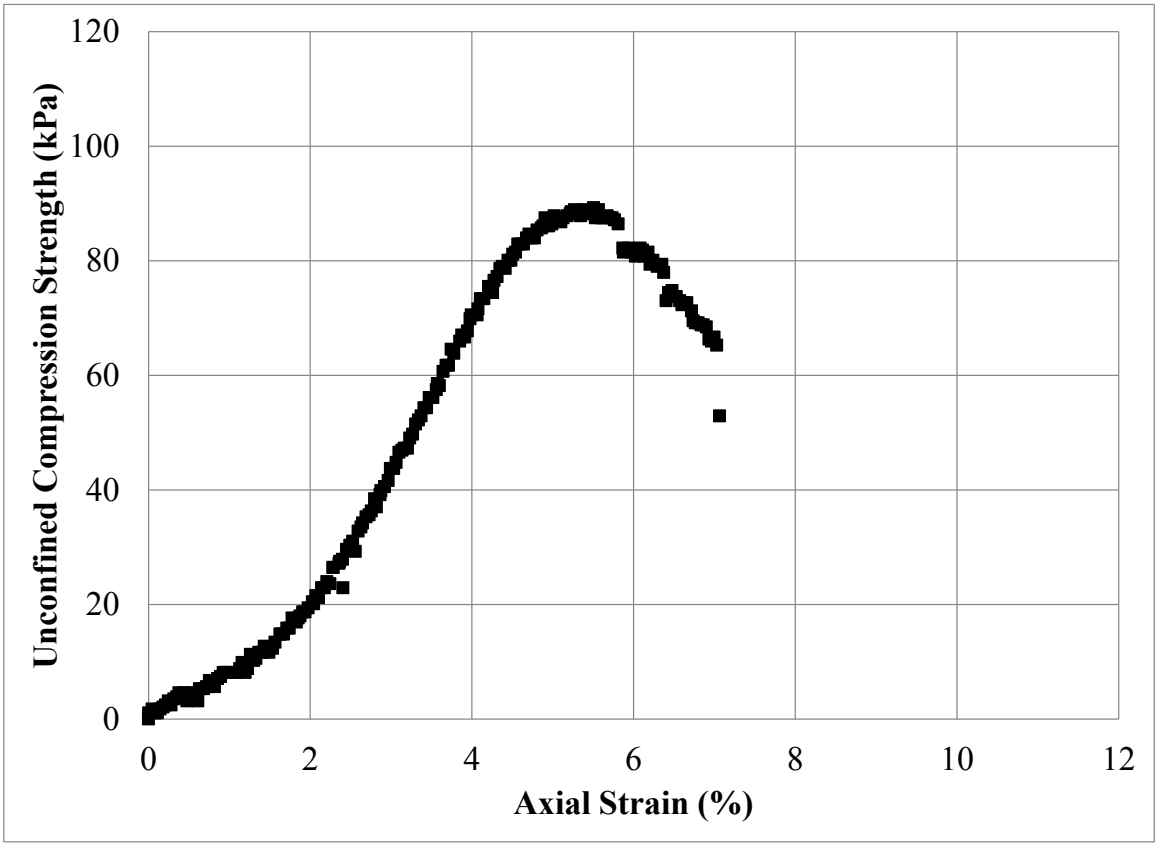

(c)

Figure C.48: Unconfined Compression Test Specimen No. 105R: (a) Photograph Prior to Testing; (b) Photograph Post Testing; and (c) Stress – Strain Data

(a)

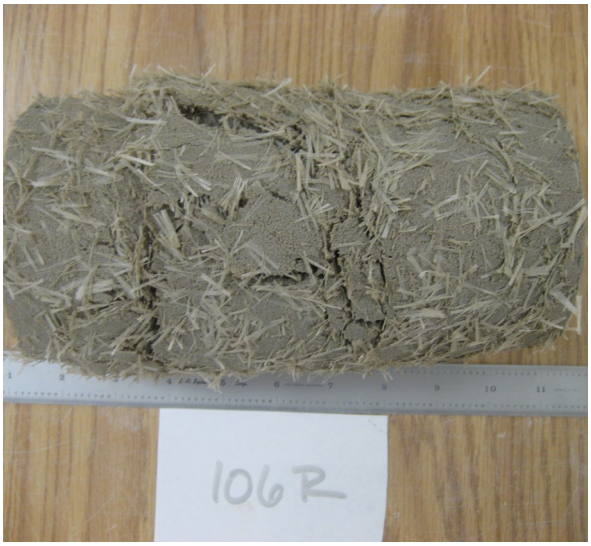

(b)

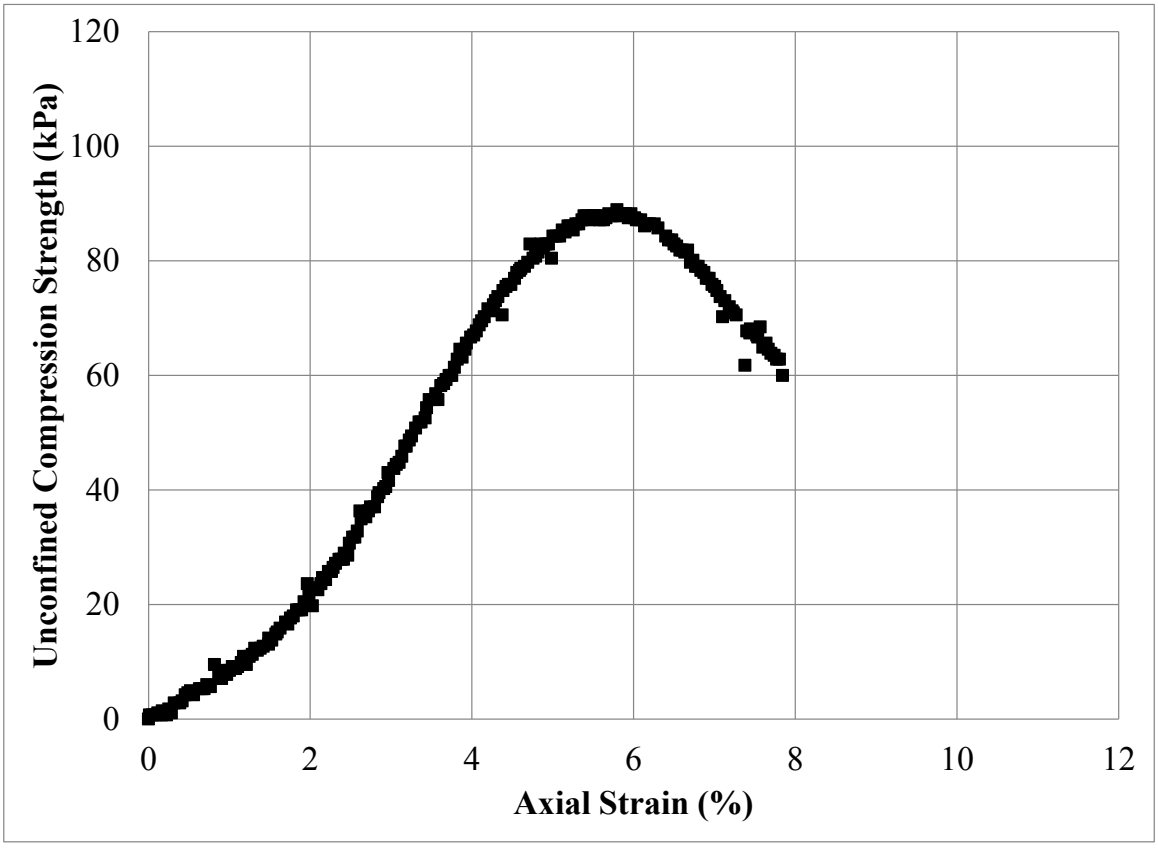

(c)

Figure C.49: Unconfined Compression Test Specimen No. 106R: (a) Photograph Prior to Testing; (b) Photograph Post Testing; and (c) Stress – Strain Data

(a)

(b)

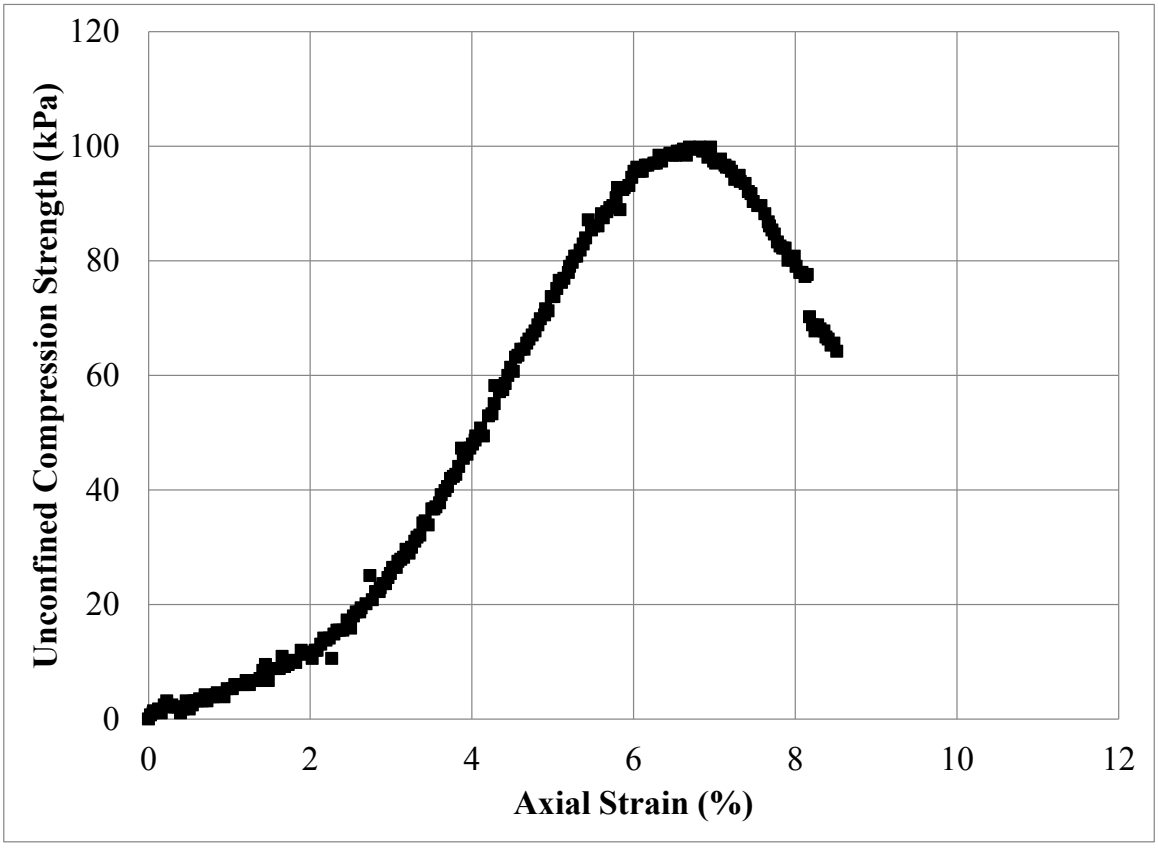

(c)

Figure C.50: Unconfined Compression Test Specimen No. 107R: (a) Photograph Prior to Testing; (b) Photograph Post Testing; and (c) Stress – Strain Data

(a)

(b)

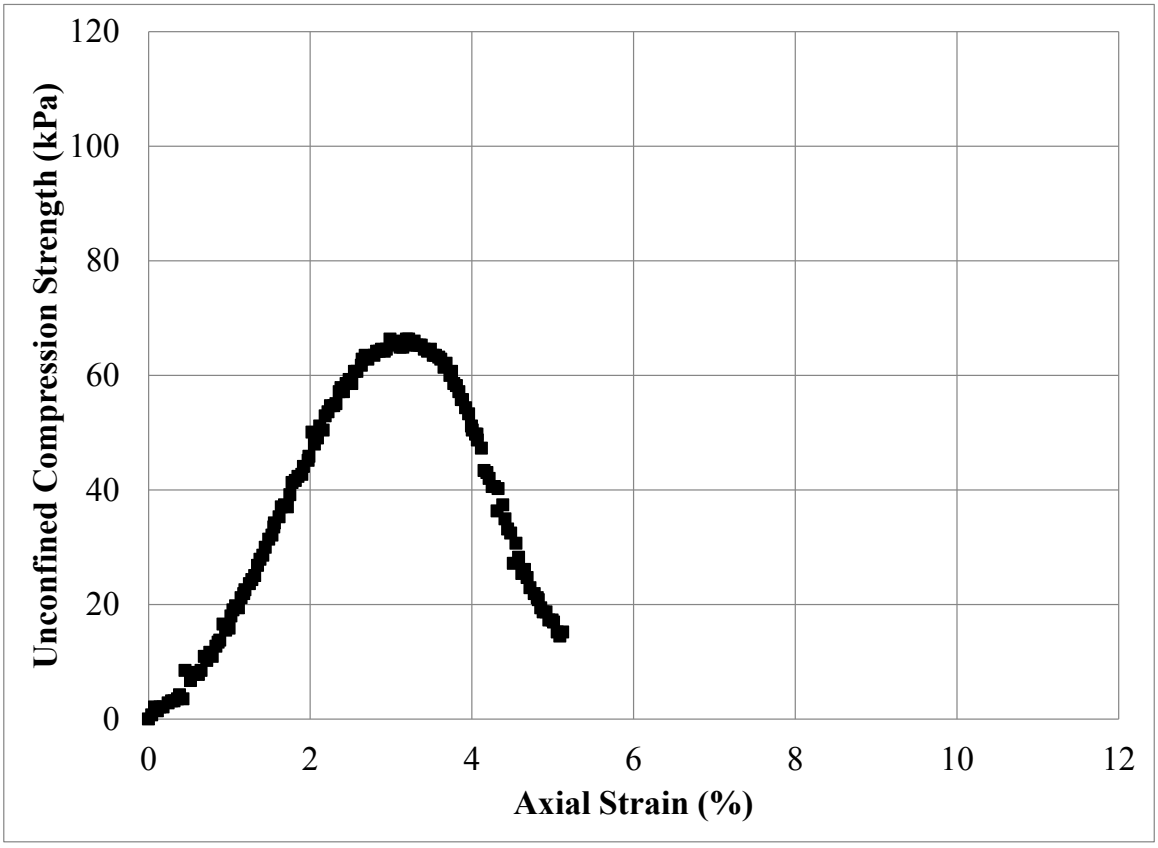

(c)

Figure C.51: Unconfined Compression Test Specimen No. 108R: (a) Photograph Prior to Testing; (b) Photograph Post Testing; and (c) Stress – Strain Data

(a)

(b)

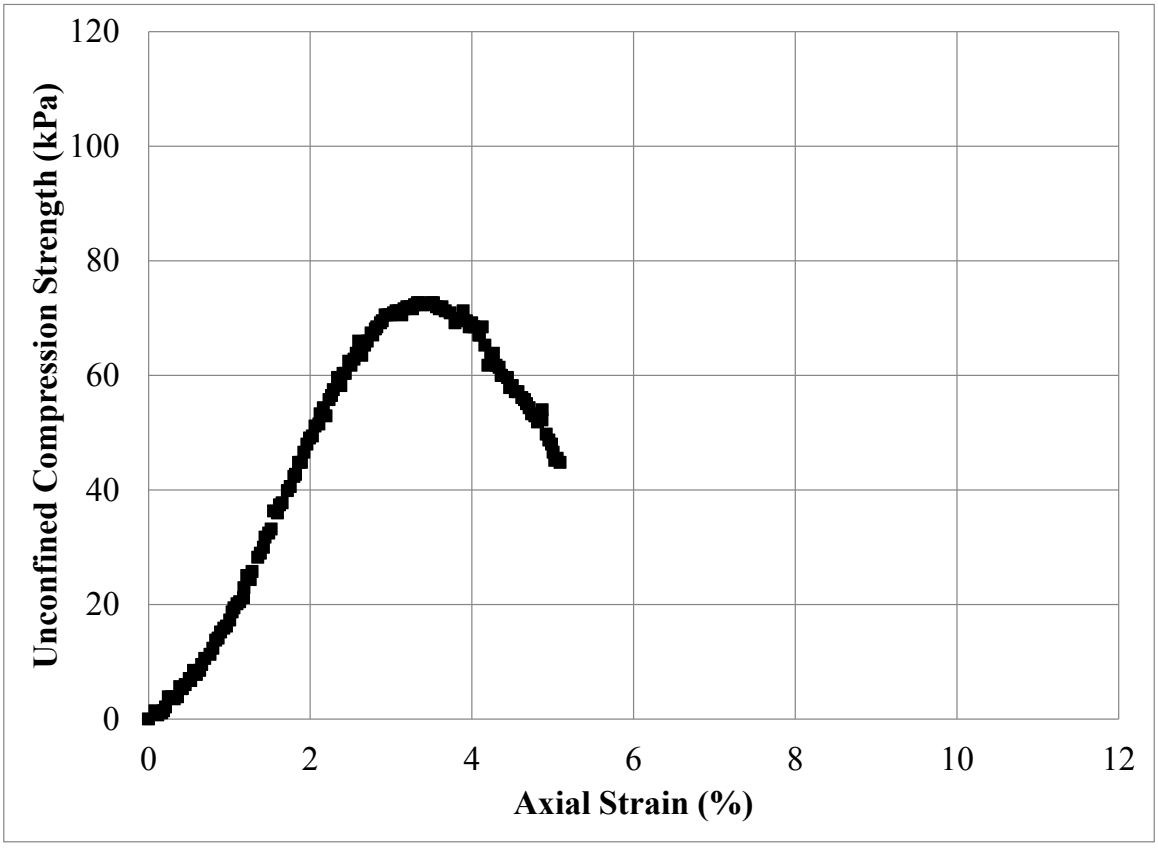

(c)

Figure C.52: Unconfined Compression Test Specimen No. 109R: (a) Photograph Prior to Testing; (b) Photograph Post Testing; and (c) Stress – Strain Data

(a)

(b)

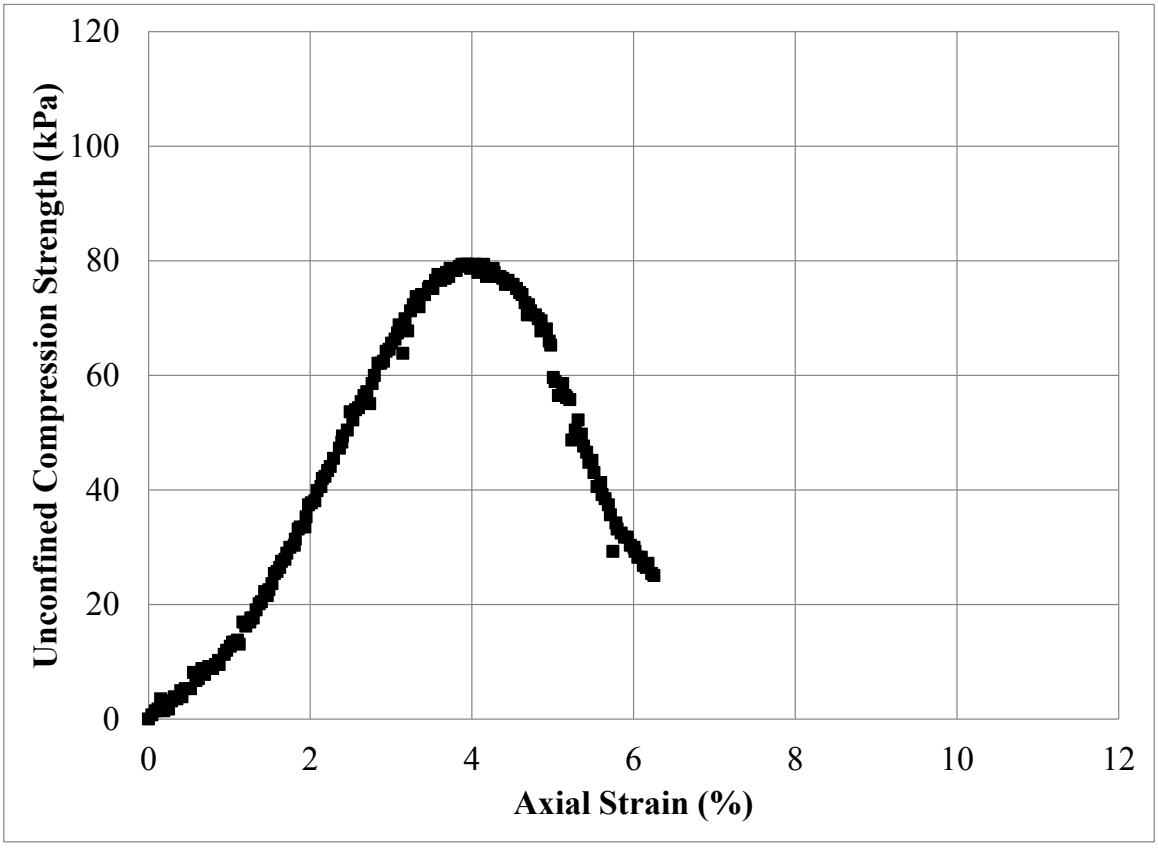

(c)

Figure C.53: Unconfined Compression Test Specimen No. 110R: (a) Photograph Prior to Testing; (b) Photograph Post Testing; and (c) Stress – Strain Data

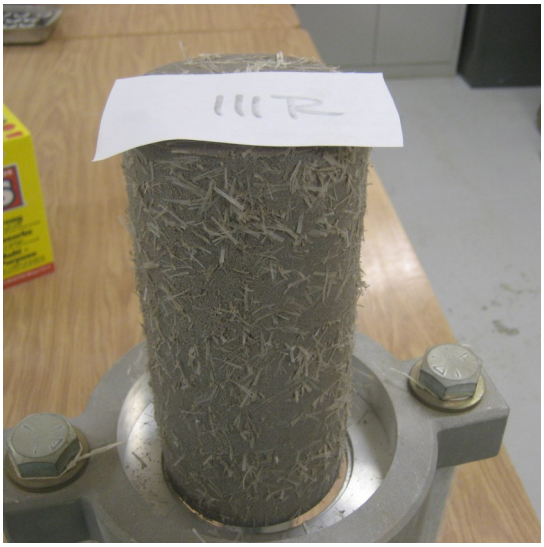

(a)

(b)

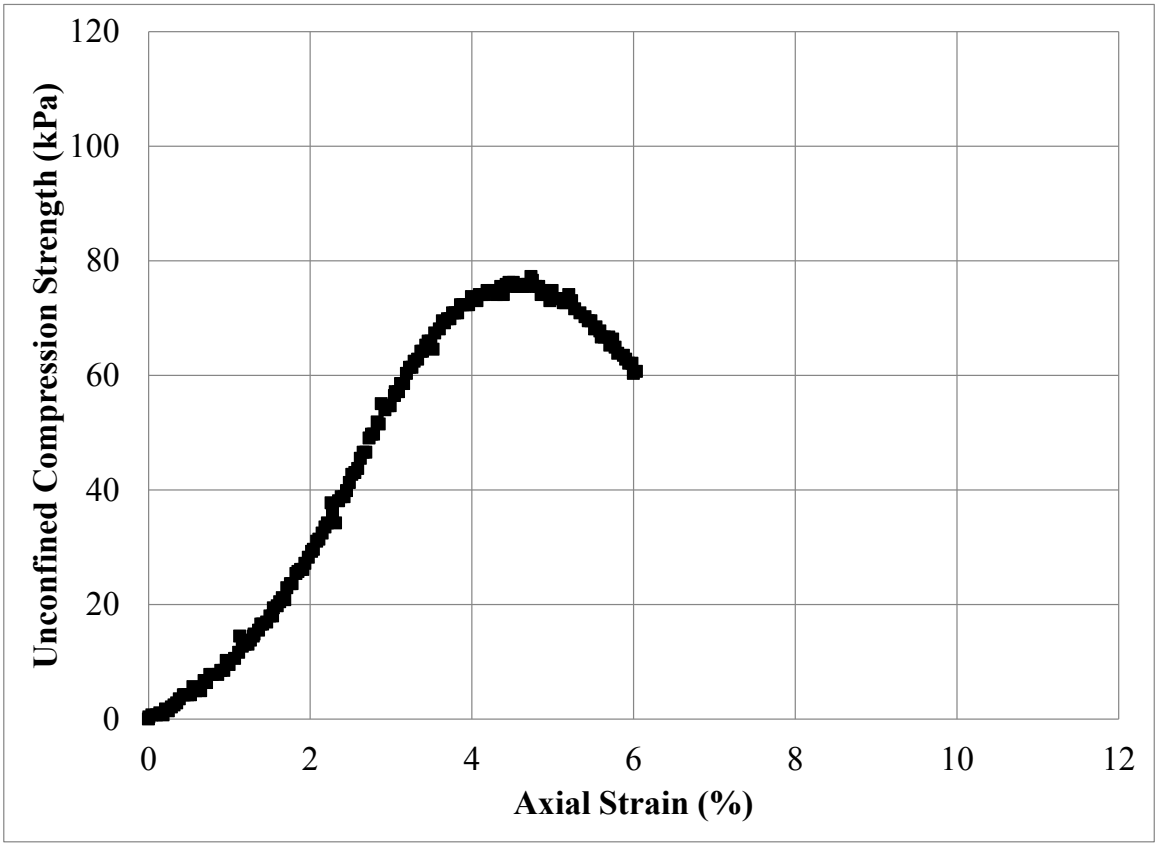

(c)

Figure C.54: Unconfined Compression Test Specimen No. 111R: (a) Photograph Prior to Testing; (b) Photograph Post Testing; and (c) Stress – Strain Data

(a)

(b)

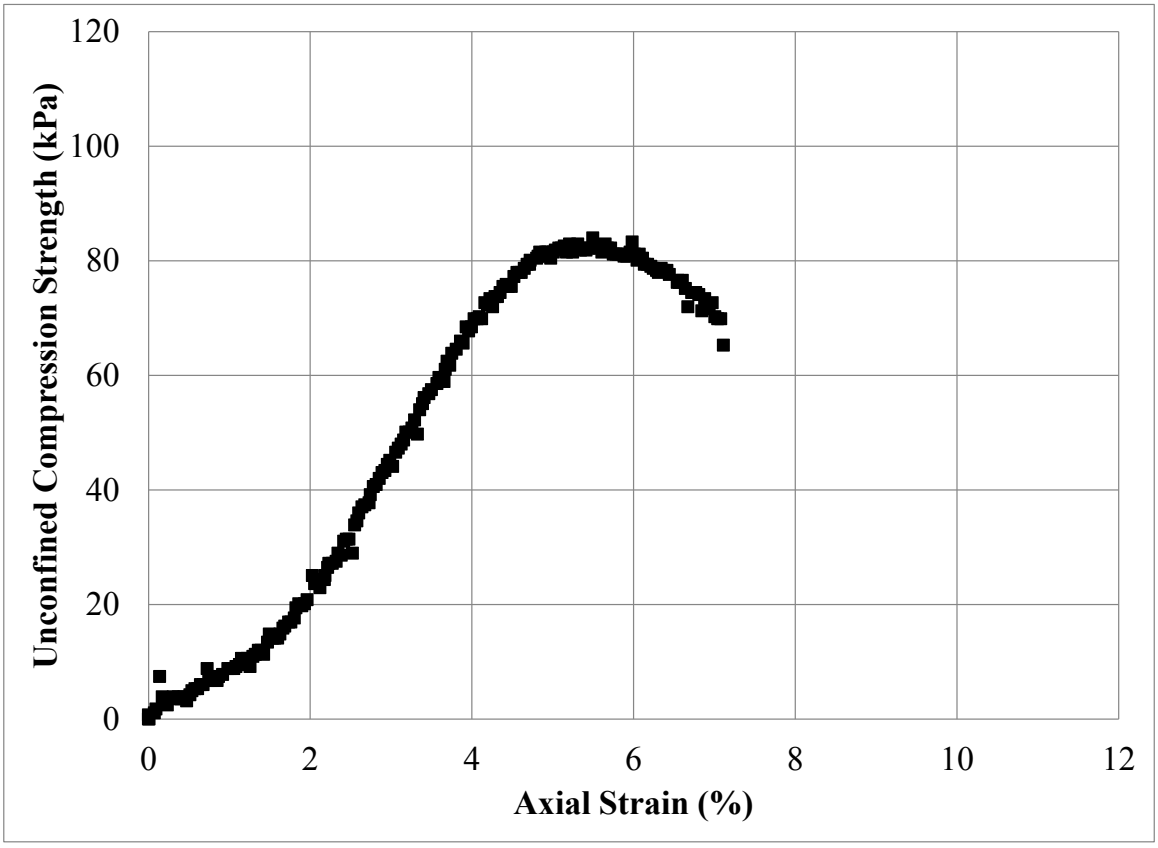

(c)

Figure C.55: Unconfined Compression Test Specimen No. 112R: (a) Photograph Prior to Testing; (b) Photograph Post Testing; and (c) Stress – Strain Data

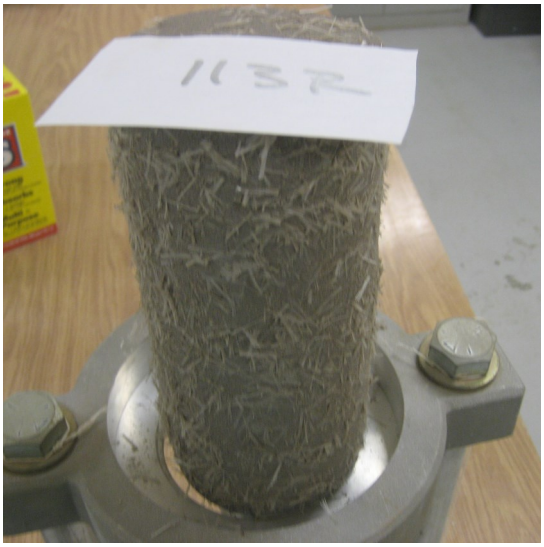

(a)

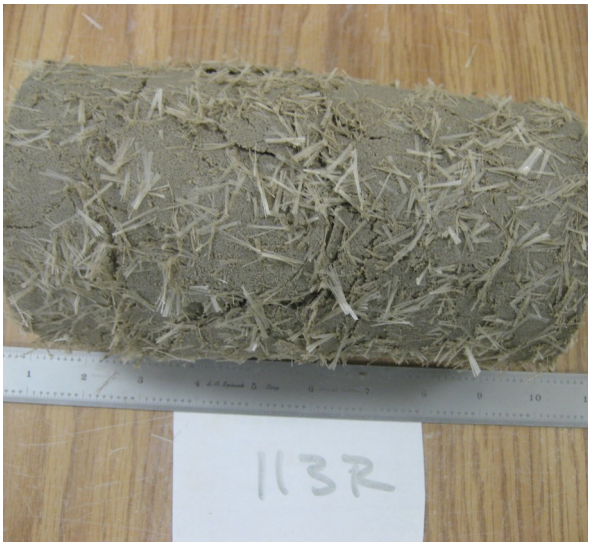

(b)

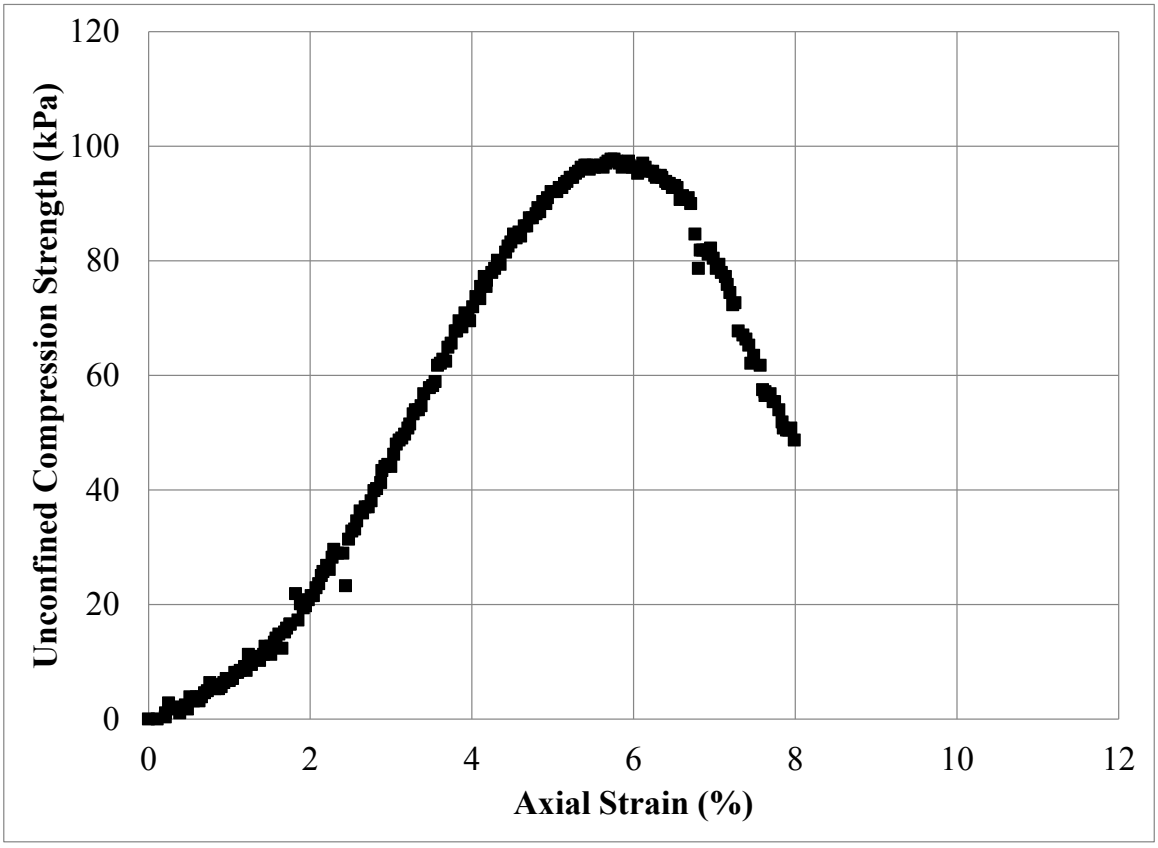

(c)

Figure C.56: Unconfined Compression Test Specimen No. 113R: (a) Photograph Prior to Testing; (b) Photograph Post Testing; and (c) Stress – Strain Data

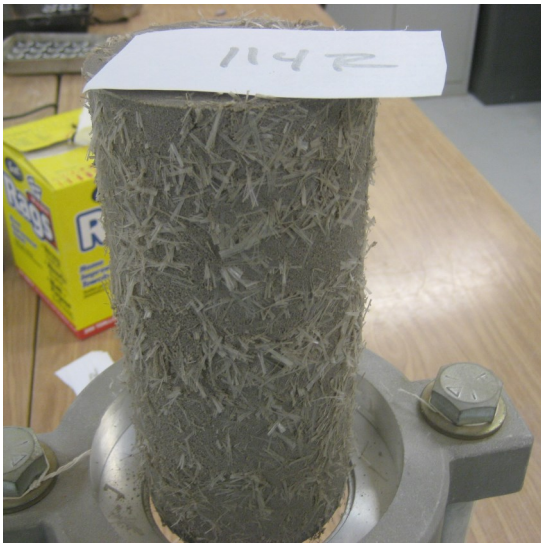

(a)

(b)

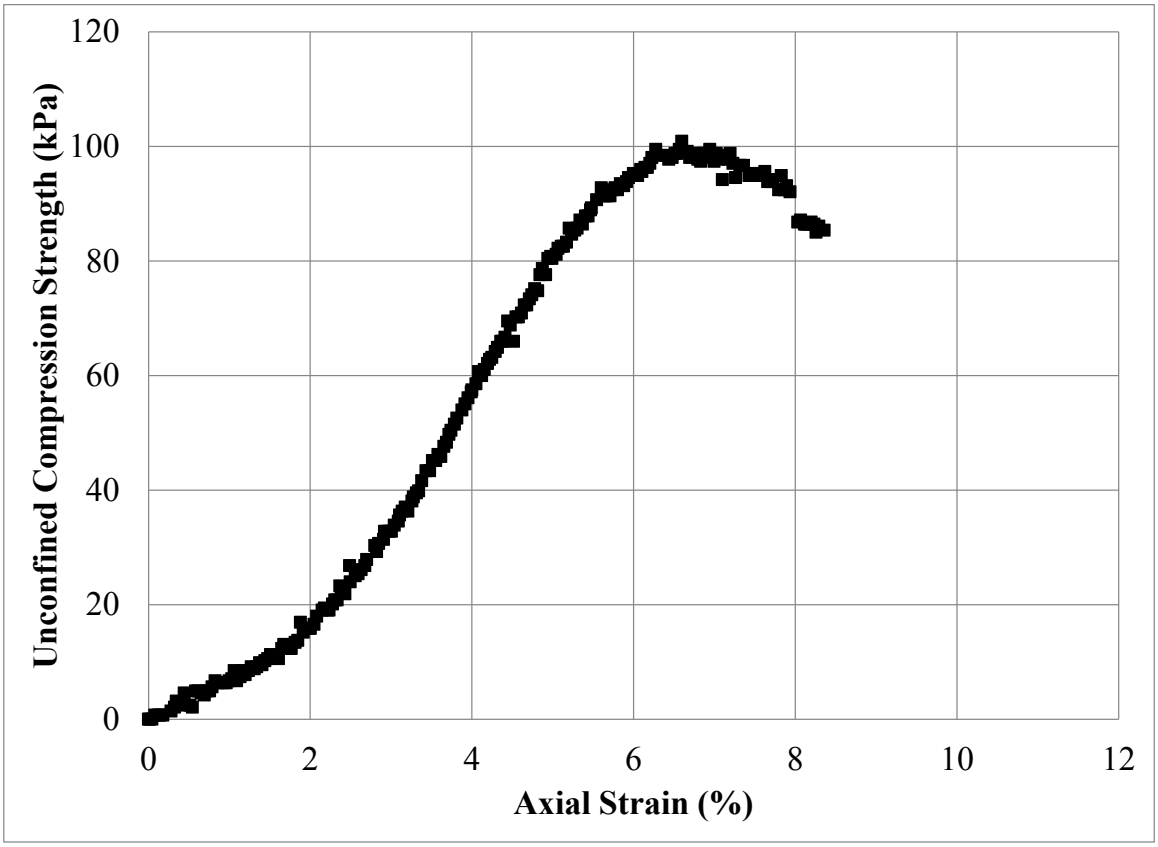

(c)

Figure C.57: Unconfined Compression Test Specimen No. 114R: (a) Photograph Prior to Testing; (b) Photograph Post Testing; and (c) Stress – Strain Data

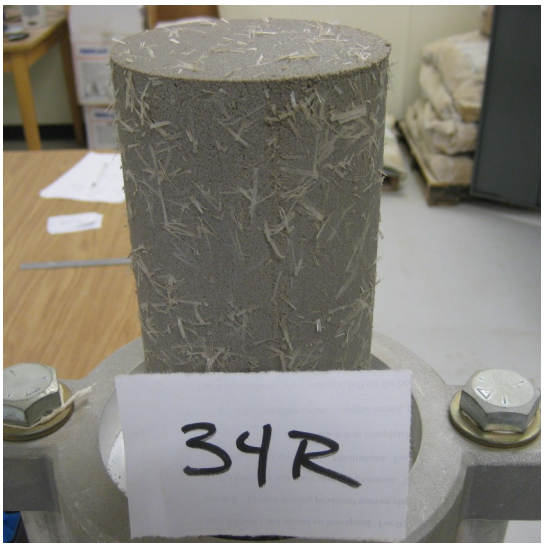

(a)

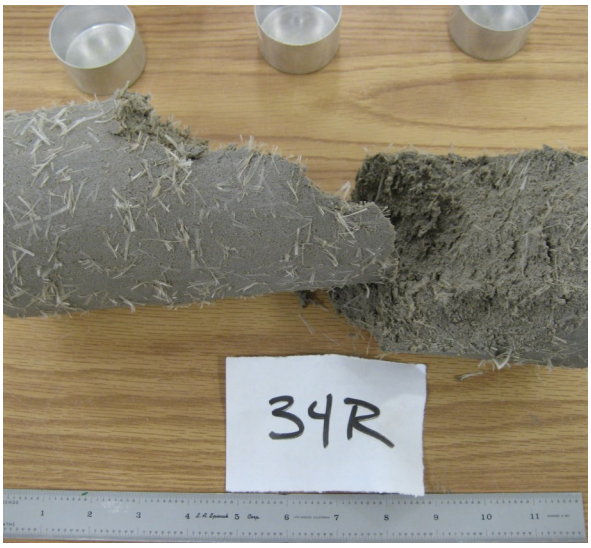

(b)

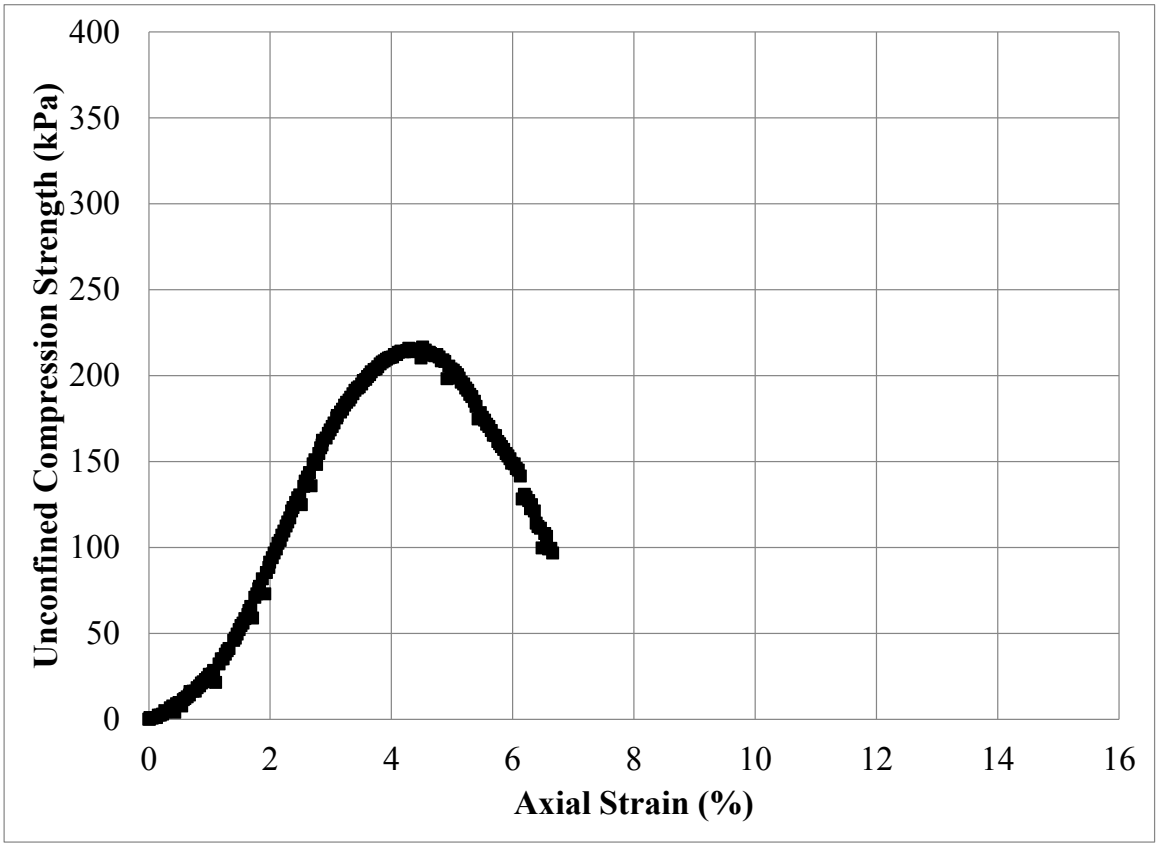

(c)

Figure C.58: Unconfined Compression Test Specimen No. 34R: (a) Photograph Prior to Testing; (b) Photograph Post Testing; and (c) Stress – Strain Data

(a)

(b)

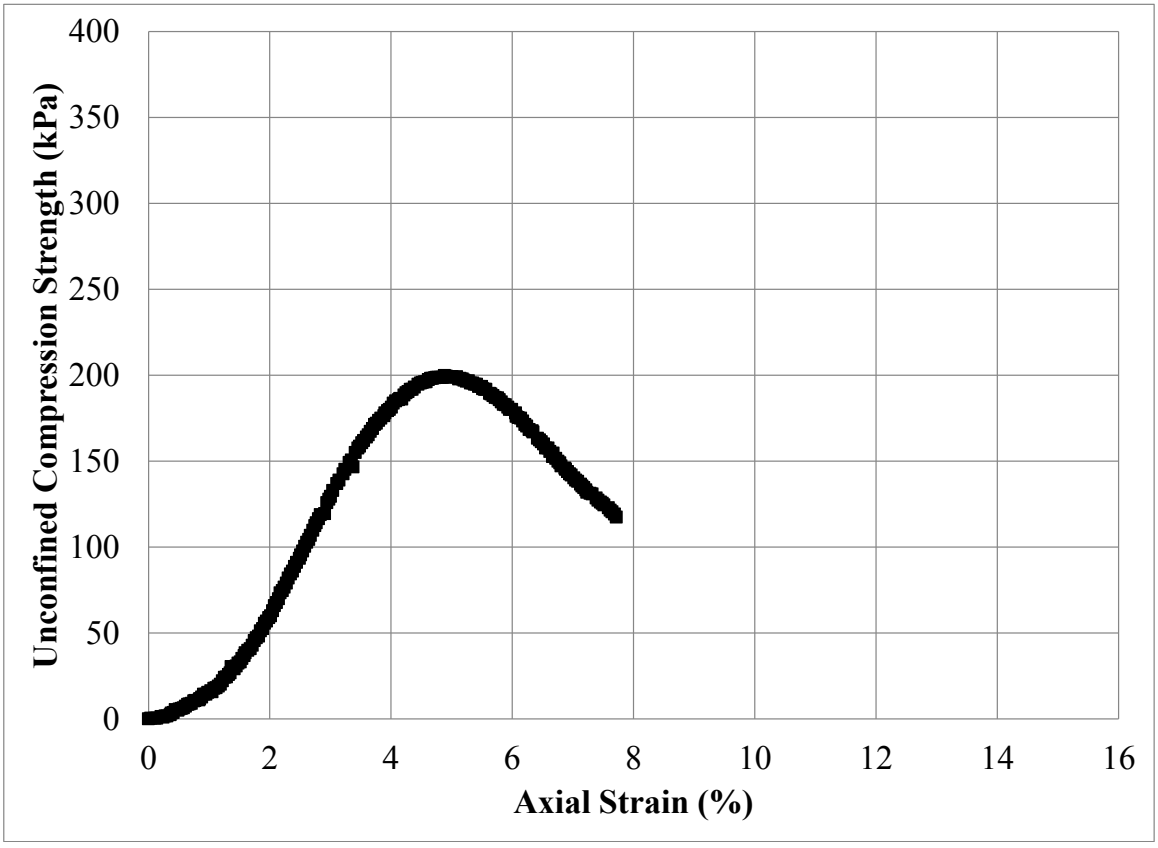

(c)

Figure C.59: Unconfined Compression Test Specimen No. 35R: (a) Photograph Prior to Testing; (b) Photograph Post Testing; and (c) Stress – Strain Data

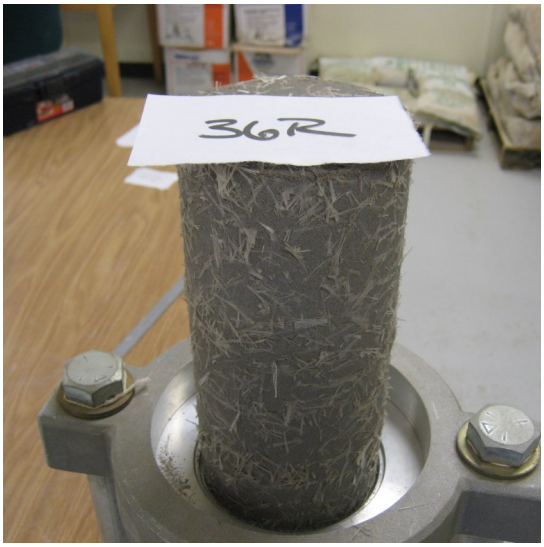

(a)

(b)

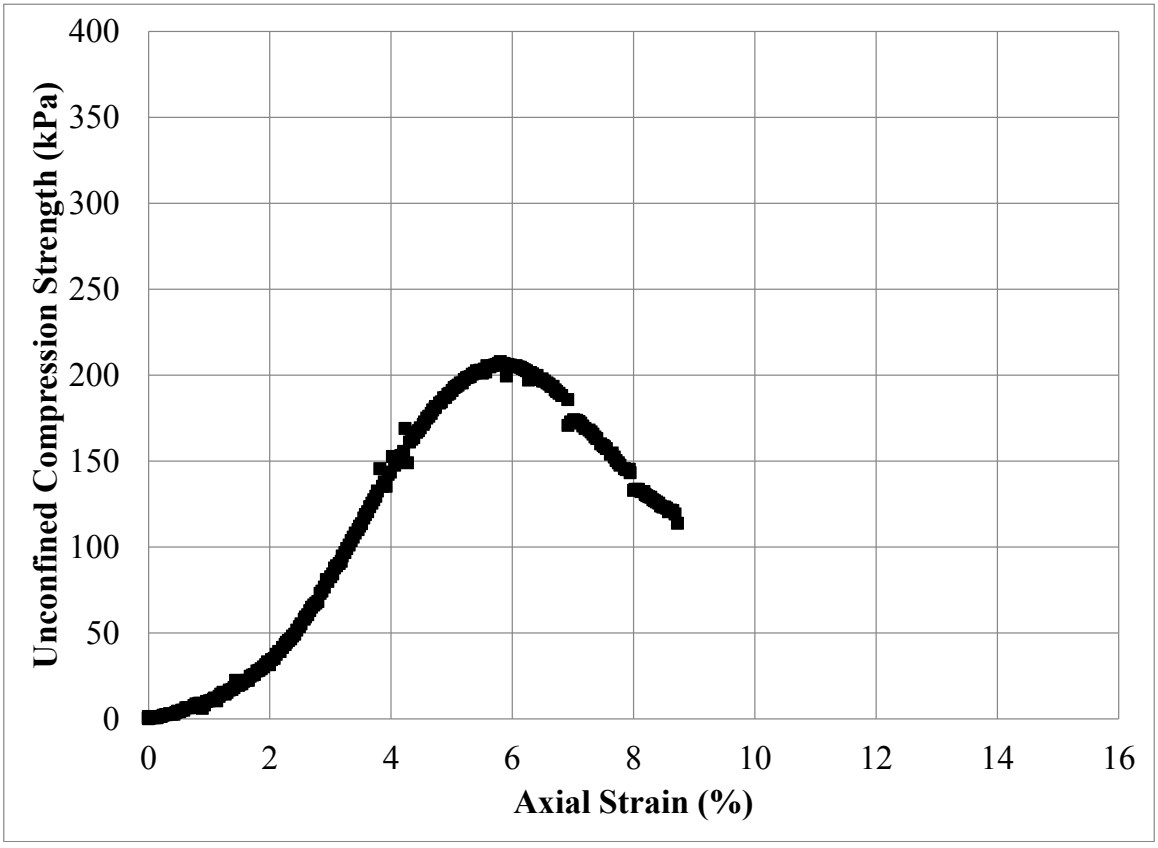

(c)

Figure C.60: Unconfined Compression Test Specimen No. 36R: (a) Photograph Prior to Testing; (b) Photograph Post Testing; and (c) Stress – Strain Data

(a)

(b)

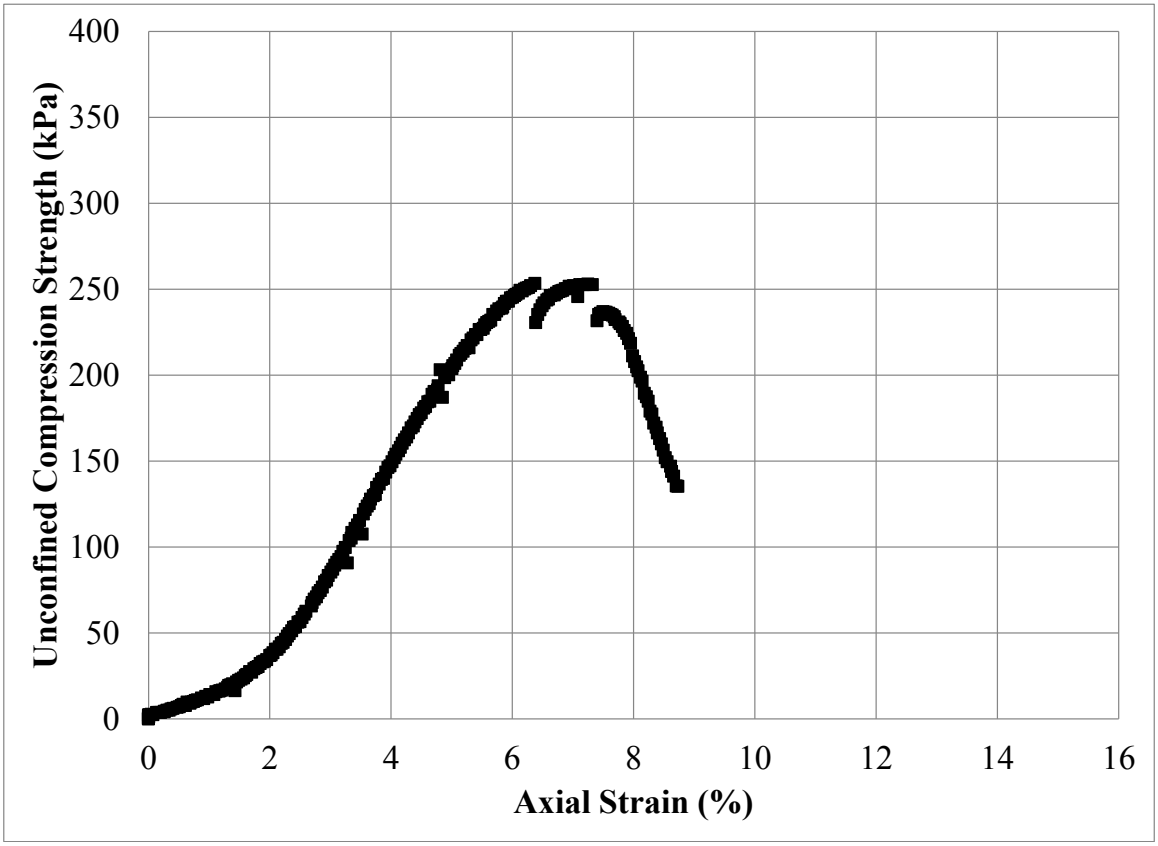

(c)

Figure C.61: Unconfined Compression Test Specimen No. 37R: (a) Photograph Prior to Testing; (b) Photograph Post Testing; and (c) Stress – Strain Data

(a)

(b)

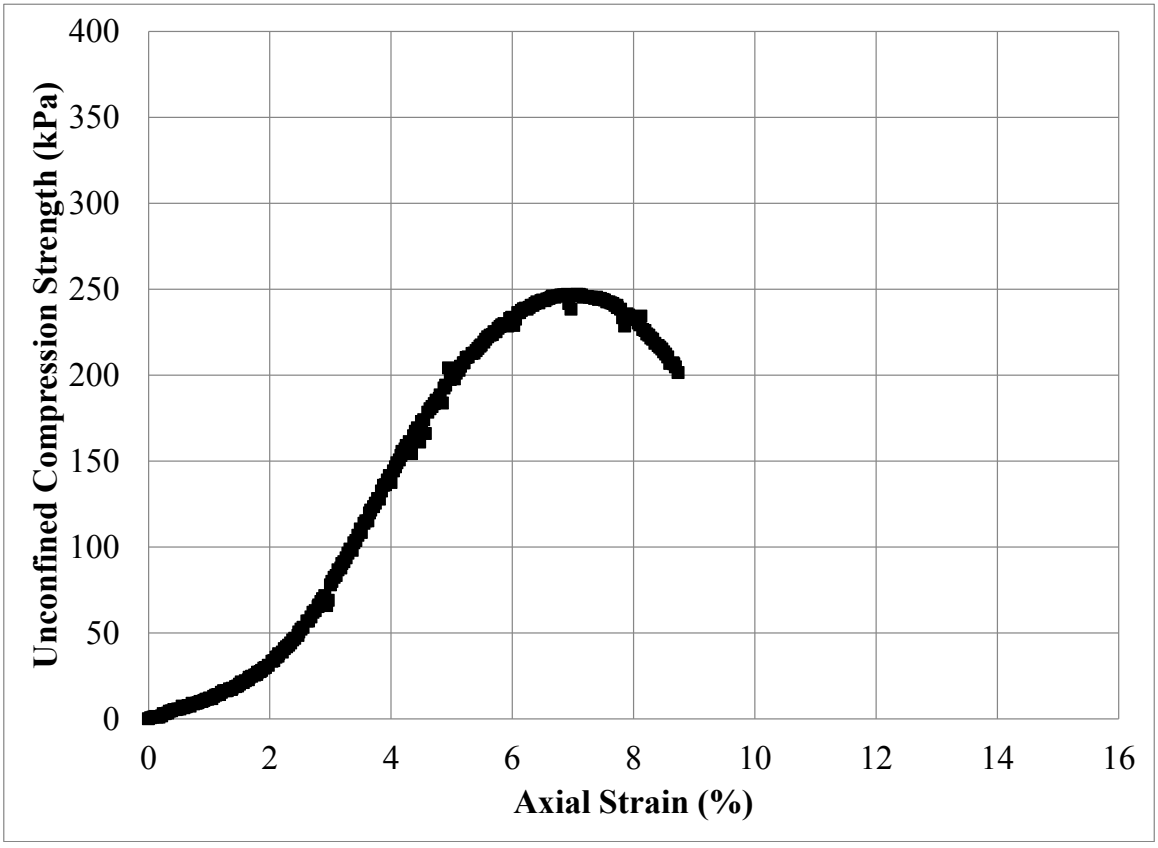

(c)

Figure C.62: Unconfined Compression Test Specimen No. 38R: (a) Photograph Prior to Testing; (b) Photograph Post Testing; and (c) Stress – Strain Data

(a)

(b)

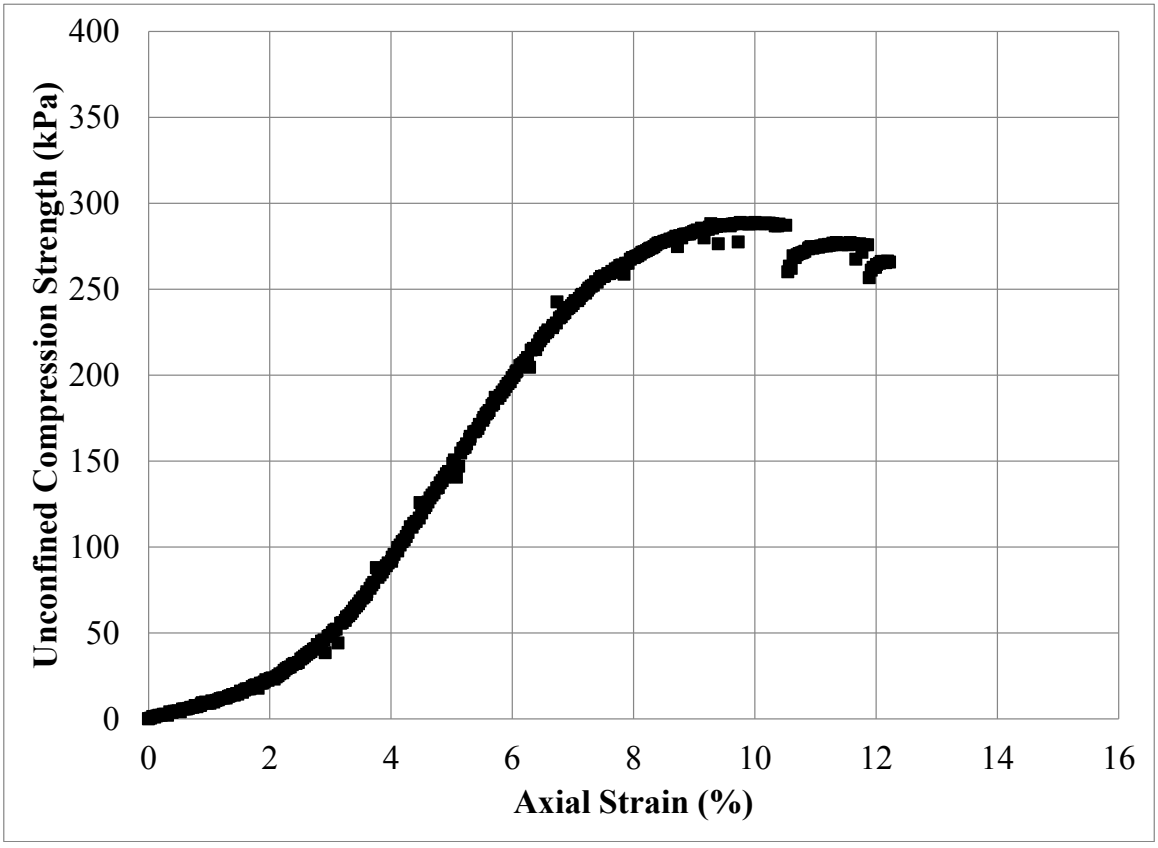

(c)

Figure C.63: Unconfined Compression Test Specimen No. 39R: (a) Photograph Prior to Testing; (b) Photograph Post Testing; and (c) Stress – Strain Data

(a)

(b)

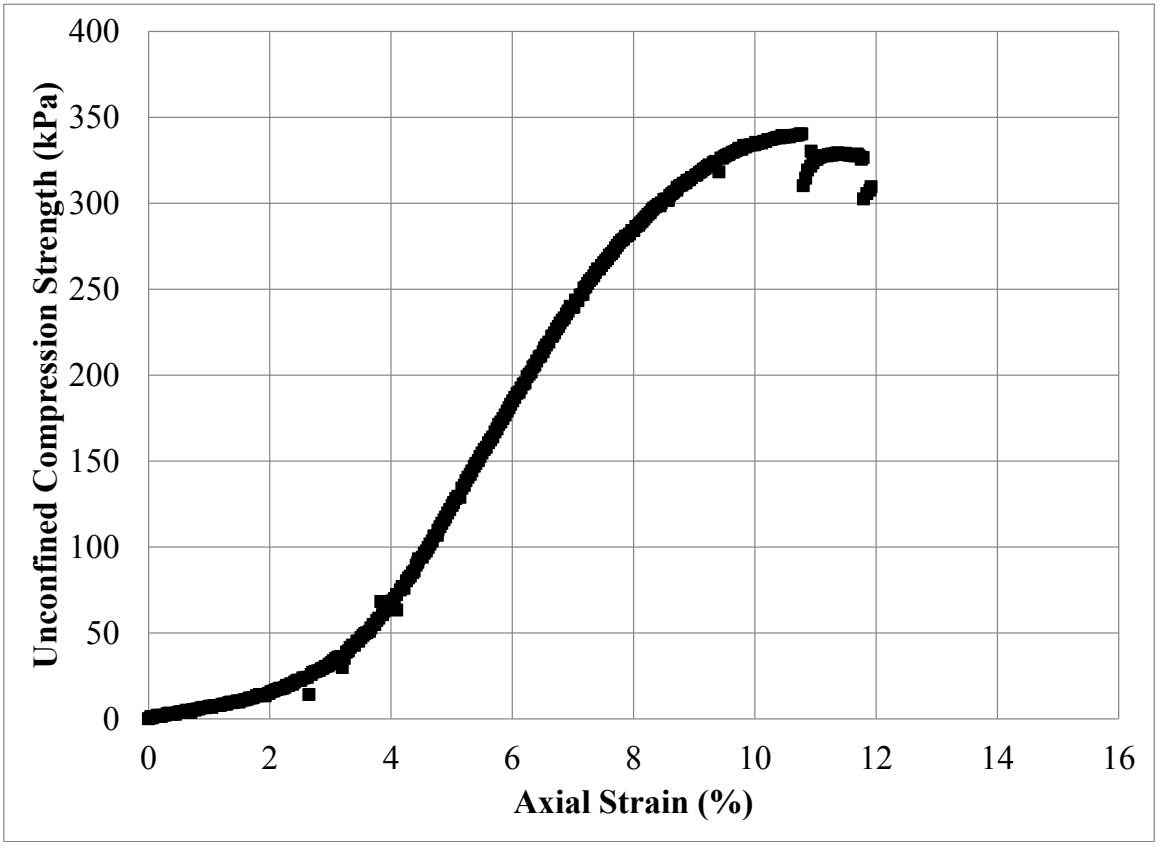

(c)

Figure C.64: Unconfined Compression Test Specimen No. 40R: (a) Photograph Prior to Testing; (b) Photograph Post Testing; and (c) Stress – Strain Data

(a)

(b)

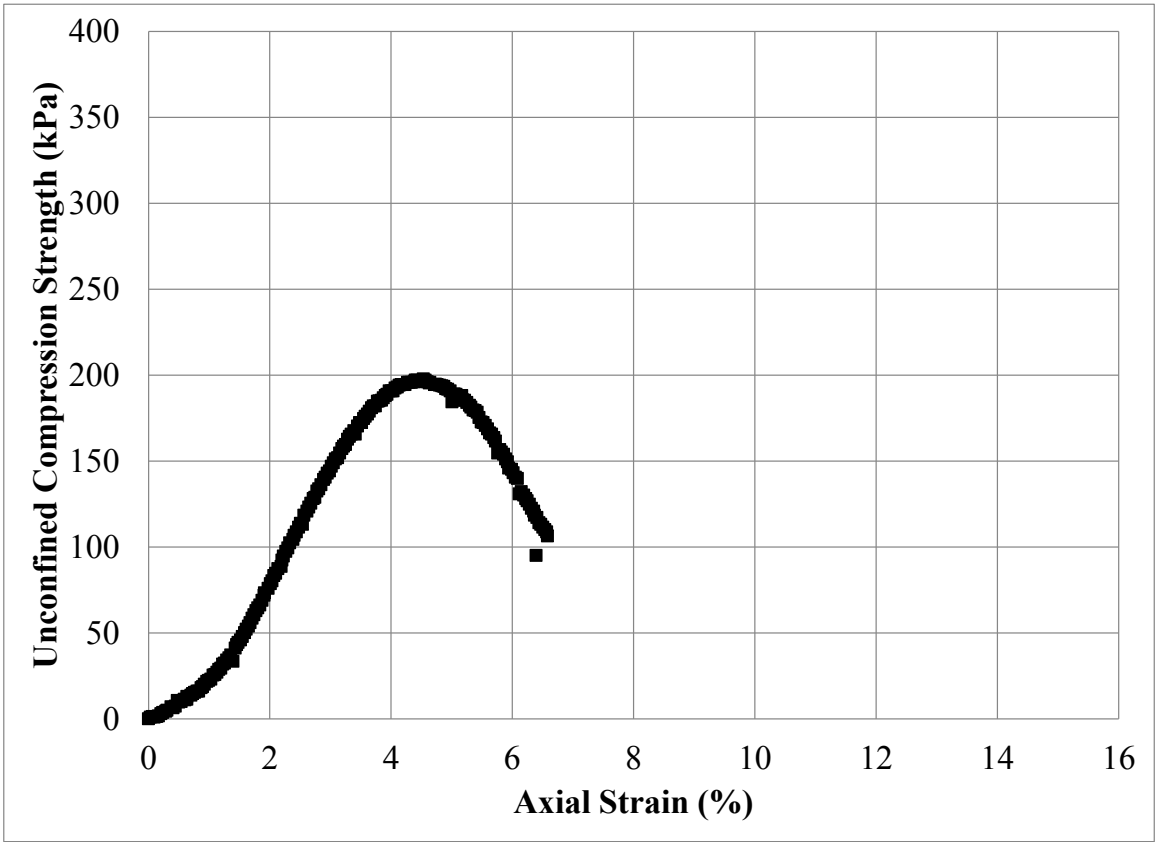

(c)

Figure C.65: Unconfined Compression Test Specimen No. 41R: (a) Photograph Prior to Testing; (b) Photograph Post Testing; and (c) Stress – Strain Data

(a)

(b)

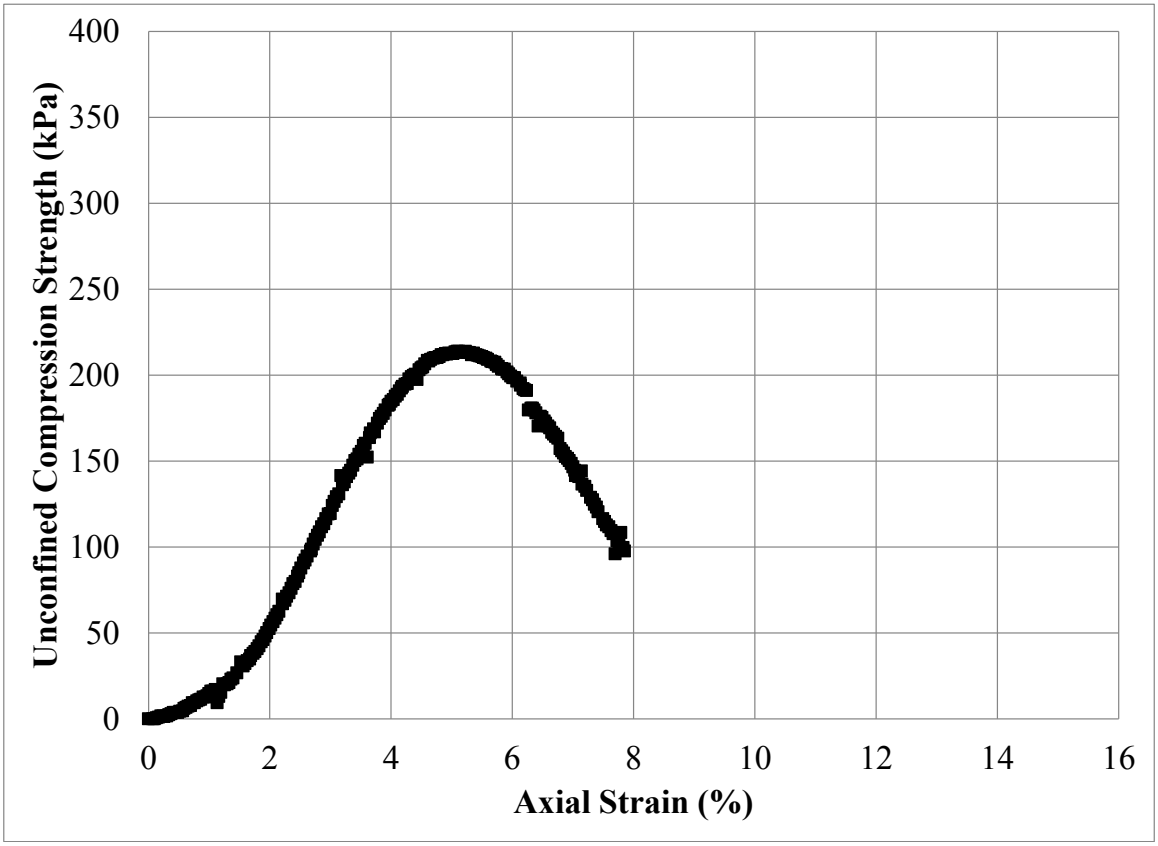

(c)

Figure C.66: Unconfined Compression Test Specimen No. 42R: (a) Photograph Prior to Testing; (b) Photograph Post Testing; and (c) Stress – Strain Data

(a)

(b)

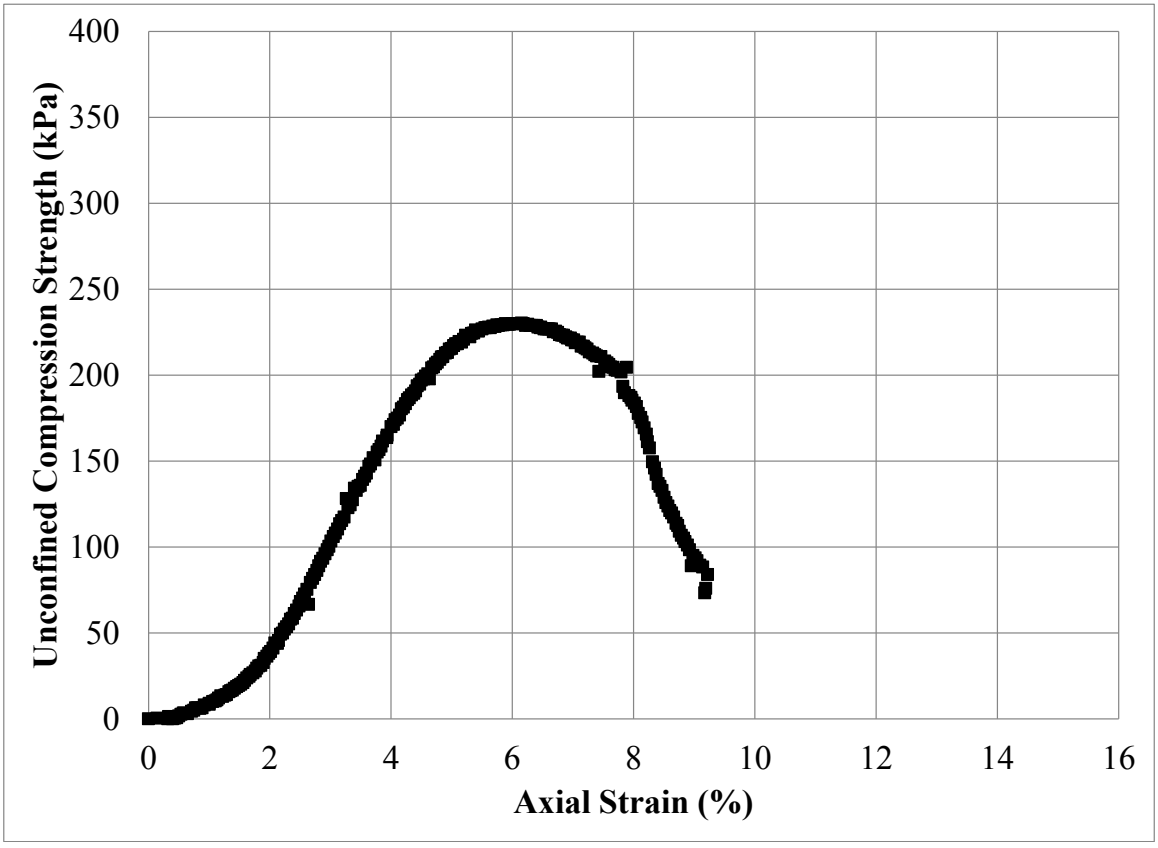

(c)

Figure C.67: Unconfined Compression Test Specimen No. 43R: (a) Photograph Prior to Testing; (b) Photograph Post Testing; and (c) Stress – Strain Data

(a)

(b)

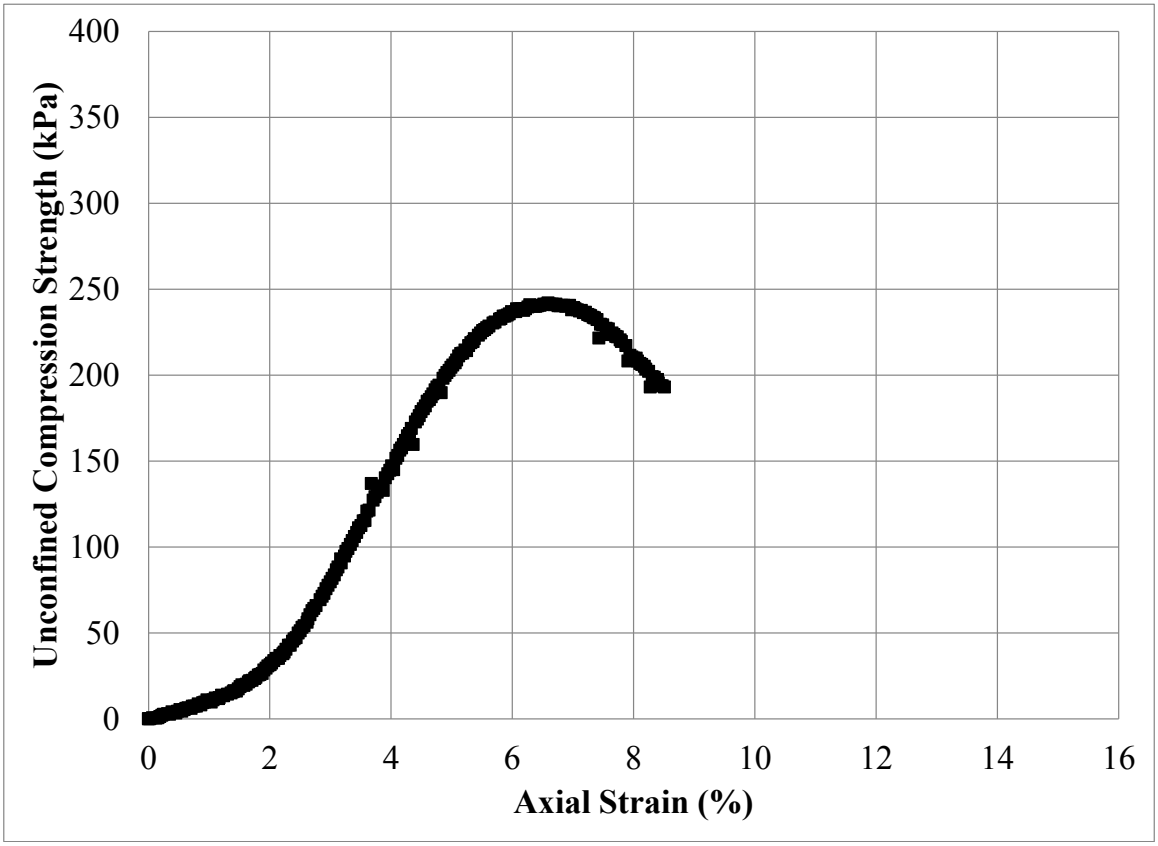

(c)

Figure C.68: Unconfined Compression Test Specimen No. 44R: (a) Photograph Prior to Testing; (b) Photograph Post Testing; and (c) Stress – Strain Data

(a)

(b)

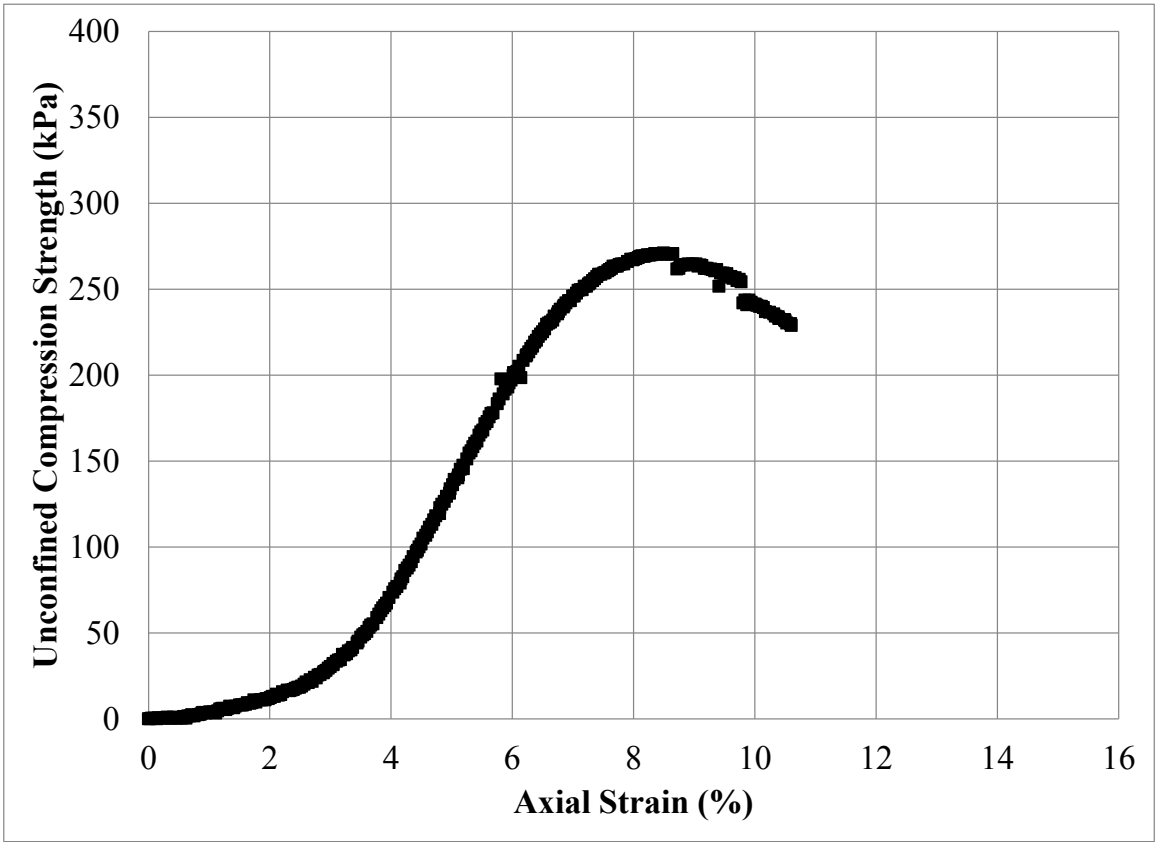

(c)

Figure C.69: Unconfined Compression Test Specimen No. 45R: (a) Photograph Prior to Testing; (b) Photograph Post Testing; and (c) Stress – Strain Data

(a)

(b)

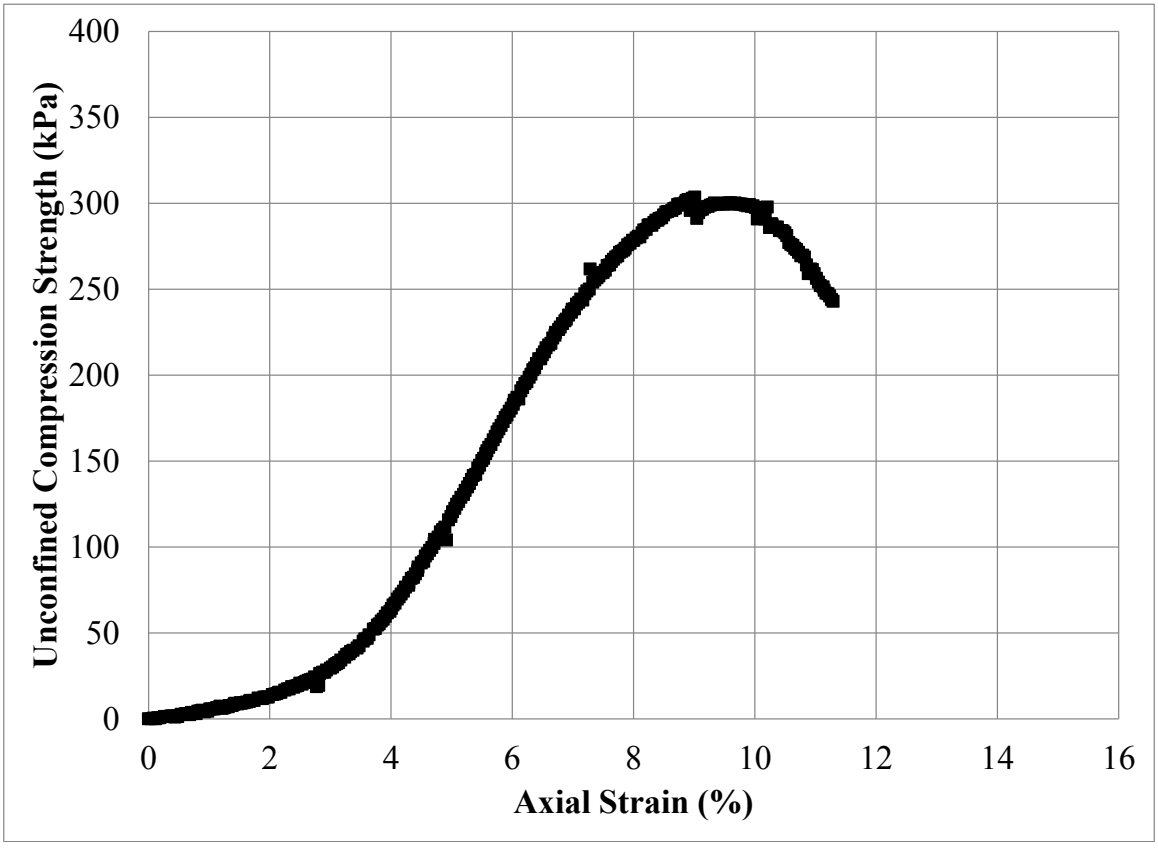

(c)

Figure C.70: Unconfined Compression Test Specimen No. 46R: (a) Photograph Prior to Testing; (b) Photograph Post Testing; and (c) Stress – Strain Data

(a)

(b)

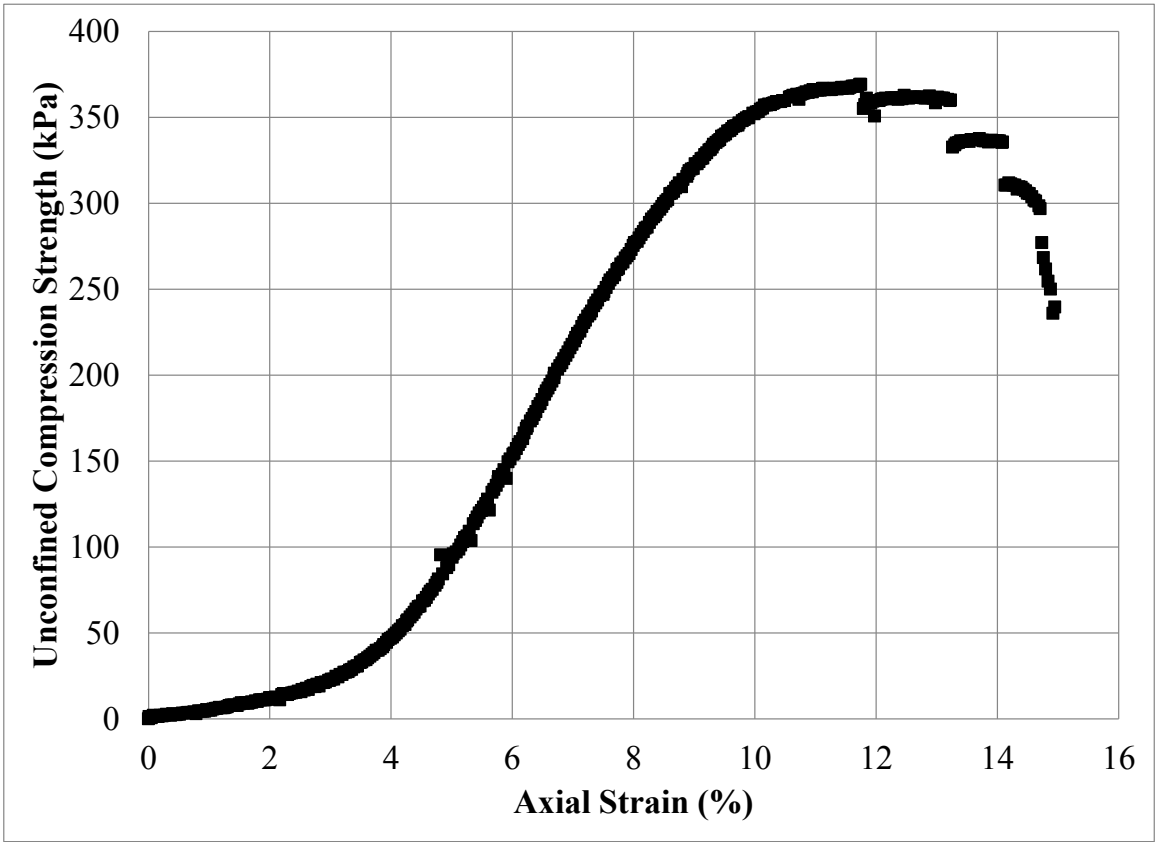

(c)

Figure C.71: Unconfined Compression Test Specimen No. 47R: (a) Photograph Prior to Testing; (b) Photograph Post Testing; and (c) Stress – Strain Data

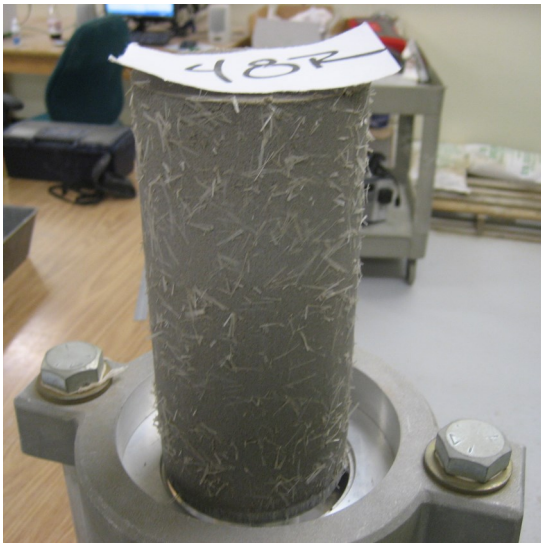

(a)

(b)

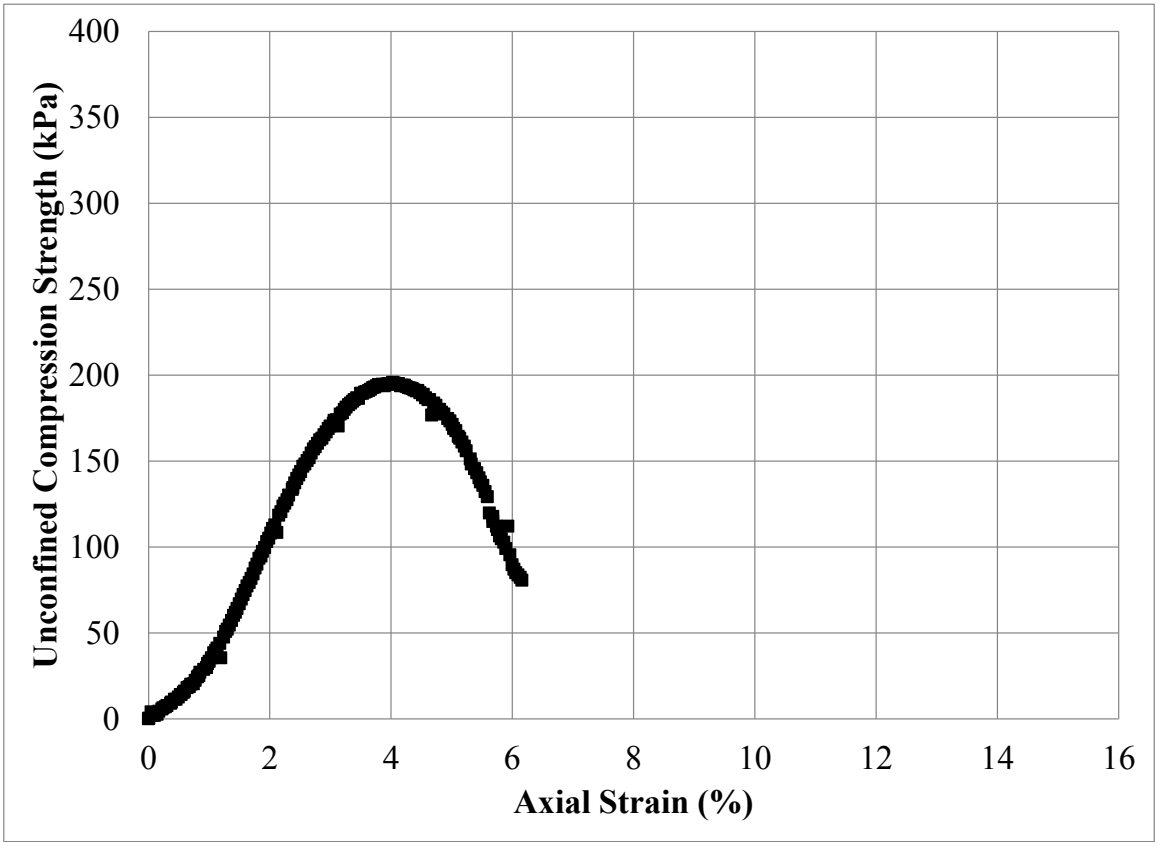

(c)

Figure C.72: Unconfined Compression Test Specimen No. 48R: (a) Photograph Prior to Testing; (b) Photograph Post Testing; and (c) Stress – Strain Data

(a)

(b)

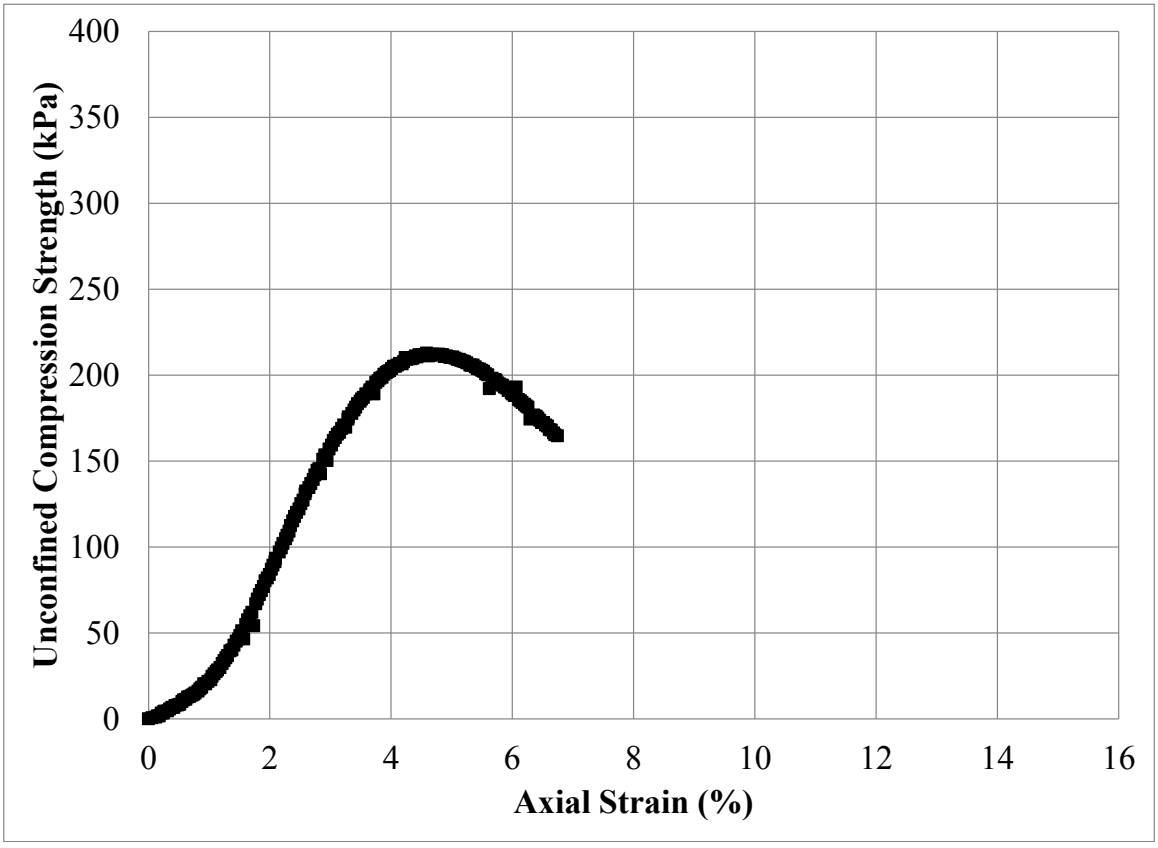

(c)

Figure C.73: Unconfined Compression Test Specimen No. 49R: (a) Photograph Prior to Testing; (b) Photograph Post Testing; and (c) Stress – Strain Data

(a)

(b)

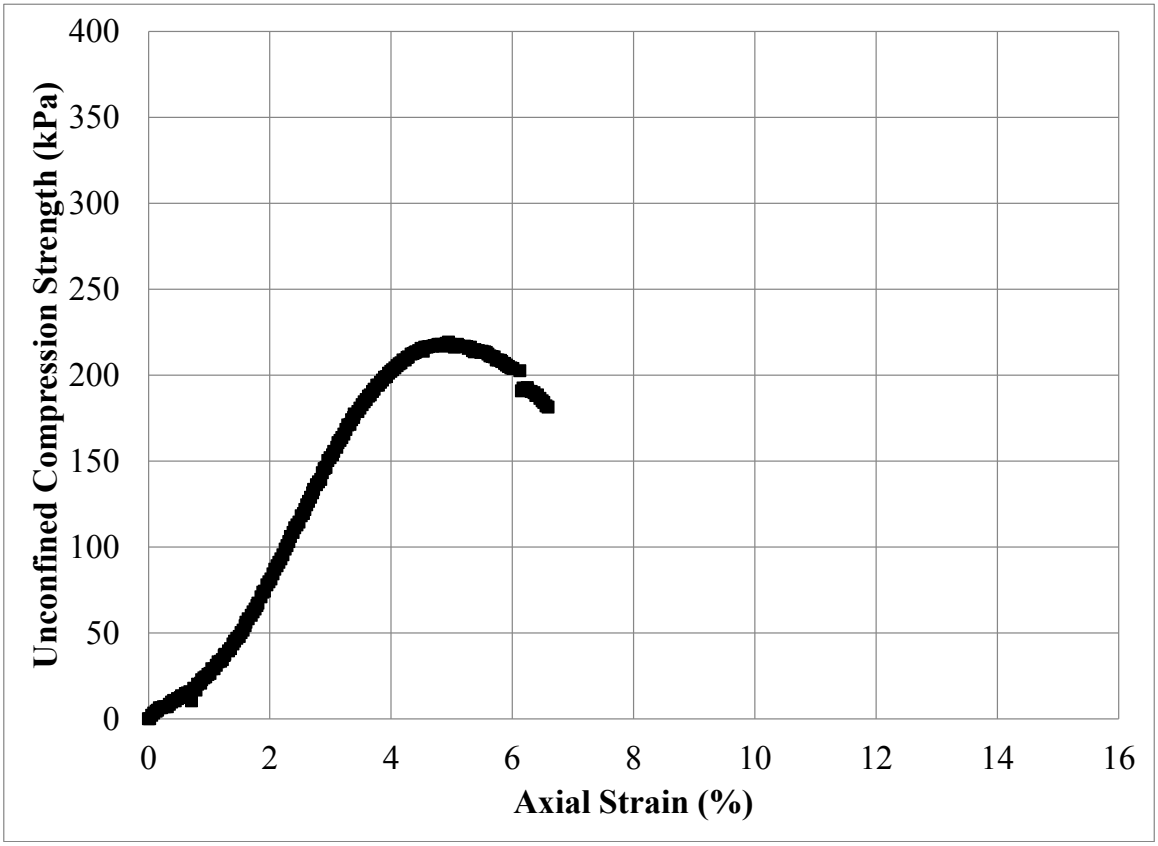

(c)

Figure C.74: Unconfined Compression Test Specimen No. 50R: (a) Photograph Prior to Testing; (b) Photograph Post Testing; and (c) Stress – Strain Data

(a)

(b)

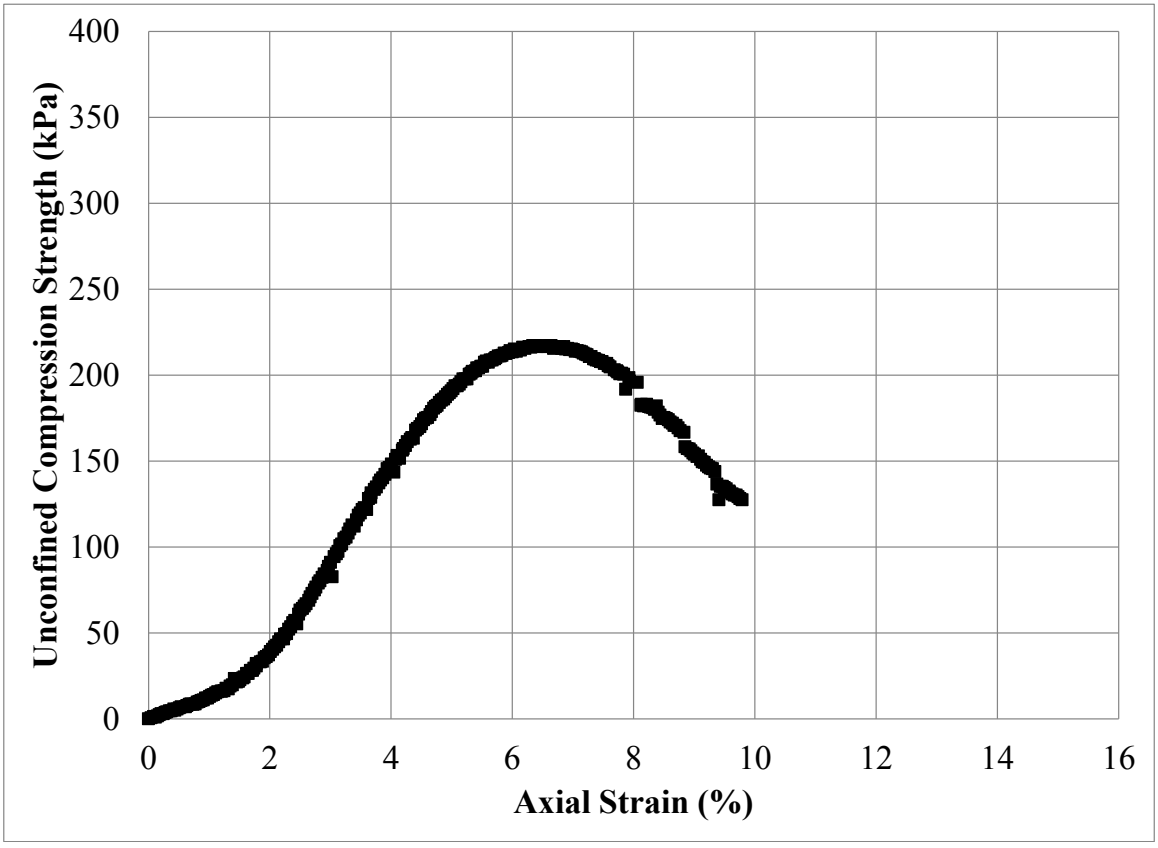

(c)

Figure C.75: Unconfined Compression Test Specimen No. 51R: (a) Photograph Prior to Testing; (b) Photograph Post Testing; and (c) Stress – Strain Data

(a)

(b)

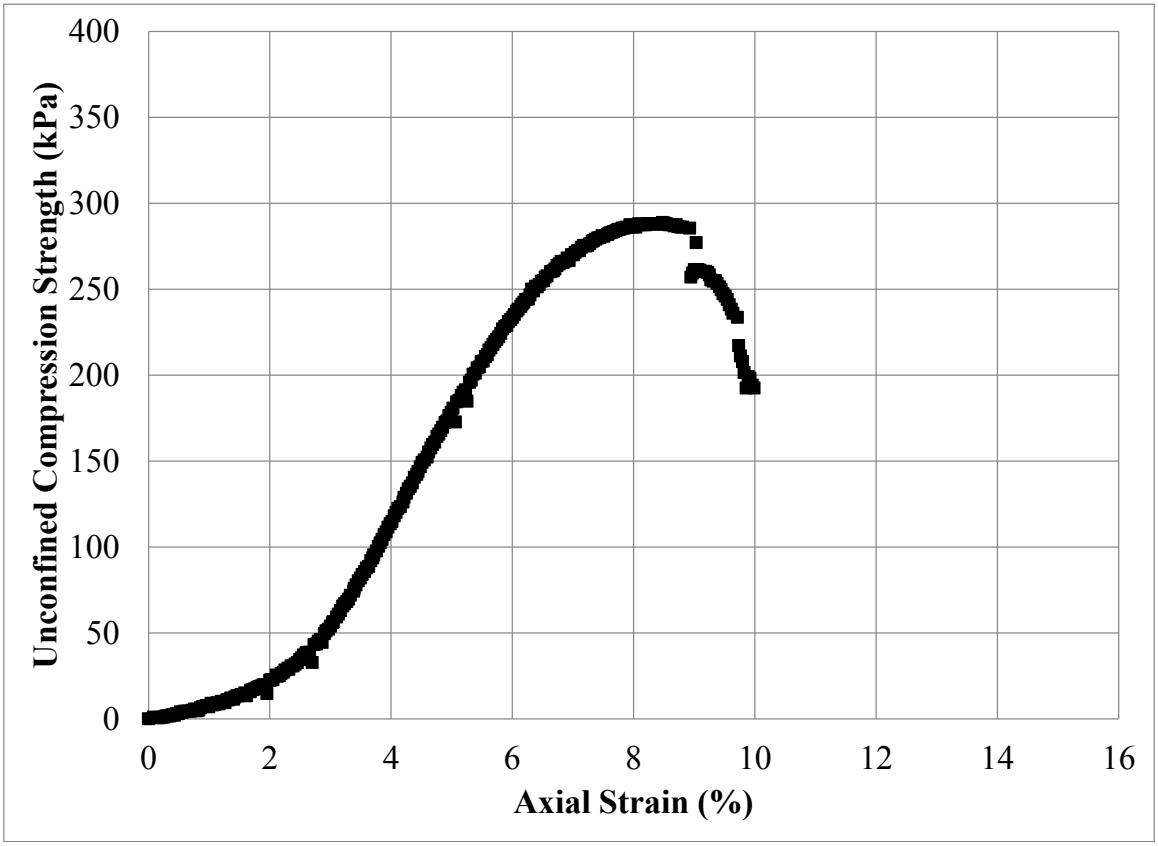

(c)

Figure C.76: Unconfined Compression Test Specimen No. 52R: (a) Photograph Prior to Testing; (b) Photograph Post Testing; and (c) Stress – Strain Data

(a)

(b)

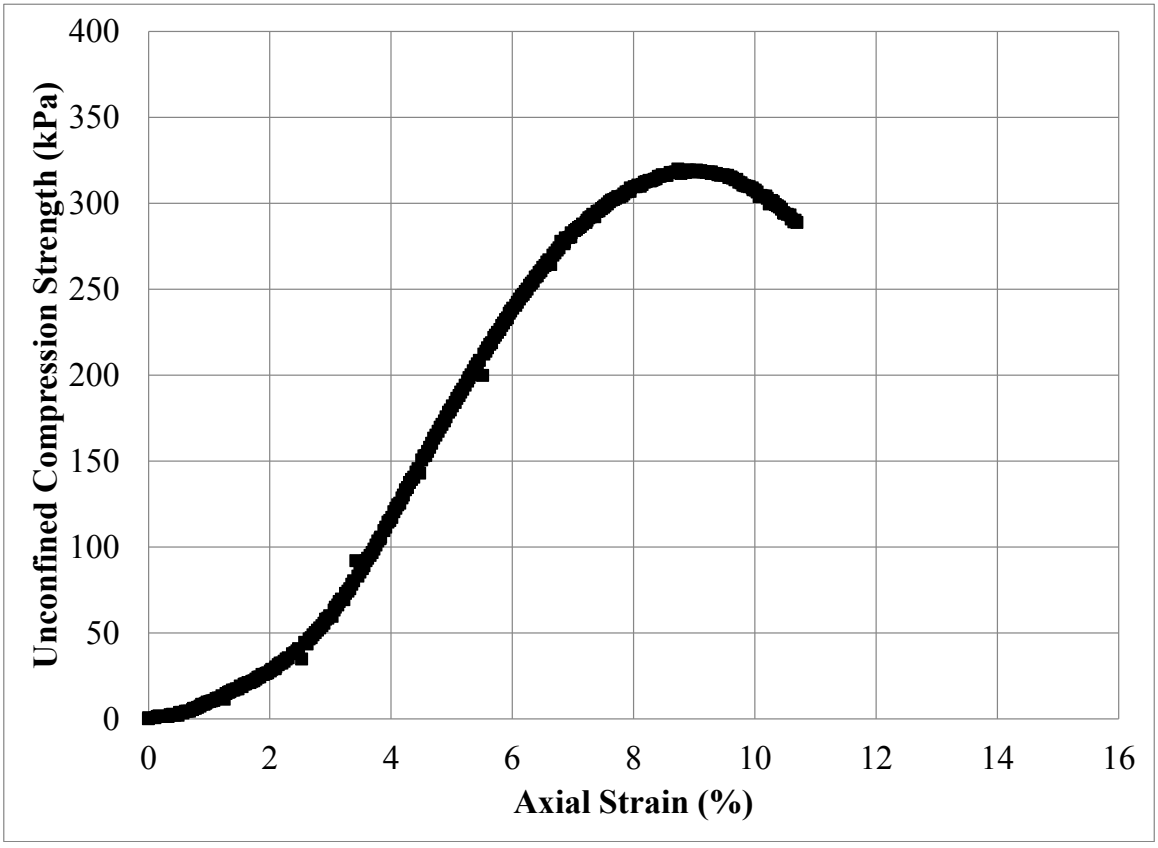

(c)

Figure C.77: Unconfined Compression Test Specimen No. 53R: (a) Photograph Prior to Testing; (b) Photograph Post Testing; and (c) Stress – Strain Data

(a)

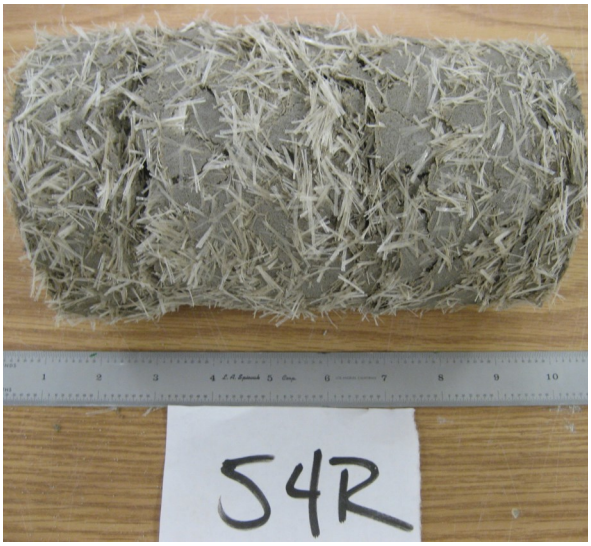

(b)

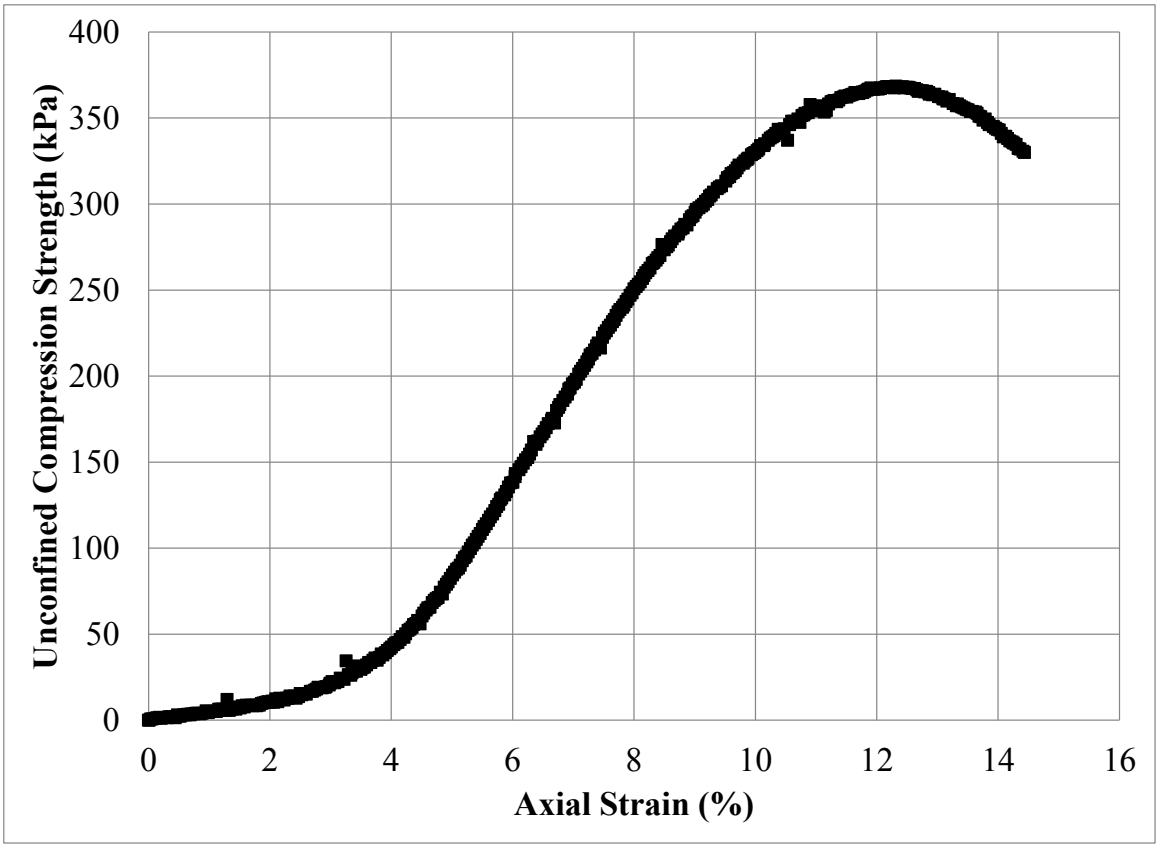

(c)

Figure C.78: Unconfined Compression Test Specimen No. 54R: (a) Photograph Prior to Testing; (b) Photograph Post Testing; and (c) Stress – Strain Data

(a)

(b)

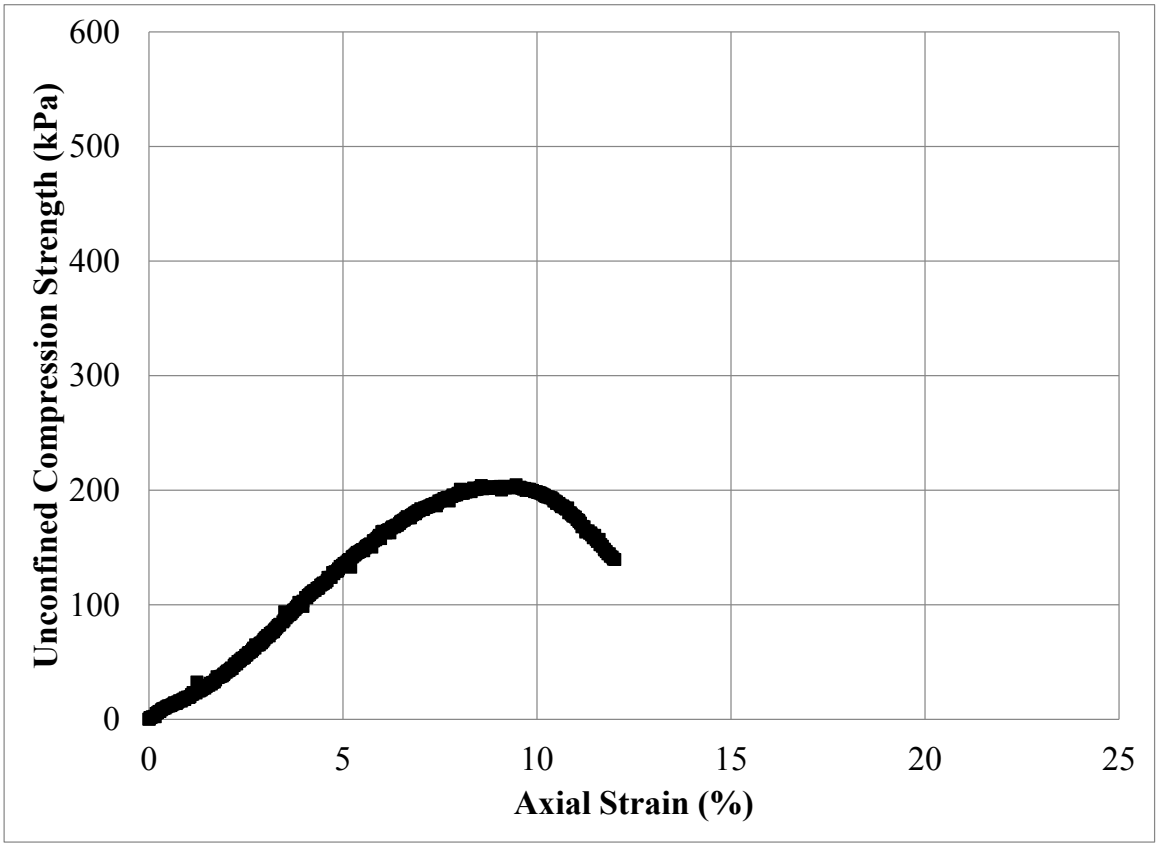

(c)

Figure C.79: Unconfined Compression Test Specimen No. 115R: (a) Photograph Prior to Testing; (b) Photograph Post Testing; and (c) Stress – Strain Data

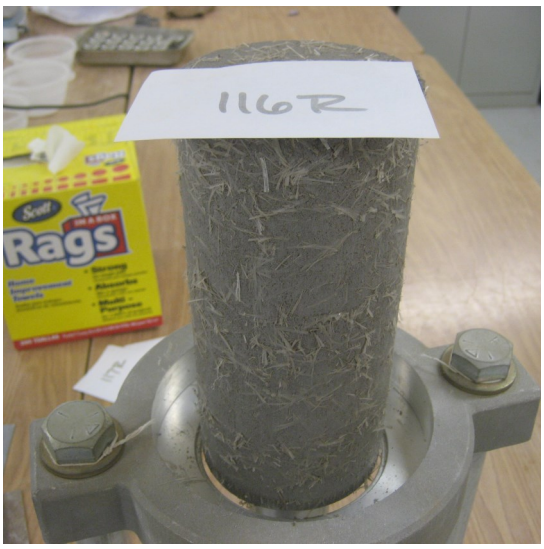

(a)

(b)

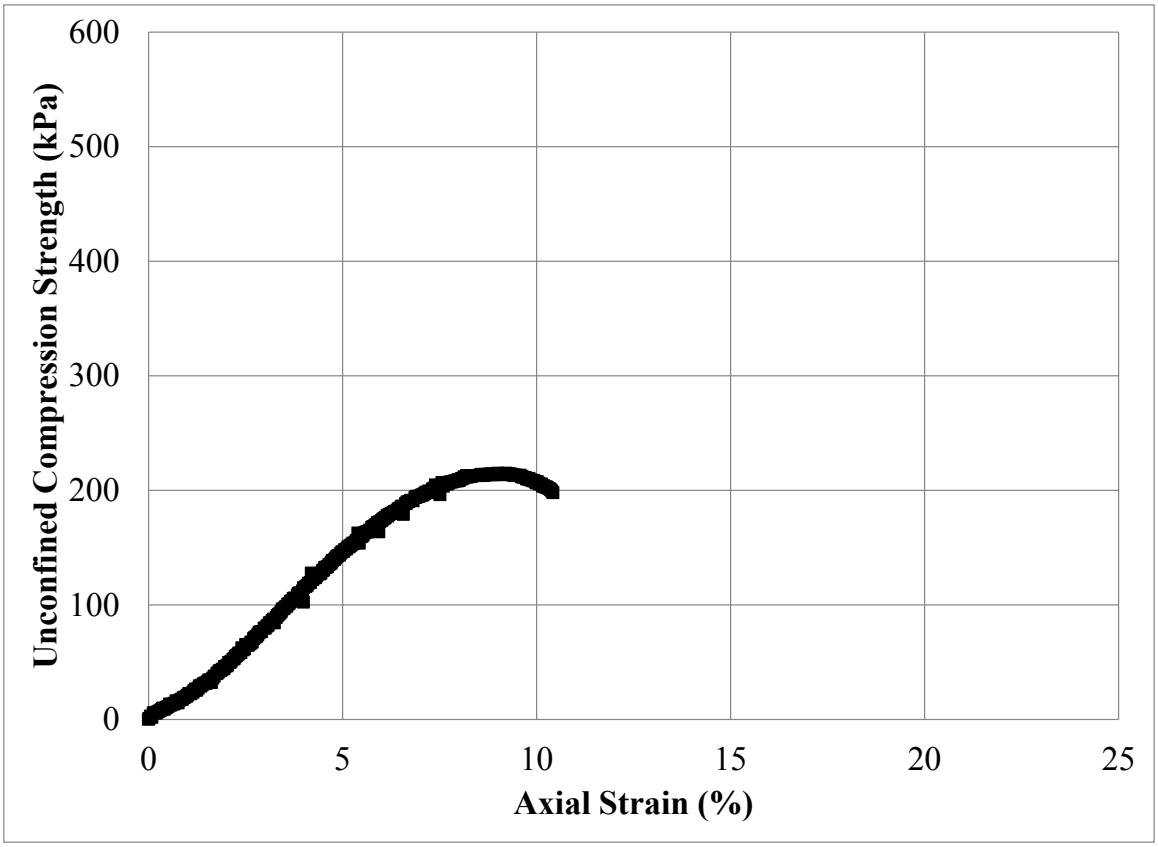

(c)

Figure C.80: Unconfined Compression Test Specimen No. 116R: (a) Photograph Prior to Testing; (b) Photograph Post Testing; and (c) Stress – Strain Data

(a)

(b)

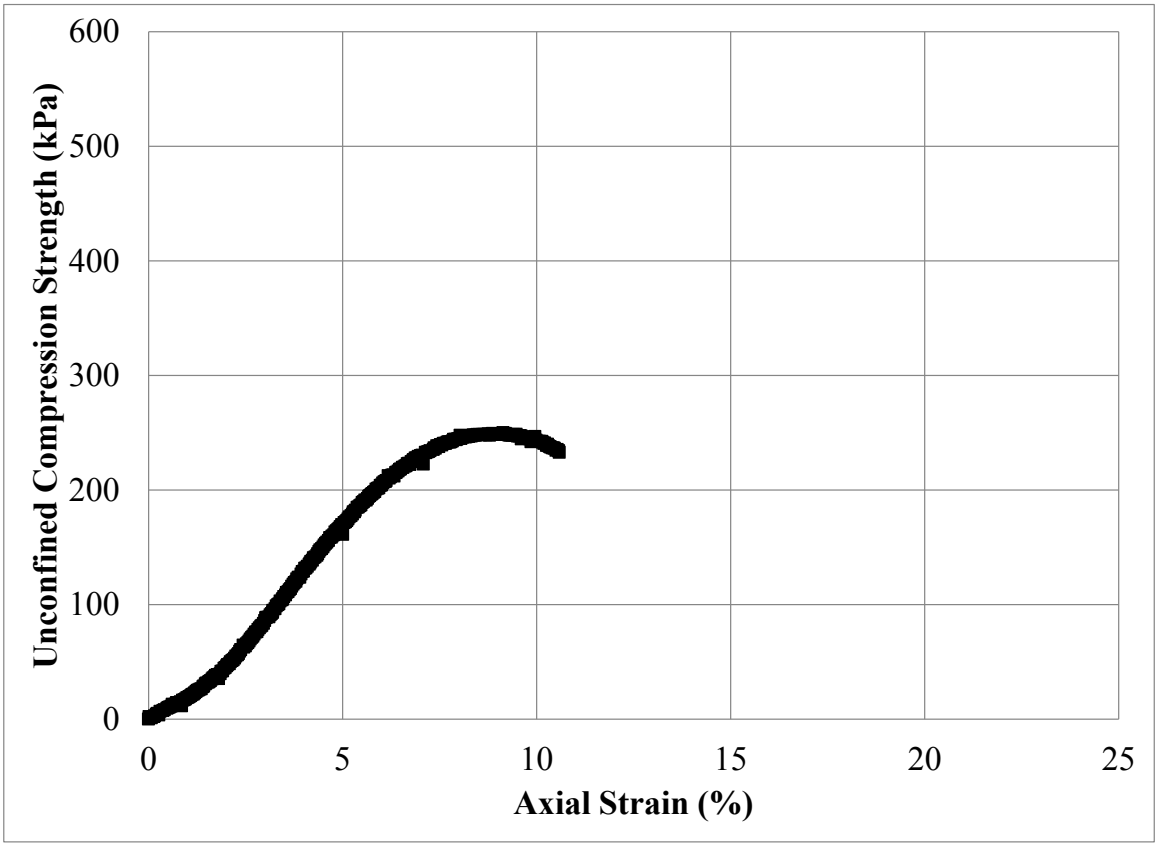

(c)

Figure C.81: Unconfined Compression Test Specimen No. 117R: (a) Photograph Prior to Testing; (b) Photograph Post Testing; and (c) Stress – Strain Data

(a)

(b)

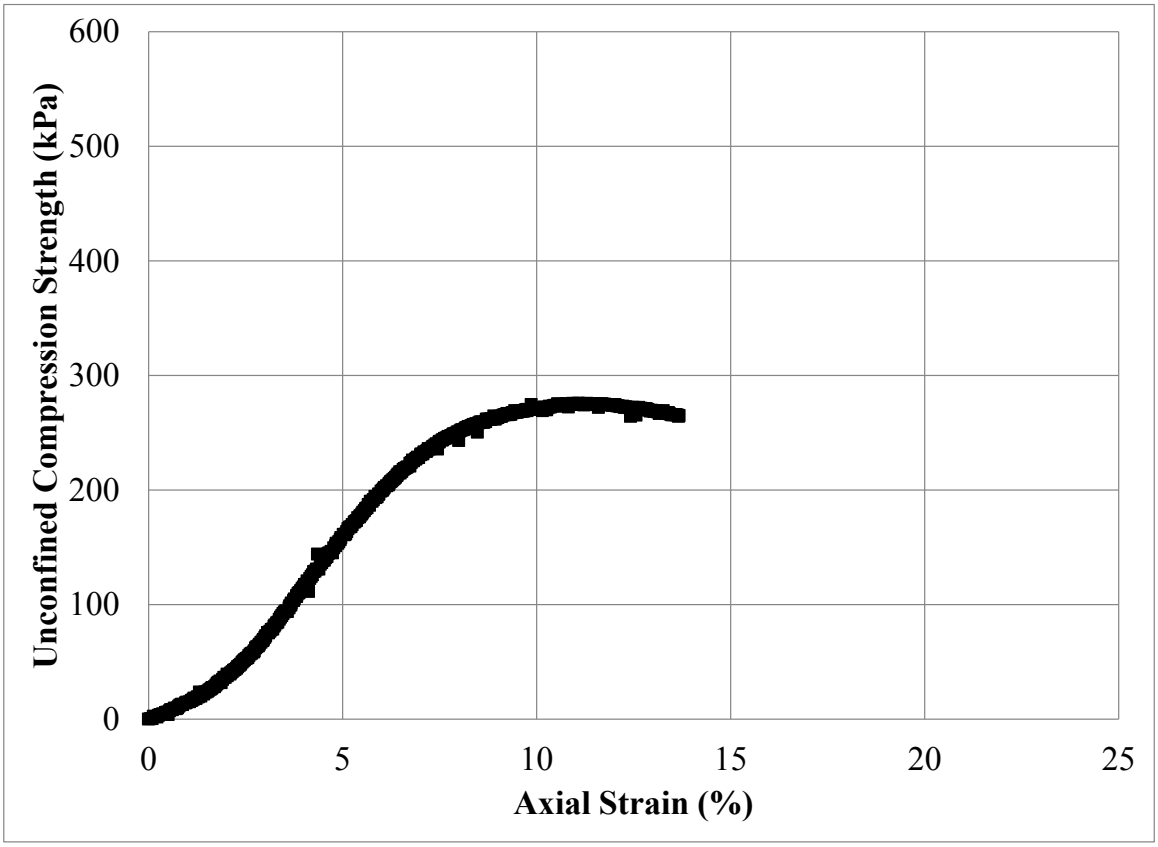

(c)

Figure C.82: Unconfined Compression Test Specimen No. 118R: (a) Photograph Prior to Testing; (b) Photograph Post Testing; and (c) Stress – Strain Data

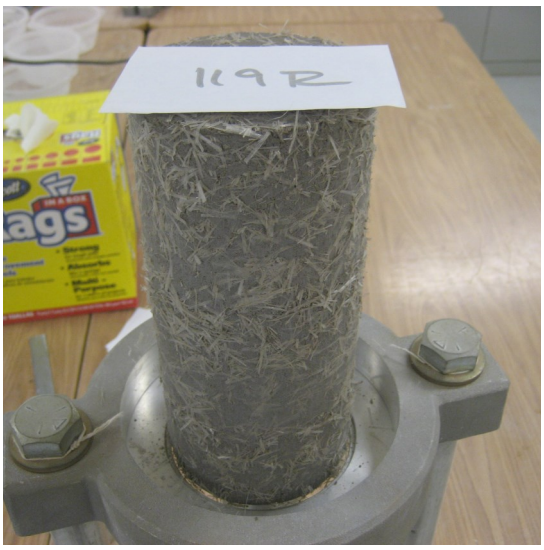

(a)

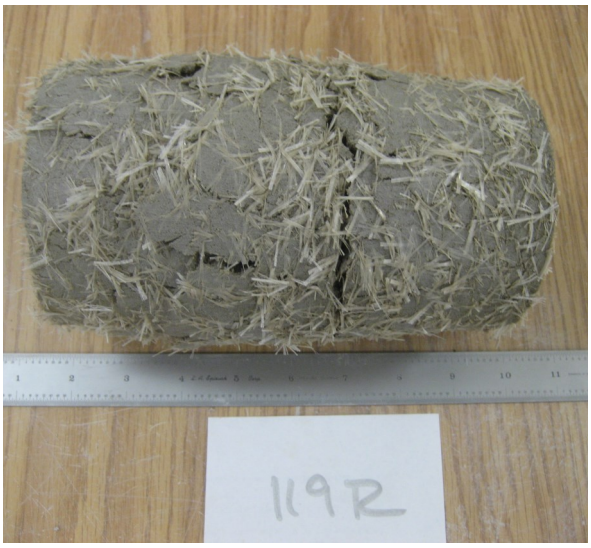

(b)

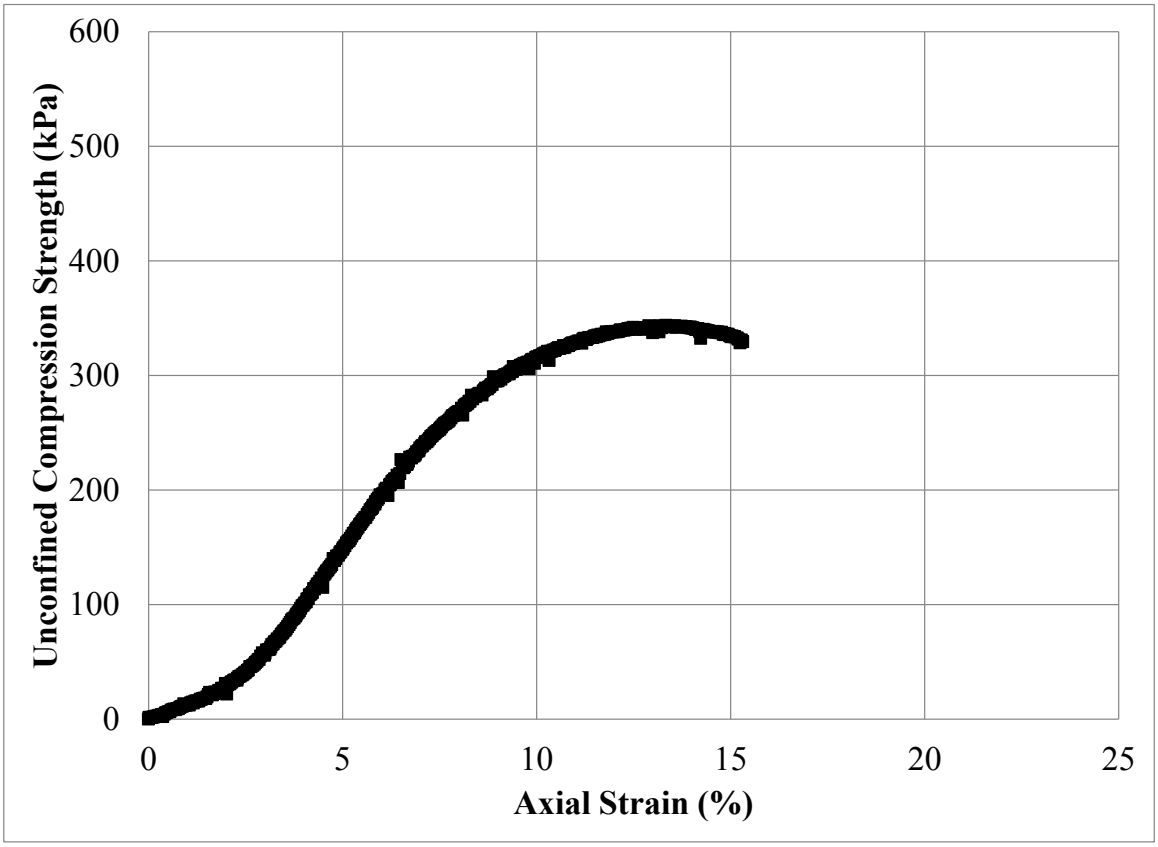

(c)

Figure C.83: Unconfined Compression Test Specimen No. 119R: (a) Photograph Prior to Testing; (b) Photograph Post Testing; and (c) Stress – Strain Data

(a)

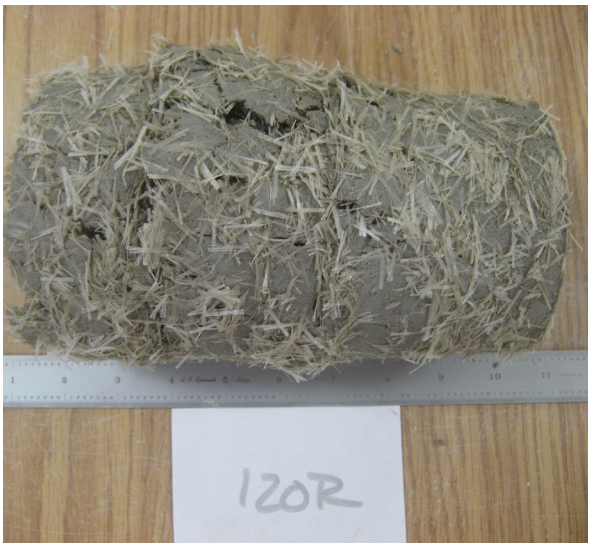

(b)

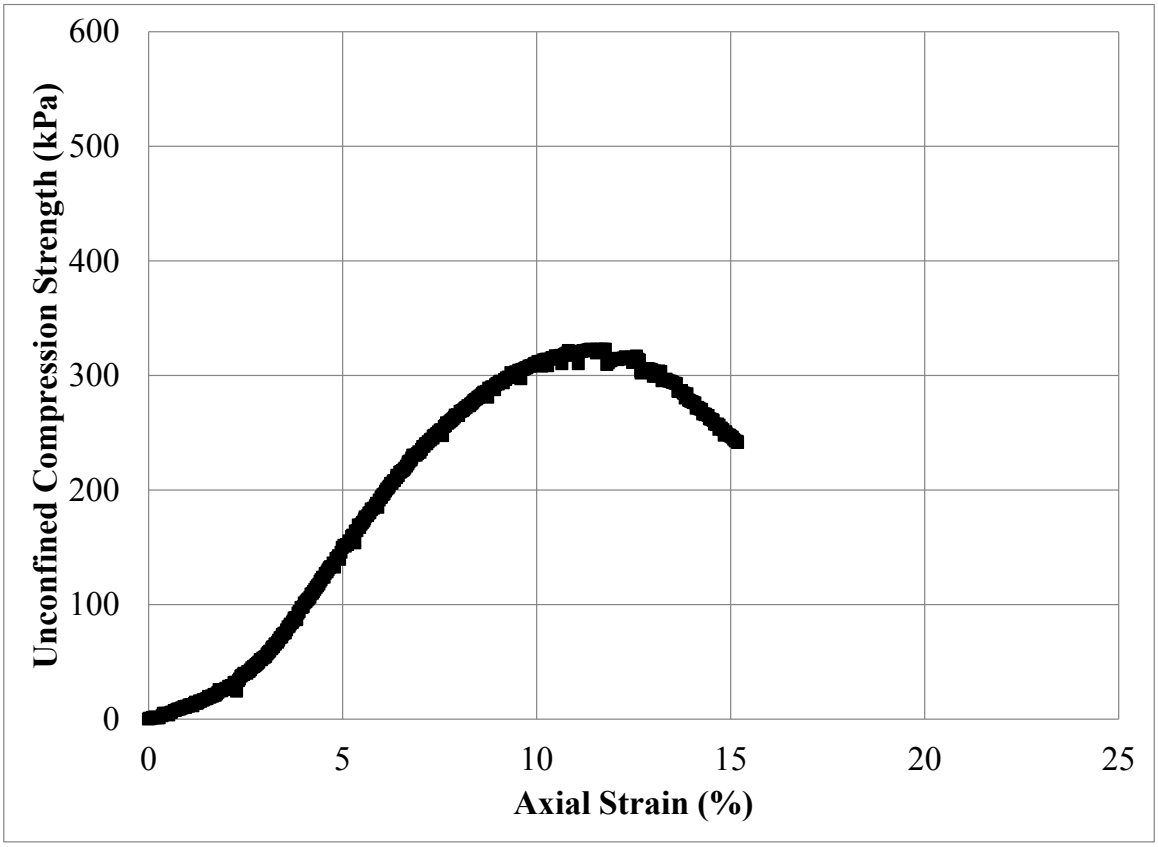

(c)

Figure C.84: Unconfined Compression Test Specimen No. 120R: (a) Photograph Prior to Testing; (b) Photograph Post Testing; and (c) Stress – Strain Data

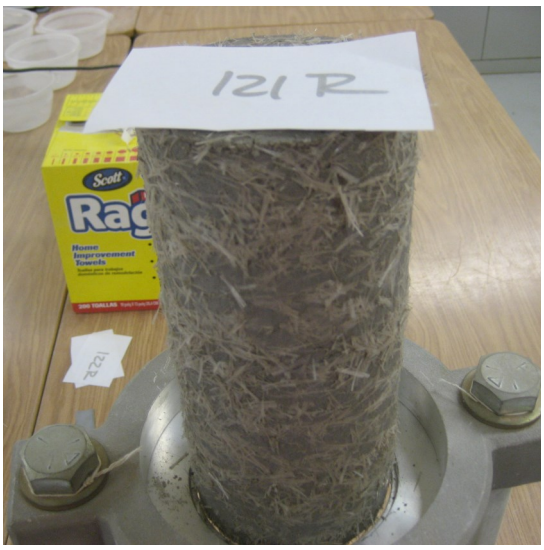

(a)

(b)

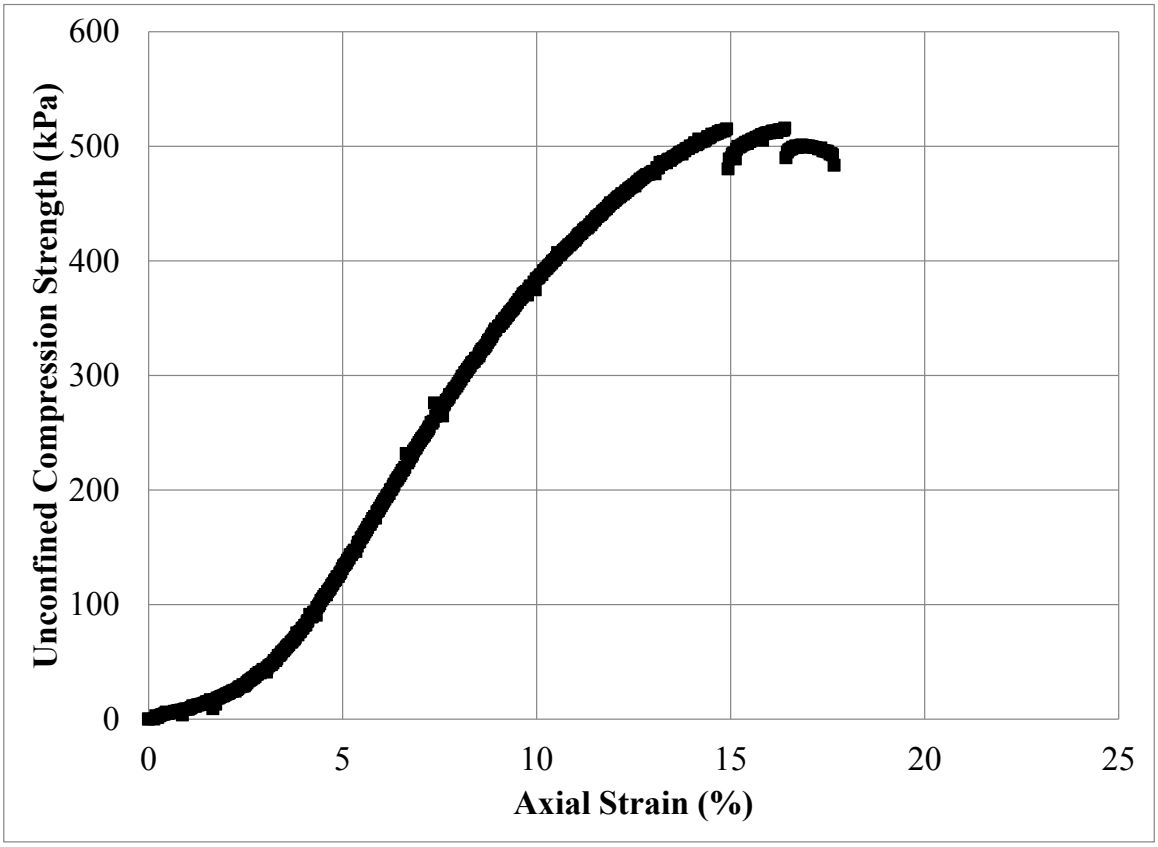

(c)

Figure C.85: Unconfined Compression Test Specimen No. 121R: (a) Photograph Prior to Testing; (b) Photograph Post Testing; and (c) Stress – Strain Data

(a)

(b)

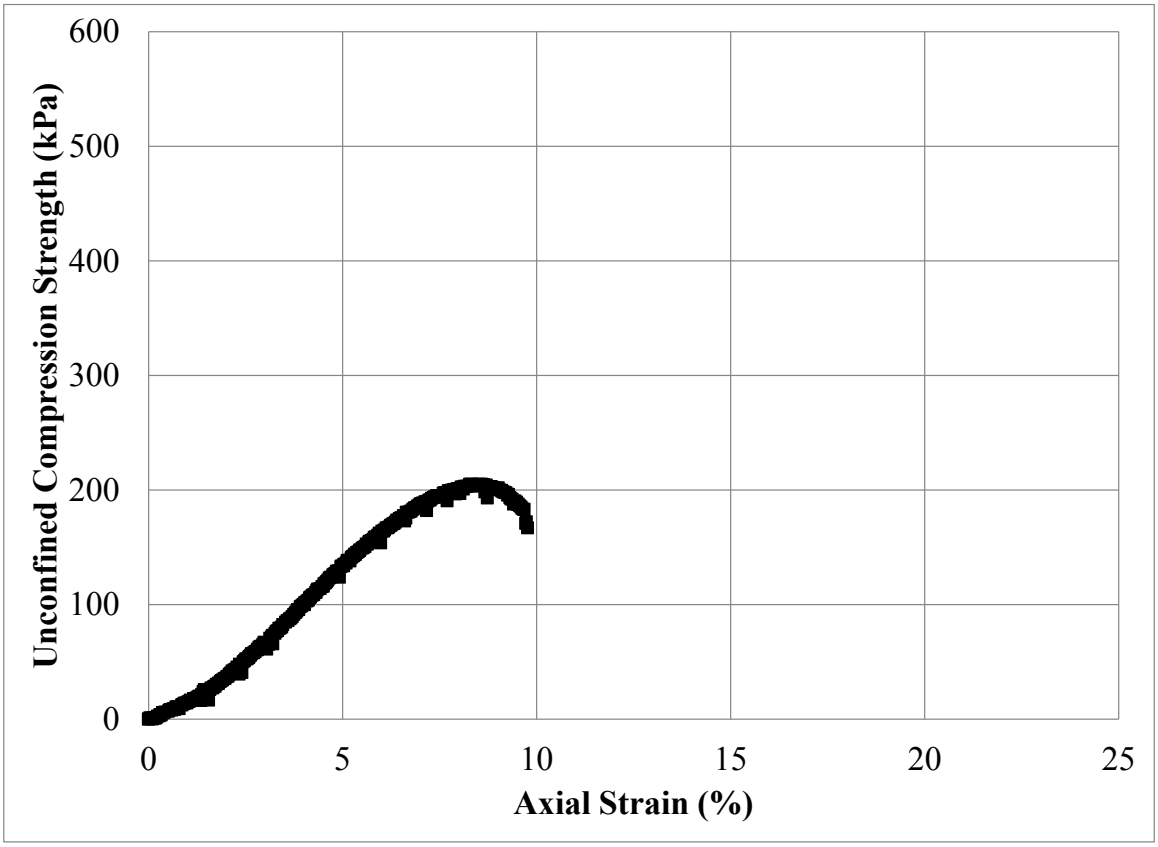

(c)

Figure C.86: Unconfined Compression Test Specimen No. 122R: (a) Photograph Prior to Testing; (b) Photograph Post Testing; and (c) Stress – Strain Data

(a)

(b)

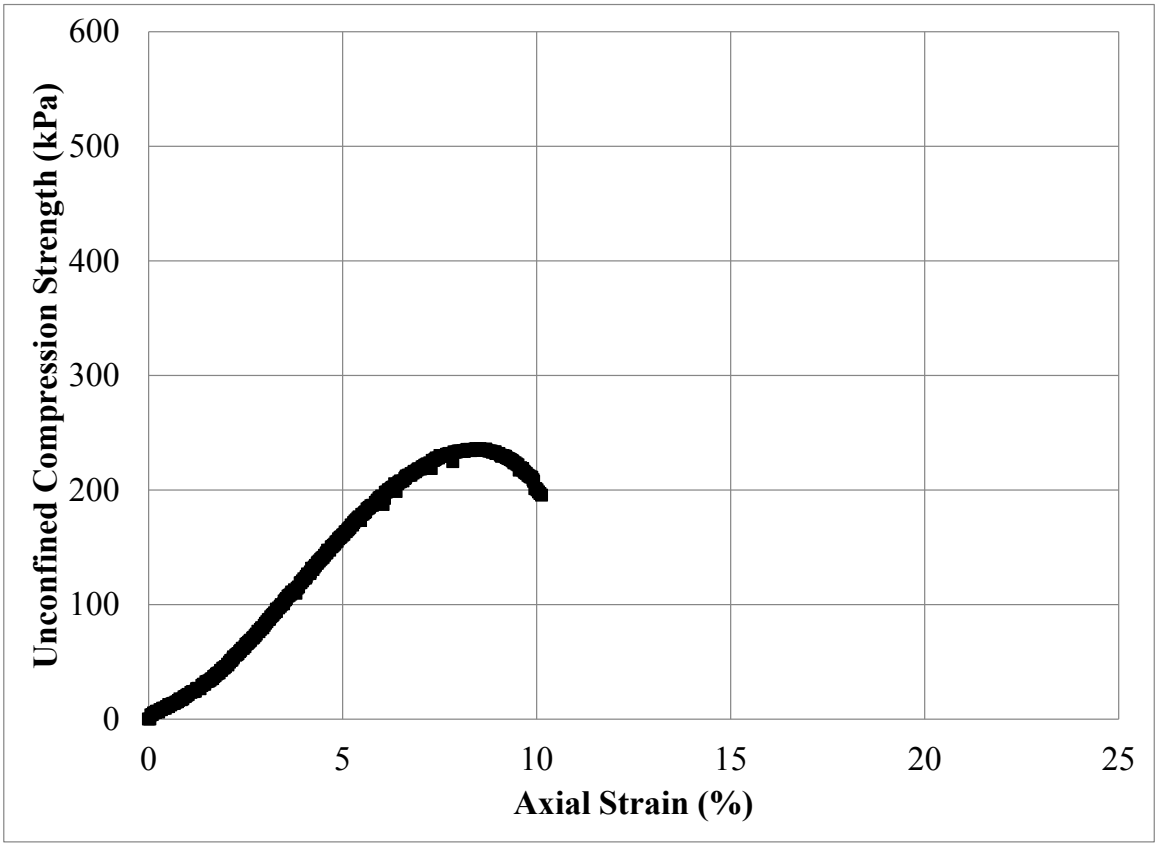

(c)

Figure C.87: Unconfined Compression Test Specimen No. 123R: (a) Photograph Prior to Testing; (b) Photograph Post Testing; and (c) Stress – Strain Data

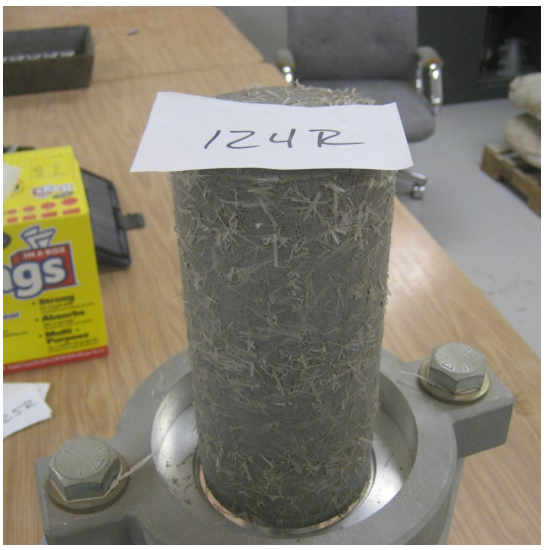

(a)

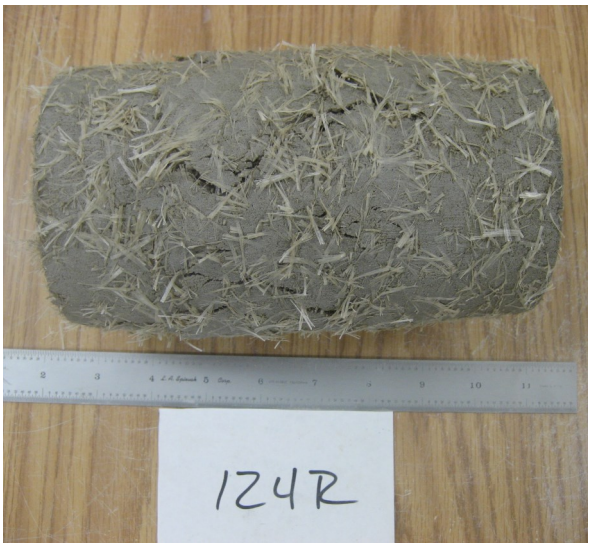

(b)

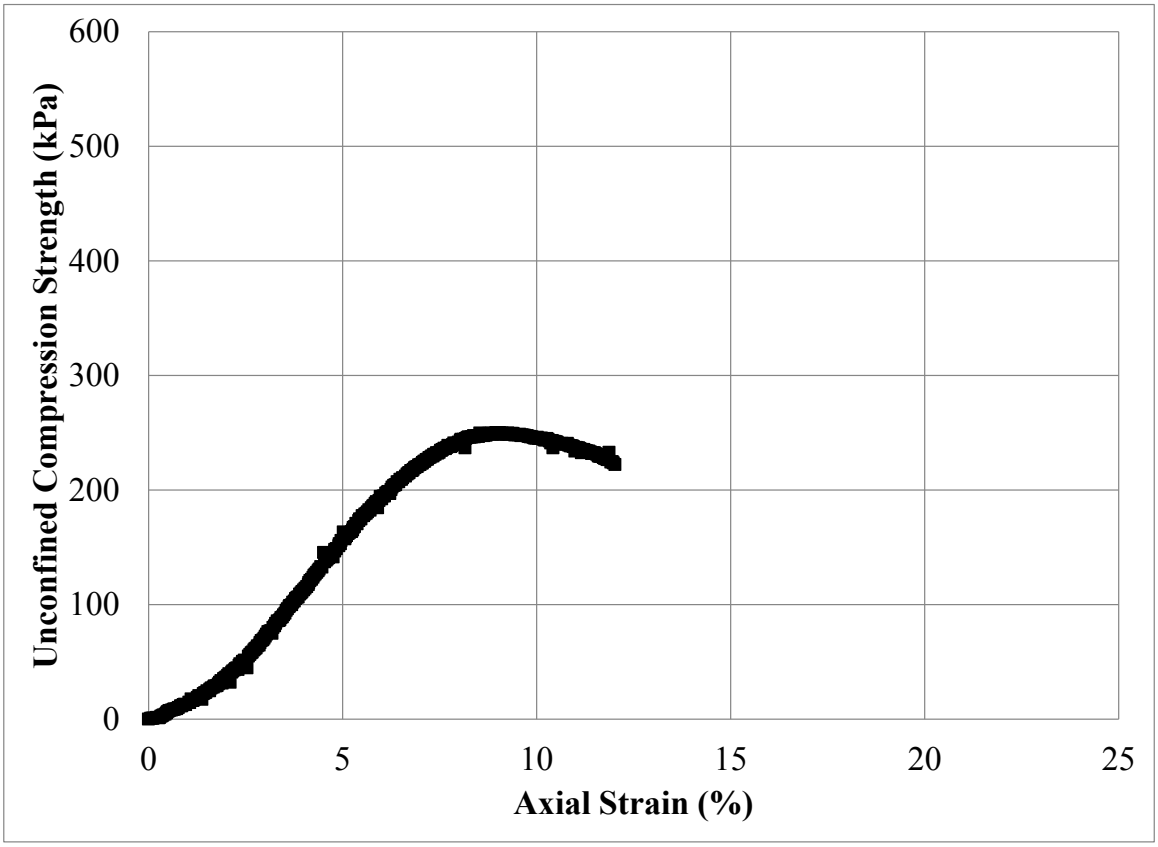

(c)

Figure C.88: Unconfined Compression Test Specimen No. 124R: (a) Photograph Prior to Testing; (b) Photograph Post Testing; and (c) Stress – Strain Data

(a)

(b)

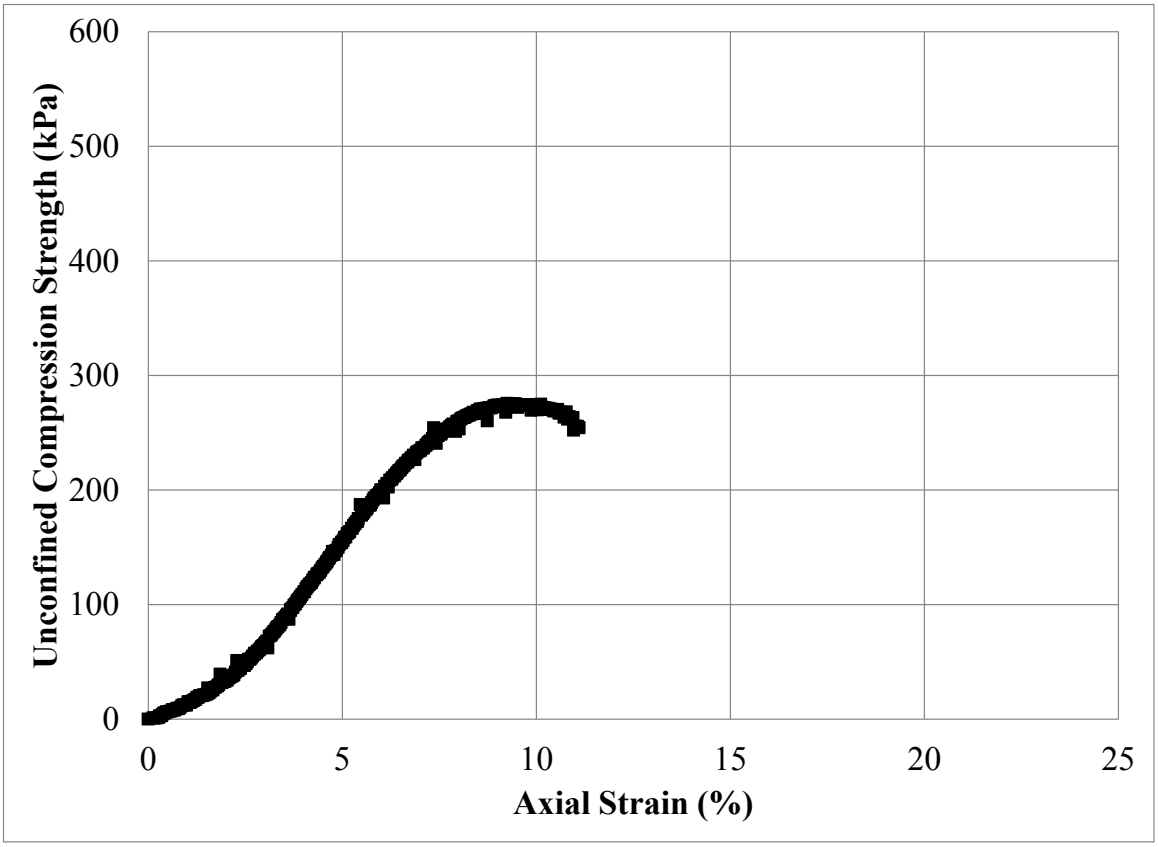

(c)

Figure C.89: Unconfined Compression Test Specimen No. 125R: (a) Photograph Prior to Testing; (b) Photograph Post Testing; and (c) Stress – Strain Data

(a)

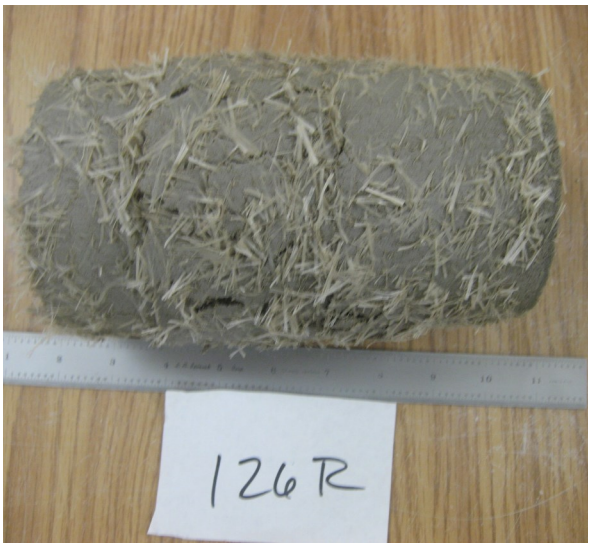

(b)

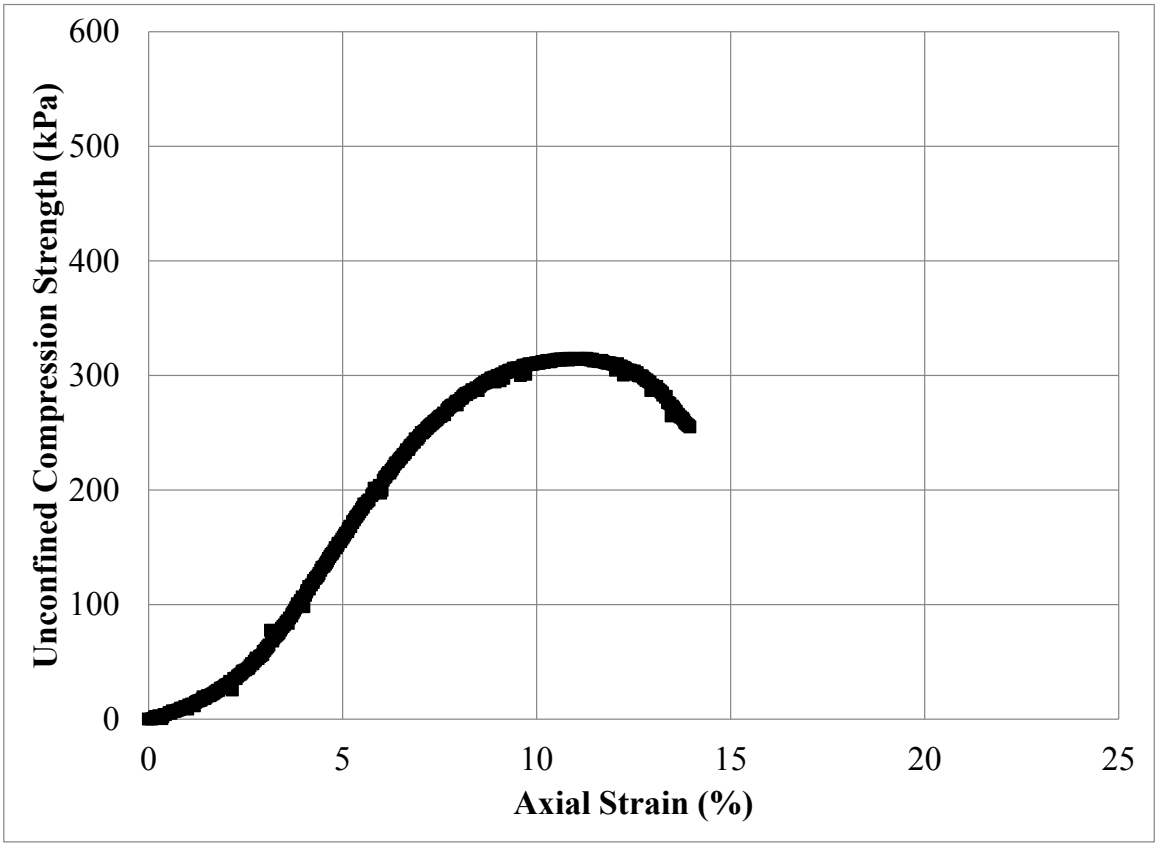

(c)

Figure C.90: Unconfined Compression Test Specimen No. 126R: (a) Photograph Prior to Testing; (b) Photograph Post Testing; and (c) Stress – Strain Data

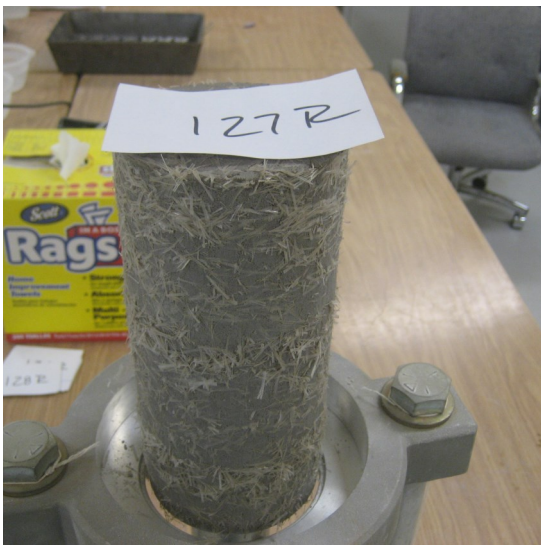

(a)

(b)

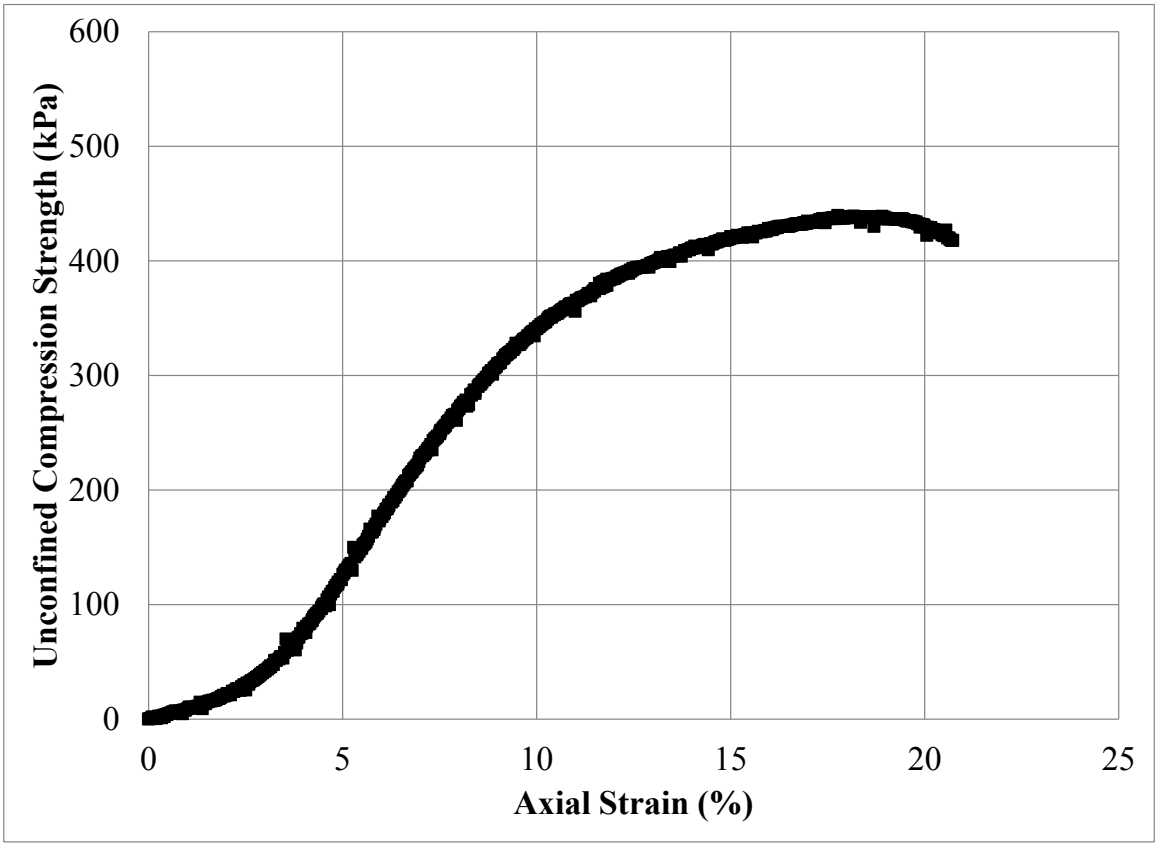

(c)

Figure C.91: Unconfined Compression Test Specimen No. 127R: (a) Photograph Prior to Testing; (b) Photograph Post Testing; and (c) Stress – Strain Data

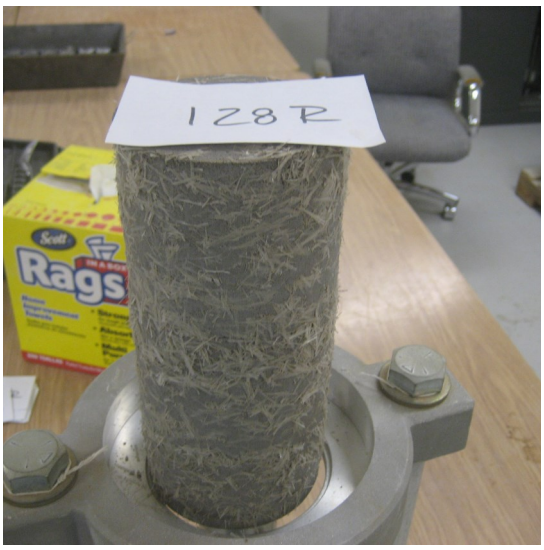

(a)

(b)

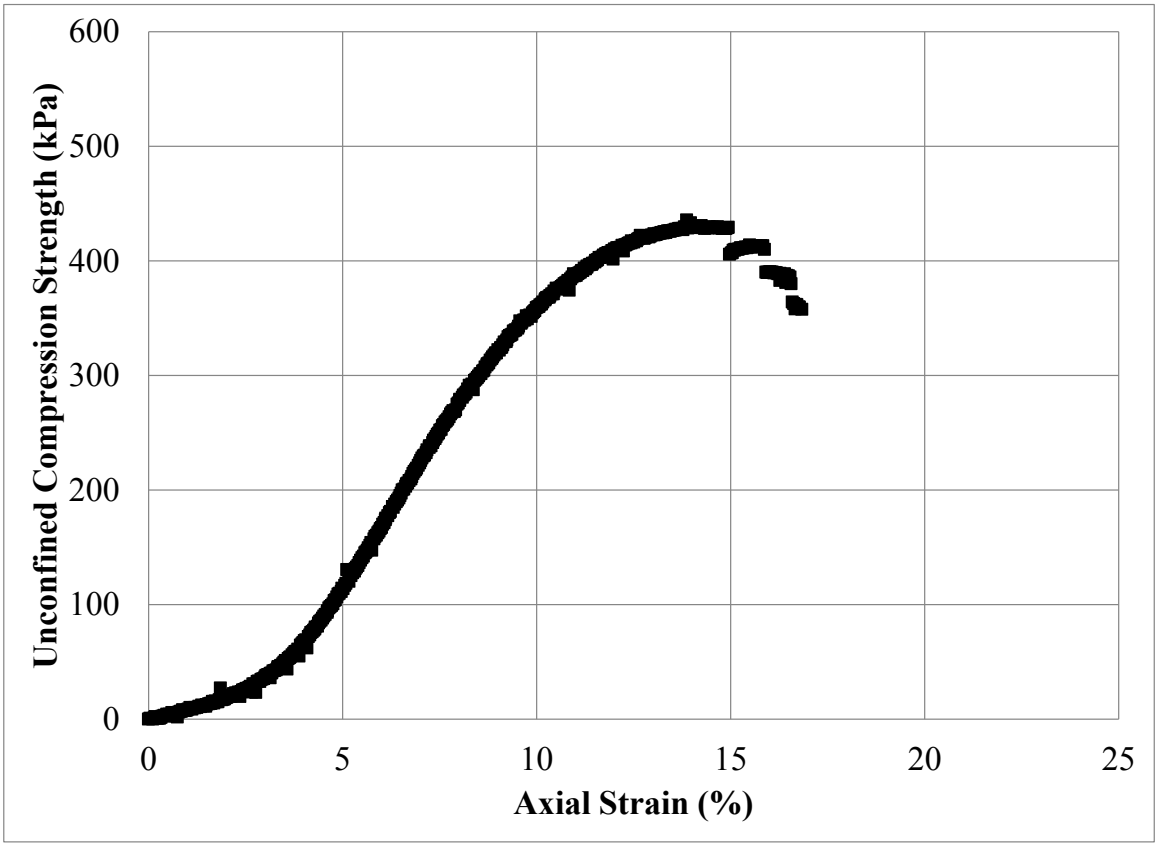

(c)

Figure C.92: Unconfined Compression Test Specimen No. 128R: (a) Photograph Prior to Testing; (b) Photograph Post Testing; and (c) Stress – Strain Data

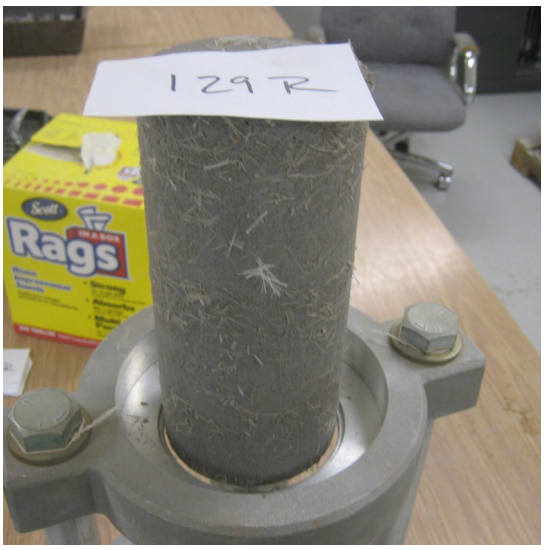

(a)

(b)

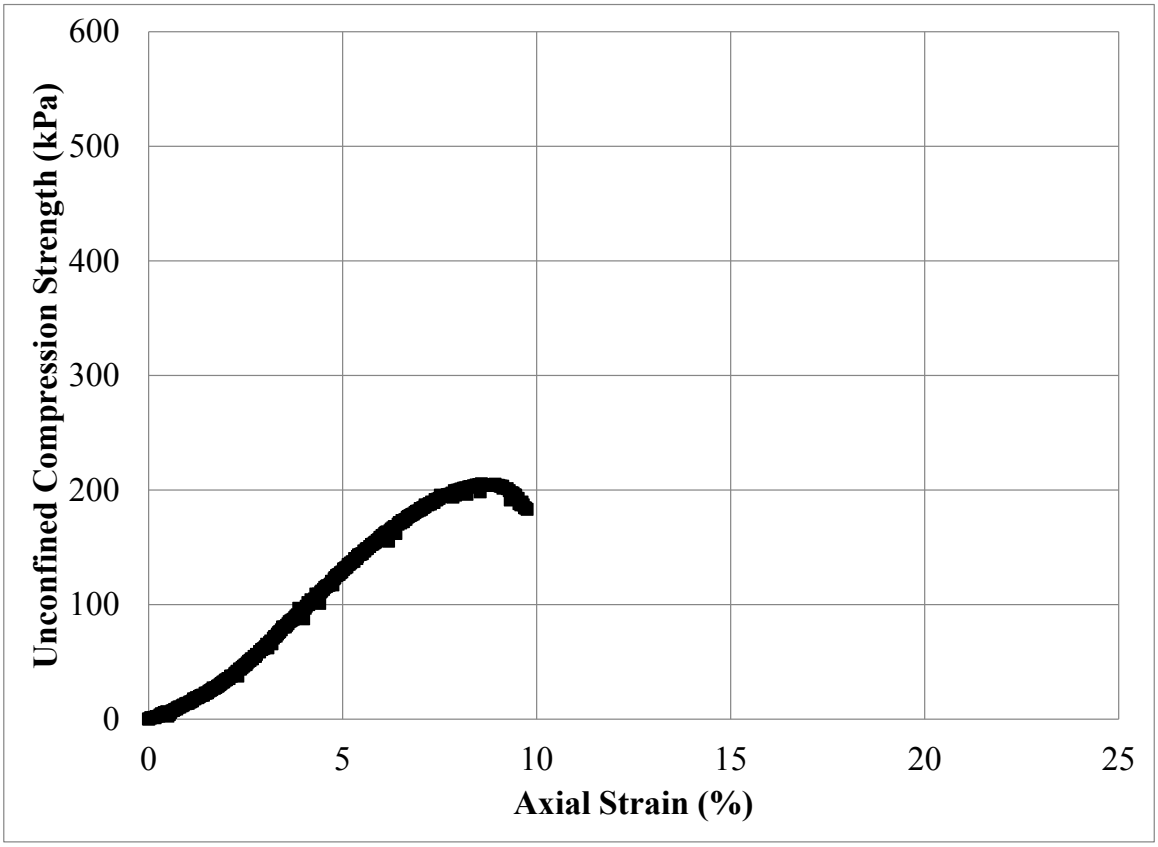

(c)

Figure C.93: Unconfined Compression Test Specimen No. 129R: (a) Photograph Prior to Testing; (b) Photograph Post Testing; and (c) Stress – Strain Data

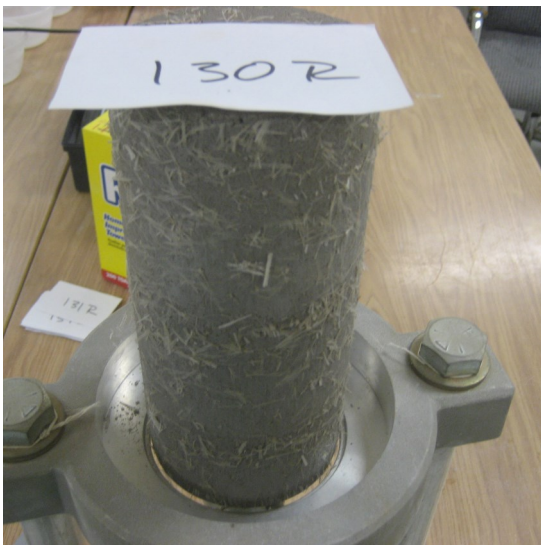

(a)

(b)

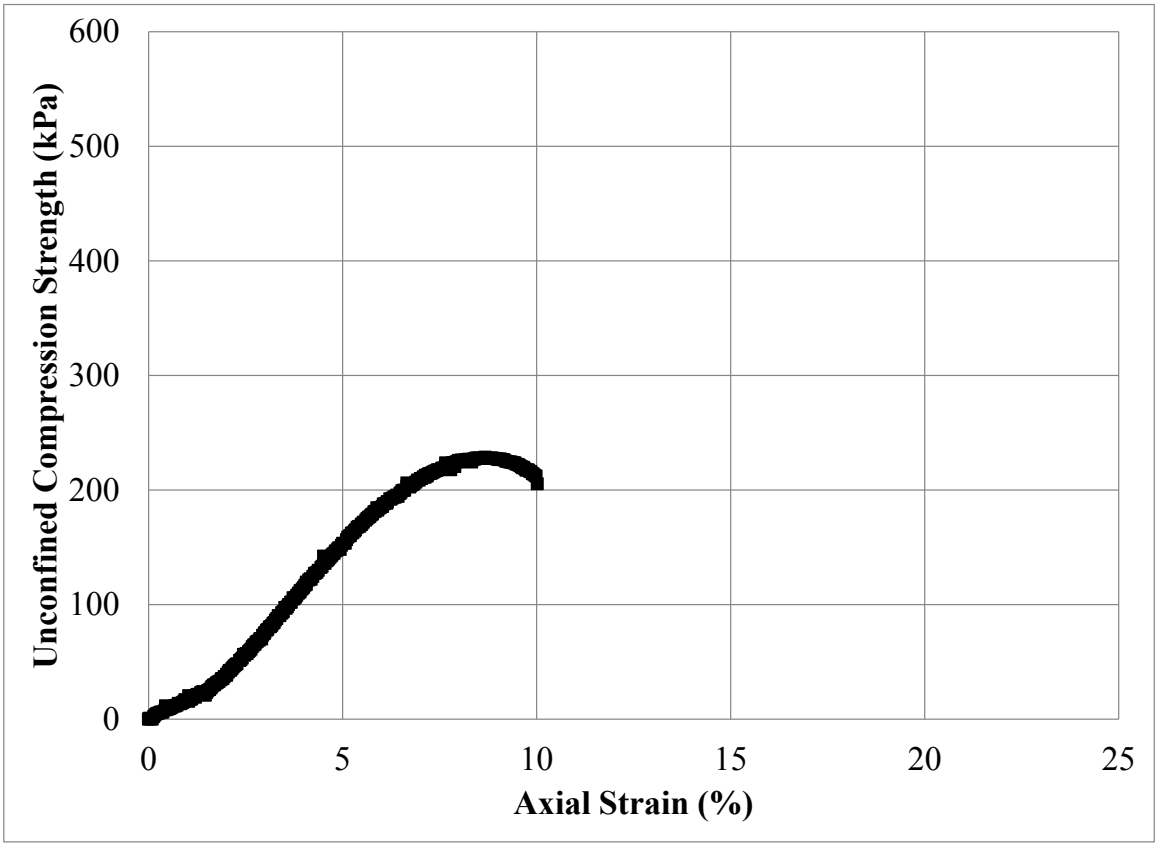

(c)

Figure C.94: Unconfined Compression Test Specimen No. 130R: (a) Photograph Prior to Testing; (b) Photograph Post Testing; and (c) Stress – Strain Data

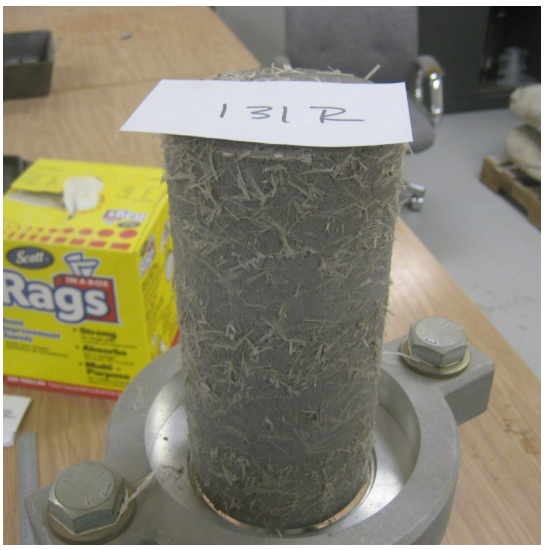

(a)

(b)

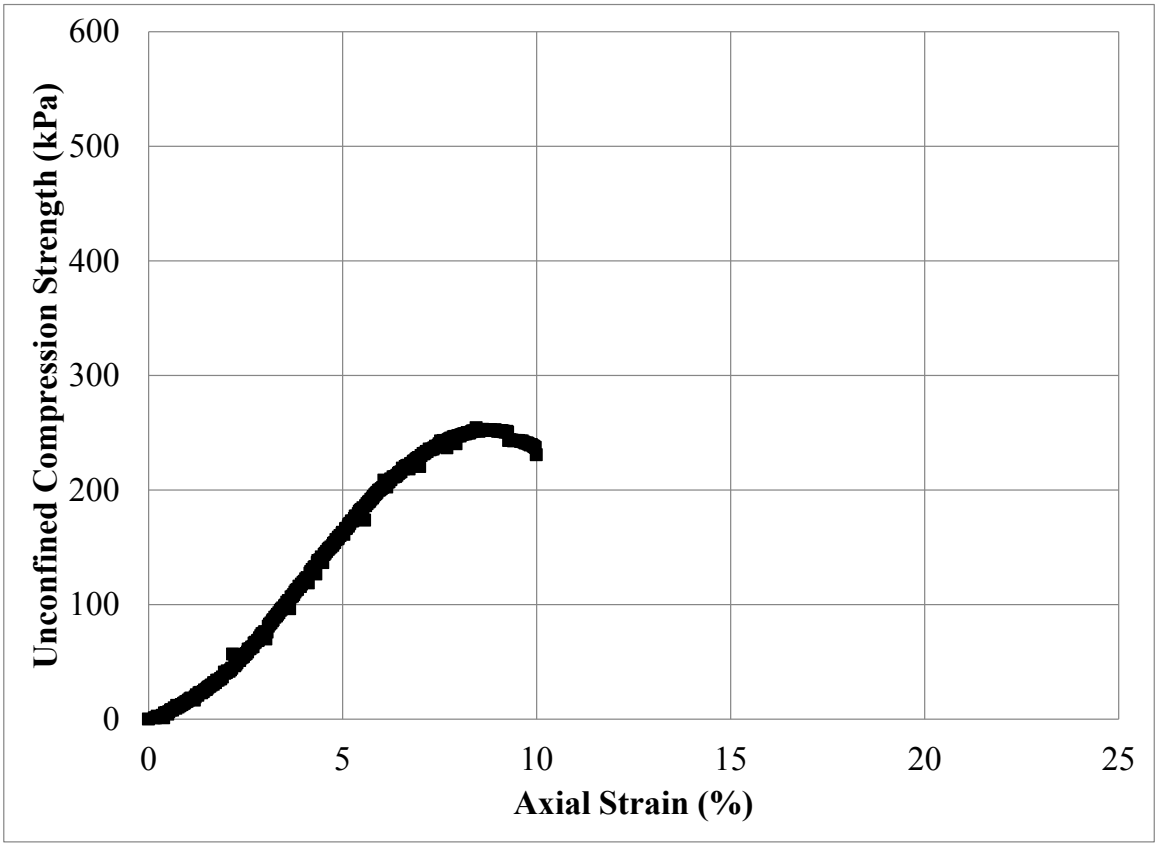

(c)

Figure C.95: Unconfined Compression Test Specimen No. 131R: (a) Photograph Prior to Testing; (b) Photograph Post Testing; and (c) Stress – Strain Data

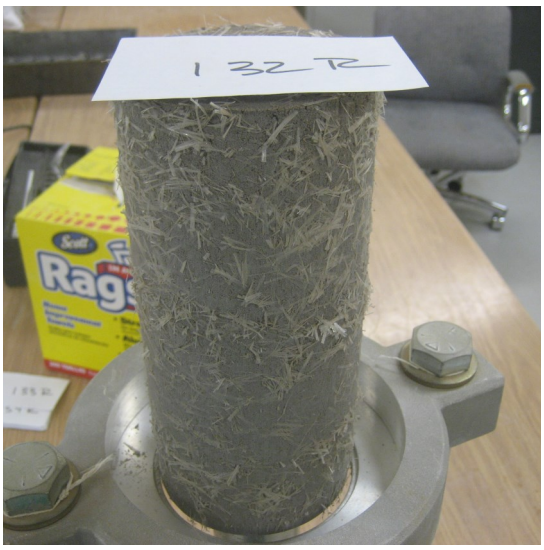

(a)

(b)

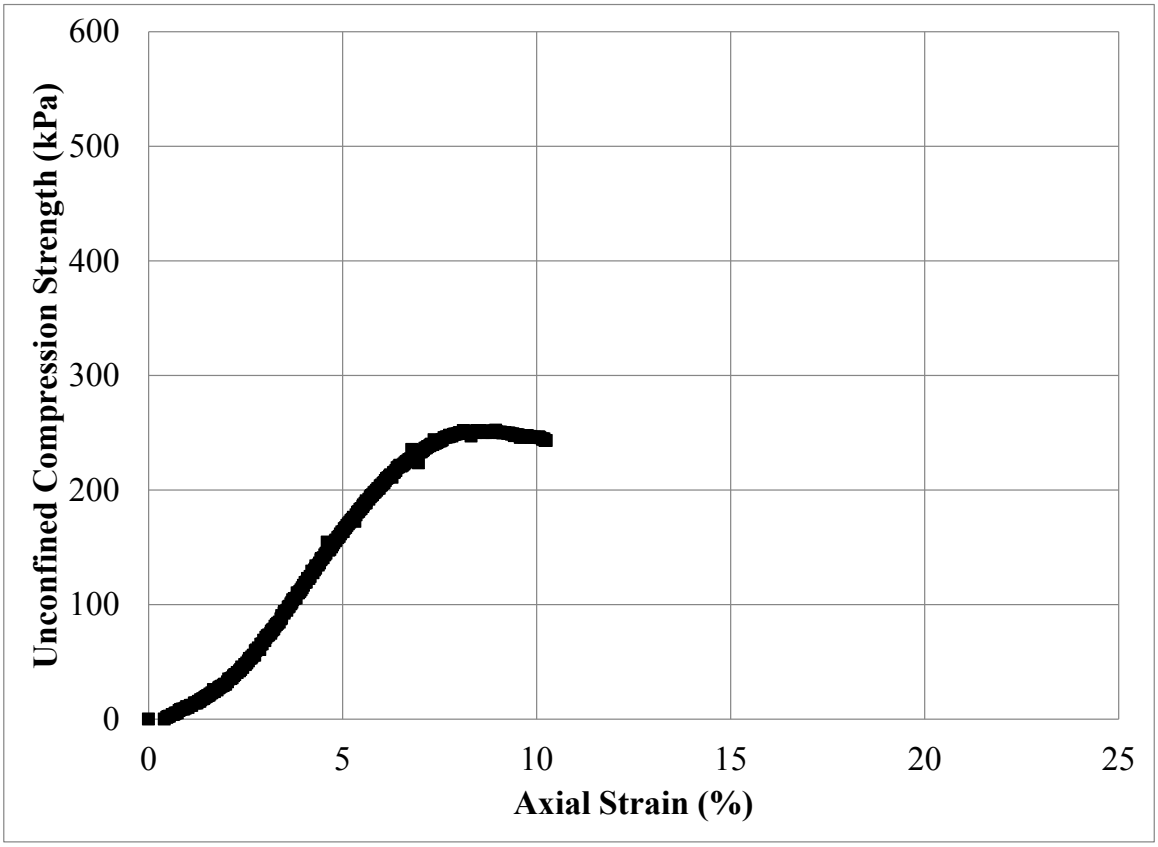

(c)

Figure C.96: Unconfined Compression Test Specimen No. 132R: (a) Photograph Prior to Testing; (b) Photograph Post Testing; and (c) Stress – Strain Data

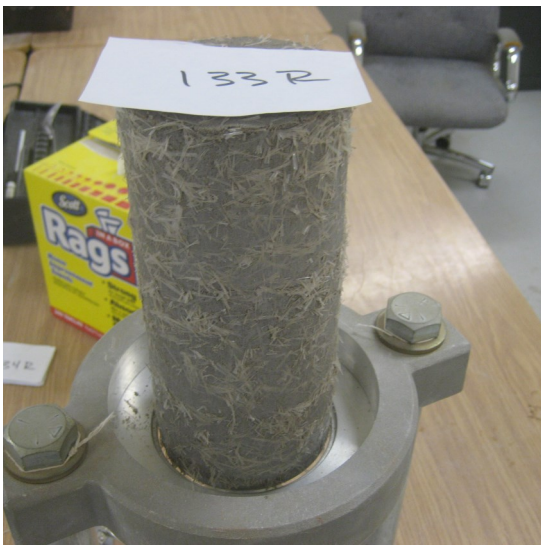

(a)

(b)

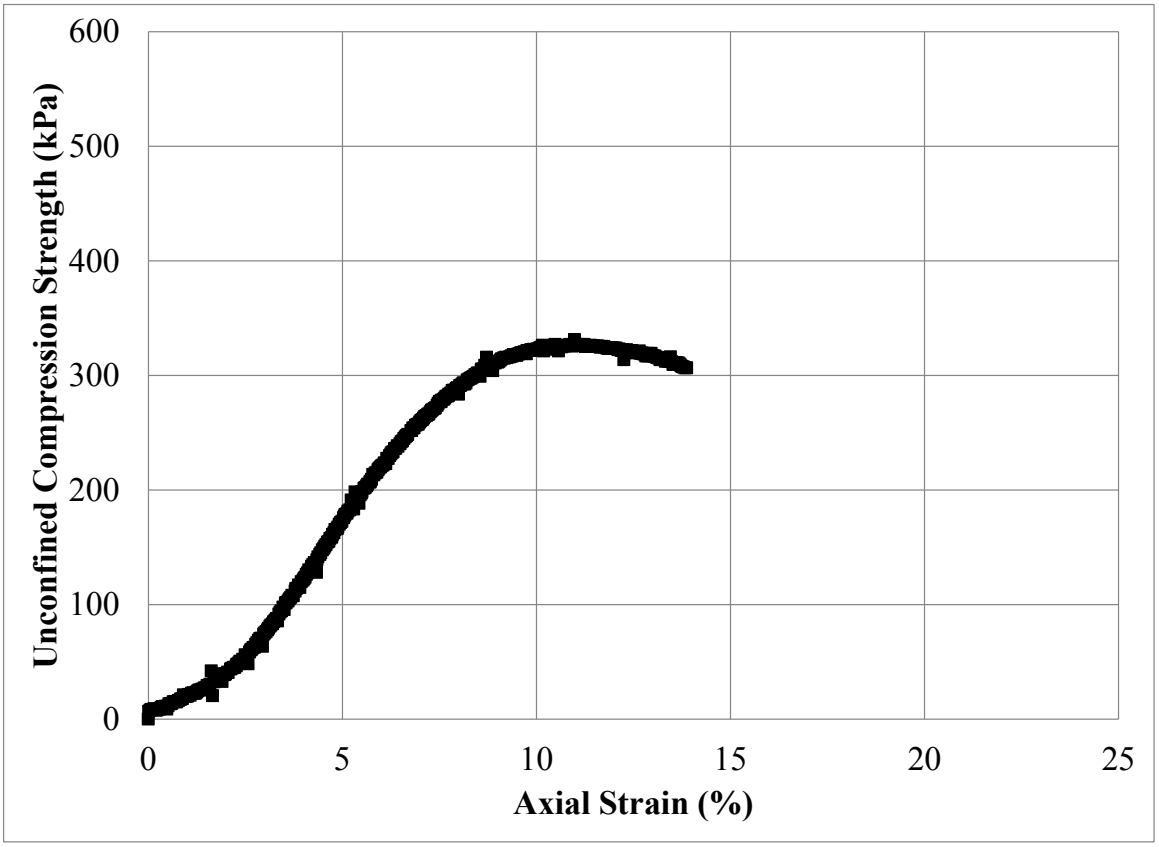

(c)

Figure C.97: Unconfined Compression Test Specimen No. 133R: (a) Photograph Prior to Testing; (b) Photograph Post Testing; and (c) Stress – Strain Data

(a)

(b)

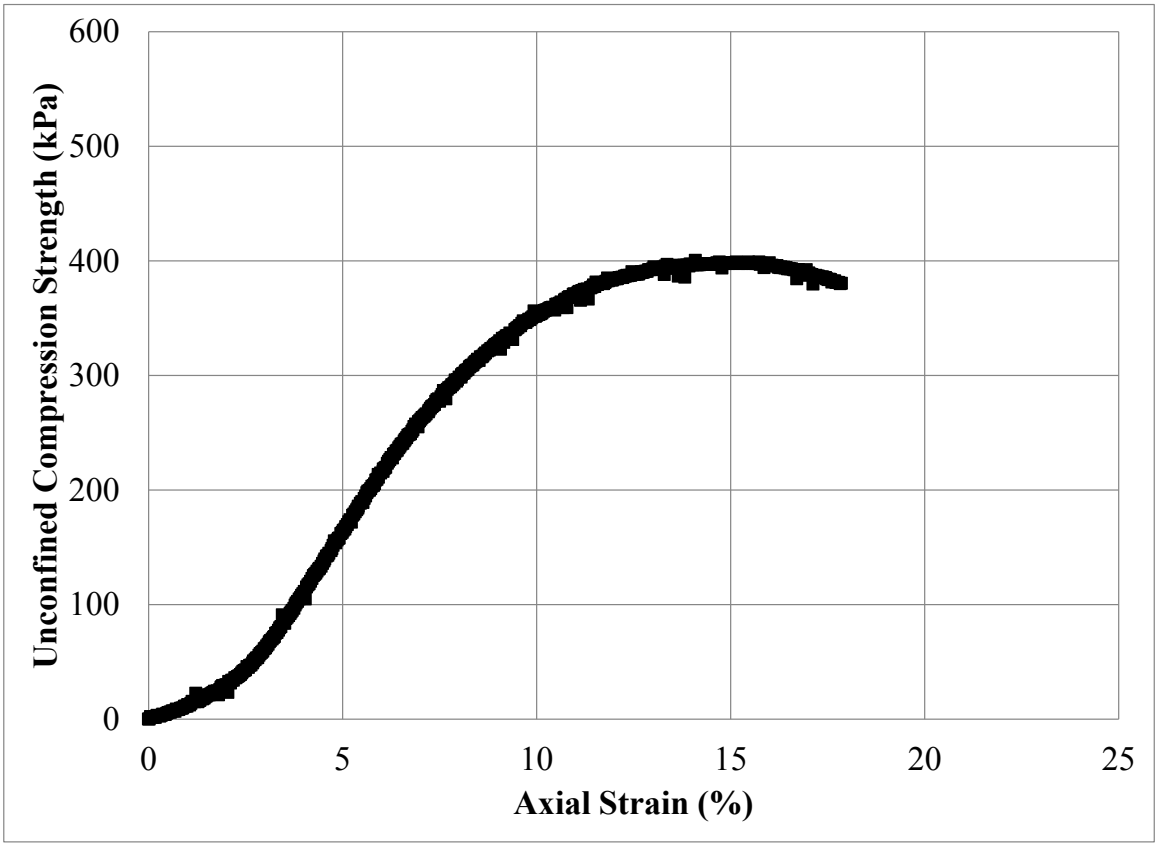

(c)

Figure C.98: Unconfined Compression Test Specimen No. 134R: (a) Photograph Prior to Testing; (b) Photograph Post Testing; and (c) Stress – Strain Data

(a)

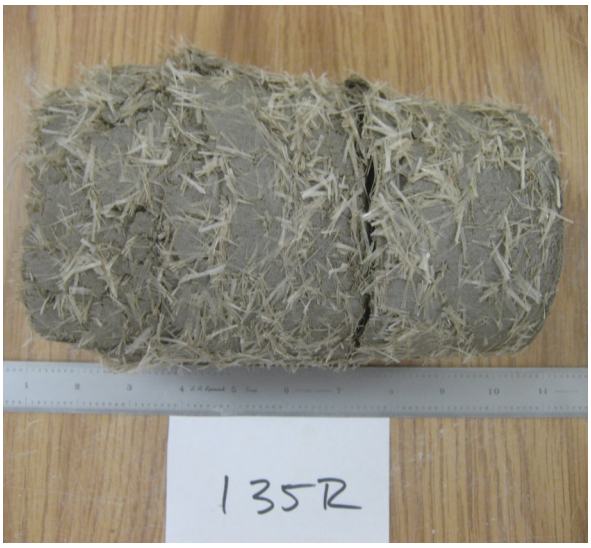

(b)

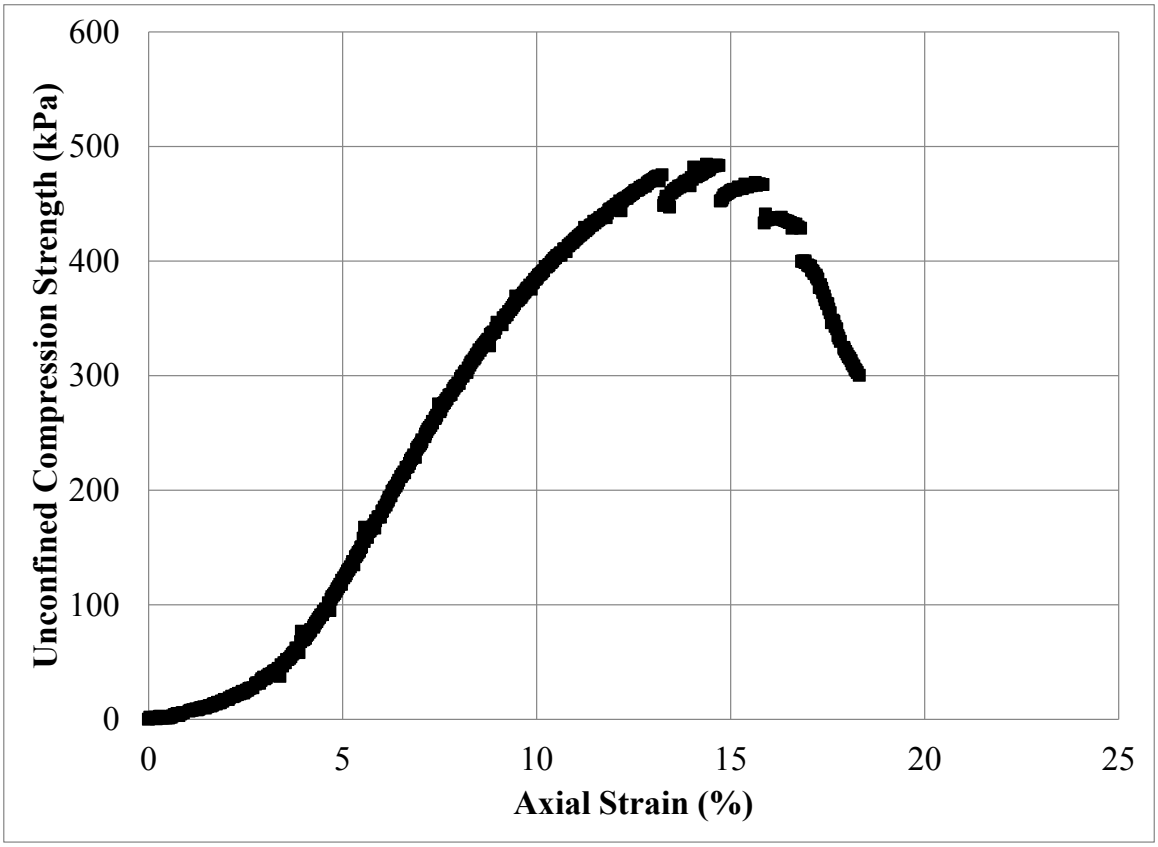

(c)

Figure C.99: Unconfined Compression Test Specimen No. 135R: (a) Photograph Prior to Testing; (b) Photograph Post Testing; and (c) Stress – Strain Data

(a)

(b)

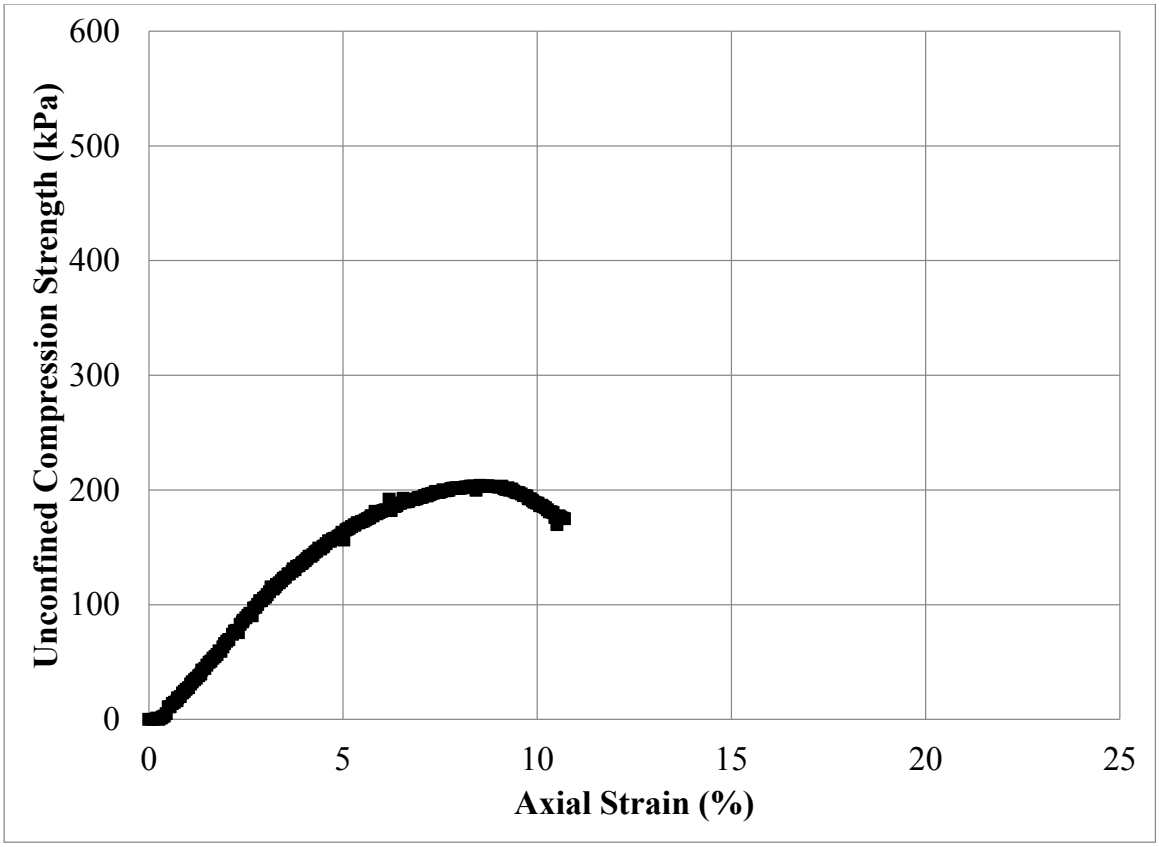

(c)

Figure C.100: Unconfined Compression Test Specimen No. 136R: (a) Photograph Prior to Testing; (b) Photograph Post Testing; and (c) Stress – Strain Data

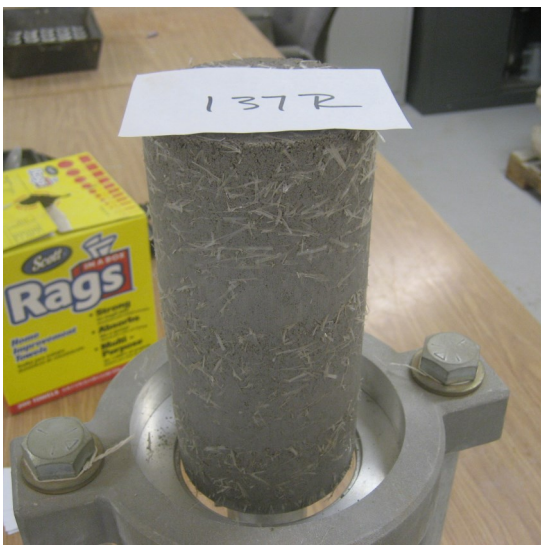

(a)

(b)

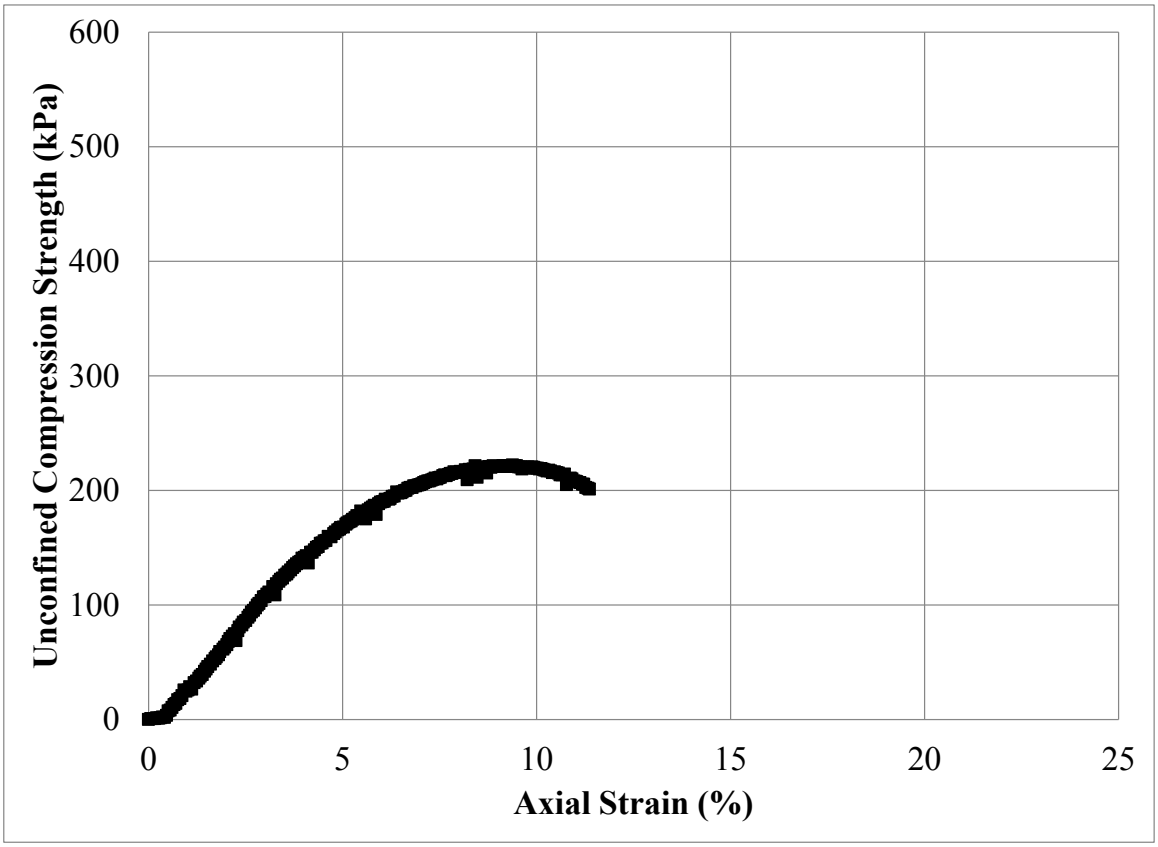

(c)

Figure C.101: Unconfined Compression Test Specimen No. 137R: (a) Photograph Prior to Testing; (b) Photograph Post Testing; and (c) Stress – Strain Data

(a)

(b)

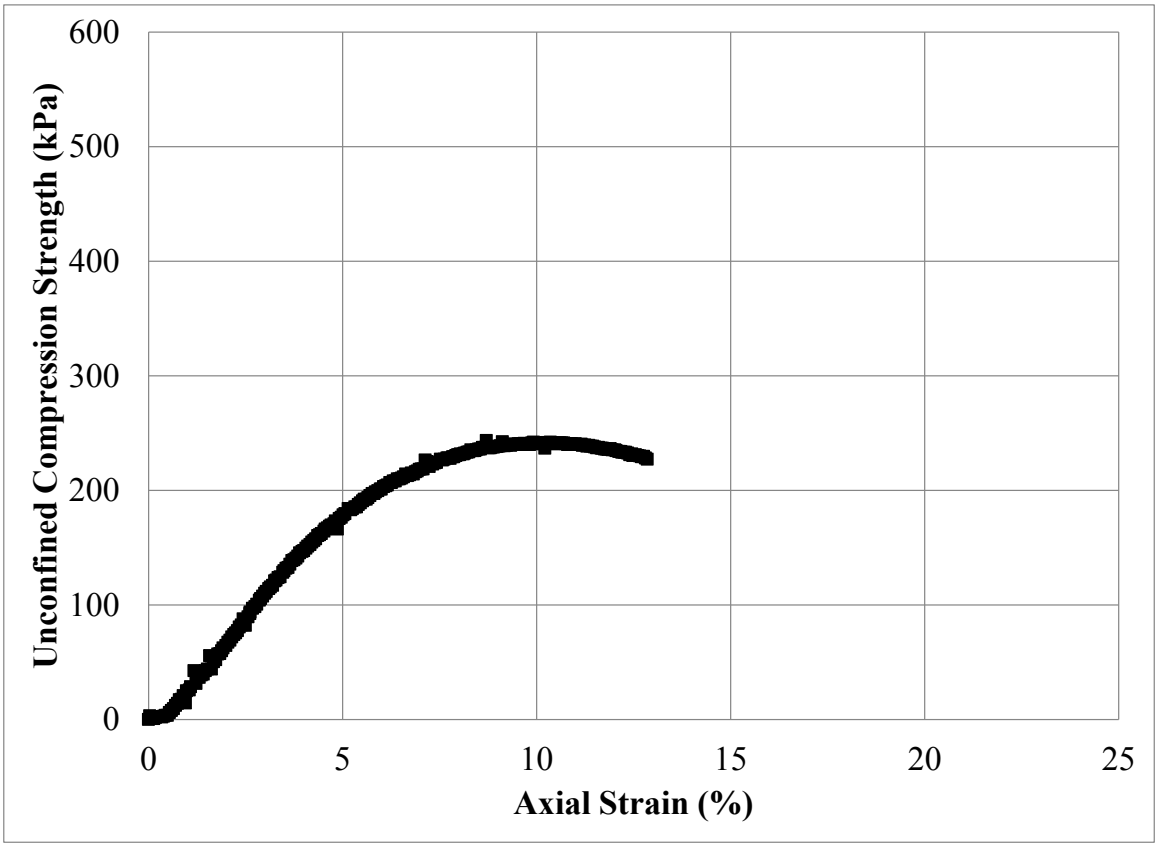

(c)

Figure C.102: Unconfined Compression Test Specimen No. 138R: (a) Photograph Prior to Testing; (b) Photograph Post Testing; and (c) Stress – Strain Data

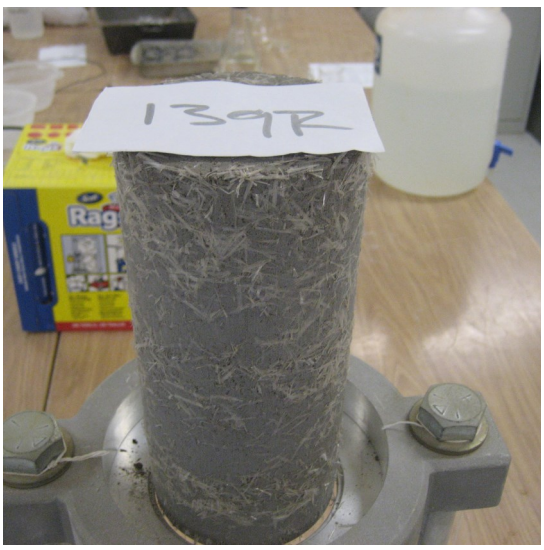

(a)

(b)

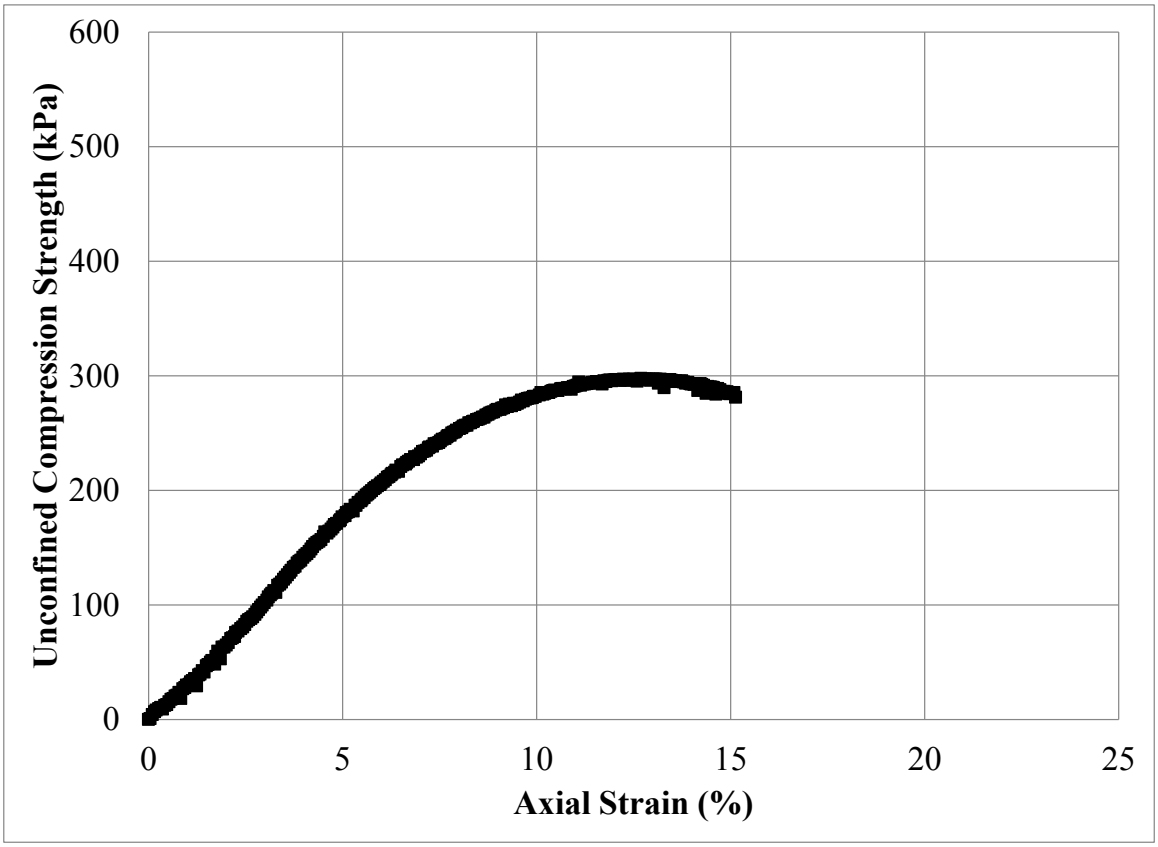

(c)

Figure C.103: Unconfined Compression Test Specimen No. 139R: (a) Photograph Prior to Testing; (b) Photograph Post Testing; and (c) Stress – Strain Data

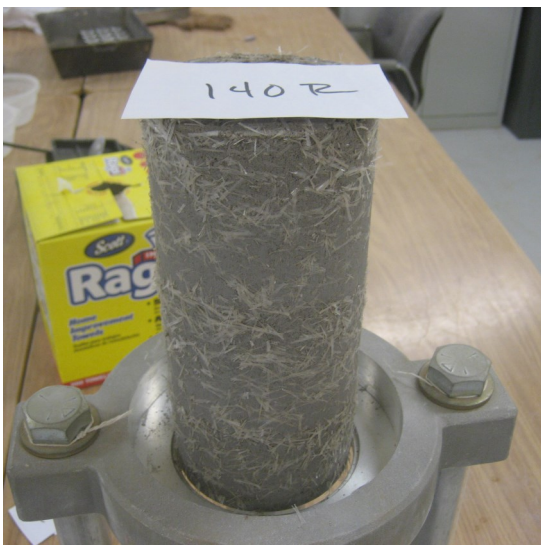

(a)

(b)

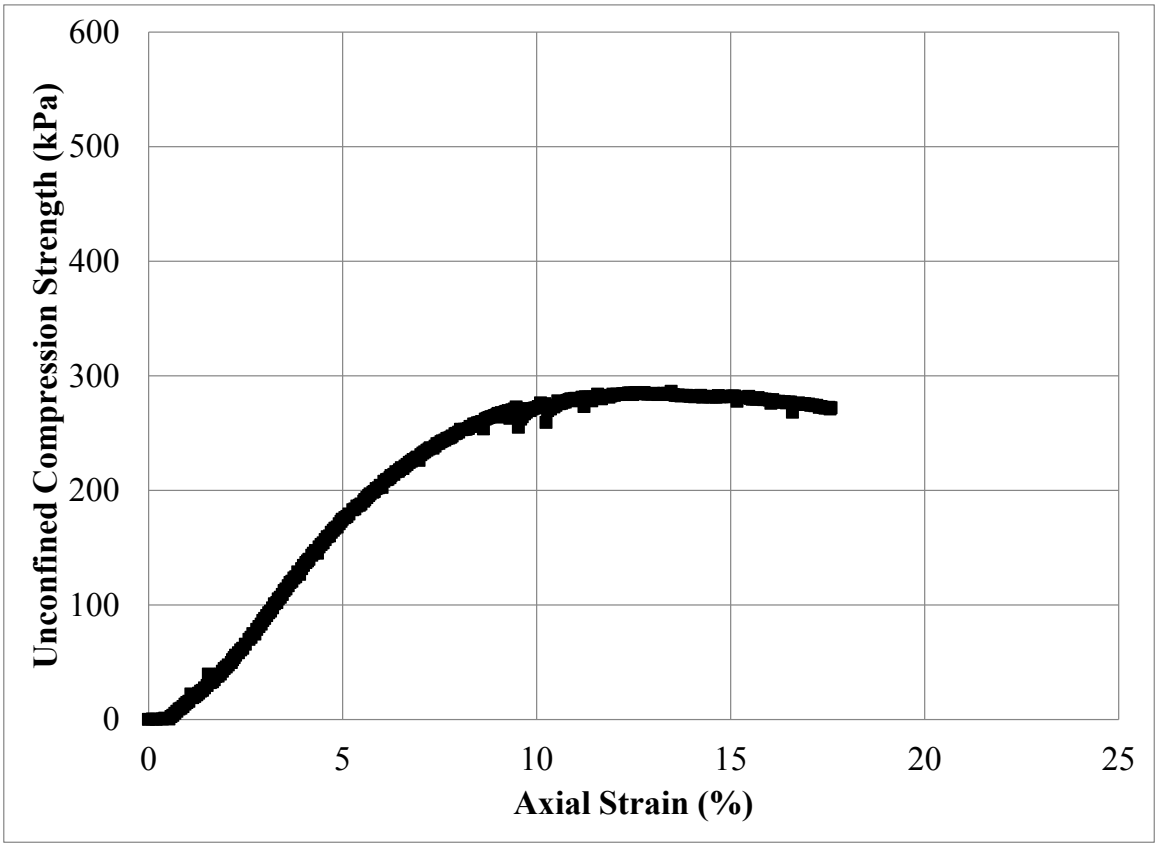

(c)

Figure C.104: Unconfined Compression Test Specimen No. 140R: (a) Photograph Prior to Testing; (b) Photograph Post Testing; and (c) Stress – Strain Data

(a)

(b)

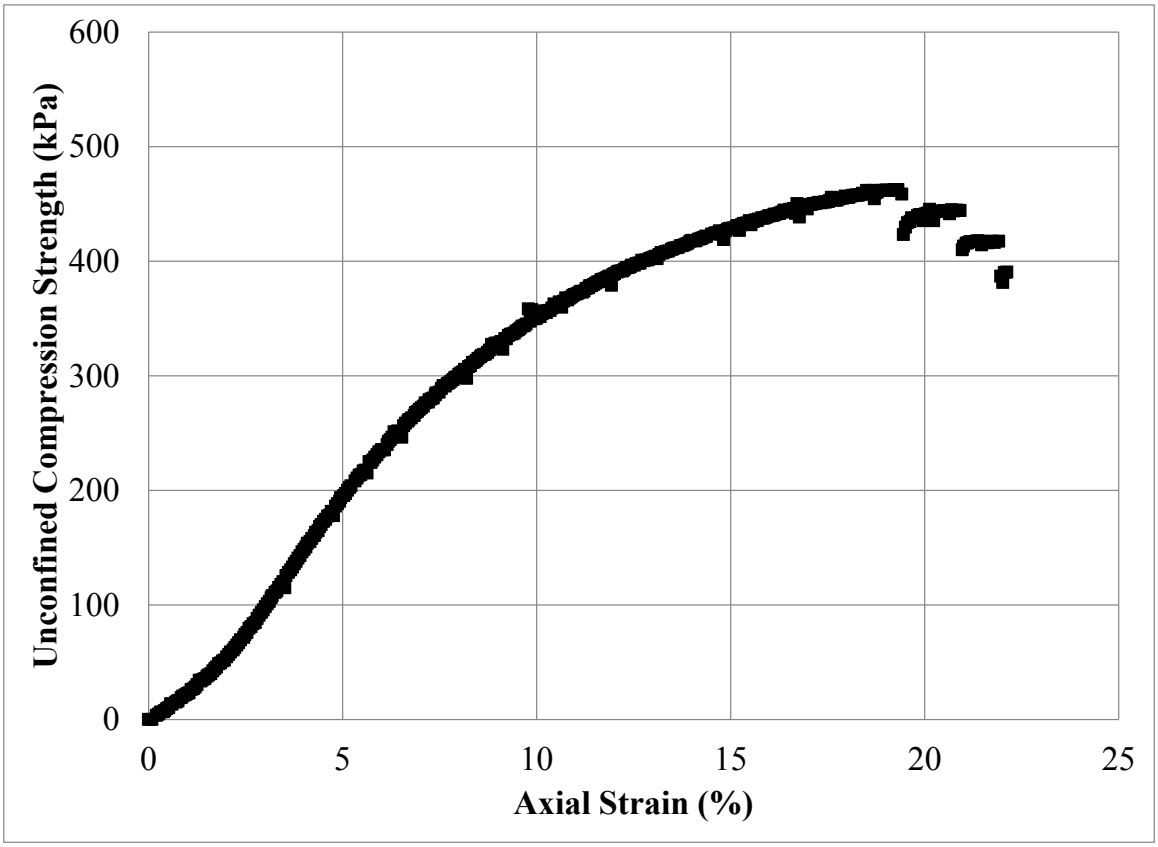

(c)

Figure C.105: Unconfined Compression Test Specimen No. 141R: (a) Photograph Prior to Testing; (b) Photograph Post Testing; and (c) Stress – Strain Data

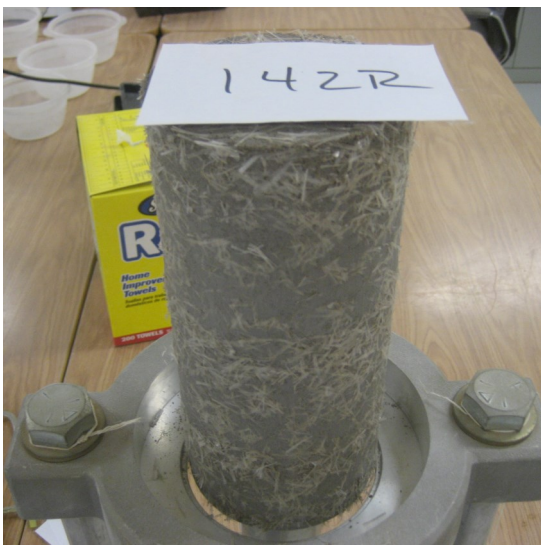

(a)

(b)

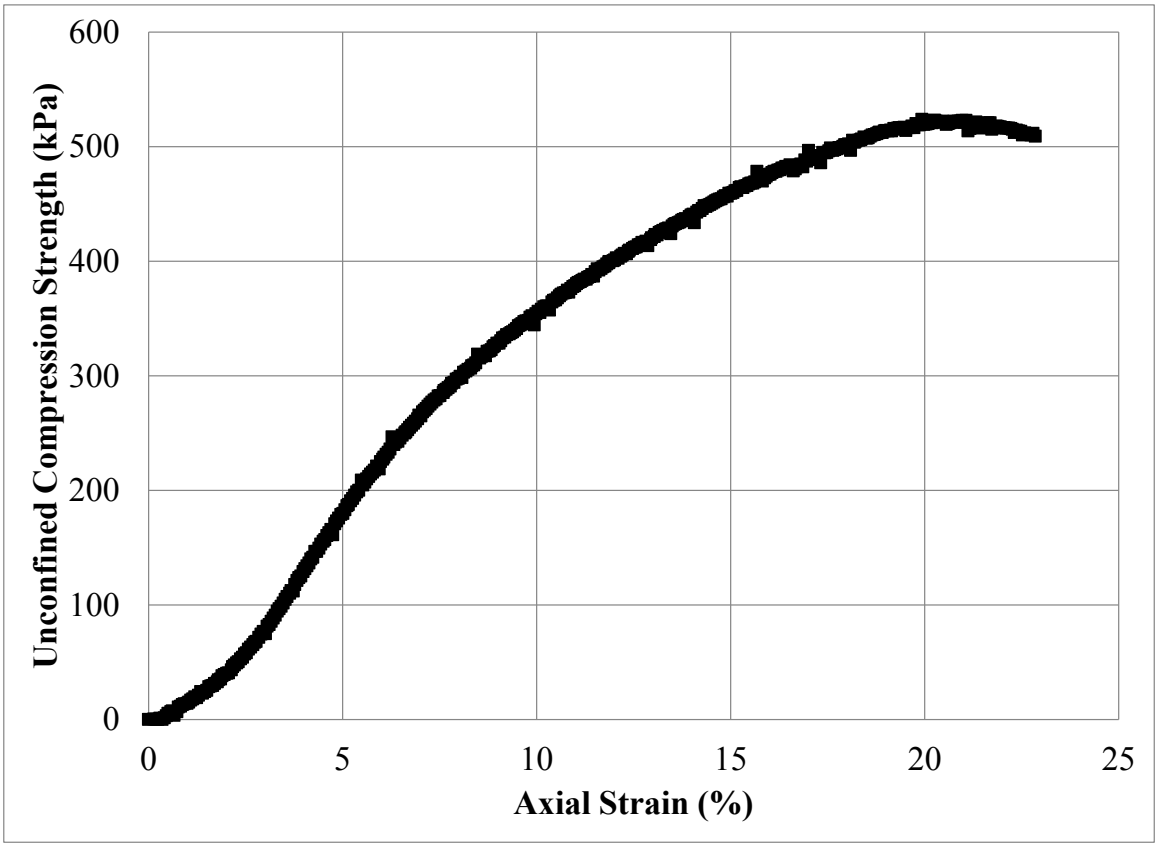

(c)

Figure C.106: Unconfined Compression Test Specimen No. 142R: (a) Photograph Prior to Testing; (b) Photograph Post Testing; and (c) Stress – Strain Data

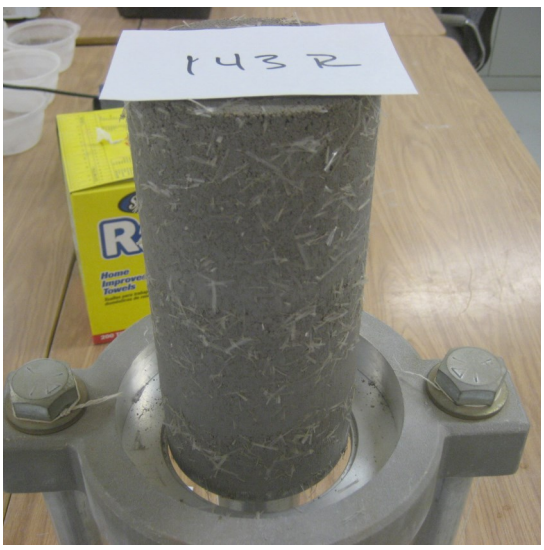

(a)

(b)

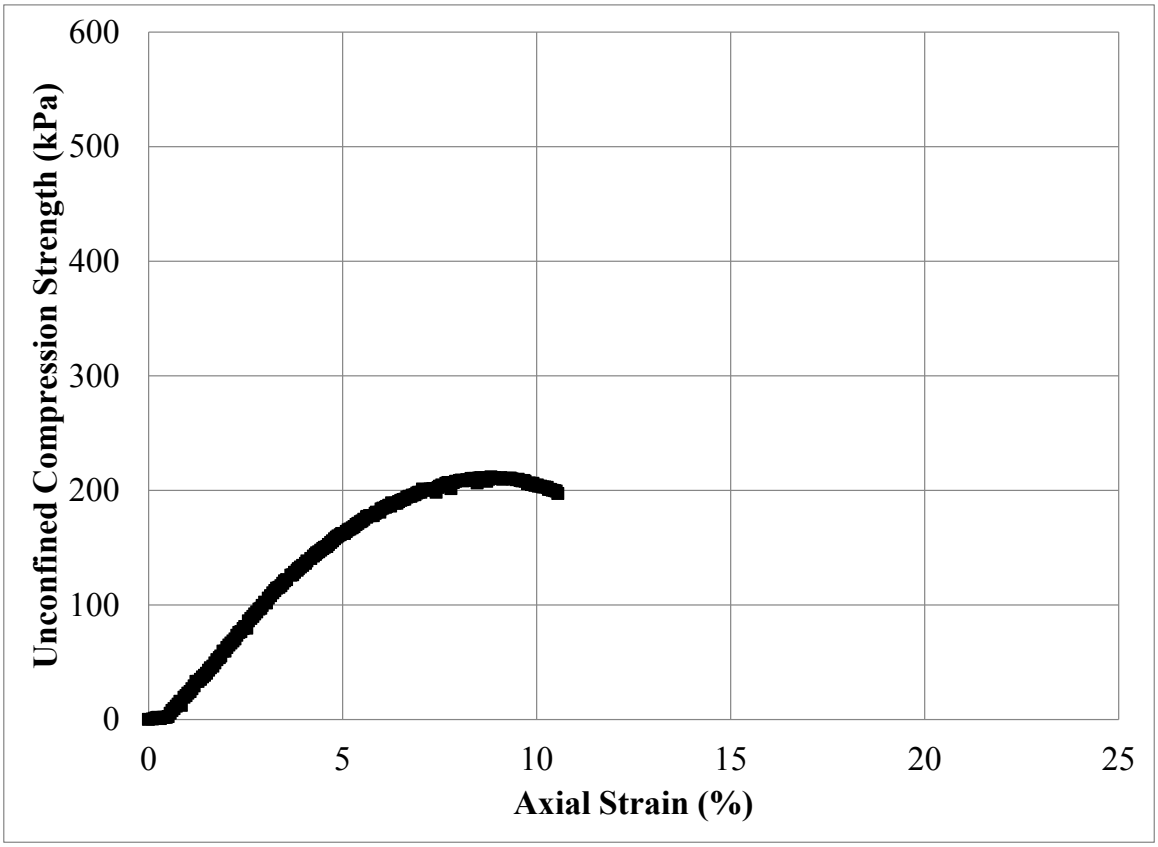

(c)

Figure C.107: Unconfined Compression Test Specimen No. 143R: (a) Photograph Prior to Testing; (b) Photograph Post Testing; and (c) Stress – Strain Data

(a)

(b)

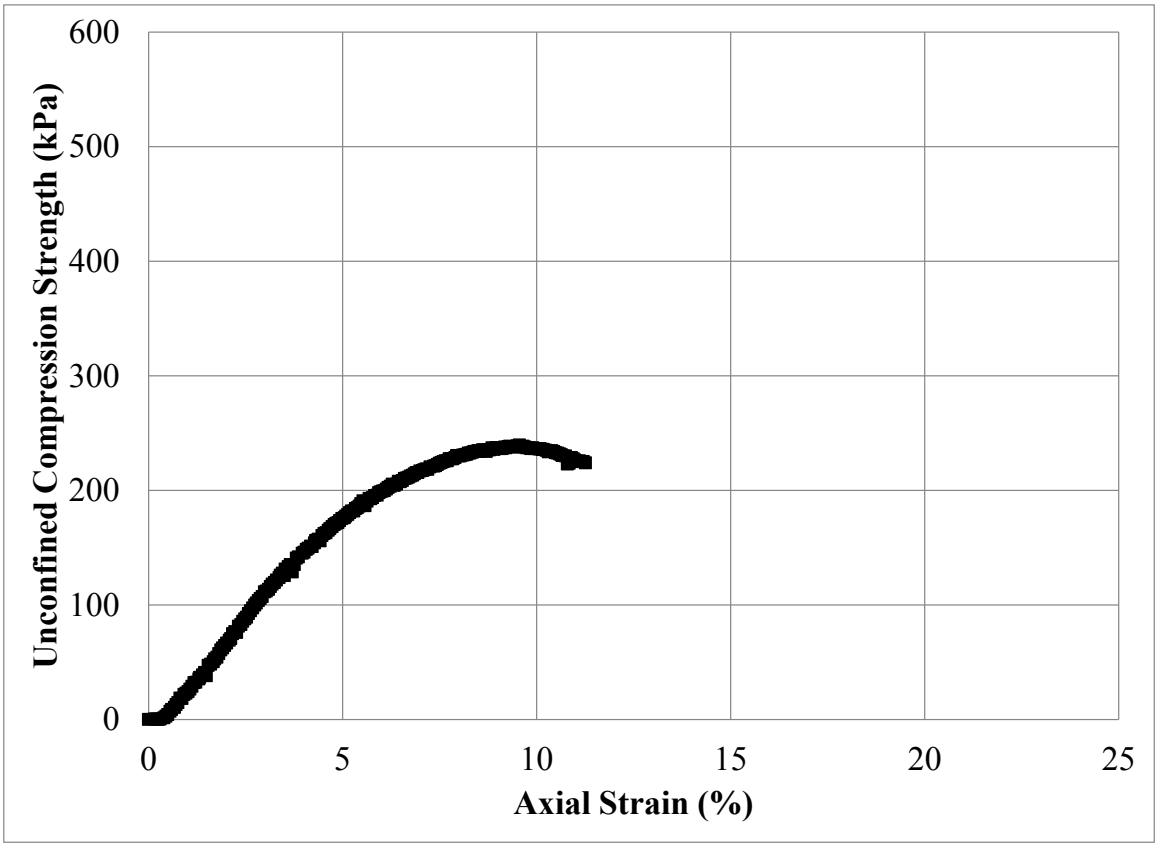

(c)

Figure C.108: Unconfined Compression Test Specimen No. 144R: (a) Photograph Prior to Testing; (b) Photograph Post Testing; and (c) Stress – Strain Data

(a)

(b)

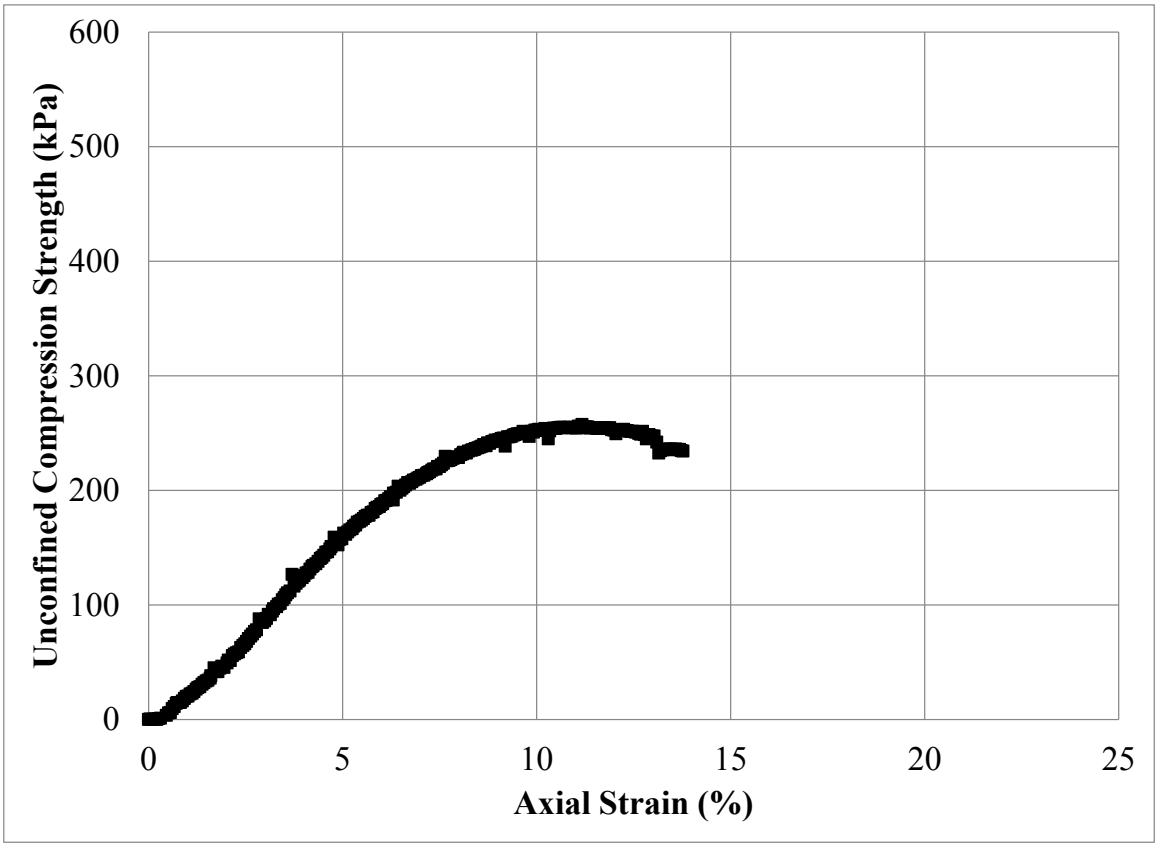

(c)

Figure C.109: Unconfined Compression Test Specimen No. 145R: (a) Photograph Prior to Testing; (b) Photograph Post Testing; and (c) Stress – Strain Data

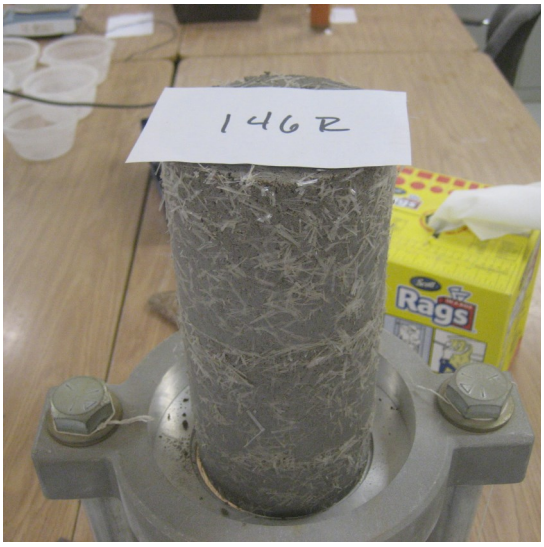

Post Test Photograph not Available

(a)

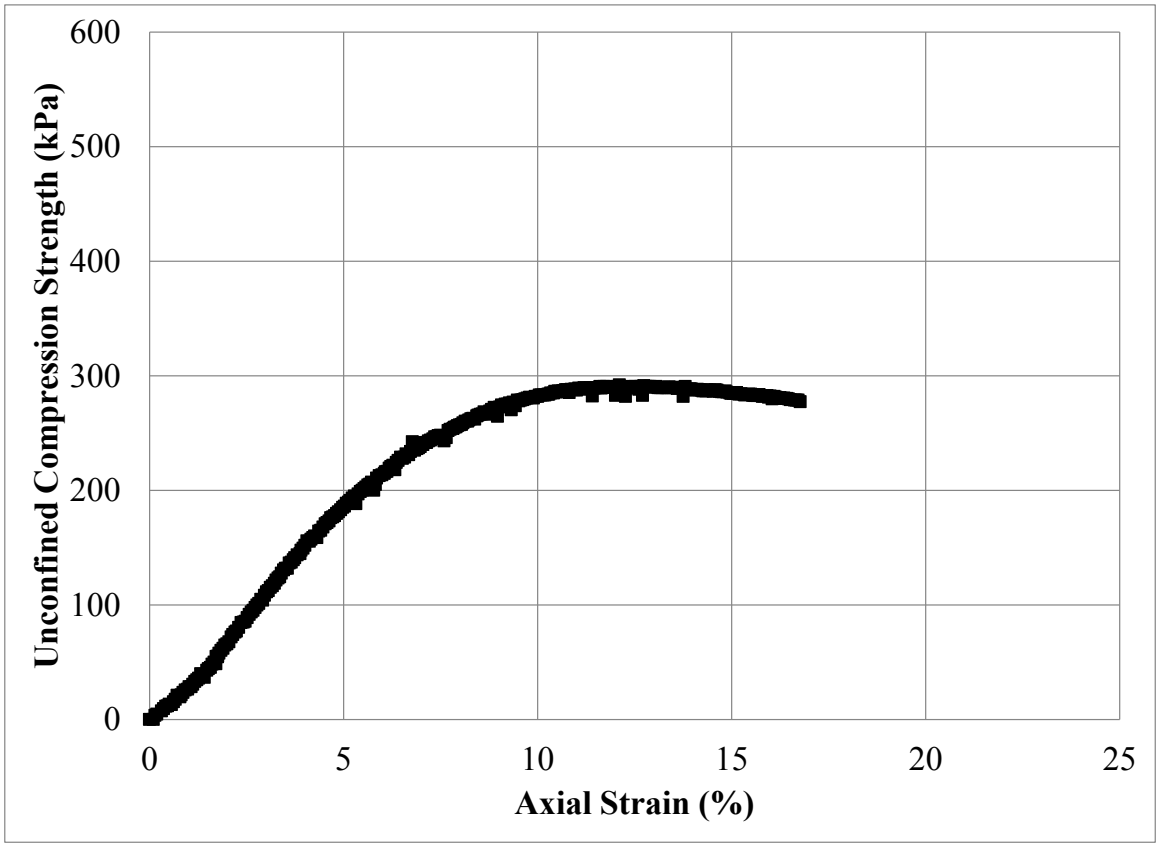

(b)

Figure C.110: Unconfined Compression Test Specimen No. 146R: (a) Photograph Prior to Testing; and (b) Stress – Strain Data

(a)

(b)

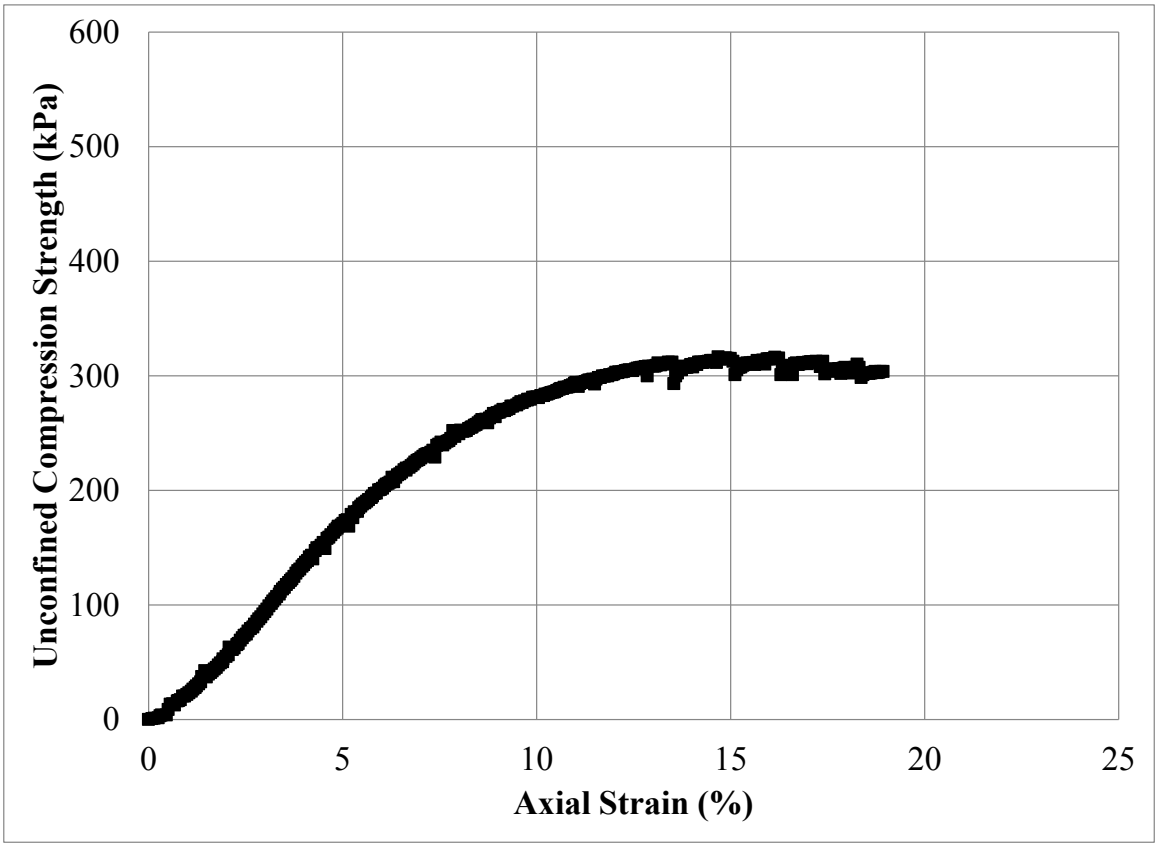

(c)

Figure C.111: Unconfined Compression Test Specimen No. 147R: (a) Photograph Prior to Testing; (b) Photograph Post Testing; and (c) Stress – Strain Data

(a)

(b)

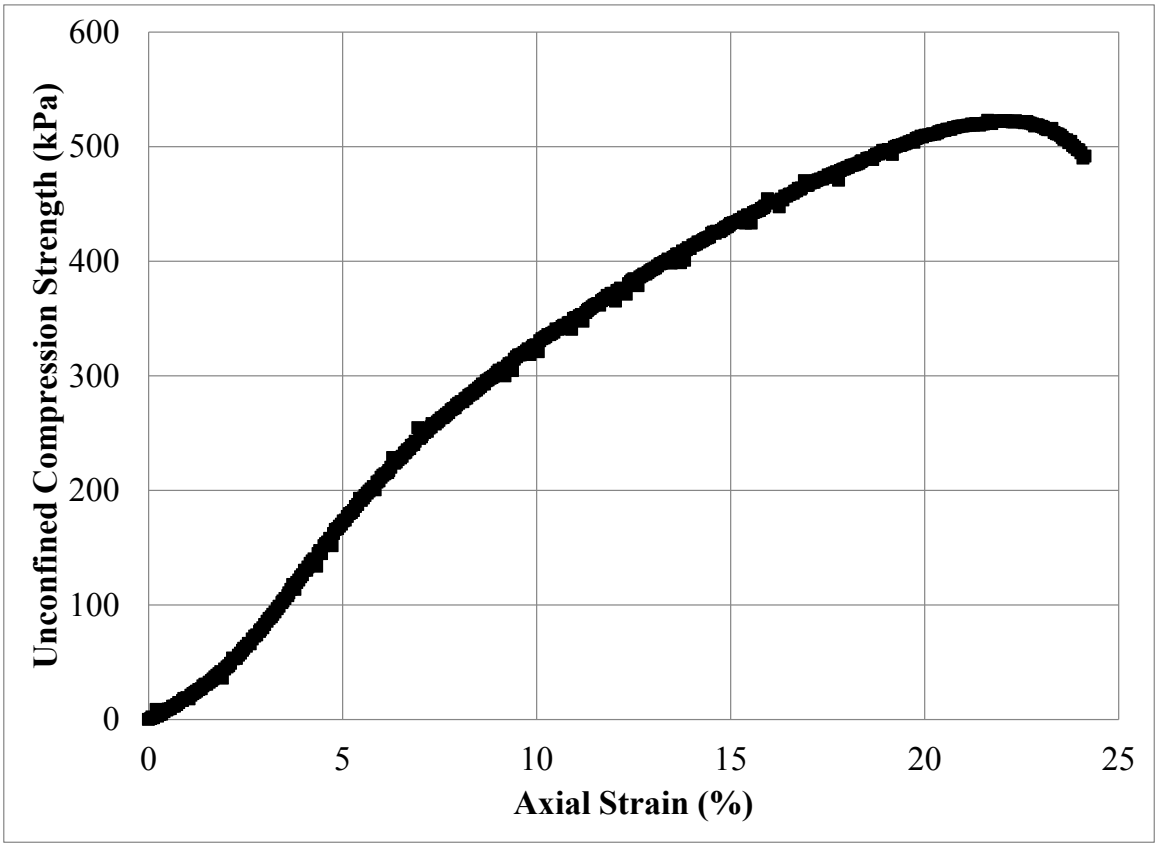

(c)

Figure C.112: Unconfined Compression Test Specimen No. 148R: (a) Photograph Prior to Testing; (b) Photograph Post Testing; and (c) Stress – Strain Data

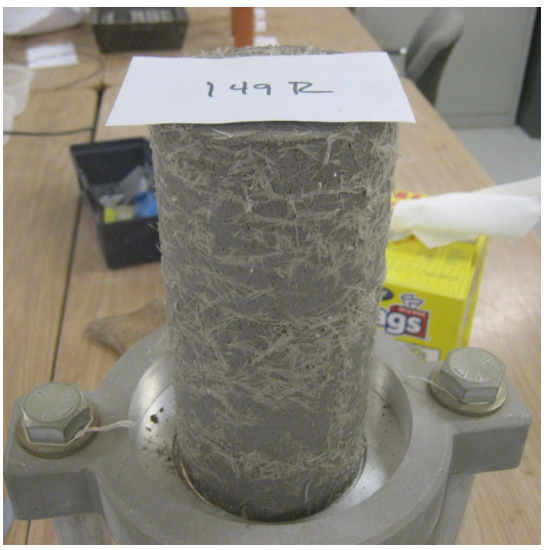

(a)

(b)

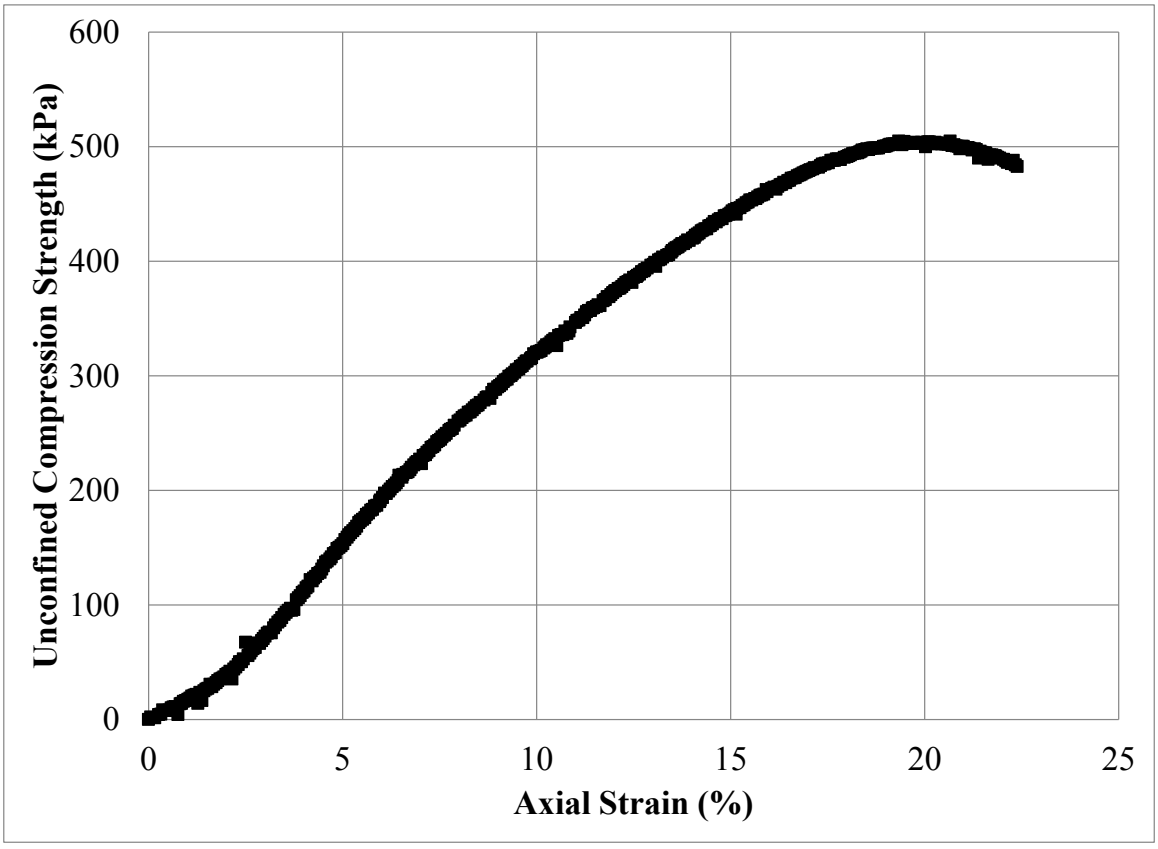

(c)

Figure C.113: Unconfined Compression Test Specimen No. 149R: (a) Photograph Prior to Testing; (b) Photograph Post Testing; and (c) Stress – Strain Data

(a)

(b)

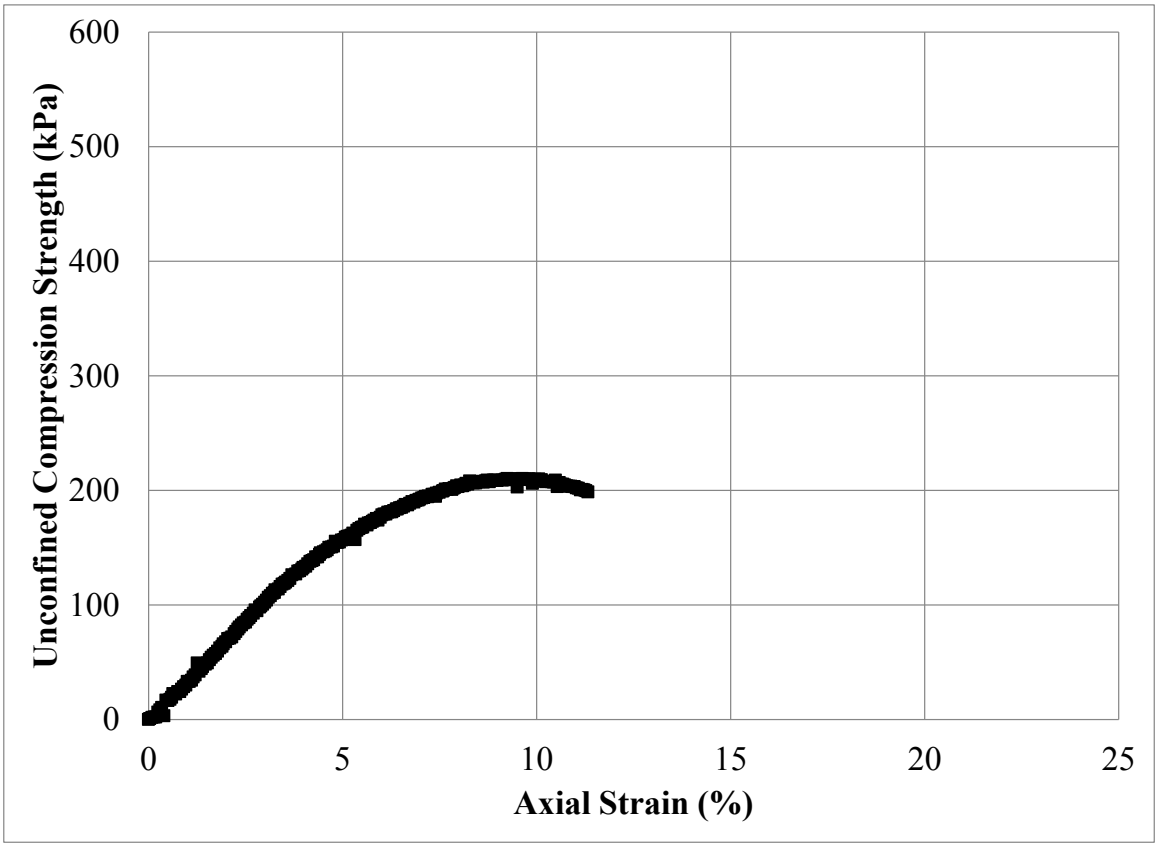

(c)

Figure C.114: Unconfined Compression Test Specimen No. 150R: (a) Photograph Prior to Testing; (b) Photograph Post Testing; and (c) Stress – Strain Data

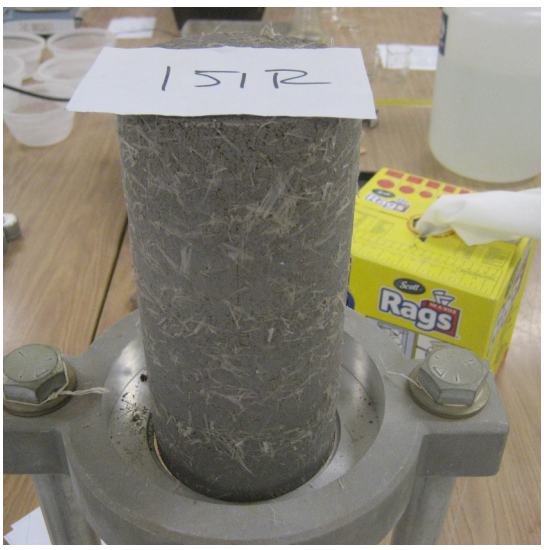

(a)

(b)

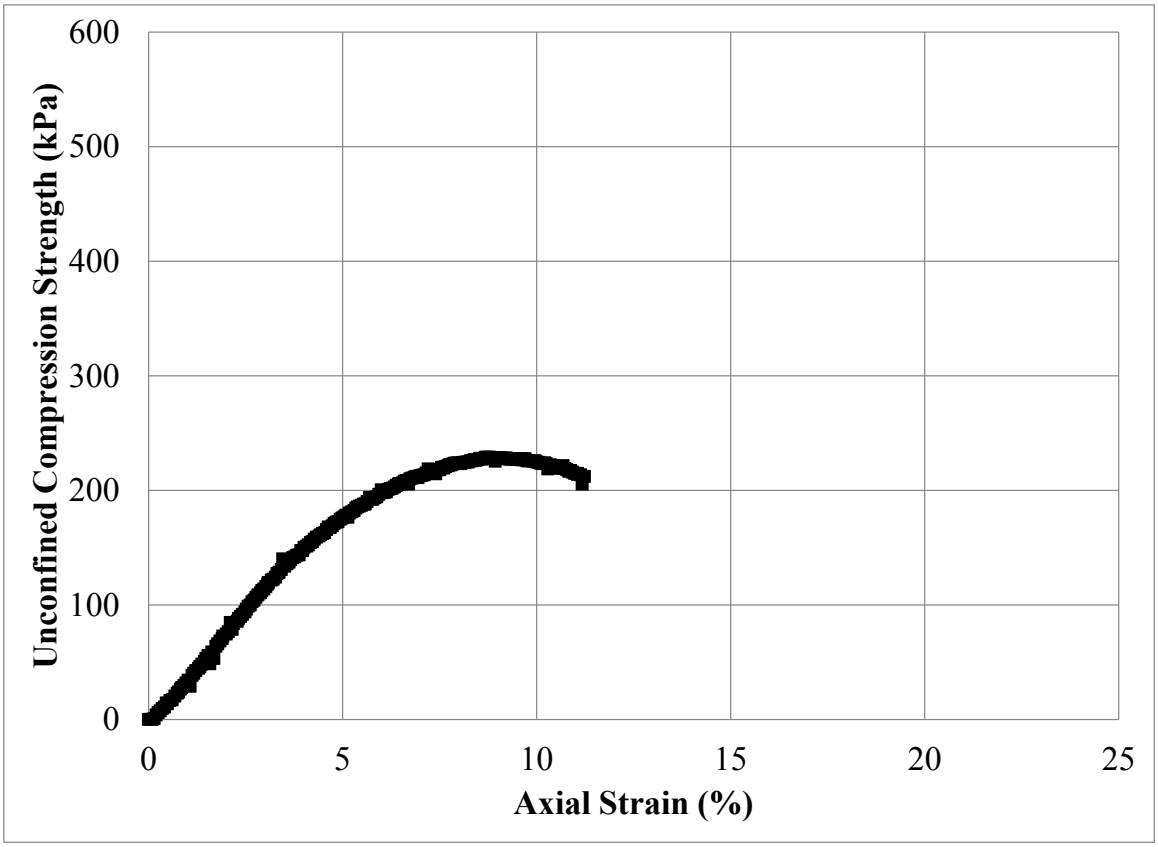

(c)

Figure C.115: Unconfined Compression Test Specimen No. 151R: (a) Photograph Prior to Testing; (b) Photograph Post Testing; and (c) Stress – Strain Data

(a)

(b)

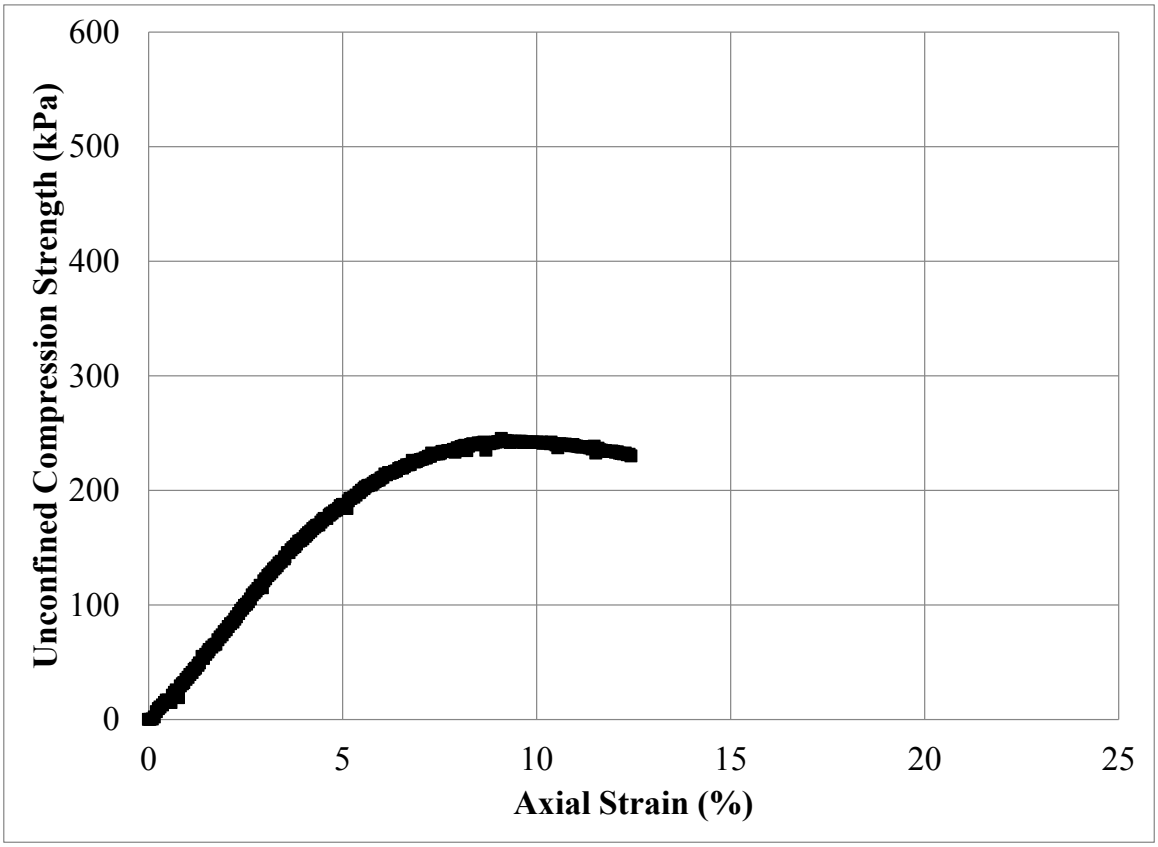

(c)

Figure C.116: Unconfined Compression Test Specimen No. 152R: (a) Photograph Prior to Testing; (b) Photograph Post Testing; and (c) Stress – Strain Data

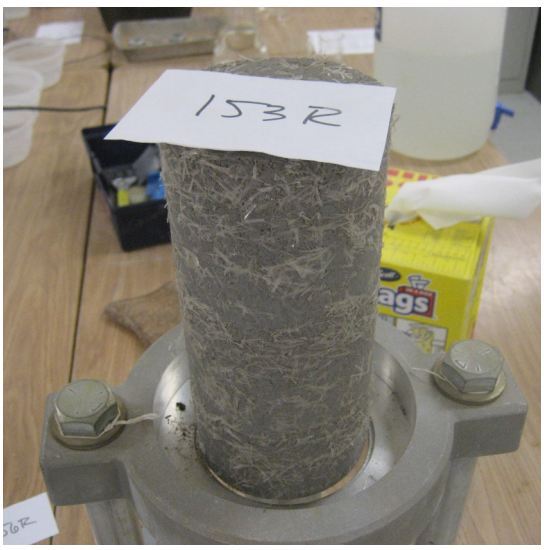

(a)

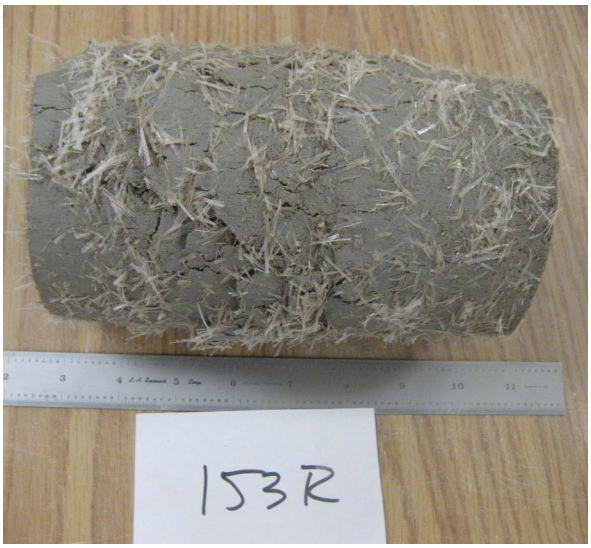

(b)

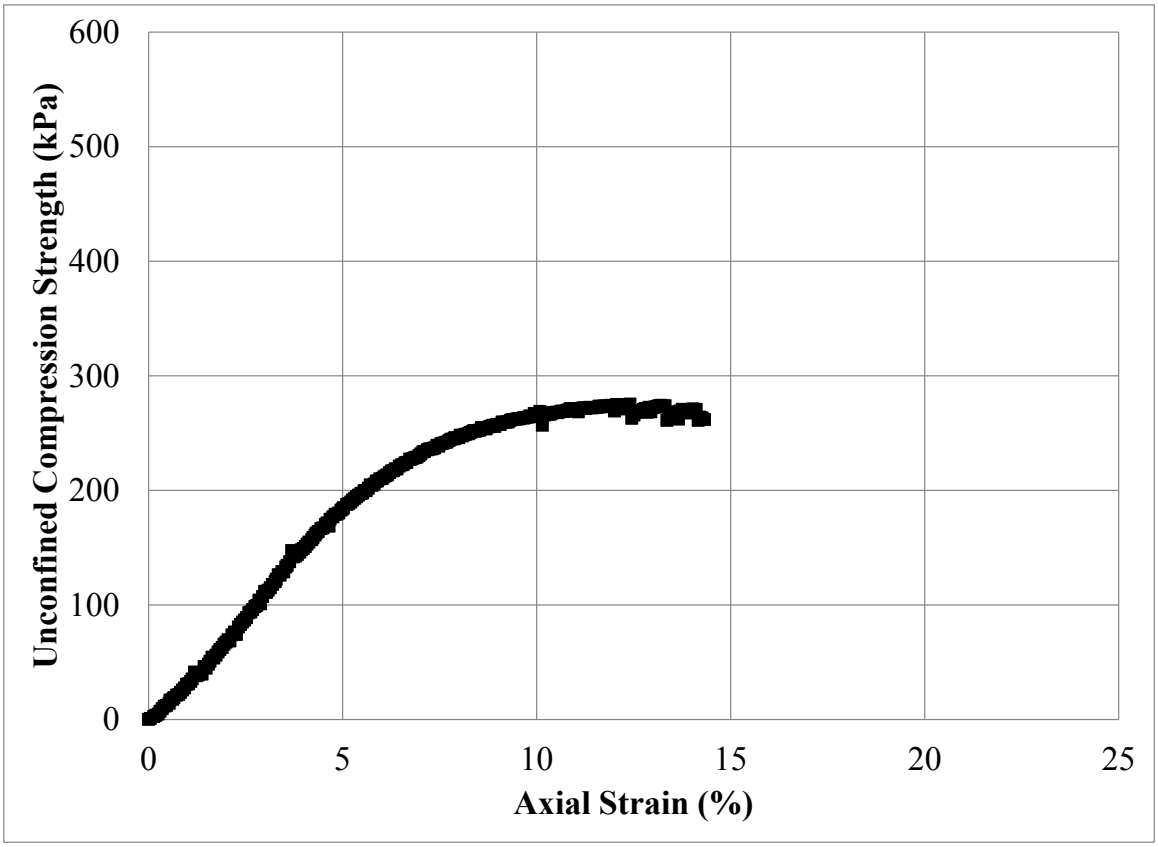

(c)

Figure C.117: Unconfined Compression Test Specimen No. 153R: (a) Photograph Prior to Testing; (b) Photograph Post Testing; and (c) Stress – Strain Data

(a)

(b)

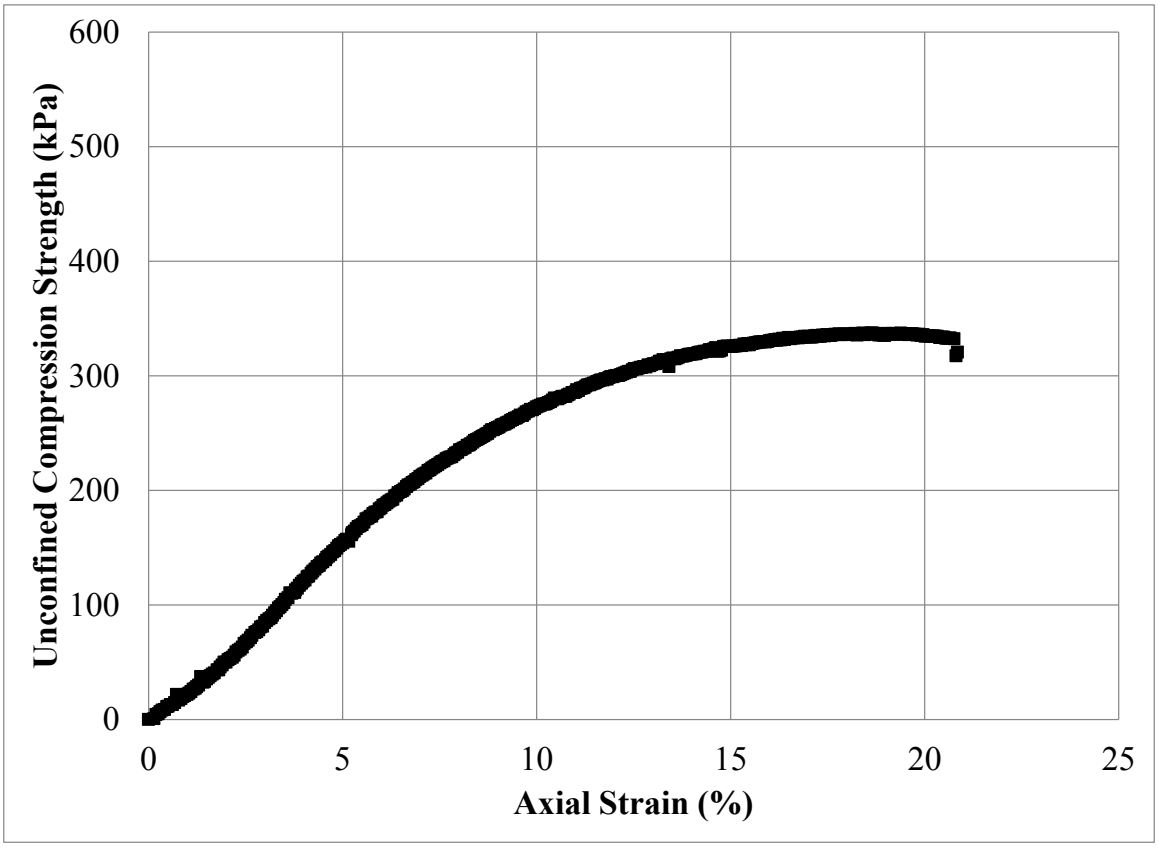

(c)

Figure C.118: Unconfined Compression Test Specimen No. 154R: (a) Photograph Prior to Testing; (b) Photograph Post Testing; and (c) Stress – Strain Data

(a)

(b)

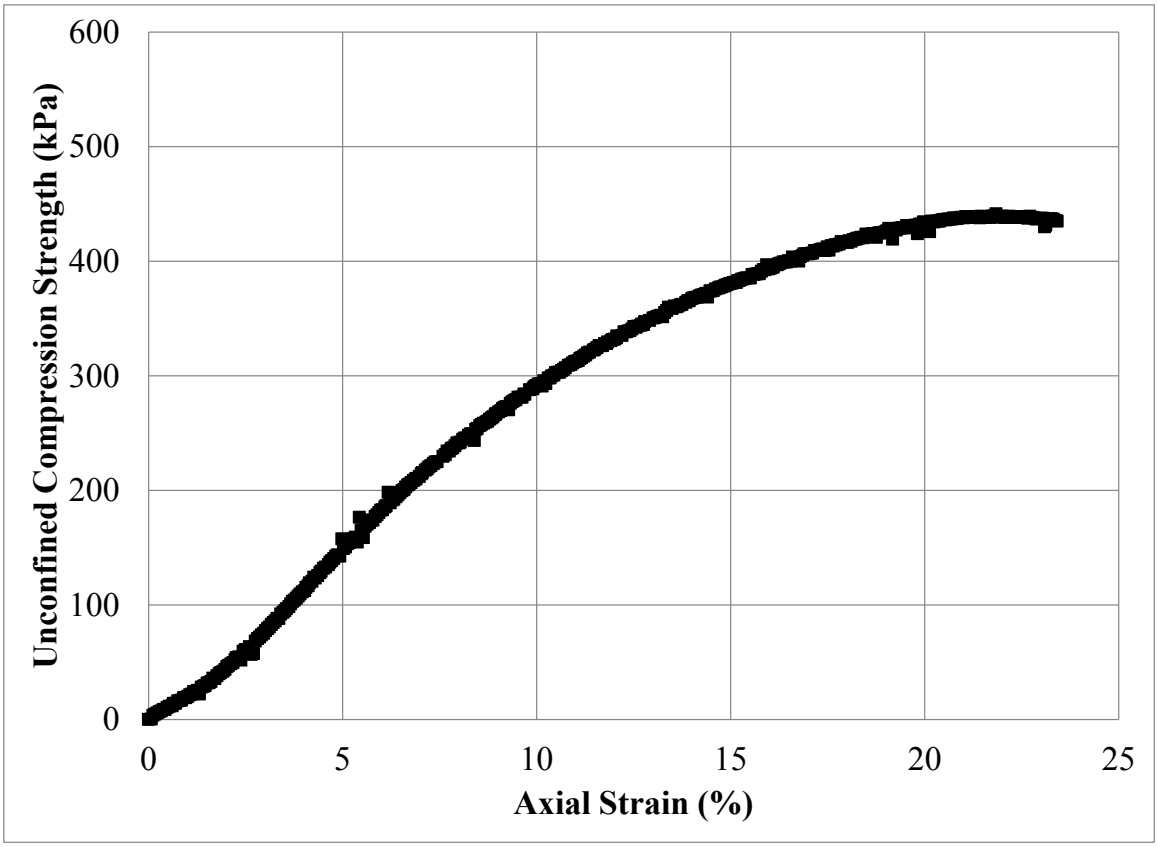

(c)

Figure C.119: Unconfined Compression Test Specimen No. 155R: (a) Photograph Prior to Testing; (b) Photograph Post Testing; and (c) Stress – Strain Data

(a)

(b)

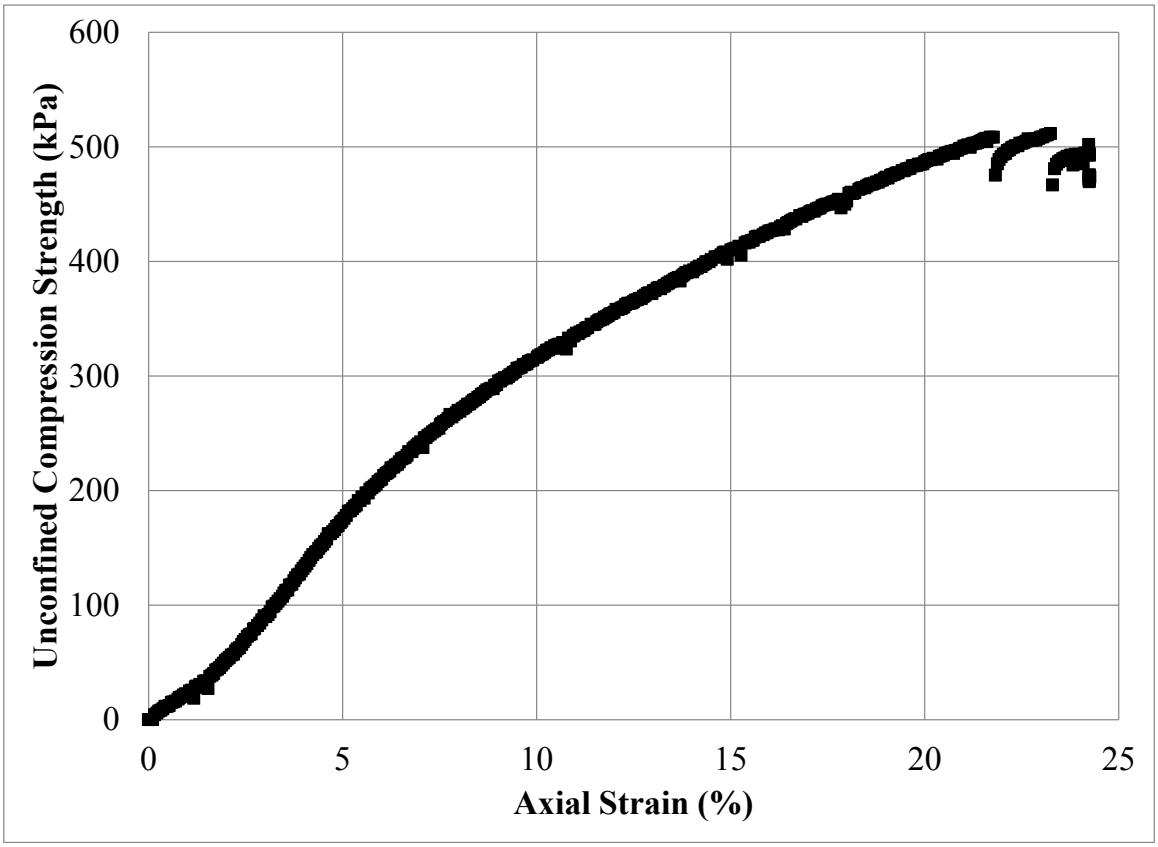

(c)

Figure C.120: Unconfined Compression Test Specimen No. 156R: (a) Photograph Prior to Testing; (b) Photograph Post Testing; and (c) Stress – Strain Data

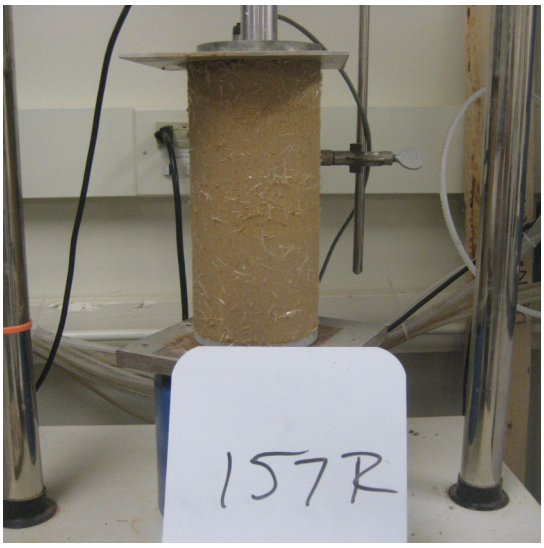

(a)

(b)

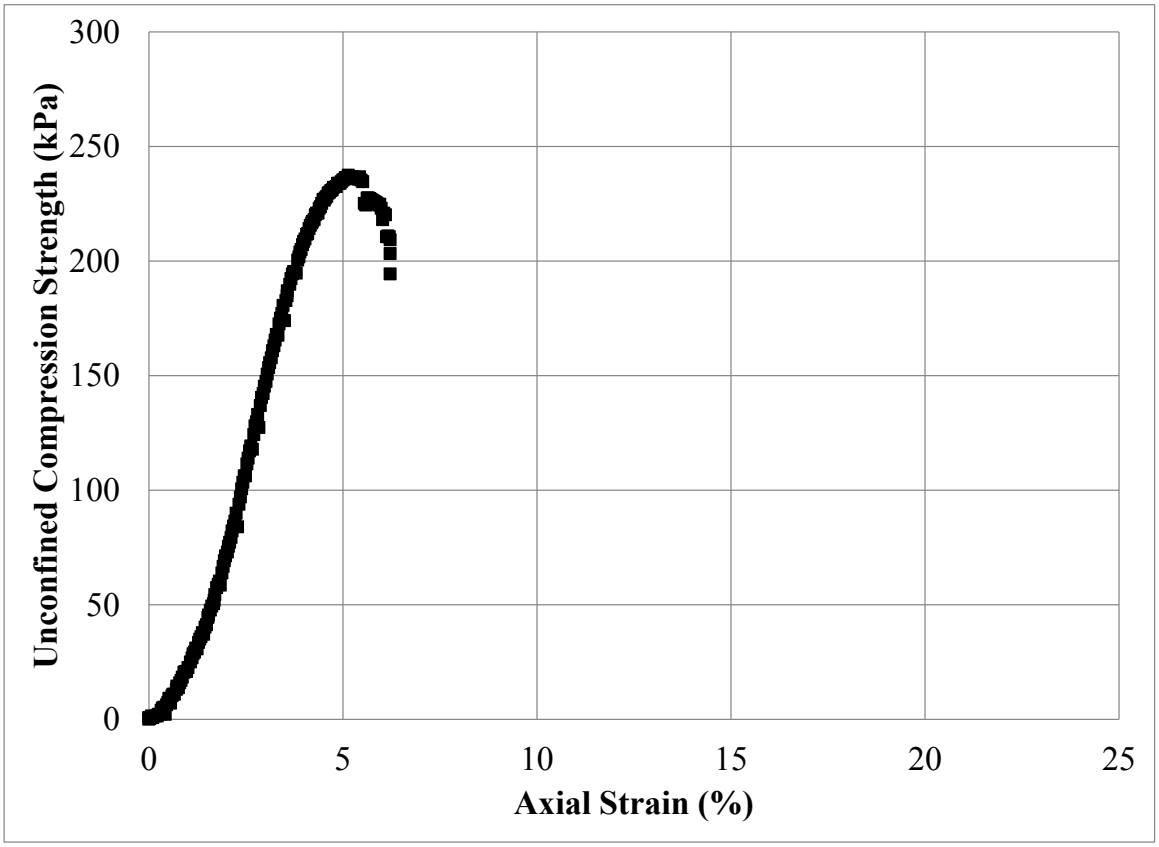

(c)

Figure C.121: Unconfined Compression Test Specimen No. 157R: (a) Photograph Prior to Testing; (b) Photograph Post Testing; and (c) Stress – Strain Data

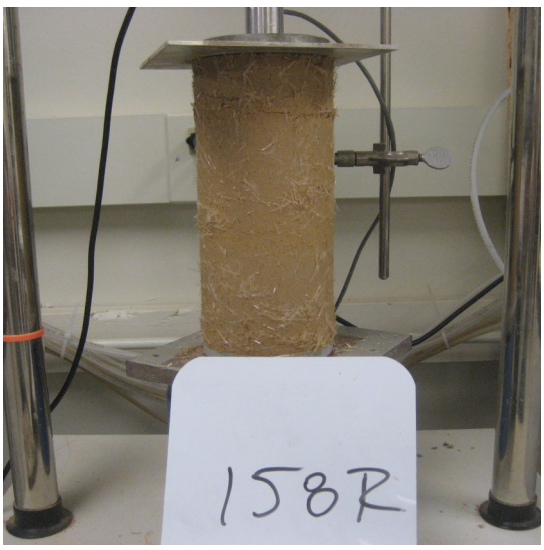

(a)

(b)

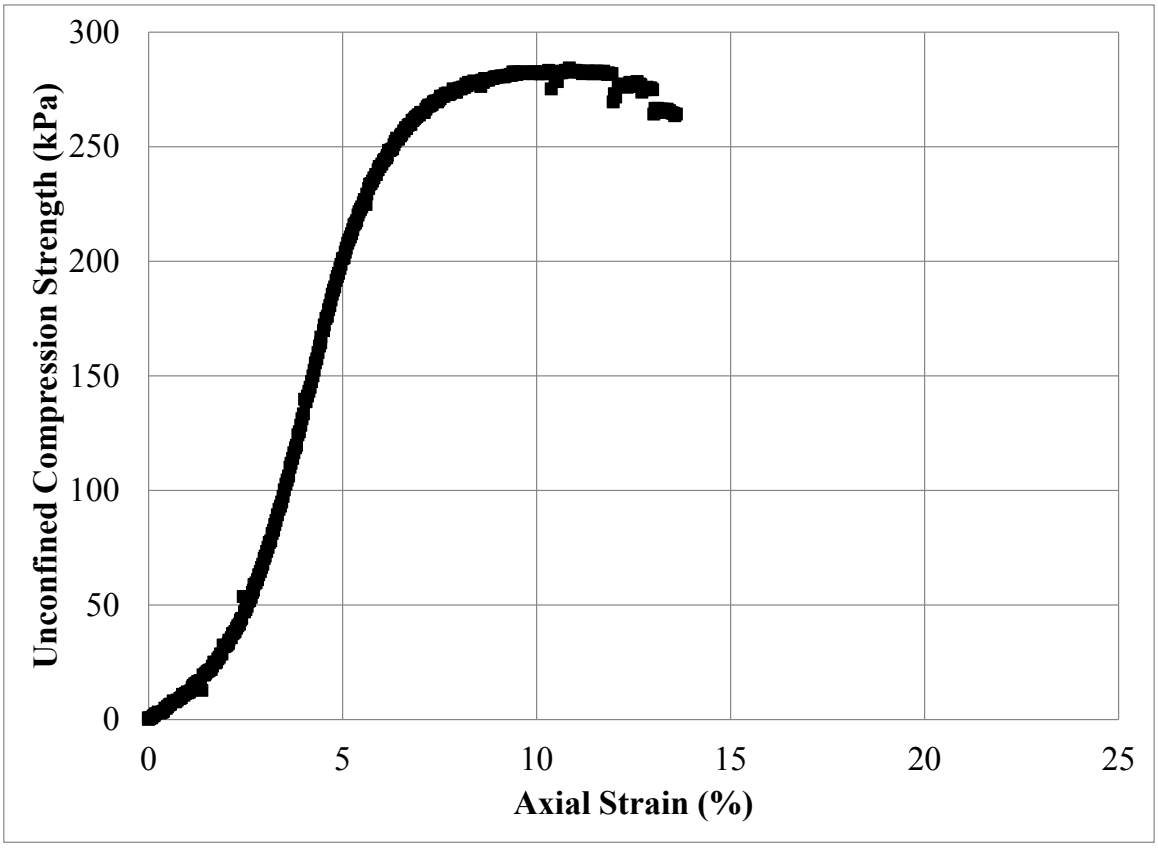

(c)

Figure C.122: Unconfined Compression Test Specimen No. 158R: (a) Photograph Prior to Testing; (b) Photograph Post Testing; and (c) Stress – Strain Data

(a)

(b)

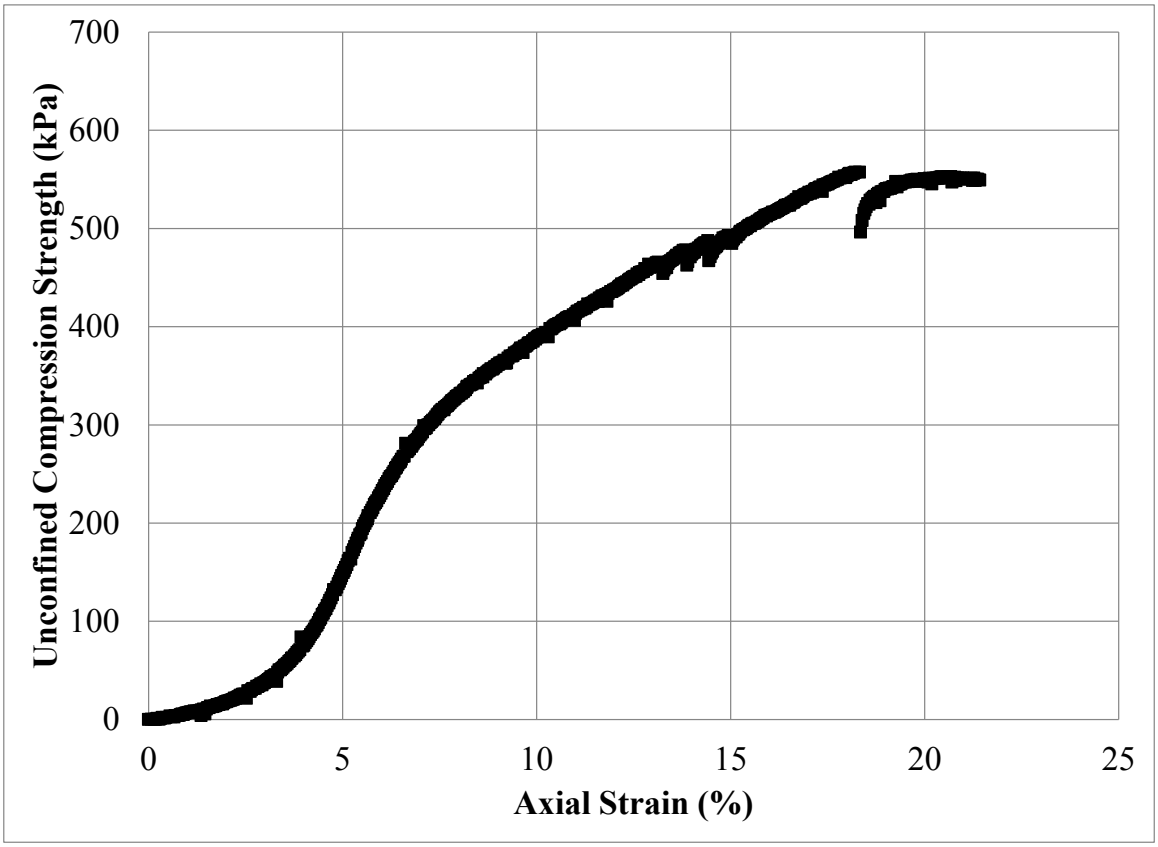

(c)

Figure C.123: Unconfined Compression Test Specimen No. 159R: (a) Photograph Prior to Testing; (b) Photograph Post Testing; and (c) Stress – Strain Data

(a)

(b)

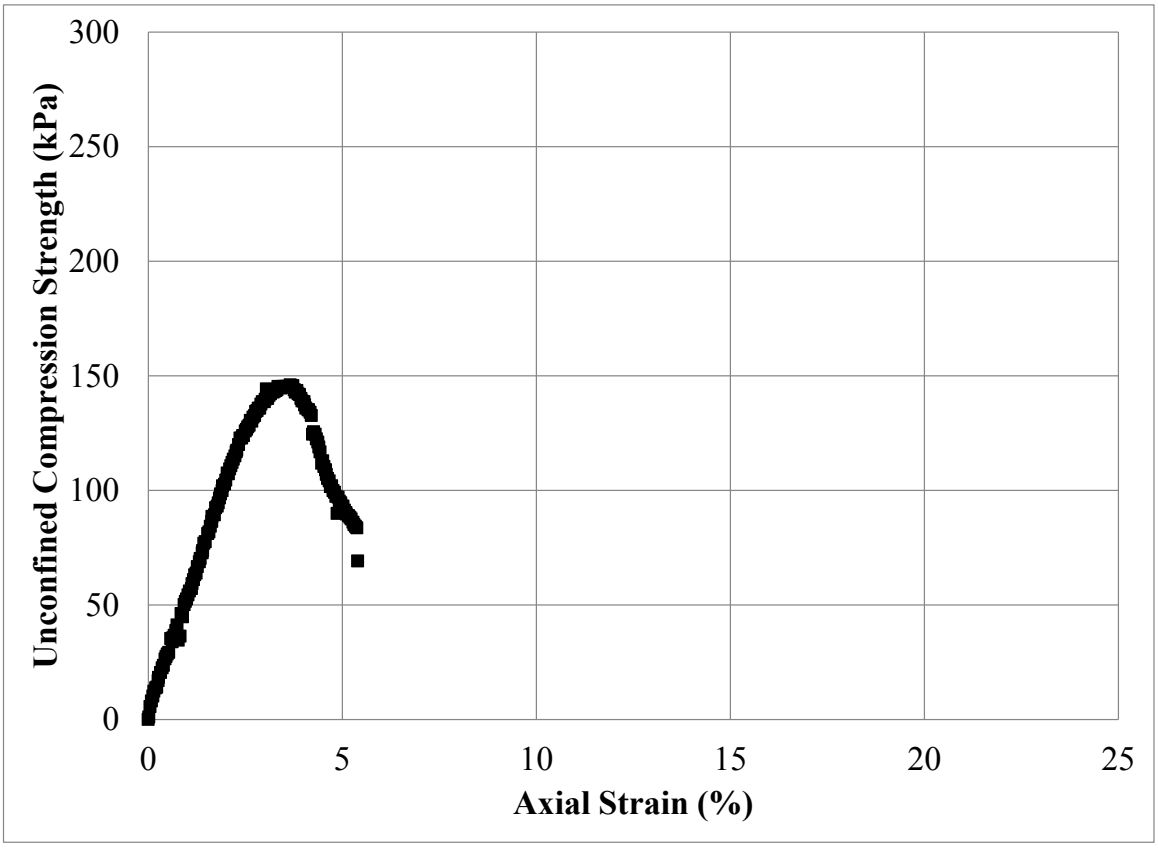

(c)

Figure C.124: Unconfined Compression Test Specimen No. 160R: (a) Photograph Prior to Testing; (b) Photograph Post Testing; and (c) Stress – Strain Data

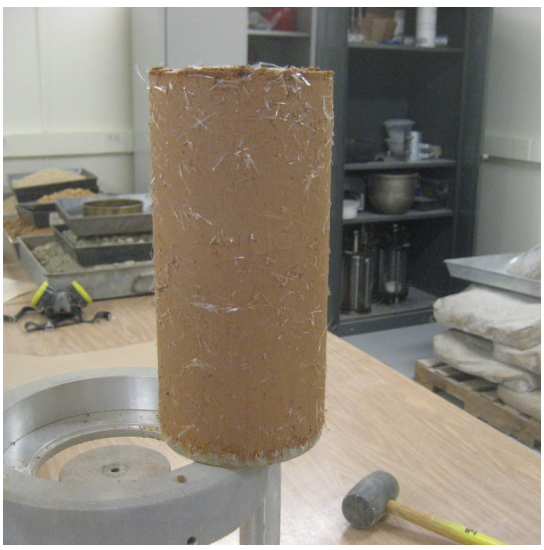

(a)

(b)

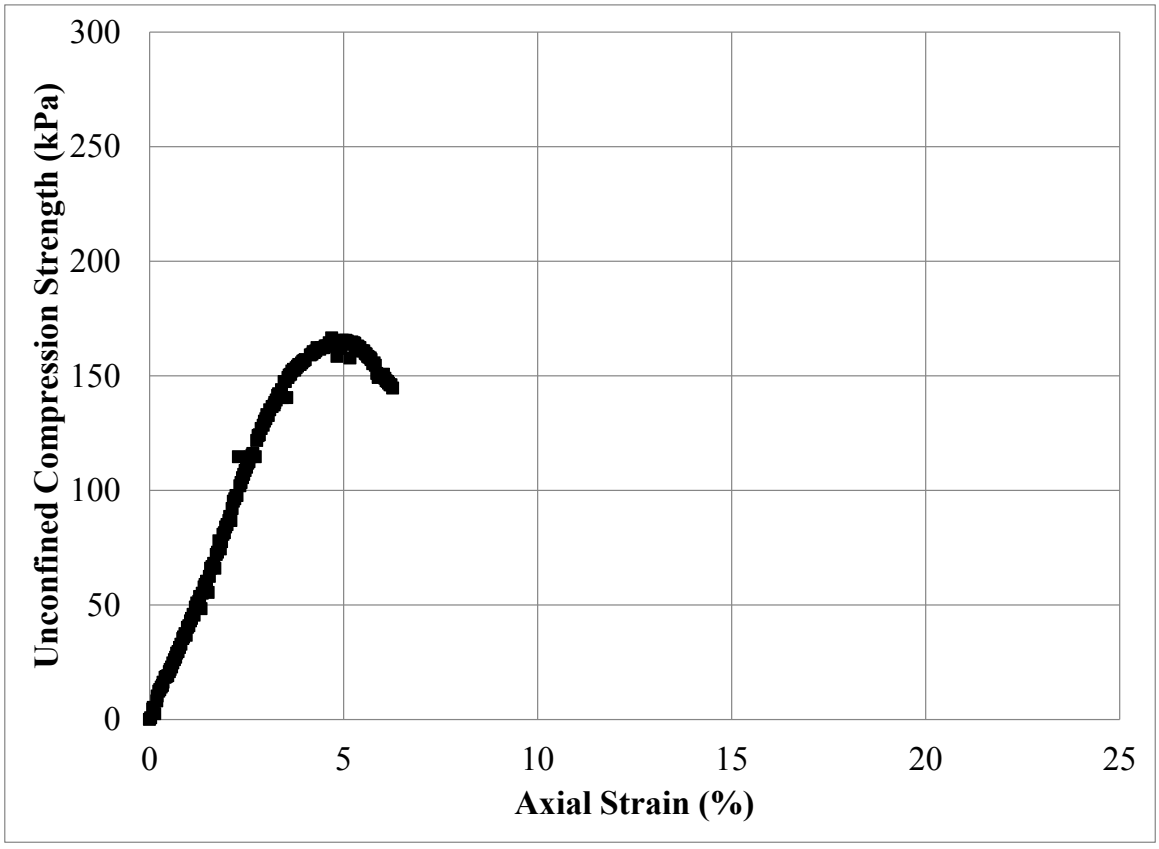

(c)

Figure C.125: Unconfined Compression Test Specimen No. 161R: (a) Photograph Prior to Testing; (b) Photograph Post Testing; and (c) Stress – Strain Data

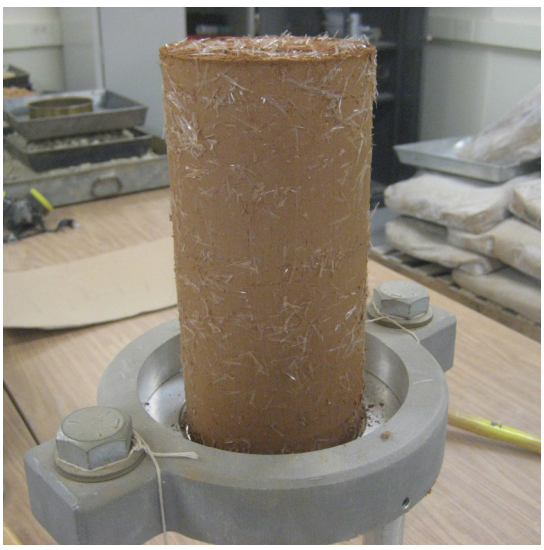

(a)

(b)

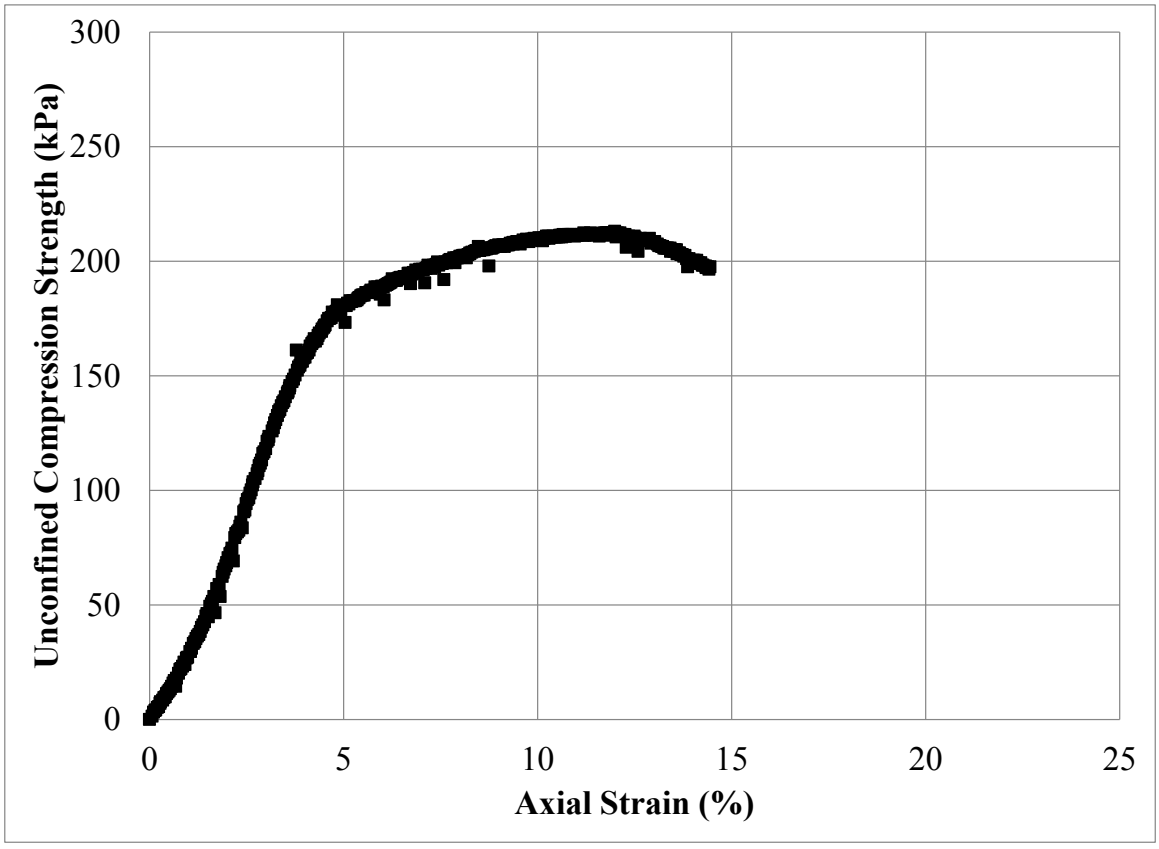

(c)

Figure C.126: Unconfined Compression Test Specimen No. 162R: (a) Photograph Prior to Testing; (b) Photograph Post Testing; and (c) Stress – Strain Data

(a)

(b)

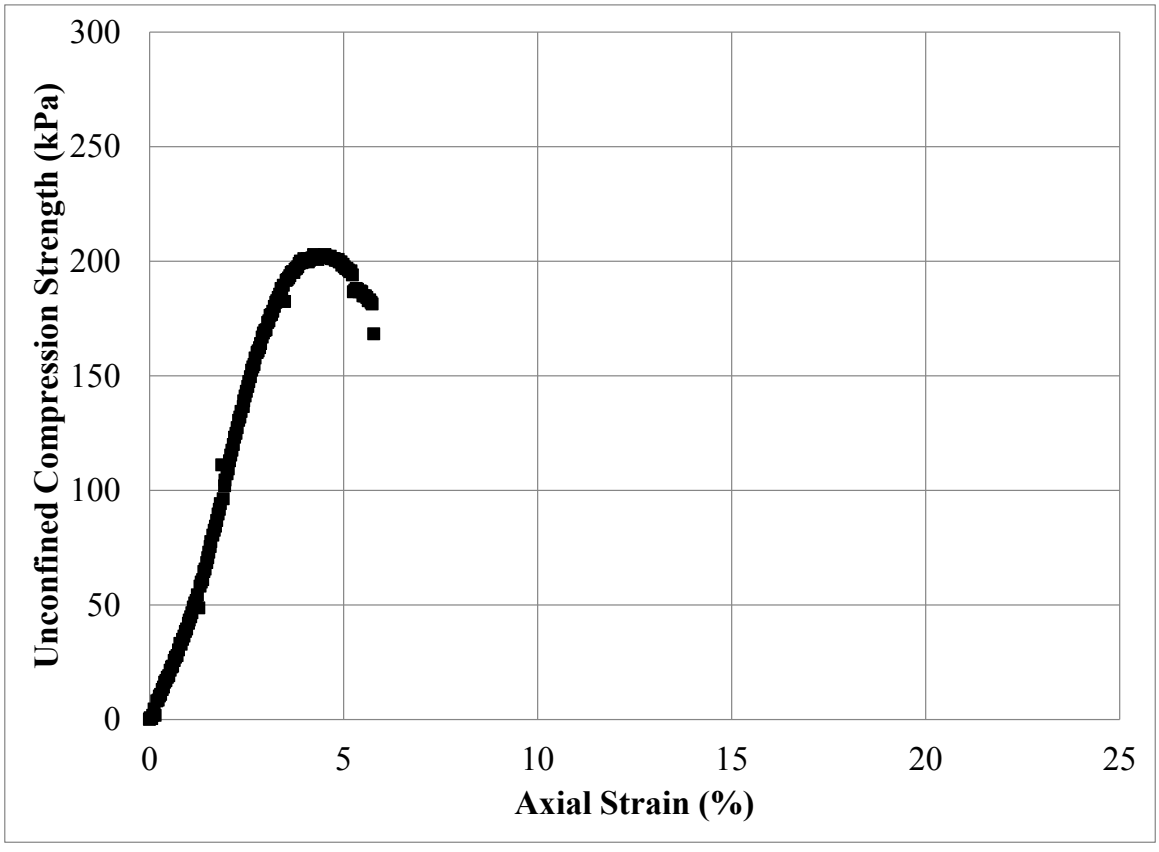

(c)

Figure C.127: Unconfined Compression Test Specimen No. 163R: (a) Photograph Prior to Testing; (b) Photograph Post Testing; and (c) Stress – Strain Data

(a)

(b)

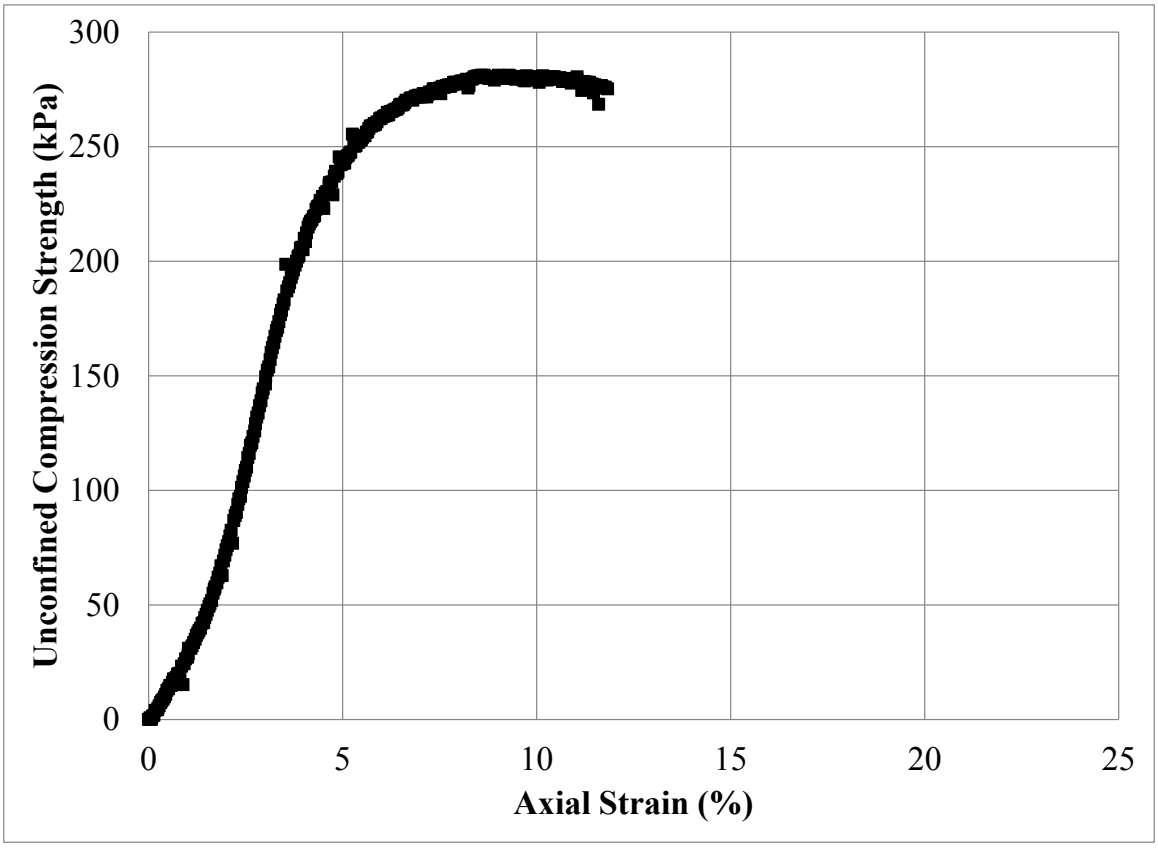

(c)

Figure C.128: Unconfined Compression Test Specimen No. 164R: (a) Photograph Prior to Testing; (b) Photograph Post Testing; and (c) Stress – Strain Data

(a)

(b)

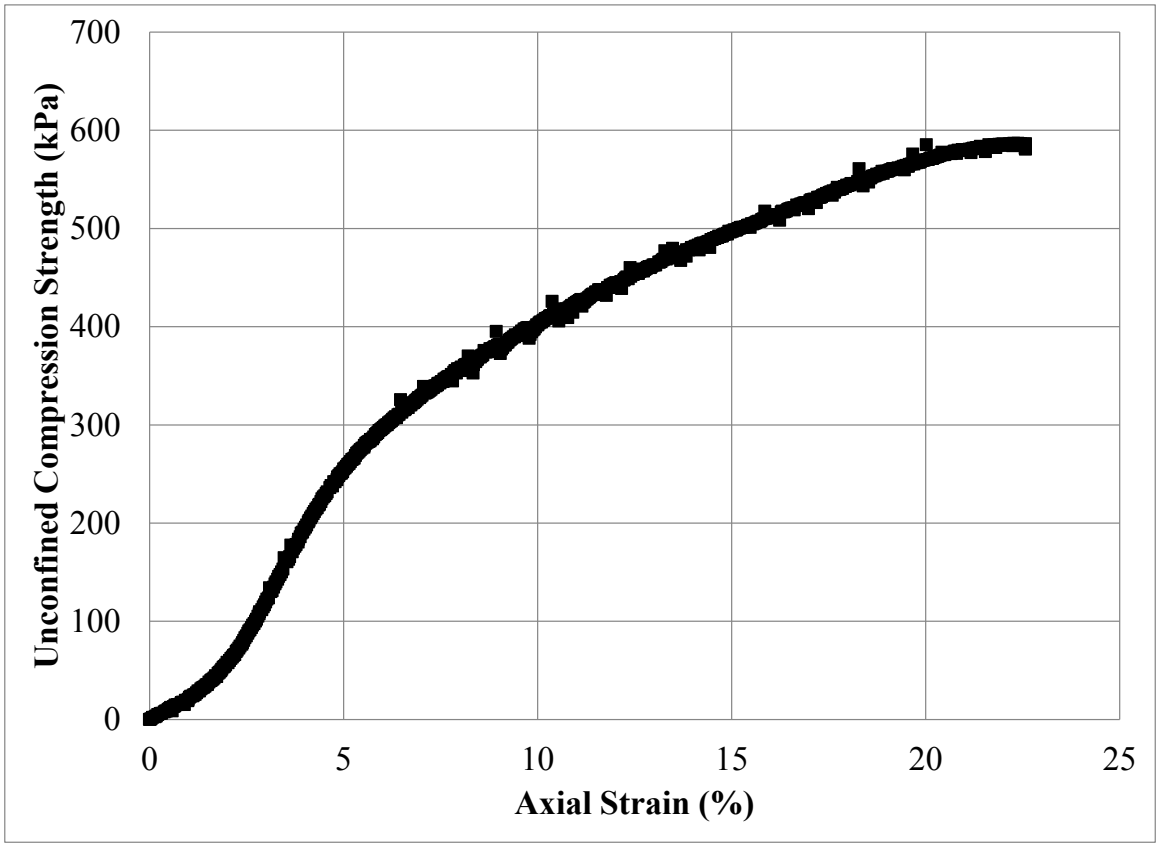

(c)

Figure C.129: Unconfined Compression Test Specimen No. 165R: (a) Photograph Prior to Testing; (b) Photograph Post Testing; and (c) Stress – Strain Data

(a)

(b)

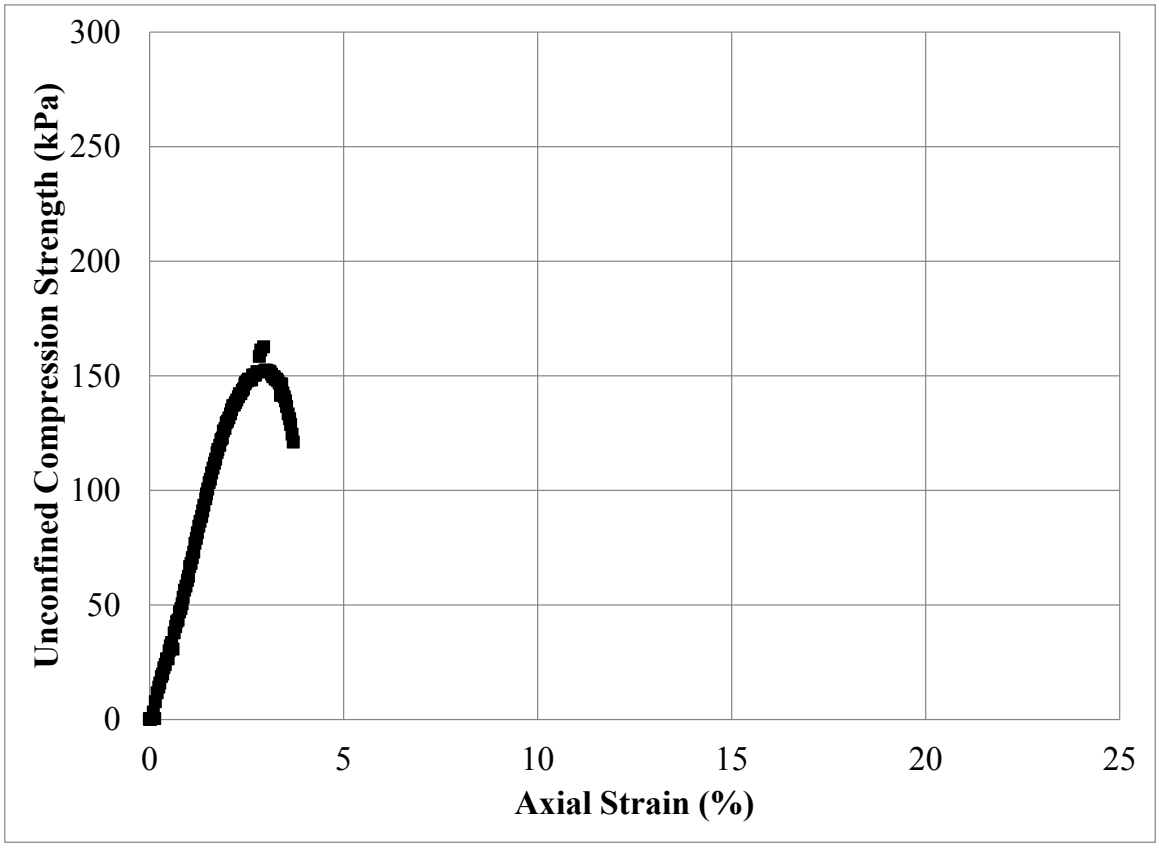

(c)

Figure C.130: Unconfined Compression Test Specimen No. 166R: (a) Photograph Prior to Testing; (b) Photograph Post Testing; and (c) Stress – Strain Data

(a)

(b)

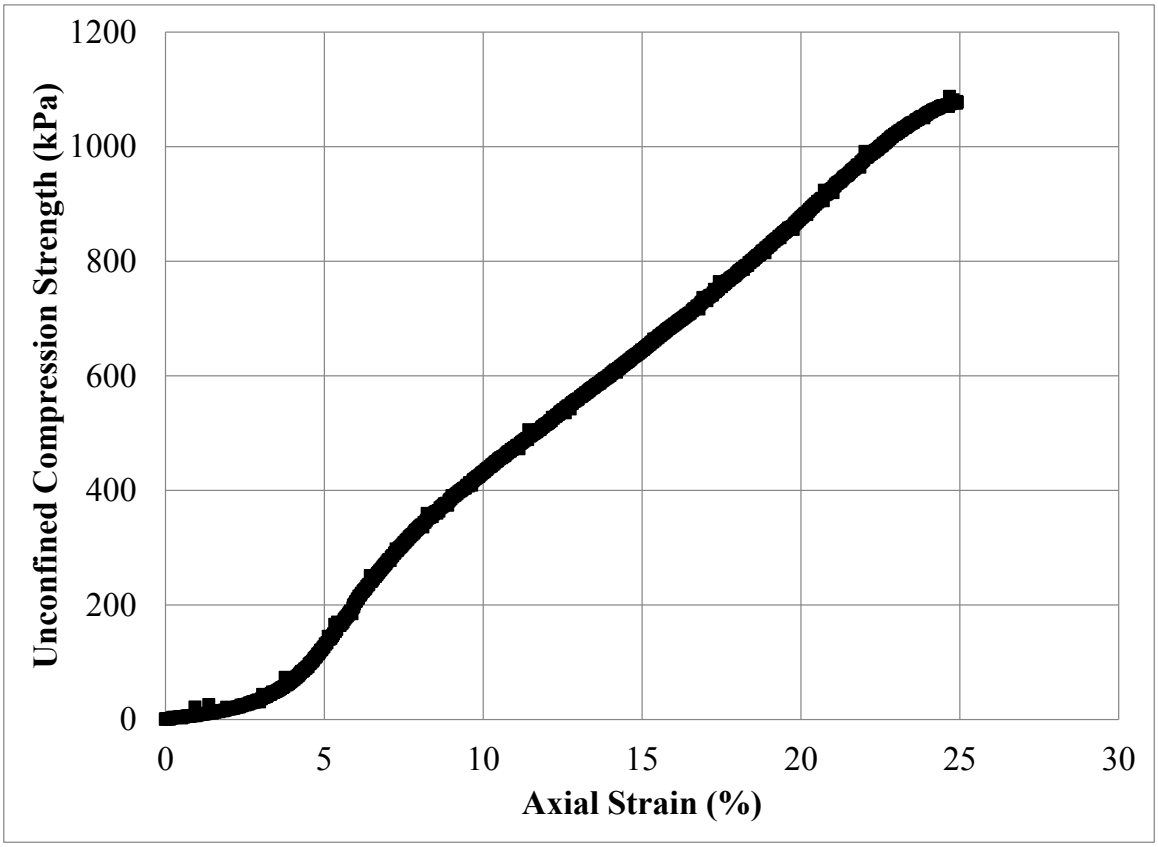

(c)

Figure C.131: Unconfined Compression Test Specimen No. 167R: (a) Photograph Prior to Testing; (b) Photograph Post Testing; and (c) Stress – Strain Data

(a)

(b)

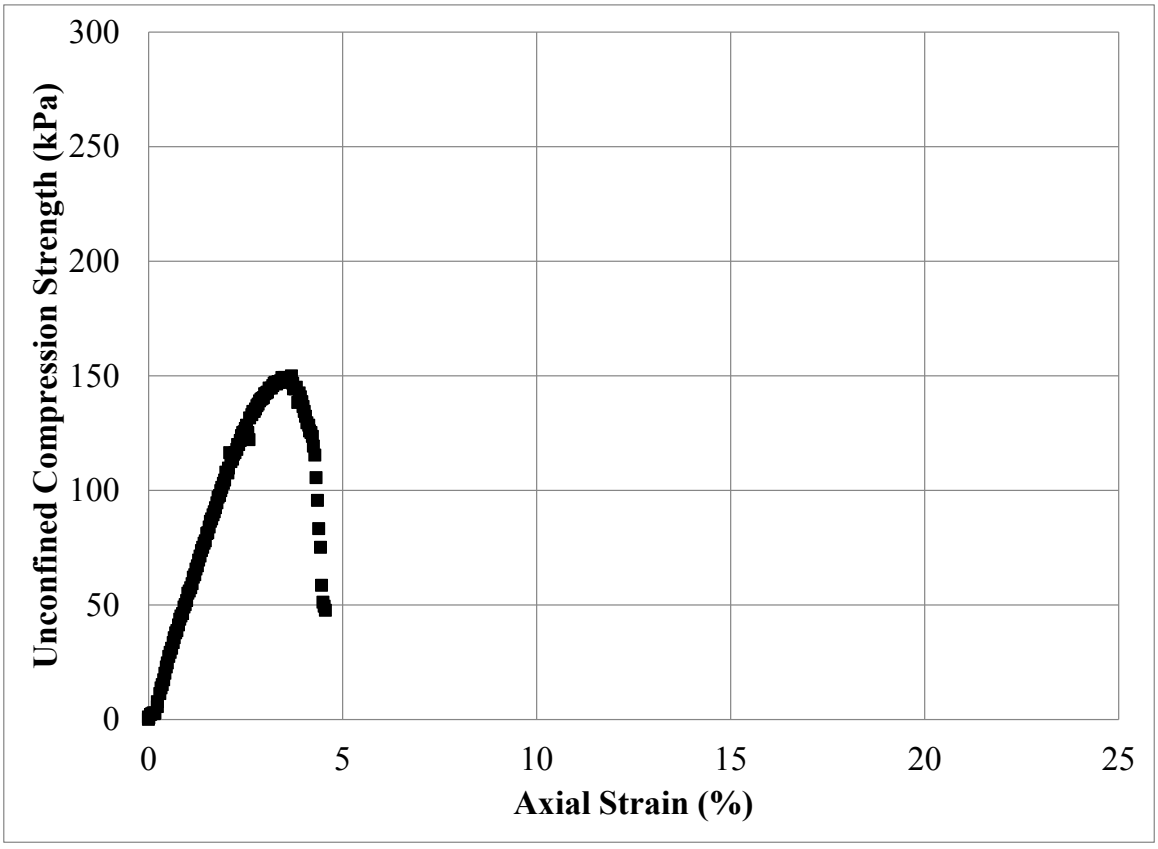

(c)

Figure C.132: Unconfined Compression Test Specimen No. 168R: (a) Photograph Prior to Testing; (b) Photograph Post Testing; and (c) Stress – Strain Data

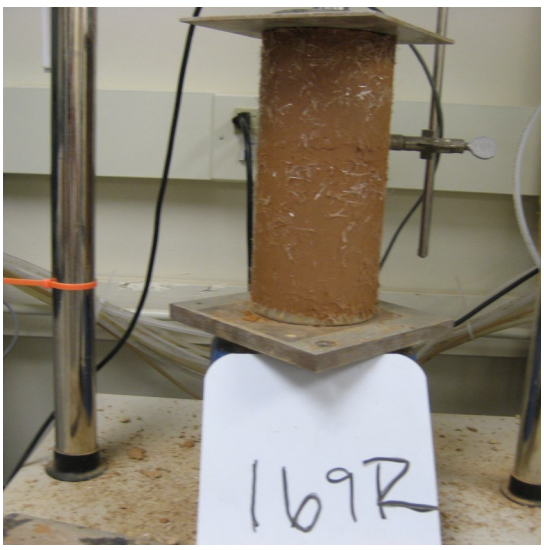

(a)

(b)

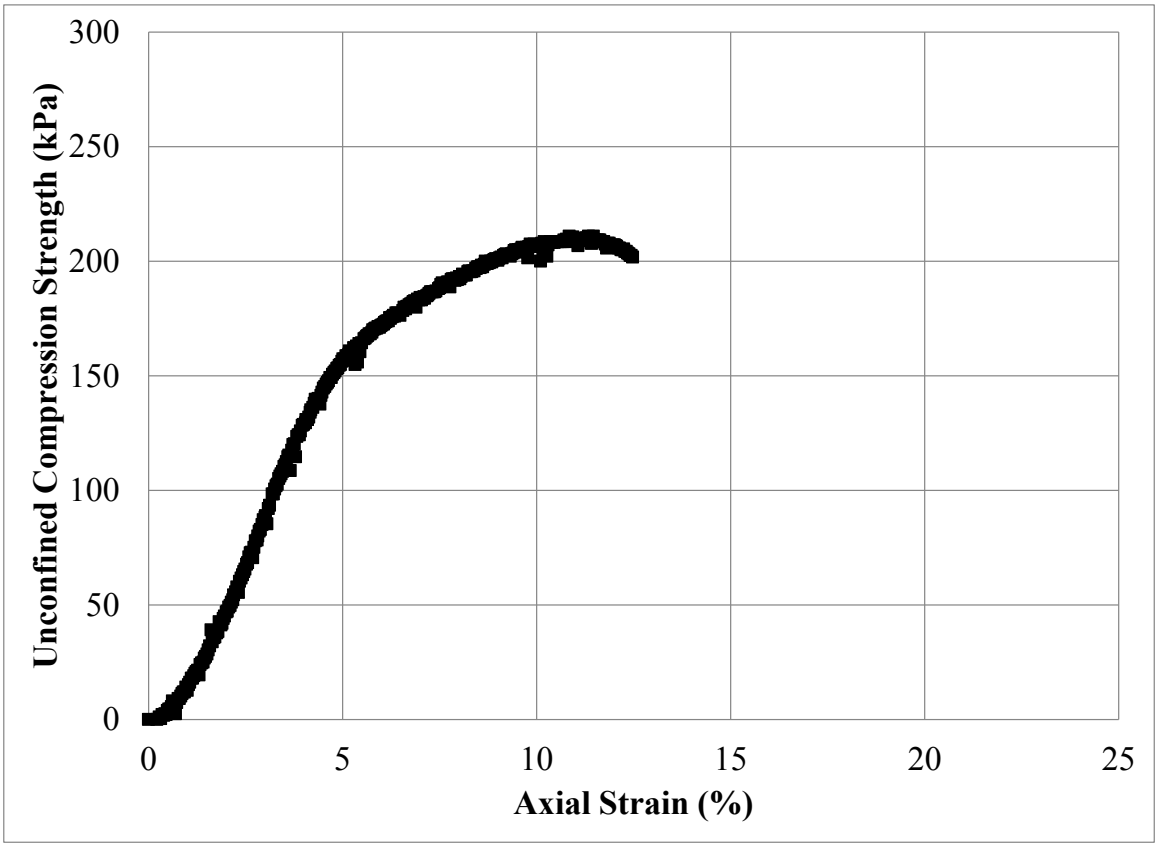

(c)

Figure C.133 Unconfined Compression Test Specimen No. 169R: (a) Photograph Prior to Testing; (b) Photograph Post Testing; and (c) Stress – Strain Data

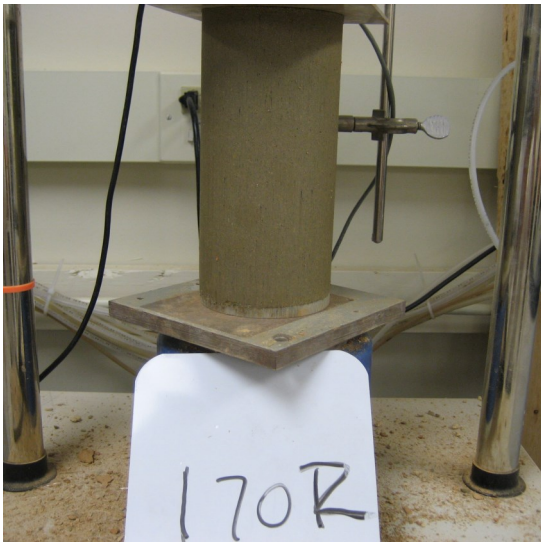

(a)

(b)

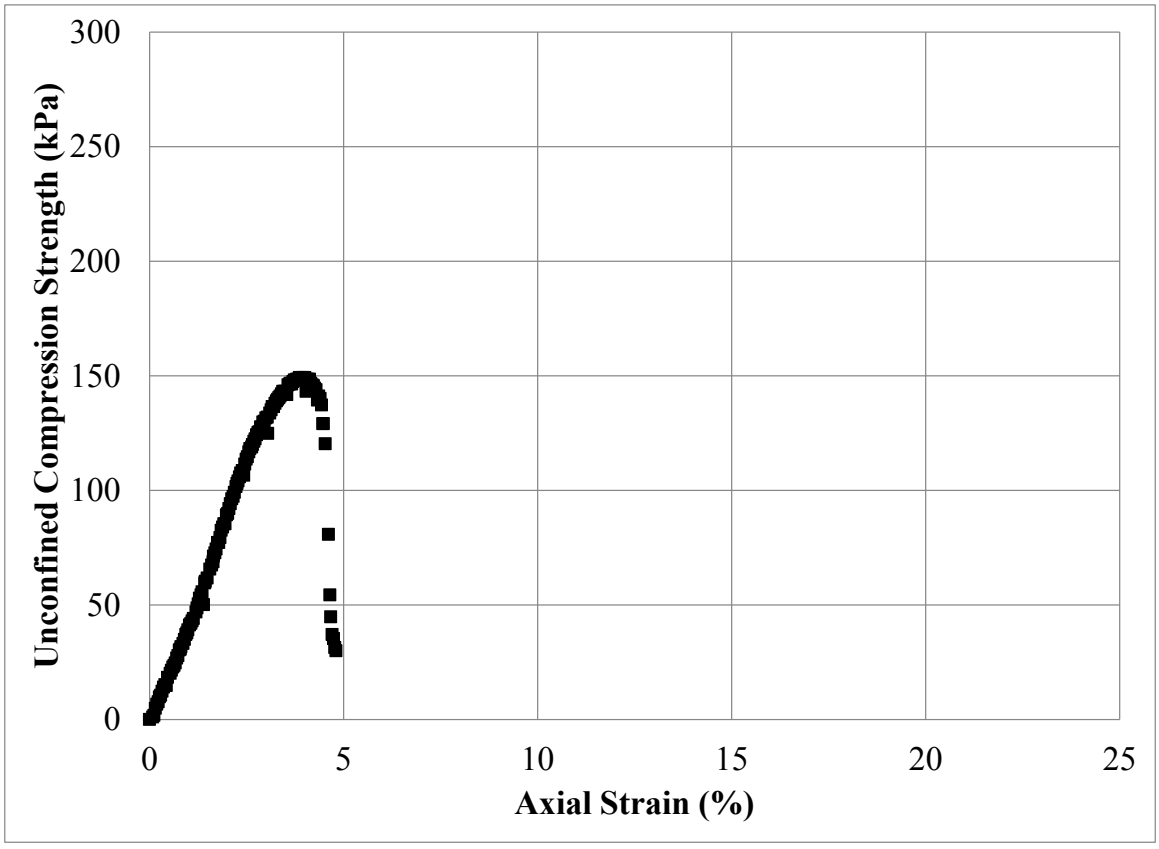

(c)

Figure C.134 Unconfined Compression Test Specimen No. 170R: (a) Photograph Prior to Testing; (b) Photograph Post Testing; and (c) Stress – Strain Data

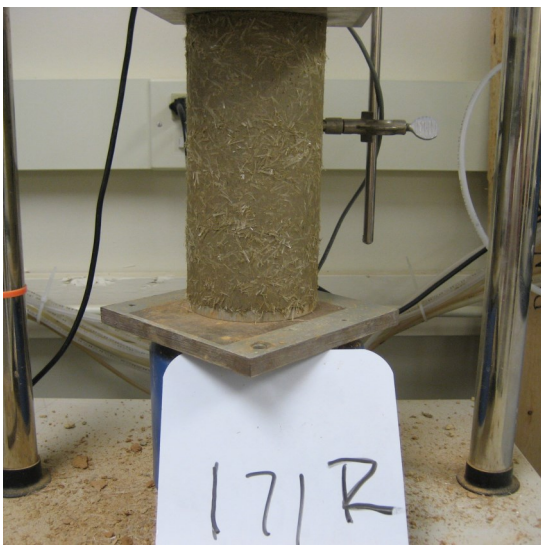

(a)

(b)

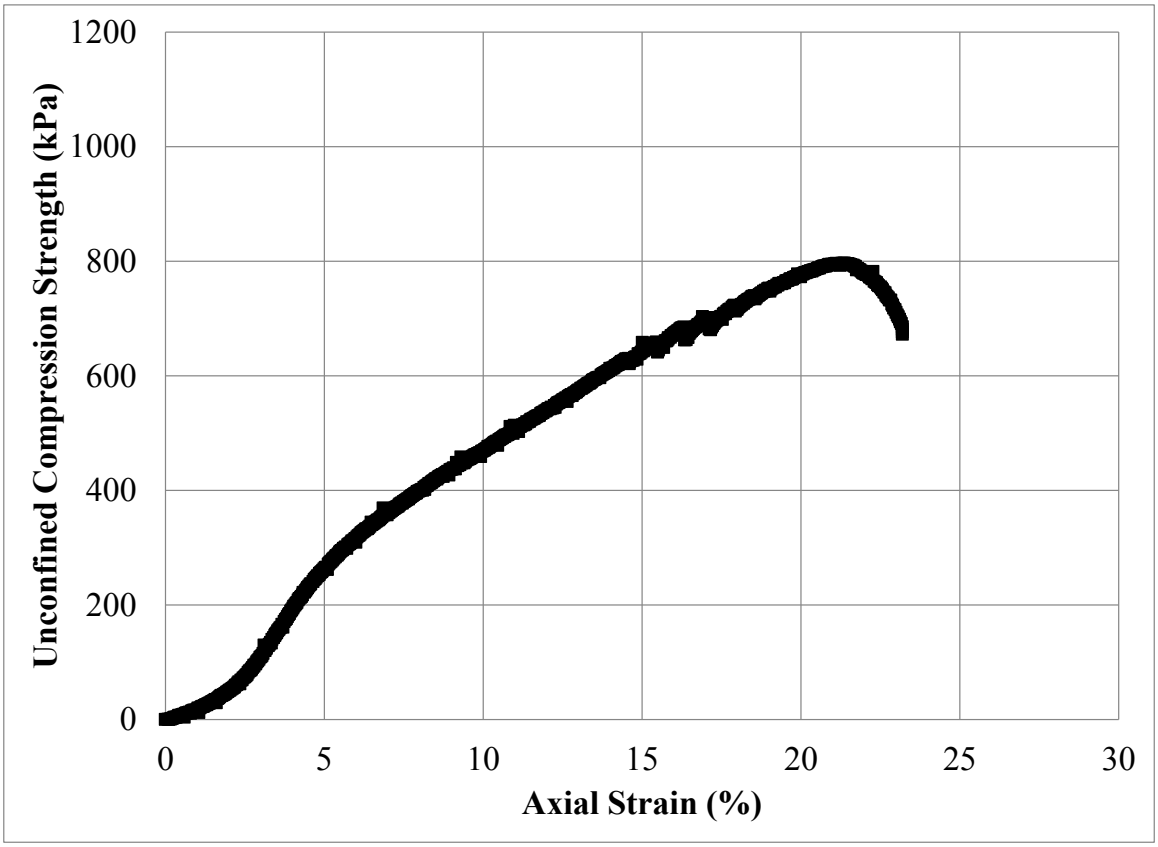

(c)

Figure C.135 Unconfined Compression Test Specimen No. 171R: (a) Photograph Prior to Testing; (b) Photograph Post Testing; and (c) Stress – Strain Data

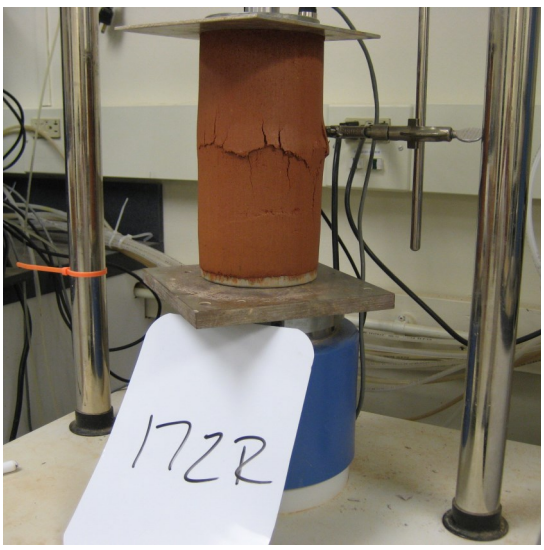

(a)

(b)

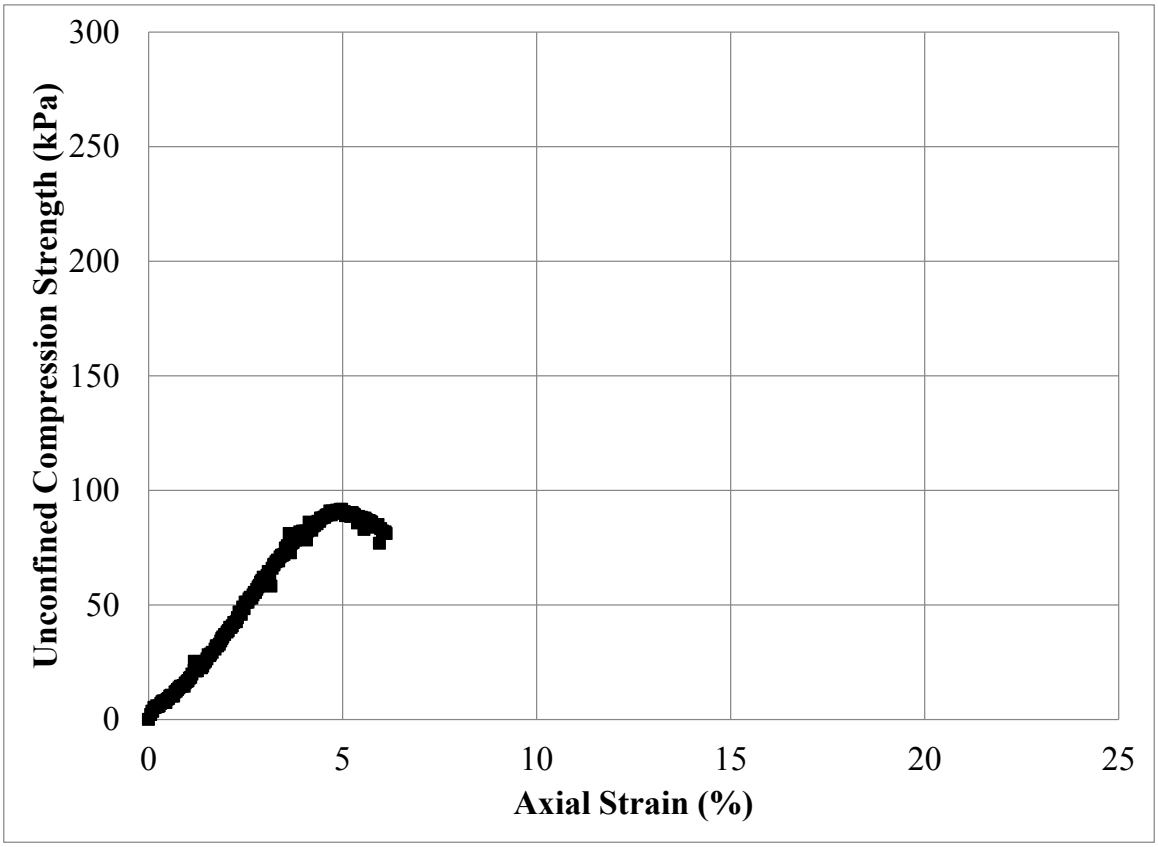

(c)

Figure C.136 Unconfined Compression Test Specimen No. 172R: (a) Photograph Prior to Testing; (b) Photograph Post Testing; and (c) Stress – Strain Data

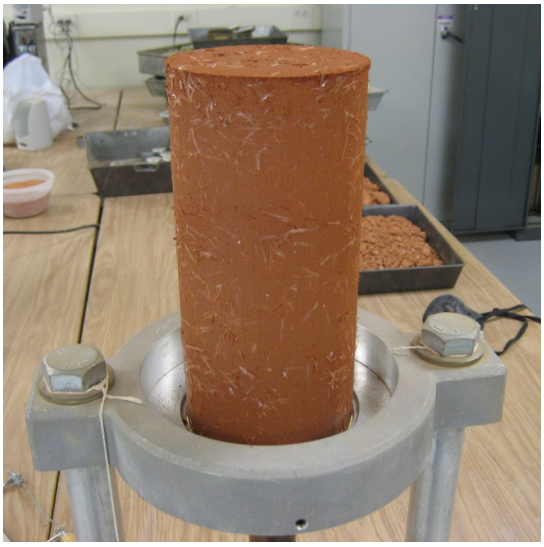

(a)

(b)

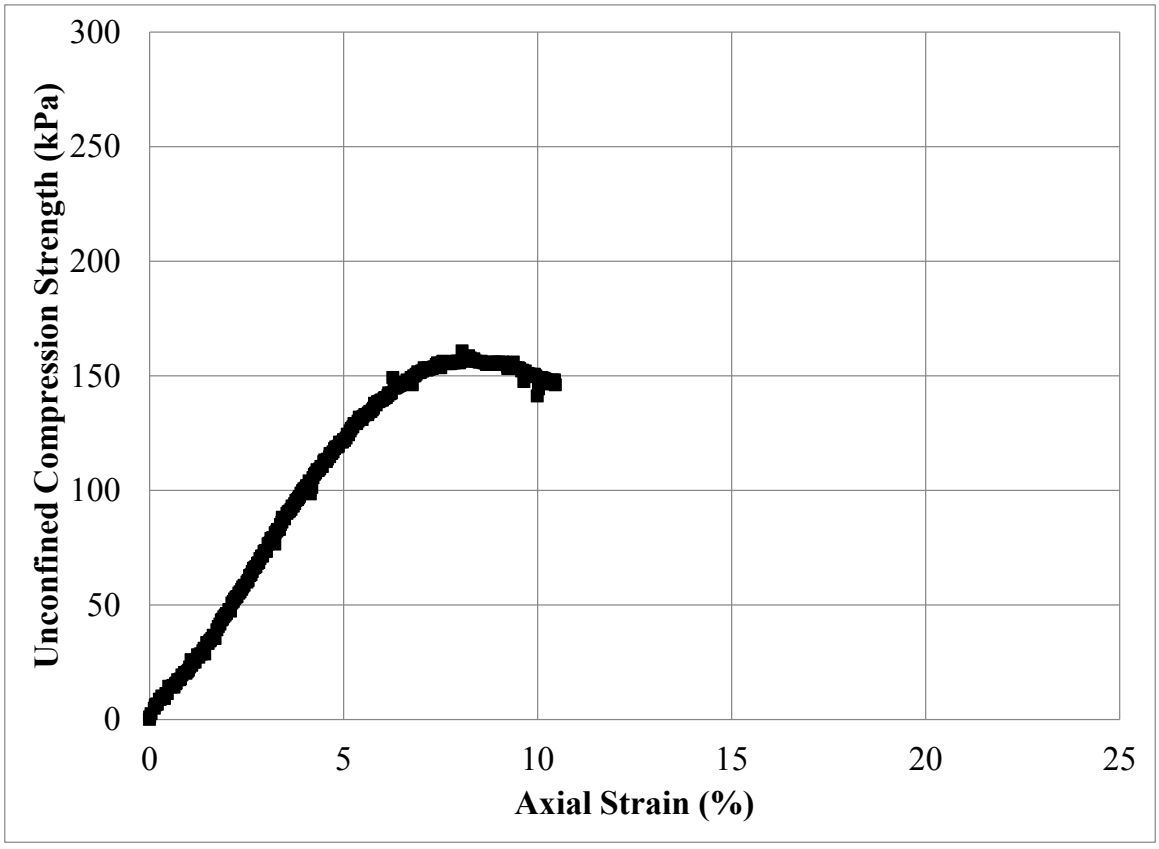

(c)

Figure C.137 Unconfined Compression Test Specimen No. 173R: (a) Photograph Prior to Testing; (b) Photograph Post Testing; and (c) Stress – Strain Data

(a)

(b)

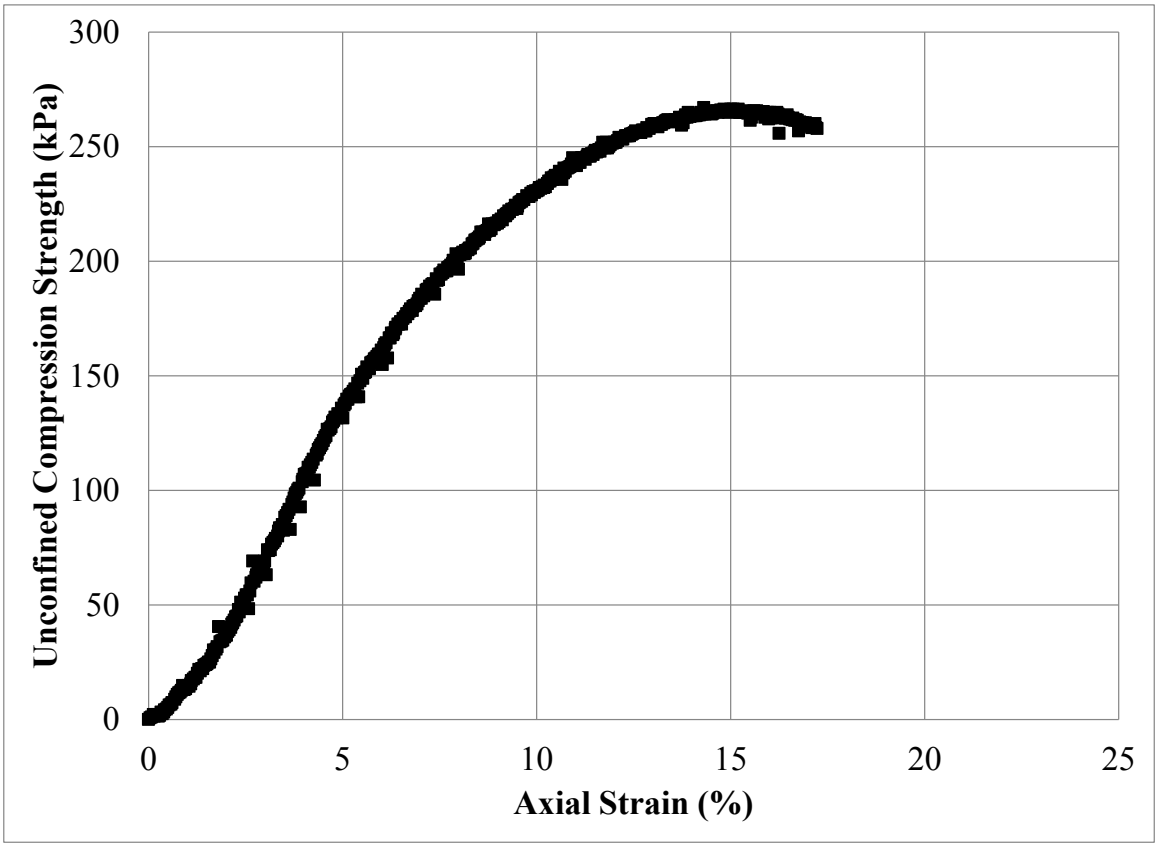

(c)

Figure C.138 Unconfined Compression Test Specimen No. 174R: (a) Photograph Prior to Testing; (b) Photograph Post Testing; and (c) Stress – Strain Data

(a)

(b)

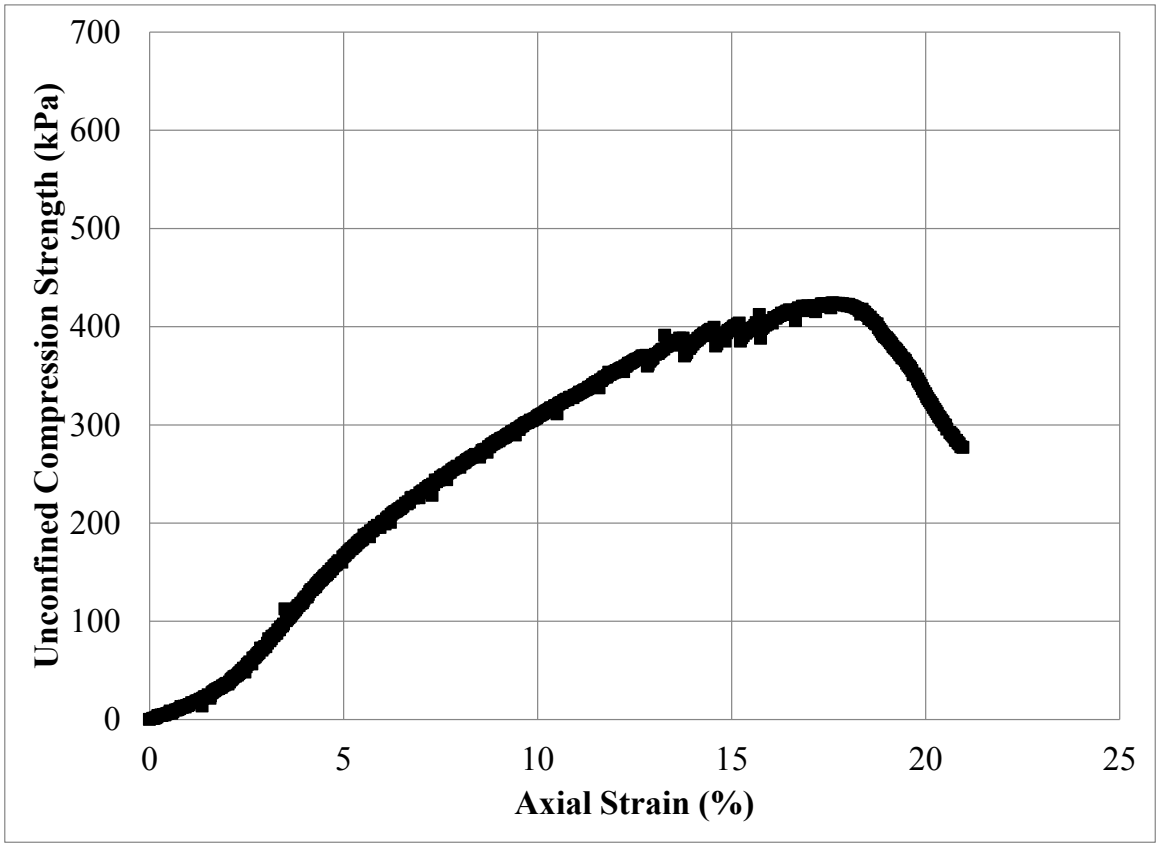

(c)

Figure C.139 Unconfined Compression Test Specimen No. 175R: (a) Photograph Prior to Testing; (b) Photograph Post Testing; and (c) Stress – Strain Data

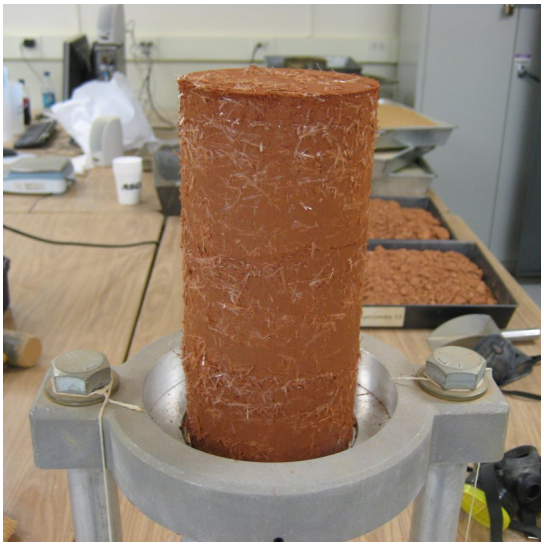

(a)

(b)

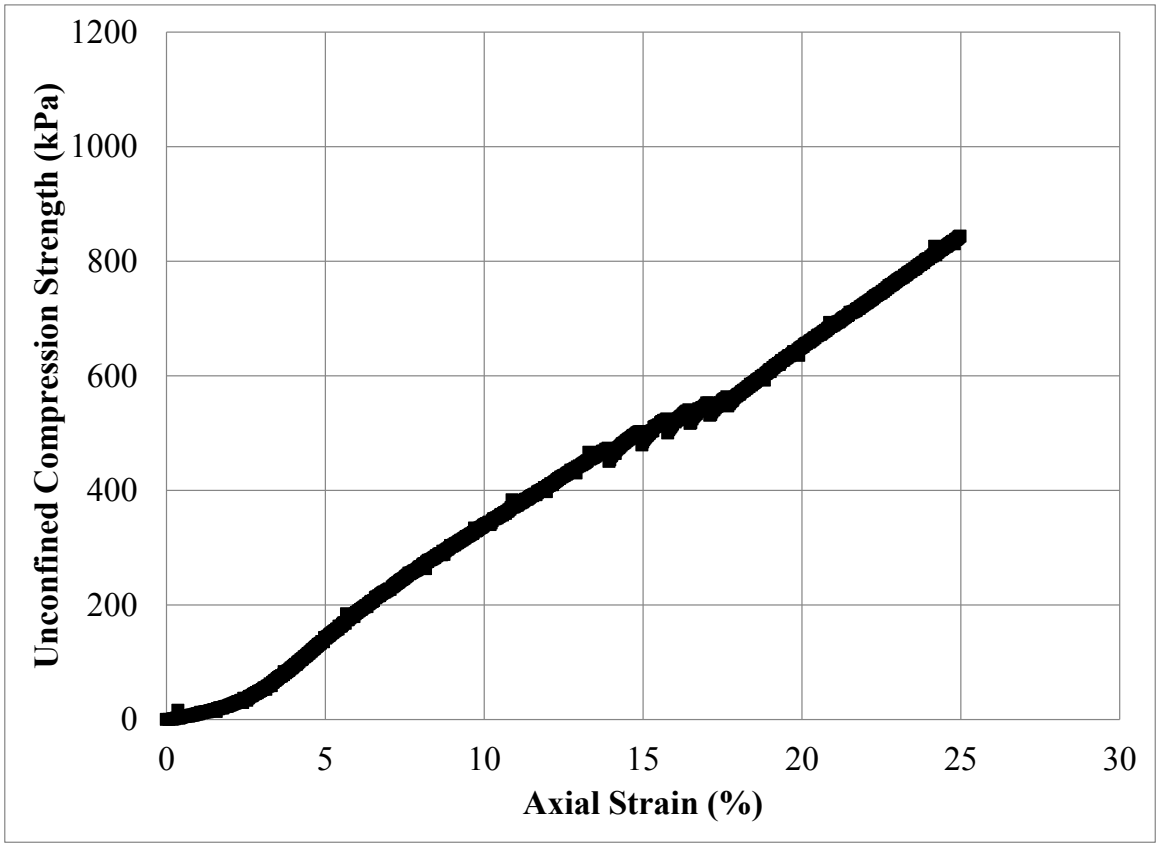

(c)

Figure C.140 Unconfined Compression Test Specimen No. 176R: (a) Photograph Prior to Testing; (b) Photograph Post Testing; and (c) Stress – Strain Data

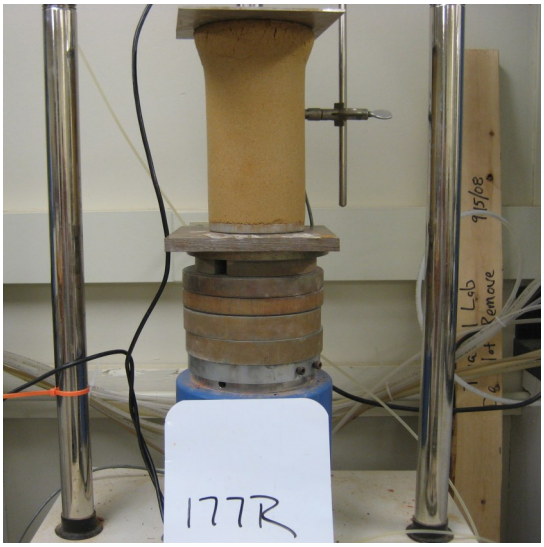

(a)

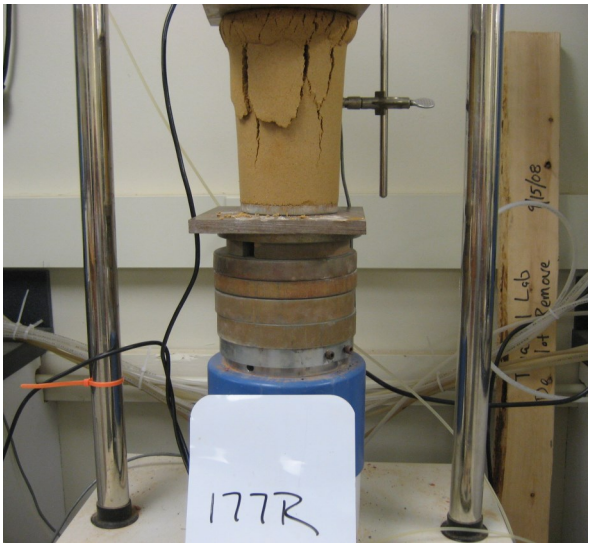

(b)

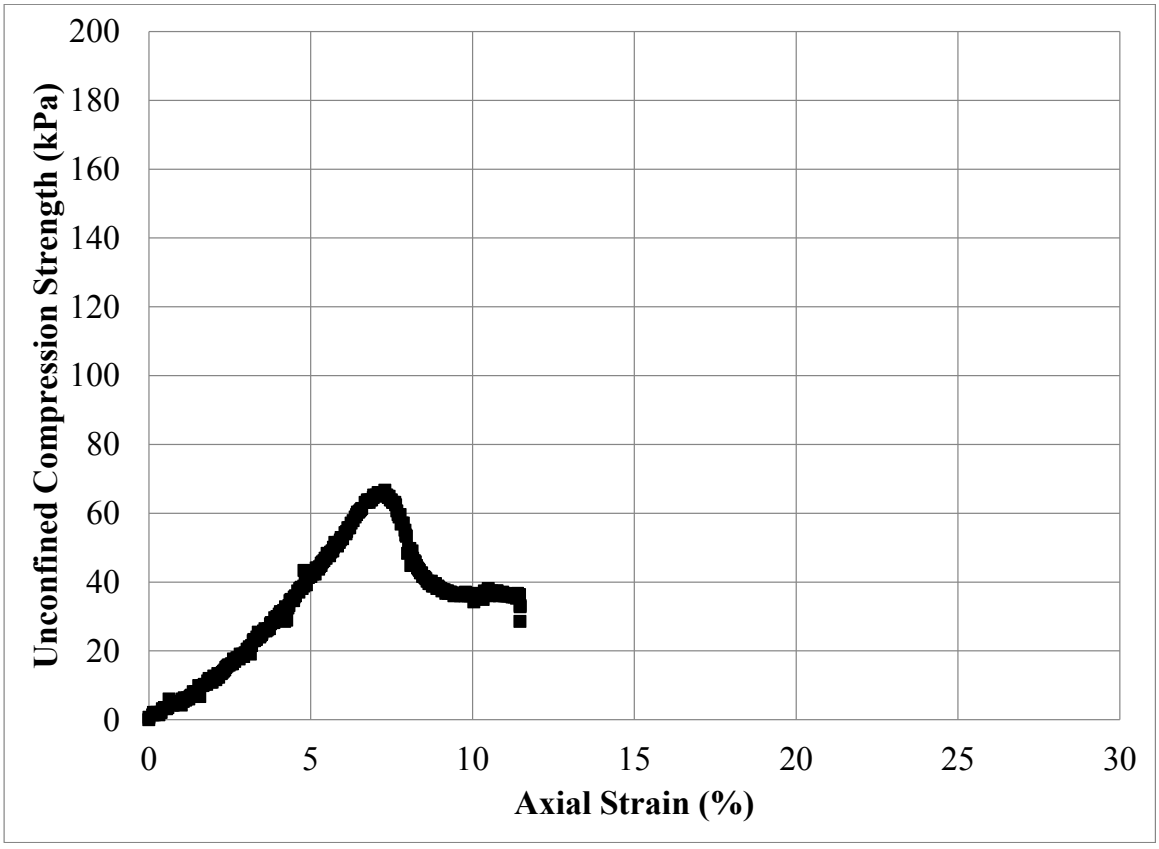

(c)

Figure C.141: Unconfined Compression Test Specimen No. 177R: (a) Photograph Prior to Testing; (b) Photograph Post Testing; and (c) Stress – Strain Data

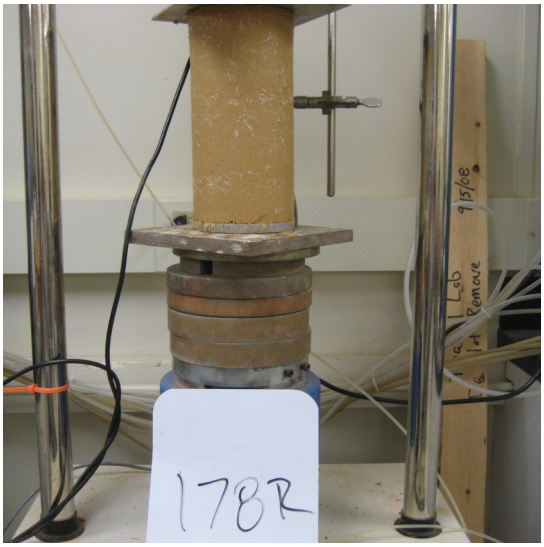

(a)

(b)

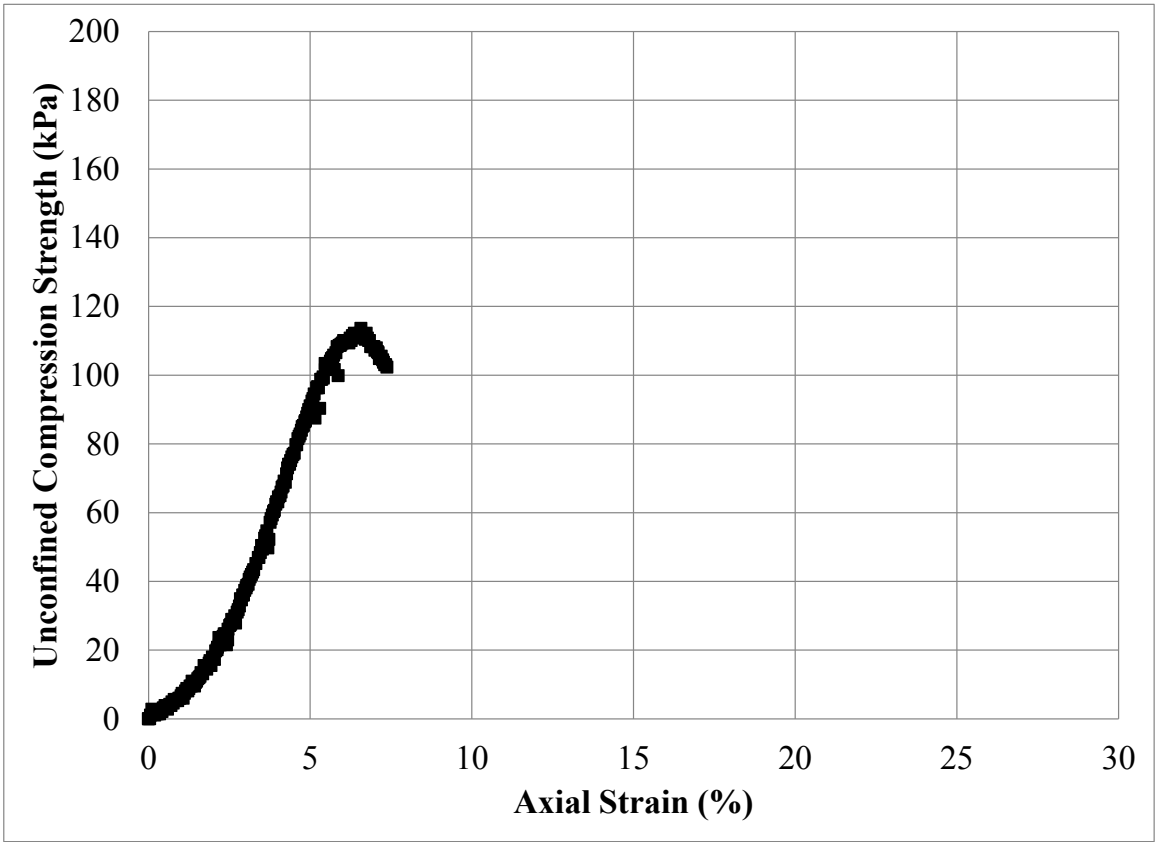

(c)

Figure C.142: Unconfined Compression Test Specimen No. 178R: (a) Photograph Prior to Testing; (b) Photograph Post Testing; and (c) Stress – Strain Data

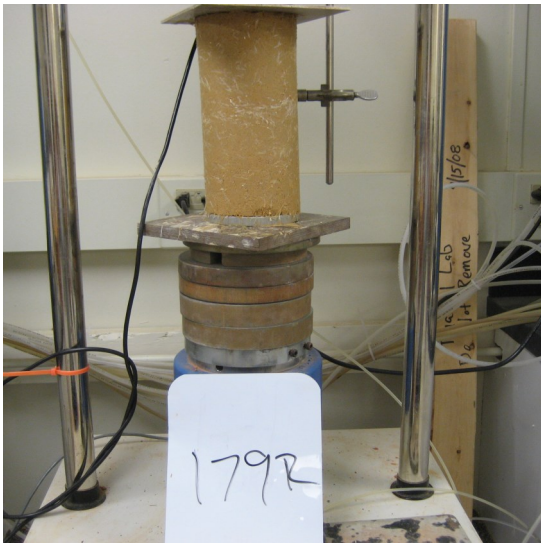

(a)

(b)

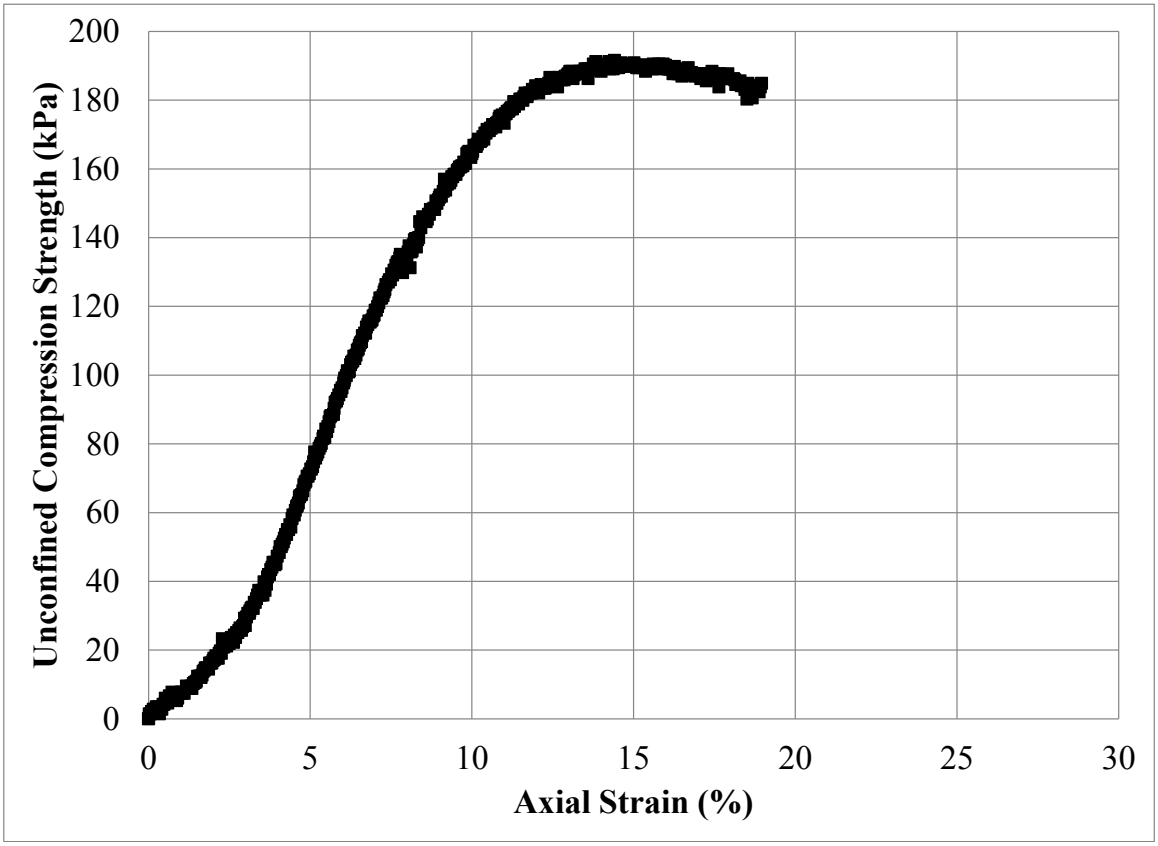

(c)

Figure C.143: Unconfined Compression Test Specimen No. 179R: (a) Photograph Prior to Testing; (b) Photograph Post Testing; and (c) Stress – Strain Data

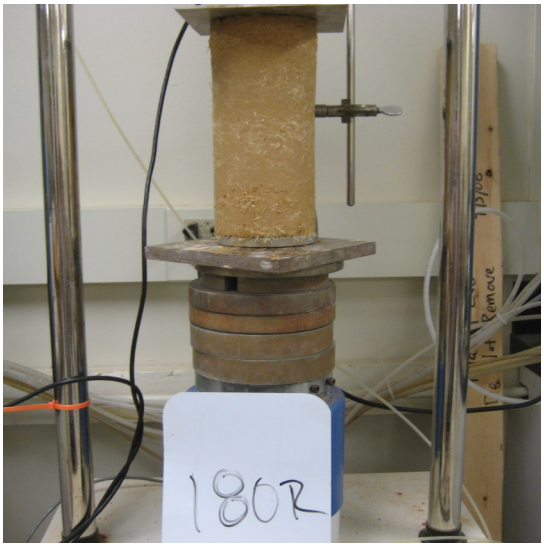

(a)

(b)

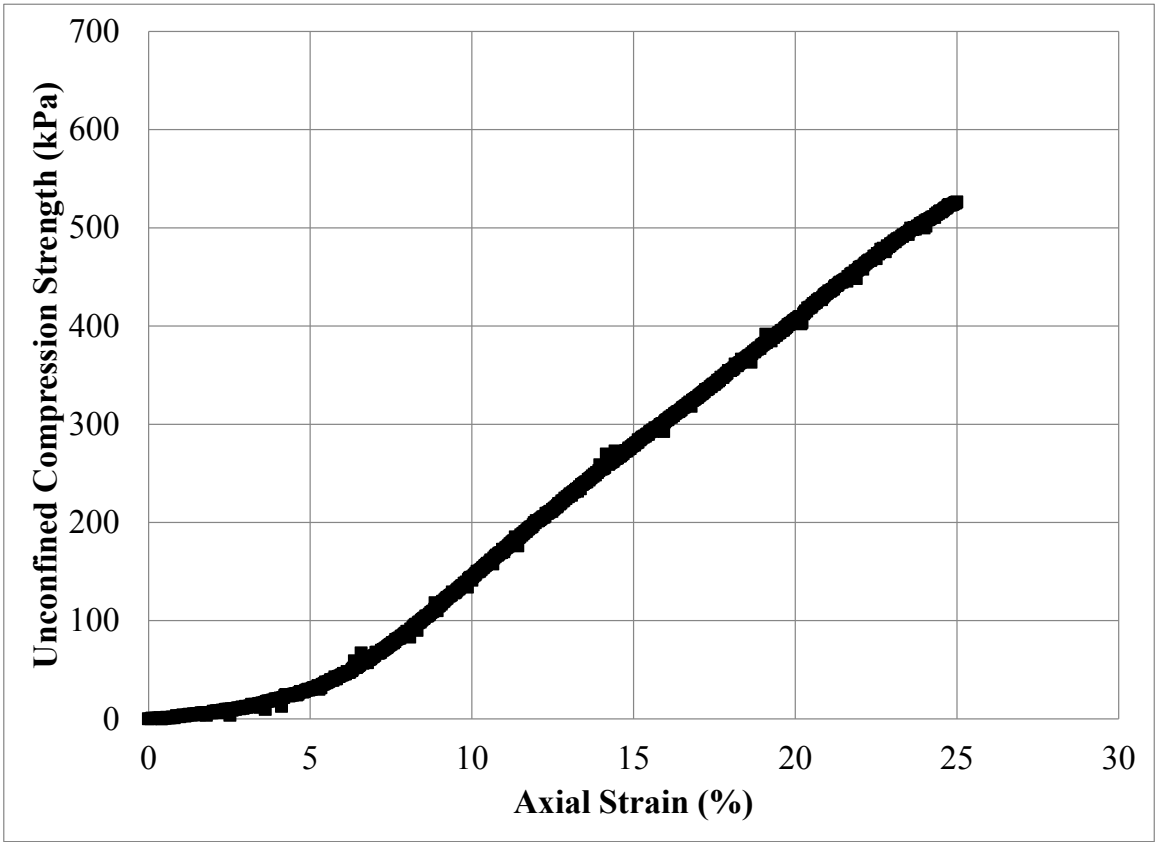

(c)

Figure C.144: Unconfined Compression Test Specimen No. 180R: (a) Photograph Prior to Testing; (b) Photograph Post Testing; and (c) Stress – Strain Data

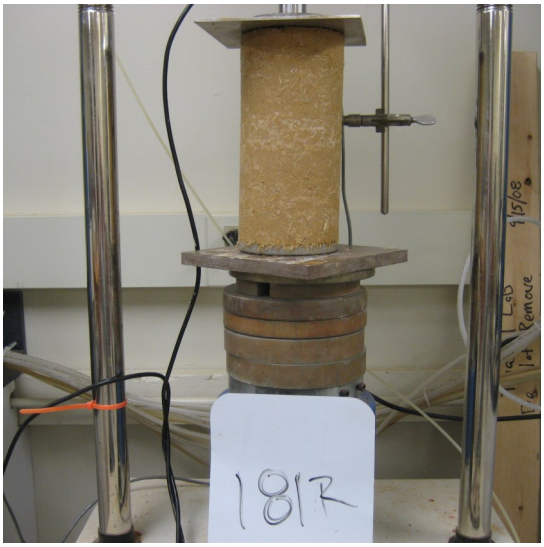

(a)

(b)

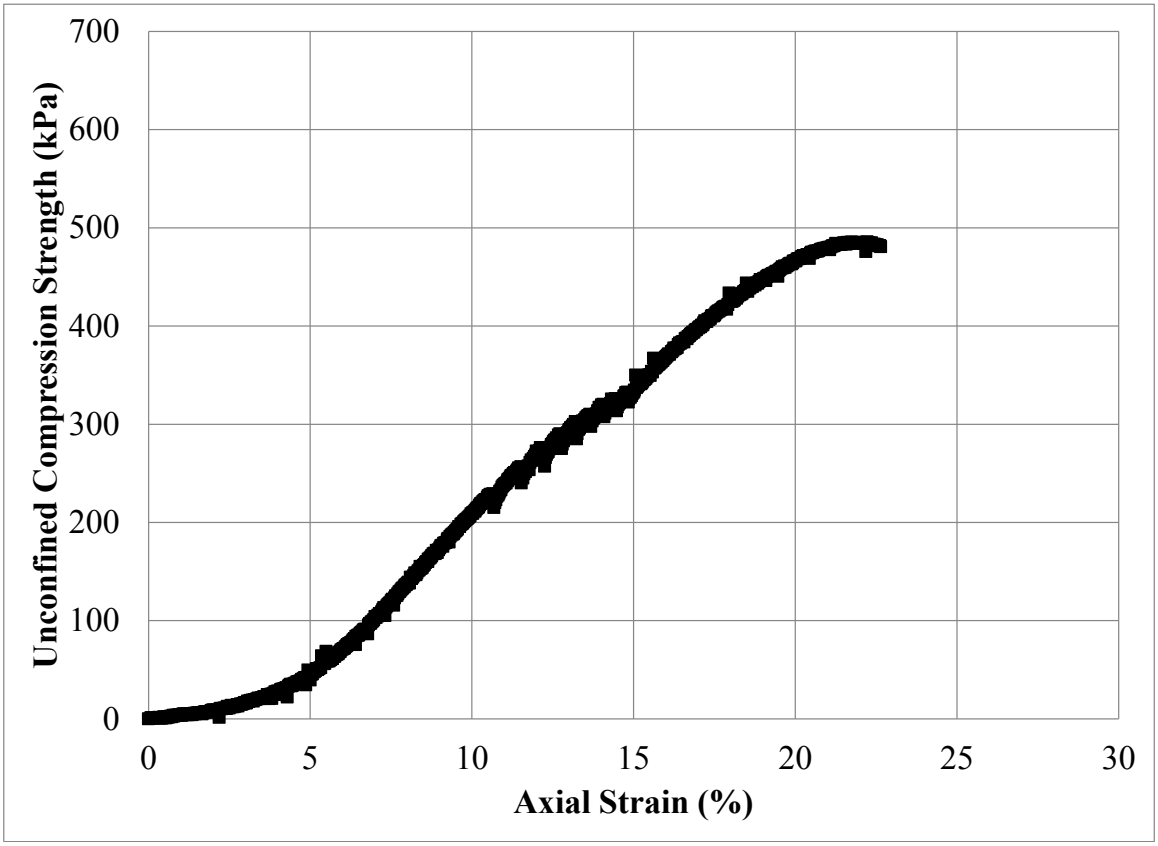

(c)

Figure C.145: Unconfined Compression Test Specimen No. 181R: (a) Photograph Prior to Testing; (b) Photograph Post Testing; and (c) Stress – Strain Data

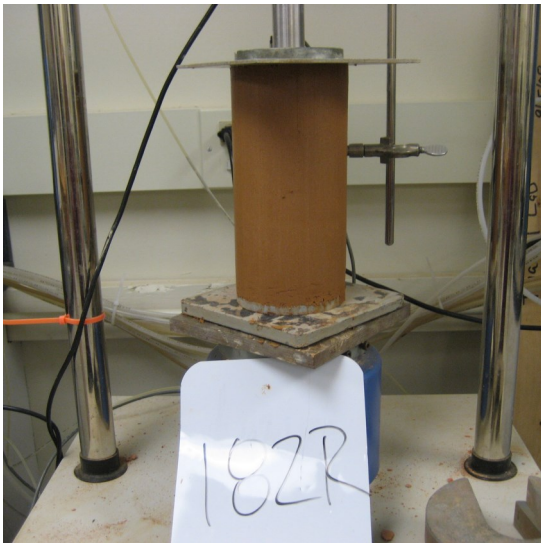

(a)

(b)

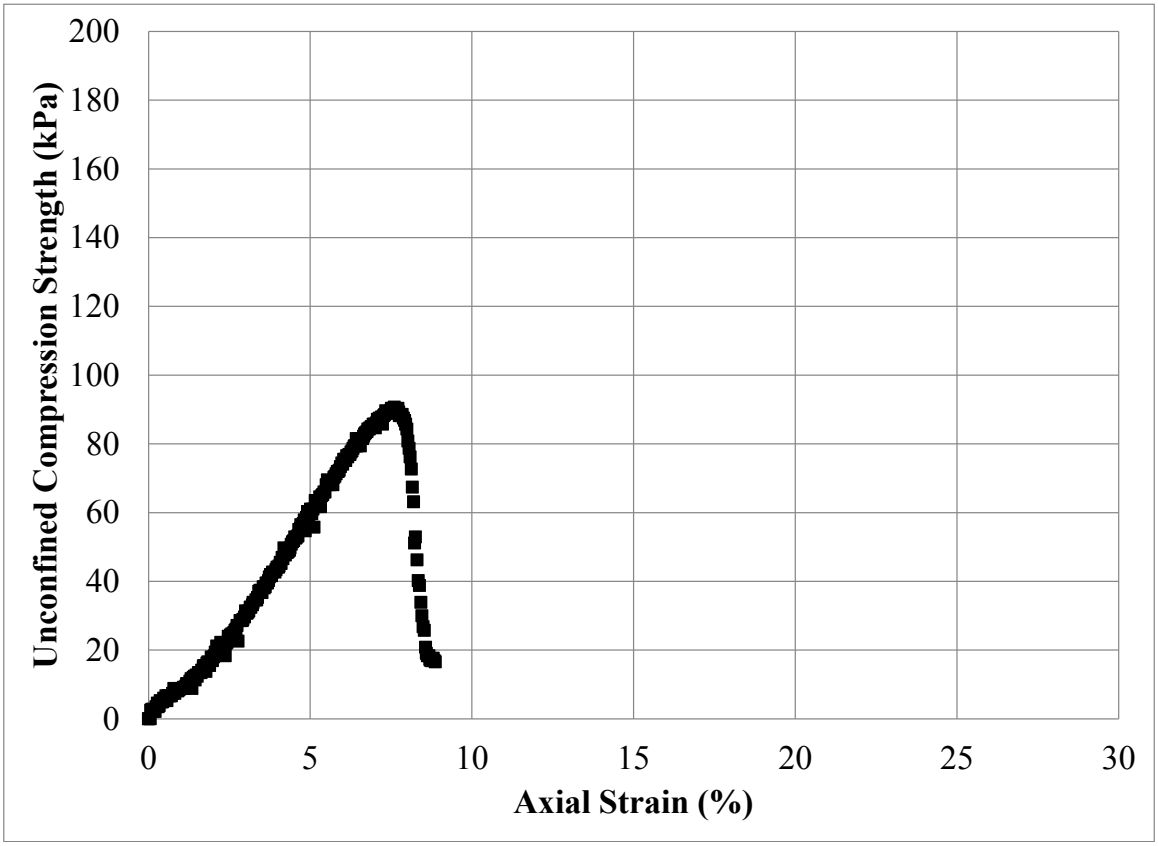

(c)

Figure C.146: Unconfined Compression Test Specimen No. 182R: (a) Photograph Prior to Testing; (b) Photograph Post Testing; and (c) Stress – Strain Data

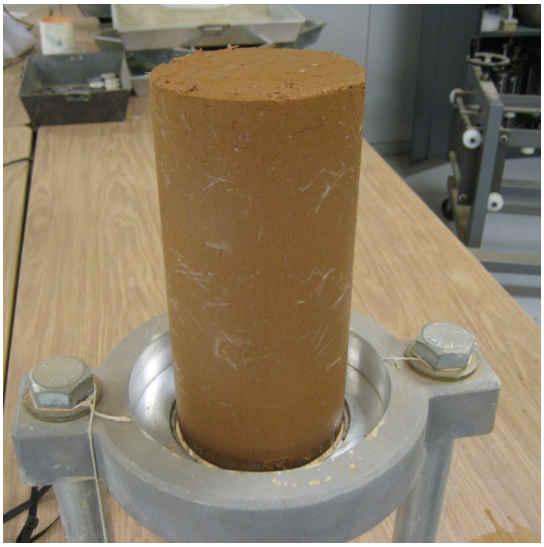

(a)

(b)

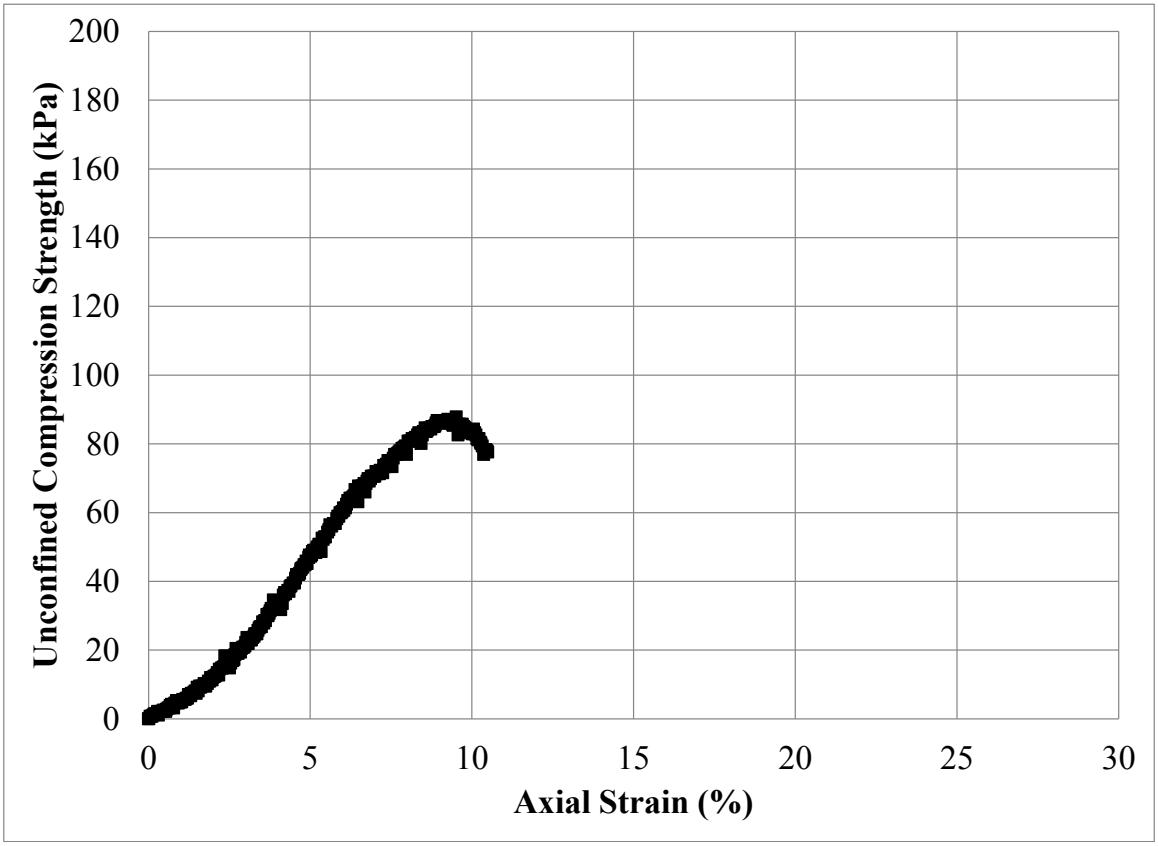

(c)

Figure C.147: Unconfined Compression Test Specimen No. 183R: (a) Photograph Prior to Testing; (b) Photograph Post Testing; and (c) Stress – Strain Data

(a)

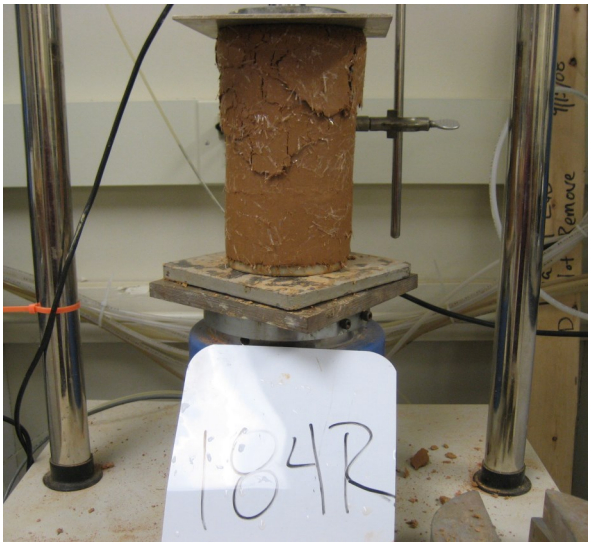

(b)

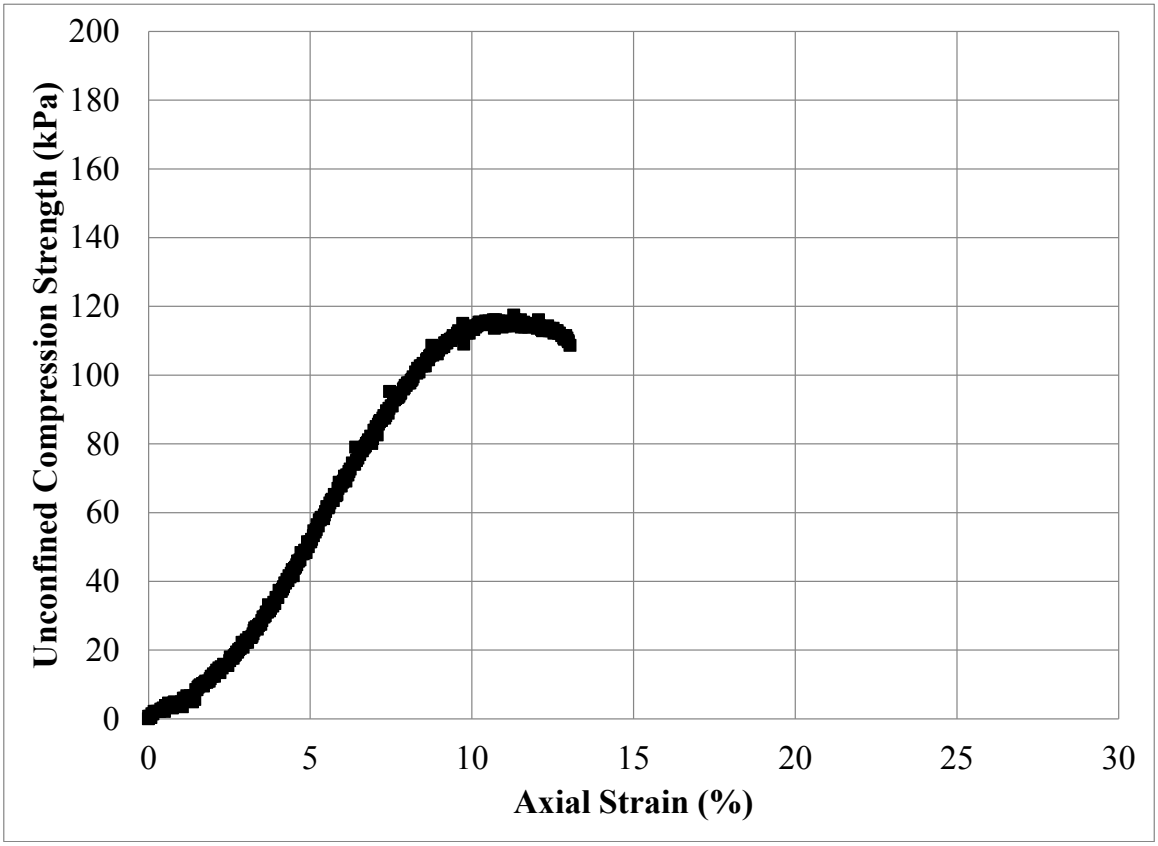

(c)

Figure C.148: Unconfined Compression Test Specimen No. 184R: (a) Photograph Prior to Testing; (b) Photograph Post Testing; and (c) Stress – Strain Data

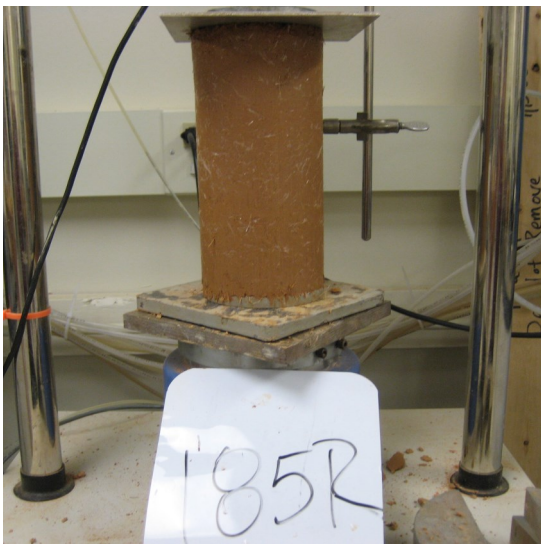

(a)

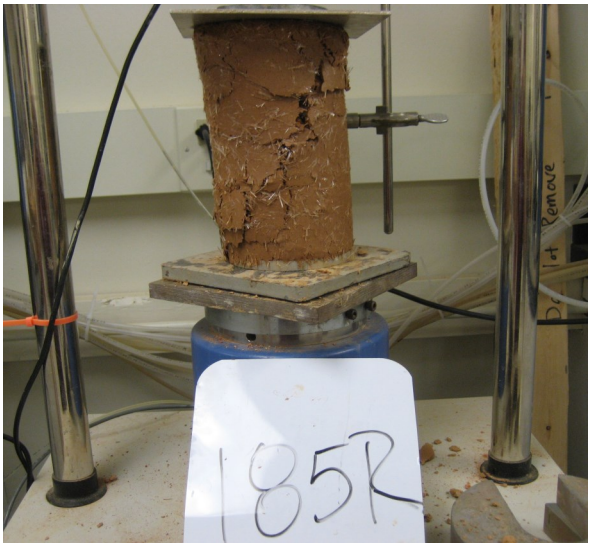

(b)

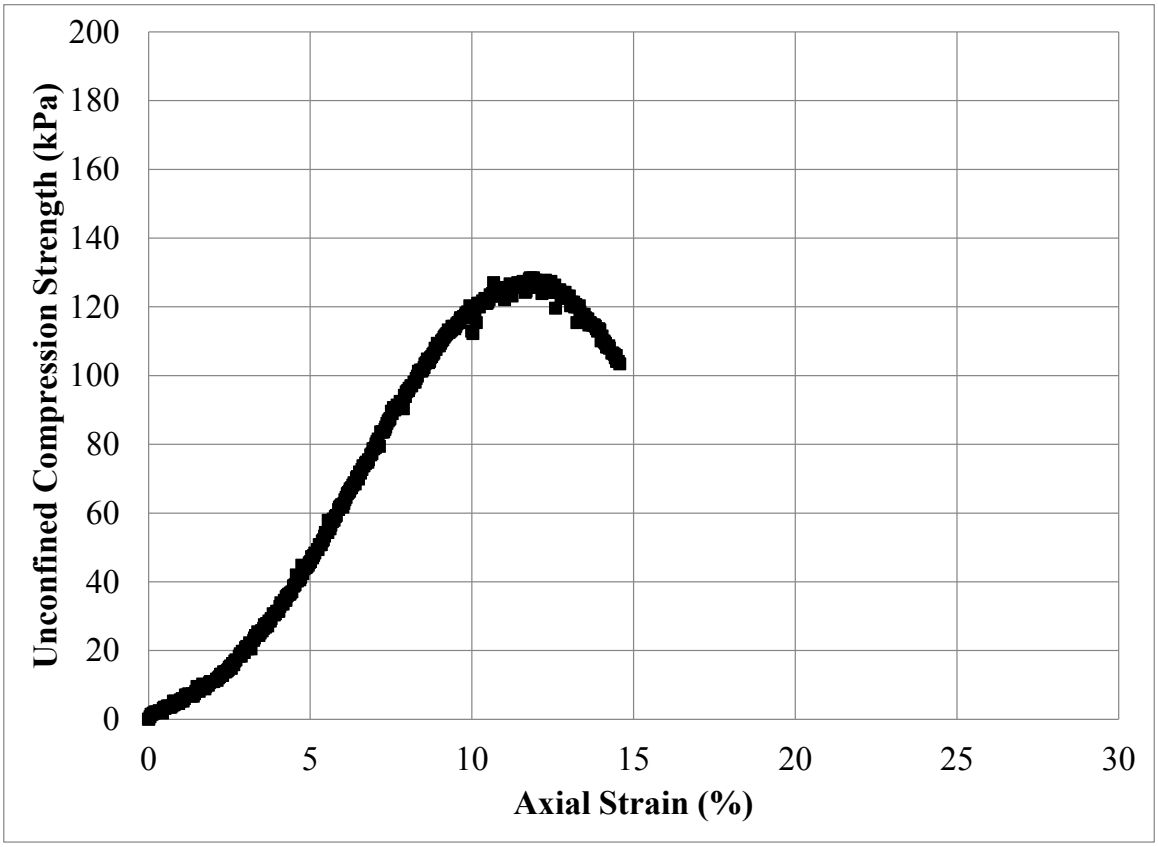

(c)

Figure C.149: Unconfined Compression Test Specimen No. 185R: (a) Photograph Prior to Testing; (b) Photograph Post Testing; and (c) Stress – Strain Data

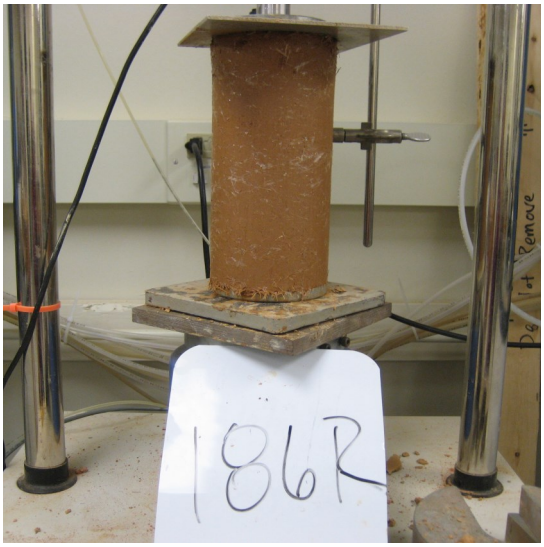

(a)

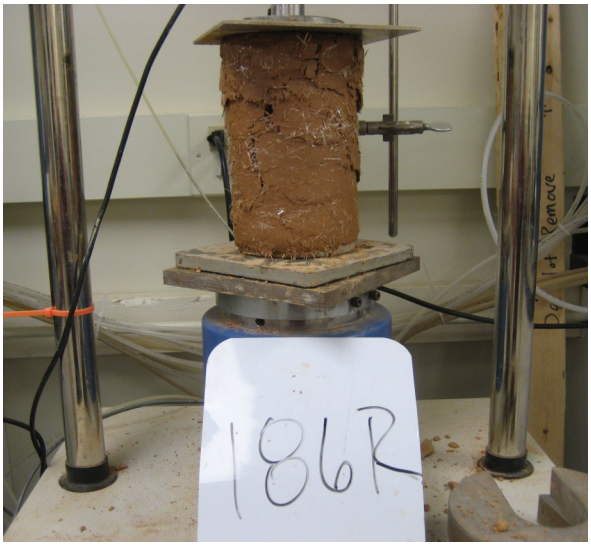

(b)

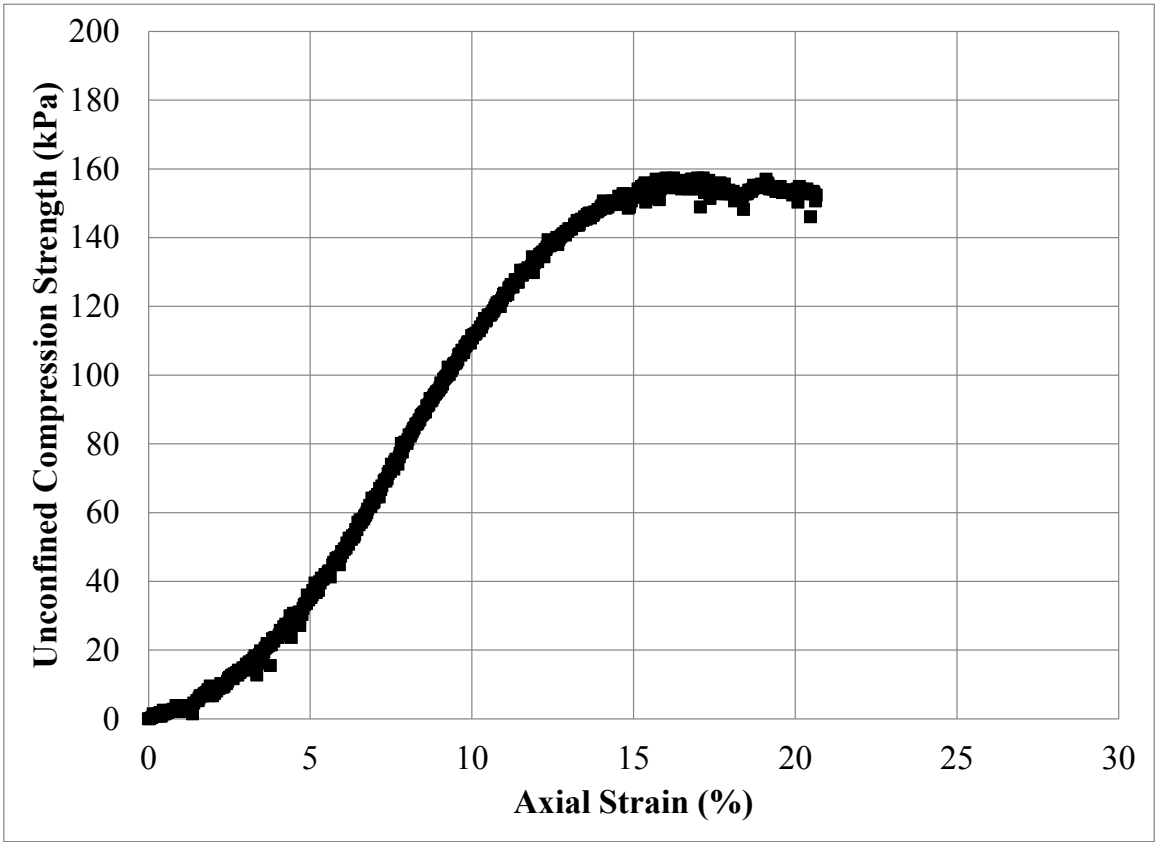

(c)

Figure C.150: Unconfined Compression Test Specimen No. 186R: (a) Photograph Prior to Testing; (b) Photograph Post Testing; and (c) Stress – Strain Data

(a)

(b)

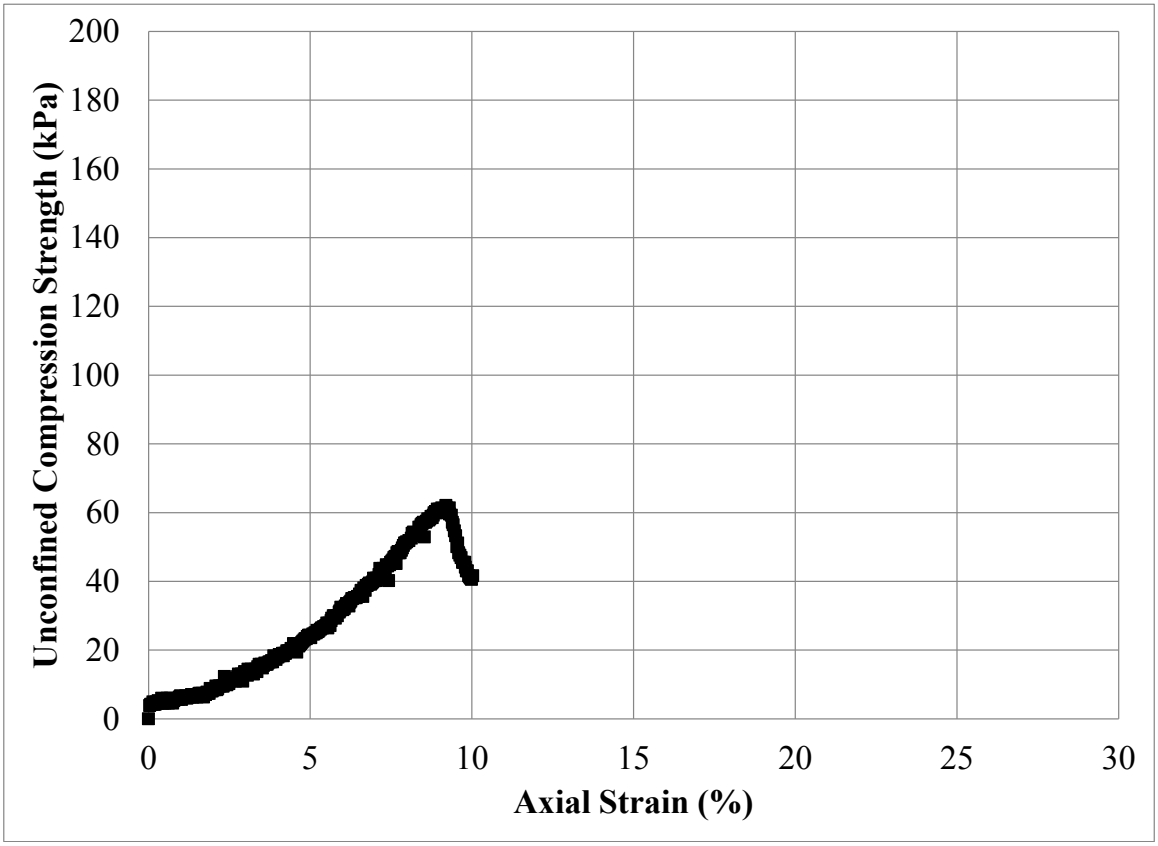

(c)

Figure C.151: Unconfined Compression Test Specimen No. 187R: (a) Photograph Prior to Testing; (b) Photograph Post Testing; and (c) Stress – Strain Data

(a)

(b)

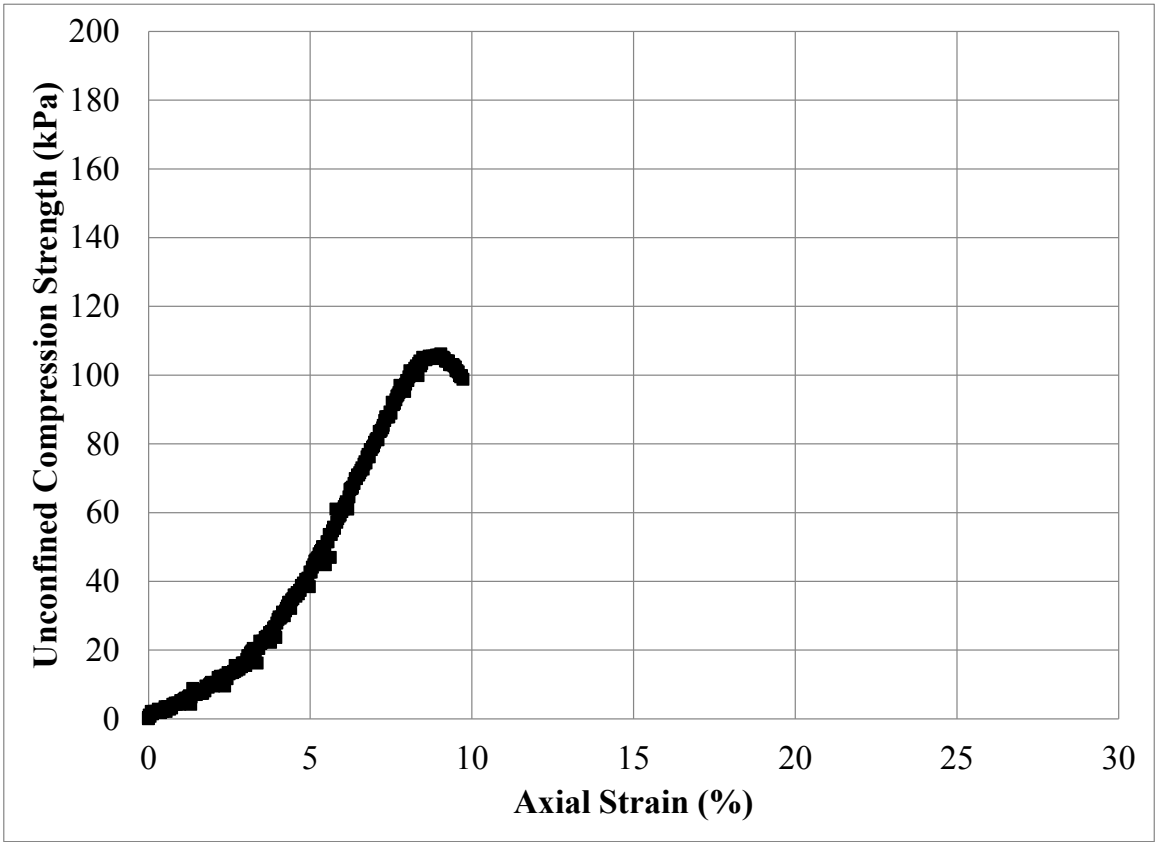

(c)

Figure C.152: Unconfined Compression Test Specimen No. 188R: (a) Photograph Prior to Testing; (b) Photograph Post Testing; and (c) Stress – Strain Data

(a)

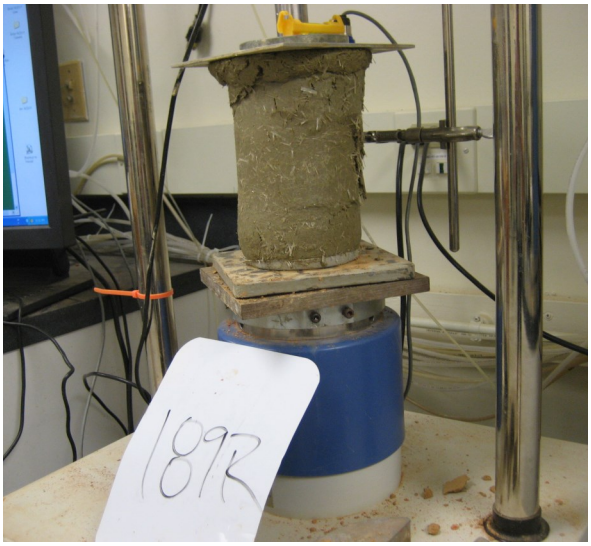

(b)

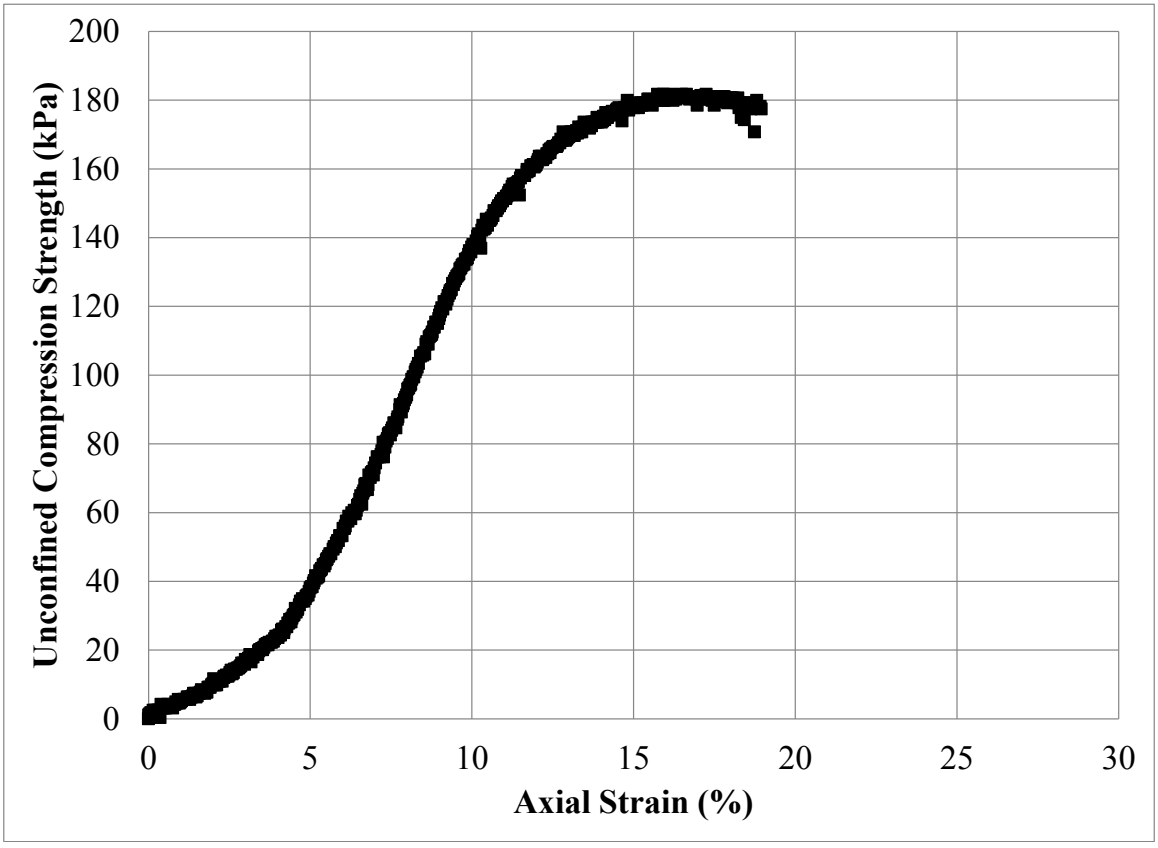

(c)

Figure C.153: Unconfined Compression Test Specimen No. 189R: (a) Photograph Prior to Testing; (b) Photograph Post Testing; and (c) Stress – Strain Data

(a)

(b)

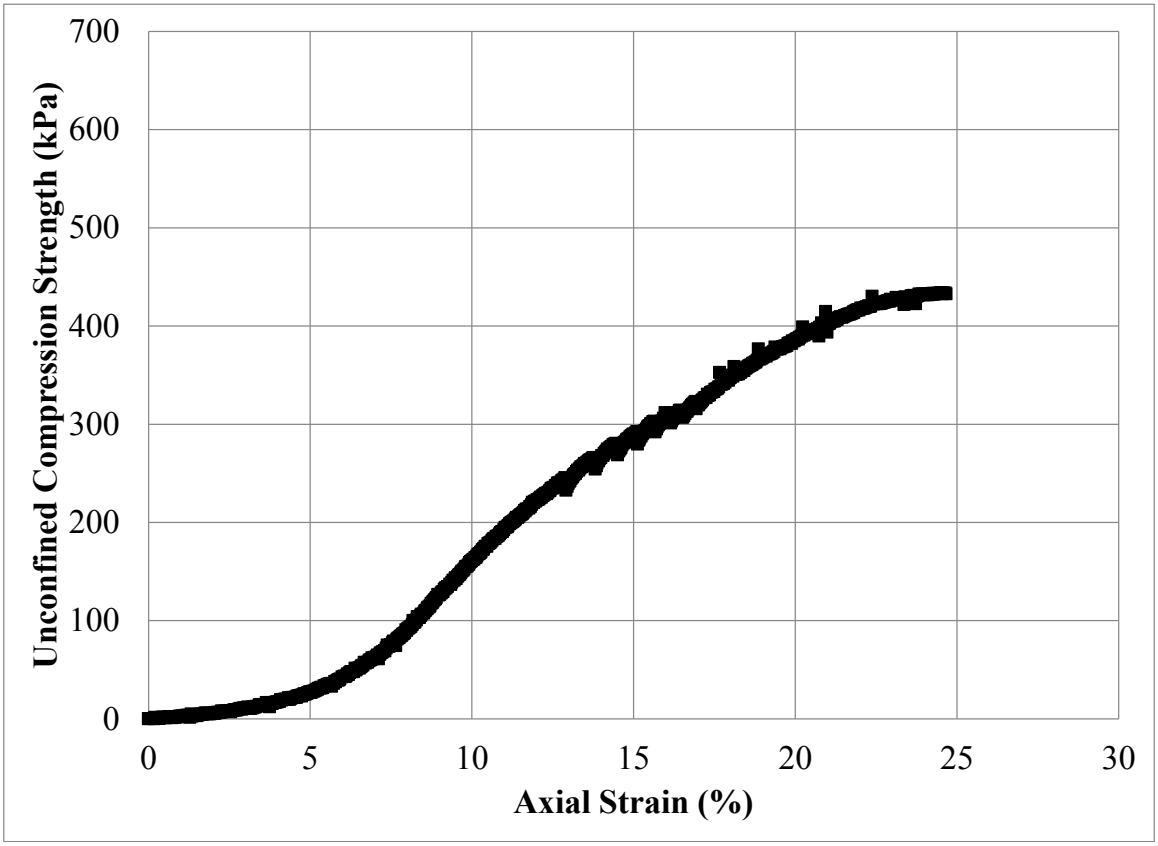

(c)

Figure C.154: Unconfined Compression Test Specimen No. 190R: (a) Photograph Prior to Testing; (b) Photograph Post Testing; and (c) Stress – Strain Data

(a)

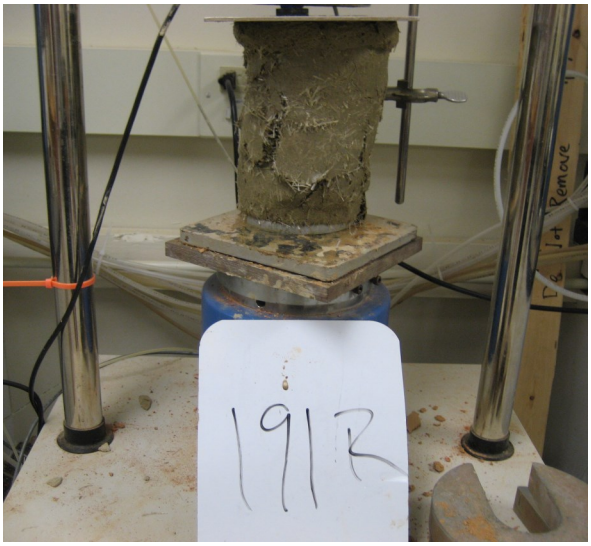

(b)

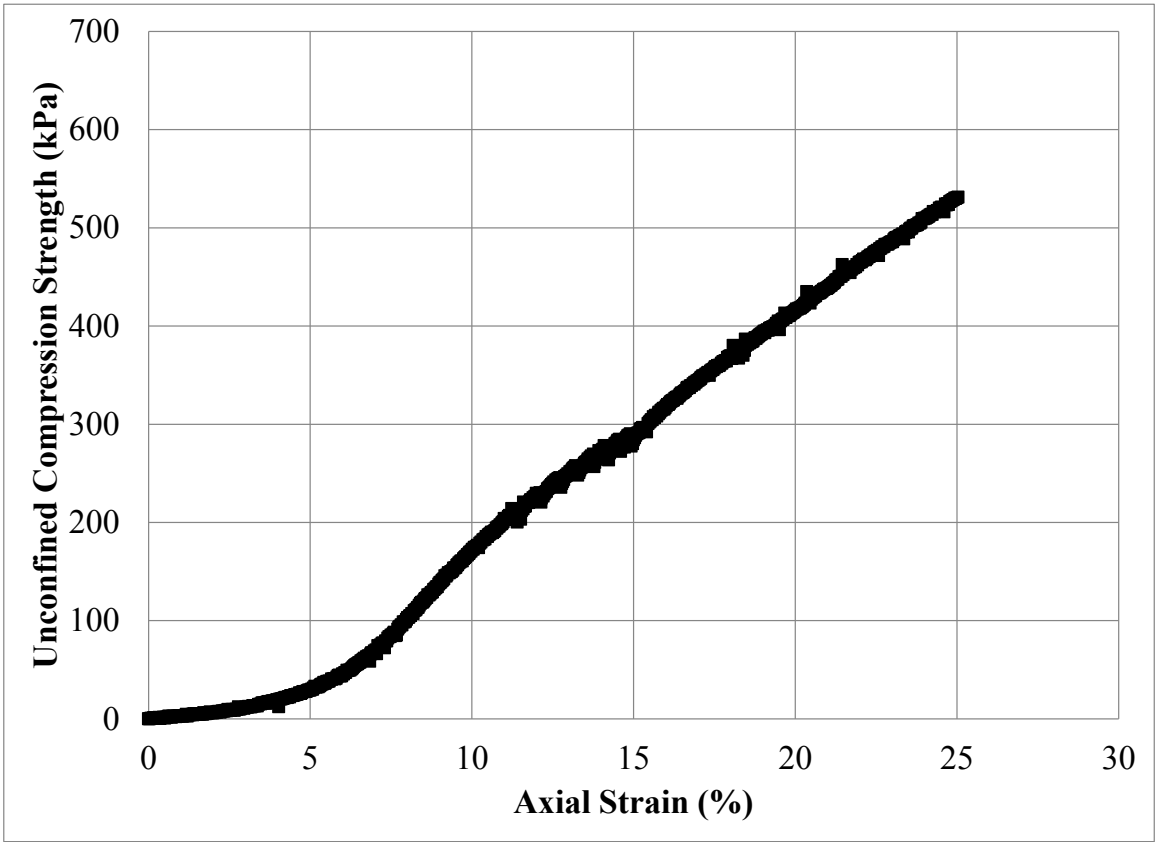

(c)

Figure C.155: Unconfined Compression Test Specimen No. 191R: (a) Photograph Prior to Testing; (b) Photograph Post Testing; and (c) Stress – Strain Data

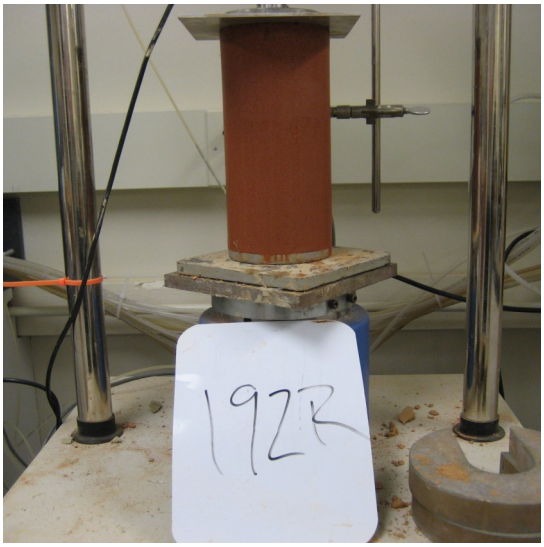

(a)

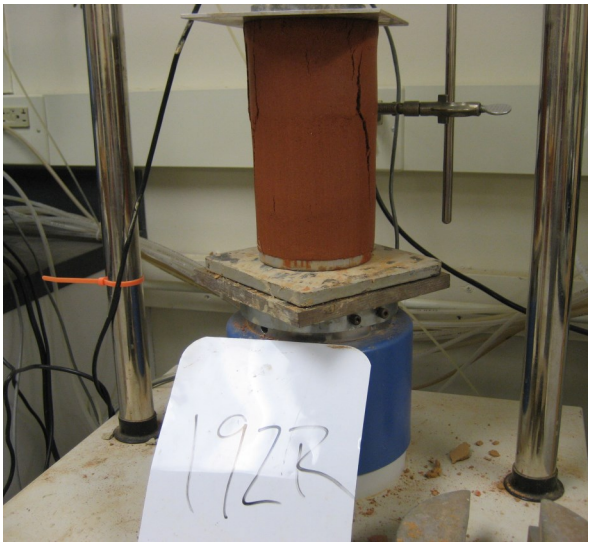

(b)

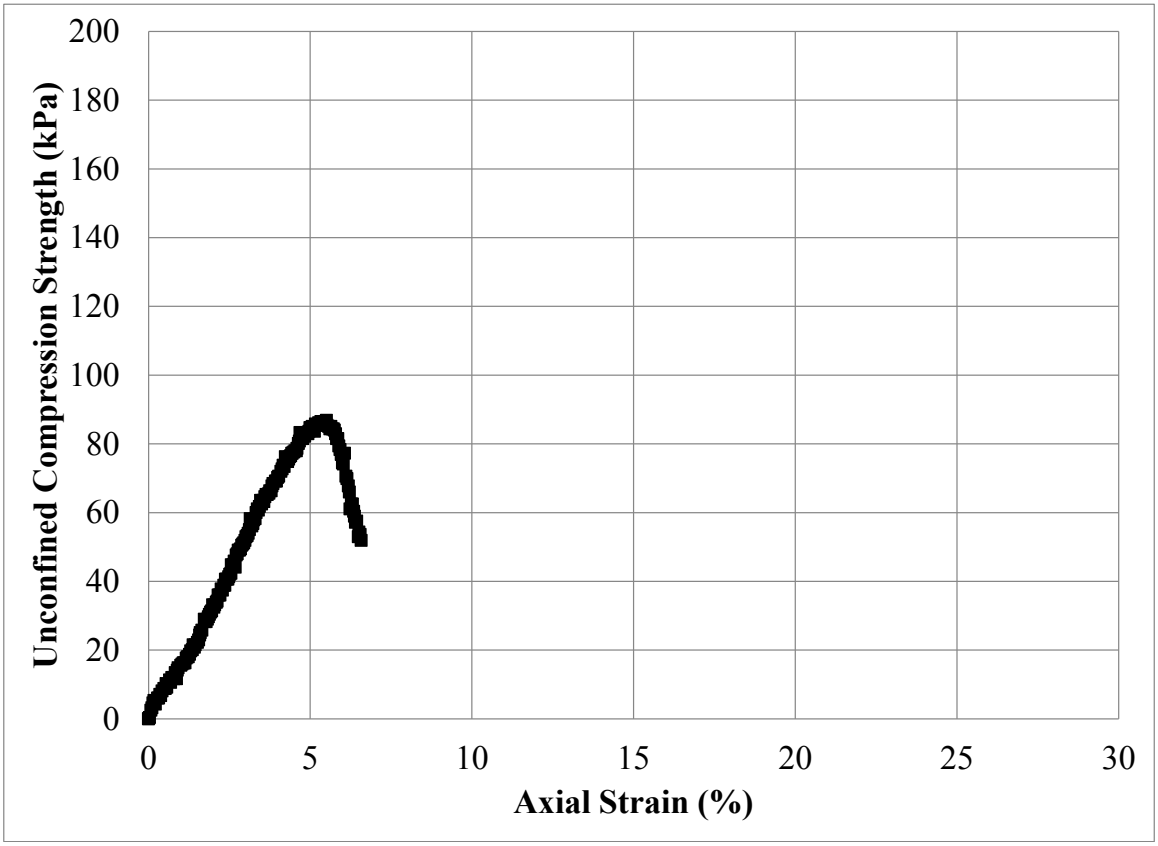

(c)

Figure C.156: Unconfined Compression Test Specimen No. 192R: (a) Photograph Prior to Testing; (b) Photograph Post Testing; and (c) Stress – Strain Data

(a)

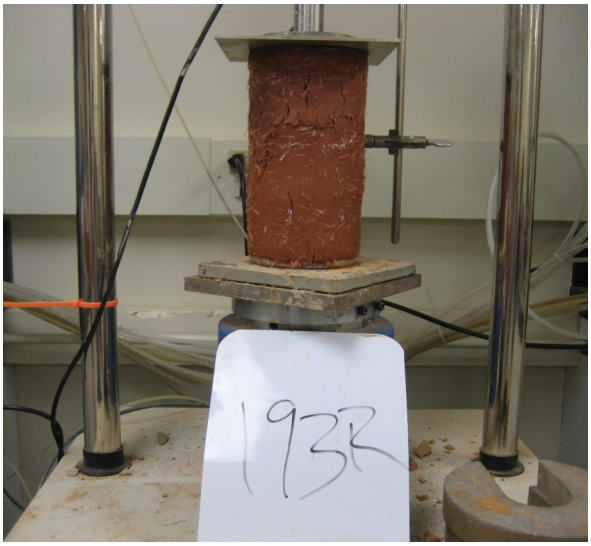

(b)

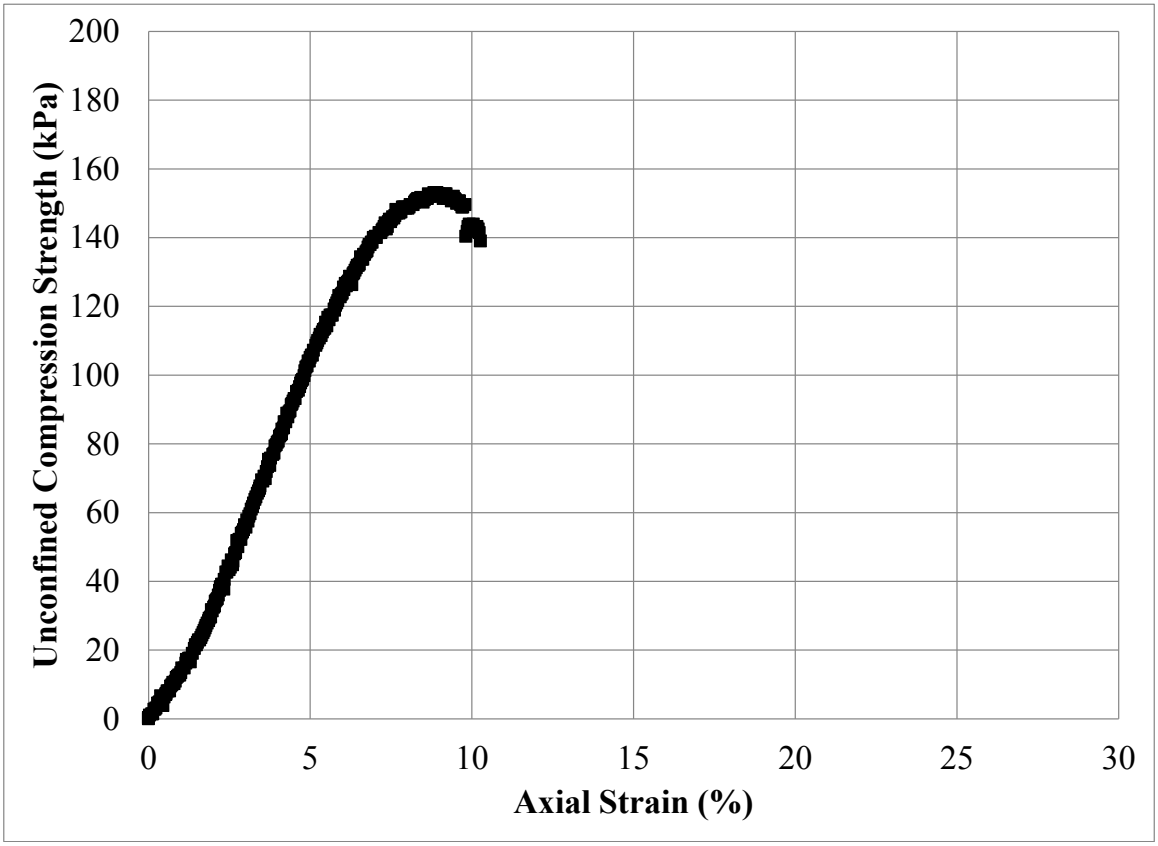

(c)

Figure C.157: Unconfined Compression Test Specimen No. 193R: (a) Photograph Prior to Testing; (b) Photograph Post Testing; and (c) Stress – Strain Data

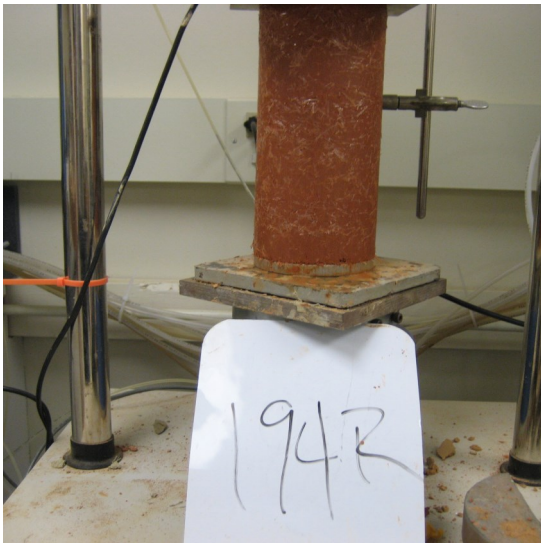

(a)

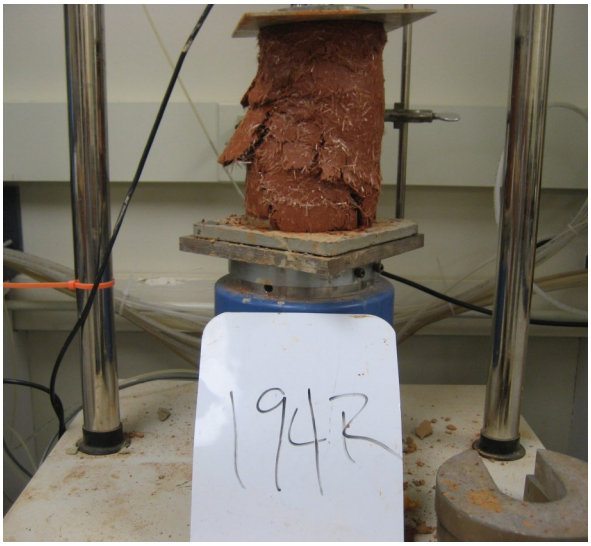

(b)

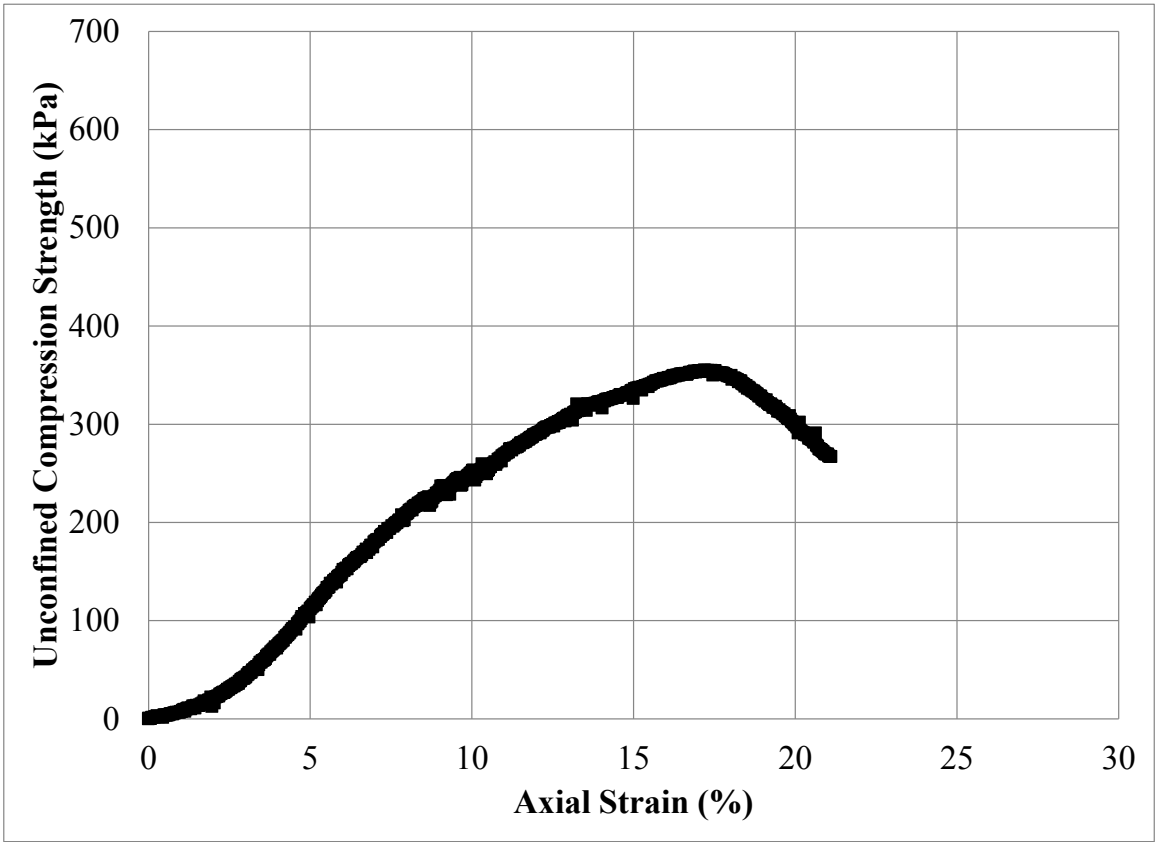

(c)

Figure C.158: Unconfined Compression Test Specimen No. 194R: (a) Photograph Prior to Testing; (b) Photograph Post Testing; and (c) Stress – Strain Data

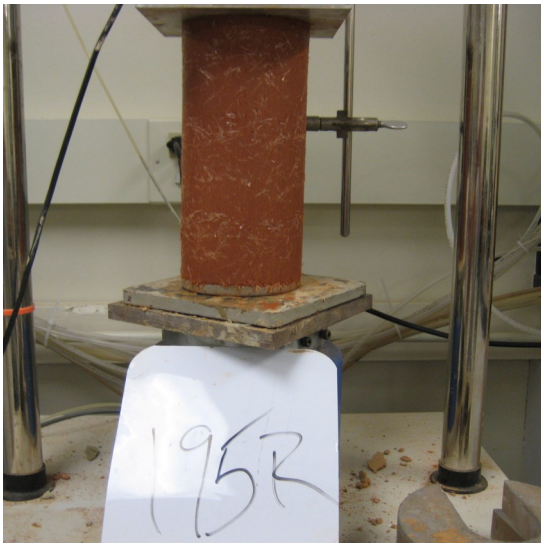

(a)

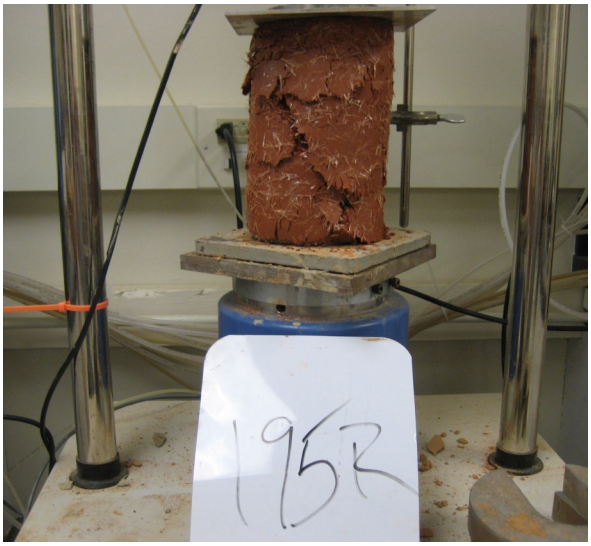

(b)

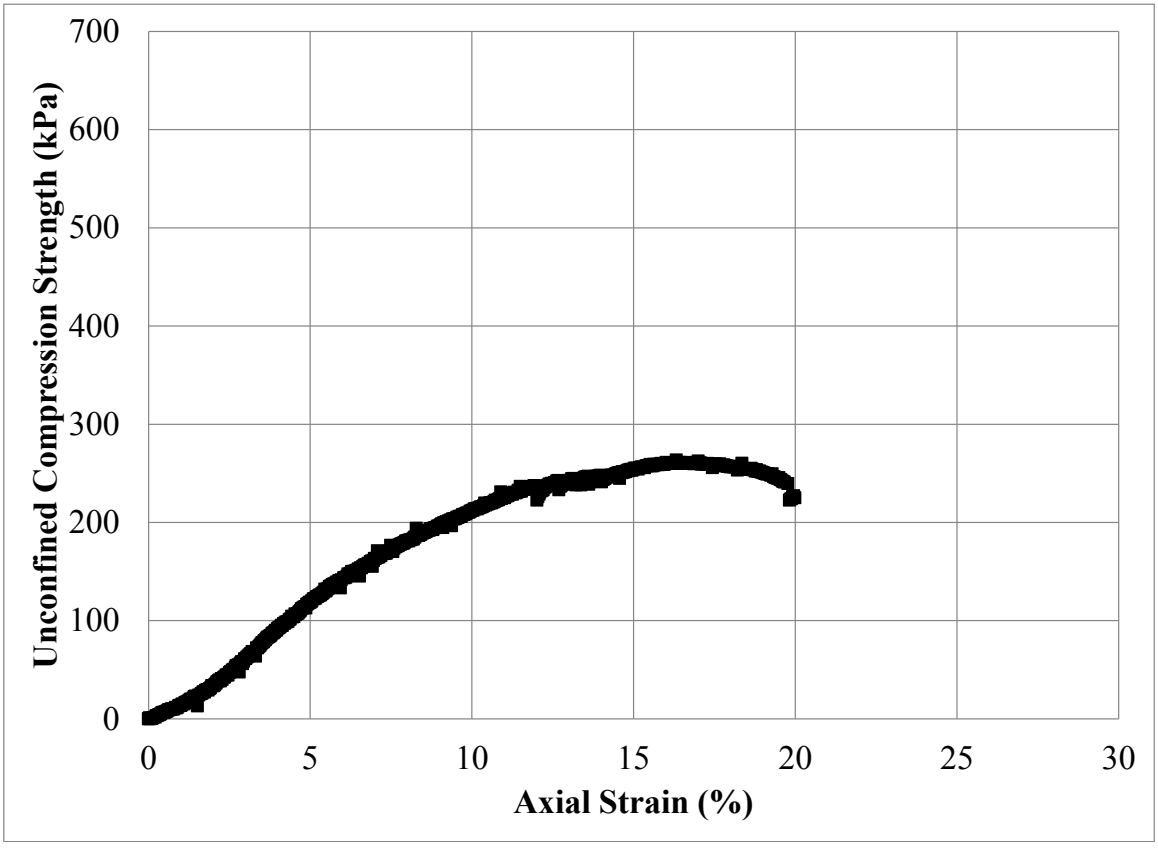

(c)

Figure C.159: Unconfined Compression Test Specimen No. 195R: (a) Photograph Prior to Testing; (b) Photograph Post Testing; and (c) Stress – Strain Data

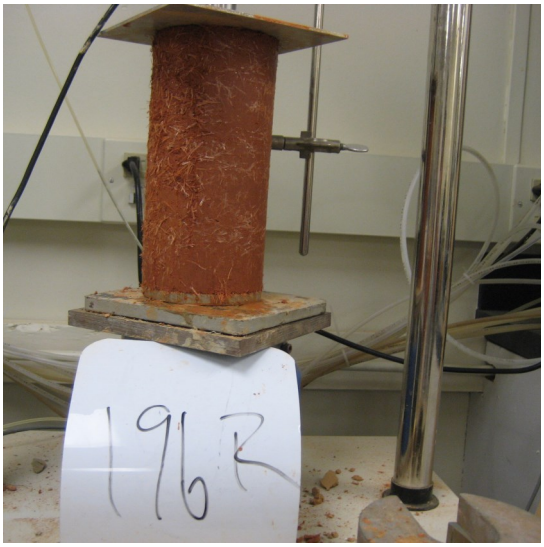

(a)

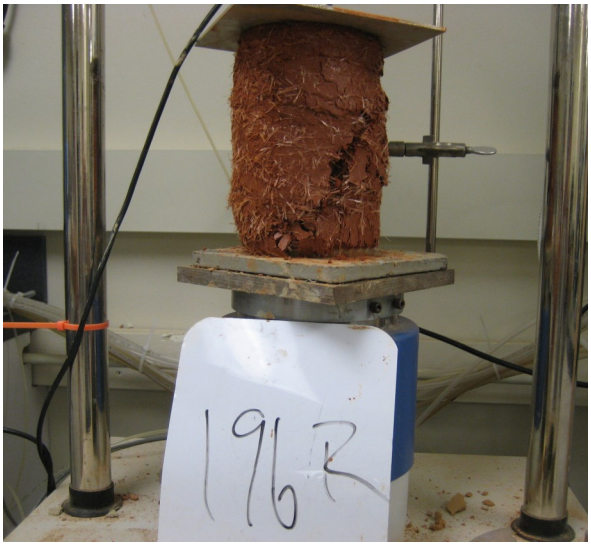

(b)

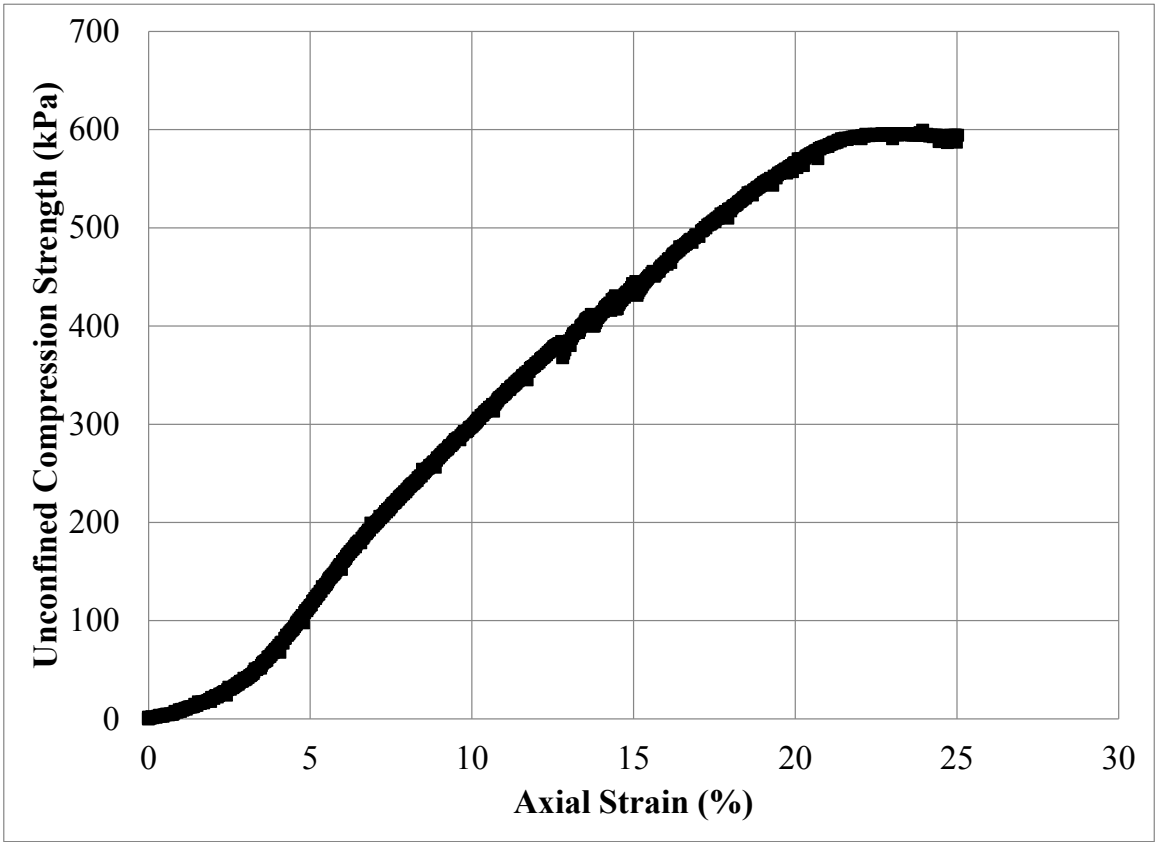

(c)

Figure C.160: Unconfined Compression Test Specimen No. 196R: (a) Photograph Prior to Testing; (b) Photograph Post Testing; and (c) Stress – Strain Data

(a)

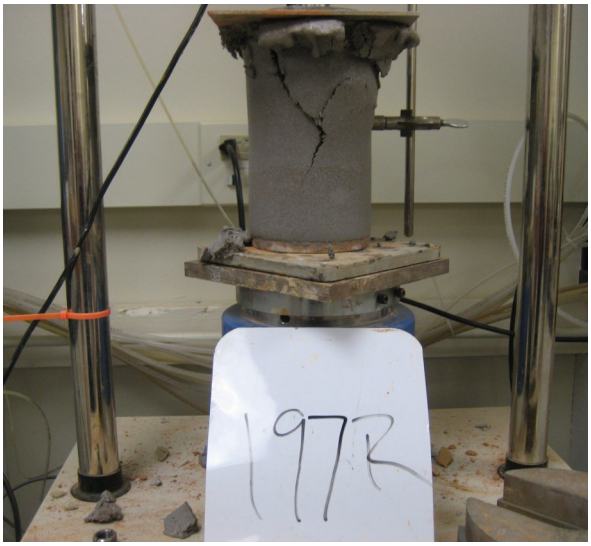

(b)

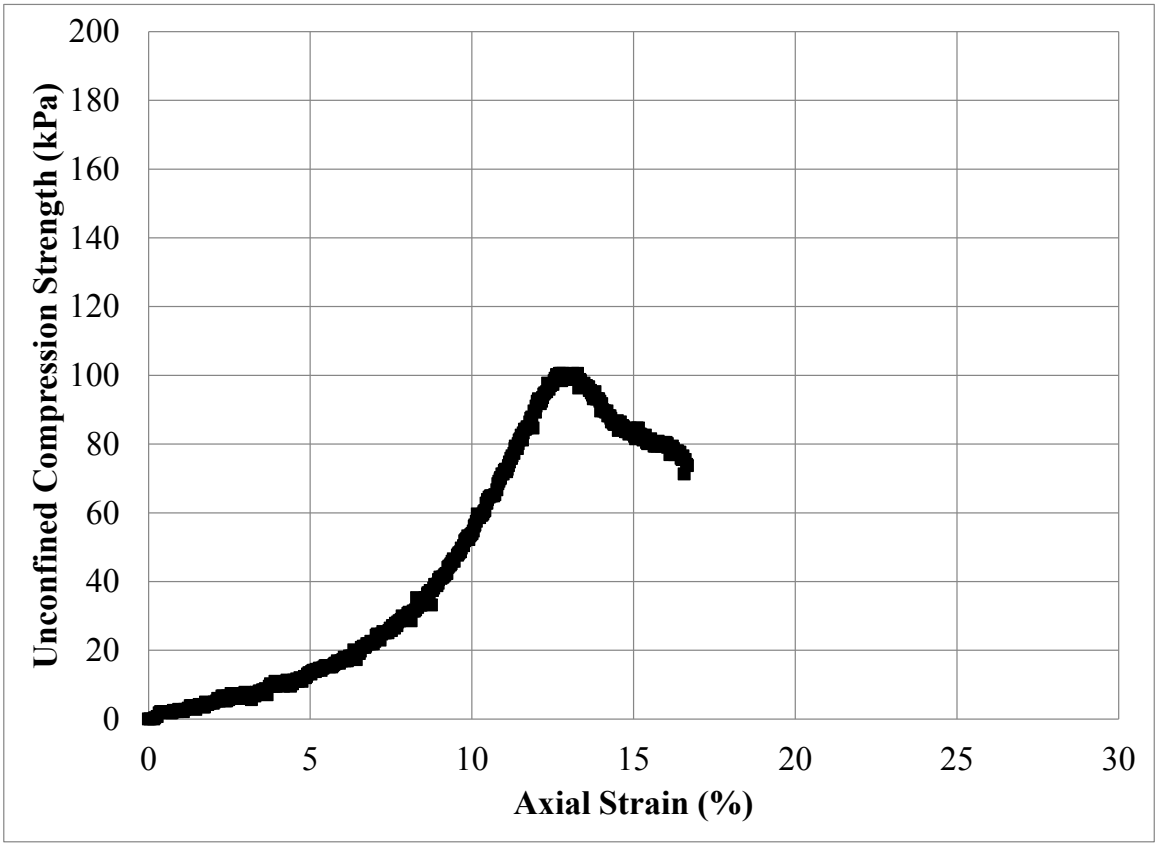

(c)

Figure C.161: Unconfined Compression Test Specimen No. 197R: (a) Photograph Prior to Testing; (b) Photograph Post Testing; and (c) Stress – Strain Data

(a)

(b)

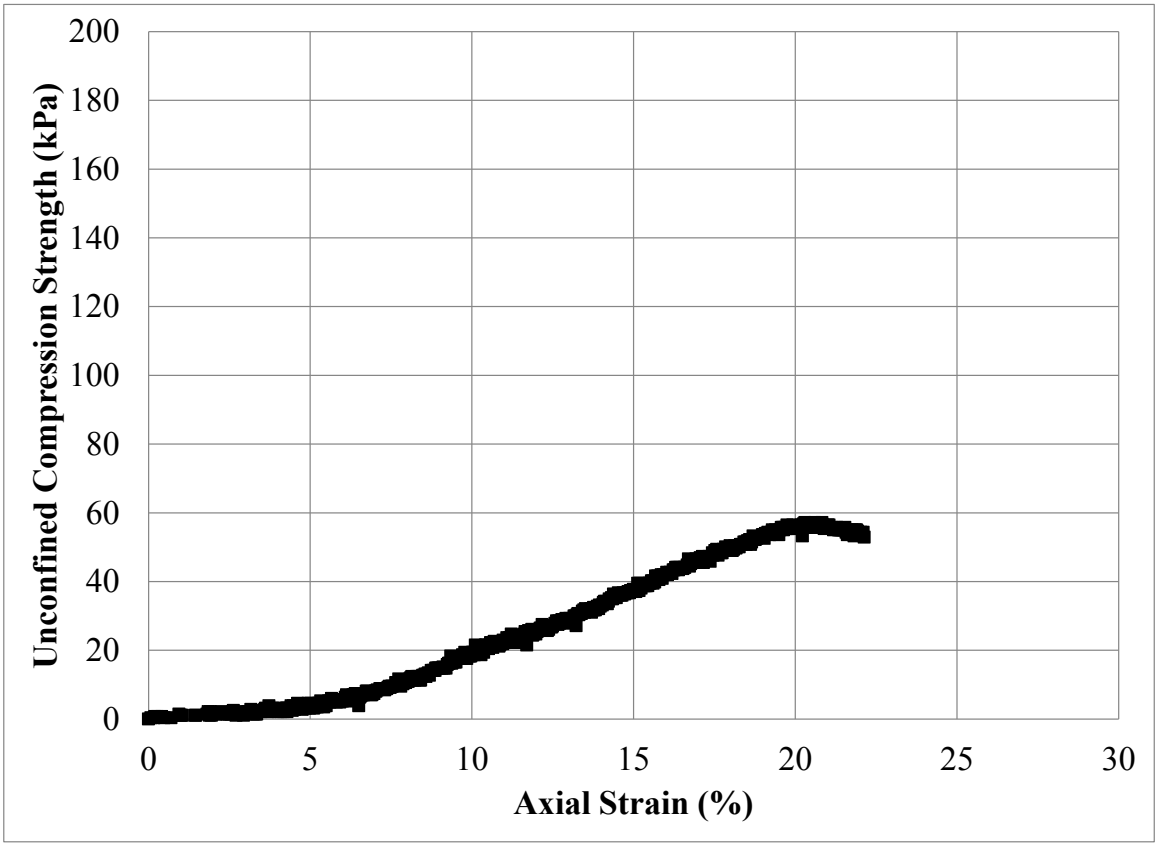

(c)

Figure C.162: Unconfined Compression Test Specimen No. 198R: (a) Photograph Prior to Testing; (b) Photograph Post Testing; and (c) Stress – Strain Data

(a)

(b)

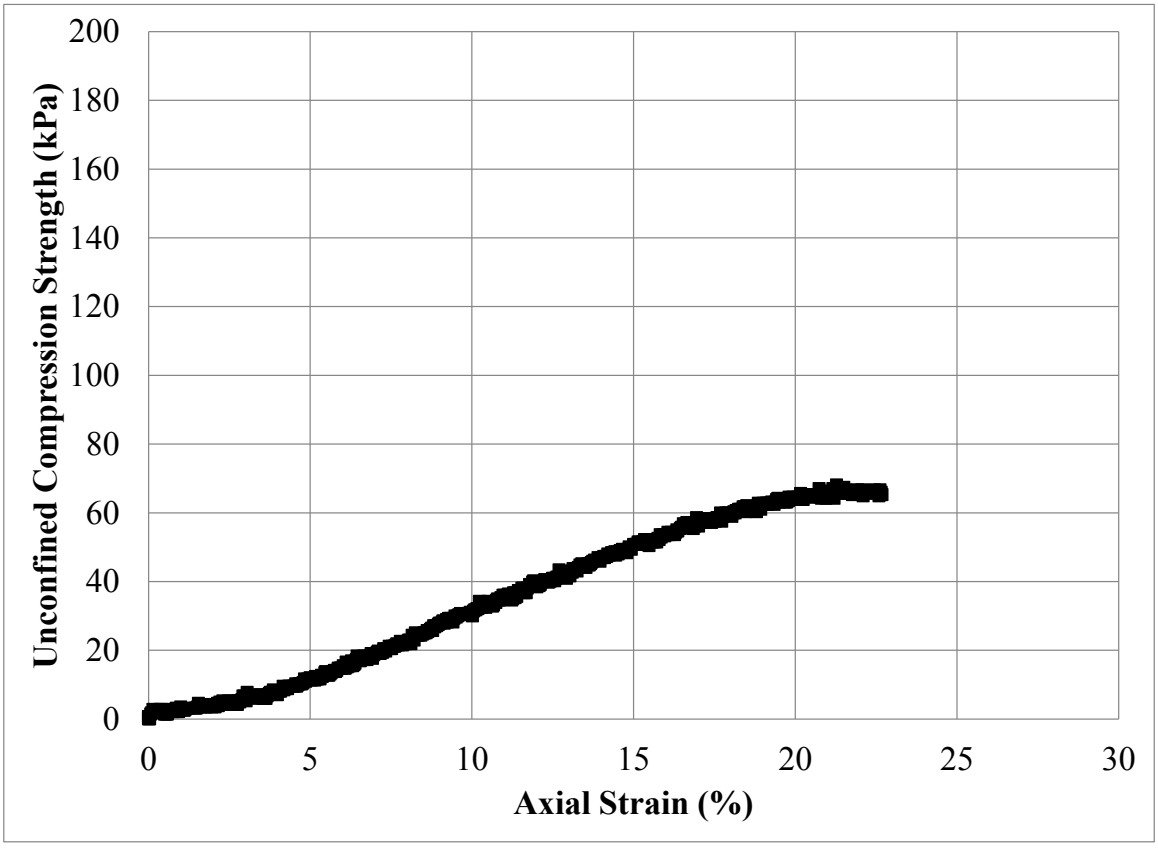

(c)

Figure C.163: Unconfined Compression Test Specimen No. 199R: (a) Photograph Prior to Testing; (b) Photograph Post Testing; and (c) Stress – Strain Data

(a)

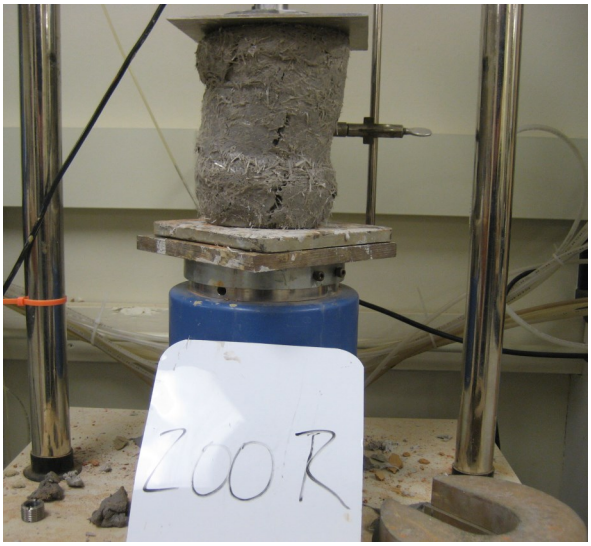

(b)

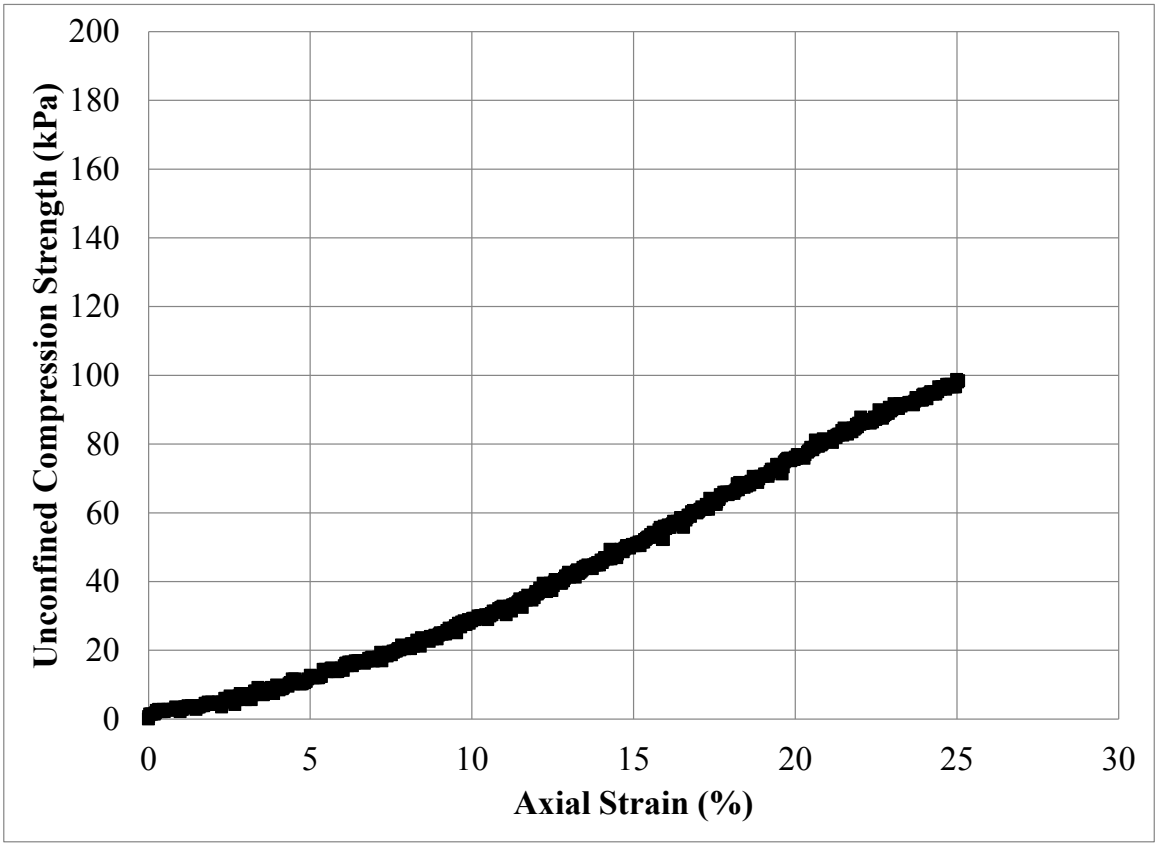

(c)

Figure C.164: Unconfined Compression Test Specimen No. 200R: (a) Photograph Prior to Testing; (b) Photograph Post Testing; and (c) Stress – Strain Data

(a)

(b)

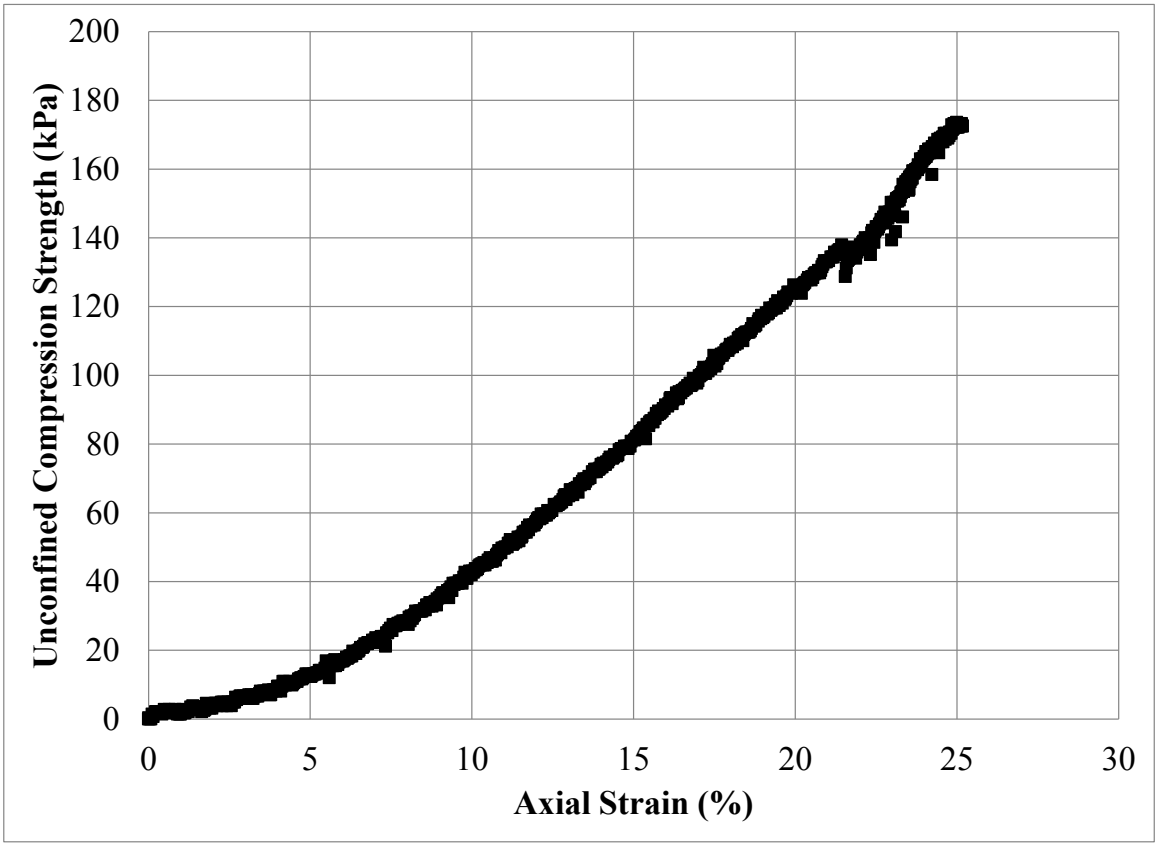

(c)

Figure C.165: Unconfined Compression Test Specimen No. 201R: (a) Photograph Prior to Testing; (b) Photograph Post Testing; and (c) Stress – Strain Data

APPENDIX D: SUMMARY OF THE TEST SPECIMEN RESULTS

Table D.1: Test Specimen Results

Specimen No.	Test Completion Date	Total Unit Weight (kN/m^3)	Water Content (%)	Peak UC Strength (kPa)	Axial Strain at Failure (mm/mm)	Degree of Saturation (%)	Group Description
19_1R	08/11/09	19.9	7.1	13.1	1.9	38	Control (0% Fiber) Vary Kaolin %
20_1R	08/11/09	21.6	9.3	187.1	4.8	57	
21_1R	08/11/09	21.5	10.9	188.1	6.8	60	
22_1R	08/11/09	22.3	10.3	187.1	8.1	67	
23_1R	08/11/09	21.4	8.3	64.9	2.6	52	
24R	07/29/09	19.9	7.0	12.7	2.6	38	
25R	07/29/09	21.4	7.9	63.3	2.8	51	
26R	07/29/09	21.5	9.5	193.4	5.2	57	
27R	07/29/09	22.3	10.1	202.8	8.6	66	
28R	07/29/09	21.6	11.2	198.5	8.5	61	
29R	07/30/09	19.9	7.0	13.4	1.8	38	
30R	07/30/09	21.3	7.7	64.9	3.1	50	
31R	07/30/09	21.6	8.8	199.1	4.8	56	
32R	07/30/09	22.3	9.9	200.1	8.0	65	
33R	07/30/09	21.6	11.2	8.1	8.1	61	
34R	08/05/09	21.6	9.0	216.5	4.5	56	20% Kaolin Vary Fiber %
35R	08/05/09	21.6	9.1	199.8	4.9	56	
36R	08/05/09	21.6	9.1	207.8	5.8	56	
37R	08/05/09	21.6	9.3	253.3	6.4	57	
38_1R	08/17/09	21.6	9.2	247.0	6.9	56	
39_1R	08/17/09	21.6	9.0	288.8	9.8	56	
40_1R	08/17/09	21.6	9.2	340.4	10.7	56	
41R	08/06/09	21.6	9.3	197.8	4.5	57	
42R	08/06/09	21.6	8.9	213.9	5.1	56	
43R	08/06/09	21.6	9.2	230.3	6.2	56	
44R	08/06/09	21.6	9.0	242.0	6.6	56	
45R	08/06/09	21.6	9.0	271.1	8.5	56	
46R	08/06/09	21.6	9.1	303.5	9.0	56	
47R	08/07/09	21.6	9.2	369.1	11.7	56	
48R	08/07/09	21.6	9.0	195.8	4.0	56	
49R	08/07/09	21.6	9.2	212.9	4.6	56	
50R	08/10/09	21.6	8.8	219.2	4.9	55	
51R	08/10/09	21.6	8.9	217.2	6.3	56	
52R	08/10/09	21.6	9.0	288.8	8.5	56	
53R	08/10/09	21.6	8.8	319.9	8.7	56	
54R	08/10/09	21.6	9.4	368.5	12.3	57	

Table D.1: Test Specimen Results (continued)

Specimen No.	Test Completion Date	Total Unit Weight (kN/m^3)	Water Content (%)	Peak UC Strength (kPa)	Axial Strain at Failure (mm/mm)	Degree of Saturation (%)	Group Description
73R	02/18/10	19.9	6.6	12.7	1.9	36	10% Kaolin Vary Fiber %
74R	02/23/10	19.9	6.7	18.0	2.7	37	
75R	02/23/10	19.9	6.5	24.0	2.8	36	
76R	02/23/10	19.9	6.7	19.7	2.4	37	
77R	02/23/10	19.9	6.5	28.9	4.2	36	
78R	02/25/10	19.9	6.4	34.6	4.0	36	
79R	02/25/10	19.8	6.3	40.9	5.3	35	
80R	02/25/10	19.9	6.6	17.3	3.0	36	
81R	02/25/10	19.9	6.4	19.8	2.9	35	
82R	02/25/10	19.8	6.3	22.2	3.2	35	
83R	05/19/10	19.8	6.3	22.6	3.7	35	
84R	05/24/10	19.9	6.9	25.8	3.9	37	
85R	05/24/10	19.9	6.8	33.9	4.7	37	
88R	05/24/10	19.9	6.8	13.4	2.3	37	
86R	05/24/10	19.9	6.9	18.3	2.3	37	
87R	05/24/10	19.9	6.9	40.2	4.5	38	
89R	05/24/10	19.9	6.8	23.6	2.9	37	
90R	05/24/10	19.9	6.7	21.9	3.3	37	
91R	05/24/10	19.9	6.7	32.5	4.0	37	
92R	05/26/10	19.9	6.9	42.7	5.2	37	
93R	05/26/10	19.9	6.7	48.7	5.3	37	
94R	05/26/10	21.3	7.8	66.3	3.6	50	15% Kaolin Vary Fiber %
95R	05/26/10	21.3	7.7	57.9	3.1	49	
96R	05/26/10	21.3	7.6	65.3	3.6	49	
97R	05/26/10	21.3	7.6	85.7	4.9	49	
98R	05/26/10	21.3	7.5	91.0	5.5	49	
99R	05/26/10	21.3	7.6	108.0	6.1	49	
100R	05/26/10	21.3	7.6	107.3	7.2	49	
101R	06/03/10	21.2	7.5	67.0	2.9	48	
102R	06/03/10	21.2	7.5	71.3	3.4	48	
103R	06/03/10	21.3	7.6	67.7	3.9	49	
104R	06/03/10	21.3	7.6	78.3	4.7	49	
105R	06/03/10	21.3	7.5	89.3	5.5	49	
106R	06/03/10	21.3	7.6	88.9	5.8	49	
107R	06/03/10	21.2	7.5	99.8	6.7	48	
108R	06/09/10	21.3	7.6	66.3	3.0	49	
109R	06/09/10	21.3	7.6	72.7	3.3	49	
110R	06/09/10	21.3	7.6	79.4	3.9	49	
111R	06/10/10	21.3	7.6	77.3	4.7	49	
112R	06/10/10	21.3	7.6	84.0	5.5	49	
113R	06/10/10	21.3	7.5	97.7	5.7	49	
114R	06/10/10	21.3	7.5	100.9	6.6	49	

Table D.1: Test Specimen Results (continued)

Specimen No.	Test Completion Date	Total Unit Weight (kN/m^3)	Water Content (%)	Peak UC Strength (kPa)	Axial Strain at Failure (mm/mm)	Degree of Saturation (%)	Group Description
115R	06/22/10	22.1	9.4	204.6	9.5	62	25% Kaolin Vary Fiber %
116R	06/22/10	22.1	9.5	214.9	9.0	63	
117R	06/22/10	22.1	9.5	250.1	9.1	63	
118R	06/22/10	22.1	9.2	275.5	10.9	62	
119R	06/22/10	22.1	9.3	343.6	13.3	62	
120R	06/23/10	22.1	9.2	322.8	11.4	61	
121R	06/23/10	22.1	9.2	515.8	16.4	61	
122R	06/29/10	22.1	9.3	205.0	8.3	62	
123R	06/29/10	22.1	9.3	236.0	8.4	62	
124R	06/29/10	22.1	9.3	250.1	8.9	62	
125R	06/29/10	22.1	9.3	275.5	9.2	62	
126R	06/29/10	22.0	9.2	314.7	10.8	61	
127R	06/29/10	22.0	9.0	439.6	17.8	60	
128R	06/29/10	22.0	9.1	435.7	13.9	61	
129R	06/29/10	22.1	9.3	205.3	8.6	62	
130R	06/29/10	22.1	9.3	228.6	8.7	62	
131R	06/29/10	22.1	9.3	254.4	8.4	62	
132R	06/29/10	22.0	9.2	252.3	8.9	61	
133R	06/30/10	22.1	9.3	331.3	11.0	62	
134R	06/30/10	22.1	9.2	400.4	14.1	61	
135R	06/30/10	22.1	9.2	484.4	14.4	61	
136R	07/07/10	21.1	10.1	203.9	8.5	55	30% Kaolin Vary Fiber %
137R	07/07/10	21.0	10.0	222.3	9.4	54	
138R	07/07/10	21.0	10.0	243.4	8.7	54	
139R	07/07/10	21.2	10.3	297.8	12.7	56	
140R	07/07/10	20.8	9.8	286.5	13.5	52	
141R	08/05/10	21.0	10.1	462.5	19.2	55	
142R	07/07/10	20.7	9.7	523.9	19.9	51	
143R	07/12/10	21.0	10.0	211.7	8.8	54	
144R	07/12/10	21.0	10.1	239.6	9.6	55	
145R	07/12/10	21.1	10.2	257.5	11.2	55	
146R	08/02/10	21.0	10.0	292.1	12.1	54	
147R	08/02/10	20.9	9.9	316.5	14.7	53	
148R	08/02/10	20.9	9.9	522.9	21.6	53	
149R	08/05/10	21.0	10.0	504.9	19.3	54	
150R	08/03/10	21.0	10.1	210.3	9.2	55	
151R	08/03/10	21.0	10.0	229.0	8.7	54	
152R	08/03/10	21.0	10.0	245.2	9.1	54	
153R	08/03/10	21.0	10.0	275.2	12.4	54	
154R	08/05/10	21.1	10.1	337.3	18.4	55	
155R	08/05/10	21.1	10.2	441.4	21.8	55	
156R	08/05/10	21.0	10.0	511.6	23.2	54	

Table D.1: Test Specimen Results (continued)

Specimen No.	Test Completion Date	Total Unit Weight (kN/m^3)	Water Content (%)	Peak UC Strength (kPa)	Axial Strain at Failure (mm/mm)	Degree of Saturation (%)	Group Description
157R	10/02/10	20.5	12.7	237.4	5.1	53*	Field Soils Vary Fiber %
158R	10/02/10	20.4	12.6	284.4	10.8	53*	
159R	10/02/10	20.3	12.4	557.4	18.2	52*	
160R	10/02/10	16.7	20.1	146.1	3.7	42*	
161R	10/02/10	16.5	19.1	166.5	4.7	40*	
162R	10/02/10	16.6	19.9	213.1	12.0	42*	
163R	10/02/10	21.4	14.5	202.9	4.2	63*	
164R	10/02/10	21.3	14.4	281.2	8.6	62*	
165R	10/03/10	21.3	14.3	586.7	22.3	61*	
166R	10/20/10	20.6	13.0	162.6	2.9	55*	
167R	10/20/10	20.3	12.4	1087.7	24.7	51*	
168R	10/20/10	16.6	20.0	149.9	3.7	42*	
169R	10/20/10	16.6	19.8	211.0	10.8	41*	
170R	10/20/10	21.6	14.8	149.2	3.9	65*	
171R	10/20/10	21.2	14.2	796.6	21.4	61*	
172R	11/17/10	20.0	22.2	91.7	4.9	61	
173R	11/17/10	19.3	22.7	160.9	8.1	57	
174R	11/17/10	19.2	22.8	267.1	14.3	56	
175R	11/17/10	19.4	22.7	424.1	17.6	57	
176R	11/17/10	19.6	22.5	843.9	25.0	59	
177R	12/07/10	22.9	17.0	66.7	7.3	78*	Field Soils Vary Fiber % 24 Hour Soak
178R	12/07/10	22.4	16.1	113.6	6.6	73*	
179R	12/07/10	22.6	16.5	191.6	14.4	75*	
180R	12/07/10	23.0	17.4	526.4	25.0	80*	
181R	12/07/10	23.1	17.4	485.8	22.2	81*	
182R	12/14/10	16.5	25.8	90.7	7.6	45*	
183R	12/14/10	16.7	25.0	87.8	9.5	46*	
184R	12/14/10	16.8	24.3	117.5	11.3	46*	
185R	12/14/10	16.7	24.8	128.4	11.8	46*	
186R	12/14/10	16.6	25.4	157.4	16.0	46*	
187R	12/15/10	23.9	17.9	62.1	9.2	90*	
188R	12/15/10	24.6	18.7	106.2	9.0	98*	
189R	12/15/10	24.3	18.3	181.7	15.7	94*	
190R	12/15/10	24.7	18.9	434.0	24.5	99*	
191R	12/15/10	24.3	18.4	531.3	25.0	94*	
192R	12/16/10	17.9	23.5	86.8	5.5	50	
193R	12/16/10	17.4	23.7	153.1	8.8	48	
194R	12/16/10	16.8	24.0	355.3	17.2	45	
195R	12/16/10	15.3	24.7	263.5	16.3	39	
196R	12/16/10	18.2	23.3	599.4	23.9	52	
197R	12/16/10	19.4	11.3	100.5	12.7	62	30% Kaolin Vary Fiber % 24 Hour Soak
198R	12/17/10	18.6	12.7	57.2	20.3	59	
199R	12/17/10	19.0	12.1	68.1	21.3	61	
200R	12/17/10	17.8	13.6	98.8	25.0	56	
201R	12/17/10	17.6	14.0	173.6	25.0	55	